

AWARD NUMBER: W81XWH-19-1-0575

TITLE: Targeting Leukemia-Initiating Cells to Improve Leukemia Treatment

PRINCIPAL INVESTIGATOR: James Croop, M.D.

CONTRACTING ORGANIZATION: TRUSTEES OF INDIANA UNIVERSITY,
980 INDIANA AVE RM 2232,
INDIANAPOLIS, IN 46202-5130.

REPORT DATE: NOVEMBER 2022

TYPE OF REPORT: FINAL REPORT

PREPARED FOR: U.S. Army Medical Research and Development Command
Fort Detrick, Maryland 21702-5012

DISTRIBUTION STATEMENT: Approved for Public Release;
Distribution Unlimited

The views, opinions and/or findings contained in this report are those of the author(s) and should not be construed as an official Department of the Army position, policy or decision unless so designated by other documentation.

REPORT DOCUMENTATION PAGE			<i>Form Approved</i> <i>OMB No. 0704-0188</i>		
Public reporting burden for this collection of information is estimated to average 1 hour per response, including the time for reviewing instructions, searching existing data sources, gathering and maintaining the data needed, and completing and reviewing this collection of information. Send comments regarding this burden estimate or any other aspect of this collection of information, including suggestions for reducing this burden to Department of Defense, Washington Headquarters Services, Directorate for Information Operations and Reports (0704-0188), 1215 Jefferson Davis Highway, Suite 1204, Arlington, VA 22202-4302. Respondents should be aware that notwithstanding any other provision of law, no person shall be subject to any penalty for failing to comply with a collection of information if it does not display a currently valid OMB control number. PLEASE DO NOT RETURN YOUR FORM TO THE ABOVE ADDRESS.					
1. REPORT DATE NOVEMBER 2022		2. REPORT TYPE Final Report		3. DATES COVERED 01 August 2019 – 31 JULY 2022	
4. TITLE AND SUBTITLE Targeting Leukemia-Initiating Cells to Improve Leukemia Treatment			5a. CONTRACT NUMBER W81XWH-19-1-0575		
			5b. GRANT NUMBER CA180318		
			5c. PROGRAM ELEMENT NUMBER		
6. AUTHOR(S) James Croop, Yan Liu, Yunlong Liu, H. Scott Boswell, and Wei Tong E-Mail: jcroop@iu.edu			5d. PROJECT NUMBER		
			5e. TASK NUMBER		
			5f. WORK UNIT NUMBER		
7. PERFORMING ORGANIZATION NAME(S) AND ADDRESS(ES) TRUSTEES OF INDIANA UNIVERSITY, 980 INDIANA AVE RM 2232, INDIANAPOLIS, IN 46202-5130.			8. PERFORMING ORGANIZATION REPORT NUMBER		
9. SPONSORING / MONITORING AGENCY NAME(S) AND ADDRESS(ES) U.S. Army Medical Research and Development Command Fort Detrick, Maryland 21702-5012			10. SPONSOR/MONITOR'S ACRONYM(S)		
			11. SPONSOR/MONITOR'S REPORT NUMBER(S)		
12. DISTRIBUTION / AVAILABILITY STATEMENT Approved for Public Release; Distribution Unlimited					
13. SUPPLEMENTARY NOTES					
14. ABSTRACT Pediatric leukemias account for almost 35% of all childhood cancers, leaving leukemia as the leading cause of cancer death for children. In addition to children, leukemia also affects adults. Adult leukemia usually occurs around age 60 and carries a very poor prognosis, with most patients live less than 18 months. Leukemia is initiated and maintained by a rare population of leukemia-initiating cells (LICs). LICs, and in particular those that are in a dormant state, are resistant to chemotherapy or targeted therapies. As we found that protein tyrosine phosphatase PRL2 is highly expressed in MLL leukemias, the objective of this proposal is to determine the effects of genetic and pharmacological inhibition of PRL2 on human leukemia-initiating cells in order to further assess its clinical potential. We found that PRL2 is essential for the self-renewal and survival of LICs expressing MLL-AF9. We developed a novel PRL2-specific inhibitor (PRLi) and found that PRLi treatment decreases the proliferation and survival of human MLL leukemia cells <i>in vitro</i> . Importantly, we found that <i>in vivo</i> PRLi treatment significantly increases the survival of MLL leukemia mice. The proposed work will facilitate the clinical application of PRL2 inhibitors in treating military personnel, veterans and their dependents with leukemia, thus improving their quality of life.					
15. SUBJECT TERMS Leukemia, leukemia-initiating cell, PRL2, PRLi, and MLL-AF9					
16. SECURITY CLASSIFICATION OF:			17. LIMITATION OF ABSTRACT	18. NUMBER OF PAGES	19a. NAME OF RESPONSIBLE PERSON USAMRDC
a. REPORT	b. ABSTRACT	c. THIS PAGE			19b. TELEPHONE NUMBER (include area code)
Unclassified	Unclassified	Unclassified	Unclassified	228	

TABLE OF CONTENTS

	<u>Page</u>
1. Introduction	4
2. Keywords	4
3. Accomplishments	4-14
4. Impact	14-15
5. Changes/Problems	15-16
6. Products	16-18
7. Participants & Other Collaborating Organizations	18-21
8. Special Reporting Requirements	21
9. Appendices	21-228

1. Introduction

This proposed research is designed to address the critical knowledge gap as identified by the **FY18 PRCRP Program: "Blood Cancers"**. Pediatric leukemias account for almost 35% of all childhood cancers, leaving leukemia as the leading cause of cancer death for children. In addition to children, leukemia also affects adults. Adult leukemia usually occurs around age 60 and carries a very poor prognosis, with most patients live less than 18 months. **Active duty military members** are frequently exposed to ionizing irradiation, chemicals, infectious agents and/or environmental carcinogens. This exposure can cause mutations in blood cells that lead to blood cancer (leukemia). For instance, there are increasing numbers of **Gulf War veterans** returning from theater with irradiation or toxin exposure-related leukemia. Despite significant progress in treating leukemia, some patient populations response poorly to conventional chemotherapy. Unfortunately, little progress has been made in treating leukemia over the past 4 decades. Clearly, new treatment strategies are urgently needed. Leukemia is initiated and maintained by a rare population of leukemia-initiating cells (LICs). LICs, and in particular those that are in a dormant state, are resistant to chemotherapy or targeted therapies. This proposal seeks to validate and pharmacologically modulate new leukemia targets with an eye toward clinical translation. As we found that protein tyrosine phosphatase PRL2 is highly expressed in MLL leukemias, the objective of this proposal is to determine the effects of genetic and pharmacological inhibition of PRL2 on human leukemia-initiating cells in order to further assess its clinical potential. We found that PRL2 is essential for the self-renewal and survival of LICs expressing MLL-AF9. We developed a novel PRL2-specific inhibitor (PRLi) and found that PRLi treatment decreases the proliferation and survival of human MLL leukemia cells *in vitro*. Importantly, we found that *in vivo* PRLi treatment significantly increases the survival of MLL leukemia mice. The proposed work will facilitate the clinical application of PRL2 inhibitors in treating military personnel, veterans and their dependents with leukemia, thus improving their quality of life.

2. Keywords

Leukemia, leukemia-initiating cells, PRL2, PRLi, targeted therapy, and MLL-AF9

3. Accomplishments

Major goals and accomplishments: From August 1, 2019, to August 31, 2022, we have carried out all experiments proposed in both Aim 1 and Aim 2. We have completed all proposed research as indicated in the Statement of Work (SOW).

Specific Aim 1: Determine the impact of genetic and pharmacological inhibition of PRL2 on leukemia-initiating cells.

Rationale: MLL-rearranged leukemias represent about 10% of all leukemia cases, including acute lymphoblastic leukemia (ALL) and acute myeloid leukemia (AML). We found that PRL2 is highly expressed in human AML with MLL translocations (**Fig. 1**). Given that elevated PRLs have been shown to promote cancer cell proliferation and survival, PRL2 may be a potential therapeutic target in MLL leukemias. Increased self-renewal potential and enhanced survival are two key behaviors of leukemia-initiating cells. The *objective* of this aim is to determine the impact of inhibiting PRL2 on LIC self-renewal and survival in MLL leukemias. Our *working hypothesis* is that inhibition of PRL2 activity will decrease LIC self-renewal and survival. To test this hypothesis, we will determine the impact of genetic and pharmacological inhibition of PRL2 on human leukemia cells with MLL translocations by employing a mouse model of human AML and Patient-Derived Xenograft (PDX) models.

Major Task 1: Determine the impact of genetic inhibition of PRL2 on human leukemia cells with MLL translocations.

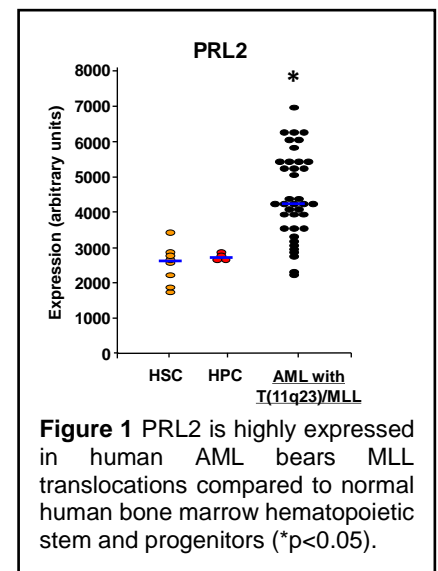
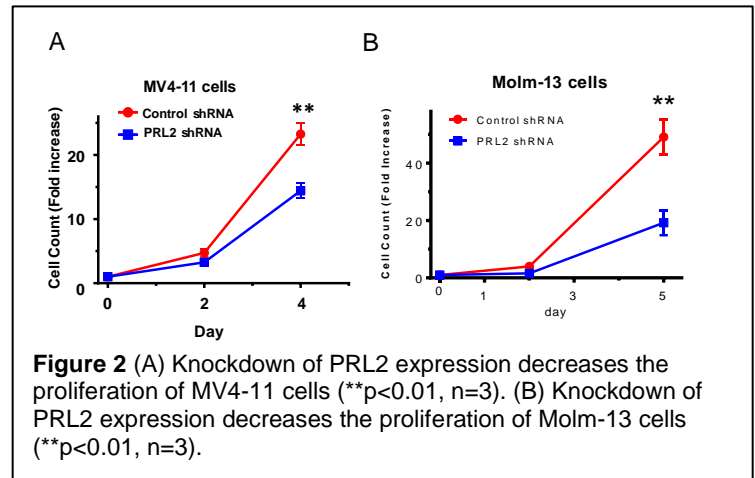
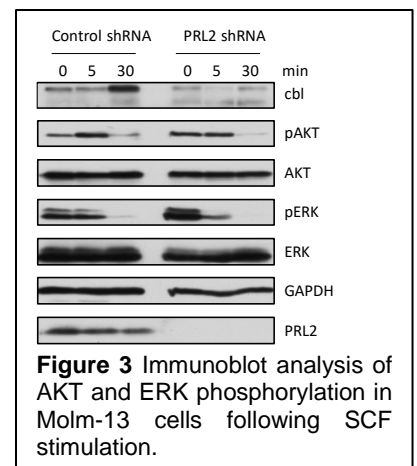


Figure 1 PRL2 is highly expressed in human AML bears MLL translocations compared to normal human bone marrow hematopoietic stem and progenitors (*p<0.05).

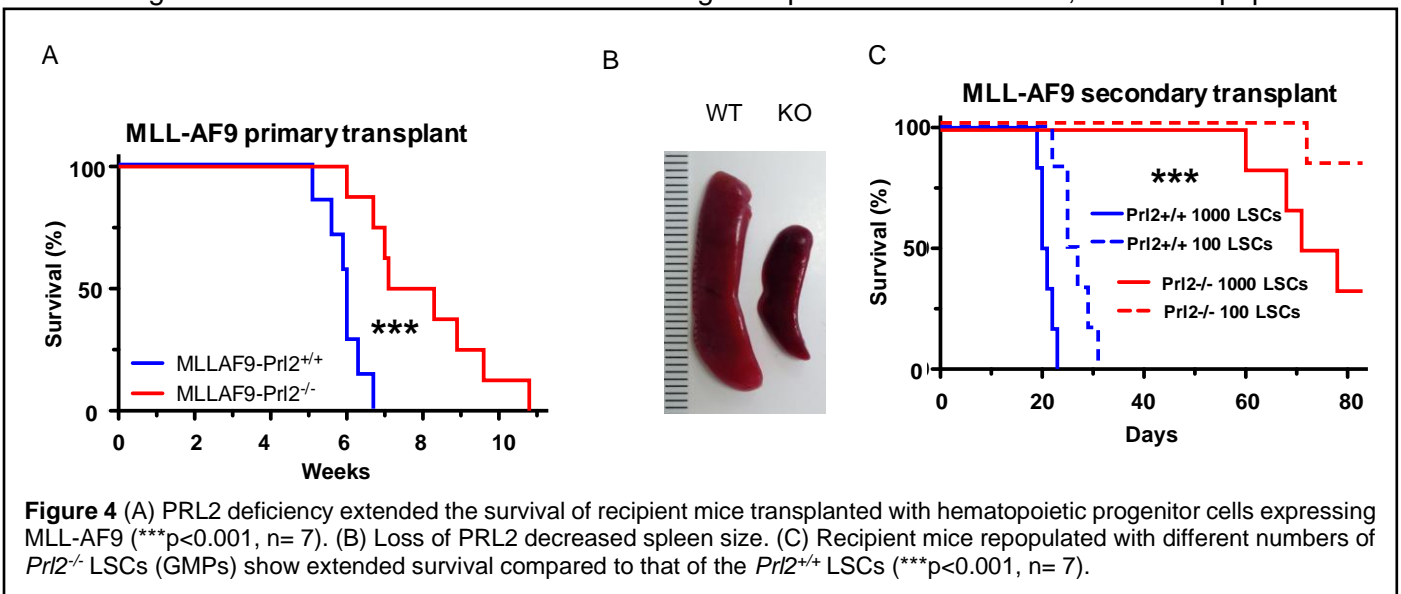
Genetic inhibition of PRL2 decreases the proliferation of human MLL leukemia cells: MV4-11 is a human B-myelomonocytic leukemia cell line with MLL-AF4 translocation and Molm-13 is a human AML cell line with MLL-AF9 translocation. To knock down PRL2 expression in human leukemia cells, we transduced human MV4-11 and Molm-13 cells with lentiviruses expressing a control shRNA (Sh-Luc) or a PRL2 shRNA. We observed downregulation of both PRL2 mRNA and protein in cells expressing PRL2 shRNA (data not shown). We found that knockdown of PRL2 using shRNA targeting PRL2 decreases the proliferation of both MV4-11 and Molm-13 cells (**Fig. 2A and 2B**). Thus, we demonstrated that PRL2 is important for the proliferation of human leukemia cells with MLL-translocations.



Genetic inhibition of PRL2 decreases the levels of pAKT and pERK in human MLL leukemia cells: To understand why PRL2 deficiency decreases leukemia cell proliferation, we examined phosphorylation of AKT and ERK in Molm-13 cells following SCF stimulation. We found that knocking down of PRL2 significantly decreases both the levels of pAKT and pERK in Molm-13 cells (**Fig. 3**). Interestingly, we also observed decreased levels of CBL, an E3 ubiquitin ligase responsible for ubiquitination of both KIT and FLT3 in hematopoietic cells, in Molm-13 cells expressing PRL2 shRNA (**Fig. 3**). These findings suggest that CBL may be involved in modulating oncogenic signaling in PRL2 null HSPCs.

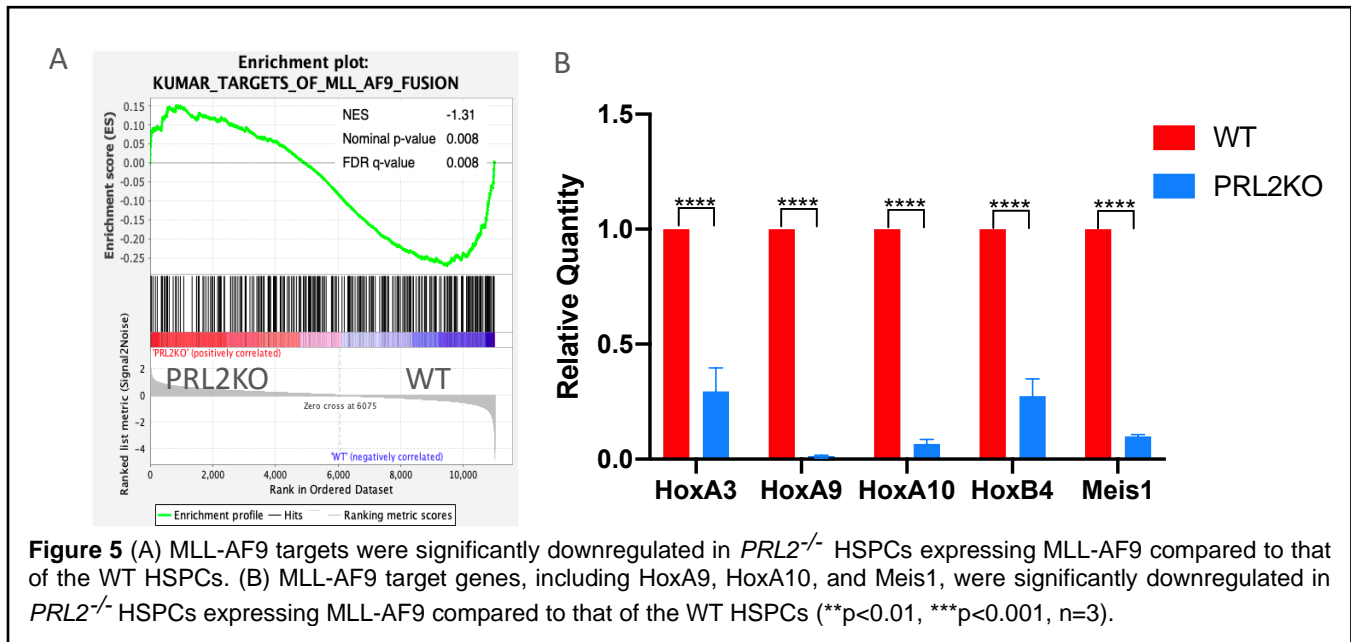


PRL2 is essential for the maintenance of MLL-AF9 driven leukemia: We utilized a well-established mouse model of human MLL leukemia-induced by MLL-AF9 to determine the role of PRL2 in the initiation and maintenance of MLL leukemias. We introduced MLL-AF9 into hematopoietic progenitor cells isolated from wild-type (WT) and *Prl2* null mice using a retrovirus carrying cDNA that encodes MLL-AF9 (MSCV-MLL-AF9-IRES-GFP). We then transplanted transduced cells (GFP⁺) into lethally irradiated recipient mice. The development of leukemia in host that received wild-type cells transduced with MLL-AF9 retrovirus was rapid, with all control animals succumbing to the disease and died 7 weeks following transplantation. In contrast, animals repopulated



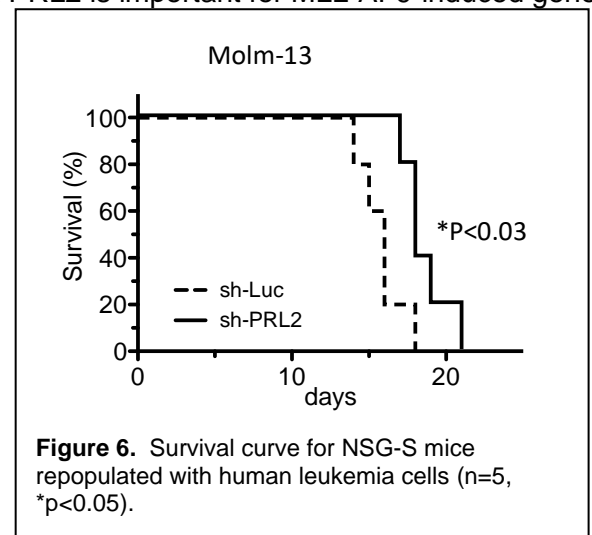
with *Prl2* null cells showed extended survival (**Fig. 4A**). Expression of MLL-AF9 causes splenomegaly in

recipient mice repopulated with WT cells and loss of PRL2 significantly decreased spleen size (**Fig. 4B**). To determine the role of PRL2 in LIC self-renewal, we performed limiting dilution transplantation assays and transplanted 100 or 1000 leukemia stem cells (GMPs) purified from the BM of primary recipients that have developed leukemia into sublethally irradiated recipient mice. While most recipient mice repopulated with *Pr12*^{+/+} cells expressing MLL-AF9 developed leukemia and died within 30 days, the recipient mice repopulated with *Pr12*^{-/-} cells displayed significant protection from disease and showed extended survival (**Fig. 4C**).



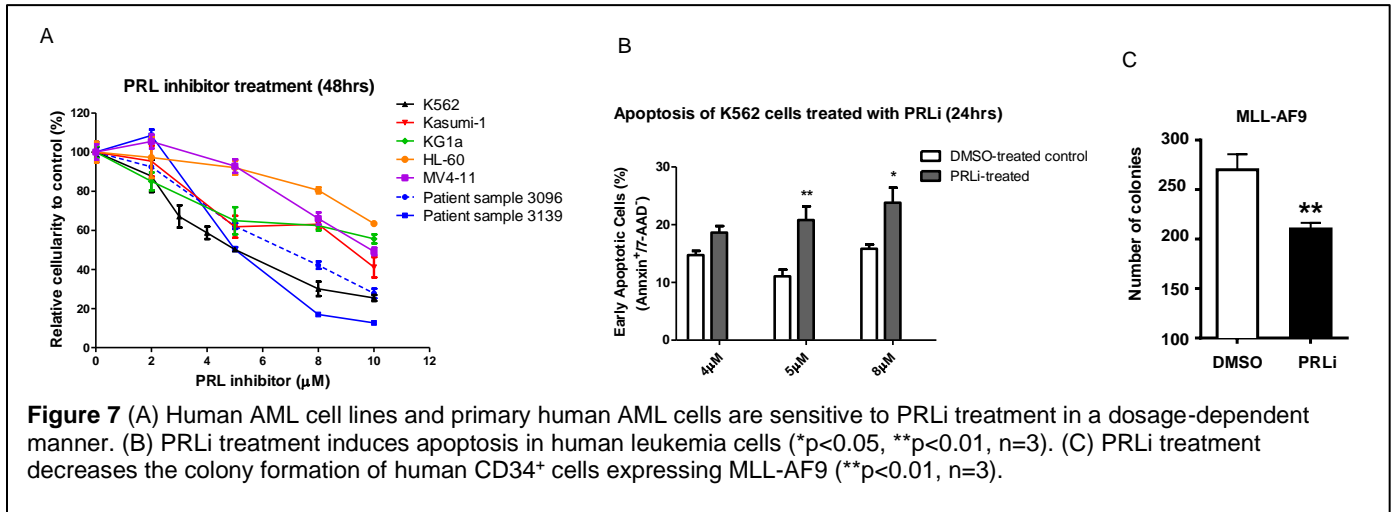
MLL-AF9 targets were significantly downregulated in *Pr12*^{-/-} HSPCs: To determine the mechanisms by which PRL2 enhances LIC self-renewal, we performed RNA-seq analysis to compare gene expression in *Pr12*^{+/+} and *Pr12*^{-/-} fetal liver HSPCs (LSKs) expressing MLL-AF9. To ensure reproducibility, three biological replicates were performed. We then employed Gene Set Enrichment Analysis (GSEA) to group potential PRL2 target genes into specific pathways important for LIC behavior. MLL-AF9 targets were significantly downregulated in *Pr12*^{-/-} HSPCs compared to *Pr12*^{+/+} HSPCs (**Fig. 5A**). We confirmed that MLL-AF9 target genes that are important for LIC self-renewal, including *HoxA9*, *HoxA10*, and *Meis1*, are downregulated in *MLL-AF9*⁺*Pr12*^{-/-} HSPCs (**Fig. 5B**). Thus, we demonstrate that PRL2 is important for MLL-AF9-induced gene expression in HSPCs.

Genetic inhibition of PRL2 prolongs the survival of human leukemia cells *in vivo*: To determine the impact of PRL2 deficiency on leukemia development *in vivo*, we have established Patient-Derived Xenograft (PDX) models. We injected 1.5 x 10⁶ Molm-13 cells expressing control shRNA (sh-Luc) or PRL2 shRNA into sublethally (2.5 Gy) irradiated immunodeficient mice (NSG-S) and monitored disease development and survival. Consistent with our findings in mouse model of human AML (**Fig. 4**), we found that knocking down of PRL2 in Molm-13 cells significantly extended the survival of NSG-S mice (**Fig. 6**). Thus, we demonstrate that genetic inhibition of PRL2 in human leukemia cells delays leukemia development and prolongs survival *in vivo*.



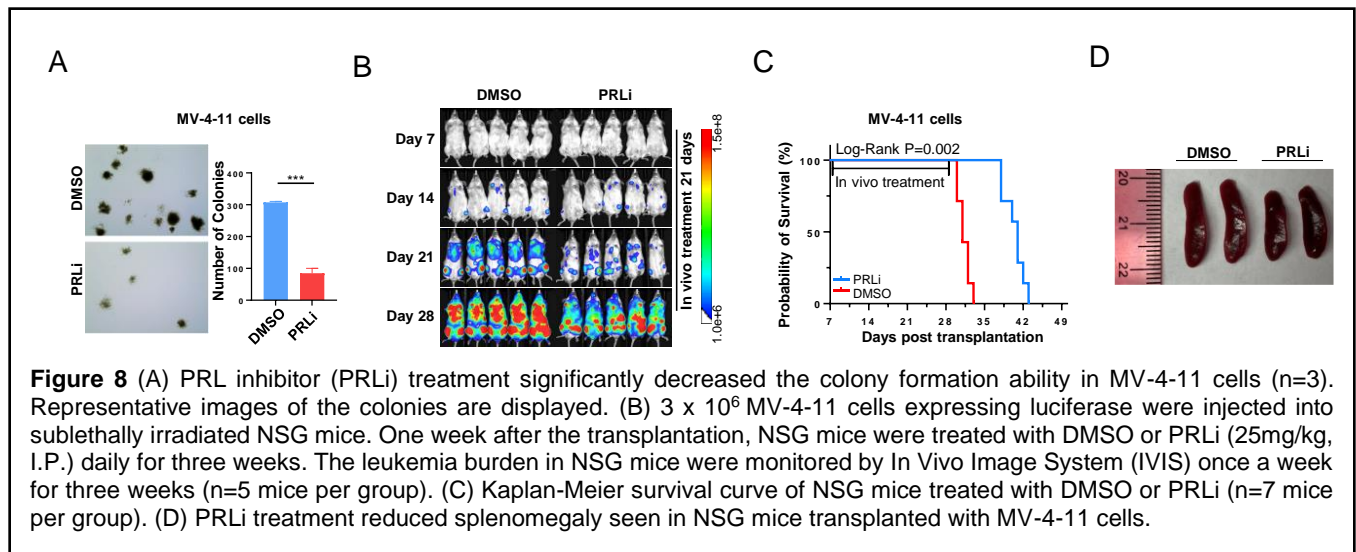
Major Task 2: Determine the impact of pharmacological inhibition of PRL2 on human leukemia cells with *MLL* translocations.

Development of a PRL2-specific inhibitor that decreases the proliferation and survival of human MLL leukemia cells: Recently, we identified a small molecule PRL2 inhibitor (PRLi) using computer-based virtual



screening. PRLi did not affect the viability of human cord blood mononuclear cells and CD34⁺ cells (data not shown). To determine the role of PRL2 in the proliferation and survival of human leukemia cells, we treated several human AML cell lines with different concentrations of PRLi and monitored cell proliferation and survival. We found that PRLi treatment of PRL2-expressing human AML cell lines resulted in decreased proliferation and survival (**Fig. 7A**). Furthermore, we found that primary human AML cells are sensitive to PRL2 inhibitor treatment in a dose-dependent manner (**Fig. 7A**). We also found that pharmacological inhibition of PRL2 function using PRLi decreases the survival of human AML cells (**Fig. 7B**). Human leukemia-initiating cells (LICs) are enriched in the CD34⁺ population of leukemia blasts. Human CD34⁺ cells expressing MLL-AF9 represent a valuable tool for studying MLL-AF9-positive AML. While DMSO treatment did not affect the colony formation of human CD34⁺ cells expressing MLL-AF9, blocking PRL2 function with PRLi decreased the colony formation of human CD34⁺ cells expressing MLL-AF9 (**Fig. 7C**).

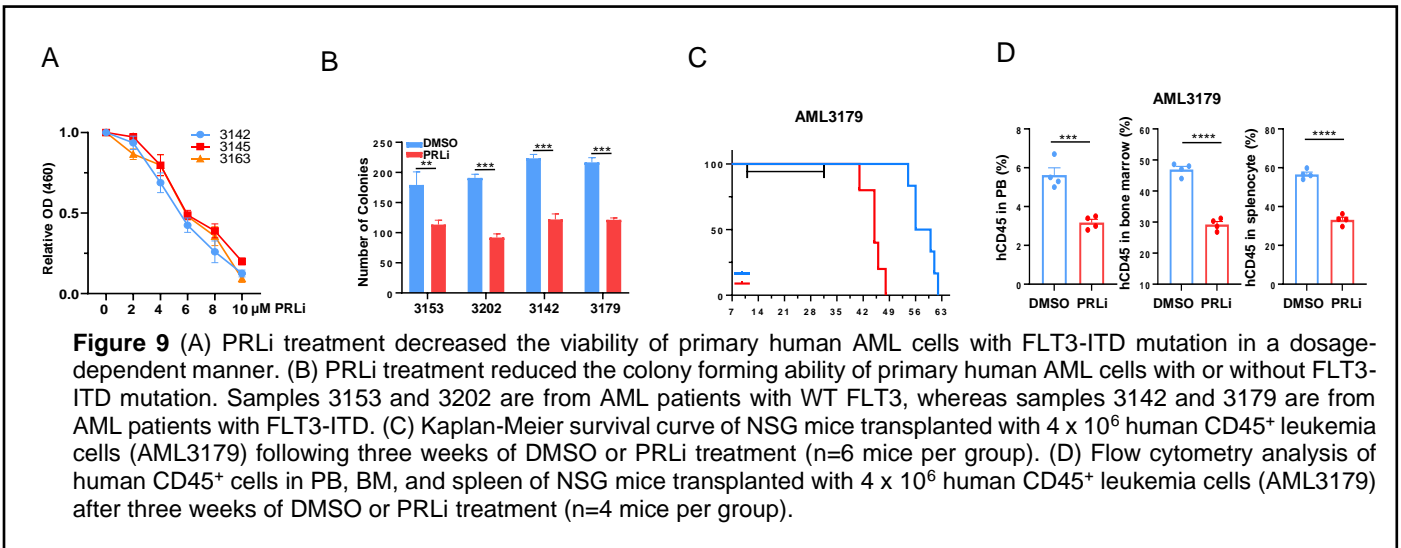
Pharmacological inhibition of PRL2 decreases leukemia burden and extends the survival of mice transplanted with human leukemia cell lines:



PRLi treatment reduces the colony formation of MV-4-11 cells (**Fig. 8A**). To determine the efficacy of PRLi on human leukemia cells *in vivo*, we transplanted luciferase-labeled MV-4-11 cells into sublethally irradiated NSG mice via tail vein injection. One week after the transplantation, we treated NSG mice with vehicle (10% DMSO) or PRLi (25 mg/kg, I.P.) daily for three weeks. Leukemia burden in NSG mice was monitored via bioluminescence imaging weekly. Serial imaging of luminescence showed that PRLi treatment dramatically decreases leukemia burden compared with the control group (**Fig. 8B**). The radiance of the NSG mice was significantly reduced after exposure to PRLi. Furthermore, PRLi

substantially extended the survival of NSG mice transplanted with human leukemia cells (**Fig. 8C**). PRLi also considerably decreased the engraftment of human leukemia cells in PB, BM, and spleen of NSG mice (data not shown). PRLi treatment significantly reduced the size and weight of spleen of NSG mice (**Fig. 8D**).

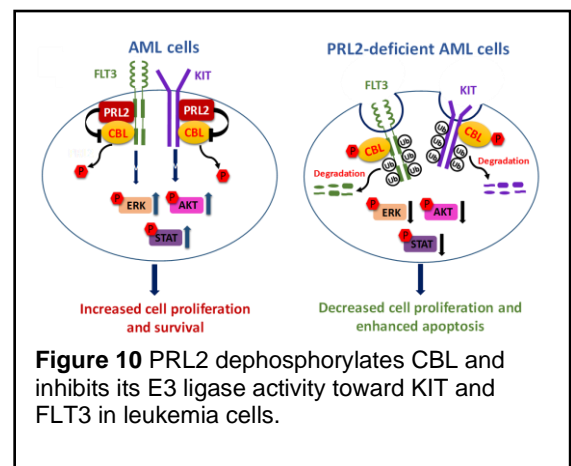
Pharmacological inhibition of PRL2 reduces leukemia burden and extends the survival of mice transplanted with primary human AML cells:



PRLi decreases the proliferation of primary human AML cells *in vitro* in a dosage-dependent manner (**Fig. 9A**). In addition, PRLi treatment decreases the colony formation of primary human AML cells with or without FLT3 mutations (**Fig. 9B**). To determine the efficacy of PRLi on primary human leukemia cells *in vivo*, we generated two patient-derived xenograft (PDX) models of FLT3-ITD positive AML in NSGS mice. 12-16 weeks post primary transplantation, we confirmed engraftment of human CD45⁺ (huCD45⁺) AML cells in NSGS mice (data not shown) and generated secondary recipients for drug administration. After confirmation of human leukemia cell engraftment in peripheral blood of NSG mice (>1% human CD45⁺ cells), NSG mice were treated with vehicle (10% DMSO) or PRLi (25 mg/kg, I.P.) daily for three weeks. PRLi substantially extended the survival of NSG mice transplanted with human CD45⁺ leukemia cells (**Fig. 9C**). PRLi also considerably decreased the engraftment of human CD45⁺ leukemia cells in PB, BM, and spleen of NSG mice at the end point of treatment (**Fig. 9D**).

Specific Aim 2: Determine the mechanisms by which PRL2 contributes to the pathogenesis of leukemia.

Rationale: Most human leukemia cells depend on aberrant receptor tyrosine kinase signaling and the subsequent downstream effectors for proliferation and survival. KIT and FLT3 are two of the major oncogenic receptor tyrosine kinases that are aberrantly activated in leukemia. We found that PRL2 enhances KIT activation in hematopoietic stem and progenitor cells following cytokine stimulation. KIT inactivation can be mediated by removal from the cell surface and intracellular degradation. Indeed, we found that PRL2 modulates KIT internalization in hematopoietic progenitor cells and leukemia cells. Further, KIT half-life is reduced in PRL2 null hematopoietic progenitor cells due to enhanced ubiquitination. The CBL family E3 ubiquitin ligases, including CBL and CBL-B, are responsible for the ubiquitination and degradation of KIT and FLT3 in hematopoietic cells. Upon SCF stimulation, KIT binds to and induces the phosphorylation of CBL proteins, which in turn act as E3 ligases, mediating the ubiquitination and degradation of KIT and themselves. We found that PRL2 showed enhanced association with CBL, KIT, and FLT3 in human



leukemia cells, suggesting that CBL may be a substrate of PRL2 in leukemia cells. We *hypothesize* that PRL2 inhibits the E3 ligase activity of CBL toward KIT and FLT3, leading to decreased ubiquitination and degradation of KIT and FLT3, thereby activating downstream signaling pathways in leukemia cells (**Fig. 10**, left panel). We further *speculate* that CBL is hyper-phosphorylated in PRL2-deficient leukemia cells, leading to enhanced ubiquitination and degradation of both KIT and FLT3 (**Fig. 10**, right panel). To test the hypothesis, we will perform four parallel experiments. First, we will determine the role of PRL2 in CBL phosphorylation in mouse HSPCs expressing MLL-AF9 and in human AML cells with MLL translocations. Second, we will determine the impact of CBL E3-dead mutant on KIT and FLT3 ubiquitination and degradation in PRL2 null hematopoietic progenitor cells. Third, we will determine the impact of CBL-deficiency on *PRL2*^{-/-} LIC self-renewal. Finally, we will determine the impact of KIT and FLT3 inhibitors on human MLL leukemia cells with high PRL2 expression.

Major Task 3: Cbl in *PRL2*^{-/-} LIC self-renewal.

PRL2 enhances oncogenic KIT and FLT3 signaling in hematopoietic progenitor cells: Previously, we discovered that PRL2 is important for SCF/KIT signaling in hematopoietic stem and progenitor cells (HSPCs). PRL2 null hematopoietic progenitor cells showed decreased KIT phosphorylation at tyrosine 703 as well as AKT and ERK phosphorylation following SCF stimulation (**Fig. 11**). Importantly, we observed decreased levels of CBL in PRL2 null HSPCs following SCF stimulation. As CBL is responsible for ubiquitination and degradation of both KIT and FLT3, these findings suggest that PRL2 enhances KIT and FLT3 activation in HSPCs through regulating CBL phosphorylation.

PRL2 is important for FLT3-ITD driven cell proliferation: To determine the role of PRL2 in oncogenic FLT3 signaling, we introduced FLT3 and FLT3-ITD into WT and PRL2 null HSPCs and performed colony formation and proliferation assays. As shown in **Figure 12A**, loss of PRL2 decreased the colony formation of HSPCs expressing FLT3-ITD, but not FLT3. We then examined the response of HSPCs to FLT3 stimulation. We found that PRL2 null HSPCs expressing FLT3-ITD show decreased proliferation both in the presence of FLT3 and in the absence of cytokine (**Fig. 12B**). Thus, we demonstrate that PRL2 is a critical mediator of FLT3-ITD signaling in hematopoietic stem and progenitor cells.

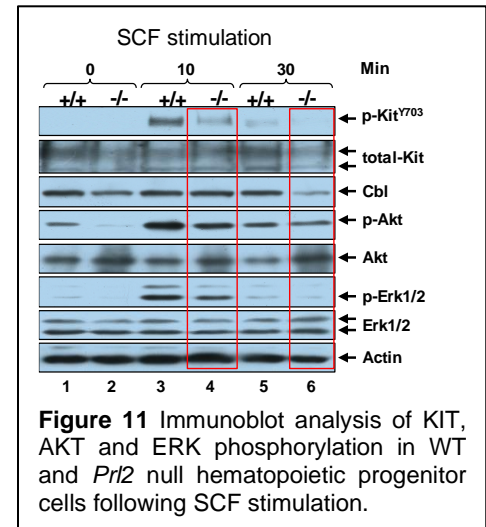
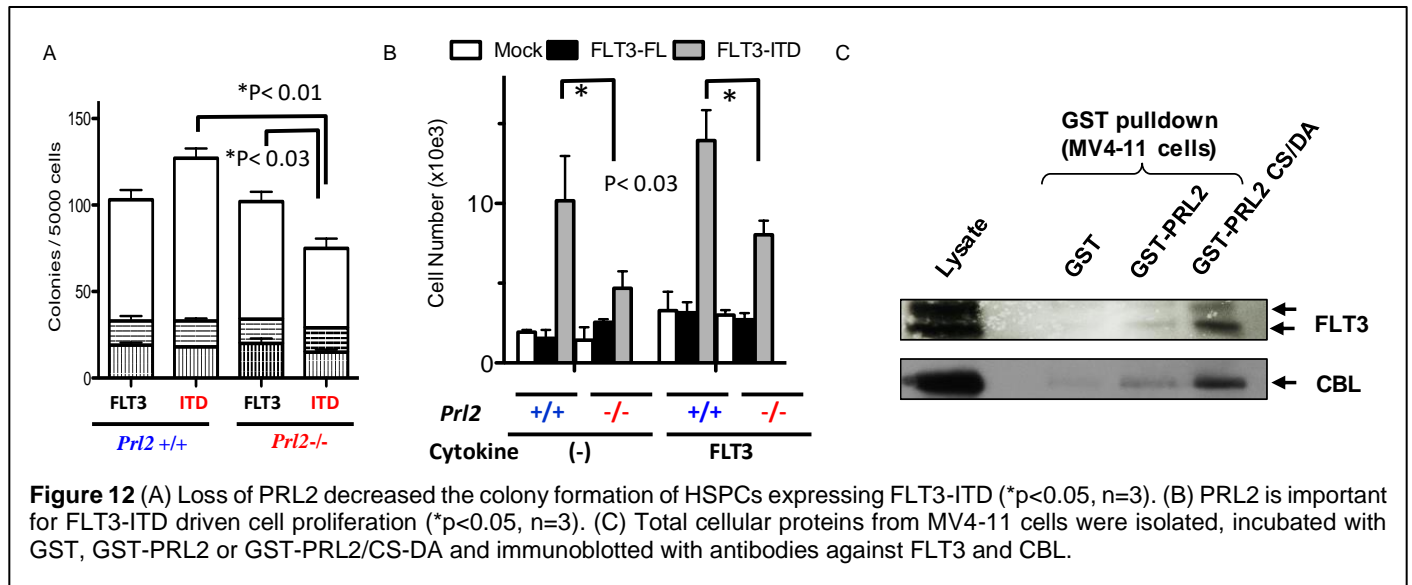


Figure 11 Immunoblot analysis of KIT, AKT and ERK phosphorylation in WT and *Prl2* null hematopoietic progenitor cells following SCF stimulation.



PRL2 interacts with CBL and FLT3 in human leukemia cells: To understand how PRL2 modulates FLT3 signaling in hematopoietic cells, we performed GST-pulldown assays using wild-type PRL2 and a substrate-trapping mutant PRL2/CS-DA. The PRL2/CS-DA mutant, in which the catalytic cysteine 101 and aspartic acid 69 were mutated to serine and alanine respectively, binds to its substrates stronger, but is

unable to catalyze substrate turnover. We found that the PRL2/CS-DA mutant shows increased association with FLT3 and CBL compared to wild-type PRL2 in human MV4-11 cells (**Fig. 12C**). Thus, CBL may be a substrate of PRL2 in human leukemia cells.

Generating *Prl2*^{-/-}*Flt3*^{ITD/+} mice: MLL-AF9 cooperates with FLT3-ITD in leukemogenesis. To determine the impact of PRL2 in MLL-AF9 and FLT3-ITD driven leukemia, we have generated *Prl2*^{-/-}*Flt3*^{ITD/+} mice. We will characterize hematopoiesis in *Prl2*^{-/-}*Flt3*^{ITD/+} and determine the impact of PRL2 deficiency on the functions of FLT3-ITD⁺ HSPCs *in vitro* and *in vivo*.

Cytokine and cytokine receptor interaction genes are downregulated in *Prl2*^{-/-} HSPCs expressing MLL-AF9:

Our RNA-seq data also revealed that cytokine and cytokine receptor interaction genes are significantly downregulated in *Prl2*^{-/-} HSPCs compared to that of the WT HSPCs (**Fig. 13A**). Notably, *Flt3* is one of the downregulated genes in *Prl2*^{-/-} HSPCs, suggesting that FLT3 signaling is diminished in PRL2-deficient LICs.

Loss of PRL2 decreases STAT5, AKT, and ERK phosphorylation in *Flt3*-ITD⁺ HSPCs: To determine the impact of PRL2 on oncogenic FLT3 signaling, we have generated *Prl2*^{-/-}*Flt3*^{ITD/+} and *Prl2*^{-/-}*Flt3*^{ITD/ITD} mice. We examined STAT5, AKT, and ERK phosphorylation and found that loss of PRL2 decreases STAT5, AKT, and ERK phosphorylation in both *Flt3*^{ITD/+} and *Flt3*^{ITD/ITD} HSPCs (**Fig. 13B**), demonstrating that PRL2 is a key mediator of FLT3 signaling in HSPCs.

Loss of PRL2 reduces splenomegaly seen in FLT3-ITD mice: FLT3-ITD KI mice develop MPN overtime and show splenomegaly. We found that loss of PRL2 significantly reduced splenomegaly seen in FLT3-ITD mice (**Fig. 14A and 14B**).

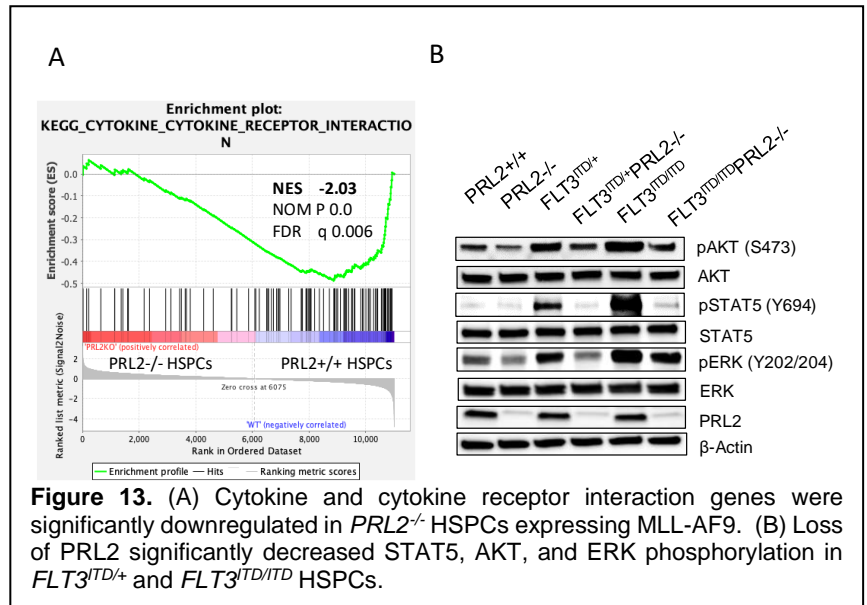


Figure 13. (A) Cytokine and cytokine receptor interaction genes were significantly downregulated in *PRL2*^{-/-} HSPCs expressing MLL-AF9. (B) Loss of PRL2 significantly decreased STAT5, AKT, and ERK phosphorylation in *FLT3*^{ITD/+} and *FLT3*^{ITD/ITD} HSPCs.

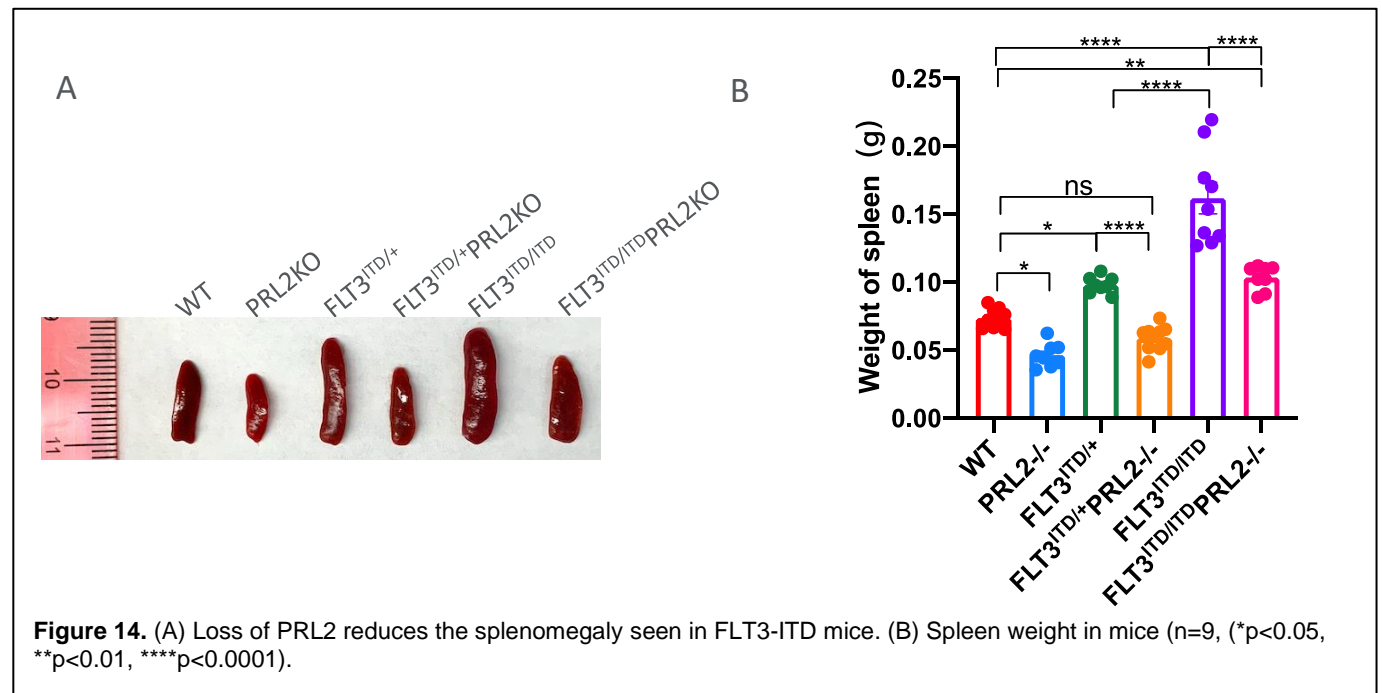


Figure 14. (A) Loss of PRL2 reduces the splenomegaly seen in FLT3-ITD mice. (B) Spleen weight in mice (n=9, (*p<0.05, **p<0.01, ****p<0.0001).

Loss of PRL2 extends the survival of FLT3^{ITD/ITD} mice: To determine the impact of PRL2 in FLT3-ITD-driven MPN, we performed bone marrow transplantation assays. We transplanted 3 x 10⁶ BM cells from PRL2^{+/+}, PRL2^{-/-}, FLT3^{ITD/+}, FLT3^{ITD/ITD}, PRL2^{-/-} FLT3^{ITD/+}, and PRL2^{-/-} FLT3^{ITD/ITD} mice into lethally irradiated recipient mice and then monitored survival and disease development in these mice. We found that loss of PRL2 significantly extends the survival of FLT3^{ITD/ITD} mice (**Fig. 15**).

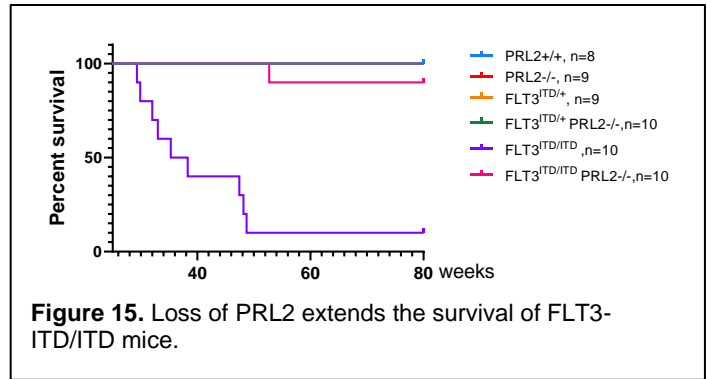


Figure 15. Loss of PRL2 extends the survival of FLT3-ITD/ITD mice.

Loss of PRL2 decreases the repopulating potential of FLT3-ITD⁺ HSPCs: We performed serial competitive BM transplantation assays and found that loss of PRL2 significantly decreases the engraftment of FLT3^{ITD/+} BM cells in both primary and secondary transplantation assays (**Fig. 16A** and data not shown), demonstrating that PRL2 is essential for the self-renewal of FLT3-ITD⁺ HSPCs *in vivo*.

Loss of PRL2 decreases replating potential of MLL-AF9⁺ FLT3-ITD⁺ HSPCs: To determine the role of PRL2 in MLL-AF9-driven leukemia, we introduced MLL-AF9 into Prl2^{-/-} FLT3^{ITD/+} HSPCs. We performed serial replating assays and found that loss of PRL2 significantly decreases the replating potential of MLL-AF9⁺ FLT3-ITD⁺ HSPCs (**Fig. 16B**), suggesting that PRL2 may be important for MLL-AF9 and FLT3-ITD-driven leukemia *in vivo*.

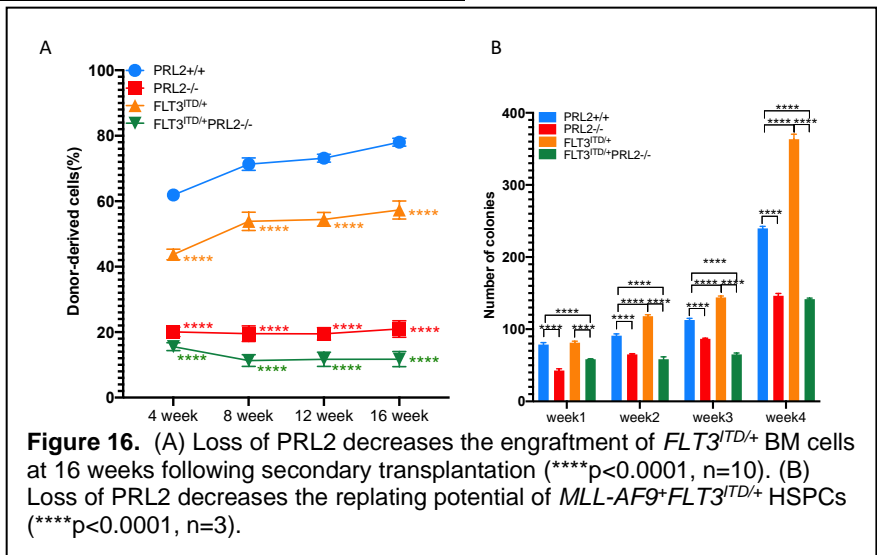


Figure 16. (A) Loss of PRL2 decreases the engraftment of FLT3^{ITD/+} BM cells at 16 weeks following secondary transplantation (****p<0.0001, n=10). (B) Loss of PRL2 decreases the replating potential of MLL-AF9⁺ FLT3^{ITD/+} HSPCs (****p<0.0001, n=3).

Major Task 4: PRL2 in CBL phosphorylation.

PRL2 associates with and dephosphorylates CBL at tyrosine 371 in leukemia cells: We confirmed

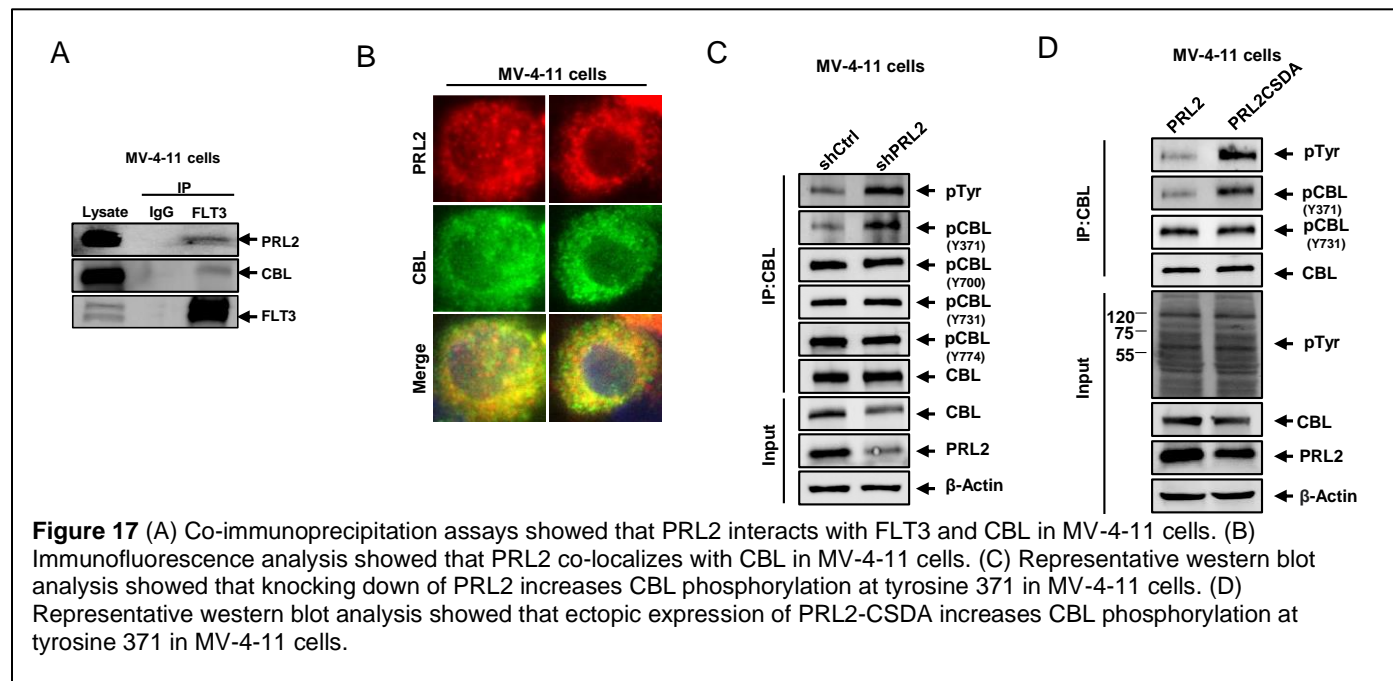
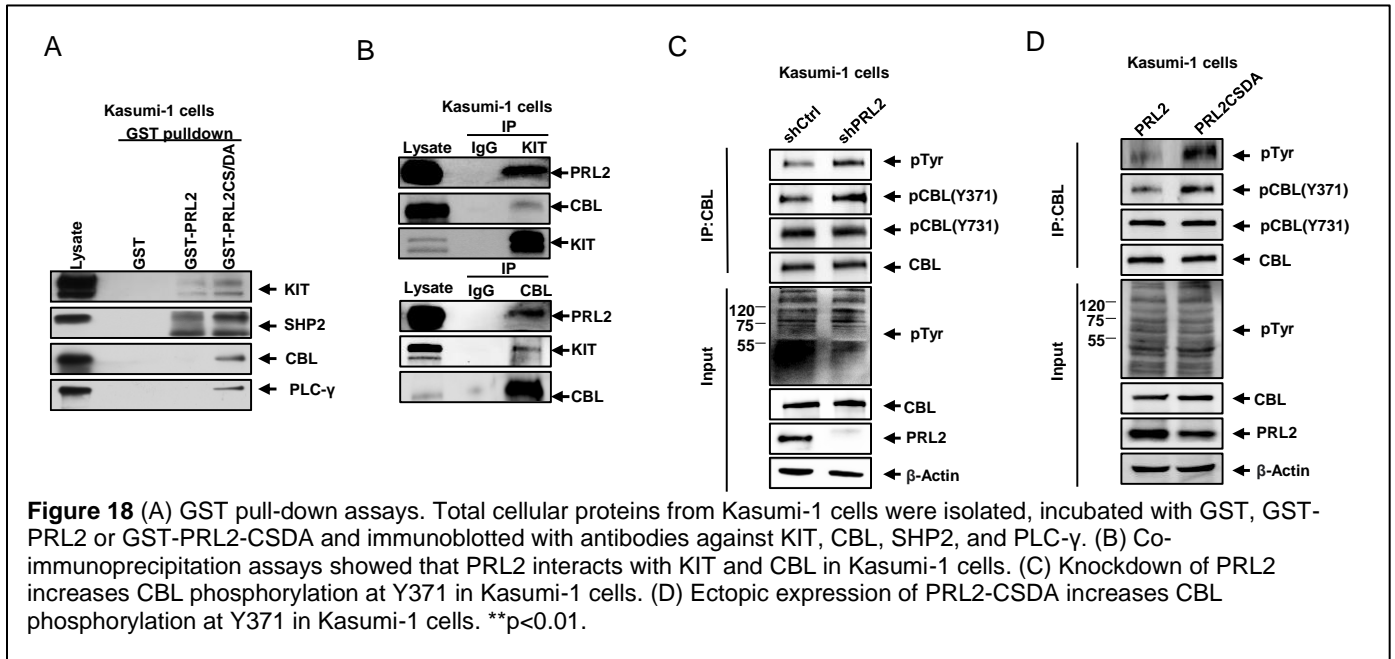


Figure 17 (A) Co-immunoprecipitation assays showed that PRL2 interacts with FLT3 and CBL in MV-4-11 cells. (B) Immunofluorescence analysis showed that PRL2 co-localizes with CBL in MV-4-11 cells. (C) Representative western blot analysis showed that knocking down of PRL2 increases CBL phosphorylation at tyrosine 371 in MV-4-11 cells. (D) Representative western blot analysis showed that ectopic expression of PRL2-CSDA increases CBL phosphorylation at tyrosine 371 in MV-4-11 cells.

that PRL2 associates with FLT3 and CBL in MV-4-11 cells using co-immunoprecipitation (Co-IP) assays

(**Fig. 17A**). We also found that PRL2 and CBL co-localizes in MV-4-11 (**Fig. 17B**). Given that CBL is an E3 ubiquitin ligase which is responsible for ubiquitination and degradation of FLT3 in hematopoietic cells, these findings suggest that CBL may be a PRL2 substrate. CBL becomes activated upon Tyrosine 371 phosphorylation, which enables it to target receptor protein tyrosine kinases for ubiquitin-mediated degradation. Indeed, we found that knockdown of PRL2 increases CBL phosphorylation at tyrosine 371, whereas the levels of CBL phosphorylation at tyrosine 700, 731, and 774 were not affected by PRL2 inhibition in MV-4-11 cells (**Fig. 17C**). We detected that ectopic expression of the catalytically inactive PRL2-CSDA mutant increases CBL phosphorylation at tyrosine 371 in MV-4-11 cells (**Fig. 17D**). Further, we found that PRLi treatment increases CBL phosphorylation at tyrosine 371 in MV-4-11 cells (data not shown). Collectively, the data presented above demonstrate that CBL is a substrate of PRL2 and that PRL2 associates with and dephosphorylates CBL at tyrosine 371 in leukemia cells. It follows that dephosphorylation of CBL at tyrosine 371 by PRL2 blocks CBL-mediated FLT3 ubiquitination and degradation, leading to heightened FLT3 signaling in leukemia cells.

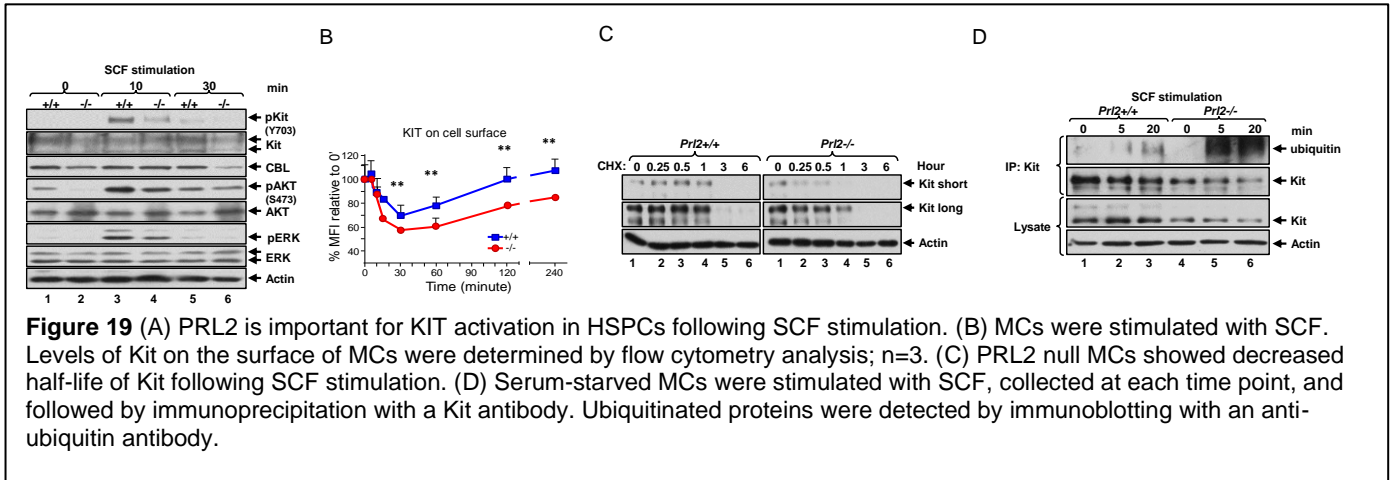


The CBL family E3 ubiquitin ligases, including CBL and CBL-B, are responsible for the ubiquitination and degradation of KIT in hematopoietic cells. In response to cytokine stimulation, CBL is phosphorylated and activated, leading to ubiquitination and degradation of KIT. However, how CBL phosphorylation is regulated in leukemia cells remains elusive. Upon SCF stimulation, KIT binds to and induces the phosphorylation of CBL proteins, which in turn act as E3 ligases, mediating the ubiquitination and degradation of KIT. We found that the catalytically inactive mutant PRL2-CSDA displays enhanced association with KIT, CBL, SHP2, and PLC- γ compared to WT PRL2 in Kasumi-1 cells (**Fig. 18A**). We confirmed the association of PRL2 with CBL and KIT in Kasumi-1 cells (**Fig. 18B**). Indeed, we found that knockdown of PRL2 increases CBL phosphorylation at tyrosine 371, whereas the levels of CBL phosphorylation at tyrosine 731 was not affected by PRL2 inhibition in both Kasumi-1 cells (**Fig. 18C**). Further, we found that ectopic expression of the PRL2-CSDA mutant also increases CBL phosphorylation at tyrosine 371 in Kasumi-1 cells (**Fig. 18D**).

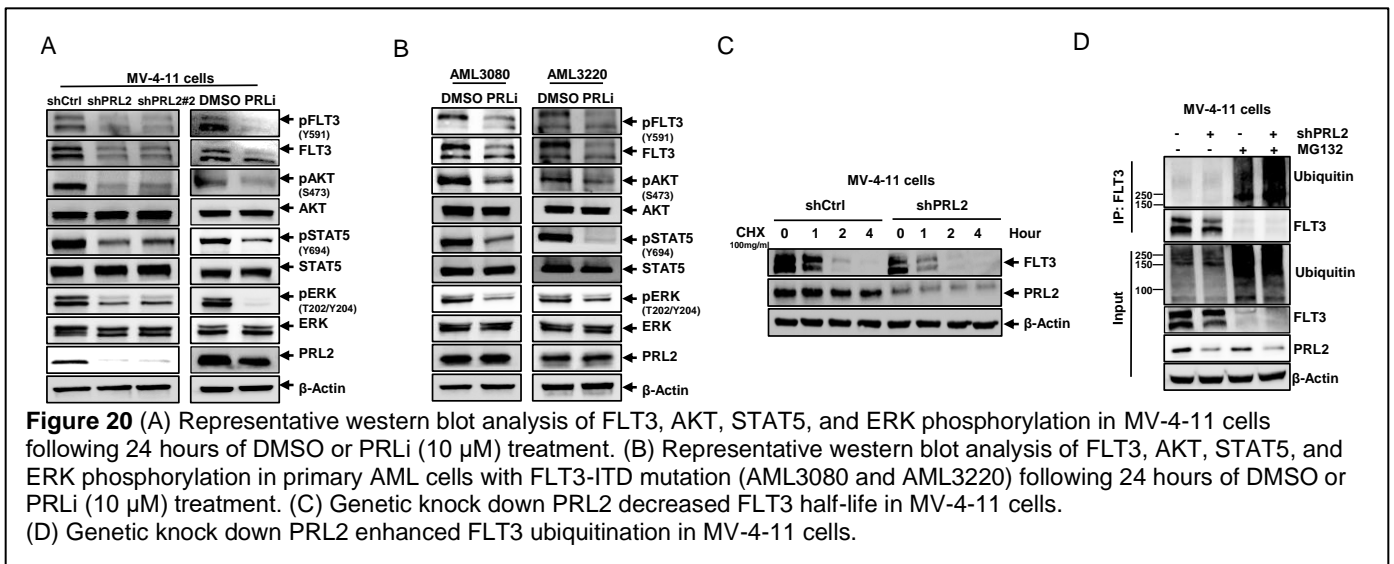
Major Task 5: CBL E3-dead mutant on KIT and FLT3 ubiquitination and degradation.

PRL2 regulates KIT and FLT3 ubiquitination and degradation: Attenuation of Kit signaling is important to obtain a suitable intensity and duration of signal transduction to meet the biological needs. There are at least three levels of Kit downregulation that function in concert: (1) tyrosine dephosphorylation, (2) inactivation of the kinase domain by serine phosphorylation, and (3) removal from the cell surface and intracellular degradation.³ We first examined Kit activation in *Prl2*^{-/-} hematopoietic stem and progenitor cells (HSPCs) following SCF stimulation. PRL2 null HSPCs showed decreased Kit phosphorylation at tyrosine 703 as well as ERK1/2 and AKT phosphorylation following SCF stimulation (**Fig. 19A**), indicating that Kit^{Y703} is not a substrate of PRL2. To further characterize Kit phosphorylation in the absence of PRL2, we utilized mast cells (MCs) derived from BM cells. Given that PKC-dependent phosphorylation is a known

negative feedback mechanism of Kit, we examined the phosphorylation status of Kit^{S744} (human S746) in MCs following SCF stimulation using a phospho-specific antibody. PRL2 null MCs showed decreased Kit phosphorylation at serine744 upon SCF stimulation (data not shown), suggesting that the negative feedback mechanism does not function in MCs. We found that Kit internalization was enhanced in *Prl2*^{-/-} MCs compared to *Prl2*^{+/+} cells following SCF stimulation (**Fig. 19B**). We then treated serum starved MCs with cycloheximide and measured the half-life of Kit protein. The half-life of Kit in *Prl2*^{-/-} MCs was significantly shorter than that of the *Prl2*^{+/+} MCs (**Fig. 19C**). Furthermore, *Prl2*^{-/-} MCs showed enhanced Kit ubiquitination compared to WT cells following SCF stimulation (**Fig. 19D**).



We observed decreased phosphorylation of AKT, STAT5, and ERK in MV4-11 and primary human AML cells isolated from NSG mice following three weeks of PRLi treatment (**Fig. 20A and 20B**). To investigate the mechanism by which PRL2 promotes FLT3 signaling, we determined the effect of PRL2 inhibition on FLT3 stability. We discovered that both knockdown of PRL2 and PRLi treatment can lead to a reduction in FLT3 protein level as a result of a decrease in FLT3 half-life in MV-4-11 cells (**Fig. 20C**). In line with this observation, we found that both knockdown of PRL2 and PRLi treatment increase FLT3 ubiquitination in MV-4-11 cells (**Fig. 20D**).

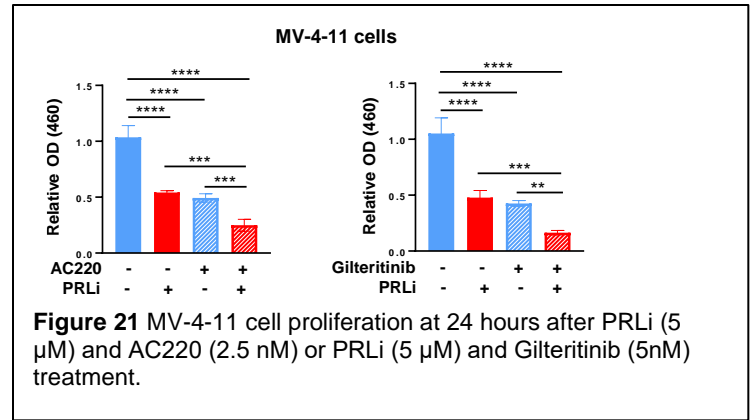


Major Task 6: Determine the impact of KIT and FLT3 inhibitors on human leukemia cells.

We showed that PRLi is synergic with KIT inhibitor AC220 or FLT3 inhibitor Gilteritinib in inhibiting the proliferation in MV-4-11 cells (**Fig. 21**).

Opportunities for training and professional development:

Dr. Yan Liu has trained four graduate students, including Sergio Barajas, Wenjie Cai, Shiyu Xiao and Christopher Borchers and three postdoctoral fellows, including Sasidhar Vemula, Yuxia Yang and Hongxia Chen, from 2019 to 2022.



Dissemination of results to communities of interest:

Invited speaker (Dr. Yan Liu):

- 2019 Chronic inflammation increases cancer development in LFS patients. Wells Center for Pediatric Research, Indiana University School of Medicine.
- 2019 Genetic and Epigenetic Regulation of Leukemia Stem Cells, University of Notre Dame, South Bend, Indiana.
- 2019 Mutant p53 drives clonal hematopoiesis through modulating epigenetic pathways, the 8th Mutant p53 Workshop, Lyon, France.
- 2019 Genetic and Epigenetic Control of Pre-leukemia Stem Cells and Leukemia Stem Cells, University of Minnesota, Minnesota.
- 2019 Understanding and Targeting of Pre-leukemia Stem Cells and Leukemia Stem Cells, Northwestern University.
- 2019 Understanding and Targeting of Pre-leukemia Stem Cells and Leukemia Stem Cells, University of Miami.
- 2020 Understanding and Targeting of Pre-leukemia Stem Cells and Leukemia Stem Cells, University of Florida.
- 2021 Understanding and Targeting of Pre-leukemia Stem Cells and Leukemia Stem Cells, Chicago Blood Club.
- 2022 Genetic and Epigenetic Control of Normal and Malignant Hematopoietic Stem Cells and Leukemia Stem Cells, Loyola University School of Medicine.

4. Impact

What was the impact on the development of the principal discipline(s) of the project?

Pediatric leukemias account for almost 35% of all childhood cancers, leaving leukemia as the leading cause of cancer death for children. In addition to children, leukemia also affects adults. Adult leukemia

usually occurs around age 60 and carries a very poor prognosis, with most patients live less than 18 months. **Active duty military members** are frequently exposed to ionizing irradiation, chemicals, infectious agents and/or environmental carcinogens. This exposure can cause mutations in blood cells that lead to blood cancer (leukemia). For instance, there are increasing numbers of **Gulf War veterans** returning from theater with irradiation or toxin exposure-related leukemia. Despite significant progress in treating leukemia, some patient populations response poorly to conventional chemotherapy. Unfortunately, little progress has been made in treating leukemia over the past 4 decades. Clearly, new treatment strategies are urgently needed.

The **long-term goal** of this research is to develop new treatments for leukemia patients that decrease relapse and improve cure rates. Given that leukemia-initiating cells (LICs), and in particular those that are in a quiescent state and capable of self-renewal, are resistant to chemotherapy or targeted therapies, the **objective** of this proposal is to develop therapeutic strategies in order to eradicate LICs and improve leukemia treatment. At the completion of this proposed work, the anticipated **short-term outcome** is to establish PRL2 as a new druggable target in leukemia treatment and provide new translational information from preclinical animal models for the development of more effective therapeutic approaches that can eliminate drug-resistant leukemia-initiating cells (LICs) and improve leukemia treatment.

The **next translation goal** would be to move PRL2 inhibitors into clinical trials for both pediatric and adult leukemia patients. This advancement will also likely to change the standard of care for patients with leukemia. To facilitate the fast transition from bench to bedside, Dr. Liu has assembled a strong translational team consisting of basic scientists and clinicians. Dr. Boswell is the Co-Investigator on this grant. He is an attending physician of the Hematology/Oncology service at the Indiana University Simon Cancer Center and the Richard Roudebush VA Medical Center. He is involved in both patient care and patient-oriented research. In addition, we will collaborate with Dr. James Croop, an attending physician of the Pediatric Hematology/Oncology section at the Riley Hospital for Children. He is involved in both patient care and patient-oriented research, as well.

Drs. Boswell and Croop have been involved in multiple clinical trials involving adult and pediatric leukemia patients at the Simon Cancer Center and Riley Hospital for Children. We will discuss a project design for moving PRL2 inhibitor into clinical trials with the Simon Cancer Center and the Riley Hospital for Children Clinical Research Program. Upon completion of this study, we believe the approach for pharmacological targeting PRL2 in LICs will allow for the commencement of efficacy and safety phase I/II clinical trials in the near term, providing novel therapeutic options for leukemia patients. Thus, the proposed research is highly translational; it will facilitate the development of novel strategies for the treatment of leukemia and other human cancers. Indeed, the translation of the discovery from the proposed studies will likely expand the horizon for both leukemia research and for patients suffering from such a life-threatening disease.

Approximately **2,000 military personnel, veterans and their dependents** are expected to develop leukemia in the United States in 2018. Within the next decade, it is expected that patients with leukemia will receive new and effective medications that can eradicate the drug resistant leukemia-initiating cells, which will significantly benefit the **US military community**. Thus, the successful completion of these studies would be expected to have a potentially important **positive impact** on **US military personnel, veterans and their family members**. In addition, the novel information gained while conducting this work will be of great value to the **military**, as these approaches will facilitate the clinical application of PRL2 inhibitors and lead to life-saving therapies, improving the quality of life of **active duty military members, military families and, the US veterans**.

What was the impact on other disciplines?

Nothing to report

What was the impact on technology transfer?

Nothing to report

What was the impact on society beyond science and technology?

Nothing to report

5. Changes/Problems

Dr. Yan Liu at the Indiana University was the PI of this award from 2019 to 2021. Dr. Liu moved to Northwestern University on April 1, 2021. Dr. James Croop at the Indiana University became the PI of this award on April 1, 2021. Dr. Yan Liu at the Northwestern University became the co-investigator (Co-I) of this award on April 1, 2021. Due to COVID pandemic, our research was significantly delayed. DOD granted one year no cost extension (NCE) to the award. The Liu lab at the Northwestern University has been working closely with Dr. James Croop at the Indiana University and completed all experiments proposed in SOW in August 2022.

6. Products

Publications, conference papers, and presentations

a. Journal publications.

1. Chen H, Bai Y, Kobayashi M, Xiao S, Cai W, Barajas S, Chen S, Miao J, Nguele Meke F, Vemula S, Ropa JP, Croop JM, Boswell HS, Wan J, Jia Y, Liu H, Li LS, Altman JK, Eklund EA, Ji P, Tong W, Band H, Huang DT, Plataniias LC, Zhang ZY, and **Liu Y***. PRL2 phosphatase enhances oncogenic FLT3 signaling via dephosphorylation of the E3 ubiquitin ligase CBL at tyrosine 371. *Blood* (In press, 2022).
2. Chen H, Bai Y, Kobayashi M, Xiao S, Cai W, Barajas S, Chen S, Miao J, Nguele Meke F, Croop JM, Boswell HS, Jia Y, Liu H, Li LS, Altman JK, Eklund EA, Ji P, Band H, Huang DT, Plataniias LC, Zhang ZY, and **Liu Y***. PRL2 phosphatase promotes oncogenic KIT signaling via dephosphorylation of the E3 ubiquitin ligase CBL. *Haematologica*. (Submitted, 2022)
3. Barajas S, Cai W, **Liu Y***. Role of p53 in regulation of hematopoiesis in health and disease. *Curr Opin Hematol*. 2022 Jul 1;29(4):194-200.
4. Yu H, Gao R, Chen S, Liu X, Wang Q, Cai W, Vemula S, Fahey AC, Henley D, Kobayashi M, Liu SZ, Qian Z, Kapur R, Broxmeyer H, Gao Z, Xi R and **Liu Y***. Bmi1 regulates Wnt signaling in hematopoietic stem and progenitor cells. *Stem Cell Rev and Rep*. 2021 Dec;17(6):2304-2313.
5. Broxmeyer HE, **Liu Y**, Kapur R. *et al*. Fate of Hematopoiesis During Aging. What Do We Really Know, and What are its Implications? *Stem Cell Rev and Rep*. 2020; (16): 1020–1048.
6. Kobayashi M, Lin Y, Mishra A, Shelly C, Gao R, Wang P, Xi R, Wenzel P, Liu Y, **Liu Y***, and Yoshimoto M. Bmi1 maintains the self-renewal property of innate -like B lymphocytes. *Journal of Immunology*. 2020 Jun 15;204(12):3262-3272. (Co-corresponding author).
7. Chen S, Wang Q, Yu H, Capitano ML, Vemula S, Nabinger SC, Gao R, Yao C, Kobayashi M, Geng Z, Fahey AC, Henley D, Liu SZ, Barajas S, Cai W, Wolf ER, Ramdas B, Cai Z, Gao H, Luo N, Sun Y, Wong TN, Link DC, Liu Y, Boswell HS, Mayo LD, Huang G, Kapur R, Yoder MC, Broxmeyer HE, Gao Z, and **Liu Y***. Mutant p53 Drives Clonal Hematopoiesis through Modulating Epigenetic Pathway. *Nature Communications*. 2019 Dec 11;10(1):5649. doi: 10.1038/s41467-019-13542-2. PMID: PMC6906427.
8. Chen S, **Liu Y***. p53 involvement in clonal hematopoiesis of indeterminate potential. *Curr Opin Hematol*. 2019 Jul;26(4):235-240. doi: 10.1097/MOH.0000000000000509.

9. Nabinger S, Chen S, Yao C, Gao R, Kobayashi M, Vemula S, Fahey AC, Wang C, Daniels C, Boswell HS, Sandusky GE, Mayo LD, Kapur R, and **Liu Y***. Mutant p53 enhances leukemia-initiating cell self-renewal to promote leukemia development. *Leukemia*. 2019 Jun;33(6):1535-1539. PMID: 30675010

a. **Books or other non-periodical, one-time publications.**

Nothing to Report

b. **Other publications, conference papers, and presentations.**

Nothing to Report

Website(s) or other Internet site(s)

Nothing to Report

Technologies or techniques

Nothing to Report

Inventions, patent applications, and/or licenses

Nothing to Report

Other Products

Identify any other reportable outcomes that were developed under this project. Reportable outcomes are defined as a research result that is or relates to a product, scientific advance, or research tool that makes a meaningful contribution toward the understanding, prevention, diagnosis, prognosis, treatment, and/or rehabilitation of a disease, injury or condition, or to improve the quality of life. Examples include:

a. *data or databases;*

Nothing to Report

b. *biospecimen collections;*

Human leukemia patient samples

c. *audio or video products;*

Nothing to Report

d. *software;*

Nothing to Report

e. *models;*

Nothing to Report

f. *educational aids or curricula;*

Nothing to Report

g. *instruments or equipment;*

Nothing to Report

h. research material (e.g., Germplasm; cell lines, DNA probes, animal models);

Cell lines: MV4-11 (control shRNA) and MV4-11 (PRL2 shRNA); Molm-13 (control shRNA) and Molm-13 (PRL2 shRNA)

Animal models: FLT3-ITD-Pr2^{-/-}, mice; Mouse models of human leukemia (MLI-AF9); and patient-derived xenograft (PDX) models of leukemia.

i. clinical interventions;

Nothing to Report

j. new business creation;

Nothing to Report

k. other.

Nothing to Report

7. Participants & Other Collaborating Organizations

What individuals have worked on the project?

- a. *Provide the following information for: (1) PDs/PIs; and (2) each person who has worked at least one person month per year on the project during the reporting period, regardless of the source of compensation (a person month equals approximately 160 hours of effort). If information is unchanged from a previous submission, provide the name only and indicate "no change."*

Name:	<i>James Croop</i>
Project Role:	<i>PI</i>
Researcher Identifier (e.g. ORCID ID):	<i>N/A</i>
Nearest person month worked:	<i>1</i>
Contribution to Project:	<i>Dr. Croop was responsible for supervising the conduct of the experiments, analyzing data, and obtaining human AML patient samples.</i>
Funding Support:	

Name:	<i>Yan Liu</i>
Project Role:	<i>Co-I</i>

Researcher Identifier (e.g. ORCID ID):	0000-0003-4878-9111
Nearest person month worked:	3
Contribution to Project:	<i>Dr. Liu supervised the conduct of the experiments, analyzed data, developed hypotheses, planned future experiments and writing, revising, and submitting manuscripts describing the findings from this project.</i>
Funding Support:	<i>NIH and Leukemia and Lymphoma Society</i>

Name:	<i>Yunlong Liu</i>
Project Role:	<i>Co-I</i>
Researcher Identifier (e.g. ORCID ID):	N/A
Nearest person month worked:	1
Contribution to Project:	<i>Dr. Liu provided statistical support for the project, including study design, sample size calculation, statistical inference, and any related requests.</i>
Funding Support:	<i>NIH</i>

Name:	<i>H Scott Boswell</i>
Project Role:	<i>Co-I</i>
Researcher Identifier (e.g. ORCID ID):	N/A
Nearest person month worked:	1
Contribution to Project:	<i>Dr. Boswell was responsible for supervising the conduct of the experiments, analyzing data, and obtaining human AML patient samples.</i>
Funding Support:	<i>NIH</i>

Name:	<i>Wei Tong</i>
Project Role:	<i>Co-I</i>
Researcher Identifier (e.g. ORCID ID):	N/A
Nearest person month worked:	2

Contribution to Project:	<i>Dr. Tong supervised the conduct of the experiments, analyzed data, developed hypotheses, planned future experiments.</i>
Funding Support:	<i>NIH and Leukemia and Lymphoma Society</i>

Name:	<i>Hongxia Chen</i>
Project Role:	<i>Postdoc</i>
Researcher Identifier (e.g. ORCID ID):	N/A
Nearest person month worked:	<i>12</i>
Contribution to Project:	Dr. Chen generated mouse models of human AML and determined the impact of genetic and pharmacological inhibition of PRL2 on leukemia treatment. He designed and conducted the experiments listed in this proposal.
Funding Support:	

Has there been a change in the active other support of the PD/PI(s) or senior/key personnel since the last reporting period?

Nothing to Report

What other organizations were involved as partners?

- i. **Organization Name:** University of Pennsylvania
- ii. **Location of Organization:** *Philadelphia*
- iii. **Partner's contribution to the project** (*identify one or more*)

1. **Financial support;**

Nothing to Report

2. **In-kind support** (*e.g., partner makes software, computers, equipment, etc., available to project staff*);

Nothing to Report

3. **Facilities** (*e.g., project staff use the partner's facilities for project activities*);

Nothing to Report

4. **Collaboration** (*e.g., partner's staff work with project staff on the project*);

Dr. Wei Tong's lab performed experiments and provided reagents to the study.

5. **Personnel exchanges** (e.g., project staff and/or partner's staff use each other's facilities, work at each other's site); and

Nothing to Report

6. **Other.**

Nothing to Report

What other organizations were involved as partners?

- i. **Organization Name: Northwestern University**
- ii. **Location of Organization:** Chicago
- iii. **Partner's contribution to the project** (identify one or more)

7. **Financial support;**

Nothing to Report

8. **In-kind support** (e.g., partner makes software, computers, equipment, etc., available to project staff);

Nothing to Report

9. **Facilities** (e.g., project staff use the partner's facilities for project activities);

Nothing to Report

10. **Collaboration** (e.g., partner's staff work with project staff on the project);

Dr. Yan Liu's lab performed experiments and provided reagents to the study.

11. **Personnel exchanges** (e.g., project staff and/or partner's staff use each other's facilities, work at each other's site); and

Nothing to Report

12. **Other.**

Nothing to Report

8. Special Reporting Requirements

COLLABORATIVE AWARDS: Not applicable

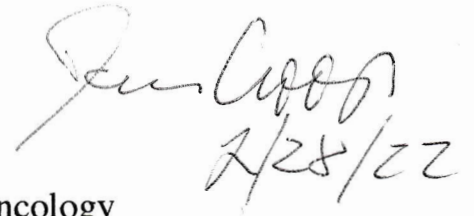
QUAD CHARTS: Not applicable

9. Appendices

A. James Croop CV

- B. Yan Liu CV
- C. Publications

Name: James Merrill Croop



Address: Section of Pediatric Hematology/Oncology
James Whitcomb Riley Hospital for Children
Room 4340
705 Riley Hospital Drive
Indianapolis, Indiana 46202

Telephone: (317) 944-8784
Fax: (317) 948-0616
Email: jcroop@iupui.edu

Place of Birth: Pittsburgh, Pennsylvania

Education:

9/71-8/74 B.A. Department of Biology, University of Pennsylvania
9/74-6/80 Ph.D. Department of Anatomy, University of Pennsylvania
9/74-6/80 M.D. School of Medicine, University of Pennsylvania

Postdoctoral Training:

7/80-6/83 Pediatric Residency
Children's Hospital of Philadelphia
7/83-6/86 Pediatric Hematology/Oncology Fellowship
Dana-Farber Cancer Institute and
Children's Hospital Medical Center, Boston

Licensure and Certification:

1982 Pennsylvania Medical License
1983 Massachusetts Medical License
1985 Diplomat, American Board of Pediatrics
1990 Diplomat, Pediatric Hematology and Oncology
1996 Recertification, Pediatric Hematology and Oncology
1997 Indiana Medical License
2014 Recertification, Pediatric Hematology and Oncology

Academic Appointments:

7/80-6/83 Assistant Instructor, Department of Pediatrics
University of Pennsylvania, School of Medicine

7/83-6/86 Research Fellow in Pediatrics, Harvard Medical School

7/86-6/88 Instructor in Pediatrics, Harvard Medical School

7/88-6/97 Assistant Professor, Department of Pediatrics,
Harvard Medical School

7/97-6/03 Associate Professor, Department of Pediatrics,
Indiana University School of Medicine

7/03- Professor, Department of Pediatrics,
Indiana University School of Medicine

Hospital Appointments:

7/86-6/88 Instructor in Medicine, The Children's Hospital, Boston

7/86-6/97 Clinical Associate in Pediatrics
Dana-Farber Cancer Institute

7/88-6/97 Associate in Medicine, Hematology/Oncology
The Children's Hospital, Boston

7/97- James Whitcomb Riley Hospital for Children, Indianapolis

Principal Clinical and Hospital Service Responsibilities:

7/86-6/97 Staff Physician, Jimmy Fund Clinic
Dana-Farber Cancer Institute

7/86-6/97 Clinic Leader, Jimmy Fund Clinic
Dana-Farber Cancer Institute

7/87-6/97 Attending Physician, Oncology Ward
The Children's Hospital, Boston

7/97- Attending Physician, Section of Hematology/Oncology
James Whitcomb Riley Hospital for Children

Visiting Appointments:

7/84-6/88 Visiting Scientist, Massachusetts Institute of
Technology, Center for Cancer Research

Clinical Investigation

- 1997-2004 Gene Therapy Working Group
Indiana University Medical Center
- 1999- 2004 Gene Therapy Working Group
Chair, Quality Assurance Committee
- 1998- Institutional Principal Investigator, COG Phase 1 Trials,
Riley Hospital for Children
- 1998-2013 Principal Investigator, A Pilot Study Of Dose-intensified
Procarbazine, CCNU, Vincristine (PCV) For Poor
Prognosis Pediatric And Adult Brain Tumors Utilizing
Fibronectin-assisted, Retroviral- Mediated Modification Of
CD34+ Peripheral Blood Cells With O6-Methylguanine
DNA Methyltransferase.
- 1998-1999 Principal Investigator, A Pilot Study of Recombinant
Human Interleukin 11 for Patients With Fanconi Anemia
and Inherited Bone Marrow Failure Syndromes.
- 1999-2004 Principal Investigator, Gene Therapy For Patients With
Fanconi Anemia: A Pilot Study. (Development Phase)
- 1999-2012 Principal Investigator, Fibronectin-Assisted, retroviral-Mediated
Transduction of CD34+ Peripheral blood Cells with gp91phox in
Patients with X-Linked Chronic Granulomatous Disease: A Phase 1
Study
- 2002-2003 Institutional PI. Phase II Irinotecan Study, Bristol Meyers.
- 2001-2004 Institutional PI. Zofran Study, GlaxoSmithKline
- 2006-2007 Principal Investigator, COG Phase I Protocol, Phase I Study of PT-
523 (Talotrexin) in Children and Adolescents with Recurrent Solid
Tumors (Development Phase).
- 2008-2009 Co-Principal Investigator, COG Phase I Protocol, Phase I Study of
GSK923295A, a centromere associated protein E (CENP-E)
inhibitor in pediatric patients with recurrent/refractory solid tumors.
- 2010--2011 Co-Principal Investigator, COG Phase I Protocol, A Phase 1 Study
of OSI-906 in Pediatric Patients with Recurrent/Refractory Solid,
including CNS, Tumors
- 2014-- Co-Principal Investigator, COG Phase I Protocol, A Phase 1
Ramucirumab, a Humanized, Monoclonal Antibody Against the
Vascular Endothelial Growth Factor-2 (VEGFR-2) Receptor in
Children with Recurrent or Refractory Solid Tumors, including
CNS Tumors.

2016- Institutional PI, A Phase 1, Multi-center, Open-label, Dose De-escalation Study to Evaluate the Safety and Efficacy of Talimogene Laherparepvec in Pediatric Subjects with Advanced Non Central Nervous System Tumors That are Amenable to Direct Injection (Amgen),

Awards and Honors:

1974 Phi Beta Kappa, University of Pennsylvania
1975-1980 Trainee, Medical Scientist Training Program
1987-1992 NIH K08 Clinical Investigator Award
1989-1990 DFCI BRSG Analysis of MDR in Drosophila
1988-1993 NIH R01 Immunological Analysis of MDR
1992-1993 DFCI BRSG Mechanisms of MDR Interactions
1992-1993 Sandoz Pharmaceutical Development Award
1992-1995 American Cancer Society Junior Faculty Award
1993-1994 DFCI BRSG Solid Tumor Models of MDR
1994-1995 DFCI BRSG Detection of MDR in vivo
1994-1997 Sandoz Pharmaceutical Research Grant
1995-1996 DFCI BRSG Characterization of Drosophila MDR Genes
1997-1998 IUPUI Cancer Center Pediatric Development Grant
1997-1998 NCCF Cancer Center Pediatric Development Grant
1997-1998 Genetics Institute Clinical Trial Grant

Invited Presentations

1987 Platform Session, American Society of Hematology
1988 Invited Lecture, Multidrug Resistance, Gordon Conference
1990 Invited Lecture, Multidrug Resistance, Gordon Conference
1991 Invited Lecture, AACR Conference on Drug Resistance
1992 Invited Lecture, Annual Drosophila Research Conference
1994 Pediatric Oncology Grand Rounds, Multidrug Resistance
1995 Pediatric Oncology Grand Rounds, Multidrug Resistance
1995 Presentation, AACR Conference on Drug Resistance
1997 Presentation, National Pediatric Blood Club, Gene Therapy
1998 Invited Lecture, AML Workshop, Hospital St. Louis, Paris
1998 Indiana University Cancer Center Grand Rounds, Gene Therapy
1998 Pediatric Grand Rounds, Riley Hospital for Children, Gene Therapy
2000 Clarian Hospital Nurses Pediatrics Seminar, Gene Therapy

2001 Indiana University Cancer Center Grand Rounds, Pediatric Oncology
2002 Pediatric Grand Rounds, Riley Hospital for Children, Phase I Studies
2006 Child Care Conference, Hematology for the Pediatrician
2011 Psi Iota Xi, Key Note Speaker, Leukemia

Teaching:

1977 Teaching Assistant in Histology
University of Pennsylvania School of Medicine
1987-1997 Resident and Medical Student Lectures
Children's Hospital, Boston
1988-1997 Laboratory Advisor, Undergraduate/Medical Students
Post-doctoral students/Thesis Advisor
1991/1995 Introduction to Clinical Medicine, Instructor
1992-1996 Tutor, The Human Body, Harvard Medical School
1992-1996 Histology Instructor, Human Body, Harvard Medical School
1999 Medical Student Clinical Trial Elective Preceptor
1999-2002 OSCE Development Committee, IUPUI School of Medicine
2005-2014 Fellow Mentoring Committees (4)
2018-2019 Fellow Mentoring Committee (1)
2020- Medical Student Mentor (4)

Committee Assignments:

1977 Admissions Committee, U of Pennsylvania School of Medicine
1992-1997 Pediatric Scientific Review Committee
Dana-Farber Cancer Institute and Boston Children's Hospital
1995, 1998 Experimental Therapeutics Study Section, NCI, Special Reader
1995-1996 Quality Improvement Committee, Dana-Farber Cancer Institute
1997-1999 Riley Children's Cancer Committee
1997-1999 Scientific Review Committee, Member
Indiana University Simon Cancer Center
1999 -2017 Chair, Scientific Review Committee
Indiana University Simon Cancer Center
1999 - Clinical Director, Pediatric Hem/Onc Clinical Research Office
1999 - Institutional Biohazard Committee, Alternate
1999-2015 Clarian/IU Health Cancer Committee
1999-2006 National Gene Vector Laboratory Advisory Committee, Alternate
1999-2017 Clinical Research Committee, IU Simon Cancer Center
2000 Inter-institutional Investigator Responsibilities, IRB Committee

2001-2004 Conflict of Interest Committee, IU School of Medicine
2001-2006 Research Subject Advocate, GCRC
2001-2003 Executive Committee, Society of Research Subject Advocates
2002-2004 Biomedical Human Subjects Research Education Committee
2001-2019 Member, COG Developmental Therapeutics Study Committee
2005-2011 Chair, COG Phase I Performance Monitoring Committee
2011- Member, COG Membership Committee
2011- Chair, COG Institutional Performance Monitoring Committee
2014-2015 Interim Director, Clinical Research Office, Simon Cancer Center
2015- Fellowship Clinical Competency Committee
2015-2019 Member, COG Developmental Therapeutics Executive Committee
2015- Member, Quality Council, Pediatric Hem/Onc Riley Hospital
2017-2018 Member, Primary Pediatric Dossier Committee, Riley Hospital
2016-2019 Member, COG Group Chair Advisory Council.
2018 - Chair, Data and Safety Monitoring Committee, Simon Cancer Center
2020- Member, Powerchart Oncology Committee, Riley Hospital
2020- Chair, Growth Factor Communication QI Committee, Riley Hospital
2020- Chair, Chemotherapy Consent Committee, Riley Hospital

Professional Societies:

1990-2008 American Association for Cancer Research
1992-2009 American Society of Hematology
1997-1999 Children's Cancer Group
1998-2008 American Society of Gene Therapy
1998- American Society of Pediatric Hematology/Oncology
1999- Children's Oncology Group

Major Research Interests:

1. Pediatric Oncology
2. Drug Development
3. Gene Therapy
4. Drug Resistance Genes
5. Hematopoietic Stem Cells

Publications

Journal Articles

1. Croop, J. and Holtzer, H. Response of myogenic and fibrogenic cells to Cytochalasin-B and Colcemid. *J. Cell Biol.* 1974; 65:271-285.
2. Holtzer, H., Croop, J., Gershon, M. and Somlyo, A. Effects of Cytochalasin B and Colcemid on cells in muscle cultures. *Am J. Anat.* 1975; 141:291-296.
3. Holtzer, H., Croop, J., Dienstman, S., Ishakawa, H. and Somlyo, A. Effects of Cytochalasin B and Colcemid on myogenic cultures. *Proc. Natl. Acad. Sci.* 1975; 72:513-517.
4. Bennett, G.S., Fellini, S., Croop, J., Otto, J., Bryan, J. and Holtzer, H. Differences among 100 A Filament subunits from different cell types. *Proc. Natl. Acad. Sci.* 1978; 75:4364-4368.
5. Schmid, E., Tapscott, S., Bennett, G.S., Croop, J., Fellini, S., Holtzer, H., and Franke, W. Differential Location of different types of intermediate sized filaments in various tissues of the chick embryo. *Differentiation* 1979; 15:27-40.
6. Croop, J., Toyama, Y., Dlugosz, A. and Holtzer, H. Selective effects of phorbol-12-myristate-13-acetate on myofibrils and 10nm filaments. *Proc. Natl. Acad. Sci.* 1980; 77:5273-5277.
7. Holtzer, H., Pacifici, M., Croop, J., Boettiger, D., Toyama, Y., Payette, R., Biehl, J., Dlugosz, A. and Holtzer, S. Properties of cell lineages as indicated by the effects of ts-RSV and TPA on the generation of cell diversity. *Fortschritte der Zell.* 1982; 26:207-225.
8. Croop, J., Dubyak, G., Toyama, Y., Dlugosz, A., Scarpa, A., and Holtzer, H. Effects of TPA on myofibril integrity and calcium content in developing myotubes. *Dev. Biol.* 1982; 89:460-474.
9. Menko, A.S., Croop, J., Toyama, Y., Holtzer, H., and Boettiger, D. The response of chicken embryo fibroblasts to Cytochalasin B is altered by RSV induced cell transformation. *Mol. and Cell. Biol.* 1982; 2:320-330.

10. Rosenberg, H., Coleman, B., Croop, J., Granowetter, L., and Evans, A. Pseudocysticerciasis in an adolescent patient. *Clin Ped* 1983; 22:708-712.
11. Croop, J., Shapiro, B., Gershon, A., and Campo, J. Arizona histiocytosis from a pet snake. *Ped Inf Disease* 1984; 3:188.
12. Gros, P., Croop, J., Roninson, I., Varshavsky, and Housman, D. Isolation and characterization of DNA Sequences Amplified in Multidrug Resistant Hamster cells. *Proc. Natl. Acad. Sci.* 1986; 83:337-341.
13. Gros, P., Ben Neriah, Y., Croop, J. and Housman, D.E. Isolation and Expression of a cDNA (mdr) that Confers Multidrug Resistance. *Nature* 1986; 323:728-731.
14. Gros, P., Fallows, D., Croop, J. and Housman, D.E. Chromosome Mediated Gene Transfer of Multidrug Resistance. *Mol. and Cell. Biol.* 1986; 6:3785-3790.
15. Gros, P., Croop, J., and Housman, D.E. Mammalian Multidrug Resistance Gene: Complete cDNA Sequence Indicates Strong Homology to Bacterial Transport Proteins. *Cell* 1986; 47:371-380.
16. Croop, J., Guild, B., Gros, P., and Housman, D. Genetics of Multidrug Resistance: Relationship of a Cloned Gene to the Complete Multidrug Resistance Phenotype. *Cancer Research* 1987; 47:5982-5988.
17. Arceci, R., Croop, J., Horwitz, S., and Housman, D. The mdr Gene is Induced and Expressed at High Levels During Pregnancy in the Secretory Epithelium of the Uterus. *Proc. Natl. Acad. Sci.* 1988; 85:4350-4354.
18. Croop, J., Raymond, M., Haber, D., Devault, A., Arceci, R., Gros, P., and Housman, D. The Three Mouse Multidrug Resistance Genes are Expressed in a Tissue Specific Manner in Normal Mouse Tissue. *Mol. Cell. Biol.* 1989; 9:1346-1350.
19. Greenberger, L. Croop, J. Horwitz, S. and Arceci, R. P-glycoproteins encoded by mdr1b in murine gravid uterus and multidrug resistant tumor cell lines are differentially glycosylated. *FEBS Letters* 1989; 257:419-421.

20. Mazzanti, R., Gatmaitan, Z., Croop, J. Shu, H., and Arias, I. Quantitative image analysis of Rhodamine 123 transport by adriamycin sensitive and resistant NIH 3T3 and human hepatocellular carcinoma (Alexander) cells. *J. Cell. Pharmacol.* 1990; 1:50-56.
21. Arceci, R., Baas, F., Raponi, R., Horwitz, S., Housman, D., and Croop, J. Multidrug resistance gene expression is controlled by steroid hormones in the secretory epithelium of the uterus. *Mol. Reprod. and Dev.* 1990; 25:101-109.
22. Gros, P., Dhir., R., Talbot, F., Croop, J., Groulx, N. A single amino acid substitution strongly modulates the activity and substrate specificity of the mouse *mdr1* and *mdr3* drug efflux pumps. *Proc. Natl. Acad. Sci.* 1991; 88:7289-7293.
23. Wu, C-t., Budding, M., Griffin, M., and Croop, J. Isolation and characterization of *Drosophila* multidrug resistance gene homologues. *Mol. Cell. Biol.* 1991; 11:3940-3948.
24. Buschman, E., Arceci, R.J., Croop, J.M. Mingxin, C., Arias, I.M., Housman, D.E., Gros, P. Isoform specific antibodies identify the bile canalicular membrane as the primary site of expression of the P-glycoprotein encoded by mouse *mdr2*. *J. Biol. Chem.* 1992; 267:18093-18099.
25. Mazzanti, R., Croop, J.M., Gatmaitan, Z., Budding, M., Steiglitz, K., Arceci, R., and Arias, I.M. Benzquinamide Inhibits P-glycoprotein Mediated Drug Efflux and Potentiates Anticancer Agent Cytotoxicity in Multidrug Resistant Cells. *Oncology Research* 1992; 4:359-365.
26. Arceci, R.J., Stieglitz, K., Bras, J., Schinkel, A., Baas, F. and Croop, J. A Monoclonal Antibody to an External Epitope of the Human MDR1 P-Glycoprotein, *Cancer Research* 1993; 53:310-317.
27. Piwnica-Worms, D., Chiu, M.L., Budding, M., Kronauge, J.F., Kramer, R.A., and Croop, J. Functional Imaging of Multidrug Resistance P-glycoprotein with and Organotechnetium Complex. *Cancer Research* 1993; 53:977-984.
28. Toppmeyer, D.L., Slapak, C.A., Croop, J., and Kufe, D.W. Role of P-Glycoprotein in Dolastatin 10 Resistance. *Biochem Pharm.* 1994; 48:609-612.

29. Piwnica-Worms, Rao, V.V., Kronauge, J.F., and Croop, J. Characterization of Multidrug Resistance P-glycoprotein Transport Function with an Organotechnetium Cation. *Biochemistry* 1995; 34:12210-12220.
30. Dunussi-Joannopoulos, K., Nickerson, P., Strom, T., Weinstein, H., Burakoff, S., Croop, J.M., and Arceci, R.J. B-7 costimulatory immunotherapy in a mouse model of acute myelogenous leukemia. *Blood*. 1996; 87:2938-2946.
31. Bosch, I., Jackson, G.R., Croop, J.M., and Cantiello, H.F. Expression of *Drosophila melaogaster* P-glycoproteins is associated with ATP-channel activity. *Amer J Physiol*. 1996; 40:C1527-C1538.
32. Croop, J.M., Tiller, G.E., Fletcher, J.A., Lux, M.L., Raab, E., Goldenson, D., Son, D., Arciniegas, S., and Wu, R.L. Isolation and Characterization of a mammalian homolog of the *Drosophila* white gene. *Gene*. 1997; 185:77-85.
33. Dunussi-Joannopoulos, K., Krenger, K., Weinstein, H., Ferrara, J., Croop, J.M. CD8+ T-cells activated during the course of murine AML elicit therapeutic responses to late B7 vaccines after cytoreductive treatment. *Blood*. 1997; 89:2915-2924.
34. Bosch, I., Dunussi-Joannopoulos, K., Wu, R.L., Furlong, S., and Croop, J.M. Phosphatidylcholine and phosphatidylethanolamine are substrates of human MDR1 P-glycoprotein. *Biochemistry*. 1997; 36:5685-5694.
35. Bosch, I., Crankshaw, C.L., Piwnica-Worms, D, Croop, J.M. Characterization of Functional Assays of P-glycoprotein Transport Activity. *Leukemia*. 1997; 11:1131-1137.
36. Dunussi-Joannopoulos, K., Dranoff, G., Weinstein, H., Ferrara, J., Bierer, B. E., Croop, J.M. Gene Immunotherapy in murine Acute Myeloid Leukemia: Granulocyte-Macrophage colony-stimulating factor tumor cell vaccines elicit more potent antitumor immunity compare with B7 family and other cytokine vaccines. *Blood*. 1998; 91:222-230.
37. Barbarics, E., Kronauge, J.F., Cohen, D., Davison, A., Jones, A.G. Croop, J.M. Characterization of P-glycoprotein transport and inhibition in vivo. 1998; *Cancer Res* 58:276-282.

38. Lee, G.Y., Croop, J.M. Anderson, E. Multidrug resistance gene expression correlates with progesterone production in dehydroepiandrosterone-induced polycystic and equine chorionic gonadotropin-stimulated ovaries of prepubertal rats. *Biology of Reproduction* 1998; 58:330-337.
39. Croop J.M., Cooper, R., Seshadri R., Fernandez, C., Graves, V., Kreissman, S., Smith, F.O., Cornetta, K., Williams, D.A., Abonour R. Large Scale Mobilization and Isolation of CD34+ Cells from Normal Donors. *Bone Marrow Transplantation*. 2000; 26:1271-1279.
40. Chen, J. Reeves, L. Sanburn, N., Croop, J. Willaims, D.A., Cornetta, K. Packaging cell line DNA contamination of vector supernatants: Implication for laboratory and clinical research. *Virology*. 2001; 282:186-197
41. Croop, J.M., Cooper, R., Fernandez, C., Graves, V., Kreissman S., Hanenberg, H., Smith, F.O., Cornetta K., Williams D.A. Mobilization and Collection of Peripheral Blood CD34+ Cells from Patients with Fanconi Anemia. *Blood* 2001; 98: 2917-2921
42. Kumar, M., Vik, T., Johnson, C. Southwood, M.E., Croop, J.M. Treatment, outcome and cost of care in children with idiopathic thrombocytopenic purpura. *Am J Hem* 2005; 78:181-187.
43. Cavalier M.E., Davis M.M., Croop J.M. Germline p53 mutation presenting as synchronous tumors. *Journal of Pediatric Hematology/Oncology*. 2005 27:441-443.
44. Daw N.C., Furman W.L., Stewart C.F., Iacono L.C., Krailo M., Bernstein M.L., Dancey J.E., Speights R.A., Blaney S.M., Croop J.M., Reaman G.H., Adamson P.C. Phase I and pharmacokinetic study of gefitinib in children with refractory solid tumors: a Children's Oncology Group Study. *Journal of Clinical Oncology*. 2005 23:6172-6180.
45. Cornetta K. Croop J. Dropcho E. Abonour R. Kieran MW. Kreissman S. Reeves L. Erickson LC. Williams DA. A pilot study of dose-intensified procarbazine, CCNU, vincristine for poor prognosis brain tumors utilizing fibronectin-assisted, retroviral-mediated modification of CD34+ peripheral blood cells with O6-methylguanine DNA methyltransferase. *Cancer Gene Therapy*. 2006 13:886-895.

46. Mondick J.T., Johnson BM, Haberer L.J., Sale M.E., Adamson P.C., Coté C.J., Croop J.M., Russo M.W., Barrett J.S., Hoke J.F. Population pharmacokinetics of intravenous ondansetron in oncology and surgical patients aged 1-48 months. *European Journal of Clinical Pharmacology*. 2010 66:77-86.
47. Creary S, Heiny M, Croop J, Fallon R, Vik T, Hulbert M, Knoderer H, Kumar M, Sharathkumar A. Clinical course of postthrombotic syndrome in children with history of venous thromboembolism. *Blood Coagul Fibrinolysis*. 2012 23:39-44.
48. Robertson KA, Nalepa G, Yang FC, Bowers DC, Ho CY, Hutchins GD, Croop JM, Vik TA, Denne SC, Parada LF, Hingtgen CM, Walsh LE, Yu M, Pradhan KR, Edwards-Brown MK, Cohen MD, Fletcher JW, Travers JB, Staser KW, Lee MW, Sherman MR, Davis CJ, Miller LC, Ingram DA, Clapp DW. Imatinib mesylate for plexiform neurofibromas in patients with neurofibromatosis type 1: a phase 2 trial. *Lancet Oncol*. 2012 13:1218-1224.
49. Mueller, E.L., Croop, J., Carroll, AE. Fever and neutropenia hospital discharges in children with cancer: A 2012 update. *Pediatr Hematol Oncol*. 2016 33:39-48.
50. Kobayashi M, Bai Y, Chen S, Gao R, Yao C, Cai W, Cardoso AA, Croop J, Zhang ZY, Liu Y. Phosphatase PRL2 promotes oncogenic NOTCH1-Induced T-cell leukemia. *Leukemia*. 2017 31:751-754.
51. Ragg, S, Zehentner BK, Loken MR, Croop JM. Evidence for BCR/ABL1-positive T-cell acute lymphoblastic leukemia arising in an early lymphoid progenitor cell. *Pediatric Blood & Cancer*. 2019 66:e27829, 2019
52. Crane S, Croop JM, Lee J, Walski J, Haase J. Parents' Insights into Pediatric Oncology Phase I Clinical Trials: Experiences from Their Child's Participation. *Seminars in Oncology Nursing*. 2021 37:151-162.

Reviews

1. Holtzer, H., Croop, J., Toyama, Y., Bennett, G.S., Fellini, S. and West, C. Differences in differentiation programs between presumptive myoblasts and their daughters the definitive myoblast and myotubes. In: *Plasticity of Muscle*. Pette, D. (Ed) Gruter & Co., Berlin, 1980:133-146.

2. Holtzer, H., Bennett, G.S., Tapscott, S. J., Croop, J., Dlugosz, A. and Toyama, Y. Changes in intermediate-sized filaments during myogenesis and neurogenesis. In: *International Cell Biology*. Schweiger (Ed) Springer-Verlag, Berlin, 1981:294-304.
3. Holtzer, H., Pacifici, M., Payette, R., Croop, J., Dlugosz, A. and Toyama, Y. TPA reversibly blocks the differentiation of chick myogenic, chondrogenic and melanogenic cells. In : *Carcinogenesis*, Vol. 7, Hecker, E., et. al. (Ed) Raven Press, N.Y., 1982:347-357.
4. Holtzer, H., Bennett, G.S., Tapscott, S.J., Croop, J., and Toyama, Y. Intermediate-size filaments: Changes in synthesis and distribution in cells of the myogenic and neurogenic lineages. *Cold Spring Harb Symp* 1982; 46:317-329.
5. Housman, D., Croop, J., Mukaiyama, T., Abelson, H., Roninson, I., and Gros, P. A molecular genetics approach to the problem of drug resistance in chemotherapy. In: *New Avenues in Developmental Cancer Chemotherapy*. Academic Press, 1987:503-517.
6. Croop, J., Gros, P., and Housman, D. Genetics of multidrug resistance. *J. Clin. Invest.* 1988; 81:1303-1309.
7. Croop, J. P-glycoprotein structure and evolutionary homologies. In: *Multiple Drug Resistance in Cancer*, Clynes, M. (Ed), Kluwer Academic Publishers, 1994:1-32.
8. Bosch, I., Croop J. P-glycoprotein and cancer. *BBA Reviews on Cancer Biochim Biophys Acta*, 1996; 1288:F37-F54.
9. Dunussi-Joannopoulos, K., Weinstein, H., Arceci, R.J., and Croop, J.M. B-7 Gene therapy with B7.1 and GM-CSF vaccines in a murine AML model. *J Ped Hem/Onc.* 1997 19:536-540.
10. Bosch, I., and Croop, J.M. P-glycoprotein structure and evolutionary homologies. *Cytotechnology.* 27:1-30, 1998.
11. Croop, J.M. Evolutionary relationships among ABC Transporters. *Meth. Enz.* 1998 292:101-116.

12. Abonour R, Croop, J., Cornetta, K. Multidrug-resistance gene therapy in hematopoietic cell transplantation. In, Gene Therapy of Cancer, Ed. Lattime, E.C., and Zgerson, S.L., Academic Press, San Diego, 2001 pp. 355-364.

13. Croop, J. Gene Therapy for Fanconi Anemia. Current Hematology Reports. 2003; 2:335-340

14. Williams, D.A., Croop, J., Kelley, P. Gene therapy in the treatment of Fanconi anemia, a progressive bone marrow failure syndrome. Current Opinion in Molecular Therapeutics 2005; 7:461-466.

Abstracts

1. Croop, J., Gros, P., and Housman, D. Mutational analysis of a site involved in colchicine resistance in the mouse *mdr1* gene. Proc. AACR 32:(1991).

2. Abonour, R., L. Einhorn, R. Hromas, M.J. Robertson, E. Srour, C.M. Traycoff, A. Bank, I. Kato, K. Asada, J. Croop, F.O. Smith, D.A. Williams, K. Cornetta Highly Efficient Mdr-1 Gene Transfer Into Humans Using Mobilized CD34+ Cells Transduced Over Recombinant Fibronectin CH-296 Fragment. 1998; Blood 92(Suppl):690a.

3. J.M. Croop, R. Cooper, H. Hanenberg, S. Kreissman, C. Thompson, V. Graves, F.O. Smith, D.A. Williams. Feasibility Of Large Scale Peripheral Blood CD34+ Cell Collections In Normal Donors And In Patients With Fanconi Anemia. Blood 1998; 92(Suppl):441a.

4. Pradhan, K., Berg, S.L., Liu, X., Minard, C.J., Croop, J., Reid, J.M., Fox, E., and Weigel, B.J. A dose escalation and toxicity study using pre-determined target concentration of Ramucirumab, a novel anti-angiogenic agent in children with recurrent / refractory solid tumors: A report from the children's oncology group phase I/ pilot consortium (ADV1416) 2018: Cancer Res (13 Supplement): 78

Patents

1. Croop, J.M., Gros, P., and Housman, D. DNA Sequence That Encodes the Multidrug Resistance Gene. Patent No. 5,198,344; Issued March 30, 1993.

2. Arceci, R. J., and Croop, J.M. Antibodies for P-glycoprotein encoded by the MDR1 Gene and Uses Thereof. Patent No. 5,369,009; Issue November 29, 1994.

CURRICULUM VITAE

Yan Liu, Ph.D.

Associate Professor of Medicine (Tenured)
Division of Hematology and Oncology
Department of Medicine
Feinberg School of Medicine
Co-Leader, Hematologic Malignancies Program
Robert H. Lurie Comprehensive Cancer Center
Northwestern University
Email: yan.liu@northwestern.edu

EDUCATION

- 1988-1992 **B.S.**, Jilin University, China
- 1992 - 1997 **Ph.D.**, Chinese Academy of Sciences, Beijing, China, Xuexian Peng and Jingrui Dai - Mentors
- 1998 - 2001 Postdoctoral Fellow, University of Arizona, Tucson, Arizona, Brian Larkins - Mentor
- 2001 - 2006 Research Fellow, Memorial Sloan-Kettering Cancer Center, New York, New York, Stephen Nimer - Mentor

ACADEMIC APPOINTMENTS

- 2006-2008 Research Associate, Memorial Sloan-Kettering Cancer Center, New York, NY
- 2008-2010 Senior Research Scientist, Memorial Sloan-Kettering Cancer Center, New York, NY
- 2010-2016 Assistant Professor of Pediatrics, Biochemistry and Molecular Biology (tenure-track), Indiana University School of Medicine, Indianapolis, IN
- 2016-2021 Associate Professor of Pediatrics, Biochemistry and Molecular Biology (tenured), Indiana University School of Medicine, Indianapolis, IN
- 2011-2021 Member, Indiana University Simon Cancer Center
- 2011-2021 Member, Indiana University/NIDDK Cooperative Center of Excellence in Hematology (CCEH)
- 2021-present Associate Professor of Medicine (tenured), Feinberg School of Medicine, Northwestern University, Chicago, IL
- 2021-present Co-Leader, Hematologic Malignancies Program, Robert H. Lurie Comprehensive Cancer Center

PROFESSIONAL ORGANIZATIONS

- 2002-present Member, American Society of Hematology (ASH)
- 2007-present Member, International Society for Stem Cell Research (ISSCR)
- 2011-present Member, International Society for Experimental Hematology (ISEH)
- 2011-present Member, Chinese Biological Investigators Society (CBIS)
- 2015-present Member, Society of Chinese Bioscientists in America (SCBA)
- 2016-present Faculty Member, Faculty of 1000 Medicine

PROFESSIONAL SERVICE

- 2013-present Member, NYSTEM Study Section, New York State Department of Health and the Empire State Stem Cell Board
- 2013-2017 Member, the Early Career Reviewer (ECR) program at the Center for Scientific Review (CSR), National Institutes of Health
- 2013-present Foreign Expert (Member), Hematology Study Section, National Natural Science Foundation of China (NSFC), China.
- 2014-present Member, Career Development Award (CDA) Program, International Human Frontier Science Program Organization (HFSP), France
- 2015-present Reviewer, St. Baldrick's Foundation, USA
- 2017 Ad hoc Reviewer, Cancer Genetics (CG) Study Section, NIH
- 2019-present Reviewer, Leukemia Research Foundation (LRF), USA

HONORS AND AWARDS

- 2009 International Society for Stem Cell Research (ISSCR) Travel Award
- 2010 NYSTEM Idea Award
- 2012 Showalter Research Trust Fund New Investigator Award
- 2013 DOD/PRCRP Career Development Award
- 2013 American Cancer Society (ACS) New Investigator Award

2014 Elsa U. Pardee Foundation New Investigator Award

2014 St. Baldrick's Foundation Scholar Award

2014 Alex's Lemonade Stand Foundation Research Award

2016 Leukemia Research Foundation (LRF) New Investigator Award

2016 Children's Leukemia Research Association Research Award

2016 Showalter Research Trust Fund Young Scholar Award

2017 St. Baldrick's Foundation Extended Scholar Award

2017 NIH/NIA R56 Award

2018 DOD/BMFRP Idea Development Award

2018 NIH/NIDDK R56 Award

2018 St. Baldrick's Foundation Extended Scholar Award

2019 NIH/NHLBI R01 Award

2019 DOD/PRCRP Idea Development Award

2019 Leukemia & Lymphoma Society (LLS) TRP Award

2019 Showalter Research Trust Fund Scholar Award

RESEARCH SUPPORT

CURRENT ACTIVE SUPPORT:

R01HL150624 (PI: Liu) 07/15/19-06/30/23 3.6 calendar
NIH/NHLBI

Molecular mechanisms underlying clonal expansion of hematopoietic stem cells
Role: Principal Investigator

6581-20 (PI: Liu) 07/01/19-06/30/23 0.6 calendar

Leukemia & Lymphoma Society (LLS) TRP Grant
Development of therapeutic strategy for the treatment of MDS
Role: Principal Investigator

F31HL160120 (PI: Barajas) 01/01/22-12/31/24
NIH/NHLBI

Mutant p53 in pathogenesis of myelodysplastic syndromes
Role: Sponsor/Mentor

Innovation Challenge Award (PIs: Liu and Yue) 01/01/22-12/31/22

Robert H. Lurie Cancer Center
Mutant p53 remodels epigenetic landscape and rewires three-dimensional DNA topology to alter gene expression in leukemia cells
Role: Principal Investigator

H Foundation Core Usage Pilot Project Award (PI: Liu) 08/10/21-08/12/22
Robert H. Lurie Cancer Center
Identify and validate proteins interacting with tumor suppressor p53 and protein tyrosine phosphatase PRL2 in human leukemia cells
Role: Principal Investigator

PENDING SUPPORT:

R01 DK134788-01 (PIs: Liu and Halene) 09/01/22-08/31/27 2.4 calendar
NIH/NIDDK
Understanding and targeting mutant p53 in myelodysplastic syndromes
Role: Principal Investigator

BM210041 (PIs: Liu and Halene) 10/01/22-09/30/25 1.2 calendar
DOD/BMFRP Investigator-initiated Award
Understanding and targeting mutant p53 in myelodysplastic syndromes
Role: Principal Investigator

LLS SCOR (PIs: Eklund, Ji and Liu) 10/01/22-09/30/27 1.8 calendar
Leukemia & Lymphoma Society (LLS) TRP Grant
Molecular mechanisms of inflammation-driven clonal progression in myelodysplastic syndromes
Role: Principal Investigator of project #3

COMPLETED SUPPORT:

Startup Fund (PI, Liu) 11/01/10-10/31/15
Indiana University School of Medicine (IUSM)
p53 in normal and malignant hematopoiesis
Role: Principal Investigator

R56AG052501 (PI, Liu) 09/15/17-08/31/18 2.4 calendar
NIH/NIA
Mutant p53 rejuvenates aged stem cells through modulating epigenetic regulators
Role: Principal Investigator

R56DK119524 (PI, Liu) 09/15/18-08/31/19 1.2 calendar
NIH/NIDDK
Molecular mechanisms underlying clonal expansion of hematopoietic stem cells
Role: Principal Investigator

W81XWH-13-1-0187 (PI: Liu) 07/01/13-06/30/15 2.4 calendar
DOD/PRCRP Career Development Award
Modulating Leukemia-initiating Cell Quiescence to Improve Leukemia Treatment
Role: Principal Investigator

W81XWH-18-1-0265	(PI, Liu)	07/01/18-03/31/21	1.2 calendar
DOD/BMFRP Idea Development Award			
Targeting Mutant p53 in Myelodysplastic Syndromes Role: Principal Investigator			
NCE			
W81XWH-19-1-0575	(PI: Liu)	08/01/19-07/30/22	2.4 calendar
DOD/PRCRP Idea Development Award			
Leukemia-initiating Cells to Improve Leukemia Treatment Role: Principal Investigator			
NCE			
R01 AI121197-01A1	(PI: Yoshimoto)	06/13/16-05/31/17	1.2 calendar
NIH/NIAID			
Embryonic origin and self-renewal of B-1a cells			
Role: Co-investigator			
R56AI110831	(PI: Yoshimoto)	03/10/15 – 02/29/17	1.2 calendar
NIH/NIAID			
Embryonic origin and self-renewal of B-1a cells			
Role: Co-investigator			
1F32CA203049-01	(PI: Nabinger)	07/01/16 – 6/30/18	
NIH/NCI			
Targeting PRL2 Phosphatase in acute myeloid leukemia			
Role: Mentor			
Scholar Award	(PI: Liu)	07/01/19-03/31/21	
Ralph and Grace Showalter Research Trust Fund			
Role: Principal Investigator			
Scholar Award	(PI: Liu)	07/11/14-12/31/19	7.2
St. Baldrick's Foundation			calendar
Targeting PRL2 phosphatase in T cell acute lymphoblastic leukemia			
Role: Principal Investigator			
NCE			
New Investigator Award	(PI: Liu)	01/01/14-12/31/14	1.2 calendar
Elsa U. Pardee Foundation			
Targeting PRL2 in Acute Myeloid Leukemia			
Role: Principal Investigator			
New Investigator Award	(PI: Liu)	07/01/16-12/31/17	
Leukemia Research Foundation			
Targeting PRL2 phosphatase in Acute Myeloid Leukemia			
Role: Principal Investigator			
Research Grant	(PI: Liu)	07/01/12-06/30/13	1.2 calendar
Showalter Research Trust Fund			
The role of gain-of-function mutant p53 in hematopoietic stem cell self-renewal			

Role: Principal Investigator

Young Scholar Award (PI: Liu) 7/01/16-6/30/18 1.2 calendar
Showalter Research Trust Fund
The role of Polycomb repressive complex 1 in hematopoietic stem cells
Role: Principal Investigator

Research Grant (PI: Liu) 06/01/13-05/31/14
American Cancer Society and Indiana University Simon Cancer Center The
role of PRL2 Phosphatase in Acute Myeloid Leukemia
Role: Principal Investigator

Research Grant (PI: Liu) 01/01/16-12/31/16 0.6 calendar
Children's Leukemia Research Association
Targeting PRL2 in acute myeloid leukemia
Role: Principal Investigator

Research Grant (PI: Liu) 09/02/14-08/31/15
Alex's Lemonade Stand Foundation
Targeting PRL2 phosphatase in pediatric acute myeloid leukemia
Role: Principal Investigator

Research Grant (PI: Liu) 10/01/11-09/30/12
NIDDK Cooperative Center of Excellence in Hematology (CCEH) The
role of mutant p53 in hematopoietic stem cell self-renewal
Role: Principal Investigator

Research Grant (PI: Liu) 7/01/16-6/30/17
NIDDK Cooperative Center of Excellence in Hematology (CCEH)
Polycomb repressive complex 1 in hematopoietic stem cells
Role: Principal Investigator

Research Grant (PI: Liu) 07/01/11-12/31/12
Indiana University Simon Cancer Center (IUSCC)
Targeting mutant p53 to improve leukemia treatment
Role: Principal Investigator

Research Grant (PI: Liu) 10/01/18 - 02/28/19
Wells Center for Pediatric Research/IUSM
Molecular mechanisms underlying clonal expansion of hematopoietic stem cells
Role: Principal Investigator

Research Grant (PI: Liu) 01/01/19 -12/31/19
Wells Center for Pediatric Research/IUSM
Molecular mechanisms of stem cell aging and pathogenesis of age-related diseases
Role: Principal Investigator

Biomedical Research Grant (PI: Liu) 07/1/13 - 06/30/14
Indiana University School of Medicine (IUSM)
Bmi1 is a key regulator of Wnt signaling in hematopoietic stem cells
Role: Principal Investigator

Biomedical Research Grant (PI: Liu) 03/1/11 - 02/28/12
Indiana University School of Medicine (IUSM)
The role of Bmi1 in hematopoietic stem cell self-renewal
Role: Principal Investigator

RSFG Grant (PI: Liu) 7/01/16-6/30/17
Indiana University-Purdue University Indianapolis
Mutant p53 rejuvenates aged stem cells through modulating epigenetic regulators
Role: Principal Investigator

Research Support Funds Grants Award (PI: Liu) 07/01/13-06/30/14
Indiana University-Purdue University Indianapolis
The role of mutant p53 in acute myeloid leukemia
Role: Principal Investigator

Seed Fund (PIs: Liu and Mayo) 01/1/18 - 02/28/19
Wells Center for Pediatric Research
Genotoxic stresses in mutant p53-driven MDS pathogenesis
Role: Principal Investigator

Seed Fund (PI: Liu) 06/1/15 - 12/31/15
Wells Center for Pediatric Research
PRL2 phosphatase as a novel therapeutic target in Acute Myeloid Leukemia
Role: Principal Investigator

Pilot Grant (PI: Liu) 5/01/15-4/30/16
Indiana University Simon Cancer Center (IUSCC)
Targeting mutant p53 to improve leukemia treatment
Role: Principal Investigator

Pilot Project Grant (PI: Liu) 07/01/12-12/31/13
Indiana University Simon Cancer Center (IUSCC)
The role of Bmi1 in the pathogenesis of myelodysplastic syndromes
Role: Principal Investigator

Research Grant (PI: Kobayashi) 07/01/14 - 06/30/15
Ralph W. and Grace M. Showalter Research Trust Fund
Targeting PRL2 in Acute Myeloid Leukemia
Role: Mentor

Biomedical Research Grant (PI: Kobayashi) 11/1/15 - 10/31/16
Indiana University School of Medicine (IUSM)
Targeting PRL2 phosphatase in Acute Myeloid Leukemia
Role: Mentor

Research Grant (PI: Kobayashi) 06/01/14 - 05/31/15
American Cancer Society and Indiana University Simon Cancer Center
The role of PRL2 Phosphatase in the pathogenesis of T-ALL
Role: Mentor

Pilot Project Grant (PI: Kobayashi) 11/01/14 - 10/30/15
NIDDK Cooperative Center of Excellence in Hematology (CCEH) The
role of PRL2 Phosphatase in T cell development
Role: Mentor

PUBLICATIONS (*Corresponding author)

PUBLICATIONS SUBMITTED/IN PREPARATION

1. Vemula S, Chen S, Barajas S, Nabinger SC, Schmitz DA, Chen H, Yang Y, Cai W, Xiao S, Gayatri S, Capitano ML, Ropa JP, Zhang Y, Henley D, Fahey A, Wan J, Perna F, de Andrade KC, Khincha PP, Kapur R, Jia Y, Liu H, Abaza Y, Altman JK, Eklund EA, Ji P, Yue F, Halene S, Vaughan DE, Plataniias LC, Abdel-Wahab O, Croker BA, Mayo LD, Savage SA, **Liu Y***. Inflammatory stress drives p53 mutant clonal hematopoiesis via activating the NLRP1 inflammasome. *Leukemia* (Submitted, 2022)
2. Chen H, Bai Y, Kobayashi M, Xiao S, Cai W, Barajas S, Chen S, Miao J, Nguele Meke F, Croop JM, Boswell HS, Jia Y, Liu H, Li LS, Altman JK, Eklund EA, Ji P, Band H, Huang DT, Plataniias LC, Zhang ZY, and **Liu Y***. PRL2 phosphatase promotes oncogenic KIT signaling via dephosphorylation of the E3 ubiquitin ligase CBL. *Haematologica*. (Submitted, 2022)
3. Olivos D, Hauck P, Jacobsen M, Sandusky G, **Liu Y**, and Mayo L. Emergence of Tumor-Initiating Cells with the Loss of Mdm2. *Molecular Cancer research* (In revision, 2022).

PEER-REVIEWED PUBLICATIONS

1. Chen H, Bai Y, Kobayashi M, Xiao S, Cai W, Barajas S, Chen S, Miao J, Nguele Meke F, Vemula S, Ropa JP, Croop JM, Boswell HS, Wan J, Jia Y, Liu H, Li LS, Altman JK, Eklund EA, Ji P, Tong W, Band H, Huang DT, Plataniias LC, Zhang ZY, and **Liu Y***. PRL2 phosphatase enhances oncogenic FLT3 signaling via dephosphorylation of the E3 ubiquitin ligase CBL at tyrosine 371. *Blood* (In press, 2022)
2. Barajas S, Cai W, **Liu Y***. Role of p53 in regulation of hematopoiesis in health and disease. *Curr Opin Hematol*. 2022 Jul 1;29(4):194-200.
3. Yu H, Gao R, Chen S, Liu X, Wang Q, Cai W, Vemula S, Fahey AC, Henley D, Kobayashi M, Liu SZ, Qian Z, Kapur R, Broxmeyer H, Gao Z, Xi R and **Liu Y***. Bmi1 regulates Wnt signaling in hematopoietic stem and progenitor cells. *Stem Cell Rev and Rep*. 2021 Dec;17(6):2304-2313.
4. Broxmeyer HE, **Liu Y**, Kapur R. *et al*. Fate of Hematopoiesis During Aging. What Do We Really Know, and What are its Implications? *Stem Cell Rev and Rep*. 2020; (16): 1020–1048.

5. Kobayashi M, Lin Y, Mishra A, Shelly C, Gao R, Wang P, Xi R, Wenzel P, Liu Y, **Liu Y***, and Yoshimoto M. Bmi1 maintains the self-renewal property of innate -like B lymphocytes. *Journal of Immunology*. 2020 Jun 15;204(12):3262-3272. (**Co-corresponding author**).
6. Chen S, Wang Q, Yu H, Capitano ML, Vemula S, Nabinger SC, Gao R, Yao C, Kobayashi M, Geng Z, Fahey AC, Henley D, Liu SZ, Barajas S, Cai W, Wolf ER, Ramdas B, Cai Z, Gao H, Luo N, Sun Y, Wong TN, Link DC, Liu Y, Boswell HS, Mayo LD, Huang G, Kapur R, Yoder MC, Broxmeyer HE, Gao Z, and **Liu Y***. Mutant p53 Drives Clonal Hematopoiesis through Modulating Epigenetic Pathway. *Nature Communications*. 2019 Dec 11;10(1):5649. doi: 10.1038/s41467-019-13542-2. PMID: 316906427.
7. Chen S, **Liu Y***. p53 involvement in clonal hematopoiesis of indeterminate potential. *Curr Opin Hematol*. 2019 Jul;26(4):235-240. doi: 10.1097/MOH.0000000000000509.
8. Nabinger S, Chen S, Yao C, Gao R, Kobayashi M, Vemula S, Fahey AC, Wang C, Daniels C, Boswell HS, Sandusky GE, Mayo LD, Kapur R, and **Liu Y***. Mutant p53 enhances leukemia-initiating cell self-renewal to promote leukemia development. *Leukemia*. 2019 Jun;33(6):1535-1539. PMID: 30675010
9. Cai Z, Kotzin JJ, Ramdas R, Chen S, Nelanuthala S, Palam LR, Pandey R, Mali RS, **Liu Y**, Kelley MR, Sandusky G, Mohseni M, Williams A, Henao-Mejia J, and Kapur R. Downregulation of *Morrbid* in Tet2-deficient preleukemic cells overcomes resistance to inflammatory stress and mitigates clonal hematopoiesis. *Cell Stem Cell*. 2018 Dec 6;23(6):833-849.e5. PMID:30526882
10. Chen S and **Liu Y***. Battle in stem cell niches: canonical versus non-canonical Wnt signaling. *Journal of Leukocyte Biology*. 2018 Mar;103(3):377-379. PubMed PMID: 29393968.
11. Chen S, Gao R, Yao C, Kobayashi M, Liu SZ, Yoder MC, Broxmeyer HE, Kapur R, Boswell HS, Mayo LD, and **Liu Y***. Genotoxic stresses promotes the clonal expansion of hematopoietic stem cells expressing mutant p53. *Leukemia*. 2018 Mar;32(3):850-854. PMID:305842141
12. Sayar H, **Liu Y***, Cripe LD, Wilson-Weekes AM, Weisenbach J, Cangany M, Sargent KJ, Nassiri M, Li L, Al Baghdadi Y, Gupta S, Suvannasankha A, Gao R, Pan F, Shanmugam R, Goswami C, Xu M, Boswell HS. Consecutive Epigenetically-active Agent Combinations act in ID1-RUNX3-TET2 and HOXA pathways for Flt3ITD+ve AML. *Oncotarget*. 2017 Dec 25;9(5):5703-5715. PubMed PMID: 29464028; PubMed Central PMCID: PMC5814168. **Co-corresponding author**
13. Yao C, Kobayashi M, Chen S, Nabinger S, Gao R, Liu SZ, Asai T, and **Liu Y***. Necdin modulates leukemia-initiating cell quiescence and chemotherapy response. *Oncotarget*. 2017; 8:87607-87622. PMID: 285675657.
14. Kobayashi M, Chen S, Bai Y, Yao C, Gao R, Sun XJ, Mu C, Twigg TA, Yu ZH, Boswell HS, Yoder M, Kapur R, Mulloy J, Zhang ZY, and **Liu Y***. Phosphatase PRL2 promotes AML1-ETO-induced acute myeloid leukemia. *Leukemia*. 2017 June; 31(6):1453-1457. PubMed PMID: 28220038. PMID:305695226

15. Kobayashi M, Bai Y, Yoshimoto M, Gao R, Chen S, Yao C, Dong Y, Zhang L, Rodriguez S, Carlesso N, Yoder MC, Kapur R, Kaplan MK, Lacorazza HD, Zhang ZY, and **Liu Y***. Protein tyrosine phosphatase PRL2 mediates Notch and Kit signals in early T cell progenitors. *Stem Cells*. 2017 Apr;35(4):1053-1064. PMID: PMC5367971.
16. Kobayashi M, Bai Y, Chen S, Gao R, Yao C, Cai W, Croop J, Zhang ZY and **Liu Y***. Phosphatase PRL2 promotes oncogenic Notch-induced T cell leukemia. *Leukemia*. 2017 Mar;31(3):751-754. PMID:PMC5695227
17. Chen S, Gao R, Kobayashi M, Yu H, Yao C, Kapur R, Yoder M, and **Liu Y***. Pharmacological inhibition of AKT activity in human CD34+ cells enhances their engraftment in immunodeficient mice. *Experimental Hematology*. 2017 Jan;45:74-84. PubMed Central PMID: PMC5859321.
18. Ghosh J, Kobayashi M, Ramdas B, Chatterjee A, Ma P, Mali RS, Carlesso N, **Liu Y**, Plas DR, Chan RJ, and Kapur R. S6K1 regulates Stem Cell Self-Renewal and Leukemia Maintenance. *Journal of Clinical Investigation*. 2016 Jul 1;126(7):2621-5. PMID:PMC4922705.
19. Gao R, Chen S, Kobayashi M, Yu H, Young SK, Soltis A, Zhang Y, Wan Y, Vemula S, Fraenkel E, Cantor A, Xu Y, Yoder MC, Wek R, Kapur R, Ellis S, Zhu X and **Liu Y***. Bmi1 promotes erythropoiesis through regulating ribosome biogenesis. *Stem Cells*. 2015 Mar;33(3):925-38. PMID:PMC4380436.
20. Chatterjee A, Ghosh J, Ramdas B, Mali RS, Martin H, Kobayashi M, Vemula S, Canela VH, Waskow ER, Visconte V, Tiu RV, Smith CC, Shah N, Bunting KD, Boswell HS, **Liu Y**, Chan RJ, Kapur R. Regulation of Stat5 by FAK and PAK1 in Oncogenic FLT3- and KIT-Driven Leukemogenesis. *Cell Reports*. 2014 Nov 20;9(4):1333-1348. PMID:PMC4380442.
21. Kobayashi M, Shelly WC, Seo W, Vemula S, **Liu Y**, Kapur R, Taniuchi I, Yoshimoto M. Functional B-1 progenitor cells are present in the hematopoietic stem cell deficient embryo and depend on Cbfb for their development. *Proc Natl Acad Sci U S A*. 111(33):12151-6, 2014. PMID: PMC4143017
22. Kobayashi M, Chen S, Gao R, Bai Y, Zhang ZY, and **Liu Y***. Phosphatase of regenerating liver in hematopoietic stem cell self-renewal and hematological malignancies. *Cell Cycle*, 2014;13(18): 2827-2835. PMID: PMC4614371
23. Kobayashi M, Bai Y, Dong Y, Yu H, Chen S, Gao R, Zhang L, Yoder MC, Kapur R, Zhang ZY and **Liu Y***. PRL2/PTP4A2 phosphatase is important for hematopoietic stem cell self-renewal. *Stem Cells*. 32(7):1956-67, 2014. PMID: PMC4063874.
24. Vu LP, Perna F, Wang L, Voza F, Figueroa ME, Tempst P, Erdjument-Bromage H, Gao R, Chen S, Paietta E, Deblasio T, Melnick A, **Liu Y**, Zhao X and Nimer SD. PRMT4 blocks myeloid differentiation by assembling a methyl-RUNX1-dependent repressor complex. *Cell Reports*. 5(6):1625-38, 2013. PMID: PMC4073674
25. Sabelli PA, **Liu Y**, Dante RA, Lizarraga LE, Nguyen HN, Brown SW, Klingler JP, Yu J, LaBrant E, Layton TM, Feldman and Larkins BA. Control of Cell Proliferation, Endoreduplication, Cell Size and Cell Death by the Retinoblastoma-Related Pathway in

- Maize Endosperm. *Proc Natl Acad Sci U S A*. 110(19):E1827-36, 2013. PMCID: PMC3651506
26. **Liu Y***, Yu H, Nimer SD. PI3K-Akt pathway regulates polycomb group protein and stem cell maintenance. *Cell Cycle*. 12(2):199-200, 2013. PMCID: PMC3757235.
 27. Asai T, **Liu Y** and Nimer SD. Necdin, a p53 target, in normal and cancer stem cells. *Oncotarget*. 4(6):806-7, 2013. PMCID: PMC3757235
 28. **Liu Y***, Liu F, Yu H, Zhao X, Sahsida G, Deblasio A, Chen Z, Lin HK, Di Giandomenico S, Elf SE, Yang YY, Miyata Y, Huang G, Menendez S, Mellinshoff I, Pandolfi PP, Hedvat CV and Nimer SD. Akt Phosphorylates the Transcriptional Repressor Bmi1 to Block Its Association with Tumor Suppressing *Ink4a-Arf* locus. *Science Signaling*, October 23; 5, ra77, 2012. PMCID: PMC3784651. **Co-corresponding author**
 29. Vemula S, Shi J, Mali RS, Ma P, **Liu Y**, Hanneman P, Koehler KR, Hashino E, Wei L, and Kapur R. ROCK1 functions as a critical regulator of stress erythropoiesis and survival by regulating p53. *Blood*, Oct 4; 120(14):2868-78, 2012. PMCID: PMC3466968
 30. Hu P, Nebreda AR, **Liu Y**, Carlesso N, Kaplan M, Kapur R. P38 α negatively regulates T helper type 2 responses by orchestrating multiple TCR-associated signals. *Journal of Biological Chemistry*, Sep 28; 287(40): 33215-26, 2012. PMCID: PMC3460427
 31. Asai T, **Liu Y**, Di Giandomenico S, Bae N, Xu H, Nadiaye-Lobry D, Deblasio A, Menendez S, Antipin J, Reva B, Wevrick R, and Nimer SD. Necdin, a p53 target gene, regulates hematopoietic stem/progenitor cell quiescence and response to genotoxic stress. *Blood*, Aug 23;120(8):1601-12, 2012. PMCID: PMC3429304. **Co-first author**.
 32. Hu P, Carlesso N, Xu M, **Liu Y**, Nebreda AR, Takemoto C, and Kapur R. Genetic evidence for critical roles of P38 α in regulating mast cell differentiation and chemotaxis through distinct mechanisms. *J. Biol. Chem*, June 8;287(24):20258-69, 2012. PMCID: PMC3370208
 33. Huang G, Zhao X, Wang L, Elf S, Xu H, Zhao X, Sashida G, **Liu Y**, Lee J, Menendez S, Yang Y, Yan Y, Zhang P, Tenen DG, Osato M, Hsieh J, and Nimer SD. The ability of MLL to bind RUNX1 and methylate H3K4 at PU.1 regulatory regions is impaired by MDS/AML-associated RUNX1/AML1 mutations. *Blood*, Dec 15;118(25):6544-52, 2011. PMCID: PMC3242717
 34. Asai T, **Liu Y**, Bae N, and Nimer SD. The p53 tumor suppressor protein regulates hematopoietic stem cell fate. *J Cell Physiol*, Sep; 226(9):2215-21, 2011. PMCID: PMC3575444.
 35. Sashida G, Bae N, Di Giandomenico S, Asai T, Gurvich N, Bazzoli E, **Liu Y**, Huang G, Zhao X, Menendez S, Nimer SD. (2011). The Mef/Elf4 transcription factor fine tunes the DNA damage response. *Cancer Research*, July 15; 71(14): 4857-65, 2011. PMCID: PMC4073677
 36. Sashida G, Bazzoli E, Menendex S, **Liu Y**, and Nimer SD. The oncogenic role of the ETS transcription factors MEF and ERG. *Cell Cycle*, Sep 1; 9(17):3457-9, 2010. PMCID: PMC3230474

Kettering Institute Scientific Colloquium, New York, NY.

- 2007 Regulation of Hematopoietic Stem Cell Quiescence - a Novel Role for p53. The 49th American Society of Hematology (ASH) Conference, Atlanta, GA.
- 2009 Using cord blood to identify cell cycle regulatory targets for treating leukemia. The 7th Annual International Umbilical Cord Blood Transplantation Symposium, Los Angeles.
- 2009 Necdin regulates hematopoietic stem cell quiescence. The 7th Annual International Society for Stem Cell Research (ISSCR), Barcelona, Spain.
- 2009 Molecular Basis of Hematopoietic Stem Cell Quiescence and Self Renewal. Children's Hospital Oakland Research Institute, Oakland, CA.
- 2010 Molecular Basis of Hematopoietic Stem Cell Quiescence and Self Renewal. Rochester University School of Medicine, Rochester, NY.
- 2010 Molecular Basis of Hematopoietic Stem Cell Quiescence and Self Renewal. New York University School of Medicine. New York, NY.
- 2010 Molecular Basis of Hematopoietic Stem Cell Quiescence and Self Renewal. St. Jude Children's Research Hospital
- 2010 Molecular Basis of Hematopoietic Stem Cell Quiescence and Self Renewal. Department of Pediatrics, Indiana University School of Medicine, Indianapolis, IN.
- 2011 Molecular basis of hematopoietic stem cell quiescence and self-renewal. Institute of Hematology & Blood Diseases Hospital, Chinese Academy of Medical Sciences, Tianjin, China
- 2011 Akt-mediated phosphorylation of Bmi1 regulates hematopoietic stem cell self-renewal. Midwest Blood Club, Cincinnati, Ohio
- 2012 Molecular basis of hematopoietic stem cell self-renewal and leukemogenesis. National Institute of Biological Sciences, Beijing, China
- 2012 Molecular basis of hematopoietic stem cell self-renewal and leukemogenesis. Tsinghua University, Beijing, China
- 2012 Molecular basis of hematopoietic stem cell quiescence and self-renewal. Department of Biochemistry and Molecular Biology seminar, Indiana University, Indianapolis, IN
- 2012 Molecular basis of hematopoietic stem cell self-renewal and leukemogenesis. Neonatology morning conference, Department of Pediatrics, Indiana University.
- 2012 Akt-mediated phosphorylation of Bmi1 inhibits hematopoietic stem cell self-renewal. Midwest Blood Club, Indianapolis, Indiana

- 2013 PRL2 maintains hematopoietic stem and progenitor cells through regulating SCF/KIT signaling. Midwest Blood Club, Cincinnati, Ohio
- 2013 Bmi1 regulates hematopoietic stem cell self-renewal and lineage commitment. Center of Excellence of Molecular Hematology, Indiana University
- 2013 Bmi1 regulates ribosome biogenesis during erythroid differentiation. The 55th American Society of Hematology (ASH) Conference, New Orleans, LA.
- 2014 PRL2 phosphatase in normal and malignant hematopoiesis. Institute of Hematology & Blood Diseases Hospital, Chinese Academy of Medical Sciences, Tianjin, China
- 2014 Polycomb group protein Bmi1 regulates hematopoietic stem cell self-renewal and differentiation. National Institute of Biological Sciences, Beijing, China
- 2015 Polycomb Repressive Complex 1 enhances HSC self-renewal through repressing the canonical Wnt signaling pathway. Midwest Blood Club, French Lick, Indiana
- 2015 Gain-of-function Mutant p53 enhances HSC self-renewal. Keystone Symposia, Hematopoiesis (B6), Keystone, CO.
- 2015 Polycomb Repressive Complex 1 enhances HSC self-renewal through repressing the canonical Wnt signaling pathway. The 57th American Society of Hematology (ASH) Conference, Orlando, FL.
- 2016 Epigenetic Control of Hematopoietic Stem Cells. Institute of Health, Chinese Academy of Sciences, Shanghai, China
- 2016 Epigenetic Control of Hematopoietic Stem Cells. Fudan University, Shanghai, China
- 2016 Mutant p53 drives the development of pre-leukemic HSCs through modulating epigenetic regulators. The 11th Bi-annual Chinese Biological Investigator Society (CBIS), Chengdu, China
- 2016 Epigenetic Control of Hematopoietic Stem Cells. Penn State College of Medicine, Hershey, PA
- 2016 Genetic and Epigenetic Control of Hematopoietic Stem Cells. Wells Center for Pediatric Research, Indiana University.
- 2016 PRL2 Phosphatase Is a Key Mediator of Oncogenic Cytokine Signaling in Leukemia Stem Cells. The 58th American Society of Hematology (ASH) Conference, San Diego, CA.
- 2016 Polycomb Repressive Complex 1 in Hematopoietic Stem Cell Self-renewal and Differentiation. NIDDK Cooperative Center of Excellence in Hematology (CCEH) Meeting. Seattle, WA.

- 2017 Gain of function mutant p53 drives the development of pre-leukemic HSCs through epigenetic modulations, Indiana University Cancer Research Day Symposium.
- 2018 Genetic and Epigenetic Control of Hematopoietic Stem Cell Expansion and pathogenesis of MDS. Wells Center for Pediatric Research, Indiana University School of Medicine.
- 2018 Understanding and Targeting Mutant p53 in Hematological Malignancies. Simon Cancer Center, Indiana University School of Medicine.
- 2018 PRL2 phosphatase in normal and malignant hematopoiesis. Cooperative Center of Excellence in Hematology, Indiana University School of Medicine.
- 2018 Developing Novel Therapeutic Approaches to improve childhood leukemia treatment, the St. Baldrick's Foundation, CA
- 2018 Mutant p53 promotes hematopoietic stem and progenitor cell expansion through interacting with epigenetic modulator EZH2. The 60th American Society of Hematology (ASH) Conference, San Diego, CA.
- 2018 Developing Novel Therapeutic Approaches to improve leukemia treatment, Indiana Science and Technology Club, IN
- 2019 Chronic inflammation increases cancer development in LFS patients. Wells Center for Pediatric Research, Indiana University School of Medicine.
- 2019 Genetic and Epigenetic Regulation of Leukemia Stem Cells, University of Notre Dame, South Bend, Indiana.
- 2019 Mutant p53 drives clonal hematopoiesis through modulating epigenetic pathways, the 8th Mutant p53 Workshop, Lyon, France.
- 2019 Genetic and Epigenetic Control of Pre-leukemia Stem Cells and Leukemia Stem Cells, University of Minnesota, Minnesota.
- 2019 Understanding and Targeting of Pre-leukemia Stem Cells and Leukemia Stem Cells, Northwestern University.
- 2019 Understanding and Targeting of Pre-leukemia Stem Cells and Leukemia Stem Cells, University of Miami.
- 2020 Understanding and Targeting of Pre-leukemia Stem Cells and Leukemia Stem Cells, University of Florida.
- 2021 Understanding and Targeting of Pre-leukemia Stem Cells and Leukemia Stem Cells, Chicago Blood Club.
- 2022 Genetic and Epigenetic Control of Normal and Malignant Hematopoietic Stem Cells and Leukemia Stem Cells, Loyola University School of Medicine.

PROFESSIONAL SERVICE

EDITORIAL BOARD:

2014 to present	International Journal of Neonatal Science and Therapeutics
2014 to present	Journal of Stem Cell Research and Transplantation
2014 to present	Stem Cells Research, Development and Therapy
2014 to present	Journal of Stem Cells and Translational Investigation
2014 to present	Pediatrics and Neonatal Biology
2016 to present	Cancer Translational Medicine
2020 to present	Leukemia & Lymphoma

REVIEWER FOR JOURNALS: Cell Stem Cell, JCI, PNAS, Blood, Leukemia, Stem Cells, Journal of Leukocyte Biology, BMC Cell Biology, PLoS ONE, Frontiers in Oncology, Cancer Biotherapy & Radiopharmaceutics, Molecular and Cellular Biochemistry, Tumor Biology, Journal of Hematology and Oncology Research, In Vitro Cellular & Developmental Biology, International Journal of Biochemistry and Molecular Biology, Oncotarget, Blood Advances, and Cell Communication and Signaling.

UNIVERSITY SERVICE

INSTITUTIONAL COMMITTEE:

2012 to 2017	Member, Institutional Animal Care and Use Committee (IACUC), Indiana University School of Medicine
2017 to 2020	Member, Graduate Faculty Council, Indiana University

REVIEWER FOR GRANTS:

2011	IUSCC ITRAC pilot project
2012	Simon Clinical Research pilot project
2013	IUSCC Pancreatic Center pilot project
2013	IUSCC Bioinformatics Core Pilot projects
2013-2016	IUSM Wright Scholarship
2015	Indiana CTSI Core Pilot projects
2017	IUSCC ITRAC pilot project

2017	IUSCC Associate Member pilot project
2018	IUSCC Associate Member pilot project
2018	Wells Center Translational Research Grant
2019	Wells Center Translational Research Grant

OTHER SERVICE:

2012 to 2016	Associate Editor, the Wells Center Newsletter
2012	Poster Judge, Research Day, Department of Biochemistry and Molecular Biology, March 2012
2013 - 2017	Poster Judge, Cancer Research Day, Indiana University Cancer Research Day
2013 - 2015	Panelist and Judge, Wells Center Summer Intern Program, Oral Presentation
2013 -2015	Poster Judge, Student Research Program in Academic Medicine Poster Presentations
2013	Interview prospective international graduate students for the IBMG program, IUSM, March 2013
2014 -2018	Career Panelist, Molecular Medicine in Action (MMIA) program, IUSM

TEACHING ASSIGNMENTS

UNDERGRADUATE SUMMER STUDENTS AND MEDICAL STUDENTS:

2007	Youyang Yang, Summer Student, Harvard University
2008-2009	Narae Bae, Graduate Student, Cornell University
2011	Joel Pollack, Undergraduate Student, Wells Center Summer Intern program, Boston University
2012	Sisi Chen, Graduate Student, Indiana University School of Medicine
2012	Zhixiang Zhang, Undergraduate Student, Wells Center Summer Intern program, Indiana University
2012	Awahngie Akwo, Medical Student, SRPAM program, Indiana University

- 2013 Levi Hadley, Undergraduate Student, Wells Center Summer Intern program, Indiana University
- 2013 Hyewon Hwang, Undergraduate Student, CEMH Summer Intern Program, Inje University, Korea
- 2014 Wenjing Cai, Undergraduate Student, Indiana University
- 2014 Chen Mu, Medical Student, SRPAM program, Indiana University
- 2015 Taylor Twiggs, Medical Student, SRPAM program, Indiana University
- 2015 Christine Wang, Medical Student, Wells Center Summer Intern program, Indiana University
- 2016 Cecil Daniels, Undergraduate Student, Undergraduate Research for Prospective Physician-Scientists, Indiana University
- 2017 David Schmitz, Medical Student, SRPAM program, Indiana University
- 2017 Aidan Fahey, Graduate student, Ulster University at Coleraine
- 2018 Odelia Satchivi, Undergraduate Student, Indiana University
- 2018 Danielle Henley, Undergraduate Student, University of South Alabama
- 2018 Sergio Barajas, Graduate Student, Indiana University School of Medicine
- 2019 Wenjie Cai, Graduate Student, Indiana University School of Medicine
- 2019 Katherine Strube, Undergraduate Student, Butler University
- 2019 Javona Freeman, Undergraduate Student, Indiana University

GRADUATE SCHOOL THESIS COMMITTEES:

- 2011-2012 Wenjuan Liao, PhD Candidate, Department of Biochemistry and Molecular Biology, IUSM
- 2017-2018 Yang Lin, PhD Candidate, Department of Biochemistry and Molecular Biology, IUSM
- 2017-2018 Aidan Fahey, Graduate student, Ulster University at Coleraine, UK
- 2020-2021 Aditi Khatpe, PhD Candidate, Department of Biochemistry and Molecular Biology, IUSM

Ph.D. THESIS DIRECTOR:

- 2012-2018 Sisi Chen, PhD Candidate, Department of Biochemistry and Molecular Biology, IUSM
- 2019-2021 Wenjie Cai, PhD Candidate, Department of Biochemistry and Molecular Biology, IUSM
- 2019-2021 Sergio Barajas, PhD Candidate, Department of Biochemistry and Molecular Biology, IUSM
- 2020-2021 Christopher Borchers, PhD Candidate, Department of Biochemistry and Molecular Biology, IUSM
- 2020-2021 Shiyu Xiao, PhD student, Department of Biochemistry and Molecular Biology, IUSM
- 2021-present Shiyu Xiao, PhD Candidate, Department of Medicine, Northwestern University Feinberg School of Medicine
- 2021-present Wenjie Cai, PhD Candidate, Visiting Predoctoral Fellow, Department of Medicine, Northwestern University Feinberg School of Medicine
- 2021-present Sergio Barajas, PhD Candidate, Visiting Predoctoral Fellow, Department of Medicine, Northwestern University Feinberg School of Medicine

POSTDOCTORAL FELLOWS:

- 2003-2006 Jinjuan Yao, MD & PhD, Postdoctoral Fellow, MSKCC
- 2004-2005 Yasuhiko Miyata, MD & PhD, Postdoctoral Fellow, MSKCC
- 2005-2006 Goro Sashida, MD & PhD, Postdoctoral Fellow, MSKCC
- 2007-2008 Fabiana Perna, MD, Postdoctoral Fellow, MSKCC
- 2008-2010 Takashi Asai, MD & PhD, Postdoctoral Fellow, MSKCC
- 2011-2013 Hao Yu, PhD, Postdoctoral Fellow, Indiana University School of Medicine
- 2011-2015 Rui Gao, PhD, Postdoctoral Fellow, Indiana University School of Medicine
- 2011-2016 Michihiro Kobayashi, MD & PhD, Postdoctoral Fellow, Indiana University School of Medicine
- 2015-2017 Chonghua Yao, MD & PhD, Postdoctoral Fellow, Indiana University School of Medicine
- 2014-2018 Sarah Nabinger, PhD, Postdoctoral Fellow, Indiana University School of Medicine

2017-2021	Sasidhar Vemula, PhD, Postdoctoral Fellow, Indiana University School of Medicine
2019-2021	Yuxia Yang, PhD, Postdoctoral Fellow, Indiana University School of Medicine
2019-2021	Hongxia Chen, MD & PhD, Postdoctoral Fellow, Indiana University School of Medicine
2021-present	Hongxia Chen, MD & PhD, Department of Medicine, Northwestern University Feinberg School of Medicine

AWARDS TO STUDENTS AND POSTDOCTORAL FELLOWS:

F32 Award	Sarah Nabinger, PhD, Postdoctoral Fellow Mentor, Yan Liu, PhD., NIH/NCI 2016-2018
New Investigator Award	Sisi Chen, Graduate Student; Mentor, Yan Liu, PhD, 45 th International Society for Experimental Hematology (ISEH) Annual Meeting, 2016
Abstract Achievement Award	Sisi Chen, Graduate Student; Mentor, Yan Liu, PhD, the 59 th American Society of Hematology (ASH) Conference, Atlanta, GA, 2017.
Abstract Achievement Award	Sarah Nabinger, PhD, Postdoctoral Fellow; Mentor, Yan Liu, PhD, the 57 th American Society of Hematology (ASH) Conference, Orlando, FL, 2015.
Abstract Achievement Award	Sisi Chen, Graduate Student; Mentor, Yan Liu, PhD, the 57 th American Society of Hematology (ASH) Conference, Orlando, FL, 2015.
Abstract Achievement Award	Sisi Chen, Graduate Student; Mentor, Yan Liu, PhD, the 56 th American Society of Hematology (ASH) Conference, San Francisco, CA, 2014.
Abstract Achievement Award	Michihiro Kobayashi, MD, PhD, Postdoctoral Fellow; Mentor, Yan Liu, PhD, the 55 th American Society of Hematology (ASH) Conference, New Orleans, LA, 2013.
Graduate Student Travel Award	Sisi Chen, Graduate Student; Mentor, Yan Liu, PhD, IUPUI, 2016.
Graduate Student Travel Award	Sisi Chen, Graduate Student; Mentor, Yan Liu, PhD, IUPUI, 2014.
Honorary Mention	Sisi Chen, Graduate Student; Mentor, Yan Liu, PhD, Biochemistry Research Day, IUSM, 2014.

Honorary Mention	Sisi Chen, Graduate Student; Mentor, Yan Liu, PhD, Biochemistry Research Day, IUSM, 2017.
Honorary Mention	Sisi Chen, Graduate Student; Mentor, Yan Liu, PhD, Indiana University Cancer Research Day, 2015.
Oral presentation First Prize	Chen Mu, Medical Student; Mentor, Yan Liu, PhD, the Summer Research Program in Academic Medicine (SRPAM), Indiana University, 2014.
Oral presentation First Prize	Taylor Twiggs, Medical Student; Mentor, Yan Liu, PhD, the Summer Research Program in Academic Medicine (SRPAM), Indiana University, 2015.
Oral presentation Second Prize	Christine Wang, Medical Student; Mentor, Yan Liu, PhD, Wells Center Summer Intern program, Indiana University, 2015.

GRADUATE TEACHING ASSIGNMENTS:

Developmental Genetics-G726 Spring 2012, Lecture 8: Hematopoiesis
Role: Instructor

Developmental Genetics-G726 Spring 2013, Lecture 8: Hematopoiesis
Role: Instructor

Clinical Problem Solving-X604 Spring 2013, Cases: 5-8
Role: Instructor

Clinical Problem Solving-X604 Spring 2014, Cases: 5-8
Role: Instructor

Clinical Problem Solving-X604 Spring 2015, Cases: 5-8
Role: Instructor

Stem Cell Biology-G720 Spring 2015, Lecture 8: Cancer Stem Cells
Role: Instructor

Stem Cell Biology-G720 Spring 2016, Lecture 8: Cancer Stem Cells
Role: Instructor

Stem Cell Biology-G720 Spring 2017, Lecture 8: Cancer Stem Cells
Role: Instructor

Stem Cell Biology-G720 Spring 2019, Lecture 8: Cancer Stem Cells
Role: Instructor

Stem Cell Biology-G720 Spring 2020, Lecture 8: Cancer Stem Cells
Role: Instructor

Stem Cell Biology-G720 Spring 2021, Lecture 8: Cancer Stem Cells
Role: Instructor

1 **PRL2 phosphatase enhances oncogenic FLT3 signaling via dephosphorylation of the E3 ubiquitin**
2 **ligase CBL at tyrosine 371**

3
4 Hongxia Chen^{1,2,16#}, Yunpeng Bai^{3#}, Michihiro Kobayashi⁴, Shiyu Xiao², Wenjie Cai^{2,4}, Sergio Barajas^{2,4},
5 Sisi Chen⁴, Jinmin Miao³, Frederick Nguete Meke³, Sasidhar Vemula⁴, James P. Ropa⁵, James M. Croop⁴,
6 H. Scott Boswell⁶, Jun Wan⁷, Yuzhi Jia⁸, Huiping Liu^{8,9}, Loretta S. Li^{9,10}, Jessica K. Altman^{2,9}, Elizabeth
7 A. Eklund^{2, 9, 11}, Peng Ji^{9,12}, Wei Tong¹³, Hamid Band¹⁴, Danny T. Huang¹⁵, Leonidas C. Platanias^{2,9,11},
8 Zhong-Yin Zhang^{3*}, and Yan Liu^{2,9*}

9 ¹Department of Hematology and Oncology, Chongqing University Three Gorges Hospital, Chongqing,
10 China; ²Department of Medicine, Feinberg School of Medicine, Northwestern University, Chicago, IL;
11 ³Department of Medicinal Chemistry and Molecular Pharmacology, Center for Cancer Research, and
12 Institute for Drug Discovery, Purdue University, West Lafayette, IN; ⁴Department of Pediatrics, Herman
13 B Wells Center for Pediatric Research, Indiana University School of Medicine, Indianapolis, IN;
14 ⁵Department of Microbiology and Immunology, Indiana University School of Medicine, Indianapolis, IN;
15 ⁶Department of Medicine, Indiana University School of Medicine, Indianapolis, IN; ⁷Department of
16 Medical Genetics, Indiana University, Indianapolis, IN; ⁸Department of Pharmacology, Feinberg School
17 of Medicine, Northwestern University, Chicago, IL; ⁹Robert H. Lurie Comprehensive Cancer Center,
18 Chicago, IL; ¹⁰Department of Pediatrics, Feinberg School of Medicine, Northwestern University,
19 Chicago, IL; ¹¹Department of Medicine, Jesse Brown VA Medical Center, Chicago, IL; ¹²Department of
20 Pathology, Feinberg School of Medicine, Northwestern University, Chicago, IL; ¹³Children's Hospital of
21 Philadelphia, University of Pennsylvania School of Medicine, Philadelphia, PA; ¹⁴Department of
22 Genetics, University of Nebraska Medical Center, Omaha, NB; ¹⁵Cancer Research UK Beatson Institute
23 and Institute of Cancer Sciences, University of Glasgow, Glasgow, United Kingdom; ¹⁶School of
24 Medicine, Chongqing University, Chongqing, China.

25 # These authors contributed equally to the paper

26 *Correspondence: zhang-zy@purdue.edu; yan.liu@northwestern.edu

27 **KEY POINTS**

28

29 Genetic and pharmacological inhibition of PRL2 significantly reduce the burden of FLT3-ITD-driven
30 leukemia and extend leukemic mice survival.

31

32 PRL2 dephosphorylates CBL at tyrosine 371 and blocks CBL-mediated FLT3 ubiquitination and
33 degradation, leading to enhanced STAT5, AKT, and ERK signaling in leukemia cells.

34

35 **Abstract**

36 Acute myeloid leukemia (AML) is an aggressive blood cancer with poor prognosis. FLT3 is one of the
37 major oncogenic receptor tyrosine kinases aberrantly activated in AML. While protein tyrosine
38 phosphatase PRL2 is highly expressed in some subtypes of AML compared to normal human
39 hematopoietic stem and progenitor cells (HSPCs), the mechanisms by which PRL2 promotes
40 leukemogenesis are largely unknown. We discovered that genetic and pharmacological inhibition of PRL2
41 significantly reduce the burden of FLT3-ITD-driven leukemia and extend the survival of leukemic mice.
42 Further, we found that PRL2 enhances oncogenic FLT3 signaling in leukemia cells, promoting their
43 proliferation and survival. Mechanistically, PRL2 dephosphorylates the E3 ubiquitin ligase CBL at
44 tyrosine 371 and attenuates CBL-mediated ubiquitination and degradation of FLT3, leading to enhanced
45 FLT3 signaling in leukemia cells. Thus, our study reveals that PRL2 enhances oncogenic FLT3 signaling
46 in leukemia cells through dephosphorylation of CBL and will likely establish PRL2 as a novel druggable
47 target for AML.

48

49

50

51

52 **Introduction**

53 Acute myeloid leukemia (AML) is an aggressive blood cancer with poor prognosis.¹⁻³ Some human
54 leukemia cells depend on aberrant receptor tyrosine kinase activation and the downstream effectors for
55 proliferation and survival.⁴⁻⁵ FMS-like tyrosine kinase receptor-3 (FLT3) is one of the major oncogenic
56 receptor tyrosine kinases aberrantly activated in AML.⁶⁻⁷ Activating *FLT3* mutations, including internal
57 tandem duplications in *FLT3* (*FLT3-ITD*), are seen in approximately 30% of AML patients and confer a
58 poor prognosis.⁶⁻⁷ Despite substantial efforts devoted to the development of FLT3 inhibitors, the
59 effectiveness of these inhibitors as a single agent in AML has been limited and development of drug
60 resistance in leukemia patients is always a concern.⁶⁻⁹ The resistance to targeted therapies seen in AML
61 patients may be associated with a rare population of leukemia-initiating cells (LICs) or leukemia stem
62 cells (LSCs) that are capable of self-renewal and initiating leukemia.¹⁰⁻¹⁴

63 The CBL family E3 ubiquitin ligases, including CBL and CBL-b, are responsible for the ubiquitination
64 and degradation of FLT3 in hematopoietic cells.¹⁵ CBL is a tumor suppressor in hematological
65 malignancies. Indeed, loss of both *CBL* and *CBL-b* results in fetal myeloproliferative neoplasms (MPN)
66 in mice.¹⁶⁻¹⁸ Both somatic and germline *CBL* mutations are frequently found in myeloid malignancies,
67 including juvenile myelomonocytic leukemia (JMML), myelodysplastic syndromes (MDS), MPN, and
68 AML.¹⁹⁻²² In response to cytokine stimulation, CBL is phosphorylated and activated.¹⁵ However, how
69 CBL phosphorylation is downregulated in leukemia cells is largely unknown.

70 The phosphatases of regenerating liver (PRL1, 2 and 3) are members of the protein tyrosine phosphatase
71 (PTP) family that are being pursued as biomarkers and therapeutic targets in human cancers.²³⁻²⁶ PRL2,
72 also known as PTP4A2, is essential for hematopoietic stem and progenitor cell (HSPC) proliferation and
73 promotes AML1-ETO-induced leukemia.^{27, 28} In addition, PRL2 regulates T cell development and
74 promotes oncogenic NOTCH1-induced T-cell leukemia.^{29, 30} While *PRL2* is highly expressed in some
75 subtypes of AML compare to normal human HSPCs,²⁸ the mechanisms by which PRL2 promotes
76 leukemogenesis are unclear. In this study, we discovered that PRL2 dephosphorylates CBL at tyrosine

77 371 and inhibits its E3 ubiquitin ligase activity toward FLT3, leading to decreased ubiquitination of FLT3,
78 and activation of FLT3-induced downstream signaling pathways in leukemia cells.

79 **Methods**

80 Detailed methodology is provided in the Supplemental Information (Available on the Blood Web site).

81 **Mice**

82 Wild type C57BL/6 (CD45.2⁺), B6.SJL (CD45.1⁺), C3H/HeJ, and *Flt3*^{+/*ITD*} mice were purchased from the
83 Jackson Laboratories. *Pr12*^{+/*+*}, *Pr12*^{-/*-*}, *Flt3*^{+/*ITD*}, *Flt3*^{+/*ITD*}*Pr12*^{-/*-*}, *Flt3*^{*ITD*/*ITD*} and *Flt3*^{*ITD*/*ITD*}*Pr12*^{-/*-*} mice were
84 maintained in the Indiana and Northwestern University Animal Facility and kept in Thorensten units with
85 filtered germ-free air. Embryonic day 14.5 (E14.5) fetal liver cells (*Pr12*^{+/*+*} and *Pr12*^{-/*-*}) were isolated from
86 pregnant *Pr12*^{+/*-*} female mice that were mated with *Pr12*^{+/*-*} male mice. The Institutional Animal Care and
87 Use Committee (IACUC) of Indiana University School of Medicine and Northwestern University
88 Feinberg School of Medicine approved all experimental procedures.

89 **Statistical Analysis**

90 The animal sample size was based on previous studies evaluating the roles of PRL2 in leukemia and
91 POWER analysis.^{26,27} Using Chi-Square analysis, 7 mice per group will provide 80% POWER in
92 detecting difference with 95% difference. Gehan-Breslow-Wilcoxon test was used for Kaplan-Meier
93 survival curves. Other data were analyzed by paired or unpaired t test or analysis of variance for nonlinear
94 distributions using GraphPad Prizm 9. Results are expressed as the mean ± standard error of the mean
95 (SEM) for at least triplicate experiments. P values of < 0.05 were regarded as statistically significant
96 which was calculated by GraphPad Prism9. *p<0.05, **p<0.01, ***p < 0.001, ****p < 0.0001. Further
97 details about methods are available in supplementary information.

98 **Data Sharing Statement**

99 RNA-seq data are available at GEO under accession number GSE208136.

100 **Results**

101 **FLT3 mutated AML patients with high *PRL2* expression have reduced overall survival**

102 To determine the role of *PRL2* (*PTP4A2*) in the pathogenesis of human AML, we first analyzed the
103 published TCGA ([https://www.cancer.gov/about-nci/organization/ccg/research/structural-](https://www.cancer.gov/about-nci/organization/ccg/research/structural-genomics/tcga)
104 [genomics/tcga](https://www.cancer.gov/about-nci/organization/ccg/research/structural-genomics/tcga)) dataset and found that *PRL2* expression is higher in intermediate and poor risk AML
105 compared to favorable risk AML (Figure 1A). *PRL2* expression is also higher in dead AML patients
106 compared to AML patients that are alive (Figure 1B). We then analyzed the dataset from cBioPortal
107 (<https://www.cbioportal.org>) and found that *PRL2* levels are higher in patients with cytogenetic and
108 central nerve system (CNS) relapse (Figure 1C; supplemental Figure 1A). We defined *PRL2* expression
109 above median as high *PRL2* expression group and below median as low *PRL2* expression group. Notably,
110 AML patients with high *PRL2* expression have reduced overall survival compared to AML patients with
111 low *PRL2* expression (Supplemental Figure 1B). In AML bearing poor cytogenetic risk, patients with
112 high *PRL2* expression have reduced overall survival compared to patients with low *PRL2* expression
113 (Figure 1D; supplemental Figure 1C-D). Next, we performed DEG (differentially expressed gene)
114 analysis to compare gene expression in a subset of AML patients with high or low *PRL2* expression. There
115 are 790 genes upregulated and 948 genes downregulated in AML patients with high *PRL2* expression
116 (Figure 1E). Gene Set Enrichment Analysis (GSEA) revealed that AML, AML prognosis, leukemia stem
117 cell (LSC), and hematopoietic stem cell (HSC) gene signatures are enriched in AML patients with high
118 *PRL2* expression (Figure 1F). In addition, pathways associated with *FLT3* as well as its downstream
119 effectors, including *STAT5A*, *PI3K/AKT*, and *ERK1/ERK2*, are enriched in *PRL2* high group (Figure
120 1G-H).

121

122 We then analyzed *PRL2* expression in AML patients with or without *FLT3* mutations using GSE15434
123 and cBioPortal dataset and found that AML patient with *FLT3* mutations have higher *PRL2* expression

124 compared to AML patients negative for *FLT3* mutations (Figure 1I; supplemental Figure 1E). In AML
125 patients without *FLT3* mutations, *PRL2* expression did not appear to affect overall survival (Supplemental
126 Figure 1F). However, in *FLT3* mutation positive AML, patients with high *PRL2* expression have reduced
127 overall survival compared to patients with low *PRL2* expression (Figure 1J). Taken together, these clinical
128 data suggest that high *PRL2* expression may be a prognostic marker in *FLT3*-mutated AML.

129 **PRL2 deficiency alters FLT3 mediated gene transcription in murine hematopoietic stem and** 130 **progenitor cells**

131 To gain insights into the molecular mechanisms underlying the role of PRL2 in hematopoietic stem and
132 progenitor cells (HSPCs), we performed RNA-seq analysis to compare gene expression in *Prl2*^{+/+} and
133 *Prl2*^{-/-} E14.5 (Embryonic day 14.5) fetal liver cells which are enrich with HSPCs. Approximately 400 genes
134 were significantly downregulated, and 75 genes were significantly upregulated in *Prl2*^{-/-} fetal liver cells,
135 respectively (Figure 2A). We then employed GSEA analysis to group potential PRL2 target genes into
136 specific pathways important for HSPC behavior. Notably, long-term hematopoietic stem cells, receptor
137 tyrosine kinase signaling, PI3K/AKT signaling, and ERK signaling gene signatures were significantly
138 downregulated in *Prl2* null fetal liver cells (Figure 2B). In addition, receptor regulator activity, receptor
139 complex, positive regulation of receptor tyrosine kinase signaling, and positive regulation of ERK
140 signaling gene signatures were significantly down regulated in *Prl2* null fetal liver cells (Figure 2C-D).
141 We utilized STRING 11.5 to perform protein association network analysis on genes downregulated in
142 *Prl2* null fetal liver cells and observed strong interconnection between downregulated genes with FLT3
143 and its downstream proteins in *Prl2* null fetal liver cells (Figure 2E). We confirmed that the expression of
144 genes interacting with the FLT3 signaling pathway was downregulated in *Prl2* null fetal liver cells (Figure
145 2F), *Prl2* null fetal liver Kit⁺ cells (supplemental Figure 2A), as well as *Prl2* null bone marrow Lin⁻ cells
146 (Figure 2G). Loss of *Prl2* significantly decreased AKT, STAT5 and ERK phosphorylation in fetal liver
147 cells (Figure 2H; supplemental Figure 2B) and bone marrow Lin⁻ cells (Figure 2I; supplemental Figure
148 2C).

149 **Loss of *Prl2* decreases the self-renewal capability of FLT3-ITD positive hematopoietic stem and**
150 **progenitor cells**

151 To determine the role of PRL2 in FLT3-ITD-mediated hematopoietic cell proliferation, we introduced
152 wild-type (WT) FLT3 or FLT3-ITD mutant into Lin⁻ cells purified from WT and *Prl2* null mice and found
153 that *Prl2* null Lin⁻ cells expressing FLT3-ITD exhibit decreased proliferation compared to that of the WT
154 cells both in the absence of cytokines and in the presence of FLT3 ligand (supplemental Figure 2D). As
155 expected, ectopic expression of FLT3-ITD increased the colony formation of WT HSPCs (supplemental
156 Figure 2E). While *Prl2* deficiency did not affect the colony formation of HSPCs expressing WT FLT3,
157 loss of *Prl2* decreased the colony formation of HSPCs expressing FLT3-ITD (supplemental Figure 2E).
158 These findings suggest that PRL2 is important for FLT3-ITD-mediated hematopoietic cell
159 hyperproliferation.

160
161 To further determine the impact of PRL2 on oncogenic FLT3 signaling, we have generated *Flt3^{+/ITD}Prl2^{-/-}*
162 *^{-/-}* and *Flt3^{ITD/ITD}Prl2^{-/-}* mice.³² *Prl2^{-/-}* mice show decreased body size as we previously reported;^{28,33}
163 however, expression of FLT3-ITD did not rescue the body size defect seen in the *Prl2^{-/-}* mice
164 (supplemental Figure 3A). To determine the impact of *Prl2* on hematopoiesis, we first analyzed the
165 peripheral blood (PB) and bone marrow (BM) of 8- to 12-week-old *Prl2^{+/+}*, *Prl2^{-/-}*, *Flt3^{+/ITD}*, *Flt3^{+/ITD}Prl2^{-/-}*
166 *^{-/-}*, *Flt3^{ITD/ITD}*, and *Flt3^{ITD/ITD}Prl2^{-/-}* mice. *Flt3^{ITD/ITD}* mice show increased white blood cell (WBC) counts
167 as reported,³² whereas loss of *Prl2* brought WBC counts back to normal (supplemental Figure 3B). Both
168 *Flt3^{ITD/ITD}* and *Flt3^{ITD/ITD}Prl2^{-/-}* mice are anemic, manifested by decreased red blood cell (RBC) counts
169 and reduced hemoglobin (HGB) levels in peripheral blood (supplemental Figure 3C-D). In addition,
170 *Flt3^{ITD/ITD}* mice displayed decreased levels of platelets but increased levels of basophil and monocyte
171 counts (supplemental Figure 3E-H). There is increased number of myeloid cells in PB of *Flt3^{ITD/ITD}* mice;
172 however, loss of *Prl2* mitigated this effect (supplemental Figure 3I). Both *Flt3^{+/ITD}* and *Flt3^{ITD/ITD}* mice
173 displayed increased BM cellularity compared to WT mice, whereas loss of *Prl2* brought BM cellularity

174 back to normal (supplemental Figure 3J). There are decreased number of B cells but increased number of
175 myeloid cells in the BM of *Flt3^{ITD/ITD}* mice (supplemental Figure 3K-M). Loss of *Prl2* significantly
176 reduced the number of myeloid cells in the FLT3-ITD background (supplemental Figure 3M).

177

178 We next examined the number of primitive hematopoietic stem and progenitor cells in the BM of *Prl2^{+/+}*,
179 *Prl2^{-/-}*, *Flt3^{+/ITD}*, *Flt3^{+/ITD}Prl2^{-/-}*, *Flt3^{ITD/ITD}*, and *Flt3^{ITD/ITD}Prl2^{-/-}* mice. *Flt3^{ITD/ITD}* mice have increased
180 number of long-term hematopoietic stem cells (LT-HSCs), multipotent progenitor cells (MPPs), and Lin⁻
181 Sca1⁺Kit⁺ cells (LSKs) in their BM, whereas loss of *Prl2* brought the numbers of hematopoietic stem and
182 progenitor cells (HSPCs) back to WT level (Figure 3A, C-D; supplemental Figure 3N). While loss of *Prl2*
183 decreases the number of ST-HSCs, *Prl2* deficiency has modest impact on ST-HSCs in FLT3-ITD
184 background (Figure 3B). We then performed methylcellulose colony-forming unit (CFU) assays to
185 quantify myeloid progenitor cells. While *Flt3^{ITD/ITD}* BM cells show increased colony formation, loss of
186 *Prl2* significantly decreased their ability to form colonies *in vitro* (Figure 3E), suggesting that PRL2 is
187 important for FLT3-ITD-mediated enhanced hematopoietic cell proliferation.

188

189 To examine whether *Prl2* deficiency affects *Flt3^{+/ITD}* HSPC function *in vivo*, we performed serial
190 competitive BM transplantation assays using *Prl2^{+/+}*, *Prl2^{-/-}*, *Flt3^{+/ITD}*, and *Flt3^{+/ITD}Prl2^{-/-}* BM cells
191 (CD45.2⁺). Equal numbers of donor and competitor BM cells were transplanted into lethally irradiated
192 recipient mice (supplemental Figure 4A). Sixteen weeks after primary transplantation, we found that loss
193 of *Prl2* significantly decreases the engraftment of *Flt3^{+/ITD}* BM cells (Figure 3F). Recipient mice
194 repopulated with *Flt3^{+/ITD}* BM cells showed increased levels of WBC counts, whereas loss of *Prl2* in the
195 *Flt3^{+/ITD}* background brought WBC counts back to normal (supplemental Figure 4B-C).

196

197 Analysis of the BM revealed a striking increase in the number of phenotypically defined MPPs and LSKs
198 in the recipients repopulated with *Flt3^{+/ITD}* BM cells, whereas the number of LT-HSCs and short-term

199 hematopoietic stem cells (ST-HSCs) are normal (Figure 3G-H). Loss of *Prl2* significantly reduced the
200 number of MPPs and LSKs in the *Flt3^{+/ITD}* background (Figure 3I-J; supplemental Figure 4D). We then
201 transplanted 3×10^6 BM cells isolated from the primary recipient mice repopulated with *Prl2^{+/+}*, *Prl2^{-/-}*,
202 *Flt3^{+/ITD}*, and *Flt3^{+/ITD}Prl2^{-/-}* BM cells into lethally irradiated secondary recipients (supplemental Figure
203 4E). Sixteen weeks after transplantation, *Flt3^{+/ITD}Prl2^{-/-}* cells continued to show decreased repopulating
204 ability (Figure 3K). Recipient mice repopulated with *Flt3^{+/ITD}* BM cells showed increased levels of WBC
205 counts, whereas loss of *Prl2* in the *Flt3^{+/ITD}* background brought WBC counts back to normal
206 (supplemental Figure 4F). Interestingly, we observed increased lymphocyte counts in the secondary
207 recipients repopulated with *Flt3^{+/ITD}* BM cells and loss of *Prl2* mitigated the effect (supplemental Figure
208 4G). Strikingly, loss of *Prl2* significantly decreased the number of *Flt3^{+/ITD}* ST-HSCs, MPPs, and LSKs,
209 but not LT-HSCs in the BM of secondary recipient mice (Figure 3L-O; supplemental Figure 4H).
210 Recipient mice repopulated with *Flt3^{+/ITD}* BM cells showed enlarged spleen and loss of *Prl2* rescued the
211 defect (supplemental Figure 4I-J).

212 **PRL2 is important for FLT3-ITD-induced myeloid proliferative neoplasm in mice**

213 Both *Flt3^{+/ITD}* and *Flt3^{ITD/ITD}* mice develop MPN with monocytic features.³² *Flt3^{+/ITD}* and *Flt3^{ITD/ITD}* mice
214 displayed dose-dependent development of progressive splenomegaly, whereas loss of *Prl2* significantly
215 reduced splenomegaly seen in *Flt3^{+/ITD}* and *Flt3^{ITD/ITD}* mice (Figure 4A-B). While there are increased
216 number of LSKs in the spleen of *Flt3^{+/ITD}* and *Flt3^{ITD/ITD}* mice, loss of *Prl2* mitigated the effect (Figure
217 4C).

218 To determine the hematopoietic cell intrinsic effect of PRL2 on FLT3-ITD induced MPN, we transplanted
219 3×10^6 BM cells (CD45.2⁺) isolated from *Prl2^{+/+}*, *Prl2^{-/-}*, *Flt3^{+/ITD}*, *Flt3^{+/ITD}Prl2^{-/-}*, *Flt3^{ITD/ITD}*, and
220 *Flt3^{ITD/ITD}Prl2^{-/-}* mice into lethally irradiated recipient mice (CD45.1⁺). All recipient mice repopulated
221 with *Flt3^{ITD/ITD}* BM cells developed MPN and died within 60 weeks after transplantation; however, loss
222 of *Prl2* significantly extended the survival of *Flt3^{ITD/ITD}* mice, with 50% of mice still alive at 73 weeks
223 following transplantation (Figure 4D). *Prl2* deficiency rescued anemia seen in recipient mice repopulated

224 with *Flt3^{ITD/ITD}* BM cells, manifested by increased RBC counts and HGB levels in PB (Figure 4E-F;
225 supplemental Figure 5A-B). In addition, loss of *Prl2* rescued myeloid expansion seen in PB of *Flt3^{ITD/ITD}*
226 mice (supplemental Figure 5C-G). Flow cytometric analysis further confirmed the expansion of
227 *Mac1⁺Gr1⁺* myeloid cells in PB of recipient mice repopulated with *Flt3^{+/ITD}* or *Flt3^{ITD/ITD}* BM cells and
228 loss of *Prl2* rescued the defect observed in the *Flt3^{ITD/ITD}* group (Figure 4G-H). Recipient mice
229 repopulated with *Flt3^{+/ITD}* and *Flt3^{ITD/ITD}* BM cells developed MPN, manifested by splenomegaly and
230 infiltration of maturing myeloid hyperplasia in bone marrow, spleen, and liver as well as accumulation of
231 myeloid blast cells in PB; however, these abnormalities were significantly reduced in *Flt3^{+/ITD}Prl2^{-/-}* and
232 *Flt3^{ITD/ITD}Prl2^{-/-}* mice (Figure 4I; supplemental Figure 5H). Recipient mice repopulated with *Flt3^{ITD/ITD}*
233 BM cells displayed splenomegaly, whereas loss of *Prl2* significantly reduced splenomegaly seen in
234 *Flt3^{ITD/ITD}* mice (Figure 4J).

235

236 To complement our murine studies, we ectopically expressed WT PRL2 or a catalytically inactive mutant
237 (PRL2-CSDA, where the active site C101 and D69 were mutated to S and A, respectively) in a murine
238 hematopoietic progenitor cell line 32D and performed *in vitro* and *in vivo* experiments.^{30, 34} We found
239 that ectopic expression of PRL2-CSDA decreases the proliferation of 32D cells expressing FLT3-ITD
240 (Figure 4K). We also transplanted transduced 32D cells into sublethally irradiated C3H/HeJ mice and
241 monitor their survival. While ectopic expression of PRL2 had no effect on the survival of C3H/HeJ mice
242 transplanted with FLT3-ITD expressing 32D cells, expression of PRL2-CSDA significantly extended the
243 survival of C3H/HeJ mice (Figure 4L).

244 **Genetic and pharmacological inhibition of PRL2 decreases leukemia burden and extends the**
245 **survival of mice transplanted with human leukemia cell lines**

246 MV-4-11, MOLM-13, and K562 are human AML cell lines.³⁵ To examine the impact of PRL2 deficiency
247 on human leukemia cell proliferation, we have developed two shRNAs targeting different regions of

248 human *PRL2*.^{27, 30} Both shRNAs can efficiently decrease PRL2 proteins in MV-4-11 cells (Figure 5A).
249 We focused our studies using one of the PRL2 shRNA and found that knockdown of PRL2 decreases the
250 colony formation of MV-4-11, MOLM-13, and K562 cells (Figure 5B and supplemental Figure 6A-C).
251 To determine the impact of PRL2 deficiency on leukemia development *in vivo*, we transplanted 3×10^6
252 MV-4-11 or MOLM-13 cells expressing control or PRL2 shRNA into sublethally irradiated NSG mice
253 and monitored their survival. We found that loss of PRL2 significantly extended the survival of recipient
254 mice transplanted with MV-4-11 or MOLM-13 cells (Figure 5C; supplemental Figure 6D). In addition,
255 we found genetic inhibition of PRL2 significantly decreases the engraftment of MV-4-11 cells in PB, BM,
256 and spleen of recipient mice (Figure 5D). Furthermore, knockdown of PRL2 significantly decreased
257 splenomegaly seen in recipient mice transplanted with MV-4-11 cells (Figure 5E-F).

258

259 To further substantiate the PRL2 knockdown results, we also utilized compound 43,³¹ a small molecule
260 PRL inhibitor (PRLi) that blocks PRL trimerization, which is essential for PRL function.^{31, 36, 37}
261 Consistent with previous findings,³¹ PRLi treatment reduces the colony formation of MV-4-11, MOLM-
262 13, and K562 cells (Figure 5G; supplemental Figure 6E-F). To determine the efficacy of PRLi on human
263 leukemia cells *in vivo*, we transplanted luciferase-labeled MV-4-11 cells into sublethally irradiated NSG
264 via tail vein injection. One week after the transplantation, we treated NSG mice with vehicle (10% DMSO)
265 or PRLi (25 mg/kg, I.P.) daily for three weeks. Leukemia burden in NSG mice was monitored via
266 bioluminescence imaging weekly. Serial imaging of luminescence showed that PRLi treatment
267 dramatically decreases leukemia burden compared with the control group (Figure 5H). The radiance of
268 the NSG mice was significantly reduced after exposure to PRLi (Figure 5I). Furthermore, PRLi
269 substantially extended the survival of NSG mice transplanted with human leukemia cells (Figure 5J).
270 PRLi also considerably decreased the engraftment of human leukemia cells in PB, BM, and spleen of
271 NSG mice (Figure 5K). PRLi treatment significantly reduced the size and weight of spleen of NSG mice
272 (Figure 5L-M). Finally, we found that PRLi is specific for PRL2 as it does not affect the colony formation

273 of MV-4-11, MOLM-13, and K562 cells expressing a shRNA targeting PRL2 (supplemental Figure 6G).
274 Further, PRLi inhibits the proliferation of MV-4-11 and MOLM-13 cells expressing PRL2, but not MV4-
275 11 and MOLM-13 cells expressing PRL2-CSDA (Supplementary Figure 6H).

276 **Pharmacological inhibition of PRL2 reduces leukemia burden and extends the survival of mice**
277 **transplanted with primary human AML cells**

278 PRLi decreases the proliferation of primary human AML cells *in vitro* in a dosage-dependent manner
279 (Figure 6A). In addition, PRLi treatment decreases the colony formation of primary human AML cells
280 with or without FLT3 mutations (Figure 6B). PRLi treatment also arrested primary AML cells with FLT3-
281 ITD mutation at the G0/G1 phase of the cell cycle and decreased the percentage of cells in S or G2M
282 phase (Figure 6C; supplemental Figure 6I). Further, PRLi treatment significantly increased the apoptosis
283 of primary human AML cells with FLT3-ITD mutation (Figure 6D; supplemental Figure 6J).

284

285 To determine the efficacy of PRLi on primary human leukemia cells *in vivo*, we generated two patient-
286 derived xenograft (PDX) models of FLT3-ITD positive AML in NSGS mice. 12-16 weeks post primary
287 transplantation, we confirmed engraftment of human CD45⁺ (huCD45⁺) AML cells in NSGS mice (data
288 not shown) and generated secondary recipients for drug administration. After confirmation of human
289 leukemia cell engraftment in peripheral blood of NSG mice (>1% human CD45⁺ cells), NSG mice were
290 treated with vehicle (10% DMSO) or PRLi (25 mg/kg, I.P.) daily for three weeks. PRLi substantially
291 extended the survival of NSG mice transplanted with human CD45⁺ leukemia cells (Figure 6E;
292 supplemental Figure 6K). PRLi also considerably decreased the engraftment of human CD45⁺ leukemia
293 cells in PB, BM, and spleen of NSG mice at the end point of treatment (Figure 6F; supplemental Figure
294 6L).

295 **PRL2 is a positive mediator of oncogenic FLT3 signaling in murine hematopoietic cells and human**
296 **leukemia cells**

297 To determine the impact of PRL2 on FLT3 signaling, we examined STAT5, AKT, and ERK
298 phosphorylation and found that loss of *Prl2* decreases STAT5, AKT, and ERK phosphorylation in both
299 *Flt3^{+/ITD}* and *Flt3^{ITD/ITD}* BM cells (Figure 6G). These observations suggest that PRL2 is a positive mediator
300 of FLT3-ITD signaling in hematopoietic cells. To determine the impact of PRL2 deficiency on FLT3
301 signaling in leukemia cells, we found that knock down of *PRL2* significantly decreases pFLT3, FLT3
302 expression, AKT, ERK and STAT5 phosphorylation in MV-4-11 cells (Figure 6H, left panel). In addition,
303 we showed that PRLi treatment also decreases pFLT3, FLT3 expression, AKT, ERK, STAT5, STAT3
304 and MEK phosphorylation in MV-4-11 cells (Figure 6H right panel; supplemental Figure 7A). Moreover,
305 we observed decreased pFLT3, FLT3 expression, phosphorylation of AKT, STAT5, STAT3, STAT1 and
306 MEK in K562 cells following PRLi treatment (supplemental Figure 7B), but there was no change in the
307 levels of BCR-ABL, BCR, and c-ABL (supplemental Figure 7C). We also found that PRLi treatment
308 reduces FLT3 expression and decreases the phosphorylation of AKT, ERK, and STAT5 in U937 cells
309 expressing WT FLT3 or FLT3-ITD (supplemental Figure 7D). We found that decreased phosphorylation
310 of AKT, STAT5, and ERK in MV4-11 cells expressing shPRL2 isolated from NSG mice at 4 weeks
311 following transplantation (Figure 6J left; supplemental Figure 7E left). Notably, we observed decreased
312 phosphorylation of AKT, STAT5, and ERK in MV4-11 and primary human AML cells isolated from
313 NSG mice following three weeks of PRLi treatment (Figure 6J-K; supplemental Figure 7E). While PTEN
314 is a negative regulator of the AKT signaling pathway,²⁸ PRLi treatment did not affect PTEN expression
315 in MV4-11 cells (supplemental Figure 7F). Finally, we showed that PRLi is synergic with FLT3 inhibitor
316 AC220 or Gilteritinib in inhibiting the proliferation in MV-4-11 cells (supplemental Figure 7G).

317 **PRL2 associates with and dephosphorylates CBL at tyrosine 371 in leukemia cells**

318 To investigate the mechanism by which PRL2 promotes FLT3 signaling, we determined the effect of
319 PRL2 inhibition on FLT3 stability. We discovered that both knockdown of PRL2 and PRLi treatment can

320 lead to a reduction in FLT3 protein level as a result of a decrease in FLT3 half-life in MV-4-11 cells
321 (Figure 7A; supplemental Figure 8A). In line with this observation, we found that both knockdown of
322 PRL2 and PRLi treatment increase FLT3 ubiquitination in MV-4-11 cells (Figure 7B; supplemental
323 Figure 8B).

324

325 To understand how does PRL2 promote FLT3 stabilization, we carried out substrate trapping experiments
326 to identify potential PRL2 substrates in leukemia cells. To that end, we utilized the GST-tagged PRL2-
327 CSDA mutant, which is competent for substrate binding but unable to catalyze substrate turnover.^{34, 38}

328 Indeed, we found that PRL2-CSDA shows enhanced association with CBL, FLT3, PLC γ , and SHP2
329 compared to wild-type PRL2 in MV-4-11 cells (Figure 7C). We confirmed that PRL2 associates with
330 FLT3 and CBL in MV-4-11 cells using co-immunoprecipitation (Co-IP) assays (Figure 7D). We also
331 found that PRL2 and CBL co-localizes in MV-4-11 (Figure 7E) and U2OS cells (supplemental Figure
332 8C). Given that CBL is an E3 ubiquitin ligase which is responsible for ubiquitination and degradation of
333 FLT3 in hematopoietic cells,¹⁵ these findings suggest that CBL may be a PRL2 substrate.

334

335 CBL becomes phosphorylated on several tyrosine residues following cytokine stimulation (supplemental
336 Figure 8D). To determine whether CBL can serve as a substrate for PRL2, we expressed PRL2 in 293
337 cells and found that ectopic PRL2 expression decreases CBL tyrosine phosphorylation in 293 cells (Figure
338 7F). Conversely, knockdown of PRL2 increases CBL tyrosine phosphorylation in MV-4-11 cells (Figure
339 7G). CBL becomes activated upon Tyrosine 371 phosphorylation, which enables it to target receptor
340 protein tyrosine kinases for ubiquitin-mediated degradation.^{15, 22, 39-41} Indeed, we found that knockdown
341 of PRL2 increases CBL phosphorylation at tyrosine 371, whereas the levels of CBL phosphorylation at
342 tyrosine 700, 731, and 774 were not affected by PRL2 inhibition in MV-4-11 cells (Figure 7H). We
343 detected that ectopic expression of the catalytically inactive PRL2-CSDA mutant increases CBL

344 phosphorylation at tyrosine 371 in MV-4-11 cells (Figure 7I). Further, we found that PRLi treatment
345 increases CBL phosphorylation at tyrosine 371 in MV-4-11 cells (supplemental Figure 8E).

346

347 To further examine the enzyme-substrate interaction between PRL2 and CBL at the molecular level, we
348 utilized APEX2 proximity labeling, which is a widely used method for rapid covalent labeling of
349 neighboring proteins within a 10–20 nm radius of a protein of interest in living cells.⁴²⁻⁴⁴ To that end,
350 APEX2-PRL2 fusion protein was used to perform proximity labeling to identify its interacting proteins.
351 To our satisfaction, we identified CBL as a PRL2 neighboring protein, but not the nonphosphorylatable
352 CBL^{Y371F} mutant, in live cells (Figure 7J). Consistently, the PRL2-CSDA substrate trapping mutant shows
353 enhanced association with CBL compared to the CBL^{Y371F} mutant in both HeLa and 293 cells (Figure 7K-
354 L). Notably, CBL expression is correlated with PRL2 expression in human leukemia patients
355 (supplemental Figure 8F). Collectively, the data presented above demonstrate that CBL is a substrate of
356 PRL2 and that PRL2 associates with and dephosphorylates CBL at tyrosine 371 in leukemia cells. It
357 follows that dephosphorylation of CBL at tyrosine 371 by PRL2 blocks CBL-mediated FLT3
358 ubiquitination and degradation, leading to heightened FLT3 signaling in leukemia cells.

359 **Discussion**

360 Members of the PTP family dephosphorylate target proteins and counter the activities of protein tyrosine
361 kinases to control the strength and duration of tyrosine phosphorylation mediated cellular signaling.^{45, 46}
362 FLT3 is a major oncogenic receptor tyrosine kinase aberrantly activated in leukemia.^{6, 7} PRL2 is known
363 to be overexpressed in some subtypes of AML.²⁷ In the present study, we demonstrate that PRL2 enhances
364 oncogenic FLT3 signaling and promotes leukemia cell proliferation and survival. We further establish
365 that PRL2 dephosphorylates CBL at tyrosine 371 and inhibits its E3 ligase activity toward FLT3, leading
366 to decreased ubiquitination and degradation of FLT3, thereby activating its downstream signaling
367 pathways in leukemia cells. Finally, we also show that genetic and pharmacological inhibition of PRL2

368 significantly reduce the burden of FLT3-ITD-driven leukemia and extend the survival of leukemic mice.
369 Together, our work validates PRL2 as a novel druggable target for AML.

370

371 We previously found that loss of PRL2 does not change HSC number in the BM but decreases adult
372 HSPC proliferation.²⁸ We now show that receptor tyrosine kinase, PI3K/AKT, and ERK signaling gene
373 signatures are significantly downregulated in *Prl2* null fetal liver HSPCs. In addition, loss of *Prl2*
374 significantly decreased AKT, STAT5 and ERK phosphorylation in fetal liver cells. Given that fetal liver
375 HSPCs are characterized by a massive expansion of HSCs whereas BM HSCs are much more quiescent,
376 PRL2 effect could be associated with cell proliferation instead of "stem" ability in fetal livers.

377

378 Members of the CBL family E3 ubiquitin ligases share a highly conserved N-terminal tyrosine kinase-
379 binding (TKB) domain, a short linker helical region (LHR), and a RING finger (RF) domain.¹⁵ The LHR
380 and RF domains dictate the E3 activity of CBL family members by serving as a structural platform for
381 optimal binding of a ubiquitin-conjugating enzyme E2.¹⁵ CBL's ubiquitination activity is stimulated
382 by phosphorylation of a Tyr residue in a linker helix region (LHR).³⁹⁻⁴¹ Structural and biochemical studies
383 show that phosphorylation of Tyr 371 activates CBL by inducing LHR conformational changes that
384 eliminate autoinhibition and enable direct participation of LHR phosphotyrosine in the activation of
385 E2~ubiquitin complex for catalysis.^{41,47} This activation is required for receptor tyrosine kinase
386 ubiquitination. We found that PRL2 associates with and dephosphorylates CBL in human leukemia cells
387 and that inhibition of PRL2 activity increases CBL Tyr 371 phosphorylation in human leukemia cells.
388 Our results suggest that CBL/pTyr371 is a novel PRL2 substrate in leukemia cells.

389

390 Most *CBL* mutations in myeloid malignancies are found in the RING finger domain and the linker region
391 of *CBL*.¹⁹⁻²¹ Some *CBL* mutants such as *CBL*^{Y371H} and *CBL*-70Z do not have E3 ubiquitin ligase activity
392 but compete against wild-type *CBL* and *CBL*-B, leading to prolonged activation of receptor tyrosine
393 kinases after cytokine stimulation.^{39, 40} Inactivating *CBL* mutations-mediated hematopoietic
394 transformation in AML depends on FLT3 signaling.⁴⁸ Indeed, loss of *CBL* E3 ubiquitin ligase activity
395 enhances the development of myeloid leukemia in FLT3-ITD mutant mice.⁴⁹ Further, myeloid leukemia
396 development in *CBL* RING finger mutant mice is dependent on FLT3 signaling.⁵⁰ Our finding that PRL2
397 dephosphorylates *CBL* at Tyr 371 thereby compromising *CBL*'s ability to ubiquitinate FLT3 is consistent
398 with a tumor suppressor role for *CBL* in hematological malignancies. We previously showed that PRL2
399 is important for SCF/KIT signaling in HSPCs.²⁸ Thus, decreased AKT, ERK and STAT5 phosphorylation
400 seen in *Prl2* null fetal HSPCs could be due to diminished FLT3 and KIT signaling. Given that *CBL* is the
401 E3 ligase for both FLT3 and KIT,¹⁵ it is possible that PRL2 could also promote KIT signaling in HSPCs
402 through dephosphorylation of *CBL* at tyrosine 371.

403

404 Despite substantial efforts devoted to the development of FLT3 inhibitors, the effectiveness of these
405 agents in AML has been limited.^{6-8, 51} Even though FLT3 inhibitors show relative success at prolonging
406 survival rates compared to the standards therapies, the short duration of response and therapeutic
407 resistance are still a clinical challenge in AML treatment.^{42, 51, 52} The strategies to overcome resistance
408 mutations and provide durable remissions, such as a combination of inhibitors or use of more potent FLT3
409 inhibitors, have been evaluated.⁹ Here we show that PRL2 functions upstream of FLT3 and promotes
410 oncogenic FLT3 signaling in leukemia cells by inhibiting *CBL* mediated FLT3 ubiquitination and
411 degradation. We further demonstrate that PRL2 deletion or inhibition decrease leukemia burden and
412 extends the survival of mice transplanted with human leukemia cells. Consequently, PRL2 inhibitors may
413 offer an alternative strategy for AML treatment. To therapeutically target the PRL family members in
414 cancer, we sought to exploit a unique regulatory property of the PRLs, namely their propensity for trimer

415 formation, which is required for PRL-mediated cell growth and migration.^{31, 36, 37, 53} Using structure-based
416 virtual screening we identified compound 43 (PRLi), which disrupts PRL trimerization and blocks PRL
417 induced cell proliferation and migration.³¹ PRLi displays a respectable pharmacokinetic profile and
418 exhibits not obvious toxicity to major tissues and organs in mice.³¹ Notably, PRLi did not affect the
419 viability of human cord blood mononuclear cells and CD34⁺ cells.²⁷ PRLi treatment significantly reduced
420 tumor volume in NSG mice transplanted with human melanoma cells.³¹ Furthermore, we found that both
421 human AML and acute lymphoblastic leukemia (ALL) cells are sensitive to PRLi treatment *in vitro*.^{27,30}
422 We now showed that *in vivo* PRLi treatment significantly reduces leukemia burden and extends the
423 survival of NSG mice transplanted with primary human leukemia cells with FLT3-ITD mutations. Our ex
424 vivo studies showed that FLT3 WT and FLT3 mutated primary AML samples are equally sensitive to
425 PRL2 inhibition, suggesting that there is an underlying mechanism that is different among AML samples
426 based on their mutations. PRL2 is highly expressed in some subtypes of AML²⁷ and AML patients with
427 high *PRL2* expression have reduced overall survival compared to AML patients with low *PRL2*
428 expression. It is possible that PRL2 utilizes distinct mechanisms to promote cell proliferation and enhance
429 oncogenic signaling in different cellular context. We thus demonstrate that PRL2 is a novel druggable
430 target in human AML.

431

432 **Acknowledgements**

433 Y. L. was supported by NIH R01 HL150624, R56 DK119524, R56 AG052501, DoD W81XWH-18-1-
434 0265, DoD W81XWH-19-1-0575, the Leukemia & Lymphoma Society Translational Research Program
435 award 6581-20 and the St. Baldrick's Foundation Scholar Award. Y.B. and Z.Y.Z. were supported by
436 NIH R01 CA069202 and the Robert C. and Charlotte Anderson Chair Endowment. S. B. was supported
437 by a NIH F31 Award F31HL160120. H.C. was supported by Natural Science Foundation of Chongqing
438 cstc2020jcyj-msxmX0969.

439

440 The authors would like to acknowledge the Flow Cytometry Core and In vivo Therapeutic Core
441 Laboratories at the Indiana University, which were sponsored, in part, by the NIDDK Cooperative Center
442 of Excellence in Hematology (CCEH) grant U54 DK106846.

443

444 **Authorship**

445 H.C., Y.B., M.K., Z.Y.Z., and Y.L. were responsible for the conception and/or design of the research.

446 H.C., Y.B., M.K., S.X., W.C., S.B., S.C., J.M., F.N.M., S.V., J. P. R., J.W., Y.J., H.L., P.J., Z.Y.Z, and

447 Y.L. were involved in acquisition, analysis or interpretation of data. J.M.C., H.S.B., L.S.L., J.K.A.,

448 E.A.E., W.T., H.B., D.T.H., and L.C.P. provided reagents and constructive advice to the study. H.C., Y.B.,

449 Z.Y.Z., and Y.L. wrote the manuscript. All authors read, comment on, and approved the manuscript.

450 **Declaration of Interests**

451 The authors declared no competing interests.

452

453 **References**

- 454 1. Roboz GJ. Treatment of acute myeloid leukemia in older patients. *Expert Review of Anticancer*
455 *Therapy*. 2007;7(3):285-295.
- 456 2. Roboz GJ. Current treatment of acute myeloid leukemia. *Current Opinion in Oncology*.
457 2012;24(6)
- 458 3. Burnett A, Wetzler M, Löwenberg B. Therapeutic Advances in Acute Myeloid Leukemia. *Journal*
459 *of Clinical Oncology*. 2011;29(5):487-494.
- 460 4. Toffalini F, Demoulin J-B. New insights into the mechanisms of hematopoietic cell transformation
461 by activated receptor tyrosine kinases. *Blood*. 2010;116(14):2429-2437.
- 462 5. Stirewalt DL, Meshinchi S. Receptor Tyrosine Kinase Alterations in AML – Biology and Therapy.
463 In: Nagarajan L, ed. *Acute Myelogenous Leukemia: Genetics, Biology and Therapy*. Springer New York;
464 2010:85-108.
- 465 6. Kindler T, Lipka DB, Fischer T. FLT3 as a therapeutic target in AML: still challenging after all
466 these years. *Blood*. 2010;116(24):5089-5102.
- 467 7. Swords R, Freeman C, Giles F. Targeting the FMS-like tyrosine kinase 3 in acute myeloid
468 leukemia. *Leukemia*. 2012;26(10):2176-2185.
- 469 8. Metzelder S, Wang Y, Wollmer E, et al. Compassionate use of sorafenib in FLT3-ITD–positive
470 acute myeloid leukemia: sustained regression before and after allogeneic stem cell transplantation. *Blood*.
471 2009;113(26):6567-6571.
- 472 9. Alfayez M, Kantarjian HM, Ravandi F, et al. Outcomes with Subsequent FLT3-Inhibitor (FLT3i)
473 Based Therapies in FLT3-Mutated (mu) Patients (pts) Refractory/Relapsed (R/R) to One or More Prior
474 FLT3 Inhibitor Based Therapies: A Single Center Experience. *Blood*. 2018;132:663.
- 475 10. Hope KJ, Jin L, Dick JE. Acute myeloid leukemia originates from a hierarchy of leukemic stem
476 cell classes that differ in self-renewal capacity. *Nature Immunology*. 2004;5:738-743.
- 477 11. Guzman ML, Jordan CT. Considerations for Targeting Malignant Stem Cells in Leukemia. *Cancer*
478 *Control*. 2004;11(2):97-104.

- 479 12. Kreso A, Dick JE. Evolution of the cancer stem cell model. *Cell Stem Cell*. 2014; 14: 275–91.
- 480 13. Gerber JM, Smith BD, Ngwang B, et al. A clinically relevant population of leukemic
481 CD34(+)CD38(-) cells in acute myeloid leukemia. *Blood*. 2012; 119: 3571–7.
- 482 14. Garz AK, Wolf S, Grath S, et al. Azacitidine combined with the selective FLT3 kinase inhibitor
483 crenolanib disrupts stromal protection and inhibits expansion of residual leukemia-initiating cells
484 in *FLT3*-ITD AML with concurrent epigenetic mutations. *Oncotarget*. 2017;8(65):108738-108759.
- 485 15. Thien CBF, Langdon WY. Cbl: many adaptations to regulate protein tyrosine kinases. *Nature*
486 *Reviews Molecular Cell Biology*. 2001;2(4):294-307.
- 487 16. Naramura M, Nandwani N, Gu H, Band V, Band H. Rapidly fatal myeloproliferative disorders in
488 mice with deletion of Casitas B-cell lymphoma (Cbl) and Cbl-b in hematopoietic stem cells. *Proceedings*
489 *of the National Academy of Sciences*. 2010;107(37):16274-16279.
- 490 17. An W, Nadeau SA, Mohapatra BC, et al. Loss of Cbl and Cbl-b ubiquitin ligases abrogates
491 hematopoietic stem cell quiescence and sensitizes leukemic disease to chemotherapy. *Oncotarget*.
492 2015;6(12):10498-10509.
- 493 18. An W, Mohapatra BC, Zutshi N, et al. VAV1-Cre mediated hematopoietic deletion of CBL and
494 CBL-B leads to JMML-like aggressive early-neonatal myeloproliferative disease. *Oncotarget*. 2016/09//
495 2016;7(37):59006-59016.
- 496 19. Makishima H, Cazzolli H, Szpurka H, et al. Mutations of e3 ubiquitin ligase cbl family members
497 constitute a novel common pathogenic lesion in myeloid malignancies. *J Clin Oncol*. 2009;27(36):6109-
498 6116.
- 499 20. Sanada M, Suzuki T, Shih L-Y, et al. Gain-of-function of mutated C-CBL tumour suppressor in
500 myeloid neoplasms. *Nature*. 2009/08/01 2009;460(7257):904-908.
- 501 21. Niemeyer CM, Kang MW, Shin DH, et al. Germline CBL mutations cause developmental
502 abnormalities and predispose to juvenile myelomonocytic leukemia. *Nat Genet*. 2010;42(9):794-800.

- 503 22. Nadeau SA, An W, Mohapatra BC, et al. Structural Determinants of the Gain-of-Function
504 Phenotype of Human Leukemia-associated Mutant CBL Oncogene. *J Biol Chem.* 2017;292(9):3666-
505 3682.
- 506 23. Bessette DC, Qiu D, Pallen CJ. PRL PTPs: mediators and markers of cancer progression. *Cancer*
507 *and Metastasis Reviews.* 2008;27(2):231-252.
- 508 24. Ríos P, Li X, Köhn M. Molecular mechanisms of the PRL phosphatases. *The FEBS Journal.*
509 2013;280
- 510 25. Campbell AM, Zhang Z-Y. Phosphatase of regenerating liver: a novel target for cancer therapy.
511 *Expert Opin Ther Targets.* 2014;18(5):555-569.
- 512 26. Kobayashi M, Chen S, Gao R, Bai Y, Zhang Z-Y, Liu Y. Phosphatase of regenerating liver in
513 hematopoietic stem cells and hematological malignancies. *Cell Cycle.* 2014;13(18):2827-2835.
- 514 27. Kobayashi M, Chen S, Bai Y, et al. Phosphatase PRL2 promotes AML1-ETO-induced acute
515 myeloid leukemia. *Leukemia.* 2017;31(6):1453-1457.
- 516 28. Kobayashi M, Bai Y, Dong Y, et al. PRL2/PTP4A2 phosphatase is important for hematopoietic
517 stem cell self-renewal. *Stem Cells.* 2014;32(7):1956-1967.
- 518 29. Kobayashi M, Nabinger SC, Bai Y, et al. Protein Tyrosine Phosphatase PRL2 Mediates Notch and
519 Kit Signals in Early T Cell Progenitors. *Stem Cells.* 2017;35(4):1053-1064.
- 520 30. Kobayashi M, Bai Y, Chen S, et al. Phosphatase PRL2 promotes oncogenic NOTCH1-Induced T-
521 cell leukemia. *Leukemia.* 2017;31(3):751-754.
- 522 31. Bai Y, Yu Z-H, Liu S, et al. Novel Anticancer Agents Based on Targeting the Trimer Interface of
523 the PRL Phosphatase. *Cancer Res.* 2016;76(16):4805-4815.
- 524 32. Lee BH, Tothova Z, Levine RL, et al. FLT3 mutations confer enhanced proliferation and survival
525 properties to multipotent progenitors in a murine model of chronic myelomonocytic leukemia. *Cancer*
526 *Cell.* 2007;12(4):367-380.

- 527 33. Dong Y, Zhang L, Zhang S, et al. Phosphatase of regenerating liver 2 (PRL2) is essential for
528 placental development by down-regulating PTEN (Phosphatase and Tensin Homologue Deleted on
529 Chromosome 10) and activating Akt protein. *J Biol Chem*. 2012;287(38):32172-32179.
- 530 34. Li Q, Bai Y, Lyle LT, et al. Mechanism of PRL2 phosphatase-mediated PTEN degradation and
531 tumorigenesis. *Proceedings of the National Academy of Sciences*. 2020;117(34):20538-20548.
- 532 35. Borkin D, He S, Miao H, et al. Pharmacologic inhibition of the Menin-MLL interaction blocks
533 progression of MLL leukemia in vivo. *Cancer Cell*. 2015;27(4):589-602.
- 534 36. Sun J-P, Wang W-Q, Yang H, et al. Structure and Biochemical Properties of PRL-1, a Phosphatase
535 Implicated in Cell Growth, Differentiation, and Tumor Invasion. *Biochemistry*. 2005;44(36):12009-
536 12021.
- 537 37. Sun J-P, Luo Y, Yu X, et al. Phosphatase Activity, Trimerization, and the C-terminal Polybasic
538 Region Are All Required for PRL1-mediated Cell Growth and Migration*. *Journal of Biological*
539 *Chemistry*. 2007;282(39):29043-29051.
- 540 38. Mercan F, Bennett AM. Analysis of protein tyrosine phosphatases and substrates. *Curr Protoc*
541 *Mol Biol*. 2010;Chapter 18:Unit-18.16.
- 542 39. Dou H, Buetow L, Hock A, Sibbet GJ, Vousden KH, Huang DT. Structural basis for autoinhibition
543 and phosphorylation-dependent activation of c-Cbl. *Nat Struct Mol Biol*. 2012;19(2):184-192.
- 544 40. Mohapatra B, Ahmad G, Nadeau S, et al. Protein tyrosine kinase regulation by ubiquitination:
545 Critical roles of Cbl-family ubiquitin ligases. *Biochimica et Biophysica Acta (BBA) - Molecular Cell*
546 *Research*. 2013;1833(1):122-139.
- 547 41. Ahmed SF, Buetow L, Gabrielsen M, et al. E3 ligase-inactivation rewires CBL interactome to
548 elicit oncogenesis by hijacking RTK–CBL–CIN85 axis. *Oncogene*. 2021;40(12):2149-2164.
- 549 42. Lam SS, Martell JD, Kamer KJ, et al. Directed evolution of APEX2 for electron microscopy and
550 proximity labeling. *Nat Methods*. 2015;12(1):51-54.
- 551 43. Lee S-Y, Kang M-G, Park J-S, Lee G, Ting Alice Y, Rhee H-W. APEX Fingerprinting Reveals
552 the Subcellular Localization of Proteins of Interest. *Cell Reports*. 2016;15(8):1837-1847.

- 553 44. Tan B, Peng S, Yatim SMJM, Gunaratne J, Hunziker W, Ludwig A. An Optimized Protocol for
554 Proximity Biotinylation in Confluent Epithelial Cell Cultures Using the Peroxidase APEX2. *STAR*
555 *Protocols*. 2020;1(2):100074.
- 556 45. Tonks NK. Protein tyrosine phosphatases: from genes, to function, to disease. *Nature Reviews*
557 *Molecular Cell Biology*. 2006;7(11):833-846.
- 558 46. Julien SG, Dubé N, Hardy S, Tremblay ML. Inside the human cancer tyrosine phosphatome.
559 *Nature Reviews Cancer*. 2011;11(1):35-49.
- 560 47. Dou H, Buetow L, Sibbet GJ, Cameron K, Huang DT. Essentiality of a non-RING element in
561 priming donor ubiquitin for catalysis by a monomeric E3. *Nat Struct Mol Biol*. 2013;20(8):982-986.
- 562 48. Sargin B, Choudhary C, Crosetto N, et al. Flt3-dependent transformation by inactivating c-Cbl
563 mutations in AML. *Blood*. 2007;110(3):1004-1012.
- 564 49. Taylor SJ, Thien CBF, Dagger SA, et al. Loss of c-Cbl E3 ubiquitin ligase activity enhances the
565 development of myeloid leukemia in FLT3-ITD mutant mice. *Experimental Hematology*.
566 2015;43(3):191-206.e1.
- 567 50. Rathinam C, Thien CBF, Flavell RA, Langdon WY. Myeloid Leukemia Development in c-Cbl
568 RING Finger Mutant Mice Is Dependent on FLT3 Signaling. *Cancer Cell*. 2010/10/19/ 2010;18(4):341-
569 352.
- 570 51. Kennedy VE, Smith CC. FLT3 Mutations in Acute Myeloid Leukemia: Key Concepts and
571 Emerging Controversies. *Front Oncol*. 2020;10:612880-612880.
- 572 52. Lam SSY, Leung AYH. Overcoming Resistance to FLT3 Inhibitors in the Treatment of FLT3-
573 Mutated AML. *Int J Mol Sci*. 2020;21(4):1537.
- 574 53. Bai Y, Luo Y, Liu S, et al. PRL-1 protein promotes ERK1/2 and RhoA protein activation through
575 a non-canonical interaction with the Src homology 3 domain of p115 Rho GTPase-activating protein. *J*
576 *Biol Chem*. 2011;286(49):42316-42324.

577

578

579 **Figure Legends**

580

581 **Figure 1. FLT3 mutated AML patients with high *PRL2* expression have reduced overall survival**

582 (A) Relative *PRL2* (*PTP4A2*) mRNA expression in AML patients with favorable or intermediated & poor
583 cytogenetic risk.

584 (B) Relative *PRL2* (*PTP4A2*) mRNA expression in live or dead AML patients.

585 (C) Relative *PRL2* (*PTP4A2*) mRNA expression in AML patients with or without cytogenetic relapse.

586 (D) Overall survival of poor cytogenetic risk AML patients with high (n=17) or low (n=14) *PRL2*
587 expression.

588 (E) DEGs between the *PRL2* high expression group and *PRL2* low expression group in AML. Genes with
589 $P < 0.05$ and $\text{Log}_2\text{FC} > 1$ is indicated in red and blue colors in the volcano plot. Red indicates genes
590 upregulated in the *PRL2* high expression group, whereas blue indicates genes downregulated in the
591 *PRL2* high expression group. The X-axis is the \log_2 -transformed fold change, and the Y-axis is the
592 \log_{10} -transformed P-value.

593 (F) Gene Set Enrichment Analysis (GSEA) of gene transcription between the *PRL2* high expression group
594 and *PRL2* low expression group in AML. Acute myeloid leukemia (AML), AML prognosis, leukemia
595 stem cell, and hematopoietic stem cell gene signatures were enriched in the *PRL2* high expression
596 group compared to the *PRL2* low expression group.

597 (G) GSEA showed that *FLT3*-mutated APL, *FLT3* signaling, and cytokine-cytokine receptor interaction
598 gene signatures are significantly enriched in the *PRL2* high expression group.

599 (H) GSEA showed that *STAT5A* targets, *PI3K/AKT* signaling pathway, and *ERK1/ERK2/MAPK*
600 pathway gene signatures are significantly enriched in the *PRL2* high expression group.

601 (I) Relative *PRL2* (*PTP4A2*) mRNA expression in AML patients with or without *FLT3* mutation.

602 (J) Overall survival of *FLT3* mutation positive AML patients with high (n=20) or low (n=19) *PRL2*
603 expression.

604

605 **Figure 2. Prl2 deficiency alters gene transcription in murine hematopoietic stem and progenitor**
606 **cells**

607 (A) Heat map of Prl2-regulated genes that are upregulated (red) or downregulated (blue) ($\text{Log}_2\text{FC} < -1$,
608 $\text{FDR} < 0.05$, $p < 0.05$) in *Prl2* null E14.5 (Embryonic day 14.5) fetal liver cells compared to WT fetal
609 liver cells.

610 (B) GSEA analysis of gene transcription between WT and *Prl2* null E14.5 fetal liver cells. Hematopoiesis
611 stem cell, receptor tyrosine kinases, PI3KAKT signaling pathway, and MAPK pathway gene
612 signatures were significantly downregulated in *Prl2* null E14.5 fetal liver cells.

613 (C) GSEA showed that receptor regulator activity, receptor complex, cell surface, and receptor protein
614 tyrosine kinase gene signatures were significantly downregulated in *Prl2* null E14.5 fetal liver cells.

615 (D) GSEA showed that regulation of receptor signaling pathway, positive regulation of ERK1 and ERK2
616 cascade, and positive regulation of MAPK cascade gene signatures were significantly downregulated
617 in *Prl2* null E14.5 fetal liver cells.

618 (E) STRING protein-protein interaction network between downregulated genes ($\text{Log}_2\text{FC} > 1$, $\text{FDR} < 0.5$,
619 $p < 0.05$) related to FLT3 signaling in *Prl2* null E14.5 fetal liver cells.

620 (F) Quantitative RT-PCR analysis of gene expression in WT and *Prl2* null E14.5 fetal liver cells (n=4).

621 (G) Quantitative RT-PCR analysis of gene expression in WT and *Prl2* null bone marrow Lin^- cells (n=4).

622 (H) Immunoblot analysis of AKT, STAT5, and ERK phosphorylation in WT and *Prl2* null E14.5 fetal
623 liver cells (n=3).

624 (I) Immunoblot analysis of AKT, STAT5, and ERK phosphorylation in WT and *Prl2* null bone marrow
625 Lin^- cells (n=3).

626 Mean values (\pm SEM) are shown (* $p < 0.05$, ** $p < 0.01$, and *** $p < 0.001$).

627

628 **Figure 3. Loss of Prl2 decreases the self-renewal capability of FLT3-ITD positive hematopoietic**
629 **stem and progenitor cells.**

630 (A–D) The frequency of LT-HSCs (Lin⁻Sca1⁺cKit⁺CD150⁺CD48⁻), ST-HSCs (Lin⁻Sca1⁺cKit⁺CD150⁻
631 CD48⁻), MPPs (Lin⁻Sca1⁺cKit⁺CD150⁻CD48⁺), and LSKs (Lin⁻Sca1⁺cKit⁺) in the bone marrow (BM) of
632 *Prl2*^{+/+}, *Prl2*^{-/-}, *Flt3*^{+/*ITD*}, *Flt3*^{+/*ITD*}*Prl2*^{-/-}, *Flt3*^{*ITD/ITD*} and *Flt3*^{*ITD/ITD*}*Prl2*^{-/-} mice (n=6 mice per group).
633 (E) Serial replating assays of *Prl2*^{+/+}, *Prl2*^{-/-}, *Flt3*^{+/*ITD*}, *Flt3*^{+/*ITD*}*Prl2*^{-/-}, *Flt3*^{*ITD/ITD*} and *Flt3*^{*ITD/ITD*}*Prl2*^{-/-} BM
634 cells (n=3 independent experiments performed in triplicate).
635 (F) The percentage of donor-derived cells (CD45.2⁺) in the peripheral blood (PB) of primary recipient
636 mice (n = 9-10 mice per group).
637 (G–J) The frequency of LT-HSCs, ST-HSCs, MPPs and LSKs in the BM of primary recipient mice (n=6
638 mice per group).
639 (K) The percentage of donor-derived cells in PB of secondary recipient mice (n = 9-10 mice per group).
640 (L–O) The frequency of LT-HSCs, ST-HSCs, MPPs, and LSKs in the BM of secondary recipient mice
641 (n=6 mice per group).
642 Mean values (±SEM) are shown (*p<0.05, **p<0.01, ***p < 0.001, ****p < 0.0001).

643 **Figure 4. *Prl2* is important for FLT3-ITD-induced myeloid proliferative neoplasm in mice.**

644 (A) Loss of *Prl2* reduced splenomegaly seen in *Flt3*^{+/*ITD*} and *Flt3*^{*ITD/ITD*} mice.
645 (B) The spleen weights of *Prl2*^{+/+}, *Prl2*^{-/-}, *Flt3*^{+/*ITD*}, *Flt3*^{+/*ITD*}*Prl2*^{-/-}, *Flt3*^{*ITD/ITD*} and *Flt3*^{*ITD/ITD*}*Prl2*^{-/-} mice
646 (n=6 mice per group).
647 (C) The frequency of LSKs in the spleen of *Prl2*^{+/+}, *Prl2*^{-/-}, *Flt3*^{+/*ITD*}, *Flt3*^{+/*ITD*}*Prl2*^{-/-}, *Flt3*^{*ITD/ITD*} and
648 *Flt3*^{*ITD/ITD*}*Prl2*^{-/-} mice (n=6 mice per group).
649 (D) Kaplan-Meier survival curve of lethally irradiated recipient mice transplanted with 3x10⁶ *Prl2*^{+/+},
650 *Prl2*^{-/-}, *Flt3*^{+/*ITD*}, *Flt3*^{+/*ITD*}*Prl2*^{-/-}, *Flt3*^{*ITD/ITD*} and *Flt3*^{*ITD/ITD*}*Prl2*^{-/-} BM cells (n=9-10 mice per group).
651 (E–F) Red blood cell (RBC) and hemoglobin (HGB) counts in PB of recipient mice transplanted with
652 *Prl2*^{+/+}, *Prl2*^{-/-}, *Flt3*^{+/*ITD*}, *Flt3*^{+/*ITD*}*Prl2*^{-/-}, *Flt3*^{*ITD/ITD*} and *Flt3*^{*ITD/ITD*}*Prl2*^{-/-} BM cells (n=9-10 mice per
653 group).

- 654 (G) Representative flow cytometric analysis of myeloid cells (Gr1⁺Mac1⁺) and lymphocytes in PB of
655 recipient mice repopulated with *Prl2*^{+/+}, *Prl2*^{-/-}, *Flt3*^{+/*ITD*}, *Flt3*^{+/*ITD*}*Prl2*^{-/-}, *Flt3*^{*ITD*/*ITD*} and
656 *Flt3*^{*ITD*/*ITD*}*Prl2*^{-/-} BM cells.
- 657 (H) The frequency of myeloid cells (Gr1⁺Mac1⁺), B cells (B220⁺) and T cells (CD3⁺) in PB of recipient
658 mice repopulated with *Prl2*^{+/+}, *Prl2*^{-/-}, *Flt3*^{+/*ITD*}, *Flt3*^{+/*ITD*}*Prl2*^{-/-}, *Flt3*^{*ITD*/*ITD*} and *Flt3*^{*ITD*/*ITD*}*Prl2*^{-/-} BM
659 cells (n=8 mice per group).
- 660 (I) Representative H&E (10 x) images of the peripheral blood smears, bone marrow, spleen, and liver of
661 recipient mice repopulated with *Flt3*^{*ITD*/*ITD*} or *Flt3*^{*ITD*/*ITD*}*Prl2*^{-/-} BM cells.
- 662 (J) The spleen weights of recipient mice repopulated with *Prl2*^{+/+}, *Prl2*^{-/-}, *Flt3*^{+/*ITD*}, *Flt3*^{+/*ITD*}*Prl2*^{-/-},
663 *Flt3*^{*ITD*/*ITD*} and *Flt3*^{*ITD*/*ITD*}*Prl2*^{-/-} BM cells (n=4 mice per group).
- 664 (K) Ectopic PRL2-CSDA expression decreased the proliferation of 32D cells expressing FLT3-ITD (n =
665 3).
- 666 (L) Expressing the PRL2-CSDA mutant, but not the WT PRL2, extended the survival of C3H/HeJ mice
667 transplanted with 32D cells expressing FLT3-ITD (n= 7 mice per group).
- 668 Mean values (±SEM) are shown (*p<0.05, **p<0.01, ***p < 0.001, ****p < 0.0001).

669 **Figure 5. Genetic and pharmacological inhibition of PRL2 decrease leukemia burden and extends**
670 **the survival of mice transplanted with human leukemia cell lines**

- 671 (A) Western blot analysis for PRL2 in MV-4-11 cells transduced with lentiviruses expressing a control
672 shRNA (shCtrl) or PRL2 shRNAs (shPRL2 and shPRL2#2).
- 673 (B) Knocking down of PRL2 significantly decreased the colony formation of MV-4-11 cells (n=3).
674 Representative images of the colonies are shown.
- 675 (C) Kaplan-Meier survival curve of sublethally irradiated NSG mice transplanted with 3x10⁶ MV-4-11
676 expressing shCtrl or shPRL2 (n=7 mice group).
- 677 (D) Flow cytometry quantification of GFP⁺ cells in PB, BM, and spleen of NSG mice transplanted with
678 MV-4-11 cells expressing control shRNA or shPRL2 (n=3 mice per group).

679 (E-F) The size and weight of spleen from NSG mice transplanted with MV-4-11 cells expressing control
680 shRNA or shPRL2 (n=3 mice per group).

681 (G) PRL inhibitor (PRLi) treatment significantly decreased the colony formation ability in MV-4-11
682 (n=3). Representative images of the colonies are displayed.

683 (H) 3×10^6 MV-4-11 cells expressing luciferase were injected into sublethally irradiated NSG mice. One
684 week after the transplantation, NSG mice were treated with DMSO or PRLi (25mg/kg, I.P.) daily for
685 three weeks. The leukemia burden in NSG mice were monitored by In Vivo Image System (IVIS)
686 once a week for three weeks (n=5 mice per group).

687 (I) Quantitative results from bioimaging (n=5 mice per group).

688 (J) Kaplan-Meier survival curve of NSG mice treated with DMSO or PRLi (n=7 mice per group).

689 (K) Flow cytometry analysis of human CD45⁺ cells in PB, BM, and spleen of NSG mice transplanted with
690 MV-4-11 cells after three weeks of DMSO or PRLi treatment (n=3 mice per group).

691 (L) PRLi treatment reduced splenomegaly seen in NSG mice transplanted with MV-4-11 cells.

692 (M) The spleen weights of NSG mice transplanted with MV-4-11 cells following three weeks of DMSO
693 or PRLi treatment (n=3 mice per group).

694 Mean values (\pm SEM) are shown (*p<0.05, **p<0.01, ***p < 0.001, ****p < 0.0001).

695 **Figure 6. Pharmacological inhibition of PRL2 reduces leukemia burden and extends the survival of**
696 **mice transplanted with primary human AML cells**

697

698 (A) PRLi treatment decreased the viability of primary human AML cells with FLT3-ITD mutation in a
699 dosage-dependent manner.

700 (B) PRLi treatment reduced the colony forming ability of primary human AML cells with or without
701 FLT3-ITD mutation. Samples 3153 and 3202 are from AML patients with WT FLT3, whereas samples
702 3142 and 3179 are from AML patients with FLT3-ITD.

703 (C) Cell cycle analysis of primary AML cells with FLT3-ITD mutation (AML3242) at 24 hours following
704 DMSO or PRLi (10 μ M) treatment.

705 (D) Apoptosis analysis of primary AML cells with FLT3-ITD (AML3242) at 24 hours following DMSO
706 or PRLi (10 μ M) treatment.

707 (E) Kaplan-Meier survival curve of NSG mice transplanted with 4×10^6 human CD45⁺ leukemia cells
708 (AML3179) following three weeks of DMSO or PRLi treatment (n=6 mice per group).

709 (F) Flow cytometry analysis of human CD45⁺ cells in PB, BM, and spleen of NSG mice transplanted with
710 4×10^6 human CD45⁺ leukemia cells (AML3179) after three weeks of DMSO or PRLi treatment (n=4
711 mice per group).

712 (G) Representative western blot analysis of AKT, STAT5 and ERK phosphorylation in *Prl2*^{+/+}, *Prl2*^{-/-},
713 *Flt3*^{+/*ITD*}, *Flt3*^{+/*ITD*}*Prl2*^{-/-}, *Flt3*^{*ITD*/*ITD*} and *Flt3*^{*ITD*/*ITD*}*Prl2*^{-/-} BM mononuclear cells.

714 (H) Representative western blot analysis of FLT3, AKT, STAT5 and ERK phosphorylation in MV-4-11
715 cells expressing shCtrl, shPRL2 or shPRL2#2 (Left) and following 24 hours of dimethyl sulfoxide
716 (DMSO) or 5 μ M PRLi treatment (Right).

717 (I) Representative western blot analysis of FLT3, AKT, STAT5, and ERK phosphorylation in primary
718 AML cells with FLT3-ITD mutation (AML3080 and AML3220) following 24 hours of DMSO or
719 PRLi (10 μ M) treatment.

720 (J) Representative western blot analysis of AKT, STAT5 and ERK phosphorylation in human CD45⁺ cells
721 isolated from the BM of NSG mice at 4 weeks after transplantation with MV-4-11 cells expressing
722 control shRNA or shPRL2 (Left panel, n=3 mice per group); human CD45⁺ cells in the BM of NSG
723 mice transplanted with MV-4-11 cells following three weeks of DMSO or PRLi treatment (Right
724 panel, n=3 mice per group).

725 (K) Representative western blot analysis of AKT, STAT5, and ERK phosphorylation in human CD45⁺
726 cells isolated from the BM of NSG mice transplanted with PDX cells (AML3179) following three
727 weeks of DMSO or PRLi treatment (n=3 mice per group).

728

729 **Figure 7. PRL2 associates with and dephosphorylates CBL at tyrosine 371 in leukemia cells**

730 (A) Genetic knock down PRL2 decreased FLT3 half-life in MV-4-11 cells.

731 (B) Genetic knock down PRL2 enhanced FLT3 ubiquitination in MV-4-11 cells.

732 (C) Total cellular proteins from MV-4-11 cells were isolated, incubated with GST, GST-PRL2 or GST-
733 PRL2-CSDA and immunoblotted with antibody against FLT3, CBL, SHP2, and PLC- γ .

734 (D) Co-immunoprecipitation assays showed that PRL2 interacts with FLT3 and CBL in MV-4-11 cells.

735 (E) Immunofluorescence analysis showed that PRL2 co-localizes with CBL in MV-4-11 cells.

736 (F) Representative western blot analysis showed that ectopic PRL2 expression decreases tyrosine
737 phosphorylation of CBL in 293 cells.

738 (G) Representative western blot analysis showed that knocking down of PRL2 increases the tyrosine
739 phosphorylation of CBL in MV-4-11 cells.

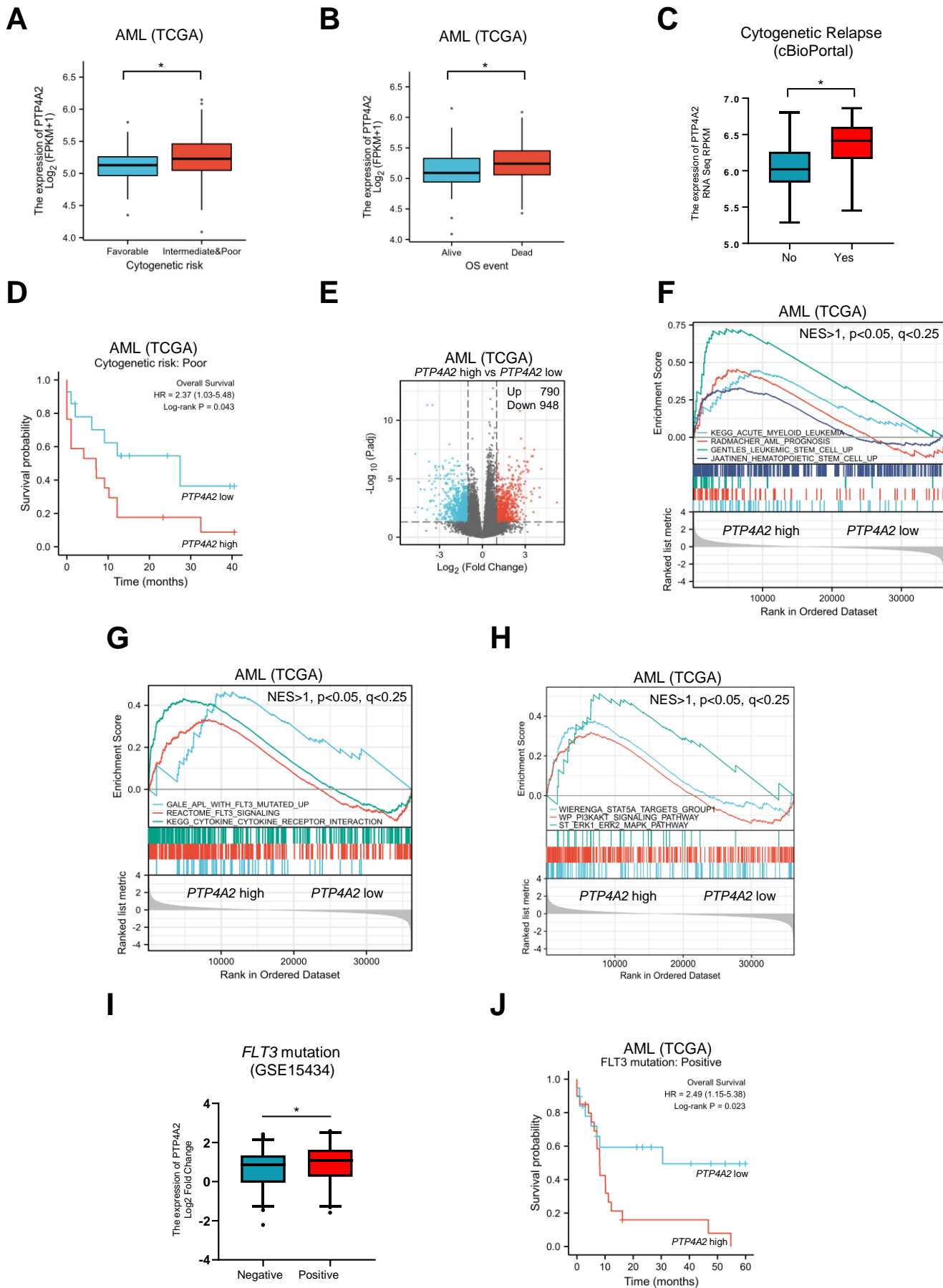
740 (H) Representative western blot analysis showed that knocking down of PRL2 increases CBL
741 phosphorylation at tyrosine 371 in MV-4-11 cells.

742 (I) Representative western blot analysis showed that ectopic expression of PRL2-CSDA increases CBL
743 phosphorylation at tyrosine 371 in MV-4-11 cells.

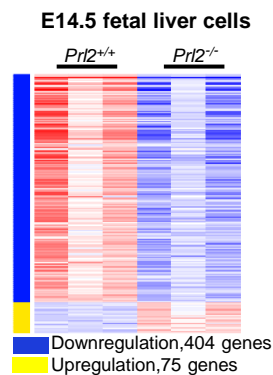
744 (J) APEX2-PRL2 proximity labeling was performed in HA-CBL or HA-Cbl^{Y371F} transiently expressed
745 293 cells stably expressing APEX2-PRL2. After labeling, biotinylated proteins are enriched with
746 neutravidin beads and examined with anti-HA and anti-PRL2 antibodies by Western blot analysis.

747 (K-L) PRL2-CSDA substrate trapping assays was performed in HA-CBL or HA- Cbl^{Y371F} transiently
748 expressed HeLa (J) or 293 (K) cells stably expressing Flag-PRL2-CSDA. After Anti-Flag pulldown,
749 bound proteins were boiled in 50 μ L Laemmli sample buffer and examined with anti-HA, anti-PRL2
750 antibodies by Western blot analysis.

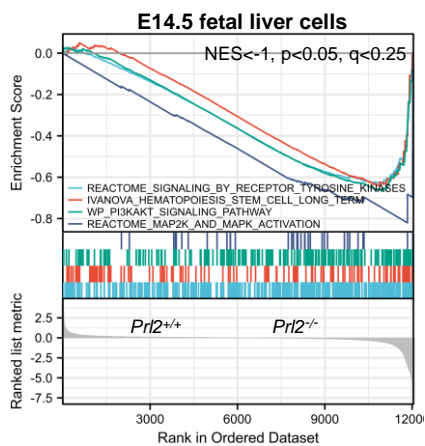
751



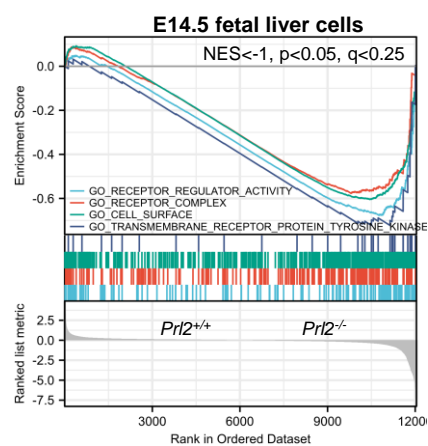
A



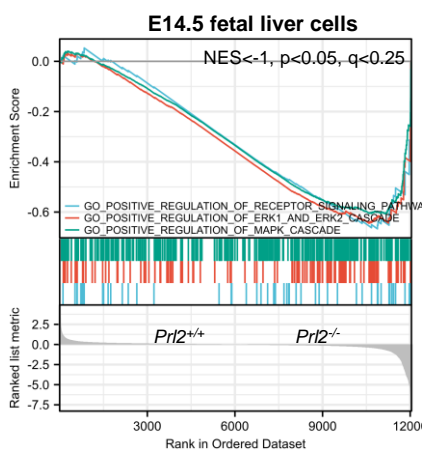
B



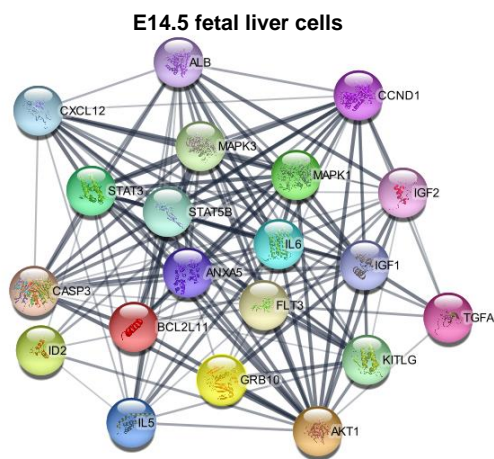
C



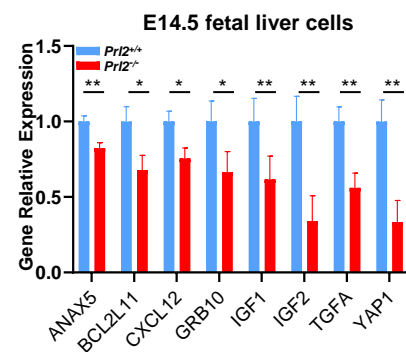
D



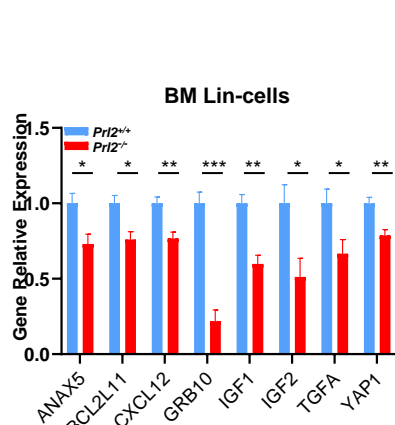
E



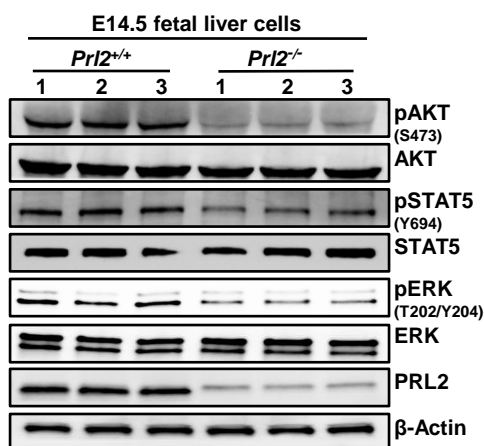
F



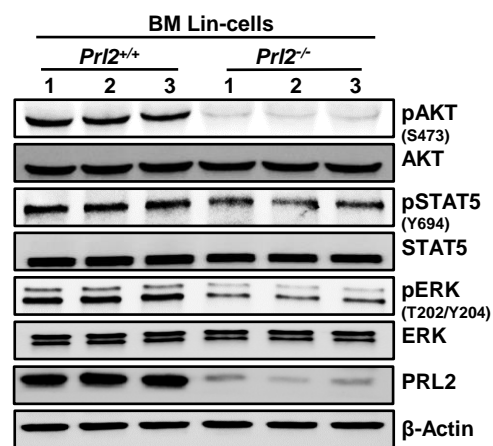
G

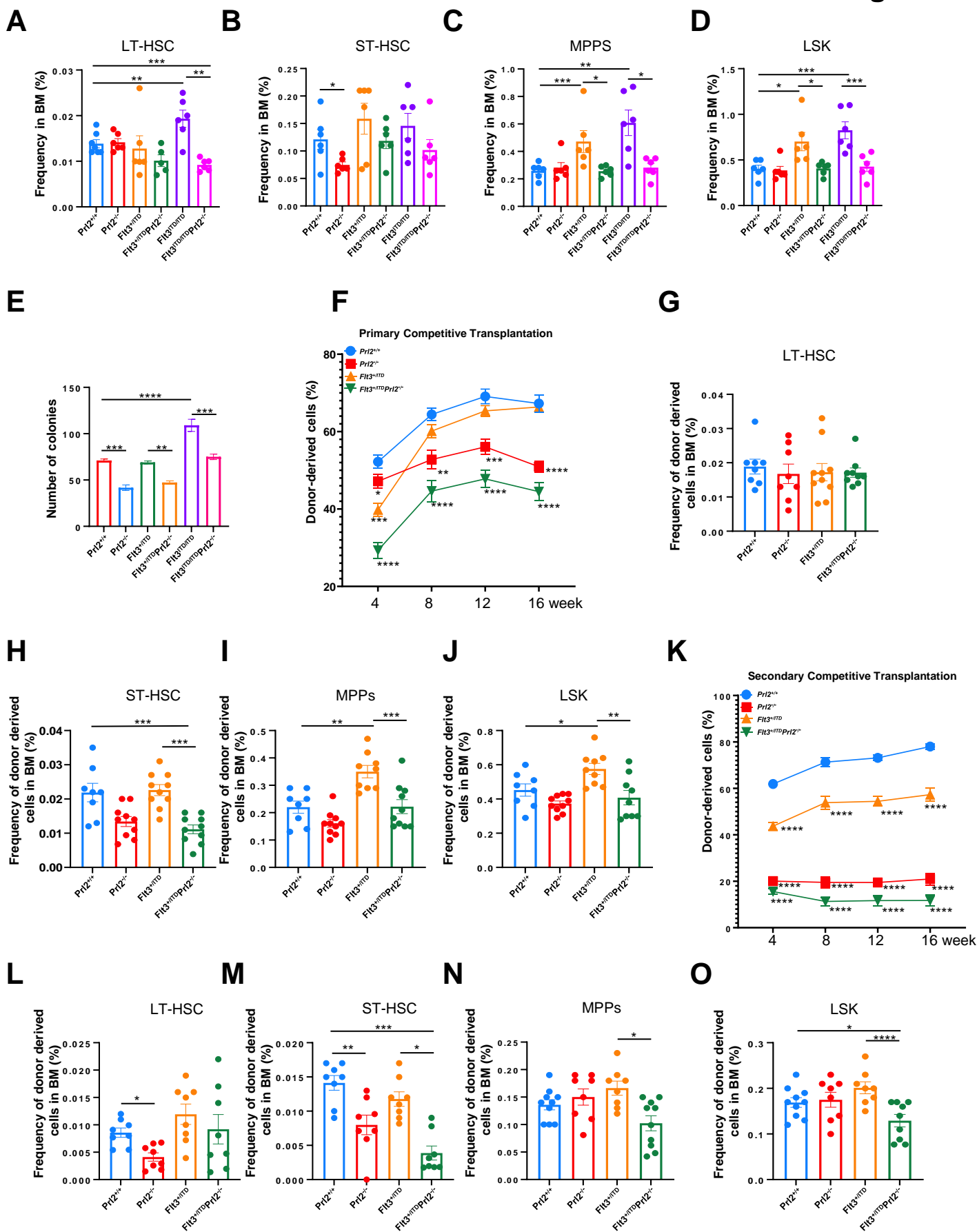


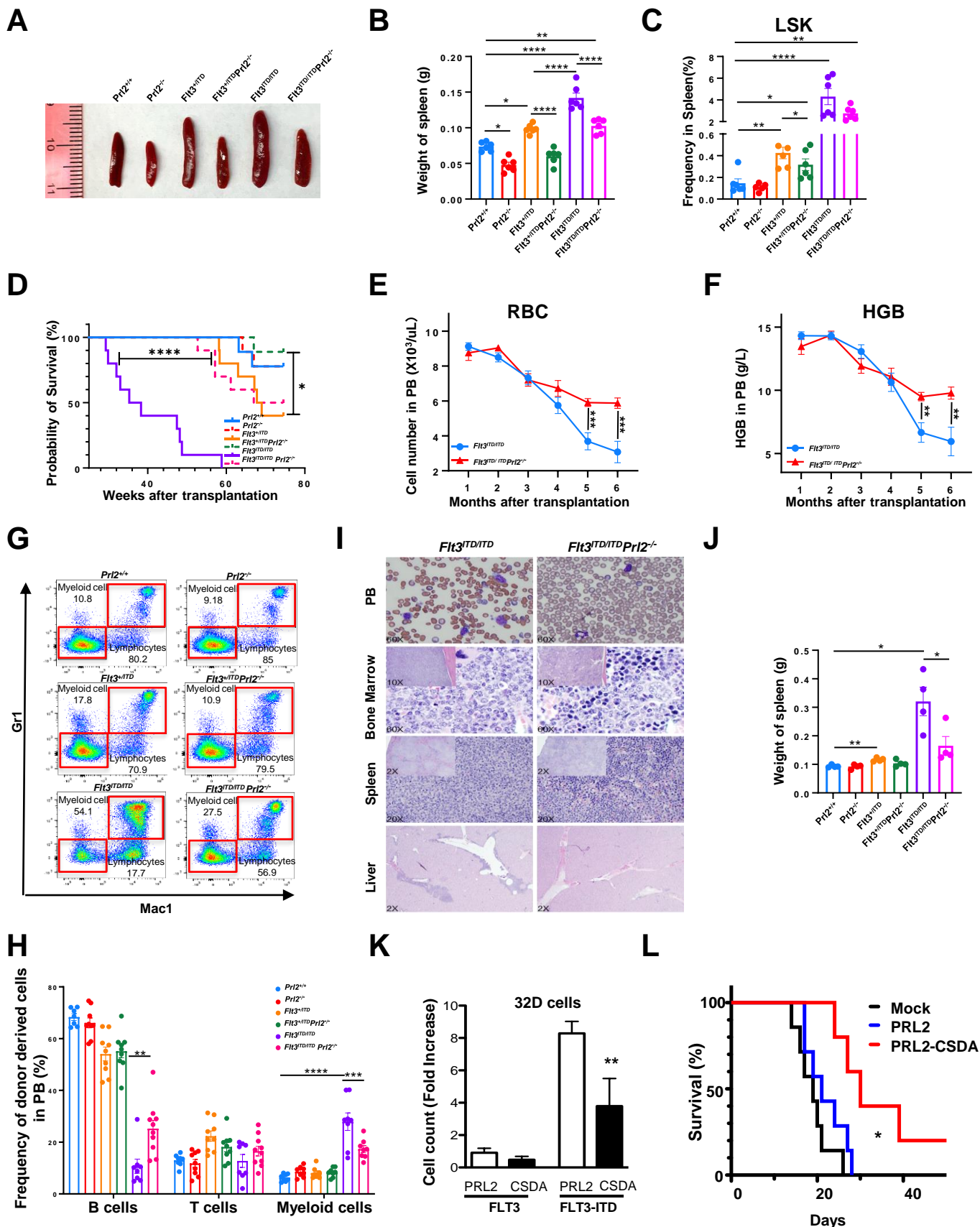
H

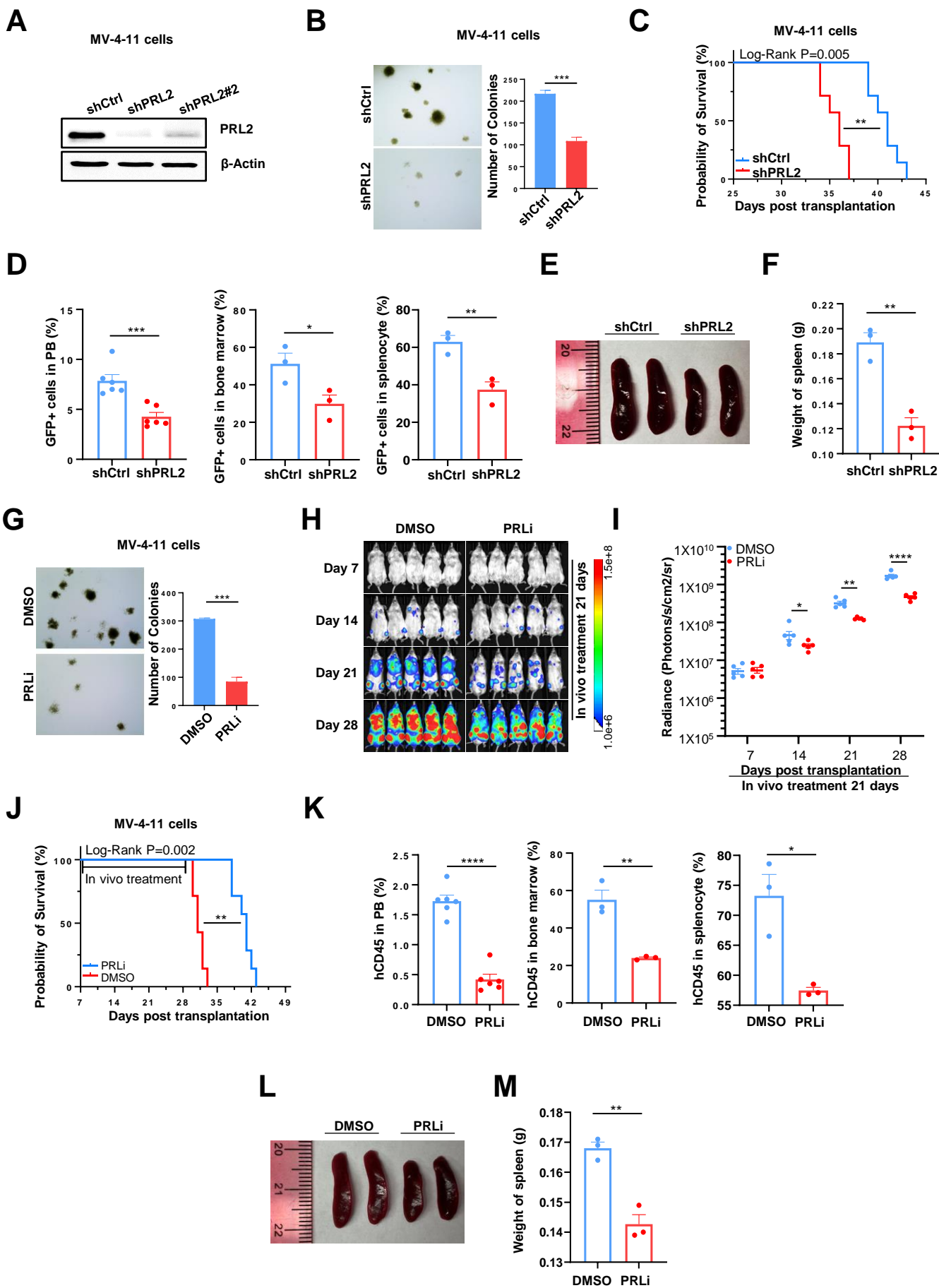


I

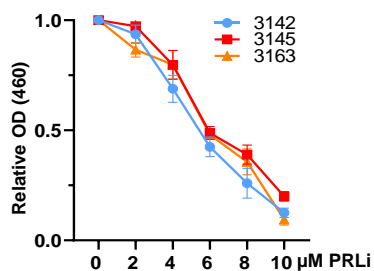




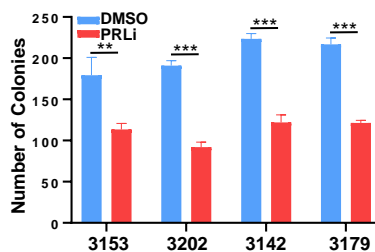




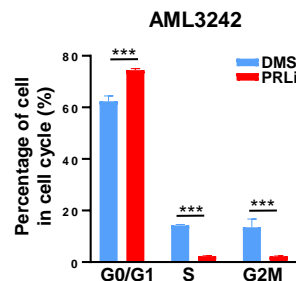
A



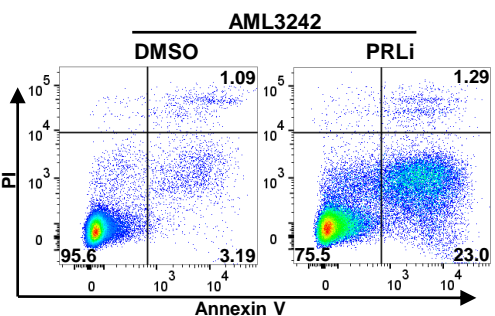
B



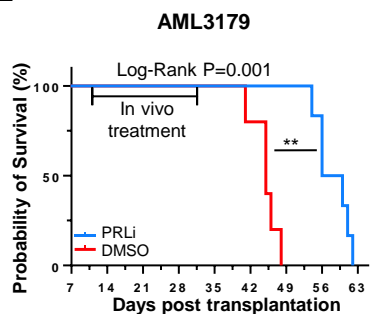
C



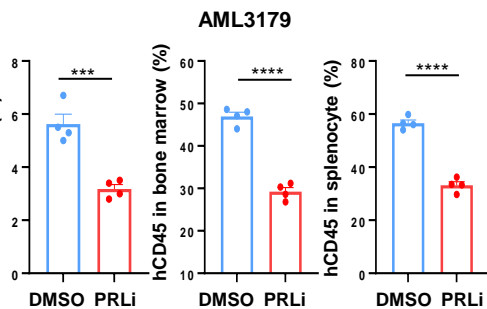
D



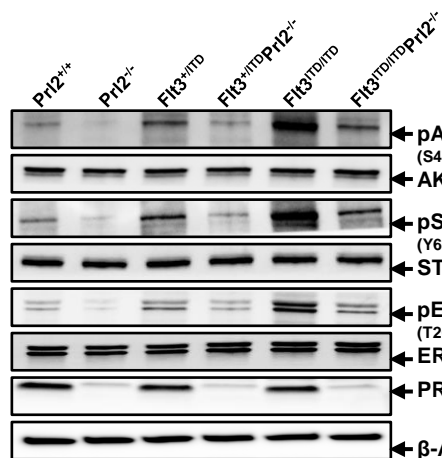
E



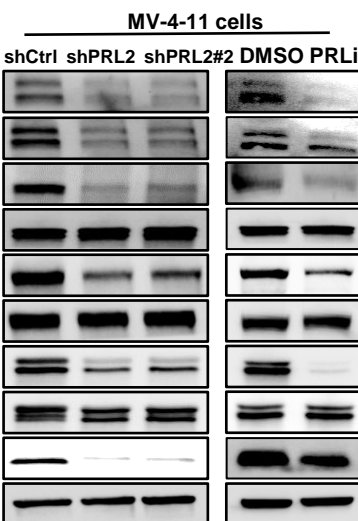
F



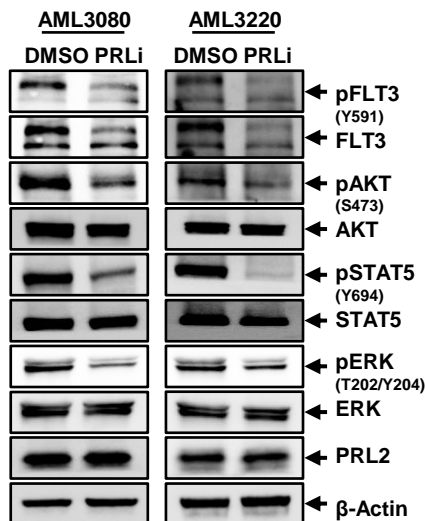
G



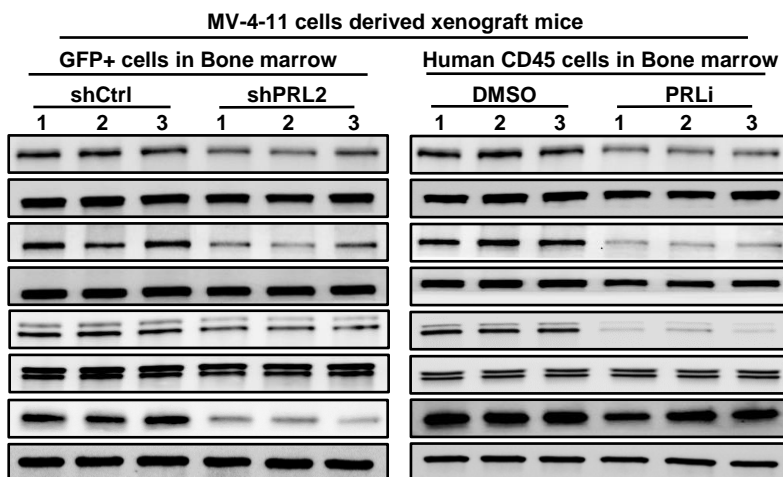
H



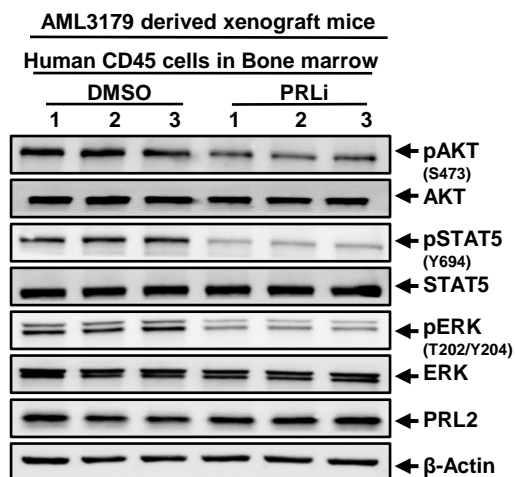
I

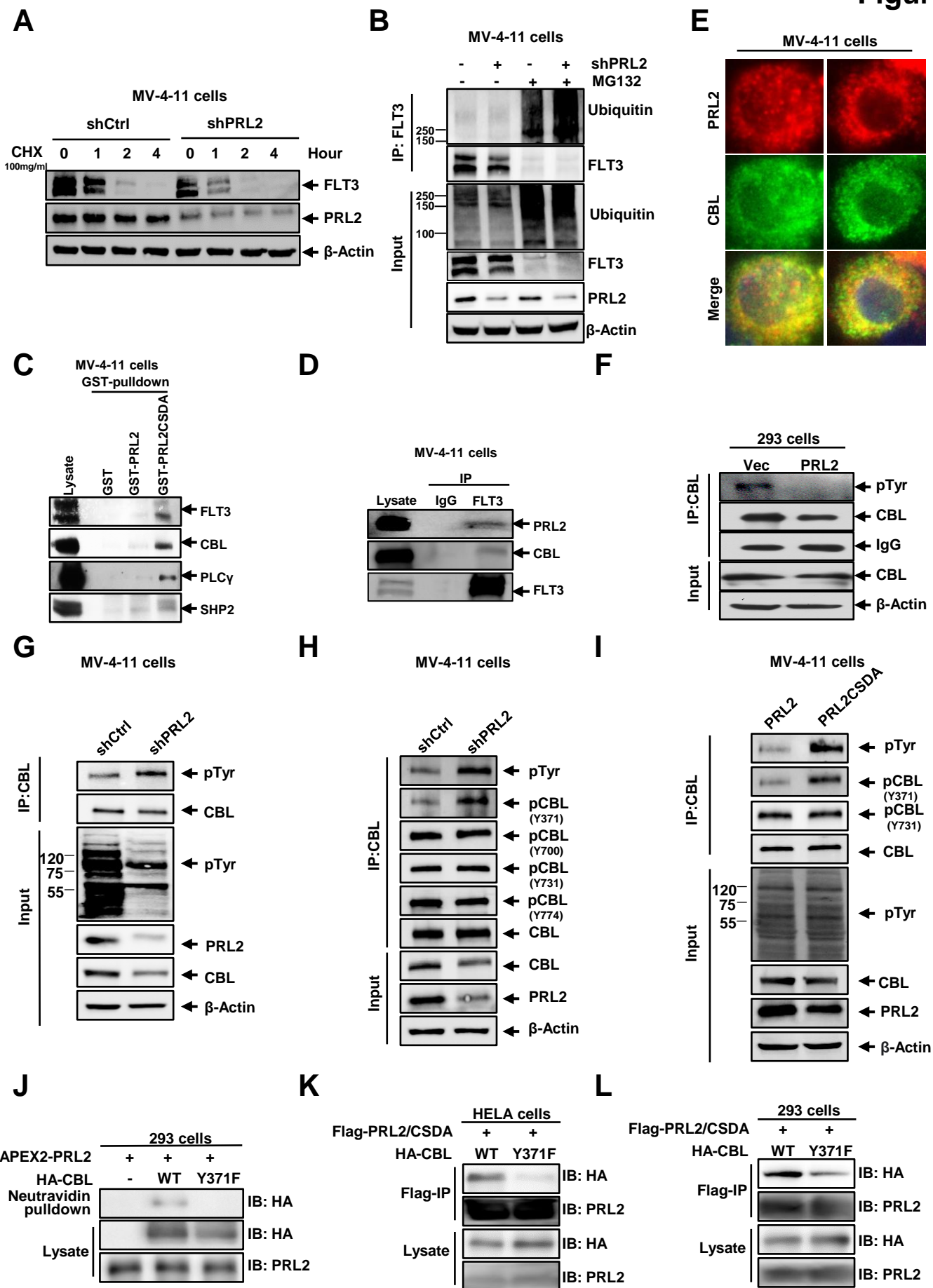


J



K





**PRL2 phosphatase enhances oncogenic FLT3 signaling via dephosphorylation of the E3 ubiquitin
ligase CBL at tyrosine 371**

Supplementary Information

Supplementary materials and methods

Human AML cell lines

Human AML cell lines, including MV-4-11, MOLM-13, K562, and U937, were obtained from ATCC (List in supplemental Table 2). All cell lines were authenticated by SRT profiling and tested for mycoplasma contamination.

Patient samples

AML samples were collected by Dr. H. Scott Boswell after informed consent. Mononuclear blasts from each sample were isolated by Ficoll (Axis-Shield) density centrifugation, and Trypan Blue Exclusion Assay was used to detect the cell viability. Protocols for sample handling and data analysis were approved by Indiana University Cancer center and Roudebush VA Medical Center Ethics Committee and were performed in compliance with the Declaration of Helsinki. Patient information is shown in supplemental Table 1.

Flow cytometry

Murine hematopoietic stem and progenitor cells were identified and evaluated by flow cytometry using a single cell suspension of bone marrow mononuclear cells (BMMCs). Hematopoietic stem and progenitors are purified based upon the expression of surface markers. BM cells were obtained from tibia, femur and iliac crest (6 from each mouse) by flushing cells out of the bone using a syringe and phosphate-buffered saline (PBS) with 2mM EDTA. Red blood cells (RBCs) were lysed by RBC lysis buffer (eBioscience) prior to staining. We defined hematopoietic stem and progenitor as well mature cells by flow cytometry markers. LT-HSCs ($\text{Lin}^- \text{Sca1}^+ \text{cKit}^+ \text{CD150}^+ \text{CD48}^-$), ST-HSCs ($\text{Lin}^- \text{Sca1}^+ \text{cKit}^+ \text{CD150}^- \text{CD48}^-$), MPPs ($\text{Lin}^- \text{Sca1}^+ \text{cKit}^+ \text{CD150}^- \text{CD48}^+$), LSKs ($\text{Lin}^- \text{Sca1}^+ \text{cKit}^+$), MyePro ($\text{Lin}^- \text{Sca1}^- \text{cKit}^+$), MEP ($\text{Lin}^- \text{Sca1}^- \text{cKit}^+ \text{CD34}^- \text{CD16/32}^-$), CMP ($\text{Lin}^- \text{Sca1}^- \text{cKit}^+ \text{CD34}^+ \text{CD16/32}^-$), and GMP ($\text{Lin}^- \text{Sca1}^- \text{cKit}^+ \text{CD34}^+ \text{CD16/32}^+$), myeloid cells ($\text{Gr1}^+ \text{Mac1}^+$), B cells (B220^+) and T cells (CD3^+). Experiments

were performed on FACS LSR IV cytometers (BD Biosciences) and analyzed by using the FlowJo_v10 software (TreeStar). All antibodies were listed in Supplementary table 2.

Transplantation assays

For competitive bone marrow transplantation assays, 5×10^5 BM cells (CD45.2⁺) isolated from *Prl2*^{+/+}, *Prl2*^{-/-}, *Flt3*^{+/*ITD*}, and *Flt3*^{+/*ITD*}*Prl2*^{-/-} mice together with 5×10^5 competitor BM cells (CD45.1⁺) were injected into lethally irradiated (9.5 Gy) B6.SJL mice (CD45.1⁺) via tail vein. At 16 weeks following primary transplantation, 3×10^6 BM cells isolated from primary recipients were transplanted into lethally irradiated secondary recipient mice (CD45.1⁺). The engraftment of donor cells in peripheral blood and bone marrow were determined by flow cytometry analysis.

To determine the impact of PRL2 deficiency on FLT3-ITD-induced MPN, 3×10^6 bone marrow cells isolated from *Prl2*^{+/+}, *Prl2*^{-/-}, *Flt3*^{+/*ITD*}, *Flt3*^{+/*ITD*}*Prl2*^{-/-}, *Flt3*^{*ITD/ITD*} and *Flt3*^{*ITD/ITD*}*Prl2*^{-/-} mice were transplanted into lethally irradiated B6.SJL mice via tail vein.

To determine the impact of PRL2 deficiency on human leukemia cells *in vivo*, 3×10^6 transduced MV-4-11 or MOLM-13 cells (GFP⁺) were injected into sublethally irradiated (2.5 Gy) NSG mice via tail vein.

To determine the efficacy of PRLi on primary human leukemia cells *in vivo*, we generated two patient-derived xenograft (PDX) models of AML in NSGS mice. 1×10^6 primary AML mononuclear cells with FLT3-ITD mutation were injected into sublethally irradiated (2.5 Gy) NSGS mice via tail vein to expand primary human AML cells *in vivo*. 12 to 16 weeks post primary transplantation, we confirmed the engraftment of human CD45⁺ (huCD45⁺) AML in NSGS mice and utilized the human CD45⁺ cell enrichment kit to isolate human cells from the bone marrow of NSGS mice. We transplanted 4×10^6 human CD45⁺ leukemia cells isolated from the BM of primary recipients into sublethally irradiated (2.5 Gy) NSG mice via tail vein injection. After confirmation of human leukemia engraftment in peripheral

blood of NSG mice (>1% human CD45⁺ cells), NSG mice were treated with vehicle (10% DMSO) or PRLi (25 mg/kg, I.P.) daily for three weeks.

PRLi treatment *in vivo*

After confirmed the human cell engraftment by checking the human CD45⁺ cells in peripheral blood reach to 1% by flow, the NSG mice start to receive the PRLi treatment. The small molecule inhibitor of PRL (PRLi, compound 43) was synthesized as described previously.³¹ PRLi were dissolved in DMSO at 25mg/ml stocking concentration saved in -80°C freezer. PRLi stock solution or DMSO was diluted in PBS before administration. 25mg/kg PRLi or DMSO was administrated by intraperitoneal injection for consecutive 21 days.

Immunoblotting analysis

Cells were washed with ice-cold PBS and lysed on ice for 30 min in lysis buffer (50 mM Tris-HCl, pH 7.4, 150 mM NaCl, 1% Triton X-100, and 10% glycerol) supplemented with a Complete Protease Inhibitor tablet (Roche Applied Science). Cell lysates were cleared by centrifugation at 15,000 rpm for 10 min. The lysate protein concentration was estimated using a BCA protein assay kit (Pierce). The protein samples were boiled with sample buffer, separated by SDS-PAGE, transferred electrophoretically to a nitrocellulose membrane, and immunoblotted with appropriate antibodies, followed by incubation with horseradish peroxidase-conjugated secondary antibodies. The blots were developed by the enhanced chemiluminescence technique (ECL kit, GE Healthcare). Representative results from at least two independent experiments are shown. Representative results from at least two independent experiments are shown. All antibodies were listed in Supplementary table 2.

***In vivo* image system**

Bioimaging of leukemia burden *in vivo* was performed by Spectral Lago System at Northwestern University Center for Advanced Microscopy generously supported by NCI CCSG P30 CA060553

awarded to the Robert H Lurie Comprehensive Cancer Center. Before imaging, Luciferin (in vivo grade, Gold Bio, CAS# 115144-35-9) was prepared in PBS, and 150 mg/kg Luciferin was injected by i.p., after 10 minutes. The signal data was analyzed by the Aura software.

Production of Retrovirus and Lentivirus

Retroviral particles were produced by transfection of Phoenix E cells with MSCV-IRES-GFP, MSCV-PRL2-IRES-GFP, MSCV-PRL2-CSDA-IRES-GFP, MSCV-FLT3-IRES-GFP, or MSCV-FLT3-ITD-IRES-GFP plasmids, according to standard protocols. Mouse hematopoietic progenitor cells were transduced on retronectin (Takara)-coated non-tissue culture plates with high-titer retroviral suspensions. Twenty-four hours after infection, GFP-positive cells were sorted by FACS. Transduced cells were then transplanted into lethally irradiated recipient mice. The presence of GFP⁺ cells in the peripheral blood was measured by flow cytometry analysis.

Lentiviral shLuciferase was a gift from Huipin Liu laboratory at the Northwestern University. Lentiviral shRNA plasmid (pLB) was purchased from Addgene (11619). Oligonucleotides targeting control (Luciferase) and human PRL2 cDNAs were cloned into the pLB plasmid. Oligonucleotide sequences are available upon request. Lentiviral particles were generated by standard method using the third-generation packaging system (pMDL, pMD2.G, and pRSV-Rev). Human AML cell lines were infected with high-titer lentiviral suspensions. 48 hours after infection, GFP-positive cells were sorted by FACS. The reduction of PRL2 proteins was determined by immunoblot analysis.

Colony formation unit assays

The colony formation of murine bone marrow Lin⁻ cells was determined in methylcellulose medium (MethoCult GF M3434, StemCell Technologies). Bone marrow Lin⁻ cells were isolated by mouse Lin⁻ cell depletion kit. Lin⁻ cells were transduced with MIGR1 (MSCV-IRES-GFP), MIGR1-FLT3 (MSCV-

FLT3-IRES-GFP), or MIGR1-FLT3-ITD (MSCV-FLT3-ITD-IRES-GFP) retrovirus. 48 hours after infection, GFP positive cells were sorted by FACS. 5×10^3 GFP⁺ cells were seed into methylcellulose medium (6-well plate). Colonies were scored after 7 days of the initial culture.

The colony formation of mice bone marrow cells was determined in methylcellulose medium (MethoCult GF M3434, StemCell Technologies) using 2×10^4 BM cells per well (6-well plate). Colonies were scored after 7 days of the initial culture.

The colony formation of human leukemia cells was determined in methylcellulose medium (MethoCult H4435, StemCell Technologies) using 1×10^3 leukemia cells or 5×10^4 primary AML patient BM cells per well (6-well plate). Colonies were scored after 10 days of culture.

Proliferation assays

Bone marrow Lin⁻ cells were transduced with MIGR1 (MSCV-IRES-GFP), MIGR1-FLT3 (MSCV-FLT3-IRES-GFP), or MIGR1-FLT3-ITD (MSCV-FLT3-ITD-IRES-GFP) retrovirus. 48 hours after infection, GFP positive cells were sorted by FACS. 2×10^6 GFP⁺ cells were cultured in serum-free medium with or without 100ng/ml human FLT3 ligand for 48 hours.

For proliferation assay using primary AML patient samples, 1×10^5 cells were treated with or without gradient concentration of PRLi in 96 well plate. After 24 hours, 10 μ l of WST-1 added to each well and incubate at 37° C for 2 hours. Experiments were performed on SpectraMax iD3.

To determine the specificity of PRLi on PRL2 in leukemia cells, MV-4-11 and MOLM-13 cells were transduced with retroviruses expressing GFP (MSCV-IRES-GFP), PRL2 (MSCV-PRL2-IRES-GFP), or PRL2-CSDA (MSCV- PRL2-CSDA -IRES-GFP). GFP positive cells were sorted by FACS. 2×10^6 GFP⁺ cells were cultured with or without 5 μ M PRLi for 7 days and cell viability was determined by Trypan blue staining.

Cell cycle analysis

Primary AML cells were harvested after treated with DMSO or PRLi (10 μ M) for 24 hours. Wash once in PBS. Add cold 70% ethanol drop wise to the pellet while vortexing and fix for 30 min at 4°C. Wash twice in PBS and spin at 850 g in a centrifuge and be careful to avoid cell loss when discarding the supernatant especially after spinning out of ethanol. Add 50 μ l of a 100 μ g/ml stock of RNase to avoid RNA. Add 200 μ l PI (from 50 μ g/ml stock solution) in each sample and incubate 15 minutes at room temperature. Wash once in PBS then perform flowcytometry analysis. Experiments were performed on FACS LSR IV cytometers (BD Biosciences) and analyzed by using the FlowJo_v10 software.

Apoptosis assays

Primary AML cells were harvested after treated with DMSO or PRLi (10 μ M) for 24 hours. Wash once in PBS. Resuspend cells in 1X Binding Buffer Solution at a final concentration of 1×10^6 cells/ml. To each 100 μ L of cell suspension, add 5 μ L of Annexin V and 5 μ L of Propidium Iodide Staining Solution. Incubate cells at room temperature for 15 minutes avoiding the light. Add 400 μ L of 1X Binding Buffer Solution. Experiments were performed on FACS LSR IV cytometers (BD Biosciences) and analyzed by using the FlowJo_v10 software.

Co-Immunofluorescence

HA-CBL was co-transfected with GFP-PRL2 in U2OS cells. 24 h after transfection, U2OS cells and MV-4-11 cells were fixed with 4% paraformaldehyde in phosphate-buffered saline (PBS) for 15 min at room temperature, permeabilized with 0.2% Triton X-100 in PBS for 10 min and blocked with BSA. Anti-HA antibody was applied to U2OS cells and Anti-CBL and anti-PRL2 antibodies were applied to MV-4-11 cells overnight at 4°C, followed by three times of washing with PBS and 1h incubation with goat anti-mouse alexa fluor 555 secondary antibody. After washing with PBS, the coverslips were mounted with

VECTASHIELD® PLUS Antifade Mounting Medium with DAPI (Vector Laboratories, H-2000-10).

Images were obtained with a Nikon Inverted Microscope Eclipse Ti-S.

GST pull down assays

1 x 10⁹ MV-4-11 cells were treated with 1 mM pervanadate for 30 minutes and collected by centrifugation. The cell pellet was lysed with 3 ml lysis buffer (20 mM Tris, pH 7.5, 100 mM NaCl, 1% Triton X-100, 10% glycerol, supplemented with 5 mM iodoacetic acid, 1 mM orthovanadate, and proteases inhibitors). 10 mM DTT was added in the lysate and incubated for 15 min on ice to inactivate any unreacted iodoacetic acid and pervanadate. Supernatant was collected by centrifugation at 14,000 g for 15 min. 25 µg GST, GST-PRL2 or GST-PRL2-CSDA were coupled to GST beads in lysis buffer, incubated at 4°C for 1h. Cell lysates were incubated with GST proteins conjugated to beads at 4 °C for 2h. The beads were pelleted and washed 3 times for 5 min with lysis buffer. Bound proteins were re-suspended in 50 µL Laemmli sample buffer, boiled for 5 min, and the samples are resolved by SDS-PAGE gels.

Immunoprecipitation (IP) assays

For Immunoprecipitation (IP), Cells were washed with ice-cold PBS and lysed on ice for 30 min in lysis buffer (50 mM Tris-HCl, pH 7.4, 150 mM NaCl, 1% Triton X-100, and 10% glycerol) supplemented with a Complete Protease and Phosphorylation Inhibitor tablet (Thermoscientific, A32961). Cell lysates were cleared by centrifugation at 15,000 rpm for 10 min. The lysate protein concentration was estimated using a BCA protein assay kit (Pierce). IP antibody plus Protein A Agarose beads (Sigma-Millipore) was added, and samples were incubated on shaker at 4 °C for overnight. After washing with lysis Buffer, the samples were ready for western blot analysis.

For the peroxidase APEX2 assay, HA-CBL or HA-CBL/Y371F were transiently expressed in 293 cells stably expressing APEX2-PRL2 with PEI. 48 h after transfection, biotin-phenol labeling was performed by changing the medium to fresh growth medium containing 2.5 mM biotin-phenol for 30 min at 37 °C

under 5% CO₂ according to previously published protocols.⁴⁴ Then, a final concentration of 0.5 mM H₂O₂ was added into the plate for 1 min. The reaction was then quenched by replacing the medium with 1X PBS containing 5 mM Trolox, 10 mM sodium ascorbate and 10 mM sodium azide. Cells were washed with PBS containing 5 mM Trolox, 10 mM sodium ascorbate and 10 mM sodium azide for three times and lysed with lysis buffer (50 mM Tris (pH 8.0), 150 mM NaCl, 10% Glycerol, 1% Triton-X-100) supplied with phosphatase inhibitor (Bimake, B15002) and protease inhibitor mixture (Roche Applied Science, 04693132001). Biotinylated proteins are enriched with neutravidin beads (Thermo Scientific, PI29202) and identified by Western blot.

For the Flag-PRL2-CSDA trapping assay, HA-CBL or HA-CBL/Y371F were transiently expressed in HEK293 cells or HeLa cells stably expressing Flag-PRL2-CSDA trapping mutant with PEI. 48 h after transfection, the cells were treated with 300 μM pervanadate for 30 min, then the medium was replaced with fresh medium for another 30 min, and the cells were washed for three time with PBS. Then the cells were lysed with 1 mL lysis buffer (50 mM Tris (pH 8.0), 150 mM NaCl, 10% Glycerol, 1% Triton-X-100) supplied with phosphatase inhibitor (Bimake, B15002) and protease inhibitor mixture (Roche Applied Science, 04693132001) on ice for 15 min and then spun at 14,000 rpm at 4 °C for 30 min, and the supernatant was transferred to a fresh tube and Flag agarose beads (Bimake, B23102) were added and incubated at 4 °C for 3 h. Beads were collected by centrifugation at 3,000 rpm for 1 min and the supernatant was removed. Beads were washed three times with 1 mL lysis buffer. Bound proteins were resuspended in 50 μL Laemmli sample buffer and boiled for 5 min, and the samples were resolved by SDS/PAGE and examined by Western blotting.

Sequencing data

Transcriptional expression data of PRL2 and all data on clinical, cytogenetic characteristics, and survival were derived from TCGA official website (<https://www.cancer.gov/about-nci/organization/ccg/research/structural-genomics/tcga>) or cBioPortal (<https://www.cbioportal.org>).

For RNA-seq assays in hematopoietic stem and progenitor cells (HSPCs), embryonic day 14.5 fetal liver cells were collected from *Prl2*^{+/-} pregnancy female. Total RNA was isolated by MiniRNA universal kit. RNA-seq was performed by Genomic Core in Indiana University. Library was prepared by Clontech SMART-Seq v4 Ultra Low Input RNA Kit, Illumina Nextera XT DNA Lib Kit. and RNA-seq was performed on Illumina NovaSeq 6000 system (Illumina, Inc.). RNA-seq data was analyzed, and the raw data was deposited in NCBI GEO (GSE208136). The Limma package in R Studio (version 4.1.0, RStudio Team (2020) was used to identify the DEGs. $P < 0.05$ and $|\log_2 \text{fold change (FC)}| > 1$ was used as the cut-off criteria for volcano plot for clinic data and heat map for fetal liver sequencing data by R Studio. All the DEGs were used to do Gene-set enrichment analysis by GSEA v4.2.2 software (<http://www.gsea-msigdb.org/gsea/index.jsp>). For HSPC sequencing data, the DEGs ($P < 0.05$ and $|\log_2 \text{fold change (FC)}| > 1$) was used to construct PPI networks with an interaction score > 0.4 by STRING (version 11.05).

Immunohistochemistry

Recipient mice repopulated with *Prl2*^{+/+}, *Prl2*^{-/-}, *Flt3*^{+ITD}, *Flt3*^{+ITD}*Prl2*^{-/-}, *Flt3*^{ITD/ITD} and *Flt3*^{ITD/ITD}*Prl2*^{-/-} BM cells mice were sacrificed at the same time. BM, liver, spleen, and PB were collected. Cellular morphology of PB smears were analyzed by May-Grünwald Giemsa staining. Bone, Liver and spleen section were stained with hematoxylin/eosin (H&E) at the Northwestern University (Chicago, IL). All slides were evaluated by conventional light-field microscopy using an optical microscope (Olympus, Japan).

Supplemental Figure Legends

Supplemental Figure 1.

(A) Relative *PRL2* (*PTP4A2*) mRNA expression in AML patients with or without CNS relapse.

(B) Overall survival of AML patients with high (n=71) or low (n=69) *PRL2* expression.

- (C) Overall survival of favorable cytogenetic risk AML patients with high (n=16) or low (n=15) *PRL2* expression.
- (D) Overall survival of intermediate cytogenetic risk AML patients with high (n=38) or low (n=38) *PRL2* expression.
- (E) Relative *PRL2* (*PTP4A2*) mRNA expression in AML patients with or without *FLT3* mutation, datasets are from cBioportal.
- (F) Overall survival of *FLT3* mutation negative AML patients with high (n=49) or low (n=48) *PRL2* expression.

Supplemental Figure 2

- (A) Quantitative RT-PCR analysis of gene expression in Kit⁺ cells from E14.5 WT and *Prl2* null fetal liver (n=4).
- (B) Image Lab software was used to calculate the gray value of each band. Graph showing the ratio of the relative density of phosphorylated protein/total protein expression and normalized with β -actin from WT and *Prl2* null fetal liver cells (n=3).
- (C) Graph showing the ratio of the relative density of phosphorylated protein/total protein expression and normalized with β -actin from WT and *Prl2* bone marrow Lin⁻ cells (n=3).
- (D) *Prl2* deficiency decreased the proliferation of hematopoietic progenitor cells expressing MIGR1-FLT3-ITD (MSCV-FLT3-ITD-IRES-GFP) both in the absence of cytokines and in the presence of FLT3 ligand (n= 3).
- (E) Wild-type FLT3 (MSCV-FLT3-IRES-GFP) or FLT3-ITD (MSCV-FLT3-ITD-IRES-GFP) were introduced into Lin⁻ cells purified from wild-type and *PRL2* null mice. Loss of *Prl2* decreased the colony formation of HSPCs expressing FLT3-ITD (n = 3). **CFU-M: Colony forming unit-macrophages, CFU-G: Colony forming unit-granulocytes, CFU-GM: Colony forming unit-granulocytes/ macrophages.**

Mean values (\pm SEM) are shown (*p<0.05, **p<0.01, and ***p<0.001).

Supplemental Figure 3

- (A) Representative body size of *Pr12*^{+/+}, *Pr12*^{-/-}, *Flt3*^{+ITD}, *Flt3*^{+ITD}*Pr12*^{-/-}, *Flt3*^{ITD/ITD} and *Flt3*^{ITD/ITD}*Pr12*^{-/-} mice.
- (B-H) White blood cell (WBC), red blood cell (RBC), hemoglobin (HGB), platelet, basophil, monocyte, and eosinophil count in peripheral blood (PB) of *Pr12*^{+/+}, *Pr12*^{-/-}, *Flt3*^{+ITD}, *Flt3*^{+ITD}*Pr12*^{-/-}, *Flt3*^{ITD/ITD} and *Flt3*^{ITD/ITD}*Pr12*^{-/-} mice (n=8 mice per group).
- (I) The frequency of myeloid cells, B cells and T cells in PB of *Pr12*^{+/+}, *Pr12*^{-/-}, *Flt3*^{+ITD}, *Flt3*^{+ITD}*Pr12*^{-/-}, *Flt3*^{ITD/ITD} and *Flt3*^{ITD/ITD}*Pr12*^{-/-} mice (n=8 mice per group).
- (J) BM cellularity of *Pr12*^{+/+}, *Pr12*^{-/-}, *Flt3*^{+ITD}, *Flt3*^{+ITD}*Pr12*^{-/-}, *Flt3*^{ITD/ITD} and *Flt3*^{ITD/ITD}*Pr12*^{-/-} mice (n=6 mice per group).
- (K-M) The frequency of myeloid, B, and T cells in the bone marrow of *Pr12*^{+/+}, *Pr12*^{-/-}, *Flt3*^{+ITD}, *Flt3*^{+ITD}*Pr12*^{-/-}, *Flt3*^{ITD/ITD} and *Flt3*^{ITD/ITD}*Pr12*^{-/-} mice (n=6 mice per group).
- (N) The frequency of myeloid progenitor (MyePro) (Lin⁻Sca1⁻cKit⁺), MEP (Lin⁻Sca1⁻cKit⁺CD34⁻CD16/32⁻), CMP (Lin⁻Sca1⁻cKit⁺CD34⁺CD16/32⁻), and GMP (Lin⁻Sca1⁻cKit⁺CD34⁺CD16/32⁺) in the BM of *Pr12*^{+/+}, *Pr12*^{-/-}, *Flt3*^{+ITD}, *Flt3*^{+ITD}*Pr12*^{-/-}, *Flt3*^{ITD/ITD} and *Flt3*^{ITD/ITD}*Pr12*^{-/-} mice (n=6).
- Mean values (\pm SEM) are shown (*p<0.05, **p<0.01, ***p < 0.001).

Supplemental Figure 4

- (A) Experimental design of primary competitive BM transplantation assays.
- (B-C) White blood cell (WBC), neutrophil, lymphocyte, and monocyte count in peripheral blood (PB) of primary transplantation recipient mice (n=8 mice per group).
- (D) The frequency of donor derived myeloid progenitor (MyePro), MEP, CMP, and GMP in the BM of primary transplantation recipient mice (n=8 mice per group).
- (E) Experimental design of secondary BM transplantation assays.

(F-G) WBC, neutrophil, lymphocyte, monocyte count in peripheral blood (PB) of the secondary transplantation recipient mice (n=8 mice per group).

(H) The frequency of donor derived myeloid progenitor (MyePro), MEP, CMP, and GMP in the BM of secondary transplantation recipient mice (n=8 mice per group).

(I-J) The size and weight of spleen of the secondary transplantation recipient mice (n=9-10 mice per group).

Mean values (\pm SEM) are shown (**p<0.01, ***p < 0.001, ****p < 0.0001).

Supplemental Figure 5

(A-G) RBC, HDB level, WBC, platelet, neutrophil, monocyte and basophil count in peripheral blood (PB) of recipient mice repopulated with *Prl2*^{+/+}, *Prl2*^{-/-}, *Flt3*^{+ITD}, *Flt3*^{+ITD}*Prl2*^{-/-}, *Flt3*^{ITD/ITD} and *Flt3*^{ITD/ITD}*Prl2*^{-/-} BM cells (n= 9-10).

(H) Representative H&E (10 \times) images of the peripheral blood smears, bone marrow, spleen, and liver of recipient mice repopulated with *Prl2*^{+/+}, *Prl2*^{-/-}, *Flt3*^{+ITD}, *Flt3*^{+ITD}*Prl2*^{-/-}, *Flt3*^{ITD/ITD} and *Flt3*^{ITD/ITD}*Prl2*^{-/-} BM cells.

Mean values (\pm SEM) are shown.

Supplemental Figure 6

(A) Western blot analysis for PRL2 in MOLM-13 and K562 cells transduced with lentiviruses expressing a control shRNA (shCtrl) or a PRL2 shRNA (shPRL2).

(B-C) Knocking down of PRL2 significantly decreased the colony formation of MOLM-13 and K562 cells (n=3). Representative images of the colonies are shown.

(D) Kaplan-Meier survival curve of sublethally irradiated NSG mice transplanted with 3 \times 10⁶ MOLM-13 cells expressing shCtrl or shPRL2 (n=7 mice group).

(E-F) PRLi treatment significantly decreased the colony formation of MOLM-13 and K562 cells (n=3). Representative images of the colonies are shown.

- (G) Colony formation of MV-4-11, MOLM-13, and K562 with or without genetic knock down of PRL2 treated with PRLi (n=3).
- (H) Proliferation of MV-4-11 and MOLM-13 cells expressing GFP, PRL2, or PRL2-CSDA in the presence or the absence of PRLi (5 μ M) (n=3).
- (I) Cell cycle analysis of primary AML cells with FLT3-ITD mutation (AML3150) at 24 hours following DMSO or PRLi (10 μ M) treatment.
- (J) Apoptosis analysis of primary AML cells with FLT3-ITD (AML3150) at 24 hours following DMSO or PRLi (10 μ M) treatment.
- (K) Kaplan-Meier survival curve of NSG mice transplanted with 4×10^6 human CD45⁺ leukemia cells (AML3242) following three weeks of DMSO or PRLi treatment (n=6 mice per group).
- (L) Flow cytometry analysis of human CD45⁺ cells in PB, BM, and spleen of NSG mice transplanted with 4×10^6 human CD45⁺ leukemia cells (AML3242) after three weeks of DMSO or PRLi treatment (n=4 mice per group).

Supplemental Figure 7

- (A) Representative western blot analysis of STAT3, STAT1 and MEK phosphorylation in MV-4-11 cells following dimethyl sulfoxide (DMSO) or PRLi treatment.
- (B) Representative western blot analysis of FLT3, AKT, STAT5, STAT3, STAT1 and MEK phosphorylation in K562 cells following dimethyl sulfoxide (DMSO) or PRLi treatment.
- (C) Representative western blot analysis of BCR-ABL, BCR, and c-ABL in K562 cells following DMSO or PRLi treatment.
- (D) Representative western blot analysis of FLT3, AKT, STAT5 and ERK phosphorylation in U937 cells expressing WT FLT3 or FLT3-ITD following DMSO or PRLi treatment.
- (E) Graph showing the ratio of the relative density of phosphorylated protein/total protein expression and normalized with β -actin in human CD45⁺ cells in BM of NSG mice 4 weeks after transplanted with MV-4-11 cells expressing control shRNA or shPRL2 (Left panel, n=3 mice per group); in human

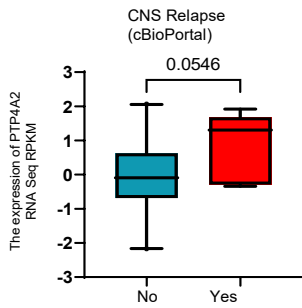
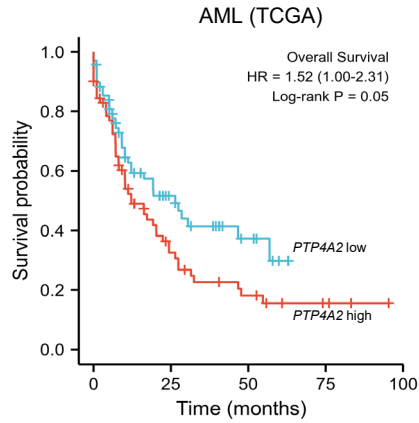
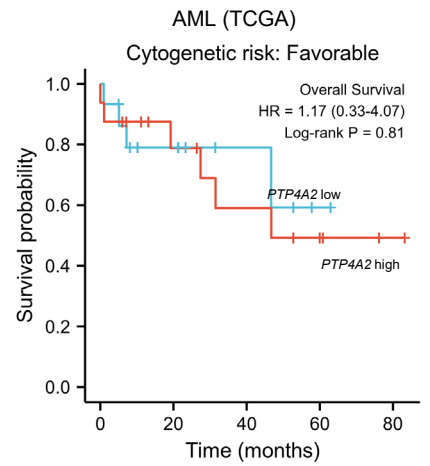
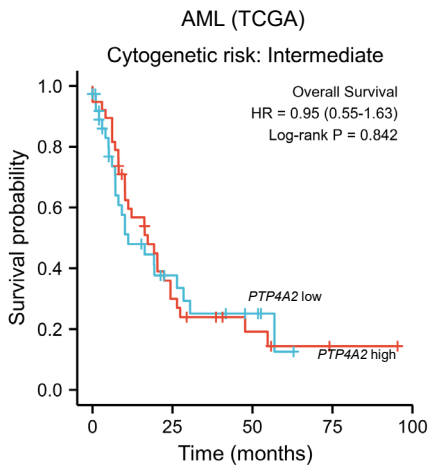
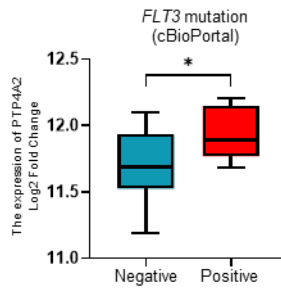
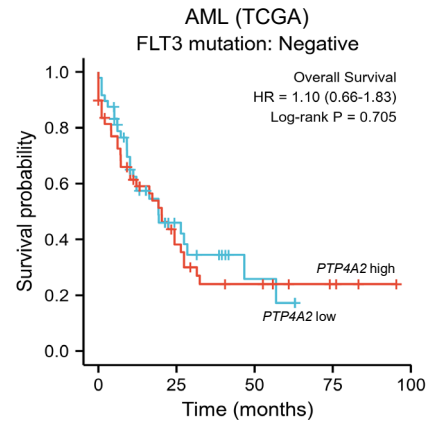
CD45⁺ cells in BM of NSG mice transplanted with MV-4-11 cells following three weeks of DMSO or PRLi treatment (Middle panel, n=3 mice per group); and in human CD45⁺ cells in BM of NSG mice transplanted with PDX cells (AML3179) following three weeks of DMSO or PRLi treatment (Right panel, n=3 mice per group).

- (F) Representative western blot analysis of PTEN levels in MV-4-11 cells expressing shCtrl or shPRL2 (Up panel) or in MV-4-11 cells following DMSO or PRLi treatment (Bottom panel).
- (G) MV-4-11 cell proliferation at 24 hours after PRLi (5 μ M) and AC220 (2.5 nM) or PRLi (5 μ M) and Gilteritinib (5nM) treatment.

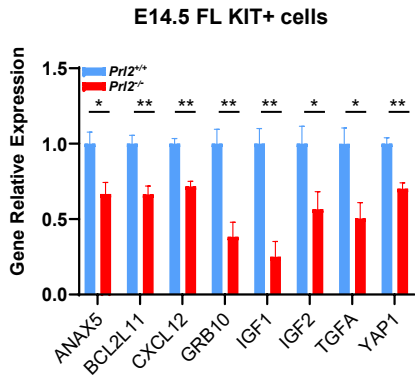
Supplemental Figure 8

- (A) PRLi treatment decreased FLT3 half-life in MV-4-11 cells.
- (B) PRLi treatment enhanced FLT3 ubiquitination in MV-4-11 cells.
- (C) Immunofluorescence analysis showed that PRL2 co-localizes with CBL in U2OS cells.
- (D) Protein structure of CBL. CBL becomes phosphorylated at Y371, Y700, Y731, and Y774 following cytokine stimulation.
- (E) Representative western blot analysis showed that PRLi treatment increases CBL phosphorylation at tyrosine 371 in MV-4-11 cells.
- (F) The mRNA level of *PRL2* and *CBL* from AML were plotted and Spearman rank-correlation analyses were performed. *PRL2* expression is positively correlated with *CBL* expression in these AML samples from TCGA dataset.

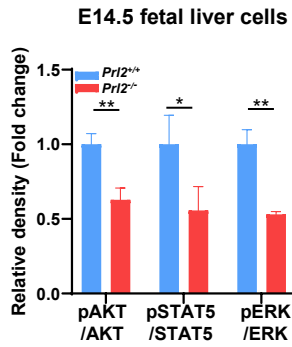
Supplementary Figure 1

A**B****C****D****E****F**

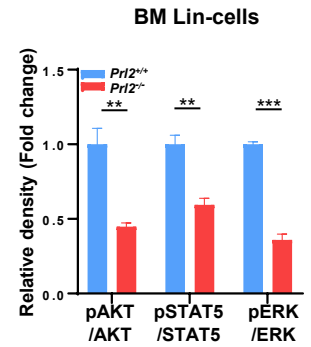
A



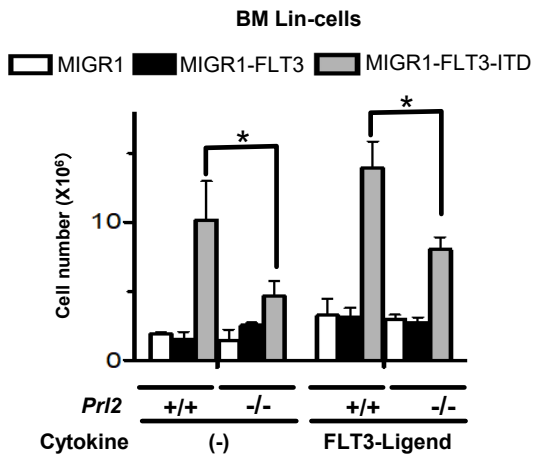
B



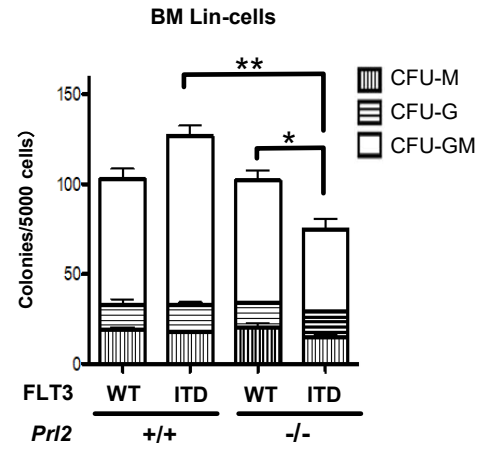
C

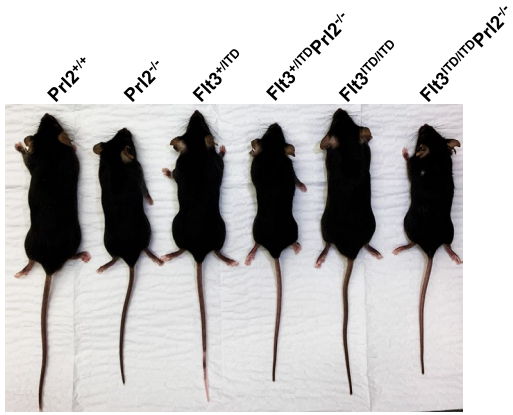
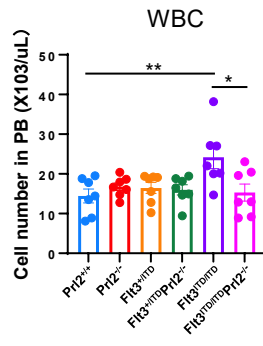
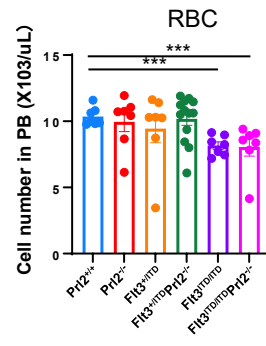
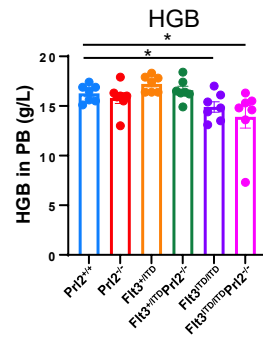
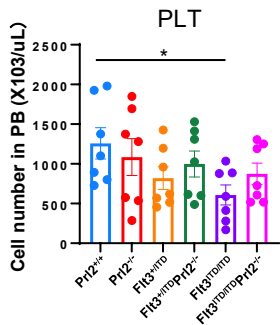
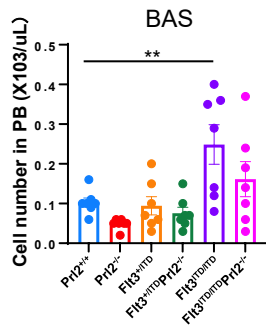
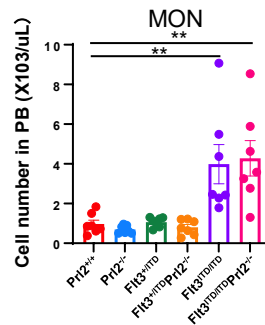
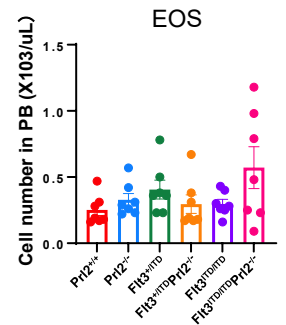
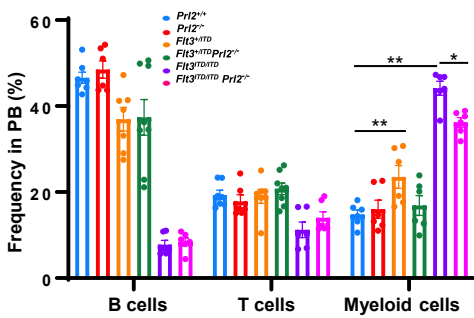
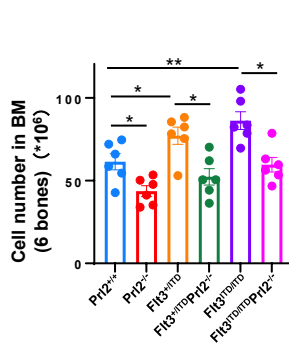
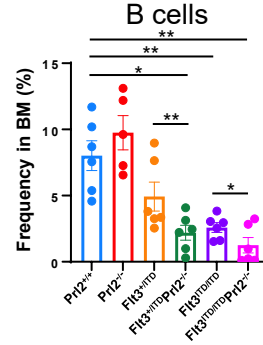
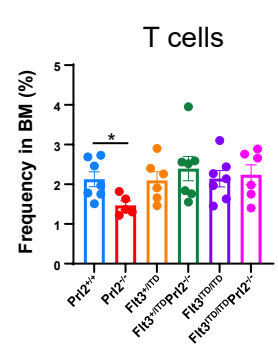
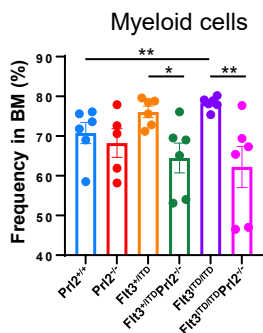
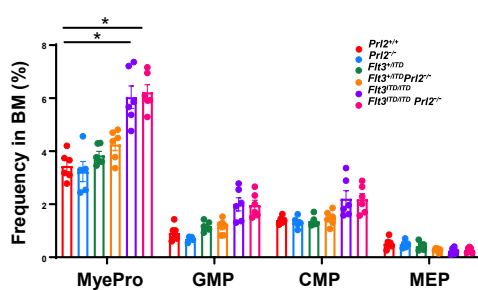


D



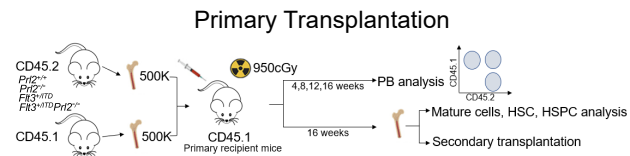
E



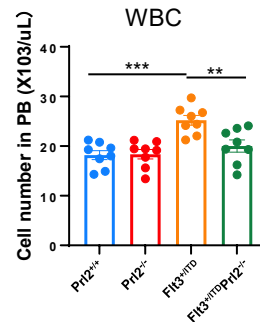
A

B

C

D

E

F

G

H

I

J

K

L

M

N


Supplementary Figure 4

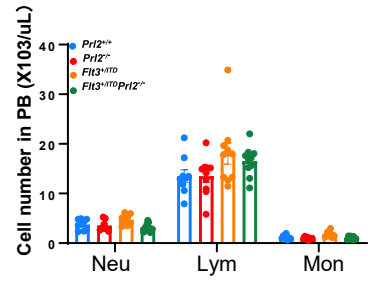
A



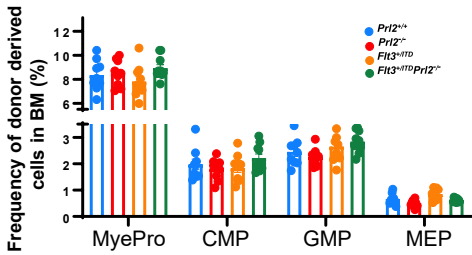
B



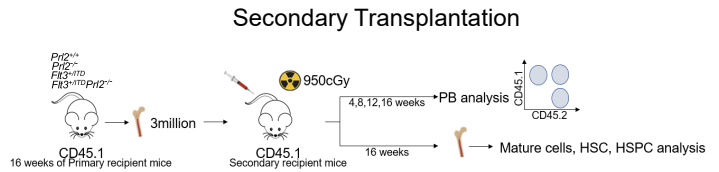
C



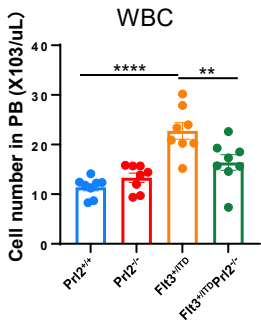
D



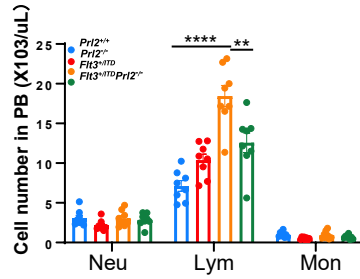
E



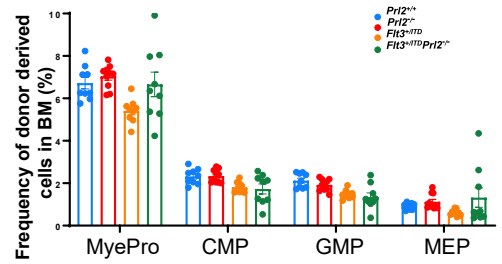
F



G



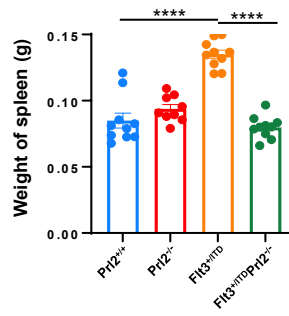
H



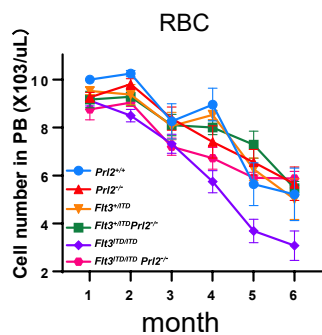
I



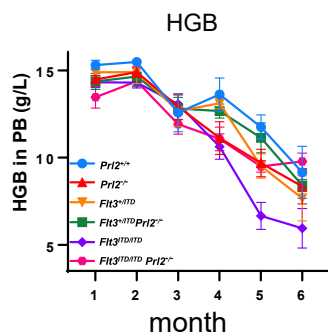
J



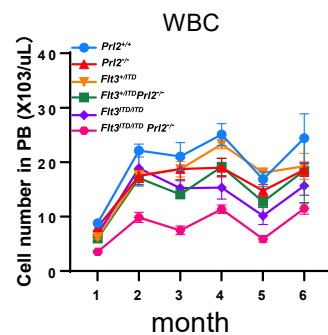
A



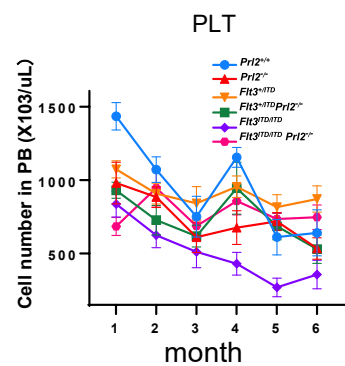
B



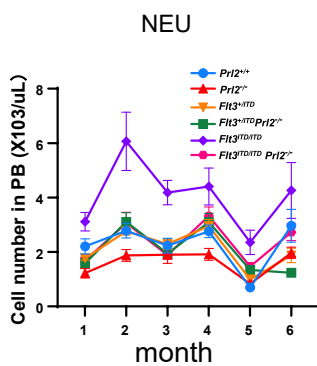
C



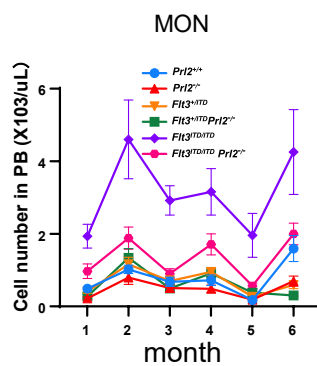
D



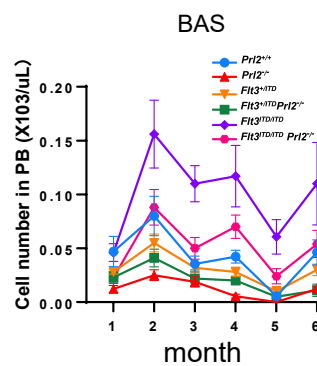
E



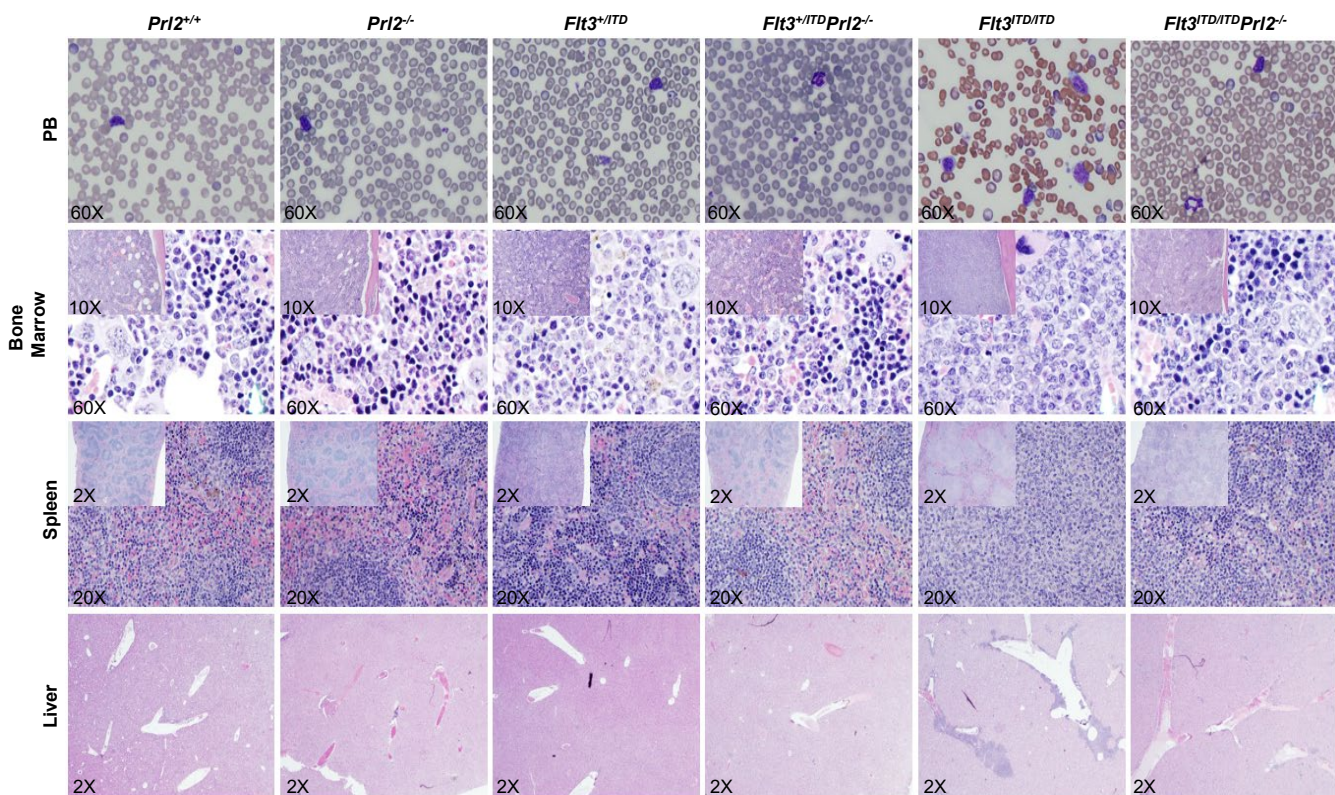
F

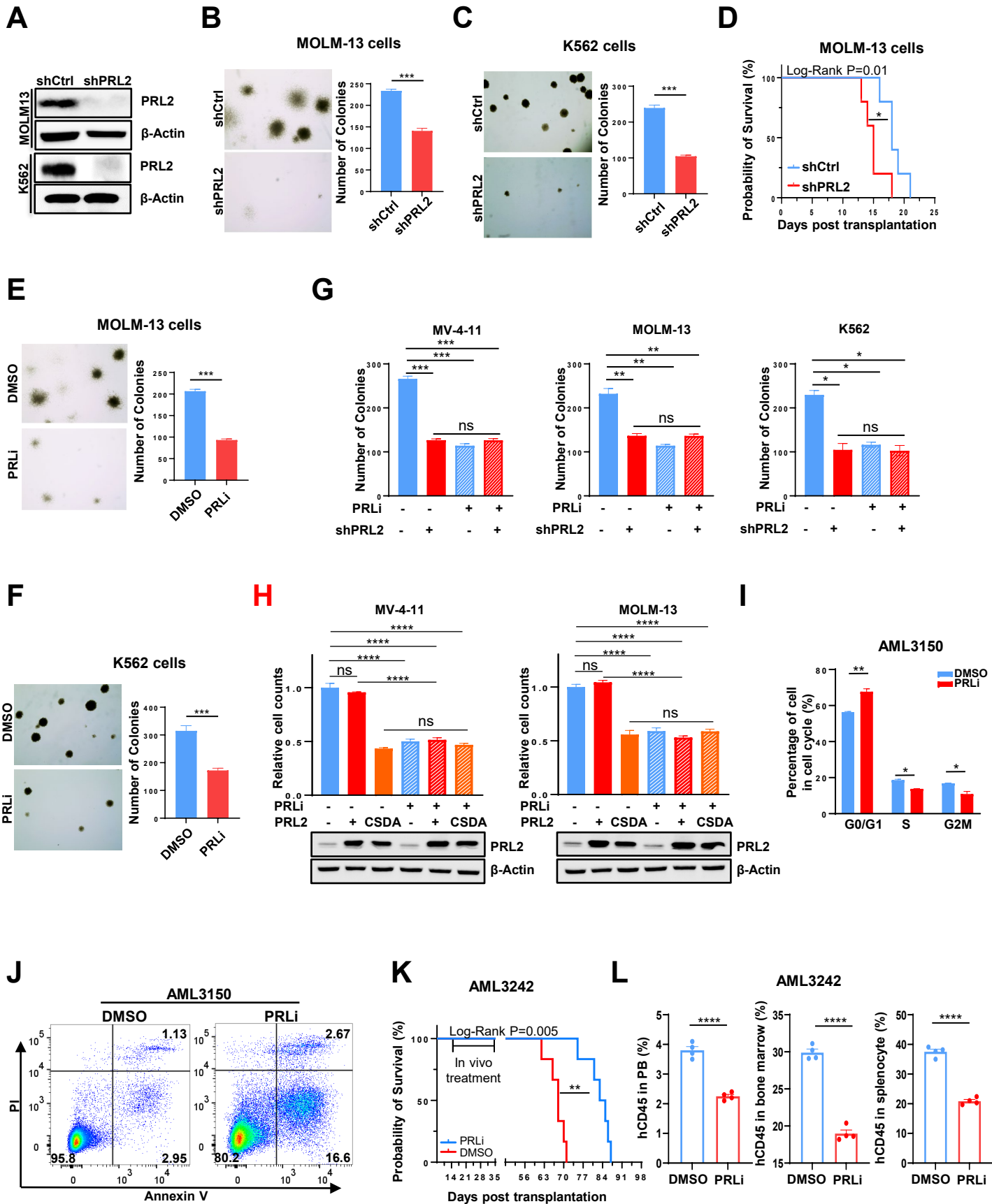


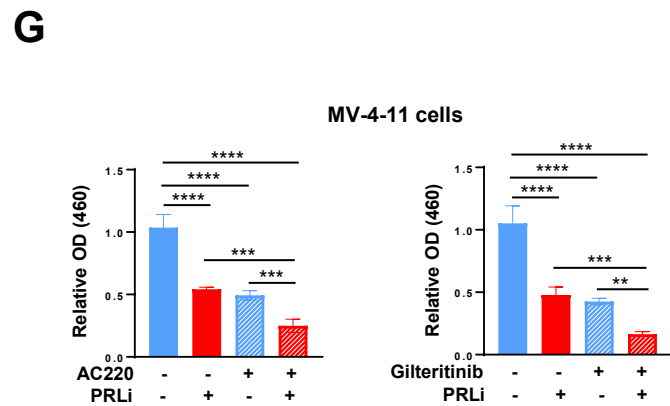
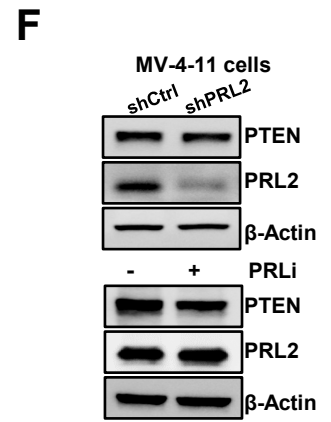
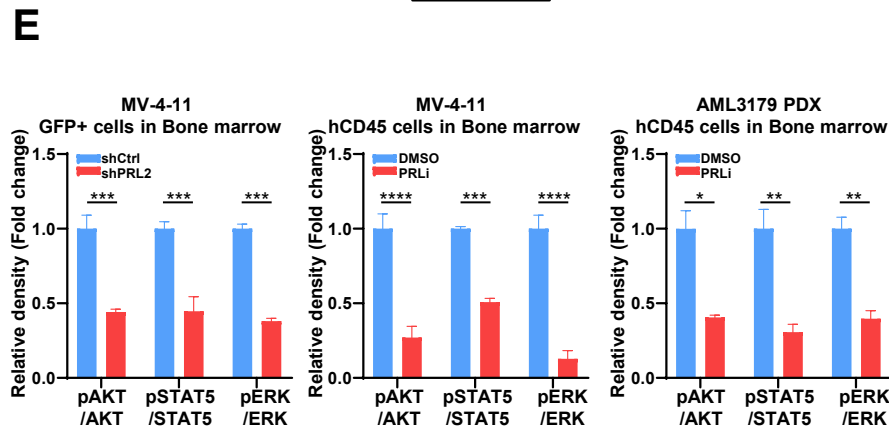
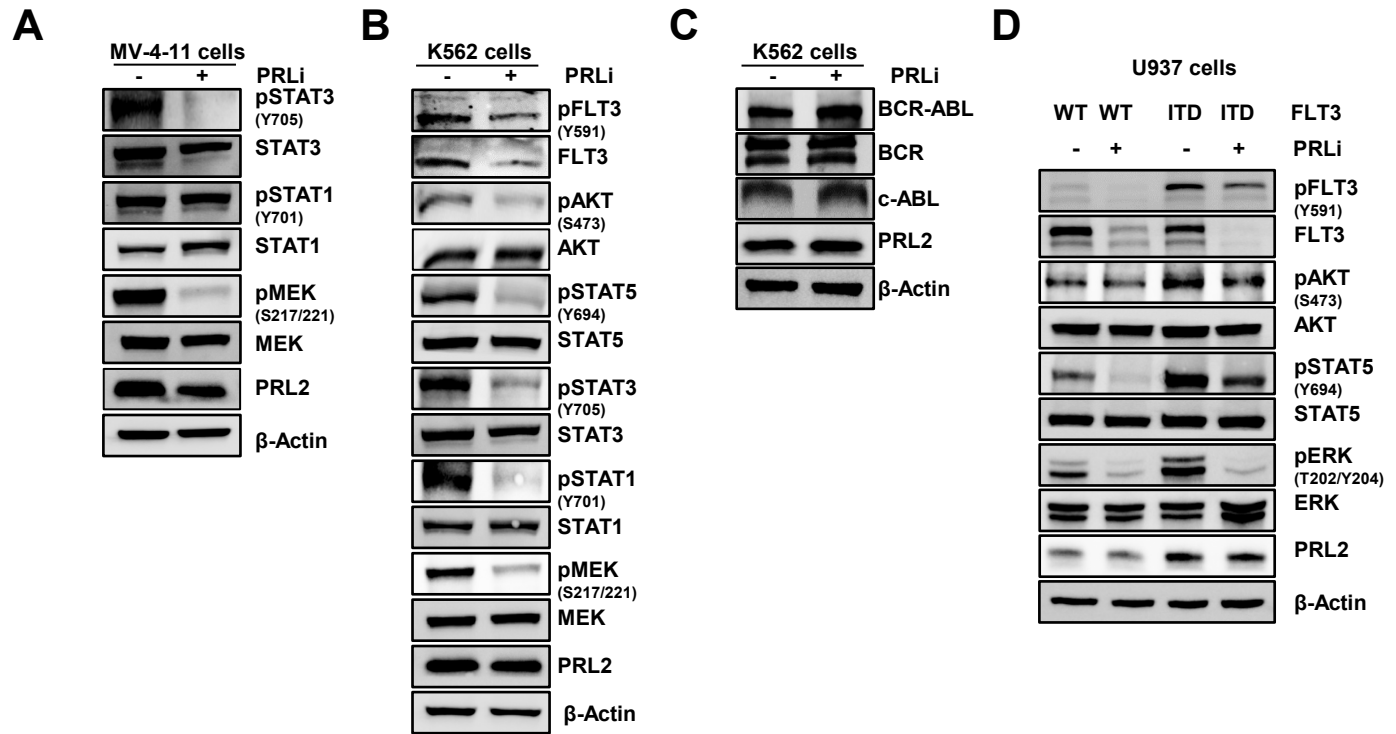
G

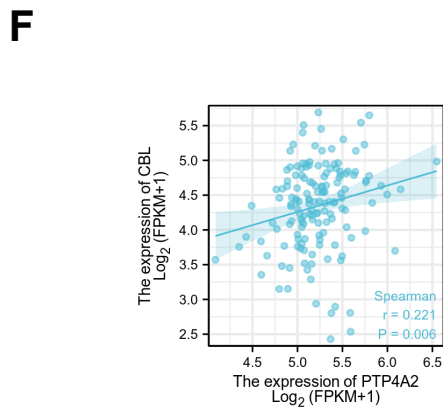
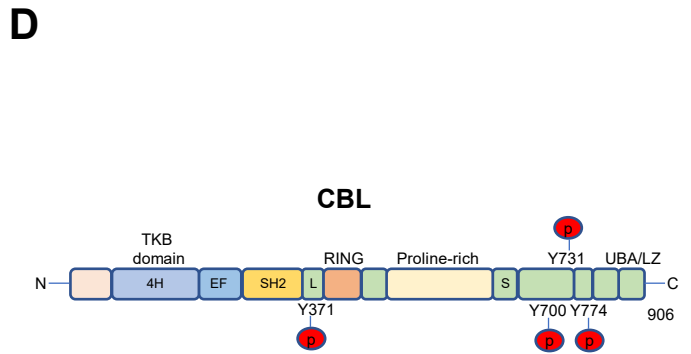
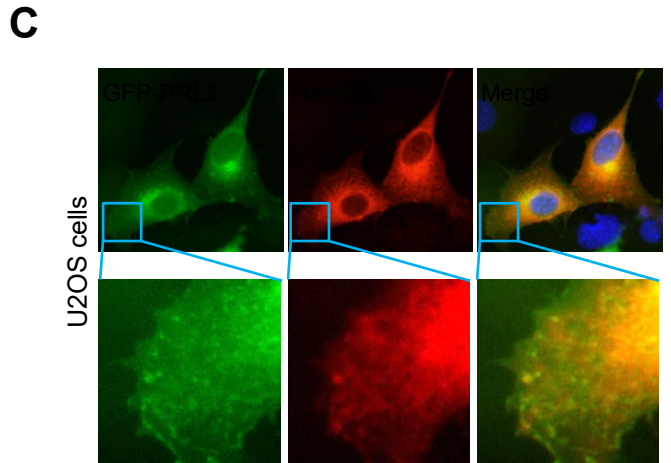
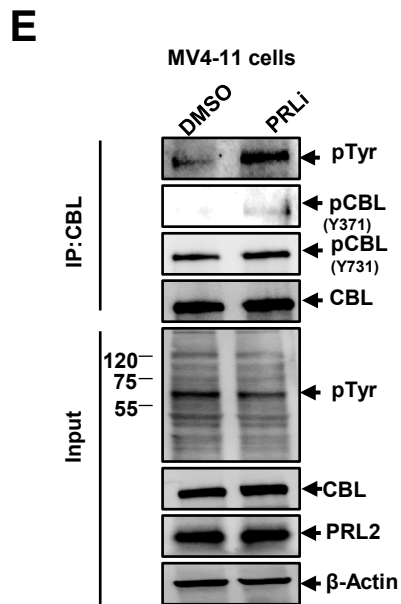
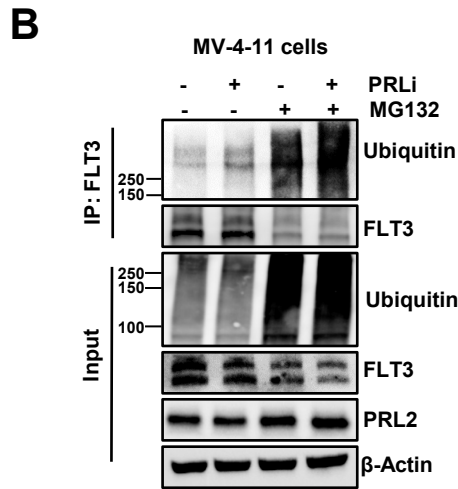
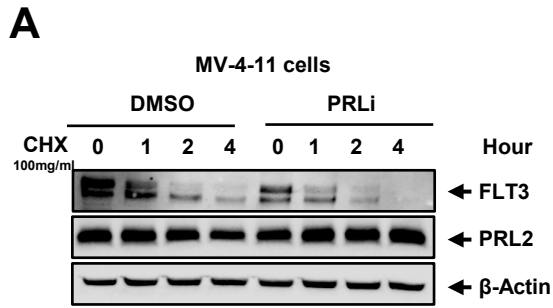


H









Supplementary Table 1. Clinical information relevant to AML patient samples

Sample#	Age	Sex	Sample type	Disease Status	Karyotype	Mutations	WBC
3142	56	F	BM	Relapse	t(12;15)[4] XX	FLT3-ITD	6.4K
3150	55	F	PB	Relapse	(46,XX)[20]//Donor (46,XY)[7]	FLT3-ITD	19.5K
3163	63	F	PB	New diagnosis	Normal karyotype	FLT3-ITD,NPM1	38K
3179	46	M	BM	Relapse	Normal karyotype	FLT3-ITD	31K
3220	33	F	BM	New diagnosis	Normal karyotype	KRAS,ASXL1,WT1, FLT3-ITD	69K
3242	56	F	BM	New diagnosis	Normal karyotype	FLT3-ITD,NPM1, PTPN11	81K
3080	37	F	BM	New diagnosis	Normal karyotype	FLT3-ITD	70K
3145	69	M	BM	New diagnosis	trisomy 8	FLT3-ITD	76K
3202	25	M	PB	New diagnosis	Normal karyotype	Negative Flt3 mutation	63k
3153	26	M	BM	Relapse	Complex	Negative Flt3 mutation	10K

BM= Bone Marrow; PB=Peripheral Blood

Supplementary Table 2. Key resources

Reagents or Resource	Source	Identifier
Western-Blot antibodies		
pAKT-S473	Cell signaling Technologies	9271
AKT	Cell signaling Technologies	4691S
pSTAT5-Y694	Cell signaling Technologies	9351
STAT5	Cell signaling Technologies	9420S
pERK-T202/Y204	Cell signaling Technologies	9101
ERK	Cell signaling Technologies	9102
β -Actin	Cell signaling Technologies	3700
Ubiquitin	Cell signaling Technologies	3936
PLCy	Cell signaling Technologies	5690
SHP2	Cell signaling Technologies	3397
CBL-human	Cell signaling Technologies	8447s
CBL-Y774	Cell signaling Technologies	3555
CBL-Y731	Cell signaling Technologies	3554
CBL-Y700	Cell signaling Technologies	8869
FLT3	Cell signaling Technologies	3462S
pFLT3	Cell signaling Technologies	3464
pSTAT3-Y705	Cell signaling Technologies	9145S
STAT3	Cell signaling Technologies	12640S
pSTAT1-Y701	Cell signaling Technologies	9167S
STAT1	Cell signaling Technologies	14994S
pMEK-Y217/221	Cell signaling Technologies	9154S
MEK	Cell signaling Technologies	4694S
Anti-mouse IgG, HRP-linked Antibody	Cell signaling Technologies	7076
Anti-rabbit IgG, HRP-linked Antibody	Cell signaling Technologies	7074
PRL2	Sigma Aldrich	05-1583
pTyr	Sigma Aldrich	05-321
CBL-Y371	Syed Feroj Ahmed et al., 2021	
CBL-mouse	Transduction	C40320
Flow Cytometry antibodies		
FITC anti-mouse/human CD45R/B220 Antibody	biolegend	103206
PE/Cy7 anti-mouse CD3 ϵ Antibody (100 μ g)	biolegend	100320
APC/Cy7 anti-mouse/human CD11b Antibody	biolegend	101226
PerCP/Cyanine5.5 anti-mouse Gr-1 Antibody	biolegend	108428
APC anti-mouse CD45.2 Antibody	biolegend	109814
PE anti-mouse CD45.1 Antibody	biolegend	110708
APC/Cy7 Streptavidin	biolegend	405208
Pacific Blue™ anti-mouse Sca-1 Antibody	biolegend	108120
PE/Cy7 anti-mouse CD117 (c-Kit) Antibody	biolegend	105814
PerCP/Cy5.5 anti-mouse CD150 Antibody	biolegend	115922
APC anti-mouse CD48 Antibody	biolegend	103412
FITC anti-mouse CD45.2 Antibody	biolegend	109806
APC/Cy7 Streptavidin	biolegend	405208
PerCP/Cyanine5.5 anti-mouse Sca-1 Antibody	biolegend	108124
PE anti-mouse CD117 (c-Kit) Antibody	biolegend	105808
antimouse CD34 APC	biolegend	128612
PE/Cy7 anti-mouse CD16/32 Antibody	biolegend	101318
Pacific Blue™ anti-mouse CD45.1 Antibody	biolegend	110722
Biotin anti-mouse Lineage Panel	biolegend	133307
PE Anti-mouse CD45	biolegend	103105
BD Pharmingen™ APC Mouse Anti-Human CD45	BD Biosciences	555485

Continue to Supplementary Table 2. Key resources

Reagents or Resource	Source	Identifier
Chemicals, Culture medium		
PRLi (Cmpd43)	Yunpeng et al. (2016)	
RIPA buffer	Sigma-Aldrich	R0278
RBC lysis buffer	Biologend	420302
Fetal Bovine Serum	GeminiBio	100-106
Antibiotic-Antimycotic	Gibco™	15240062
MethoCult™ GF M3434	Stem cell tech	M3434
MethoCult™ GF H4435	Stem cell tech	H4435
Critical commercial assays		
PureLink™ HiPure Plasmid Maxiprep Kit	Life tech corp	K210007
DNeasy Blood & Tissue Kit (50)	Qiagen	69504
MiniRNA universal kit	Qiagen	74134
MicroRNA universal kit	Qiagen	74034
FastStart Universal SYBR Green Master (Rox)	Sigma-Aldrich	4913850001
SuperScript™ IV First-Strand Synthesis System	invitrogen	18091200
Mouse Lin-cell depletion kit	Miltenyi Biotec	130-090-858
Human CD45 cell enrichment kit	Miltenyi Biotec	130-104-694
Mouse Kit+ cell selection kit	Miltenyi Biotec	130-091-224
Cell cycle kit	Abcam	ab139418
Apoptosis kit	Abcam	ab214485
Cell Proliferation Reagent WST-1	Sigma-Aldrich	11644807001
Deposited data		
RNA-seq data	Klein HU et al., 2009	GEO:GSE15434
RNA-seq data	This paper	GEO:GSE208136
TCGA	The Cancer Genome Atlas Program	https://www.cancer.gov/tcga
cBioPortal	Cerami et al., 2012 & Gao et al., 2013	https://www.cbioportal.org/
Software		
Gene set enrichment analysis	Subramanian et al. (2005)	https://www.gsea-msigdb.org/gsea/index.jsp
Rstudio 4.1.0	RStudio Team (2020)	http://www.rstudio.com/
GraphPad Prism 9	GraphPad	https://www.graphpad.com/
FlowJo_v10	BD Life Sciences	https://www.flowjo.com/solutions/flowjo/
Image J	Schneider et al., 2012	https://imagej.nih.gov/ij/
Experimental Models: Cell Lines		
MV-4-11	ATCC	CRL-9591
K562	ATCC	CCL-243
32D	ATCC	CRL-11346
293	ATCC	CRL-1573
U937	ATCC	CRL-1593.2
MOLM-13	Accegen Biotechnology	ABC-TC517S
Experimental Models: Organisms/Strains		
NOD-scid IL2Rgnull-3/GM/SF(NSGS)	The Jackson Laboratory	#013062
NOD.Cg-Prkdcscid Il2rgtm1Wjl/SzJ (NSG)	The Jackson Laboratory	#005557
B6.SJL(CD45.1+)	The Jackson Laboratory	#002014
C57BL/6 (CD45.2+)	The Jackson Laboratory	#000664
C3H/HeJ	The Jackson Laboratory	#000659

1 **PRL2 phosphatase promotes oncogenic KIT signaling in leukemia cells via dephosphorylation of**
2 **the E3 ubiquitin ligase CBL**

3
4 Hongxia Chen^{1,2,16#}, Yunpeng Bai^{3#}, Michihiro Kobayashi⁴, Shiyu Xiao², Sergio Barajas^{2,4}, Wenjie Cai^{2,4},
5 Sisi Chen⁴, Jinmin Miao³, Frederick Nguele Meke³, Chonghua Yao^{4,5}, Yuxia Yang^{4,6}, Katherine Strube⁴,
6 Odelia Satchivi⁴, Jiangmen Sun⁷, Lars Rönstrand⁷, James M. Croop⁴, H. Scott Boswell⁸, Yuzhi Jia⁹,
7 Huiping Liu^{9,10}, Loretta S. Li^{10,11}, Jessica K. Altman^{2,10}, Elizabeth A. Eklund^{2, 10, 12}, Peng Ji^{10,13}, Hamid
8 Band¹⁴, Danny T. Huang¹⁵, Leonidas C. Plataniias^{2,10,12}, Zhong-Yin Zhang^{3*}, and Yan Liu^{2,10*}

9
10 ¹Department of Hematology and Oncology, Chongqing University Three Gorges Hospital, Chongqing,
11 China. ²Department of Medicine, Northwestern University, Chicago, USA. ³Department of Medicinal
12 Chemistry and Molecular Pharmacology, Center for Cancer Research, and Institute for Drug Discovery,
13 Purdue University, West Lafayette, USA. ⁴Department of Pediatrics, Indiana University School of
14 Medicine, Indianapolis, USA. ⁵Shanghai Municipal Hospital of Traditional Chinese Medicine, Shanghai,
15 China. ⁶Department of Medical Genetics, Peking University Health Science Center, Beijing, China.
16 ⁷Division of Translational Cancer Research and Lund Stem Cell Center, Lund University, Lund, Sweden.
17 ⁸Department of Medicine, Indiana University School of Medicine, Indianapolis, USA. ⁹Department of
18 Pharmacology, Northwestern University, Chicago, USA. ¹⁰Robert H. Lurie Comprehensive Cancer
19 Center, Chicago, USA. ¹¹Department of Pediatrics, Northwestern University, Chicago, IL 60611, USA.
20 ¹²Department of Medicine, Jesse Brown VA Medical Center, Chicago, Illinois, USA. ¹³Department of
21 Pathology, Northwestern University, Chicago, USA. ¹⁴ Department of Genetics, University of Nebraska
22 Medical Center, Omaha, Nebraska, USA. ¹⁵Cancer Research UK Beatson Institute and Institute of Cancer
23 Sciences, University of Glasgow, Glasgow, United Kingdom. ¹⁶School of Medicine, Chongqing
24 University, Chongqing, China.

25 # These authors contributed equally to the paper

26 *Correspondence: zhang-zy@purdue.edu; yan.liu@northwestern.edu

27 Acute myeloid leukemia (AML) is an aggressive blood cancer with poor prognosis.¹ Most human
28 leukemia cells depend on aberrant receptor tyrosine kinase signaling and the subsequent downstream
29 effectors for proliferation and survival.² KIT is one of the oncogenic receptor tyrosine kinases that are
30 aberrantly activated in leukemia.³⁻⁴ Activating mutations in *KIT* are confined to either the extracellular
31 (exon 8 mutations) or the PTK2 domain (D816 mutations). Both classes of *KIT* mutations have been
32 identified predominantly in core binding factor (CBF) leukemia and are associated with poor prognosis
33 and reduced survival.³⁻⁵ As there are no effective therapies for leukemia patients with *KIT* mutations,⁴⁻⁵
34 novel therapeutic approaches are urgently needed to improve leukemia treatment. The **p**hosphatase of
35 **r**egenerating **l**iver (PRL) family of phosphatases, consisting of PRL1, PRL2, and PRL3, represents an
36 intriguing group of proteins that are being pursued as biomarkers and therapeutic targets in human
37 cancers, including hematological malignancies.⁶⁻⁷ PRL2, encoded by *PTP4A2* gene, is highly expressed
38 in some subtypes of AML, including AML1-ETO⁺ AML and AML with mixed lineage leukemia (MLL)
39 translocations.⁷ While PRL2 is important for SCF/KIT signaling in hematopoietic stem and progenitor
40 cells (HSPCs) and leukemia cells,⁷⁻⁸ the underlying mechanism is not fully understood.

41 Enforced KitD814V expression in HSPCs induces myeloproliferative neoplasms (MPN) in mice⁹ and we
42 found that PRL2 deficiency significantly delays the onset of MPN induced by the KitD814V in mice
43 (Figure 1A), demonstrating that PRL2 is important for KitD814V-driven MPN *in vivo*. To determine the
44 role of PRL2 (*PTP4A2*) in the pathogenesis of human AML, we analyzed the published TCGA
45 (<https://www.cancer.gov/about-nci/organization/ccg/research/structural-genomics/tcga>) dataset and
46 found that high *PRL2* expression is correlated with activation of oncogenic KIT signaling in AML (Figure
47 1B). Kasumi-1 and SKNO-1 are human AML cell lines with *KIT* mutations.⁷ To examine the impact of
48 PRL2 deficiency on human leukemia cell proliferation, we have developed two shRNAs targeting
49 different regions of human *PRL2* and showed that these shRNAs can efficiently decrease PRL2 proteins
50 in human leukemia cells.⁷ We focused our studies on one of the PRL2 shRNA and found that knockdown
51 of PRL2 decreases the colony formation of both Kasumi-1 and SKNO-1 cells (Figure 1C, *Online*

52 *Supplementary Figure S1A*). To determine the impact of PRL2 deficiency on leukemia development *in*
53 *vivo*, we transplanted 3×10^6 Kasumi-1 cells expressing control or PRL2 shRNA into sublethally-
54 irradiated NSG mice and monitored their survival. We found that loss of PRL2 significantly extended the
55 survival of recipient mice transplanted with Kasumi-1 cells (Figure 1D). Notably, genetic inhibition of
56 PRL2 significantly decreases the engraftment of Kasumi-1 cells in peripheral blood (PB), bone marrow
57 (BM), and spleen of recipient mice (Figure 1E). Furthermore, knockdown of PRL2 significantly decreased
58 splenomegaly seen in recipient mice transplanted with Kasumi-1 cells (Figure 1F).

59 To further substantiate the PRL2 knockdown results, we utilized compound 43,^{7,10} a small molecule PRL
60 inhibitor (PRLi) that blocks PRL trimerization, which is essential for PRL function. We found that PRLi
61 treatment reduces the colony formation of both Kasumi-1 and SKNO-1 cells (Figure 1G, *Online*
62 *Supplementary Figure S1B*). To determine the efficacy of PRLi on human leukemia cells *in vivo*, we
63 transplanted luciferase-labeled Kasumi-1 cells into sublethally-irradiated NSG mice via tail vein injection.
64 One week after the transplantation, we treated NSG mice with vehicle (10% DMSO) or PRLi (25 mg/kg,
65 I.P.) daily for three weeks. Leukemia burden in NSG mice was monitored via bioluminescence imaging.
66 Imaging of luminescence showed that PRLi treatment dramatically decreases leukemia burden compared
67 with the control group (Figure 1H). The radiance of the NSG mice was significantly reduced after
68 exposure to PRLi (Figure 1I). Furthermore, PRLi treatment substantially extended the survival of NSG
69 mice transplanted with human leukemia cells (Figure 1J). PRLi also considerably decreased the
70 engraftment of human leukemia cells in PB, BM, and spleen of NSG mice (Figure 1K). Finally, PRLi
71 treatment significantly reduced spleen weight of NSG mice (Figure 1L).

72 Attenuation of Kit signaling is important to obtain a suitable intensity and duration of signal
73 transduction to meet the biological needs. There are at least three levels of Kit downregulation that
74 function in concert: (1) tyrosine dephosphorylation, (2) inactivation of the kinase domain by serine
75 phosphorylation, and (3) removal from the cell surface and intracellular degradation.³ We first examined
76 Kit activation in *Prl2*^{-/-} hematopoietic stem and progenitor cells (HSPCs) following SCF stimulation.

77 PRL2 null HSPCs showed decreased Kit phosphorylation at tyrosine 703 as well as ERK1/2 and AKT
78 phosphorylation following SCF stimulation (Figure 2A), indicating that Kit^{Y703} is not a substrate of
79 PRL2. To further characterize Kit phosphorylation in the absence of PRL2, we utilized mast cells (MCs)
80 derived from BM cells (*Online Supplementary Figure S1C*).¹¹ Given that PKC-dependent
81 phosphorylation is a known negative feedback mechanism of Kit,¹² we examined the phosphorylation
82 status of Kit^{S744} (human S746) in MCs following SCF stimulation using a phospho-specific antibody.
83 PRL2 null MCs showed decreased Kit phosphorylation at serine744 upon SCF stimulation (Figure 2B),
84 suggesting that the negative feedback mechanism does not function in MCs. We found that Kit
85 internalization was enhanced in *Prl2*^{-/-} MCs compared to *Prl2*^{+/+} cells following SCF stimulation (Figure
86 2C). Importantly, PRL2 null MCs had progressively reduced Kit expression on cell surface during SCF-
87 induced differentiation (*Online Supplementary Figure S1D*). In addition, we observed reduced Kit
88 expression on the surface of human AML cell line MO7e expressing either a shRNA targeting PRL2 or
89 overexpressing a catalytically inactive PRL2-CSDA mutant (*Online Supplementary Figure S1E*). We
90 then treated serum starved MCs with cycloheximide and measured the half-life of Kit protein. The half-
91 life of Kit in *Prl2*^{-/-} MCs was significantly shorter than that of the *Prl2*^{+/+} MCs (Figure 2D).
92 Furthermore, *Prl2*^{-/-} MCs showed enhanced Kit ubiquitination compared to WT cells following SCF
93 stimulation (Figure 2E).

94 The CBL family E3 ubiquitin ligases, including CBL and CBL-B, are responsible for the ubiquitination
95 and degradation of KIT in hematopoietic cells.¹³⁻¹⁴ In response to cytokine stimulation, CBL is
96 phosphorylated and activated, leading to ubiquitination and degradation of KIT.¹³⁻¹⁵ However, how CBL
97 phosphorylation is regulated in leukemia cells remains elusive. Notably, GSEA analysis revealed that high
98 PRL2 expression is correlated with CBL signaling in human leukemia patients (Figure 2F). Upon SCF
99 stimulation, KIT binds to and induces the phosphorylation of CBL proteins, which in turn act as E3 ligases,
100 mediating the ubiquitination and degradation of KIT.¹³⁻¹⁴ We found that the catalytically inactive mutant
101 PRL2-CSDA displays enhanced association with KIT, CBL, SHP2, and PLC- γ compared to WT PRL2 in

102 Kasumi-1 cells (Figure 2G). We confirmed the association of PRL2 with CBL and KIT in Kasumi-1 and
103 SKNO-1 cells (Figure 2H, *Online Supplementary Figure S2A, B*). In addition, we found that
104 overexpression of PRL2 increases KIT levels in HEK293 cells (*Online Supplementary Figure S2C*) and
105 we confirmed the PRL2 and CBL interaction in HEK293 cells expressing KitD814V (*Online*
106 *Supplementary Figure S2D*). CBL becomes activated upon Tyrosine 371 phosphorylation, which enables
107 it to target receptor protein tyrosine kinases for ubiquitin-mediated degradation.¹⁵ Indeed, we found that
108 knockdown of PRL2 increases CBL phosphorylation at tyrosine 371, whereas the levels of CBL
109 phosphorylation at tyrosine 731 was not affected by PRL2 inhibition in both Kasumi-1 and SKNO-1 cells
110 (Figure 2I, *Online Supplementary Figure S2E*). Further, we found that ectopic expression of the PRL2-
111 CSDA mutant also increases CBL phosphorylation at tyrosine 371 in Kasumi-1 and SKNO-1 cells (Figure
112 2J, *Online Supplementary Figure S2F*).

113 In summary, we discovered that PRL2 promotes oncogenic KIT signaling by dephosphorylating CBL at
114 tyrosine 371 and inhibits its E3 ubiquitin ligase activity toward KIT, leading to decreased ubiquitination
115 of KIT and activation of downstream signaling pathways in leukemia cells. Furthermore, genetic and
116 pharmacological inhibition of PRL2 blocks oncogenic KIT driven AML *in vivo*. Our studies uncover a
117 novel mechanism that fine-tunes oncogenic KIT signaling in leukemia cells and will likely establish PRL2
118 as a druggable target in AML with *KIT* mutations.

119

120

121 **References**

- 122 1. Roboz GJ. Current treatment of acute myeloid leukemia. *Curr Opin Oncol.* 2012; 24:711-9.
- 123 2. Toffalini F, Demoulin JB. New insights into the mechanisms of hematopoietic cell transformation
124 by activated receptor tyrosine kinases. *Blood.* 2010;116:2429-2437.
- 125 3. Lennartsson J, Rönstrand L. Stem cell factor receptor/c-Kit: from basic science to clinical
126 implications. *Physiol Rev.* 2012;92:1619-49.
- 127 4. Longley BJ, Reguera MJ, Ma Y. Classes of c-KIT activating mutations: proposed mechanisms of
128 action and implications for disease classification and therapy. *Leuk Res.* 2001;25:571-576.
- 129 5. Schnittger S, Kohl TM, Haferlach T, *et al.* KIT-D816 mutations in AML1-ETO-positive AML are
130 associated with impaired event-free and overall survival. *Blood.* 2006;107:1791-9.
- 131 6. Campbell AM, Zhang ZY. Phosphatase of regenerating liver: a novel target for cancer therapy.
132 *Expert Opin Ther Targets.* 2014;18:555-69.
- 133 7. Kobayashi M, Chen S, Bai Y, Yao C, Gao R, Sun XJ *et al.* Phosphatase PRL2 promotes AML1-
134 ETO-induced acute myeloid leukemia. *Leukemia.* 2017;31:1453-1457.
- 135 8. Kobayashi M, Bai Y, Dong Y, Yu H, Chen S, Gao R *et al.* PRL2/PTP4A2 phosphatase is important
136 for hematopoietic stem cell self-renewal. *Stem Cells.* 2014; 32:1956-67.
- 137 9. Ma P, Mali RS, Martin H, *et al.* Role of intracellular tyrosines in activating KIT-induced
138 myeloproliferative disease. *Leukemia.* 2012;26:1499-506.
- 139 10. Bai Y, Yu ZH, Liu S, *et al.* Novel Anticancer Agents Based on Targeting the Trimer Interface of the
140 PRL Phosphatase. *Cancer Res.* 2016;76:4805-15.
- 141 11. Hu P, Carlesso N, Xu M, *et al.* Genetic evidence for critical roles of P38 α protein in regulating mast
142 cell differentiation and chemotaxis through distinct mechanisms. *J Biol Chem.* 2012; 287:20258-69.
- 143 12. Edling CE, Pedersen M, Carlsson L, *et al.* Haematopoietic progenitor cells utilise conventional PKC
144 to suppress PKB/Akt activity in response to c-Kit stimulation. *Br J Haematol.* 2007;136:260-8.

- 145 13. Thien CB, Langdon WY. Cbl: many adaptations to regulate protein tyrosine kinases. *Nat Rev Mol*
146 *Cell Biol.* 2001; 2:294-307.
- 147 14. Zeng S, Xu Z, Lipkowitz S, Longley JB. Regulation of stem cell factor receptor signaling by Cbl
148 family proteins (Cbl-b/c-Cbl). *Blood.* 2005;105:226-32.
- 149 15. Ahmed SF, Buetow L, Gabrielsen M, et al. E3 ligase-inactivation rewires CBL interactome to elicit
150 oncogenesis by hijacking RTK–CBL–CIN85 axis. *Oncogene.* 2021;40:2149-2164.

151 **Acknowledgements**

152
153 YL was supported by NIH R01 HL150624, R56 DK119524, R56 AG052501, DoD W81XWH-18-1-0265,
154 DoD W81XWH-19-1-0575, the Leukemia & Lymphoma Society Translational Research Program award
155 6581-20 and the St. Baldrick's Foundation Scholar Award. YB, JM, FNM, and ZYZ were supported by
156 NIH R01 CA069202 and the Robert C. and Charlotte Anderson Chair Endowment. SB was supported
157 by a NIH F31 Award F31HL160120. HC was supported by Natural Science Foundation of Chongqing
158 cstc2020jcyj-msxmX0969. The authors would like to acknowledge the Flow Cytometry Core and In vivo
159 Therapeutic Core Laboratories at the Indiana University, which were sponsored, in part, by the NIDDK
160 Cooperative Center of Excellence in Hematology (CCEH) grant U54 DK106846.

161

162 **Author Contributions**

163 HC, YB, MK, ZYZ, and YL were responsible for the conception and/or design of the research. HC, YB,
164 MK, SX, SB, WC, SC, JM, FNM, CY, YY, KS, OS, JS, LR, YJ, HL, PJ, ZYZ and YL were involved in
165 acquisition, analysis or interpretation of data. JMC, HSB, LSL, JKA, EAE, HB, DTH, and LCP provided
166 reagents and constructive advice to the study. HC, YB, ZYZ, and YL wrote the manuscript. All authors
167 read, comment on, and approved the manuscript.

168 **Competing Interests**

169 The authors declared no competing interests.

170

171 **Figure Legends**

172

173 **Figure 1. Genetic and pharmacological inhibition of PRL2 blocks oncogenic KIT driven AML *in***

174 ***vivo*.** (A) PRL2 deficiency extended the survival of recipient mice transplanted with hematopoietic

175 progenitor cells expressing KitD814V; n= 9 mice per group. (B) Signaling by KIT in disease, KIT

176 pathway, signaling by SCF-KIT, regulation of KIT signaling, KIT receptor signaling pathway were

177 enriched in the *PRL2* high expression group compared to the *PRL2* low expression group in AML. (C)

178 Knocking down of PRL2 significantly decreased the colony formation of Kasumi-1 cells; n=3 independent

179 experiments performed in duplicate. Representative images of the colonies are shown. (D) Kaplan-Meier

180 survival curve of sublethally-irradiated NSG mice transplanted with 3×10^6 Kasumi-1 expressing shCtrl or

181 shPRL2; n=6 mice per group. (E) Flow cytometry quantification of GFP⁺ cells in peripheral blood (PB),

182 bone marrow (BM), and spleen of NSG mice transplanted with Kasumi-1 cells expressing control shRNA

183 or shPRL2; n=4 mice per group. (F) The weight of spleen from NSG mice transplanted with Kasumi-1

184 cells expressing control shRNA or shPRL2; n=4 mice per group. (G) PRL inhibitor (PRLi) treatment

185 significantly decreased the colony formation of Kasumi-1 cells; n=3 independent experiments performed

186 in duplicate. Representative images of the colonies are displayed. (H) 3×10^6 Kasumi-1 cells expressing

187 luciferase were injected into sublethally irradiated NSG mice. One week after the transplantation, NSG

188 mice were treated with DMSO or PRLi (25mg/kg, I.P.) daily for three weeks. The leukemia burden in

189 NSG mice were monitored by In Vivo Image System (IVIS) once a week for three weeks (n=3 mice per

190 group). (I) Quantitative results from bioimaging; n=3 mice per group. (J) Kaplan-Meier survival curve of

191 NSG mice treated with DMSO or PRLi; n=6 mice per group. (K) Flow cytometry analysis of human

192 CD45⁺ cells in PB, BM, and spleen of NSG mice transplanted with Kasumi-1 cells after three weeks of

193 DMSO or PRLi treatment; n=4 mice per group. (L) The spleen weights of NSG mice transplanted with

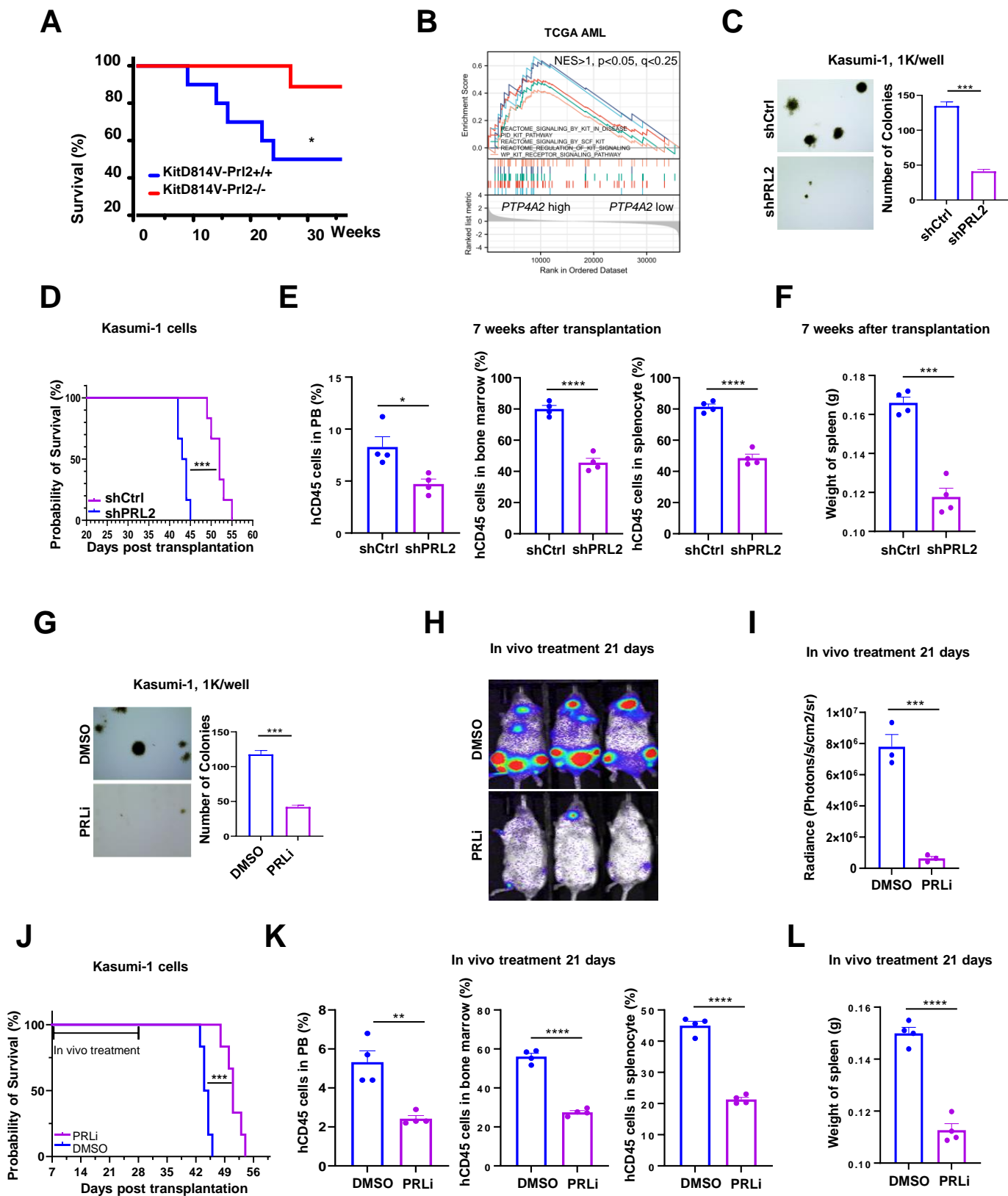
194 Kasumi-1 cells following three weeks of DMSO or PRLi treatment; n=4 mice per group. *p<0.05,

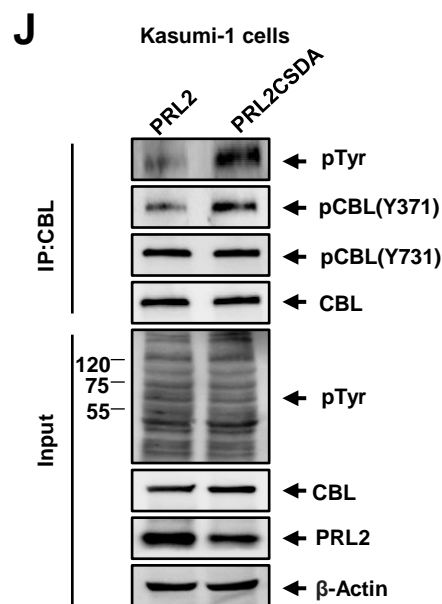
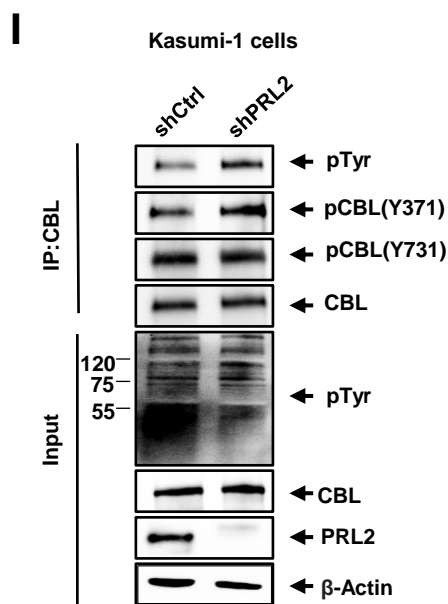
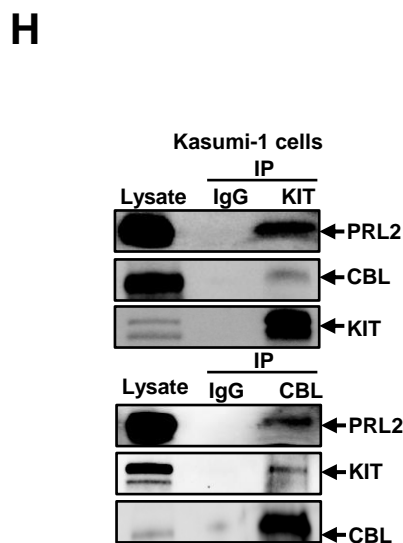
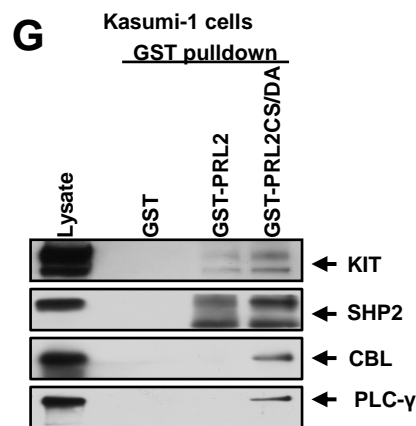
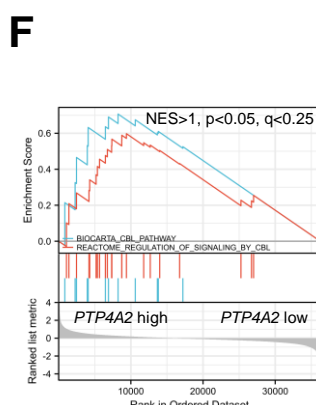
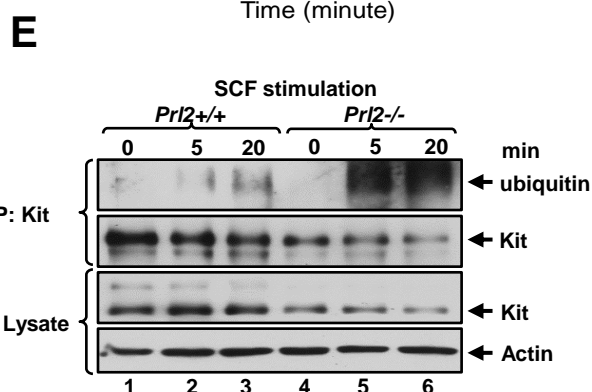
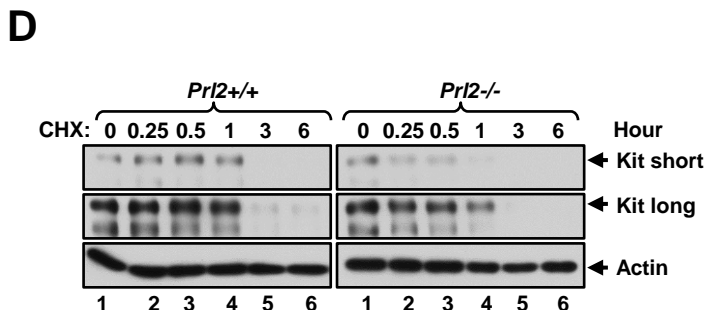
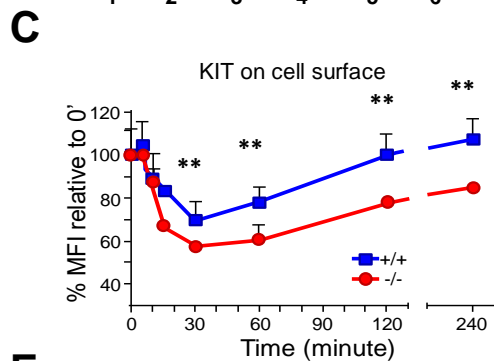
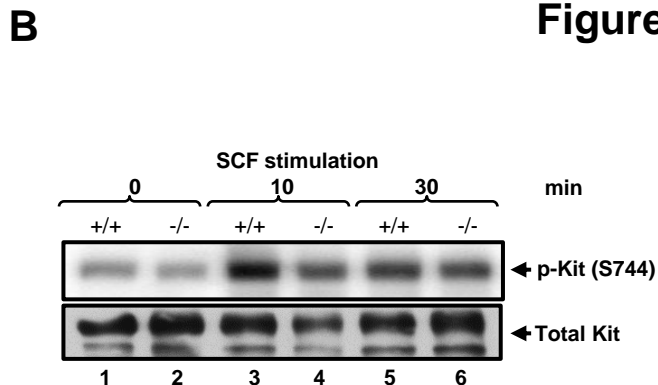
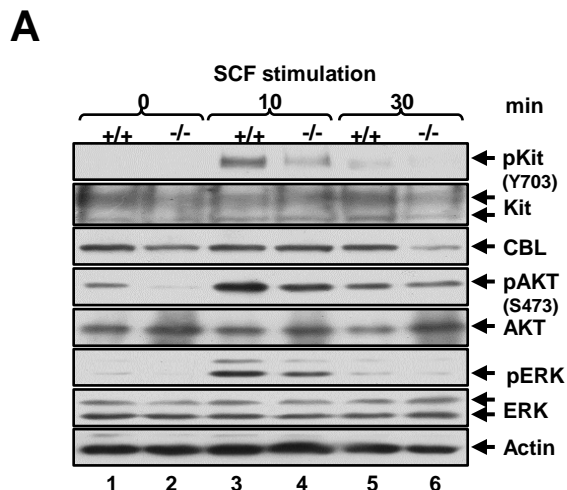
195 **p<0.01, ***p<0.001, ****p<0.0001.

196

197 **Figure 2. PRL2 enhances oncogenic KIT signaling in leukemia cells via dephosphorylating CBL at**
198 **tyrosine 371.** (A) PRL2 is important for KIT activation in HSPCs following SCF stimulation. (B) Mast
199 cells (MCs) were induced from WT and PRL2 null BM cells, serum starved, followed by stimulation of
200 SCF. Total cell lysates harvested at each time point were subjected to western blot analysis using
201 antibodies against KIT or KIT^{S746} (mouse KIT^{S744}). (C) MCs were stimulated with SCF. Levels of Kit on
202 the surface of MCs were determined by flow cytometry analysis; n=3. (D) PRL2 null MCs showed
203 decreased half-life of Kit following SCF stimulation. (E) Serum-starved MCs were stimulated with SCF,
204 collected at each time point, and followed by immunoprecipitation with a Kit antibody. Ubiquitinated
205 proteins were detected by immunoblotting with an anti-ubiquitin antibody. (F) CBL pathway and
206 regulation of signaling by CBL were enriched in the *PRL2* high expression group compared to the *PRL2*
207 low expression group in AML. (G) GST pull-down assays. Total cellular proteins from Kasumi-1 cells
208 were isolated, incubated with GST, GST-PRL2 or GST-PRL2-CSDA and immunoblotted with antibodies
209 against KIT, CBL, SHP2, and PLC- γ . (H) Co-immunoprecipitation assays showed that PRL2 interacts
210 with KIT and CBL in Kasumi-1 cells. (I) Knockdown of PRL2 increases CBL phosphorylation at Y371
211 in Kasumi-1 cells. (J) Ectopic expression of PRL2-CSDA increases CBL phosphorylation at Y371 in
212 Kasumi-1 cells. **p<0.01.

213





Supplementary Information

PRL2 phosphatase promotes oncogenic KIT signaling in leukemia cells via dephosphorylation of the E3 ubiquitin ligase CBL

Materials and Methods

Mice

B6.SJL (CD45.1⁺) and NOD.Cg-Prkdcscid Il2rgtm1Wjl/SzJ (NSG) mice were purchased from the Jackson Laboratories. *Prl2*^{+/+} and *Prl2*^{-/-} mice were maintained in the Indiana and Northwestern University Animal Facility and kept in Thorensten units with filtered germ-free air. The Institutional Animal Care and Use Committee (IACUC) of Indiana University School of Medicine and Northwestern University Feinberg School of Medicine approved all experimental procedures.

Human AML cell lines

Human AML cell lines, including Kasumi-1, SKNO-1, and MO7e were obtained from ATCC (List in table1). All cell lines were authenticated by SRT profiling and tested for mycoplasma contamination.

Transplantation assays

To determine the impact of PRL2 deficiency on KitD814V induced leukemia, 1 x 10⁶ KitD814V transduced Lin⁻ cells isolated from *PRL2*^{+/+} and *PRL2*^{-/-} mice were transplanted into lethally irradiated B6.SJL mice via tail vein.

To determine the impact of PRL2 deficiency or inhibition on human Kasumi-1 leukemia cells *in vivo*, 3 x 10⁶ transduced Kasumi-1 cells (GFP⁺) were injected into sublethally irradiated (2.5 Gy) NSG mice via tail vein. shCtrl or shPRL2 were used to study PRL2 deficiency.

PRLi treatment *in vivo*

Small molecule inhibitor of PRL (PRLi) was synthesized at the Department of Medicinal Chemistry and Pharmacology Department of the Purdue University. PRLi were dissolved in DMSO at 25mg/ml stocking concentration saved in -80°C freezer. PRLi stock solution or DMSO was diluted in PBS before administration. 25mg/kg PRLi or DMSO was administrated by intraperitoneal injection for consecutive

21 days.

***In vivo* image system**

Bioimaging of leukemia burden *in vivo* was performed by Spectral Lago System at Northwestern University Center for Advanced Microscopy generously supported by NCI CCSG P30 CA060553 awarded to the Robert H Lurie Comprehensive Cancer Center. Before imaging, Luciferin (in vivo grade, Gold Bio, CAS# 115144-35-9) was prepared in PBS, and 150 mg/kg Luciferin was injected by i.p., after 10 minutes. The signal data was analyzed by the Aura software.

Flow cytometry

To determine the engraftment in NSG mice, peripheral blood or bone marrow cells from NSG mice were obtained from tibia, femur and iliac crest (6 from each mouse) by flushing cells out of the bone using a syringe and phosphate-buffered saline (PBS) with 2mM EDTA. Red blood cells (RBCs) were lysed by RBC lysis buffer (eBioscience) prior to staining. Other cells were washed twice by PBS before staining. mCD45(103105), mCD117(105808), hCD117 (983302) FcεRIα (134316) were obtained from Biolegend. hCD45(555485) were obtained from BD Biosciences. Experiments were performed on FACS LSR IV cytometers (BD Biosciences) and analyzed by using the FlowJo_v10 software (TreeStar).

Production of Retrovirus and Lentivirus

Retroviral particles were produced by transfection of Phoenix E cells with MSCV-IRES-GFP, MSCV-PRL2-IRES-GFP, MSCV-PRL2-CSDA-IRES-GFP, MSCV-KITD814V-IRES-GFP plasmids, according to standard protocols. Mouse hematopoietic progenitor cells were transduced on retronectin (Takara)-coated non-tissue culture plates with high-titer retroviral suspensions. Twenty-four hours after infection, GFP-positive cells were sorted by FACS.

Lentiviral shLuciferase was a gift from Huipin Liu laboratory at the Northwestern University. Lentiviral

shRNA plasmid (pLB) was purchased from Addgene (11619). Oligonucleotides targeting control (Luciferase) and human PRL2 cDNAs were cloned into the pLB plasmid. Oligonucleotide sequences are available upon request. Lentiviral particles were generated by standard method using the third-generation packaging system (pMDL, pMD2.G, and pRSV-Rev). Human AML cell lines were infected with high-titer lentiviral suspensions. 48 hours after infection, GFP-positive cells were sorted by FACS. The reduction of PRL2 proteins was determined by immunoblot analysis.

Colony formation unit assays

The colony formation of human leukemia cells was determined in methylcellulose medium (MethoCult H4435, StemCell Technologies) using 1×10^3 Kaumi-1 or 5×10^4 SKNO-1 cells per well (6-well plate). Colonies were scored after 14 days of culture.

Generation of murine mast cells

We cultured low-density BM mononuclear cells from *PRL2*^{+/+} and *PRL2*^{-/-} mice in IMDM supplemented with 10% fetal calf serum (FCS; inactivated at 56°C), 2 mM L-glutamine, 1 mM pyruvate, 100 U of penicillin/ml, 100 µg of streptomycin/ml, 20 U of mIL-3/ml, and 50 U of mIL-4/ml. Nonadherent cells were transferred to fresh culture plates every 2 to 3 days for a total of at least 21 days to remove adherent macrophages and fibroblasts. The resulting cell population consisted of more than 95% BMDCs as determined by flow cytometry analysis using anti-mouse CD117 and anti-mouse FcεRIα antibody (Hu et al., 2012).

Immunoblotting analysis

Cells were washed with ice-cold PBS and lysed on ice for 30 min in lysis buffer (50 mM Tris-HCl, pH 7.4, 150 mM NaCl, 1% Triton X-100, and 10% glycerol) supplemented with a Complete Protease Inhibitor tablet (Roche Applied Science). Cell lysates were cleared by centrifugation at 15,000 rpm for 10 min. The lysate protein concentration was estimated using a BCA protein assay kit (Pierce). The

protein samples were boiled with sample buffer, separated by SDS-PAGE, transferred electrophoretically to a nitrocellulose membrane, and immunoblotted with appropriate antibodies, followed by incubation with horseradish peroxidase-conjugated secondary antibodies. The blots were developed by the enhanced chemiluminescence technique (ECL kit, GE Healthcare). Representative results from at least two independent experiments are shown. Representative results from at least two independent experiments are shown. pAKT-S473(9271), AKT(4691S), pERK-Y202/204(9101), ERK(9102), β -Actin(3700), Ubiquitin(3936), PLCy (5690), SHP2(3397), CBL-human(8447s), KIT (3074S), CBL-Y731(3554), were obtained from Cell signaling. CBL-mouse(C40320) was obtained from Transduction. PRL2(05-1583) and pTyr(05-321) were obtained from Sigma Aldrich. pCBL-Y371 and pKIT-S746 antibodies have been described previously (Edling et al., 2007; Ahmed et al., 2021).

GST pull down assays

1 x 10⁹ Kasumi-1 cells were treated with 1 mM pervanadate for 30 minutes and collected by centrifugation. The cell pellet was lysed with 3 ml lysis buffer (20 mM Tris, pH 7.5, 100 mM NaCl, 1% Triton X-100, 10% glycerol, supplemented with 5 mM iodoacetic acid, 1 mM orthovanadate, and proteases inhibitors). 10 mM DTT was added in the lysate and incubated for 15 min on ice to inactivate any unreacted iodoacetic acid and pervanadate. Supernatant was collected by centrifugation at 14,000 g for 15 min. 25 μ g GST, GST-PRL2 or GST-PRL2-CSDA were coupled to GST beads in lysis buffer, incubated at 4°C for 1h. Cell lysates were incubated with GST proteins conjugated to beads at 4 °C for 2h. The beads were pelleted and washed 3 times for 5 min with lysis buffer. Bound proteins were re-suspended in 50 μ L Laemmli sample buffer, boiled for 5 min, and the samples are resolved by SDS-PAGE gels.

Immunoprecipitation (IP) assays

For Immunoprecipitation (IP), Cells were washed with ice-cold PBS and lysed on ice for 30 min in lysis buffer (50 mM Tris-HCl, pH 7.4, 150 mM NaCl, 1% Triton X-100, and 10% glycerol) supplemented

with a Complete Protease and Phosphorylation Inhibitor tablet (Thermoscientific, A32961). Cell lysates were cleared by centrifugation at 15,000 rpm for 10 min. The lysate protein concentration was estimated using a BCA protein assay kit (Pierce). IP antibody plus Protein A Agarose beads (Sigma-Millipore) was added, and samples were incubated on shaker at 4 °C for overnight. After washing with lysis Buffer, the samples were ready for western blot analysis.

TCGA sequencing data

Transcriptional expression data of PRL2 and all data on clinical, cytogenetic characteristics, and survival were derived from TCGA official website (<https://www.cancer.gov/about-nci/organization/ccg/research/structural-genomics/tcga>). The Limma package in R Studio (version 4.1.0, RStudio Team (2020) was used to identify the DEGs between PRL2 high group (PRL2 expression above medium) and PRL2 low group (PRL2 expression below medium). $P < 0.05$ and $|\log_2 \text{fold change (FC)}| > 1$ was used as the cut-off criteria for volcano plot for clinic data and heat map for fetal liver sequencing data by R Studio. All the DEGs were used to do Gene-set enrichment analysis by GSEA v4.2.2 software (<http://www.gsea-msigdb.org/gsea/index.jsp>).

Statistical Analysis

Long rank test was used for Kaplan-Meier survival curves. Other data were analyzed by paired or unpaired t test or analysis of variance for nonlinear distributions using GraphPad Prism 9. Results are expressed as the mean \pm standard error of the mean (SEM) for at least triplicate experiments. P values of < 0.05 were regarded as statistically significant which was calculated by GraphPad Prism9. * $p < 0.05$, ** $p < 0.01$, *** $p < 0.001$, **** $p < 0.0001$.

Supplementary Figure Legends

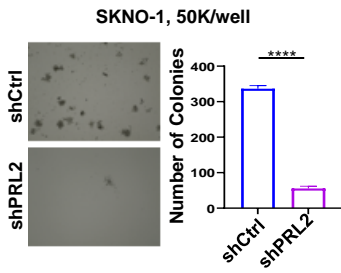
Supplementary Figure 1

(A) Knocking down of PRL2 significantly decreased the colony formation of SKNO-1 cells; n=3 independent experiments performed in duplicate. Representative images of the colonies are shown. (B) PRL inhibitor (PRLi) treatment significantly decreased the colony formation of SKNO-1 cells; n=3 independent experiments performed in duplicate. Representative images of the colonies are shown. (C) Mast cells were induced from BM cells *in vitro*. (D) Expression of KIT is progressively declined in PRL2 null MCs. MCs were induced from BM cells and KIT median fluorescent intensity (MFI) was measured by flow cytometry at each time point. (E) Knockdown of PRL2 in human AML cell line MO7e decreased the level of KIT on the cell surface (Left). MO7e cells were transduced with retroviruses expressing GFP, PRL2 or PRL2-CSDA mutant and the levels of KIT were assessed by flow cytometry analysis (Right). ****p<0.0001.

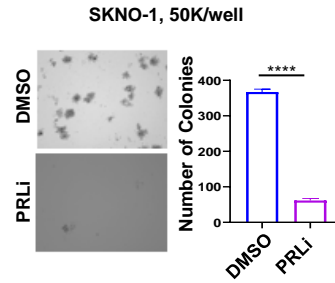
Supplementary Figure 2

(A) and (B) Co-immunoprecipitation assays showed that PRL2 interacts with KIT and CBL in SKNO-1 cells. (C) PRL2 regulates the level of KIT in a dosage-dependent manner in HEK293 cells. (D) PRL2 interacts with KitD814V and CBL in HEK293 cells. (E) Knockdown of PRL2 increases CBL phosphorylation at Y371 in SKNO-1 cells. (F) Ectopic expression of PRL2-CSDA increases CBL phosphorylation at Y371 in SKNO-1 cells.

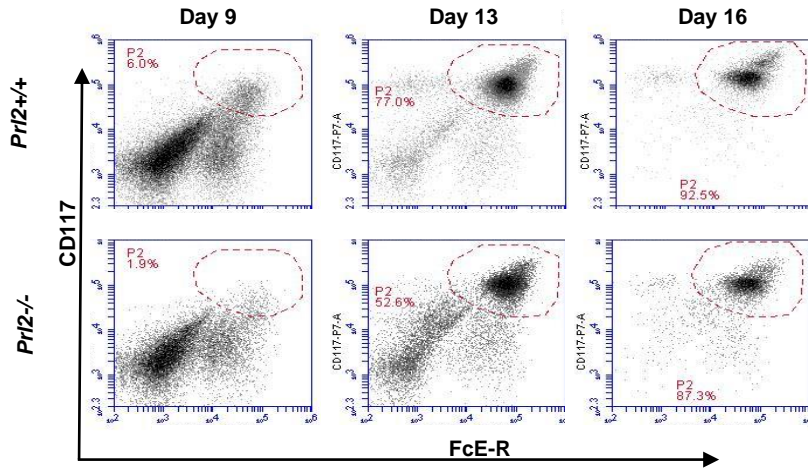
A



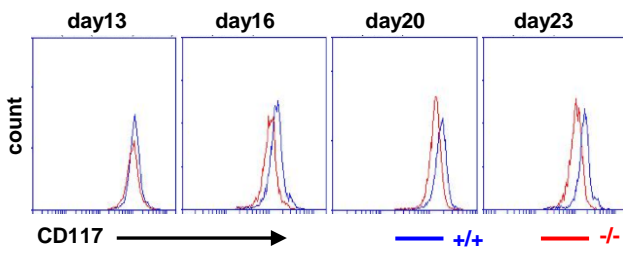
B



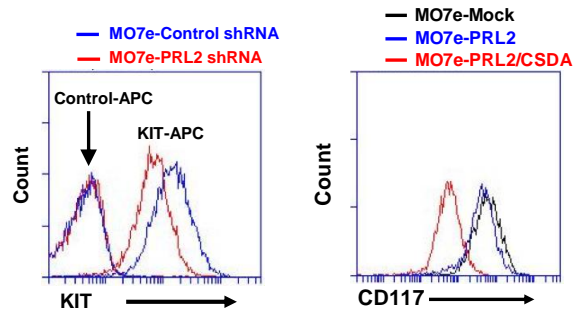
C



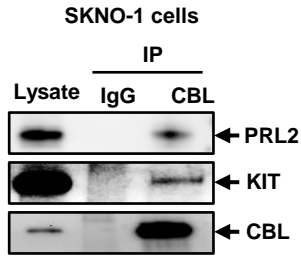
D



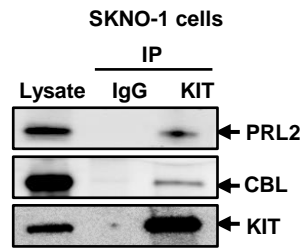
E



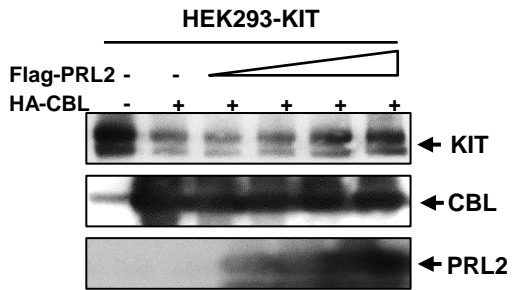
A



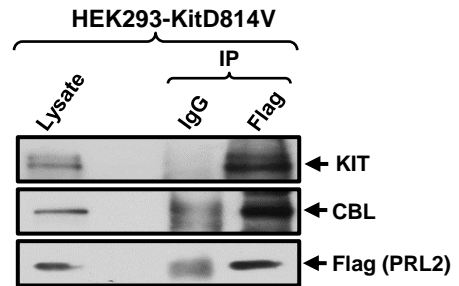
B



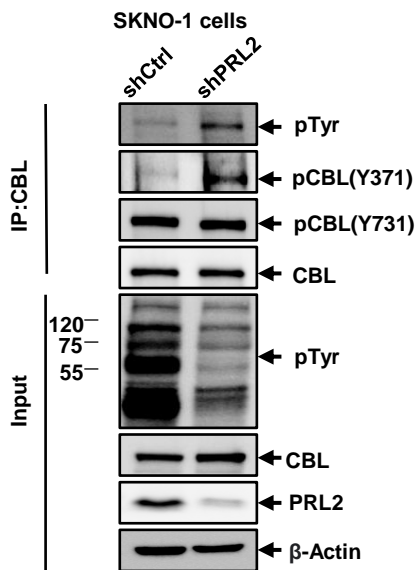
C



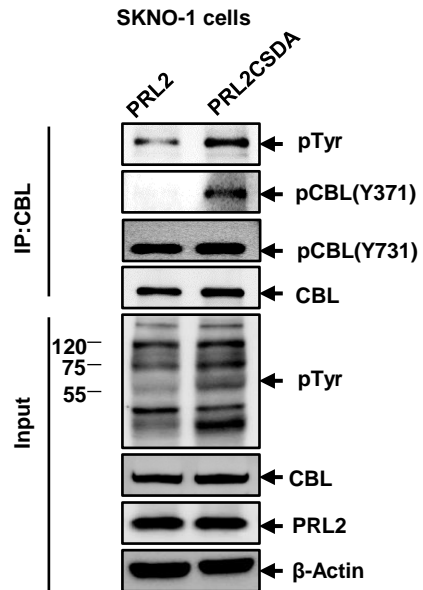
D



E



F



Leukemia (2019) 33:1535–1539
<https://doi.org/10.1038/s41375-019-0377-0>

Acute myeloid leukemia

Mutant p53 enhances leukemia-initiating cell self-renewal to promote leukemia development

Sarah C. Nabinger¹ · Sisi Chen² · Rui Gao¹ · Chonghua Yao^{1,3} · Michihiro Kobayashi¹ · Sasidhar Vemula¹ · Aidan C. Fahey¹ · Christine Wang¹ · Cecil Daniels¹ · H. Scott Boswell⁴ · George E. Sandusky⁵ · Lindsey D. Mayo¹ · Reuben Kapur¹ · Yan Liu^{1,2}

Received: 15 July 2018 / Revised: 20 December 2018 / Accepted: 24 December 2018 / Published online: 23 January 2019
© Springer Nature Limited 2019

To the Editor

Acute myeloid leukemia (AML) is an aggressive blood cancer with poor prognosis [1]. AML is thought to be initiated and maintained by a rare population of leukemia stem cells (LSCs) or leukemia-initiating cells (LICs) that have acquired the capacity for self-renewal and is blocked in their ability to differentiate by the accumulation of a series of mutations and/or epigenetic changes [2, 3]. Clinical studies show that LICs are resistant to conventional chemotherapy and/or targeted therapies [3]. Thus, there is an unmet need to elucidate the molecular mechanisms governing LIC self-renewal and develop novel therapeutic approaches that can target LICs and improve leukemia treatment [3].

The tumor suppressor p53 is a stress response protein that regulates a large number of genes in response to a variety of cellular insults, including oncogene activation,

DNA damage, and inflammation [4]. These signals activate p53 primarily through post-translational modifications that result in augmented levels of p53 protein and transactivation activity [4]. Activated p53 suppresses cellular transformation mainly by inducing growth arrest, apoptosis, DNA repair, and differentiation in damaged cells [4]. Accordingly, p53 function is always compromised in tumor cells, usually as a result of somatic mutations and deletions, which occur in approximately half of all human cancers [5]. The *TP53* gene encodes the tumor suppressor p53. The frequency of *TP53* mutations in AML is ~10%. However, in AML with complex karyotype, the frequency of *TP53* mutations and/or deletions is almost 70% [6]. While *TP53* mutations confer drug resistance and poor prognosis in AML, the role of mutant p53 in the initiation and progression of AML is largely unknown [6, 7].

We have been investigating the role of tumor suppressor p53 in normal and malignant hematopoiesis. We found that wild-type p53 maintains HSC quiescence and inhibits HSC self-renewal [8]. Codon 248 of p53 is frequently mutated in AML and p53^{R248W} has been shown to be a gain-of-function (GOF) mutant in human cancer cells as well as in animal models [6, 7, 9]. We recently reported that p53^{R248W} enhances HSC self-renewal in steady state and promotes HSC expansion following genotoxic stresses [10]. Of note, homozygous *p53*^{-/-} and *p53*^{R248W/R248W} mice develop lymphoid tumors, including lymphoma and thymoma, but not myeloid malignancies [9], suggesting that expression of mutant p53 is not sufficient for inducing myeloid leukemia in mice. This has led to a search for potential second hits that cooperate with mutant p53 in the pathogenesis of myeloid malignancies, primarily focused on using mouse models.

While coexisting mutations with *TP53* mutations in AML are limited [6, 7], previous studies indicate that *TP53* mutations co-occur with AML driver mutations in oncogenic

Supplementary information The online version of this article (<https://doi.org/10.1038/s41375-019-0377-0>) contains supplementary material, which is available to authorized users.

✉ Yan Liu
liu219@iu.edu

¹ Department of Pediatrics, Herman B Wells Center for Pediatric Research, Indiana University School of Medicine, Indianapolis, IN 46202, USA

² Department of Biochemistry and Molecular Biology, Indiana University School of Medicine, Indianapolis, IN 46202, USA

³ Department of Rheumatism, Shanghai Municipal Hospital of Traditional Chinese Medicine, Shanghai University of Traditional Chinese Medicine, Shanghai, China

⁴ Department of Medicine, Indiana University School of Medicine, Indianapolis, IN 46202, USA

⁵ Department of Pathology and Laboratory Medicine, Indiana University School of Medicine, Indianapolis, IN 46202, USA

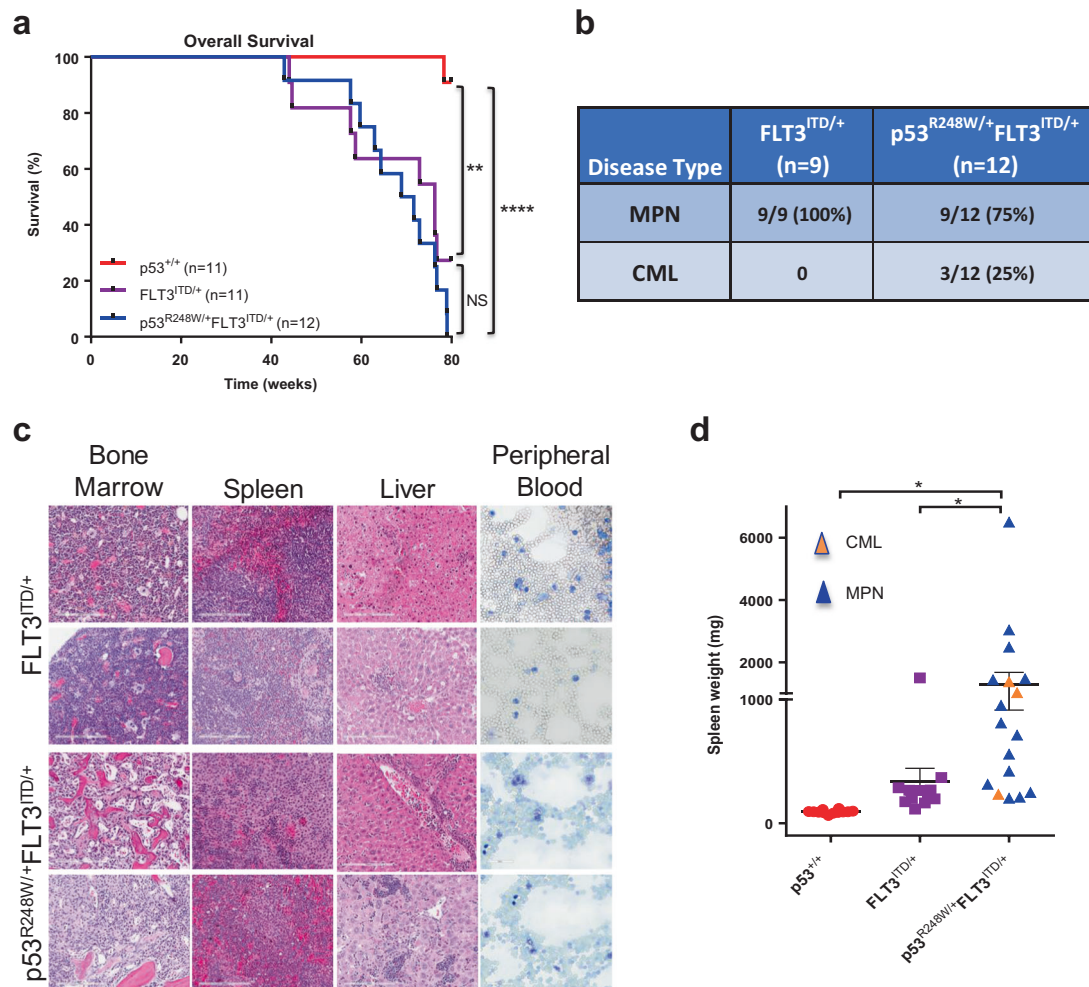


Fig. 1 Mutant p53 cooperates with FLT3-ITD in the pathogenesis of myeloid leukemia. **a** $FLT3^{ITD/+}$ and $p53^{R248W/+}FLT3^{ITD/+}$ mice show decreased survival compared to $p53^{+/+}$ mice ($n = 11$, $p53^{+/+}$; $n = 11$, $FLT3^{ITD/+}$; $n = 12$, $p53^{R248W/+}FLT3^{ITD/+}$, ** $p < 0.01$, **** $p < 0.0001$). **b** Disease spectrums in $FLT3^{ITD/+}$ and $p53^{R248W/+}FLT3^{ITD/+}$ mice were determined by pathological analysis of the bone marrow, spleen, liver, and peripheral blood ($n = 9$, $FLT3^{ITD/+}$; $n = 12$, $p53^{R248W/+}FLT3^{ITD/+}$).

c Representative H&E (20 \times) images of the bone marrow, spleen, liver, and peripheral blood smears from $FLT3^{ITD/+}$ mice with MPN and $p53^{R248W/+}FLT3^{ITD/+}$ mice with CML. **d** Spleen weight of $p53^{+/+}$, $FLT3^{ITD/+}$, and $p53^{R248W/+}FLT3^{ITD/+}$ mice. Mean values (\pm SEM) are shown ($n = 12$, $p53^{+/+}$; $n = 12$, $FLT3^{ITD/+}$; $n = 17$, $p53^{R248W/+}FLT3^{ITD/+}$, * $p < 0.05$).

signaling molecules, such as FMS-like tyrosine kinase receptor-3 (FLT3) [11]. Mutations in FLT3 have been identified in myeloid malignancies, including myeloproliferative neoplasms (MPN) and AML [12]. Internal tandem duplications in the juxtamembrane domain (FLT3-ITD) and mutations in the activating loop of FLT3 (FLT3-TKD) are seen in 30–35% of AML patients [12]. Both ITD and TKD mutations of FLT3 lead to constitutive activation of the tyrosine kinase, promoting proliferation, and survival of leukemic blasts [12]. Given that expression of FLT3-ITD in the hematopoietic compartment results in MPN in mice and that FLT3-ITD impairs HSC self-renewal in vivo [13], we reasoned that mutant p53 might synergize with FLT3-ITD in driving the development of myeloid leukemia through enhancing LIC self-renewal.

To test this hypothesis, we generated $p53^{R248W/+}FLT3^{ITD/+}$ mice and monitored overall survival and tumor development of these mice. We observed that both $FLT3^{ITD/+}$ and $p53^{R248W/+}FLT3^{ITD/+}$ mice have decreased life span compared with $p53^{+/+}$ mice (Fig. 1a). Some $p53^{R248W/+}$ mice develop myelodysplastic syndromes (MDS) with age and other $p53^{R248W/+}$ mice developed lymphoma and sarcoma based upon pathological analysis of the bone marrow (BM), spleen, liver, and peripheral blood (PB) (SC and YL, unpublished data). However, the majority of $p53^{R248W/+}FLT3^{ITD/+}$ mice developed MPN as seen in $FLT3^{ITD/+}$ mice (Fig. 1b, c and data not shown), suggesting that FLT3-ITD-induced MPN development does not depend on mutant p53. Histological observation of spleen sections from MPN mice showed disarray of normal splenic architecture with a

reduction and almost total absence of the white pulp in some cases and increased red pulp area with increased extramedullary hematopoiesis (Fig. 1c). These features appeared in conjunction with hepatosplenomegaly, variable leukocytosis and overproduction of myeloid cells in the bone marrow, spleen, and peripheral blood (Fig. 1c). We noted that the bone marrow cellularity decreased as splenomegaly increased, consistent with increased extramedullary hematopoiesis. Notably, ~25% of $p53^{R248W/+}FLT3^{ITD/+}$ mice developed chronic myeloid leukemia (CML) [14]. Upon necropsy, mice with CML displayed severe splenomegaly, and some also displayed hepatomegaly. Morphological analysis of peripheral blood smears revealed increased myeloid cells with dysplastic features (Fig. 1c). The bone marrow cellularity varied from hypocellular to hypercellular among animals. Increased number of myeloid cells (blast to immature myeloid cells) was observed in the bone marrow with extensive spread of myeloid elements in the spleen and in a few livers (Fig. 1c). While $p53^{R248W/+}FLT3^{ITD/+}$ mice showed marked splenomegaly compared with $p53^{+/+}$ and $FLT3^{ITD/+}$ mice (Fig. 1d), this is not likely due to CML development as majority of double-mutant mice developed MPN (Fig. 1b, c).

Given that patients with homozygous FLT3-ITD mutations have a more severe disease compared with those with heterozygous FLT3-ITD mutations [11, 12], we examined whether mutant p53 cooperates with homozygous FLT3-ITD mutant in leukemia development. We transplanted 3×10^6 whole bone marrow cells from $p53^{+/+}$, $FLT3^{ITD/ITD}$, or $p53^{R248W/+}FLT3^{ITD/ITD}$ mice into lethally irradiated recipient mice and measured their overall survival. Both $FLT3^{ITD/ITD}$ and $p53^{R248W/+}FLT3^{ITD/ITD}$ recipient mice had decreased life spans compared with $p53^{+/+}$ recipient mice (Figure S1a). Interestingly, ~30% of the $p53^{R248W/+}FLT3^{ITD/ITD}$ transplanted animals developed CML (Figure S1b), similar to that seen in $p53^{R248W/+}FLT3^{ITD/+}$ animals (Fig. 1b). Rest of the $p53^{R248W/+}FLT3^{ITD/ITD}$ mice developed MPN (Figure S1b).

Given that some $p53^{R248W/+}FLT3^{ITD/+}$ mice develop CML, we next examined the impact of mutant p53 on FLT3-ITD⁺ hematopoietic stem and progenitor cells (HSPCs) in order to understand the underlying mechanisms. We first analyzed peripheral blood (PB), the bone marrow (BM), and the spleen of $p53^{+/+}$, $p53^{R248W/+}$, $FLT3^{ITD/+}$, and $p53^{R248W/+}FLT3^{ITD/+}$ mice (8–12 week old). PB white blood cell (WBC) counts, BM cellularity, and spleen weight were comparable among the four groups of mice (Figures S1c, S1d, and S1e). We then examined the frequency of hematopoietic stem and progenitor cells in the BM of $p53^{R248W/+}FLT3^{ITD/+}$ mice. While the number of LT-HSCs and ST-HSCs was comparable among these mice, LSKs and MPPs were expanded in the $p53^{R248W/+}FLT3^{ITD/+}$ mice compared with that of the $p53^{+/+}$, $p53^{R248W/+}$, and $FLT3^{ITD/+}$ mice

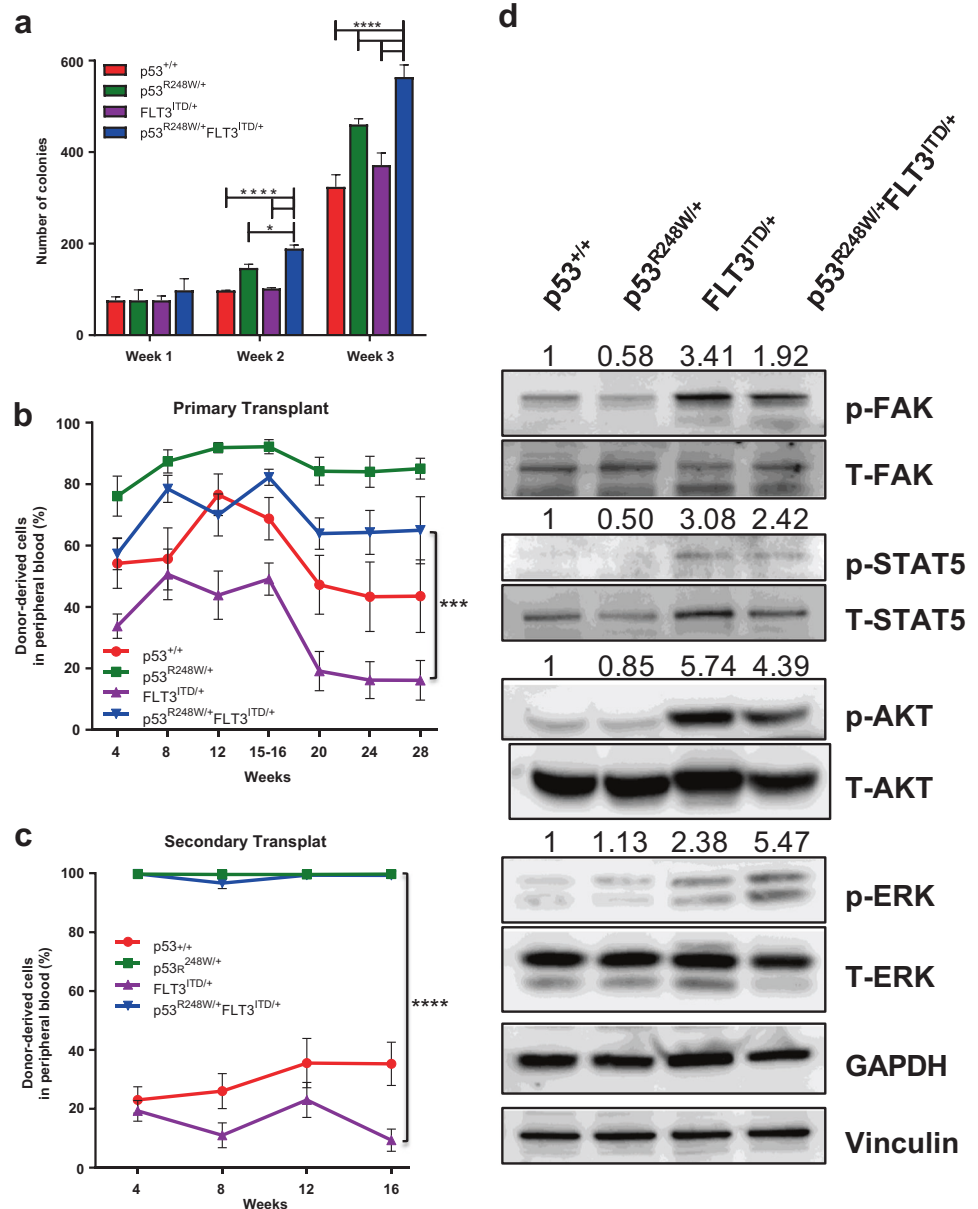
(Figure S2a). We also observed increased frequency of myeloid progenitors (Lin⁻Kit⁺ cells) in the bone marrow of $p53^{R248W/+}FLT3^{ITD/+}$ mice (Figure S2b). These findings suggest that the effects of mutant p53 and FLT3-ITD on myeloid progenitor cell expansion appears additive. However, the number of common lymphoid progenitors (CLPs) was comparable among four group of mice (Figure S2c).

FLT3 mutations have been shown to enhance the proliferation of hematopoietic stem and progenitor cells [13]. We then examined the cell cycle status of LSKs isolated from $p53^{+/+}$, $p53^{R248W/+}$, $FLT3^{ITD/+}$, and $p53^{R248W/+}FLT3^{ITD/+}$ mice. We confirmed that $FLT3^{ITD/+}$ LSKs shown enhanced proliferation compared with $p53^{+/+}$ LSKs (Figure S2d). However, mutant p53 did not alter the proliferation of $FLT3^{ITD/+}$ LSKs (Figure S2d). To determine the impact of mutant p53 on myeloid progenitors, we performed serial replating assays using BM cells from $p53^{+/+}$, $p53^{R248W/+}$, $FLT3^{ITD/+}$, and $p53^{R248W/+}FLT3^{ITD/+}$ mice. While the colony formation potential of $p53^{+/+}$ and $FLT3^{ITD/+}$ BM cells was comparable in serial replating assays, $p53^{R248W/+}FLT3^{ITD/+}$ BM cells show enhanced replating potential compared with $p53^{R248W/+}$ and $FLT3^{ITD/+}$ BM cells (Fig. 2a), suggesting that expanded myeloid progenitors in $p53^{R248W/+}FLT3^{ITD/+}$ mice are functional in vitro.

To examine the impact of mutant p53 on HSCs in vivo, we performed serial competitive bone marrow transplantation assays. We transplanted 5×10^5 donor BM cells ($p53^{+/+}$, $p53^{R248W/+}$, $FLT3^{ITD/+}$ or $p53^{R248W/+}FLT3^{ITD/+}$, and CD45.2⁺) into lethally irradiated (11 Gy) F1 recipient mice (CD45.1⁺ CD45.2⁺) along with 5×10^5 competitor BM cells (CD45.1⁺). Peripheral blood white blood cell counts were comparable among the four groups of mice following transplantation (Figure S2e). While $FLT3^{ITD/+}$ BM cells showed decreased repopulating ability compared with $p53^{+/+}$ cells 16 weeks post transplantation, $p53^{R248W/+}FLT3^{ITD/+}$ BM cells displayed enhanced engraftment compared to $FLT3^{ITD/+}$ BM cells (Fig. 2b). We then killed the recipient mice and examined the frequency of donor-derived hematopoietic stem and progenitor cells in their bone marrow. We found increased number of donor-derived LSKs in the BM of recipient mice repopulated with $p53^{R248W/+}$ BM cells compared with that of the $p53^{+/+}$ and $FLT3^{ITD/+}$ BM cells, whereas the frequency of donor-derived LSKs in the BM of recipient mice repopulated with $p53^{R248W/+}$ and $p53^{R248W/+}FLT3^{ITD/+}$ cells was comparable (Figure S2f). We found increased number of donor-derived GMPs in the BM of recipient mice repopulated with $p53^{R248W/+}FLT3^{ITD/+}$ bone marrow cells compared with that of the $FLT3^{ITD/+}$ BM cells (Figure S3a). The spleen size was comparable in recipient mice repopulated with four group of BM cells (Figure S3b).

To determine the impact of mutant p53 on the self-renewal potential of FLT3-ITD⁺ HSCs, we transplanted 3×10^6 BM cells isolated from the primary recipient mice

Fig. 2 Mutant p53 enhances the self-renewal potential of FLT3-ITD⁺ LICs. **(a)** Serial replating assays of bone marrow cells from young $p53^{+/+}$, $p53^{R248W/+}$, $FLT3^{ITD/+}$ and $p53^{R248W/+}FLT3^{ITD/+}$ mice. Mean values (\pm SD) are shown ($n = 3$, * $p < 0.05$, *** $p < 0.0001$). **(b)** $p53^{R248W/+}$ enhances the repopulating potential of $FLT3^{ITD/+}$ hematopoietic cells. Percentage of donor-derived (CD45.2⁺) cells in the peripheral blood of primary recipient mice post-transplantation, measured at 4-week intervals. Mean values (\pm SEM) are shown ($n = 7$, *** $p < 0.001$). **(c)** The percentage of donor-derived cells in the peripheral blood of secondary recipient mice. Mean values (\pm SEM) shown, ($n = 7$, $p53^{R248W/+}$ vs $FLT3^{ITD/+}$ and $FLT3^{ITD/+}$ vs $p53^{R248W/+}FLT3^{ITD/+}$, *** $p < 0.0001$). **(d)** Western blot analysis of activated and total FAK, STAT5, AKT, and ERK protein levels in $p53^{+/+}$, $p53^{R248W/+}$, $FLT3^{ITD/+}$ and $p53^{R248W/+}FLT3^{ITD/+}$ mononuclear cells differentiated into macrophage progenitors. Loading controls GAPDH and Vinculin are also shown. Quantification of phosphorylated proteins was calculated relative to total protein level and is displayed above each respective phospho-protein



repopulated with $p53^{+/+}$, $p53^{R248W/+}$, $FLT3^{ITD/+}$, or $p53^{R248W/+}FLT3^{ITD/+}$ cells into lethally irradiated secondary F1 recipients. Sixteen weeks after transplantation, $p53^{R248W/+}FLT3^{ITD/+}$ cells continued to show increased repopulating ability compared with $FLT3^{ITD/+}$ BM cells (Fig. 2c). These findings suggest that mutant p53 may promote leukemic transformation through enhancing LIC self-renewal.

To examine the impact of mutant p53 on oncogenic signaling pathways, we performed western blot analysis on macrophage progenitor cells derived from $p53^{+/+}$, $p53^{R248W/+}$, $FLT3^{ITD/+}$, or $p53^{R248W/+}FLT3^{ITD/+}$ bone marrow cells. Consistent with previous studies, cells from $FLT3^{ITD/+}$ mice had activated FAK, STAT5, and AKT (Fig. 2d). Further, expressing FLT3-ITD in a mutant p53 background

enhances activated ERK levels, but slightly decreases activated FAK and STAT5 levels (Fig. 2d). We found increased levels of FLT3 in $p53^{R248W/+}FLT3^{ITD/+}$ macrophage progenitor cells (Figure S3c). Thus, expressing FLT3-ITD in a mutant p53 background has no effect on FLT3-ITD-induced activation of signaling pathways. However, ERK inhibitor treatment decreased the replating potential of $p53^{R248W/+}$, $FLT3^{ITD/+}$, and $p53^{R248W/+}FLT3^{ITD/+}$ bone marrow cells (Figure S3d). These findings suggest that mutant p53 and FLT3-ITD may function through different signaling pathways in the pathogenesis of hematological malignancies. In future, we will elucidate the mechanisms by which mutant p53 upregulates FLT3 in HSPCs.

While *TP53* and *FLT3* mutations are rarely co-occur in MPN and AML [11], the underlying mechanisms are not known. We found that the majority of *p53*^{R248W/+} *FLT3*^{ITD/+} mice developed MPN, as seen in *FLT3*^{ITD/+} mice [13]. Further, we discovered that mutant *p53* and *FLT3*-ITD cooperate in CML development in mice. Functionally, mutant *p53* synergizes with *FLT3*-ITD to expand the myeloid progenitor cell pool and enhance the self-renewal potential of LICs. *TP53* mutations are present in both chronic and blast crisis phase of CML [15], underscoring the importance of mutant *p53* in CML pathogenesis. Delineating the role of mutant *p53* and *FLT3*-ITD in LIC self-renewal and pathogenesis of hematological malignancies may facilitate the development of novel therapeutic approaches that can improve leukemia treatment.

Acknowledgements This work was supported by the Office of the Assistant Secretary of Defense for Health Affairs, through the Bone Marrow Failure Research Program—Idea Development Award under Award No. W81XWH-18-1-0265 to YL. Opinions, interpretations, conclusions, and recommendations are those of the author and are not necessarily endorsed by the Department of Defense. This work was also supported in part by two NIH R56 Awards (R56DK119524-01 and R56AG05250), a DoD Career Development Award W81XWH-13-1-0187, a Scholar Award from the St. Baldrick's Foundation, an Elsa Pardee Foundation New Investigator Award, a Leukemia Research Foundation New Investigator Award, a Showalter Trust Fund New Investigator Award, an Alex Lemonade Stand Foundation grant, a Children's Leukemia Research Association grant, and an American Cancer Society Institutional Research Grant to YL. SCN was supported by a NIH F32 Award 1F32CA203049-01. The authors would like to acknowledge the Flow Cytometry Core and In vivo Therapeutic Core Laboratories, which were sponsored, in part, by the NIDDK Cooperative Center of Excellence in Hematology (CCEH) grant U54 DK106846. This work was supported, in part, by a Project Development Team within the ICTSI NIH/NCRR Grant Number UL1TR001108. We would like to thank Dr. Yang Xu at USCD for providing the *p53*^{R248W} mice to the study.

Author contributions SCN and YL designed the research. SCN, SC, RG, CY, MK, SV, ACF, CW, and CD performed the research. SCN, SC, and YL analyzed the data and performed the statistical analysis. GES performed pathological analysis. HSB, LDM, and RK provided reagents and constructive advice to the study. SCN, SC, and YL wrote the paper. All authors read, commented on, and approved the paper.

Compliance with ethical standards

Conflict of interest The authors declare that they have no conflict of interest.

Publisher's note: Springer Nature remains neutral with regard to jurisdictional claims in published maps and institutional affiliations.

References

1. Coombs CC, Tallman MS, Levine RL. Molecular therapy for acute myeloid leukaemia. *Nat Rev Clin Oncol*. 2016;13:305–18.
2. Hope KJ, Jin L, Dick JE. Acute myeloid leukemia originates from a hierarchy of leukemic stem cell classes that differ in self-renewal capacity. *Nat Immunol*. 2004;5:738–43.
3. Essers MA, Trumpp A. Targeting leukemic stem cells by breaking their dormancy. *Mol Oncol*. 2010;4:443–50.
4. Khoo KH, Verma CS, Lane DP. Drugging the *p53* pathway: understanding the route to clinical efficacy. *Nat Rev Drug Discov*. 2014;13:217–36.
5. Brosh R, Rotter V. When mutants gain new powers: news from the mutant *p53* field. *Nat Rev Cancer*. 2009;9:701–13.
6. Rücker FG, Schlenk RF, Bullinger L, Kayser S, Teleanu V, Kett H, et al. *TP53* alterations in acute myeloid leukemia with complex karyotype correlate with specific copy number alterations, monosomal karyotype, and dismal outcome. *Blood*. 2012;119:2114–21.
7. Prokocimer M, Molchadsky A, Rotter V. Dysfunctional diversity of *p53* proteins in adult acute myeloid leukemia: projections on diagnostic workup and therapy. *Blood*. 2017;130:699–712.
8. Liu Y, Elf SE, Miyata Y, Sashida G, Liu YH, Huang G, et al. *p53* Regulates Hematopoietic Stem Cell Quiescence. *Cell Stem Cell*. 2009;4:37–48.
9. Song H, Hollstein M, Xu Y. *p53* gain-of-function cancer mutants induce genetic instability by inactivating ATM. *Nat Cell Biol*. 2007;15:376–88.
10. Chen S, Gao R, Yao C, Kobayashi M, Liu SZ, Yoder MC, et al. Genotoxic stresses promotes the clonal expansion of hematopoietic stem cells expressing mutant *p53*. *Leukemia*. 2018;32:850–4.
11. Garg M, Nagata Y, Kanojia D, Mayakonda A, Yoshida K, Haridas Keloth S, et al. Profiling of somatic mutations in acute myeloid leukemia with *FLT3*-ITD at diagnosis and relapse. *Blood*. 2015;126:2491–501.
12. Swords R, Freeman C, Giles F. Targeting the FMS-like tyrosine kinase 3 in acute myeloid leukemia. *Leukemia*. 2012;26:2176–85.
13. Lee BH, Tothova Z, Levine RL, Anderson K, Buza-Vidas N, Cullen DE, et al. *FLT3* mutations confer enhanced proliferation and survival properties to multipotent progenitors in a murine model of chronic myelomonocytic leukemia. *Cancer Cell*. 2007;12:367–80.
14. Morse HC 3rd, Anver MR, Fredrickson TN, Haines DC, Harris AW, Harris NL, Hematopathology subcommittee of the Mouse Models of Human Cancers Consortium, et al. Bethesda proposals for classification of lymphoid neoplasms in mice. *Blood*. 2002;100:246–58.
15. Menezes J, Salgado RN, Acquadro F, Gómez-López G, Carralero MC, Barroso A, et al. *ASXL1*, *TP53* and *IKZF3* mutations are present in the chronic phase and blast crisis of chronic myeloid leukemia. *Blood Cancer J*. 2013;3:e157.

Mutant p53 drives clonal hematopoiesis through modulating epigenetic pathway

Sisi Chen^{1,2}, Qiang Wang ³, Hao Yu², Maegan L. Capitano⁴, Sasidhar Vemula², Sarah C. Nabinger², Rui Gao², Chonghua Yao^{2,5}, Michihiro Kobayashi², Zhuangzhuang Geng³, Aidan Fahey², Danielle Henley², Stephen Z. Liu⁶, Sergio Barajas¹, Wenjie Cai¹, Eric R. Wolf ², Baskar Ramdas², Zhigang Cai², Hongyu Gao⁶, Na Luo ⁷, Yang Sun ⁷, Terrence N. Wong⁸, Daniel C. Link⁸, Yunlong Liu⁶, H. Scott Boswell⁹, Lindsey D. Mayo², Gang Huang¹⁰, Reuben Kapur², Mervin C. Yoder², Hal E. Broxmeyer⁴, Zhonghua Gao^{3*} & Yan Liu^{1,2*}

Clonal hematopoiesis of indeterminate potential (CHIP) increases with age and is associated with increased risks of hematological malignancies. While *TP53* mutations have been identified in CHIP, the molecular mechanisms by which mutant p53 promotes hematopoietic stem and progenitor cell (HSPC) expansion are largely unknown. Here we discover that mutant p53 confers a competitive advantage to HSPCs following transplantation and promotes HSPC expansion after radiation-induced stress. Mechanistically, mutant p53 interacts with EZH2 and enhances its association with the chromatin, thereby increasing the levels of H3K27me3 in genes regulating HSPC self-renewal and differentiation. Furthermore, genetic and pharmacological inhibition of EZH2 decreases the repopulating potential of p53 mutant HSPCs. Thus, we uncover an epigenetic mechanism by which mutant p53 drives clonal hematopoiesis. Our work will likely establish epigenetic regulator EZH2 as a novel therapeutic target for preventing CHIP progression and treating hematological malignancies with *TP53* mutations.

¹ Department of Biochemistry and Molecular Biology, Indiana University, Indianapolis, IN 46202, USA. ² Department of Pediatrics, Herman B Wells Center for Pediatric Research, Indiana University, Indianapolis, IN 46202, USA. ³ Department of Biochemistry and Molecular Biology, the Cancer Institute, College of Medicine, Pennsylvania State University, Hershey, PA 17033, USA. ⁴ Department of Microbiology and Immunology, Indiana University, Indianapolis, IN 46202, USA. ⁵ Shanghai Municipal Hospital of Traditional Chinese Medicine, Shanghai University of Traditional Chinese Medicine, Shanghai, China. ⁶ Department of Medical Genetics, Indiana University, Indianapolis, IN 46202, USA. ⁷ Department of Ophthalmology, Indiana University, Indianapolis, IN 46202, USA. ⁸ Siteman Cancer Center, Washington University, St. Louis, MO 63110, USA. ⁹ Department of Medicine, Indiana University, Indianapolis, IN 46202, USA. ¹⁰ Division of Pathology and Experimental Hematology and Cancer Biology, Cincinnati Children's Hospital Medical Center, Cincinnati, OH, USA. *email: zgao1@pennstatehealth.psu.edu; liu219@iu.edu

Clonal hematopoiesis of indeterminate potential (CHIP), also known as age-related clonal hematopoiesis (ARCH), occurs when a single mutant hematopoietic stem and progenitor cell (HSPC) contributes to a significant clonal proportion of mature blood lineages during aging^{1–3}. CHIP is common in aged healthy individuals and associated with increased risks of hematological neoplasms, including myelodysplastic syndromes (MDS) and acute myeloid leukemia (AML)^{4–8}. CHIP is also associated with increased all-cause mortality and risk of cardio-metabolic disease^{4–6,9}. While these findings suggest that mutations identified in CHIP likely drive disease development, mechanisms by which these mutations promote HSPC expansion are largely unknown^{4–9}.

Most individuals with CHIP carry hematological malignancy-associated mutations, including *DNMT3A*, *TET2*, *ASXL1*, *JAK2*, and *TP53*^{4–6}. The *TP53* gene, which encodes the tumor suppressor protein p53, ranks in the top five among genes that were mutated in CHIP^{4–6,10–12}. p53 bears the usual hallmarks of a transcription factor and regulates a large number of genes in response to a variety of cellular insults, including oncogene activation, DNA damage, and inflammation, to suppress tumorigenesis^{13,14}. *TP53* mutations and deletions were found in approximately half of all human cancers, including hematological malignancies^{13,14}. Recently, somatic *TP53* mutations were identified in CHIP^{4–6}. *TP53* mutations were also commonly found in therapy-related CHIP^{10,12}. Interestingly, some individuals with Li-Fraumeni syndrome (LFS), who carry germline *TP53* mutations, develop MDS and AML as they age^{14,15}. Indeed, somatic *TP53* mutations are present in 10% of MDS and AML cases and in 30% of secondary MDS and AML patients arising after exposure to radiation or chemotherapy^{2,16–19}. While *TP53* mutations are associated with adverse clinical outcomes in MDS and AML^{2,16–19}, how mutant p53 drives the pathogenesis of hematological malignancies are not fully understood.

We have been investigating the role of p53 in normal and malignant hematopoiesis. We discovered that wild-type (WT) p53 maintains hematopoietic stem cell (HSC) quiescence and identified Necdin as a p53 target gene that regulates DNA damage response (DDR) in HSCs^{20,21}. We extended our research to mutant p53 to generate additional knowledge in order to develop therapeutic strategies that can enhance our abilities to prevent CHIP progression and treat hematological diseases. We discovered that mutant p53 enhances the repopulating potential of HSPCs²², similar to what has been reported previously^{23,24}. While clinical studies suggest that expansion of HSPCs with *TP53* mutations predisposes the elderly to hematological neoplasms^{4–6,10–12}, the role of *TP53* mutations in CHIP progression remains elusive.

Polycomb group (PcG) proteins are epigenetic regulators that have been implicated in stem cell maintenance and cancer development^{25–28}. Genetic and biochemical studies indicate that PcG proteins exist in at least two protein complexes, Polycomb repressive complex 2 (PRC2) and Polycomb repressive complex 1 (PRC1), that act in concert to initiate and maintain stable gene repression^{25–28}. EZH2, a key component of PRC2 complex, catalyzes the trimethylation of lysine 27 of histone H3 (H3K27me3) in cells²⁷. While EZH2 plays important roles in HSCs and MDS development^{16,29,30}, its regulation in HSPCs is not fully understood.

In the present study, we discovered that mutant p53 confers a competitive advantage to HSPCs following transplantation and promotes HSPC expansion after radiation-induced stress. Mechanistically, mutant p53 interacts with EZH2 and enhances its association with the chromatin, thereby increasing the levels of H3K27me3 in genes regulating HSPC self-renewal and differentiation. Thus, we have uncovered an epigenetic mechanism by which mutant p53 drives clonal hematopoiesis.

Results

TP53 mutations identified in CHIP enhance HSPC functions.

TP53 ranks in the top five among genes that were mutated in CHIP (Fig. 1a)^{4–6,10–12}. Approximately 90% of somatic *TP53* mutations in CHIP are missense mutations in the DNA-binding domain (DBD) of the p53 protein (Fig. 1b)^{4–6,10–12}. The most frequently mutated codon in p53 was 248, followed by codons 273, 220, and 175 (Fig. 1c). *TP53* mutation spectrums in CHIP are similar to hematological malignancies. Different mutant p53 proteins have been shown to exhibit distinct functions in promoting cancer initiation, progression, or metastasis¹⁴. To determine the impact of *TP53* mutations on HSPC functions, we introduced eight hot-spot *TP53* mutations identified in CHIP^{4–6,10–12} (Fig. 1c), into WT mouse HSPCs using retrovirus-mediated transduction and performed in vitro and in vivo assays (Fig. 1d). Ectopic expression of some mutant p53, including p53^{R248W}, p53^{R248Q}, p53^{R175H}, p53^{R273H}, p53^{C238Y}, and p53^{Y220C}, enhanced the replating potential of WT HSPCs compared to control viruses (MIGR1) transduced cells (Fig. 1e).

p53^{R248W}, p53^{R273H}, and p53^{Y220C} are hot-spot *TP53* mutations in CHIP, MDS, and AML and predict leukemia development^{4–6,10–12,17–19}. These mutations have also been shown to gain oncogenic properties in mouse models of human cancer^{14,31–33}. We introduced p53^{R248W}, p53^{R273H}, or p53^{Y220C} into WT HSPCs (CD45.2⁺) using retrovirus-mediated transduction, and then transplanted transduced cells (GFP⁺) together with competitor bone marrow (BM) cells (CD45.1⁺) into lethally irradiated recipient mice. We observed increased number of GFP⁺ cells in peripheral blood (PB) of recipient mice repopulated with HSPCs expressing mutant p53 compared to that of control viruses transduced cells at 16 weeks following transplantation (Fig. 1f). Increases in total GFP⁺ cells in PB at 16 weeks from mice with mutant p53 proteins were highly suggestive of enhanced HSPC repopulating potential.

p53 is important for HSC survival following genotoxic stress and p53 null HSCs are less sensitive to irradiation as manifested by decreased apoptosis²⁰. We found that ectopic expression of p53^{R248W}, p53^{R273H}, or p53^{Y220C} in WT HSPCs resulted in decreased apoptosis following 2 Gy irradiation (Fig. 1g), suggesting that HSPCs expressing these mutant p53 proteins are not sensitive to radiation-induced stress.

TP53 mutations in CHIP confer competitive advantage to HSPCs.

Given that codon 248 of the p53 protein (p53^{R248}) is most frequently mutated in CHIP, MDS, and AML^{4,6,10–12,18,19}, we focused our investigation on p53^{R248W} in hematopoiesis. Since overexpression of mutant p53 from an MSCV promoter may not reflect accurate function when expressed at physiological levels, we utilized the p53^{R248W} knock-in mice, where p53^{R248W} was introduced into the humanized p53 knock-in (*HUPKI*) allele in mice, expressing human p53 mutant protein from the endogenous murine *Trp53* promoter³³. The *HUPKI* allele encodes a human/mouse chimeric protein consisting primarily of human p53 sequence (amino acids 33–332) flanked by the conserved extreme amino and carboxyl-termini of mouse p53³⁴. *HUPKI* mice were described as p53^{+/+} mice in the text.

Since the majority of *TP53* mutations in CHIP are mono-allele missense mutations (Fig. 1b)^{4–6,10–12}, we utilized heterozygous mutant mice (p53^{R248W/+}) to investigate the biological impact of mutant p53 on primitive HSPC populations. As nonsense, frameshift, and splice site mutations result in *TP53* deletions¹⁴, we also included p53^{+/-} and p53^{-/-} mice in the experiments. We first analyzed the BM of p53^{+/+}, p53^{+/-}, p53^{-/-}, and p53^{R248W/+} mice and found that BM cellularity is comparable among these mice (Supplementary Fig. 1a). We observed increased number of

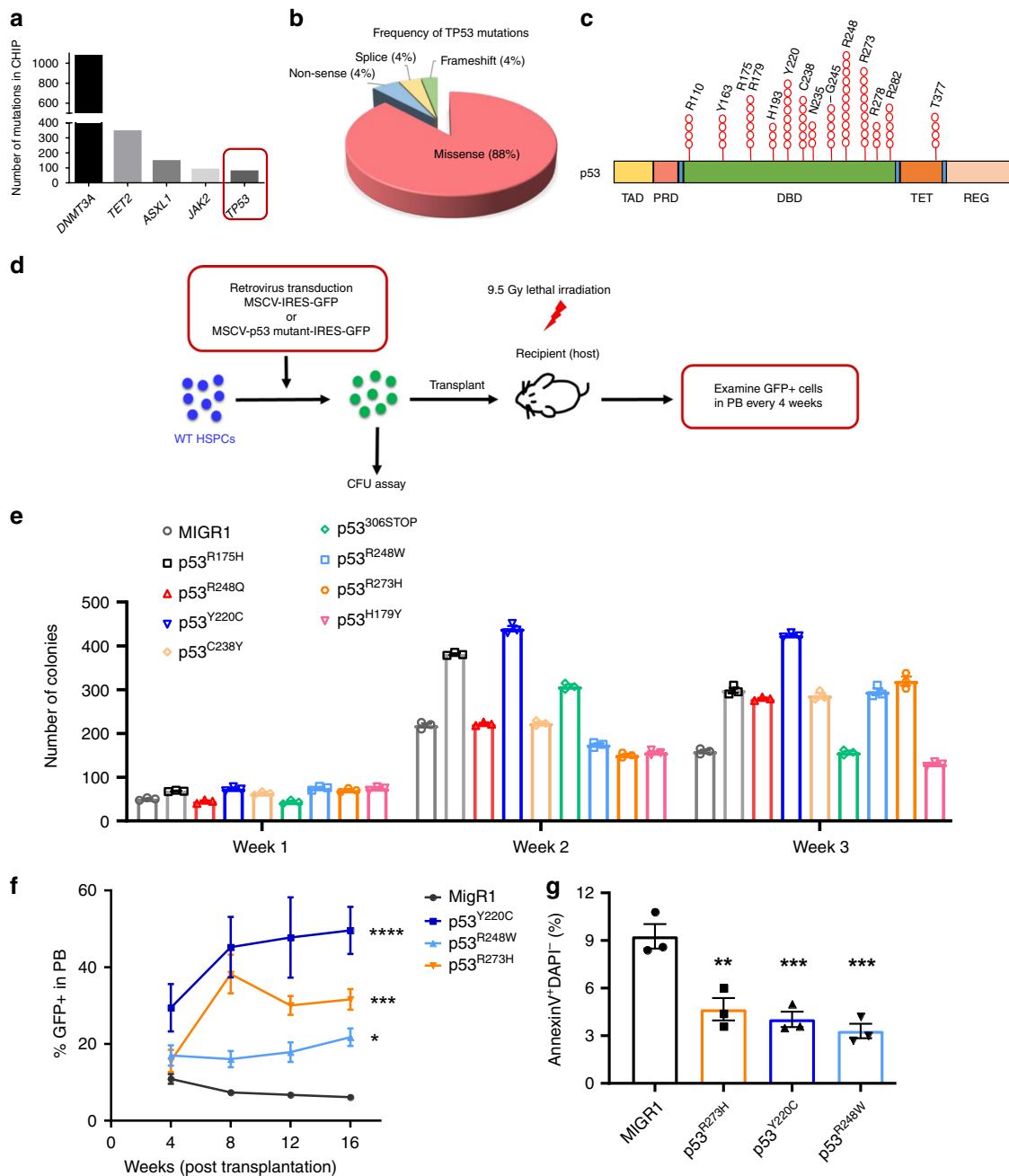
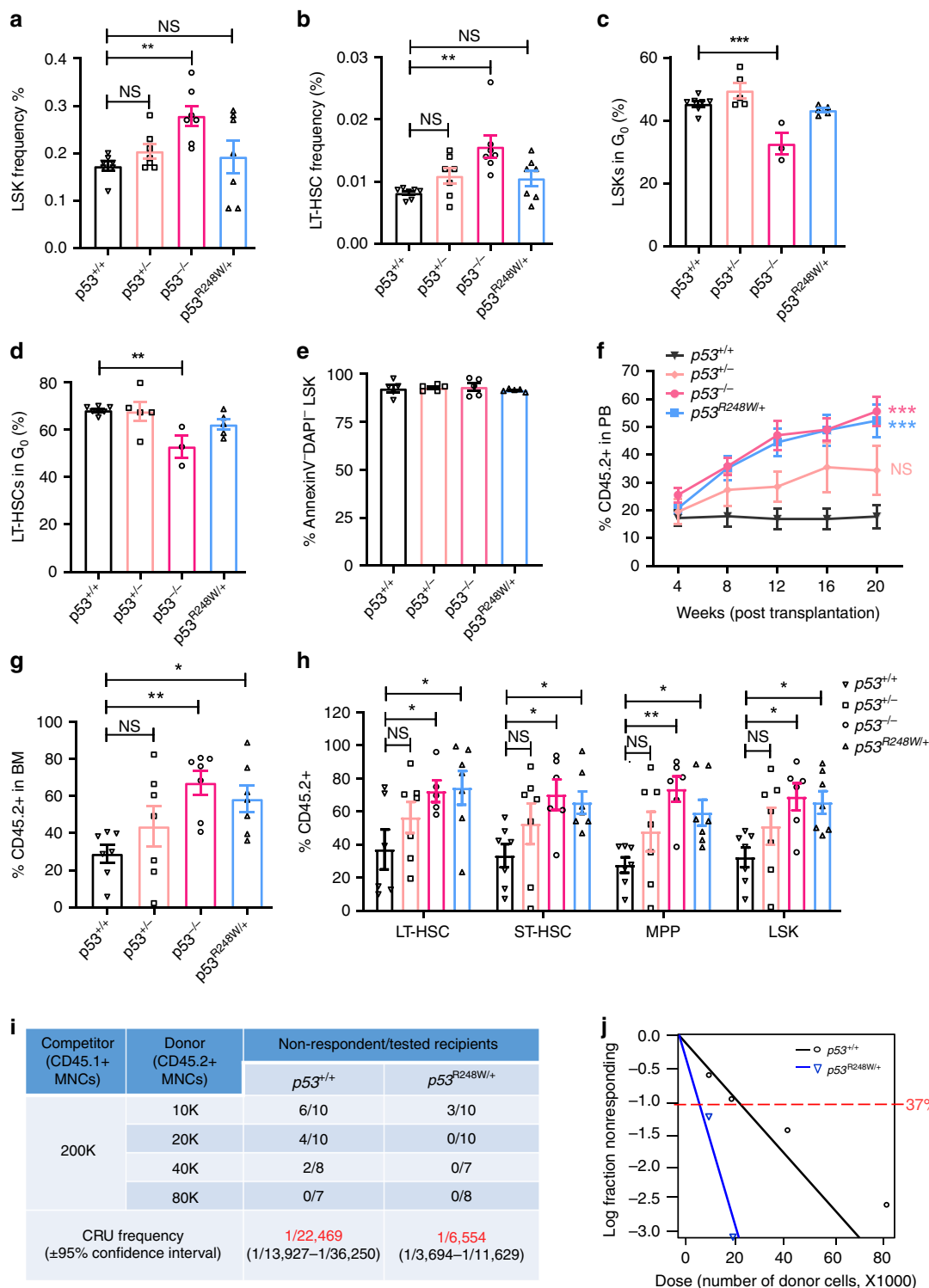


Fig. 1 *TP53* mutations identified in CHIP enhance HSPC repopulating potential. **a** Tumor suppressor gene *TP53* ranks in the top five among genes that were mutated in clonal hematopoiesis with indeterminate potential (CHIP). **b** Pie chart representing different types of *TP53* mutations identified in CHIP. **c** *TP53* mutations in CHIP are enriched in the DNA-binding domain (DBD) of the p53 protein. TAD, transactivation domain; PRD, proline-rich domain; DBD, DNA-binding domain; TET, tetramerization domain; and REG, carboxy-terminal regulatory domain. **d** Several hot-spot *TP53* mutations identified in CHIP were introduced into wild-type hematopoietic stem and progenitor cells (HSPCs) using retrovirus-mediated transduction. In vitro and in vivo stem and progenitor cell assays were then performed using sorted GFP (green fluorescent protein)-positive cells. **e** Serial replating assays of HSPCs expressing different mutant p53 proteins. The methylcellulose cultures were serially replated, weekly, for 3 weeks; $n = 3$ independent experiments performed in duplicate. **f** Percentage of GFP⁺ cells in the peripheral blood (PB) of recipient mice following competitive transplantation; $n = 3-5$ mice per group. **g** HSPCs expressing mutant p53 proteins were assessed for apoptosis at 24 h after radiation (2 Gy); $n = 3$ independent experiments. Data are represented as mean \pm SEM. *P*-values were calculated using two-way ANOVA (analysis of variance) with Dunnett's multiple comparisons test in **e** and **f**, one-way ANOVA with Dunnett's multiple comparisons test in **g**; * $P < 0.05$, ** $P < 0.01$, *** $P < 0.001$, **** $P < 0.0001$. Source data are provided as a Source Data file.

LSKs and LT-HSCs in the BM of $p53^{-/-}$ mice as reported²⁰; however, $p53^{R248W}$ affects neither the frequency nor the number of HSPCs in the BM (Fig. 2a, b, and Supplementary Fig. 1b, c). While loss of p53 decreases the quiescence of LSKs and LT-HSCs²⁰, mutant p53 does not affect HSPC quiescence (Fig. 2c, d). In addition, we observed similar number of apoptotic HSPCs in

$p53^{+/+}$, $p53^{+/-}$, $p53^{-/-}$, and $p53^{R248W/+}$ mice in steady state (Fig. 2e). Thus, mutant p53 does not affect the frequency, quiescence, or the survival of HSPCs when expressed at physiological levels.

Hematopoietic transplantation is a cellular stressor that has been shown to promote the expansion of mutant HSPCs^{12,35,36}.



We recently reported that $p53^{R248W}$ enhances the repopulating potential of BM cells²². To further establish that the enhanced repopulating potential is HSC intrinsic, we purified HSCs (CD48⁻CD150⁺LSKs, CD45.2⁺) from $p53^{+/+}$, $p53^{+/-}$, $p53^{-/-}$, and $p53^{R248W/+}$ mice and performed HSC transplantation assays. Both $p53^{-/-}$ and $p53^{R248W/+}$ HSCs exhibited a substantially higher contribution to PB production compared to $p53^{+/+}$ and $p53^{+/-}$ HSCs at 20 weeks following primary transplantation (Fig. 2f). In addition, the percentage of donor-derived hematopoietic cells and HSPCs in the BM of recipient mice repopulated

with $p53^{-/-}$ and $p53^{R248W/+}$ HSCs was significantly higher than that of the $p53^{+/+}$ HSCs (Fig. 2g, h). Mutant p53 did not affect myeloid and lymphoid differentiation in PB and the BM of recipient mice following HSC transplantation (Supplementary Fig. 1d, e).

To determine the impact of mutant p53 on HSC self-renewal, we performed secondary BM transplantation assays. We found that both $p53^{-/-}$ and $p53^{R248W/+}$ HSCs continue to show enhanced engraftment compared to $p53^{+/+}$ and $p53^{+/-}$ HSCs at 20 weeks following secondary transplantation. Interestingly,

Fig. 2 $p53^{R248W/+}$ confers a competitive advantage to HSPCs. **a** The frequency of Lin⁻Sca1⁺Kit⁺ cells (LSKs) in the bone marrow (BM) of $p53^{+/+}$, $p53^{+/-}$, $p53^{-/-}$, and $p53^{R248W/+}$ mice; $n = 7$ mice per genotype. **b** The frequency of long-term hematopoietic stem cells (LT-HSCs) in the BM of $p53^{+/+}$, $p53^{+/-}$, $p53^{-/-}$, and $p53^{R248W/+}$ mice; $n = 7$ mice per genotype. **c** The quiescence of LSKs was determined by Ki67 and DAPI (4',6-diamidino-2-phenylindole) staining followed by flow cytometry analysis; $n = 3-7$ mice per genotype. **d** The quiescence of LT-HSCs was determined by Ki67 and DAPI staining and flow cytometry analysis; $n = 3-7$ mice per genotype. **e** The apoptosis of LSKs was determined by Annexin V and DAPI staining and flow cytometry analysis; $n = 5$ mice per genotype. **f** Percentage of donor-derived cells in PB of recipient mice at 20 weeks following HSC transplantation; $n = 7$ mice per group. **g** Percentage of donor-derived cells in the BM of recipient mice at 20 weeks following HSC transplantation; $n = 7$ mice per group. **h** Percentage of donor-derived LT-HSCs, short-term hematopoietic stem cells (ST-HSCs), multi-potent progenitors (MPPs), and LSKs in the BM of recipient mice repopulated with $p53^{+/+}$, $p53^{+/-}$, $p53^{-/-}$, or $p53^{R248W/+}$ HSCs; $n = 7$ mice per genotype. **i** Measuring the number of functional HSCs in the BM of $p53^{+/+}$ and $p53^{R248W/+}$ mice utilizing limiting dilution transplantation assays. Recipients with <2% donor-derived cells in the peripheral blood were defined as non-respondent; $n = 7-10$ mice per group. $P = 0.00114$. **j** Poisson statistical analysis of data from Fig. 2i using L-Calcul software. Shapes represent the percentage of negative mice for each dose of cells. Solid lines indicate the best-fit linear model for each dataset. Data are represented as mean \pm SEM. P -values were calculated using one-way ANOVA with Dunnett's multiple comparisons test in **a**, **b**, **c**, **d**, **e**, **g**, and **h**, two-way ANOVA with Dunnett's multiple comparisons test in **f**, and χ^2 test in **i** and **j**; * $P < 0.05$, ** $P < 0.01$, *** $P < 0.001$. Source data are provided as a Source Data file.

$p53^{+/-}$ HSCs show increased repopulating potential compared to $p53^{+/+}$ HSCs in secondary transplantation assays (Supplementary Fig. 1f). We observed increased number of donor-derived hematopoietic cells in the BM of secondary recipients repopulated with $p53^{+/-}$, $p53^{-/-}$, and $p53^{R248W/+}$ cells compared to $p53^{+/+}$ cells (Supplementary Fig. 1g). However, neither *TP53* mutation nor *p53*-deficiency alters terminal differentiation of HSCs (Supplementary Fig. 1h).

To enumerate the numbers of functional HSCs in the BM of $p53^{R248W/+}$ mice, we performed competitive BM transplantation experiments with limiting-dilution of donor cells. The frequency of competitive repopulation units (CRU) in the BM of $p53^{R248W/+}$ mice is three- to four-fold higher than that of the $p53^{+/+}$ mice (Fig. 2i, j). Enhanced repopulating potential of $p53^{R248W/+}$ BM cells could be due to changes in homing capacities of donor cells. We performed homing assays but did not detect difference in the frequency of donor-derived cells in the BM of recipient mice repopulated with $p53^{R248W/+}$ BM cells compared to $p53^{+/+}$ BM cells (Supplementary Fig. 1i, j). Taken together, we demonstrate that mutant *p53* identified in CHIP confers a competitive advantage to HSPCs following transplantation.

***TP53* mutations promote HSPC survival following radiation.**

Therapy-related CHIP in patients with non-hematologic cancers is common and associated with adverse clinical outcomes^{10,12}. Cytotoxic therapy results in the expansion of clones carrying *TP53* mutations^{10,12,37}. Indeed, we found that chemotherapy treatment expands HSPCs expressing mutant *p53*²². Given that HSPCs expressing mutant *p53* are not sensitive to radiation (Fig. 1g), we then examined the impact of radiation on mutant HSPC expansion. We generated mixed BM chimeras containing both $p53^{R248W/+}$ (CD45.2⁺) and $p53^{+/+}$ (CD45.1⁺) cells with a 1:10 ratio of mutant to WT cells. Eight weeks following transplantation, recipient mice were treated with or without 5 Gy total body irradiation (TBI) (Fig. 3a). We found that mutant BM cells outcompeted $p53^{+/+}$ cells, and became clonally dominant following TBI (Fig. 3b). Further, TBI significantly increased frequency of mutant HSPCs in BM of recipient mice (Fig. 3c, d). Thus, we demonstrate that radiation promotes the expansion of HSPCs with mutant *p53*.

To determine the impact of radiation on $p53^{+/+}$ and $p53^{R248W/+}$ mice, we irradiated these mice and monitored their survival. While most $p53^{+/+}$ mice died 5 weeks following 9 Gy TBI, most $p53^{R248W/+}$ mice were still alive (Supplementary Fig. 2a). Further, $p53^{R248W/+}$ HSCs show decreased apoptosis both in vitro and in vivo following 2 Gy irradiation (Fig. 3e, f). Using phosphorylation of histone H2AX (γ H2AX) as an indicator of DNA damage, we found that $p53^{+/+}$ HSCs stained positive for γ H2AX, whereas

$p53^{R248W/+}$ HSCs were largely devoid of γ H2AX foci (Supplementary Fig. 2b, c).

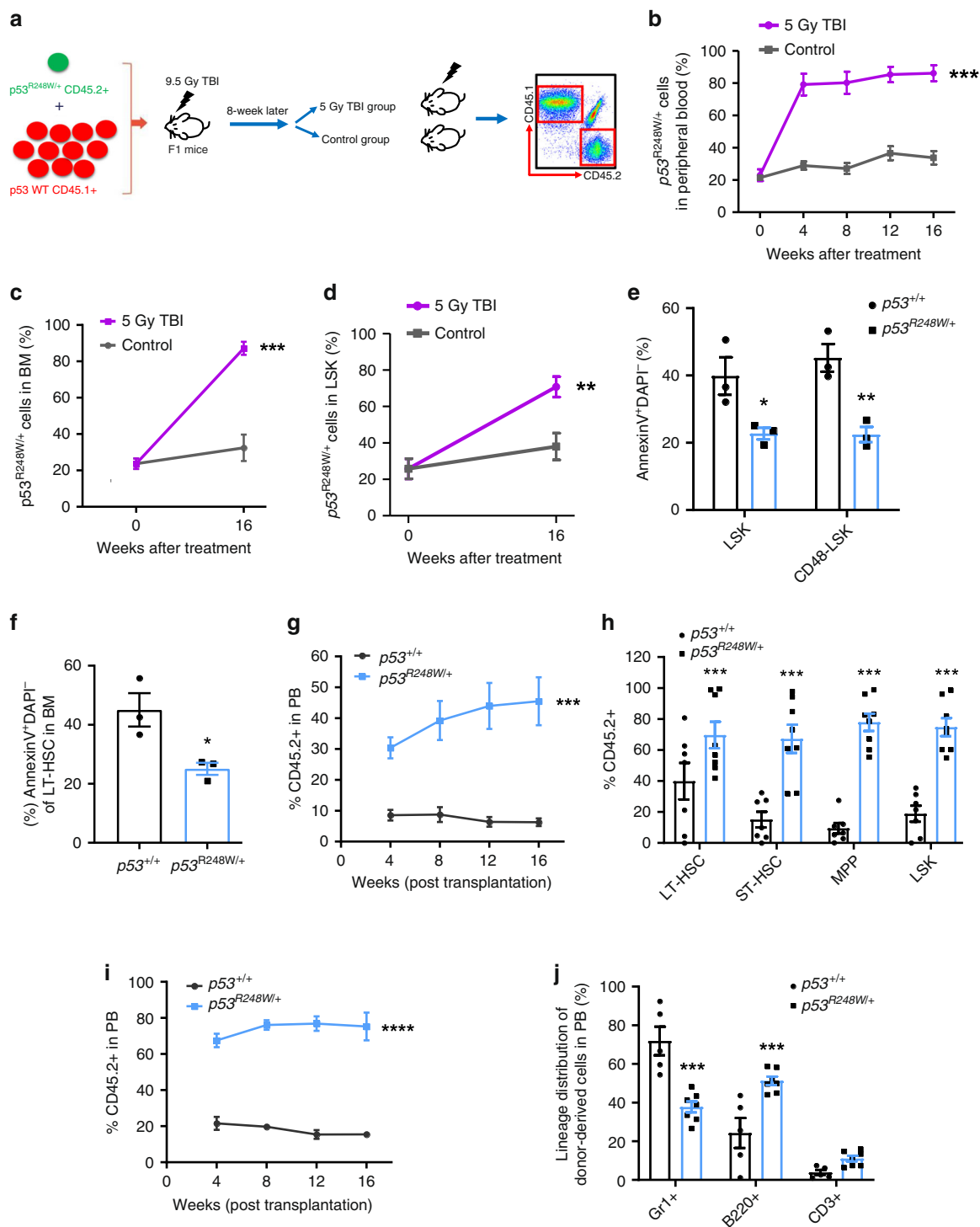
To determine the impact of radiation on $p53^{R248W/+}$ HSPC function in vivo, we treated $p53^{+/+}$ and $p53^{R248W/+}$ mice with 2 Gy TBI. Two hours following TBI, we isolated live BM cells from irradiated mice and performed competitive transplantation assays. Irradiated mutant BM cells displayed enhanced repopulating potential in primary transplantation assays compared to irradiated WT cells (Fig. 3g). We observed increased number of donor-derived HSPCs in the BM of primary recipient mice repopulated with live $p53^{R248W/+}$ BM cells (Fig. 3h and Supplementary Fig. 2d). Sixteen weeks after secondary transplantation, $p53^{R248W/+}$ cells continued to show increased repopulating ability (Fig. 3i). While mutant *p53* had no effect on multilineage differentiation in PB of primary recipient mice (Supplementary Fig. 2e), we found decreased myeloid differentiation and increased B cell differentiation in the PB of secondary recipient mice repopulated with mutant BM cells (Fig. 3j). Thus, we demonstrate that *TP53* mutations identified in CHIP confer resistance to radiation, leading to the selective expansion of *TP53*-mutant HSPCs.

HSC and AML signatures were enriched in *p53* mutant HSPCs.

WT *p53* is a transcription factor that activates the transcription of several target genes in HSCs, including *p21* and *Necdin*^{20,21}. However, we found that mutant *p53* does not alter the expression of *p21* and *Necdin* in HSCs (Fig. 4a). To understand how mutant *p53* enhances HSPC self-renewal, we performed transcript profiling (using RNA-seq studies and quantitative real-time PCR (qRT-PCR) analysis) to compare gene expression in HSPCs isolated from $p53^{+/+}$ and $p53^{R248W/+}$ mice. We employed Gene Set Enrichment Assays (GSEA) to group potential mutant *p53* target genes into specific pathways important in HSPC behavior. HSC and AML signatures were significantly enriched in *p53* mutant HSPCs compared to $p53^{+/+}$ HSPCs (Supplementary Fig. 3a, b). Several pathways important for HSC maintenance, including Regulation of hematopoiesis, Hematopoietic organ development, Immune response, and Positive regulation of cytokine response, were significantly enriched in $p53^{R248W/+}$ HSPCs compared to $p53^{+/+}$ HSPCs (Supplementary Fig. 3c). Collectively, the gene expression profiling data suggest that mutant *p53* modulates specific pathways associated with HSC maintenance and leukemogenesis.

EZH2 targets were downregulated in *p53* mutant HSPCs.

While we found that several hundred genes are either upregulated or downregulated in *p53* mutant HSPCs compared to WT HSPCs, how mutant *p53* regulates gene expression in HSPCs is



unknown. Recent studies revealed that some mutant p53 proteins increase the expression of epigenetic factors, including *MLL1*, *MLL2*, and *MOZ* (*KAT6A*), in human cancer cells³⁸. *MLL1* and *MLL2* are key components of the MLL complexes that confer histone H3K4 trimethylation (H3K4me3), which is an active histone mark important for gene expression^{39,40}. *MOZ* is a histone acetyltransferase and mediates histone H3K9 acetylation (H3K9ac)^{41,42}. However, we found that the expression of *MLL1*, *MLL2*, and *MOZ* is comparable in p53 WT and mutant HSPCs (Supplementary Fig. 3d), suggesting mutant p53 may utilize other mechanisms to modulate gene expression in hematopoietic cells.

Interestingly, RNA-seq assays revealed that genes that only marked by H3K27me3 were negatively enriched with significance in mutant HSPCs compared to that of the WT HSPCs (Fig. 4b, left panel). EZH2 target gene signature (without EZH1 compensation) was also negatively enriched with significance in mutant HSPCs (Fig. 4b, right panel). However, loss of p53 in HSPCs did not significantly change EZH2 target gene signature (Supplemental Fig. 3e). Western blot analysis showed increased levels of H3K27me3 in p53 mutant HSPCs compared to WT HSPCs (Fig. 4c). Further, *p53*^{R248W/+} HSPCs displayed higher levels of H3K27me3 compared to *p53*^{+/+} HSPCs quantified by flow cytometry analysis (Fig. 4d).

Fig. 3 $p53^{R248W/+}$ confers a survival advantage to HSPCs after radiation. **a** BM chimeras were generated by transplanting a 1:10 ratio of $p53^{R248W/+}$ cells (CD45.2⁺) to $p53^{+/+}$ cells (CD45.1⁺) into irradiated recipient mice (CD45.1⁺CD45.2⁺). After hematopoietic reconstitution (8 weeks), mice were treated with or without 5 gray (Gy) total body irradiation (TBI). **b** Percentage of $p53^{R248W/+}$ (CD45.2⁺) cells in PB of recipient mice following TBI treatment; $n = 7$ mice per group. **c** Percentage of $p53^{R248W/+}$ cells (CD45.2⁺) in the BM of recipient mice at 16 weeks following TBI treatment; $n = 7$ mice per group. **d** Percentage of $p53^{R248W/+}$ LSK cells (CD45.2⁺) in the BM of recipient mice at 16 weeks following TBI treatment; $n = 7$ mice per group. **e** Hematopoietic stem and progenitor cells from $p53^{+/+}$ and $p53^{R248W/+}$ mice were assessed for apoptosis 2 h after 2 Gy TBI; $n = 3$ mice per group. **f** HSCs purified from the BM of $p53^{+/+}$ and $p53^{R248W/+}$ mice were treated with 2 Gy TBI and then assessed for apoptosis; $n = 3$ mice per group. **g** Competitive transplantation assays using BM cells isolated from $p53^{+/+}$ and $p53^{R248W/+}$ mice treated with 2 Gy TBI. Two hours following TBI, we isolated BM cells from irradiated mice and transplanted 500,000 live BM cells together with equal number of competitor BM cells into lethally irradiated recipient mice. The percentage of donor-derived cells in the PB of recipient mice; $n = 7-8$ mice per group. **h** Percentage of donor-derived LT-HSCs, ST-HSCs, MPPs, and LSK cells in the PB of the primary recipient mice 16 weeks following transplantation; $n = 7-8$ mice per group. **i** Contribution of $p53^{+/+}$ and $p53^{R248W/+}$ BM cells to recipient mouse PB in secondary transplantation assays; $n = 5-7$ mice per group. **j** Lineage contribution of donor-derived cells in the PB of secondary recipient mice 16 weeks following transplantation; $n = 5-7$ mice per group. Data are represented as mean \pm SEM. *P*-values were calculated using two-way ANOVA with Bonferroni's multiple comparisons test in **b**, **e**, **g**, **i**, and **j**, unpaired *t*-test with Welch's correction in **c**, **d**, **f**, and **h**; **P* < 0.05, ***P* < 0.01, ****P* < 0.001, *****P* < 0.0001. Source data are provided as a Source Data file.

To further understand how mutant p53 modulates gene expression in hematopoietic cells, we performed H3K27me3 ChIP-seq assays in HSPCs from $p53^{+/+}$ and $p53^{R248W/+}$ mice. As expected, H3K27me3 is enriched at the transcription start site (TSS). Large regions of H3K27me3 enrichments are also found covering entire gene regions as well as intragenic regions. We found that p53 mutant HSPCs exhibited significantly higher levels of H3K27me3 at TSS compared to that of the WT HSPCs (Fig. 4e). The heat map of H3K27me3 ChIP-seq also revealed that many genes show increased H3K27me3 enrichment in mutant HSPCs compared to that of the WT HSPCs (Fig. 4f). The majority of H3K27me3 peaks (2582 out of 2669) in WT HSPCs are overlapped with H3K27me3 peaks in p53 mutant HSPCs (Supplementary Fig. 4a). By using the same enrichment threshold, we obtained 1232 additional peaks in mutant HSPCs. These peaks are likely targeted by H3K27me3 in WT cells but failed to reach the threshold. Indeed, these peaks show a similar pattern of fold enrichment between mutant and WT HSPCs (Supplementary Fig. 4b). We also observed increased H3K27me3 enrichment in other genes in p53 mutant HSPCs (Supplementary Fig. 4c, d).

Increased levels of H3K27me3 were found in genes regulating HSC self-renewal and differentiation, including *Cebpa* and *Gadd45g*⁴³⁻⁴⁵, in $p53^{R248W/+}$ HSPCs compared to $p53^{+/+}$ HSPCs (Fig. 4f, g). The transcription factor C/EBP alpha is required for granulopoiesis and frequently disrupted in human AML. Loss of *Cebpa* enhances HSC repopulating capability and self-renewal^{43,44}. Tumor suppressor GADD45G induces HSC differentiation following cytokine stimulation, whereas loss of GADD45G enhances the self-renewal potential of HSCs⁴⁵. We confirmed that there were increased levels of H3K27me3 at both *Cebpa* and *Gadd45g* genes by ChIP experiments (Fig. 4h). Consistently, both *Cebpa* and *Gadd45g* were significantly down-regulated in $p53^{R248W/+}$ HSCs compared to $p53^{+/+}$ HSPCs (Fig. 4i, j).

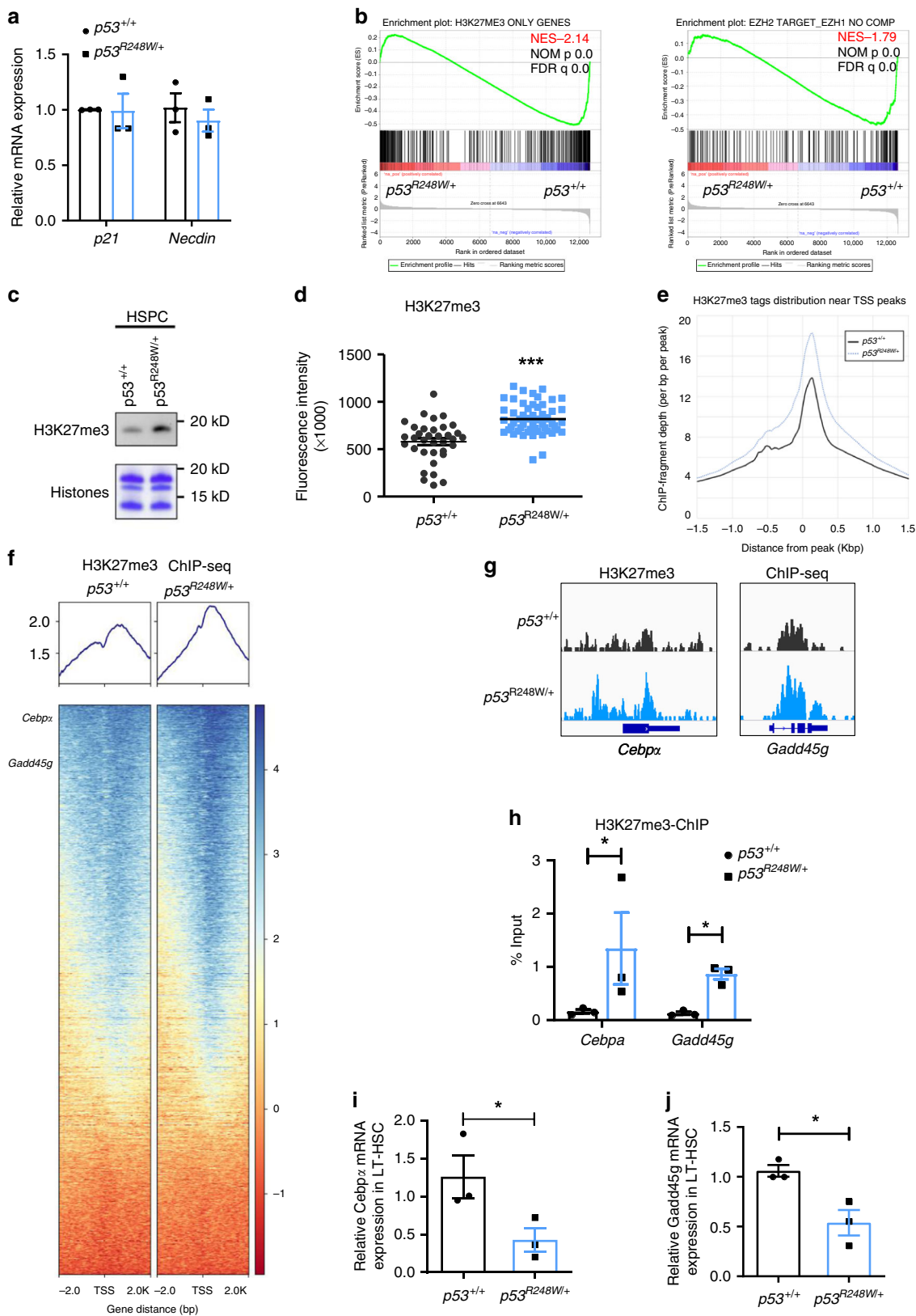
Stimulation of WT HSPCs with thrombopoietin (TPO) dramatically increased *Gadd45g* expression; however, TPO treatment only modestly increased *Gadd45g* expression in p53 mutant HSPCs (Supplementary Fig. 5a), suggesting that mutant p53 may repress *Gadd45g* expression upon cytokine stimulation. To determine the impact of Gadd45g on HSPC function in vitro, we introduced *Gadd45g* into BM cells from $p53^{+/+}$ and $p53^{R248W/+}$ mice using retroviruses and performed colony formation as well as transplantation assays. We found that ectopic *Gadd45g* expression decreases the colony formation of p53 mutant BM cells (Supplementary Fig. 5b). Further, ectopic *Gadd45g* expression decreased the engraftment of p53 mutant BM cells in vivo (Supplementary Fig. 5c). Given that loss of Gadd45g increases HSC self-renewal⁴⁵, it is possible that inactivation of Gadd45g is responsible for increased self-

renewal and colony formation seen in p53 mutant HSPCs. We also found that ectopic *Cebpa* expression decreases the colony formation of p53 mutant BM cells (Supplementary Fig. 5d). These data suggest that mutant p53 may repress gene expression in HSPCs through increasing the levels of H3K27me3.

Mutant p53 enhances the association of EZH2 with the chromatin. The PRC2 complex consists of EZH2/EZH1, EED, and SUZ12²⁷. While the levels of EZH2 was modestly increased in mutant HSPCs, the expression of other PRC2 core components was comparable between p53 WT and mutant HSPCs (Supplementary Fig. 6a). As the protein levels of PRC2 complex in mouse HSPCs were very low, we determined the impact of mutant p53 on the expression of PRC2 complex in murine hematopoietic progenitor 32D cells. We found that ectopic expression of mutant p53, but not WT p53, increased levels of H3K27me3 in 32D cells (Fig. 5a). However, ectopic expression of neither WT nor mutant p53 affected the protein levels of PRC2 core components in 32D cells (Supplementary Fig. 6b). Thus, the increased H3K27me3 in p53 mutant HSPCs may not be due to increased expression of catalytic components of PRC2, including EZH2 and EZH1, or other components of the PRC2 complex.

We then tested whether mutant p53 interacts with EZH2. We performed co-immunoprecipitation assays and found that several mutant p53 proteins, including $p53^{R248W}$, $p53^{R273H}$, and $p53^{R175H}$, displayed enhanced association with EZH2 compared to WT p53 (Fig. 5b). The recruitment and displacement of the PRC2 complex on chromatin are a dynamic process and tightly regulated to activate or repress transcription²⁵⁻²⁸. Genome-wide H3K27me3 ChIP-seq assays revealed that the majority of H3K27me3 peaks in p53 mutant HSPCs are overlapped with that of the WT HSPCs (Fig. 4e, f, Supplementary Fig. 4a), suggesting that mutant p53 may enhance the association of EZH2 with the chromatin, thereby increasing the levels of H3K27me3. To test this, we examine the co-localization of p53 and Ezh2 in p53 WT and mutant HSPCs utilizing the ImageStream flow cytometry analysis. The median fluorescent intensity (MFI) of p53 and Ezh2 in the nucleus was comparable between $p53^{+/+}$ and $p53^{R248W/+}$ HSPCs (Supplementary Fig. 6c, d). However, we found that mutant p53, but not WT p53, show increased co-localization with Ezh2 in the nucleus (Fig. 5c, d).

To determine whether mutant p53 enhances the association of Ezh2 with the chromatin, we separated proteins in p53 WT and mutant HSPCs into cytosol, nuclear cytosol, and chromatin bound fractions. While EZH2 was present in the cytosol of both p53 WT and mutant HSPCs, we observed increased levels of Ezh2 in the chromatin bound fraction of p53 mutant HSPCs compared to that of the p53 WT HSPCs (Fig. 5e). We then performed p53 and EZH2 ChIP assays in $p53^{+/+}$ and $p53^{R248W/+}$ HSPCs



(Lin⁻Kit⁺ cells) and found that both mutant p53 and EZH2 show increased association with *Cebpa* (Supplementary Fig. 6e, f). Thus, we demonstrate that mutant p53 interacts with EZH2 and enhances its association with the chromatin, thereby increasing the levels of H3K27me3 in HSPCs.

Inhibiting EZH2 decreases p53 mutant HSPC expansion. Hematopoietic-specific deletion of *Ezh2* impairs HSC self-renewal and terminal differentiation³⁰. To determine the functional impacts of mutant p53 and Ezh2 interaction on hematopoiesis, we generated *p53*^{R248W/+}*Ezh2*^{fl/fl}-*Mx1Cre*⁺ mice³⁰. While Ezh2-

Fig. 4 EZH2 targets were significantly downregulated in p53 mutant HSPCs. **a** Quantitative reverse transcription polymerase chain reaction (RT-PCR) analysis of mRNA levels of p53 target genes, including *p21* and *Necdin*, in HSCs; $n = 3$ biological replicates. **b** Gene Set Enrichment Assays (GSEA) analysis shows that EZH2 targets were significantly downregulated in p53 mutant HSPC compared to $p53^{+/+}$ HSPCs. **c** p53 mutant HSPCs display increased levels of H3K27me3 (trimethylation at lysine 27 of histone H3) determined by immuno-blot analysis. **d** Lineage depleted HSPCs were stained with SLAM (signaling lymphocyte activation molecule) surface markers (CD48 and CD150) before fixation. Median fluorescence intensity of H3K27me3 in $p53^{+/+}$ and $p53^{R248W/+}$ HSCs ($\text{Lin}^{-}\text{Sca1}^{+}\text{Kit}^{+}\text{CD48}^{-}\text{CD150}^{+}$ cells) was detected by ImageStream flow cytometry analysis. $p53^{+/+}$ $n = 35$ cells, $p53^{R248W/+}$ $n = 52$ cells. **e** H3K27me3 ChIP-seq (chromatin immunoprecipitation sequencing) tag density in $p53^{+/+}$ and $p53^{R248W/+}$ HSPCs, centered on TSS (transcription start site). **f** Heat map shows genes in HSPCs marked by H3K27me3. **g** Genome browser views of H3K27me3 ChIP-seq profiles of *Cebpa* (CCAAT/enhancer-binding protein alpha) and *Gadd45g* (growth arrest and DNA-damage-inducible 45 gamma). **h** H3K27me3 enrichment on *Cebpa* and *Gadd45g* genes in $p53^{+/+}$ and $p53^{R248W/+}$ HSPCs were examined by H3K27me3-ChIP assays; $n = 3$ independent experiments. **i** Quantitative RT-PCR analysis of mRNA levels of *Cebpa* in $p53^{+/+}$ and $p53^{R248W/+}$ LT-HSCs; $n = 3$ biological replicates. **j** Quantitative RT-PCR analysis of mRNA levels of *Gadd45g* in $p53^{+/+}$ and $p53^{R248W/+}$ LT-HSCs; $n = 3$ biological replicates. Data are represented as mean \pm SEM. P -values were calculated using unpaired t test with Welch's correction in **a** and **d**, paired t -test in **h**, **i**, and **j**, and GSEA software in **b**; * $P < 0.05$, *** $P < 0.001$. Source data are provided as a Source Data file.

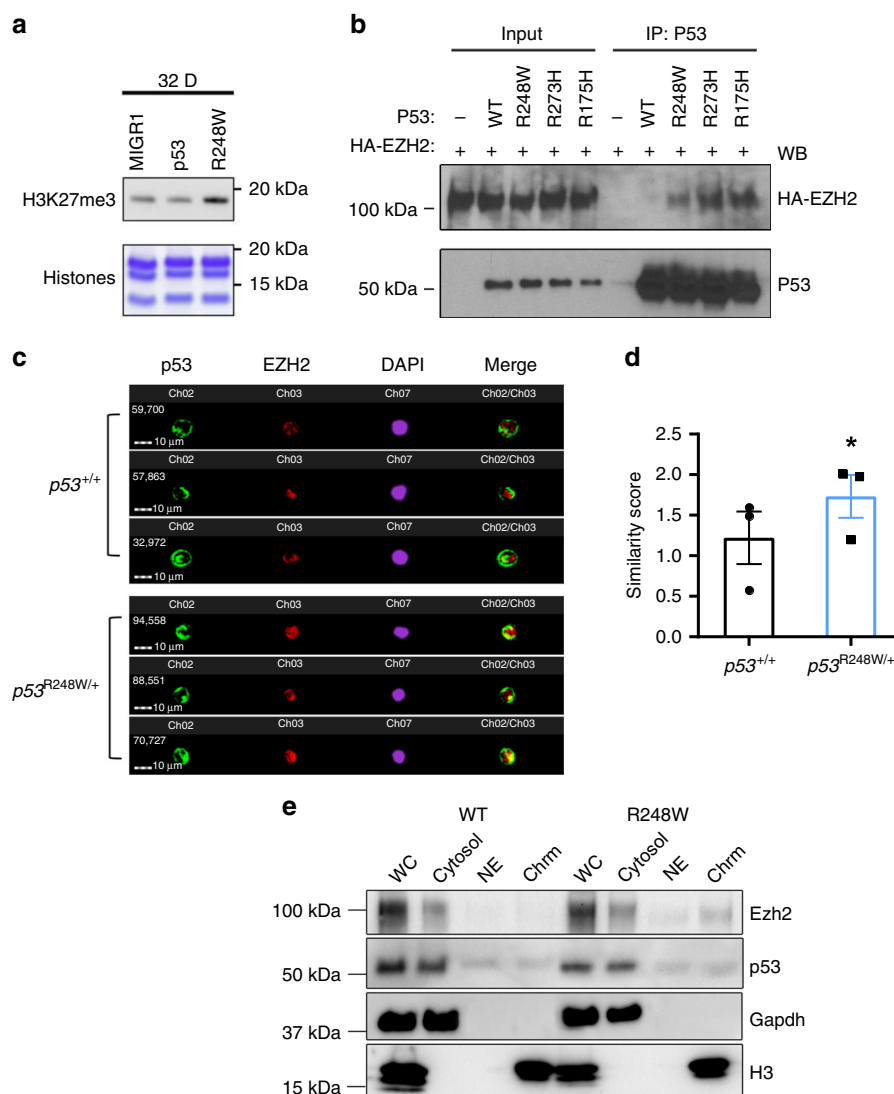


Fig. 5 Mutant p53 enhances the association of EZH2 with the chromatin in HSPCs. **a** 32D cells expressing mutant p53, but not wild-type (WT) p53, displayed increased levels of H3K27me3 as determined by immuno-blot analysis. **b** Several mutant p53 proteins, but not wild-type p53, show enhanced association with EZH2 as assayed by co-IP (co-immunoprecipitation) experiments. **c** Mutant p53 and EZH2 localization in HSPCs ($\text{Lin}^{-}\text{Sca1}^{+}\text{Kit}^{+}\text{CD150}^{+}$) as determined by ImageStream flow cytometry analysis. **d** Quantification of p53 and Ezh2 co-localization in the nucleus of HSPCs ($\text{Lin}^{-}\text{Sca1}^{+}\text{Kit}^{+}\text{CD150}^{+}$). A similarity feature determined the amount of overlay between p53 and Ezh2 within the DAPI mask. The higher the similarity score is, the more co-localized staining is within the nucleus; $n = 3$ biological replicates. **e** Cellular fractionation shows increased EZH2 association with the chromatin fraction in p53 mutant HSPCs. The absence of Gapdh (glyceraldehyde 3-phosphate dehydrogenase) and exclusive distribution of histone H3 in the chromatin fraction indicates no cross contamination between different cellular compartments. WC whole cell extract, Cyto cytosol, NE nuclear cytosol, Chrm chromatin. Data are represented as mean \pm SEM. P -values were calculated using paired t -test in **d**; * $P < 0.05$. Source data are provided as a Source Data file.

deficiency did not affect *Cebpa* and *Gadd45g* expression, *Ezh2* deficiency brought the expression of *Cebpa* and *Gadd45g* back to normal in the mutant *p53* background (Fig. 6a and Supplementary Fig. 7a).

To determine the impact of genetic inhibition of *Ezh2* on *p53* mutant HSPC function in vitro, we performed serial replating assays using BM cells from *p53*^{+/+}, *Ezh2*^{f/+}-*Mx1Cre*⁺, *p53*^{R248W/+}, and *p53*^{R248W/+}*Ezh2*^{f/+}-*Mx1Cre*⁺ mice following polyinosinic:polycytidylic acid (pI:pC) treatment. We found that *Ezh2*-deficiency brings the replating potential of *p53* mutant BM cells back to the WT cell level (Fig. 6b). To determine the impact of *Ezh2* deficiency on HSPC function in vivo, we performed competitive BM transplantations. We treated recipient mice with pI:pC at 8 weeks after transplantation to delete *Ezh2* and then examined donor cell engraftment every 4 weeks for 20 weeks. *p53*^{R248W/+} BM cells exhibited a substantially higher contribution to PB production compared to *p53*^{+/+} cells at 20 weeks following pI:pC treatment, whereas loss of *Ezh2* decreased the engraftment of mutant BM cells to the WT cell level (Fig. 6c). While both the frequency and the absolute number of donor-derived HSPCs in the BM of recipient mice repopulated with *p53*^{R248W/+} BM cells was significantly higher than that of the WT cells, the frequency and the number of donor-derived HSPCs in the BM of recipient mice repopulated with *p53*^{+/+} and *p53*^{R248W/+}*Ezh2*^{-/-} BM cells were comparable (Fig. 6d, e). In addition, we observed decreased number of donor-derived CMPs and MEPs in the BM of recipient mice repopulated with *p53*^{R248W/+}*Ezh2*^{-/-} BM cells compared to that of the *p53*^{R248W/+} BM cells (Supplementary Fig. 7b, c), whereas the number of donor-derived GMPs was comparable in the BM of recipient mice repopulated with *p53*^{R248W/+} cells and *p53*^{R248W/+}*Ezh2*^{-/-} cells (Supplementary Fig. 7d). To determine the impact of *Ezh2*-deficiency on mutant HSC self-renewal, we performed secondary BM transplantation assays and found that *EZH2*-deficiency decreases the repopulating potential of *p53*^{R248W/+} HSCs following secondary transplantation assays (Fig. 6f).

To determine the effect of pharmacological inhibition of *Ezh2* activity on mutant *p53* HSPCs, we treated *p53*^{+/+} and *p53*^{R248W/+} BM cells with DMSO or *EZH2* specific inhibitor EPZ011989⁴⁶ and performed serial replating assays. While *EZH2* inhibitor had no effect on the colony formation of WT BM cells, *EZH2* inhibitor treatment decreased the replating potential of *p53*^{R248W/+} BM cells to the WT level (Fig. 6g). Thus, we demonstrate that *EZH2* is important for mutant *p53* HSPC functions both in vitro and in vivo.

Discussion

WT *p53* is a transcription factor that activates the transcription of target genes to mediate DNA damage repair, growth arrest, or apoptosis^{13,47}. Most TP53 mutations observed in human cancers abrogate or attenuate the binding of *p53* to its consensus DNA sequence (*p53* responsive element) and impede transcriptional activation of *p53* target genes¹⁴. However, we found that mutant *p53* does not alter the expression of *p53* target genes, including *p21* and *Necdin*, in HSCs (Fig. 4a). Genome-wide transcriptome assays revealed that HSC and AML signatures are enriched in *p53* mutant HSPCs, which is different from gene expression signatures regulated by the WT *p53* protein^{20,47}. Thus, our findings provide experimental evidence that TP53 mutations identified in CHIP regulate gene expression in a distinct manner compared to WT *p53*.

Some mutant *p53* proteins have been shown to promote cancer development through modulating gene transcription¹⁴. Dysregulated epigenetic control has been implicated in HSC aging and the pathogenesis of hematological malignancies^{16,48–50}. RNA-seq

assays revealed that *Ezh2* target genes are significantly down-regulated in *p53*^{R248W/+} HSPCs compared to *p53*^{+/+} HSPCs. We observed increased levels of H3K27me3 in *p53* mutant HSPCs. Further, H3K27me3 ChIP-seq assays revealed that *p53* mutant HSPCs exhibit significantly high levels of H3K27me3. Genes important for HSC self-renewal and differentiation, including *Cebpa* and *Gadd45g*^{43–45}, were occupied with increased levels of H3K27me3 in *p53* mutant HSPCs. Thus, mutant *p53* may enhance HSPC self-renewal through increasing the levels of H3K27me3 in genes involved in HSC self-renewal and differentiation.

Then, how does mutant *p53* enhance H3K27me3 in HSPCs? One possible mechanism is that mutant *p53* upregulates the expression of the core PRC2 components, thereby increasing PRC2 activity. However, the expression of the core PRC2 components was comparable between *p53* WT and mutant HSPCs. Mutant *p53* is incapable of binding to its normal binding sites and has been shown to be targeted by interactions with other transcription factors, including ETS family and SREBP^{14,38}. We discovered that several mutant *p53* proteins show enhanced association with *EZH2* compared to WT *p53*. H3K27me3 ChIP-seq assays revealed that the increase in *EZH2*-dependent H3K27me3 is broad across genes, pointing toward an alternative *EZH2*/PRC2 targeting strategy or an increase in enzymatic activity but with normal targeting mechanisms. As shown in Supplementary Fig. 4a, 96.7% H3K27me3 peaks in WT cells also show H3K27me3 occupation in *p53* mutant cells. Although additional peaks are enriched in *p53* mutant cells, they are indeed associated with H3K27me3 in WT cells as well albeit lower enrichment. Further, we found that mutant *p53* interacts with *EZH2* and enhances its association with the chromatin in HSPCs. Thus, mutant *p53* appears to enhance H3K27me3 occupation rather than change its genome-wide distribution in HSPCs.

While the PRC2 complex controls dimethylation and trimethylation of H3K27, the Jumonji domain containing-3 (*Jmjd3*, *KDM6B*) and ubiquitously transcribed X-chromosome tetratricopeptide repeat protein (*UTX*, *KDM6A*) have been identified as H3K27 demethylases that catalyze the demethylation of H3K27me2/3^{51,52}. Decreased activity of *KDM6A*/*UTX* and *JMJD3* may be an alternative mechanism leading to increased *EZH2* activity. Future studies will be needed to investigate the potential impact of *UTX* and *JMJD3* on regulating H3K27me3 in *p53* mutant HSPCs.

Most of *TP53* mutations in human cancer result in either partial or complete loss of tumor suppressor function¹⁴. Some mutant *p53* proteins acquire new oncogenic properties that are independent of WT *p53*, known as the gain-of-function (GOF) properties¹⁴. Most GOF properties are believed to stem from binding of mutant *p53* to cellular proteins such as transcription factors and altering their activity¹⁴. These (neomorphic) GOF properties can be experimentally demonstrated in the absence of a functional WT *p53*. Homozygous *p53*^{R248W/R428W} and *p53*^{R273H/R273H} mice developed novel tumors compared to *p53*^{-/-} mice^{31,33}, demonstrating that some mutant *p53* proteins have enhanced oncogenic potential beyond the simple loss of *p53* function. WT *p53* has not been shown to be associated with *EZH2* activity or H3K27me3. RNA-seq assays revealed that PRC2-related gene signature was not significantly different between *p53*^{+/+} and *p53*^{-/-} HSPCs, which is different from what we observed in *p53* mutant HSPCs, suggesting that loss of WT *p53* may affect neither *EZH2* activity nor H3K27me3 in HSPCs. Ectopic expression of mutant *p53*, but not WT *p53*, enhances H3K27me3 in 32D cells. Further, we found that several mutant *p53* proteins show enhanced association with *EZH2* compared to WT *p53*. While both loss of *p53* (*p53*^{-/-}) and mutant *p53* (*p53*^{R248W/+}) enhances HSC repopulating potential, our data

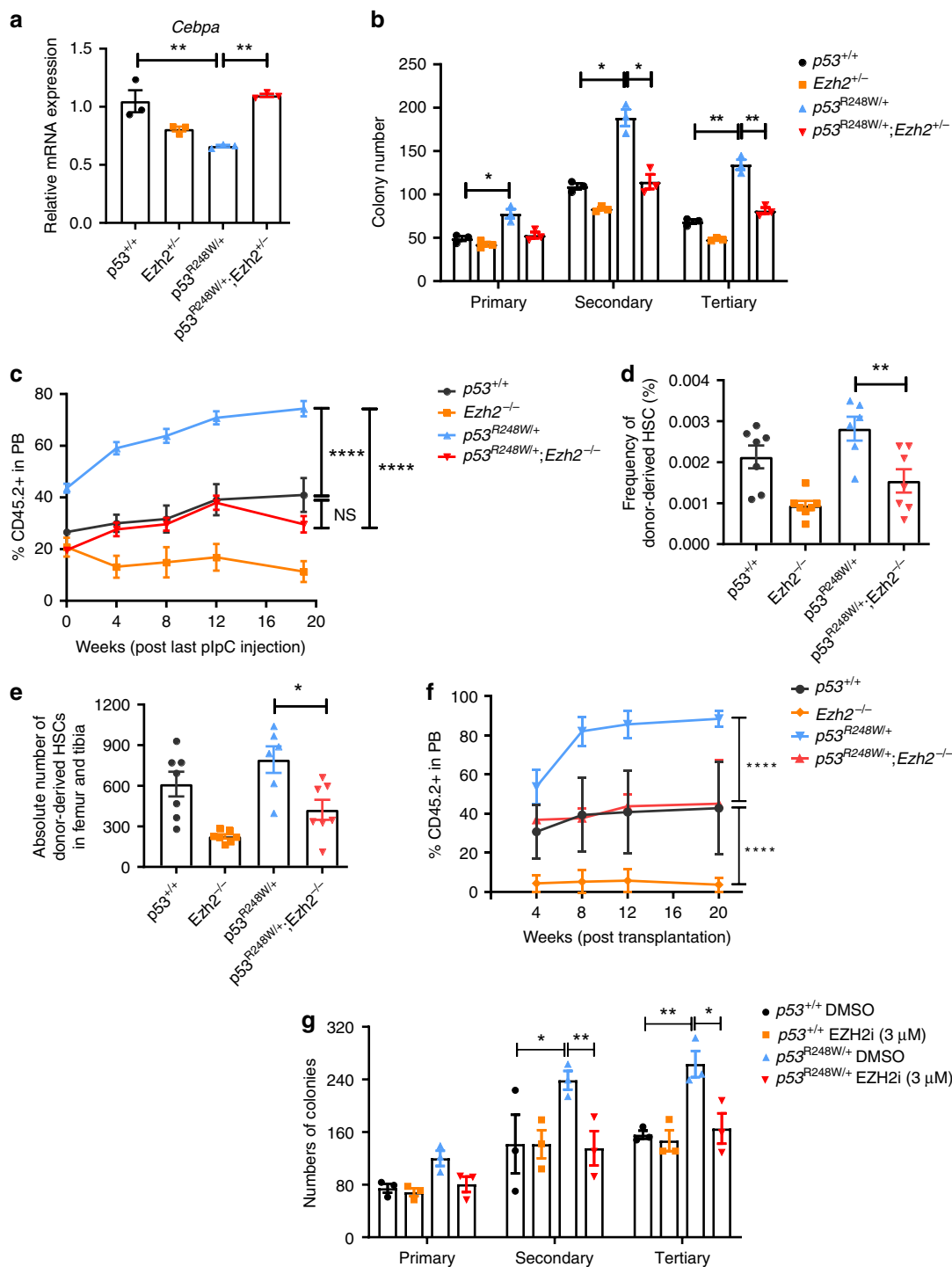


Fig. 6 Loss of EZH2 decreases the repopulating potential of p53 mutant HSPCs. **a** *Cebpa* expression in $p53^{+/+}$, $Ezh2^{-/-}$, $p53^{R248W/+}$, and $p53^{R248W/+};Ezh2^{-/-}$ HSPCs; $n = 3$ biological replicates. **b** Serial replating assays of BM cells from $p53^{+/+}$, $Ezh2^{-/-}$, $p53^{R248W/+}$ and $p53^{R248W/+};Ezh2^{-/-}$ mice; $n = 3$ independent experiments. **c** Percentage of donor-derived cells in the PB of recipient mice at 20 weeks following pl:pC (polyinosinic:polycytidylic acid) treatment; $n = 7$ mice per group. **d** Percentage of donor-derived HSCs in the BM of recipient mice at 20 weeks following pl:pC treatment; $n = 6-7$ mice per group. **e** The absolute number of donor-derived HSCs in the BM of recipient mice at 20 weeks following pl:pC treatment; $n = 6-7$ mice per group. **f** Percentage of donor-derived cells in the PB of recipient mice at 20 weeks following secondary transplantation; $n = 7$ mice per group. **g** Serial replating assays using $p53^{+/+}$ and $p53^{R248W/+}$ BM cells treated with DMSO (dimethyl sulfoxide) or EZH2 inhibitor (3 μ M); $n = 3$ independent experiments. Data are represented as mean \pm SEM. *P*-values were calculated using one-way ANOVA with Tukey's multiple comparisons test in **a**, **d**, and **e**, two-way ANOVA with Tukey's multiple comparison test in **b**, **c**, **f**, and **g**; **P* < 0.05, ***P* < 0.01, *****P* < 0.0001. Source data are provided as a Source Data file.

suggest that increased levels of H3K27me3 in p53 mutant HSPCs is likely due to the presence of the mutant allele, but not the result of losing WT p53 activity. While a dominant-negative (DN) effect has been shown to drive selection of *TP53* missense mutations in

myeloid malignancies⁵³, GOF mutant p53 appears to play an important role in myeloid leukemia³². Our work suggests that both DN and GOF properties may contribute to enhanced HSC self-renewal seen in $p53^{R248W/+}$ mice.

Clinical studies revealed that hematopoietic clones harboring specific mutations in individuals with CHIP may expand over time^{4–6}. However, how different cellular stressors affect clonal expansion is largely unknown. Recently, two different stressors, including hematopoietic transplantation and cytotoxic therapy, have been shown to expand hematopoietic clones^{10,12,22,35–37}. We discovered that *TP53* mutations identified in CHIP confer a competitive advantage to HSPCs following transplantation. *TP53* mutations are associated with prior exposure to chemotherapy^{10,12} and we observed that *TP53* mutations confer radiation resistance, leading to selective expansion of *TP53*-mutant HSPCs. Recently, *PPM1D* mutations were found in CHIP, especially in patients previously exposed to chemotherapy^{10,12,35,36}. *PPM1D* is a phosphatase that negatively regulates p53 and several proteins involved in the DDR pathway^{54,55}. While *PPM1D* mutations result in the expansion of *PPM1D*-mutant hematopoietic cells following chemotherapy treatment^{35,36}, they do not confer competitive advantage to HSPCs following BM transplantation^{12,35,36}. Thus, p53 and *PPM1D* appear to play distinct roles in driving clonal hematopoiesis.

While we have identified a stem cell intrinsic mechanism by which mutant p53 drives clonal hematopoiesis, recent studies indicate that mutations identified in CHIP may utilize cell extrinsic mechanisms to promote clonal hematopoiesis^{56,57}. We will investigate the cell extrinsic mechanisms by which mutant p53 drives CHIP in the future. Some individuals with CHIP developed AML with age^{2,3}. However, the role of mutant p53 in the initiation and progression of AML is largely unknown^{18,58}. We recently reported that mutant p53 synergizes with FLT3-ITD in leukemia development⁵⁹. We will elucidate the mechanisms by which mutant p53 drives leukemia development.

In summary, we discovered that *TP53* mutations drive clonal hematopoiesis in response to distinct cellular stressors. Mechanistically, mutant p53 interacts with EZH2 and enhances its association with the chromatin, increasing the levels of H3K27me3 in genes regulating HSPC self-renewal and differentiation. EZH2 is rarely mutated in CHIP^{4–6} and we found that genetic and pharmacological inhibition of EZH2 decrease the repopulating potential of p53 mutant HSPCs. Thus, our work will likely establish epigenetic regulator EZH2 as a novel therapeutic target for preventing CHIP progression and treating hematological malignancies with *TP53* mutations.

Methods

Mice. The HUPKI (*p53*^{+/+}) and *p53*^{R248W/+} mice used in our studies have been backcrossed to the C57BL/6 background for 12 generations^{22,33}. All young *p53*^{+/+}, *p53*^{+/-}, *p53*^{-/-}, and *p53*^{R248W/+} and *Ezh2*^{Fl/F}.*Mx1-Cre*⁺ mice used in these studies are 8–12 weeks old and are tumor free. WT C57BL/6 (CD45.2⁺), B6.SJL (CD45.1⁺), and F1 mice (CD45.2⁺ CD45.1⁺) mice were obtained from an on-site core breeding colony. We have complied with all relevant ethical regulations for animal testing and research. All animal-related experiments have received ethical approval from the Indiana University Institutional Animal Care and Use Committee (IACUC). All mice were maintained in the Indiana University Animal Facility according to IACUC-approved protocols.

Generation of retroviruses and infection of HSPCs. Retroviral vectors were produced by transfection of Phoenix E cells with the MIGR1 control or MIGR1 full-length mutant p53 cDNA plasmids, according to standard protocols. Mouse HSPCs were infected with high-titer retroviral suspensions in the presence of Retronectin. Forty-eight hours after infection, the GFP-positive cells were sorted by FACS^{20,21}.

Stem and progenitor cell assays. Clonogenic progenitors were determined in methylcellulose medium (MethoCult GF M3234, StemCell Technologies) using 2 × 10⁴ BM cells per well (6-well plate). Colonies were scored after 7 days of the initial culture, and all cells were collected and washed twice in PBS. Subsequently cells were cultured in the same medium. Colony scoring and replating were repeated every 7 days for at least two times^{20,21}.

Flow cytometry. Murine HSPCs were identified and evaluated by flow cytometry using a single cell suspension of bone marrow mononuclear cells (BMMCs). Hematopoietic stem and progenitors are purified based upon the expression of surface markers: LT-HSC (Lin⁻ Sca1⁺ Kit⁺ CD48⁻ CD150⁺), ST-HSC (Lin⁻ Sca1⁺ Kit⁺ CD48⁻ CD150⁻), MPP (Lin⁻ Sca1⁺ Kit⁺ CD48⁺ CD150⁻), CMP (Lin⁻ Sca1⁻ Kit⁺ CD16/32^w CD34^{high}), GMP (Lin⁻ Sca1⁻ Kit⁺ CD16/32^w CD34^{high}), and MEP (Lin⁻ Sca1⁻ Kit⁺ CD16/32^w CD34^{low}). BM cells were obtained from tibia, femur, and iliac crest (6 from each mouse) by flushing cells out of the bone using a syringe and phosphate-buffered saline (PBS) with 2 mM EDTA. Red blood cells (RBCs) were lysed by RBC lysis buffer (eBioscience) prior to staining. Experiments were performed on FACS LSR IV cytometers (BD Biosciences) and analyzed by using the FlowJo software (TreeStar).

Ki-67 staining. BM cells were stained for cell surface markers as described above. After staining, cells were washed with 0.2% BSA in PBS, fixed and permeabilized using Cytofix/Cytoperm buffer (BD Biosciences) and then incubated with PE-conjugated-antibody against Ki-67 (BD Biosciences) for more than 30 min on ice. Cells were washed, incubated with 4',6-diamidino-2-phenylindole (DAPI) (Sigma) and acquired using LSR IV flow cytometer machine^{20,21}. Data analysis was performed using FlowJo software.

Hematopoietic cell transplantation. For HSC transplantation, we injected 200 CD48⁻ CD150⁺ LSK cells from *p53*^{+/+}, *p53*^{+/-}, *p53*^{-/-}, and *p53*^{R248W/+} mice (CD45.2⁺) plus 3 × 10⁵ competitor BM cells (CD45.1⁺) into lethally irradiated F1 mice (CD45.1⁺ CD45.2⁺). The percentage of donor-derived (CD45.2⁺) cells in PB was analyzed every 4 weeks after transplantation as described above. Twenty weeks following transplantation, we harvested BM cells from recipient mice and performed flow cytometry analysis to evaluate HSC repopulating capability. For secondary transplantation assays, 3 × 10⁶ BM cells from mice repopulated with *p53*^{+/+}, *p53*^{+/-}, *p53*^{-/-}, and *p53*^{R248W/+} HSCs were transplanted into lethally irradiated F1 mice.

For the competitive BM repopulation assays, we injected 5 × 10⁵ BM cells from *p53*^{+/+} and *p53*^{R248W/+} mice (CD45.2⁺) plus 5 × 10⁵ competitor BM cells (CD45.1⁺) into 9.5 Gy lethally irradiated F1 mice (CD45.1⁺ CD45.2⁺). PB was obtained by tail vein bleeding every 4 weeks after transplantation, RBC lysed, and the PB mononuclear cells stained with anti-CD45.2 FITC and anti-CD45.1 PE, and analyzed by flow cytometry. Sixteen weeks following transplantation, BM cells from recipient mice were analyzed to evaluate donor chimerisms in BMs. For secondary transplantation, 3 × 10⁶ BM cells from mice reconstituted with *p53*^{+/+} or *p53*^{R248W/+} BM cells were injected into 9.5 Gy lethally irradiated F1 mice (CD45.1⁺ CD45.2⁺).

Limiting dilution assays. Different doses (10,000, 20,000, 40,000, 80,000) of BM cells from *p53*^{+/+} and *p53*^{R248W/+} mice (CD45.2⁺) together with 200,000 competitor cells (CD45.1⁺) were transplanted into lethally irradiated (9.5 Gy) F1 recipient mice (CD45.2⁺ CD45.1⁺). The percentage of donor-derived (CD45.2⁺) cells were analyzed 16-weeks following transplantation as described above. HSC frequency was calculated using L-Calcul software (StemCell Technologies Inc.) and ELDA software (bioinf.wehi.edu.au/software/elda/). Poisson statistics was used to calculate the *P* value.

Homing assays. A total of 1 × 10⁷ *p53*^{+/+} and *p53*^{R248W/+} BM cells (CD45.2⁺) were injected into lethally irradiated recipient mice (CD45.1⁺). BM cells were harvested 18 h following injection and the frequency of donor-derived cells (CD45.2⁺) was evaluated by flow cytometry.

Quantitative real-time PCR. Total RNA was extracted from cells using RNeasy Plus Micro Kit (Qiagen) and cDNA was prepared from total RNA using SuperScript IV First-Strand cDNA Synthesis Kit (Invitrogen Life Technologies) and oligo (dT) primers, following manufacturer's instructions. qRT-PCR assay was performed by using the 7500 Real Time PCR machine (Applied Biosystems) with FastStart Universal SYBR Green Master (ROX) (Roche).

ImageStream flow cytometry analysis. To quantify γ-H2Ax foci in HSPCs, lineage-depleted BM cells were first stained with antibodies against appropriate HSPC surface markers, then fixed and permeabilized using the Cytofix/Cytoperm Kit (BD Biosciences), as described by the manufacturer, and finally stained with an Alexa-488-conjugated anti-γ-H2Ax antibody (Cell Signaling Technology).

To quantify the intensity of H3K27me3 in HSPCs, lineage-depleted BM cells were first stained with antibodies against HSPC surface markers, then fixed and permeabilized using the Cytofix/Cytoperm Kit (BD Biosciences), as described by the manufacturer, and finally stained with an Alexa-488-conjugated anti-H3K27me3.

For quantitative image analysis of p53 and *Ezh2* co-localization within the nucleus, fluorescent cell images (×40) were acquired using an ImageStream flow cytometry system (Amnis; Seattle, WA, <http://www.amnis.com>). Between 171 and 554 Lin⁻ Sca1⁺ cKit⁺ CD150⁺ cell images were analyzed per sample using IDEAS software (Amnis; Seattle, WA, <http://www.amnis.com>). In focus cells were evaluated after gating on live, single, Lin⁻ Sca1⁺ cKit⁺ CD150⁺ cells. Utilizing DAPI staining, we were able to create a nucleus mask and instruct the program to only look at the staining of p53 and *Ezh2* within the DAPI/nucleus mask. Bright detail intensity of

FITC-p53, PE-Ezh2, and DAPI staining was used to quantify mean and geo mean intensity and co-localization within the nucleus. A similarity feature determined the amount of overlay between p53 and Ezh2 within the DAPI mask. The higher the similarity score is, the more co-localized the staining within the nucleus.

Co-IP. H1299 cells (p53 null) were co-transfected with FLAG-HA-EZH2 and WT or mutant p53, respectively, or transfected with FLAG-HA-EZH2 alone. Nuclear extract (NE) was prepared from these cells and incubated with a polyclonal p53 antibody (FL393, Santa Cruz) prior to addition of protein G beads. After overnight incubation, beads were then washed five times and eluted with glycine (0.1 M, pH 2.0), and then neutralized by adding Tris solution (1.5 M, pH 8.8). The eluates were mixed with SDS sample buffer and analyzed by SDS-PAGE, followed by immunoblotting⁶⁰.

Cellular fractionation. Briefly, p53^{+/+} and p53^{R248W/+} HSPCs were harvested and lysed in Buffer A (10 mM Tris-HCl, pH 7.9, 1.5 mM MgCl₂, 10 mM KCl, 0.5 mM DTT, 0.2 mM PMSF, 1 µg/ml pepstatin A, 1 µg/ml leupeptin, 1 µg/ml aprotinin). The cell lysate was then homogenized by a dounce homogenizer for 10 strokes and centrifuged at 4 °C and 15,000×g for 10 min. The supernatant was saved as the cytosolic fraction. The pellet was washed with Buffer A and then re-suspended with Buffer C (20 mM Tris-HCl, pH 7.9, 25% glycerol, 420 mM NaCl, 1.5 mM MgCl₂, 0.2 mM EDTA, 0.5 mM DTT, 0.2 mM PMSF, 1 µg/ml pepstatin A, 1 µg/ml leupeptin, 1 µg/ml aprotinin) and dounced for 10 strokes. Suspension was rotated at 4 °C for 30 min and centrifuged at 4 °C and 7500×g for 5 min. The supernatant was saved as the nucleoplasmic fraction. The pellet was saved as the chromatin fraction and re-suspended with Buffer C. Cell fractions were mixed with SDS sample buffer and heated at 95 °C for 5 min⁶¹. Whole-cell extraction, nucleoplasmic, and chromatin extractions were sonicated for 15 s using a probe sonicator before loading to SDS-PAGE.

RNA sequencing. Total RNA is extracted from LSKs using RNeasy MicroPlus Kit (Qiagen). Then the mRNA is enriched with the oligo(dT) magnetic beads (for eukaryotes), and is fragmented into short fragments (about 100 bp). With random hexamer-primer, the first strand of cDNA is synthesized, and then the second strand is synthesized. The double-strand cDNA is purified with magnetic beads. The ends of the double strand cDNA are repaired, and a single nucleotide A (adenine) is added to the 3'-ends. Finally, sequencing adaptors are ligated to the fragments. The ligation products are amplified with PCR. For quality control, RNA and library preparation integrity are verified using Agilent 2100 BioAnalyzer system and ABI StepOnePlus Real-Time PCR System. RNA sequencing library was then constructed and then sequenced with HiSeq 4000.

Gene Set Enrichment Analysis (GSEA) was performed on gene sets from the Molecular Signatures Database (MSigDB, <https://www.broadinstitute.org/msigdb>) and additional gene sets curated from publications. Gene sets with FDR q-value <0.05 were considered significantly enriched.

ChIP sequencing. Lin⁻Kit⁺ cells were fixed with 1% formaldehyde for 15 min and quenched with 0.125 M glycine. Chromatin was isolated by the addition of lysis buffer, followed by disruption with a Dounce homogenizer. Lysates were sonicated and the DNA sheared to an average length of 300–500 bp. Genomic DNA (Input) was prepared by treating aliquots of chromatin with RNase, proteinase K and heat for de-crosslinking, followed by ethanol precipitation. Pellets were resuspended and the resulting DNA was quantified on a NanoDrop spectrophotometer. An aliquot of chromatin (10 µg, spiked-in with 200 ng of Drosophila chromatin) was precleared with protein A agarose beads (Invitrogen). Genomic DNA regions of interest were isolated using 4 µg of antibody against Histone H3K27me3 (clone: 39155, Active Motif). Antibody against H2Av (0.4 µg) was also present in the reaction to ensure efficient pull-down of the spike-in chromatin⁶². Complexes were washed, eluted from the beads with SDS buffer, and subjected to RNase and proteinase K treatment. Crosslinks were reversed by incubation overnight at 65 °C, and ChIP DNA was purified by phenol–chloroform extraction and ethanol precipitation.

Illumina sequencing libraries were prepared from the ChIP and Input DNAs by the standard consecutive enzymatic steps of end-polishing, dA-addition, and adaptor ligation. After a final PCR amplification step, the resulting DNA libraries were quantified and sequenced on Illumina's NextSeq 500 (75 nt reads, single end). Reads were aligned consecutively to the mouse genome (mm10) and to the Drosophila genome (dm3) using the BWA algorithm (default settings). Duplicate reads were removed and only uniquely mapped reads (mapping quality >= 25) were used for further analysis. The number of mouse alignments used in the analysis was adjusted according to the number of Drosophila alignments that were counted in the samples that were compared. Mouse alignments were extended in silico at their 3'-ends to a length of 200 bp, which is the average genomic fragment length in the size-selected library, and assigned to 32-nt bins along the genome. The resulting histograms (genomic "signal maps") were stored in bigWig files. H3K27me3 enriched regions were identified using the SICER algorithm with a MaxGap parameter setting of 600 bp. Signal maps and peak locations were used as input data to Active Motifs proprietary analysis program, which creates Excel tables containing detailed information on sample comparison, peak metrics, peak locations, and gene annotations.

Statistical information. Statistical analysis was performed with GraphPad Prism 8 software (GraphPad software, Inc.). All data are presented as mean ± standard error of the mean (SEM). The sample size for each experiment and the replicate number of experiments are included in the figure legends. Statistical analyses were performed using Student's *t* test where applicable for comparison between two groups, and a one-way ANOVA test or two-way ANOVA was used for experiments involving more than two groups. Statistical significance was defined as **P* < 0.05, ***P* < 0.01, ****P* < 0.001, *****P* < 0.0001; ns, not significant.

Reporting summary. Further information on research design is available in the Nature Research Reporting Summary linked to this article.

Data availability

All RNA-seq and ChIP-seq data from this study were deposited in the Gene Expression Omnibus (GEO) with the accession number of [GSE137126](https://www.ncbi.nlm.nih.gov/geo/query/acc.cgi?acc=GSE137126). The source data underlying all figures are provided as Source Data files. All other remaining data are available within the article and Supplemental Files, or available from the authors upon request.

Received: 19 March 2019; Accepted: 11 November 2019;

Published online: 11 December 2019

References

1. Steensma, D. P. et al. Clonal hematopoiesis of indeterminate potential and its distinction from myelodysplastic syndromes. *Blood* **126**, 9–16 (2015).
2. Spiering, A. S., Gibson, C. J. & Ebert, B. L. The genetics of myelodysplastic syndrome: from clonal haematopoiesis to secondary leukaemia. *Nat. Rev. Cancer* **17**, 5–19 (2017).
3. Jan, M., Ebert, B. L. & Jaiswal, S. Clonal hematopoiesis. *Semin. Hematol.* **54**, 43–50 (2017).
4. Genovese, G. et al. Clonal hematopoiesis and blood-cancer risk inferred from blood DNA sequence. *N. Engl. J. Med.* **371**, 2477–2487 (2014).
5. Jaiswal, S. et al. Age-related clonal hematopoiesis associated with adverse outcomes. *N. Engl. J. Med.* **371**, 2488–2498 (2014).
6. Xie, M. et al. Age-related mutations associated with clonal hematopoietic expansion and malignancies. *Nat. Med.* **20**, 1472–1478 (2014).
7. Young, A. L., Challen, G. A., Birmann, B. M. & Druley, T. E. Clonal haematopoiesis harbouring AML-associated mutations is ubiquitous in healthy adults. *Nat. Commun.* **7**, 12484 (2016).
8. Zink, F. et al. Clonal hematopoiesis, with and without candidate driver mutations, is common in the elderly. *Blood* **130**, 742–752 (2017).
9. Jaiswal, S. et al. Clonal hematopoiesis and risk of atherosclerotic cardiovascular disease. *N. Engl. J. Med.* **13**, 111–121 (2017).
10. Coombs, C. C. et al. Therapy-related clonal hematopoiesis in patients with non-hematologic cancers is common and associated with adverse clinical outcomes. *Cell Stem Cell* **21**, 374–382.e4 (2017).
11. Xia, J. et al. Somatic mutations and clonal hematopoiesis in congenital neutropenia. *Blood* **131**, 408–416 (2018).
12. Wong, T. N. et al. Cellular stressors contribute to the expansion of hematopoietic clones of varying leukemic potential. *Nat. Commun.* **9**, 455 (2018).
13. Levine, A. J. & Oren, M. The first 30 years of p53: growing ever more complex. *Nat. Rev. Cancer* **9**, 749–758 (2009).
14. Brosh, R. & Rotter, V. When mutants gain new powers: news from the mutant p53 field. *Nat. Rev. Cancer* **9**, 701–713 (2009).
15. Talwalkar, S. S. et al. Myelodysplastic syndromes arising in patients with germline TP53 mutation and Li-Fraumeni syndrome. *Arch. Pathol. Lab Med.* **134**, 1010–1015 (2010).
16. Bejar, R. et al. Clinical effect of point mutations in myelodysplastic syndromes. *N. Engl. J. Med.* **364**, 2496–2506 (2011).
17. Peller, S. & Rotter, V. TP53 in hematological cancer: low incidence of mutations with significant clinical relevance. *Hum. Mutat.* **21**, 277–284 (2003).
18. Rücker, F. G. et al. TP53 alterations in acute myeloid leukemia with complex karyotype correlate with specific copy number alterations, monosomal karyotype, and dismal outcome. *Blood* **119**, 2114–2121 (2012).
19. Welch, J. S. et al. TP53 and decitabine in acute myeloid leukemia and myelodysplastic syndromes. *N. Engl. J. Med.* **375**, 2023–2036 (2016).
20. Liu, Y. et al. p53 Regulates hematopoietic stem cell quiescence. *Cell Stem Cell* **4**, 37–48 (2009).
21. Asai, T. et al. Necdin, a p53 target gene, regulates the quiescence and response to genotoxic stress of hematopoietic stem/progenitor cells. *Blood* **120**, 1601–1612 (2012).
22. Chen, S. et al. Genotoxic stresses promotes the clonal expansion of hematopoietic stem cells expressing mutant p53. *Leukemia* **32**, 850–854 (2018).
23. Bondar, T. & Medzhitov, R. p53-Mediated Hematopoietic Stem and Progenitor Cell Competition. *Cell Stem Cell* **6**, 309–322 (2010).

24. Marusyk, A., Porter, C. C., Zaberezhnyy, V. & DeGregori, J. Irradiation Selects for p53-Deficient Hematopoietic Progenitors. *PLoS Biology* **8**, e1000324 (2010).
25. Valk-Lingbeek, M. E., Bruggeman, S. W. & van Lohuizen, M. Stem cells and cancer; the polycomb connection. *Cell* **118**, 409–418 (2004).
26. Sparmann, A. & van Lohuizen, M. Polycomb silencers control cell fate, development and cancer. *Nat. Rev. Cancer* **6**, 846–856 (2006).
27. Bracken, A. P. & Helin, K. Polycomb group proteins: navigators of lineage pathways led astray in cancer. *Nat. Rev. Cancer* **9**, 773–784 (2009).
28. Simon, J. A. & Kingston, R. E. Mechanisms of polycomb gene silencing: knowns and unknowns. *Nat. Rev. Mol. Cell. Biol.* **10**, 697–708 (2009).
29. Xie, H. et al. Polycomb repressive complex 2 regulates normal hematopoietic stem cell function in a developmental-stage-specific manner. *Cell Stem Cell* **14**, 68–80 (2014).
30. Mochizuki-Kashio, M. et al. Dependency on the polycomb gene *Ezh2* distinguishes fetal from adult hematopoietic stem cells. *Blood* **118**, 6553–6561 (2012).
31. Olive, K. P. et al. Mutant p53 gain of function in two mouse models of Li-Fraumeni syndrome. *Cell* **119**, 847–860 (2004).
32. Loizou, E. et al. A gain-of-function p53-mutant oncogene promotes cell fate plasticity and myeloid leukemia through the pluripotency factor FOXH1. *Cancer Discov.* **9**, 962–979 (2019).
33. Song, H., Hollstein, M. & Xu, Y. p53 gain-of-function cancer mutants induce genetic instability by inactivating ATM. *Nat. Cell. Biol.* **15**, 376–388 (2007).
34. Luo, J. L. et al. Knock-in mice with a chimeric human/murine p53 gene develop normally and show wild-type p53 responses to DNA damaging agents: a new biomedical research tool. *Oncogene* **20**, 320–328 (2001).
35. Hsu, J. I. et al. PPM1D mutations drive clonal hematopoiesis in response to cytotoxic chemotherapy. *Cell Stem Cell* **23**, 700–713.e6 (2018).
36. Kahn, J. D. et al. PPM1D-truncating mutations confer resistance to chemotherapy and sensitivity to PPM1D inhibition in hematopoietic cells. *Blood* **132**, 1095–1105 (2018).
37. Wong, T. N. et al. Role of TP53 mutations in the origin and evolution of therapy-related acute myeloid leukaemia. *Nature* **518**, 552–555 (2015).
38. Zhu, J. et al. Gain-of-function p53 mutants co-opt chromatin pathways to drive cancer growth. *Nature* **525**, 206–211 (2015).
39. Krivtsov, A. V. & Armstrong, S. A. MLL translocations, histone modifications and leukaemia stem-cell development. *Nat. Rev. Cancer* **7**, 823–833 (2007).
40. Rao, R. C. & Dou, Y. Hijacked in cancer: the KMT2 (MLL) family of methyltransferases. *Nat. Rev. Cancer* **15**, 334–346 (2015).
41. Voss, A. K., Collin, C., Dixon, M. P. & Thomas, T. Moz and retinoic acid coordinately regulate H3K9 acetylation, Hox gene expression, and segment identity. *Dev. Cell* **17**, 674–686 (2009).
42. Sun, X. J., Man, N., Tan, Y., Nimer, S. D. & Wang, L. The role of histone acetyltransferases in normal and malignant hematopoiesis. *Front. Oncol.* **5**, 108 (2015).
43. Zhang, P. et al. Enhancement of hematopoietic stem cell repopulating capacity and self-renewal in the absence of the transcription factor C/EBP alpha. *Immunity* **21**, 853–863 (2004).
44. Pulikkan, J. A., Tenen, D. G. & Behre, G. C/EBPα deregulation as a paradigm for leukemogenesis. *Leukemia* **31**, 2279–2285 (2017).
45. Thalheimer, F. B. et al. Cytokine-regulated GADD45G induces differentiation and lineage selection in hematopoietic stem cells. *Stem Cell Rep.* **3**, 34–43 (2014).
46. Campbell, J. E. et al. EPZ011989, a potent, orally-available EZH2 inhibitor with robust in vivo activity. *ACS Med. Chem. Lett.* **6**, 491–495 (2015).
47. Kenzelmann Broz, D. et al. Global genomic profiling reveals an extensive p53-regulated autophagy program contributing to key p53 responses. *Genes Dev.* **27**, 1016–1031 (2013).
48. Lindsley, R. C. & Ebert, B. L. Molecular pathophysiology of myelodysplastic syndromes. *Annu. Rev. Pathol.* **8**, 21–47 (2013).
49. Sun, D. et al. Epigenomic profiling of young and aged HSCs reveals concerted changes during aging that reinforce self-renewal. *Cell Stem Cell* **14**, 673–688 (2014).
50. Beerman, I. & Rossi, D. J. Epigenetic control of stem cell potential during homeostasis, aging, and disease. *Cell Stem Cell* **16**, 613–625 (2015).
51. Van der Meulen, J., Speleman, F. & Van Vlierberghe, P. The H3K27me3 demethylase UTX in normal development and disease. *Epigenetics* **9**, 658–668 (2014).
52. Burchfield, J. S., Li, Q., Wang, H. Y. & Wang, R. F. JMJD3 as an epigenetic regulator in development and disease. *Int. J. Biochem. Cell Biol.* **67**, 148–157 (2015).
53. Boettcher, S. et al. A dominant-negative effect drives selection of TP53 missense mutations in myeloid malignancies. *Science* **365**, 599–604 (2019).
54. Fiscella, M. et al. Wip1, a novel human protein phosphatase that is induced in response to ionizing radiation in a p53-dependent manner. *Proc. Natl Acad. Sci. USA* **94**, 6048–6053 (1997).
55. Lu, X. et al. The type 2C phosphatase Wip1: an oncogenic regulator of tumor suppressor and DNA damage response pathways. *Cancer Metastasis Rev.* **27**, 123–135 (2008).
56. Fuster, J. J. et al. Clonal hematopoiesis associated with TET2 deficiency accelerates atherosclerosis development in mice. *Science* **355**, 842–847 (2017).
57. Cai, Z. et al. Inhibition of inflammatory signaling in Tet2 mutant preleukemic cells mitigates stress-induced abnormalities and clonal hematopoiesis. *Cell Stem Cell* **23**, 833–849 (2018).
58. Prokocimer, M., Molchadsky, A. & Rotter, V. Dysfunctional diversity of p53 proteins in adult acute myeloid leukemia: projections on diagnostic workup and therapy. *Blood* **130**, 699–712 (2017).
59. Nabinger, S. C. et al. Mutant p53 enhances leukemia-initiating cell self-renewal to promote leukemia development. *Leukemia* **33**, 1535–1539 (2019).
60. Gao, Z. et al. PCGF homologs, CBX proteins, and RYBP define functionally distinct PRC1 family complexes. *Mol. Cell* **45**, 344–356 (2012).
61. Wang, Q. et al. WDR68 is essential for the transcriptional activation of the PRC1-AUTS2 complex and neuronal differentiation of mouse embryonic stem cells. *Stem Cell Res.* **33**, 206–214 (2018).
62. Egan, B. et al. An alternative approach to ChIP-seq normalization enables detection of genome-wide changes in histone H3 lysine 27 trimethylation upon EZH2 inhibition. *PLoS ONE* **11**, e0166438 (2016).

Acknowledgements

This work was supported by the Office of the Assistant Secretary of Defense for Health Affairs, through the Bone Marrow Failure Research Program—Idea Development Award under Award No. W81XWH-18-1-0265 to Y.L. Opinions, interpretations, conclusions, and recommendations are those of the author and are not necessarily endorsed by the Department of Defense. This work was also supported in part by R01HL150624, R56DK119524, R56AG05250, and a Leukemia & Lymphoma Society (LLS) Translational Research Program Grant 6581–20 to Y.L. S.C.N. was supported by a NIH F32 Award 1F32CA203049. The authors would like to acknowledge the Flow Cytometry Core and In vivo Therapeutic Core Laboratories, which were sponsored, in part, by the NIDDK Cooperative Center of Excellence in Hematology (CEEH) grant U54 DK106846. This work was supported, in part, by a Project Development Team within the ICTSI NIH/NCRR Grant Number UL1TR001108. We would like to thank Dr. Yang Xu at USC for providing the p53^{R248W} mice and Dr. Daniel G Tenen at Harvard Medical School for providing the *Cebpa* plasmid to the study.

Author contributions

S.C., Z.G., and Y.L. conceived the concept, designed the experiments, analyzed and interpreted the data, and wrote the manuscript. S.C., Q.W., H.Y., M.L.C., S.V., S.C.N., R.G., C.Y., M.K., Z.G., A.F., D.H., S.Z.L., S.B., W.C., E.R.W., B.R., Z.C., and N.L. performed the experiments. Q.W. performed the ChIP-seq data analysis. H.G. and Yunlong L performed the RNA-seq data analysis. Y.S., T.N.W., D.C.L., H.S.B., L.D.M., G.H., R.K., M.C.Y., and H.E.B. provided reagents and constructive advice to the study.

Competing interests

The authors declare no competing interests.

Additional information

Supplementary information is available for this paper at <https://doi.org/10.1038/s41467-019-13542-2>.

Correspondence and requests for materials should be addressed to Z.G. or Y.L.

Peer review information *Nature Communications* thanks Peter Adams and the other, anonymous, reviewer(s) for their contribution to the peer review of this work. Peer reviewer reports are available.

Reprints and permission information is available at <http://www.nature.com/reprints>

Publisher's note Springer Nature remains neutral with regard to jurisdictional claims in published maps and institutional affiliations.



Open Access This article is licensed under a Creative Commons Attribution 4.0 International License, which permits use, sharing, adaptation, distribution and reproduction in any medium or format, as long as you give appropriate credit to the original author(s) and the source, provide a link to the Creative Commons license, and indicate if changes were made. The images or other third party material in this article are included in the article's Creative Commons license, unless indicated otherwise in a credit line to the material. If material is not included in the article's Creative Commons license and your intended use is not permitted by statutory regulation or exceeds the permitted use, you will need to obtain permission directly from the copyright holder. To view a copy of this license, visit <http://creativecommons.org/licenses/by/4.0/>.



Versatile by design

Deriving precursor cells from embryonic and induced pluripotent stem cells is no trivial task. Discover how researchers across the world have used the Sony MA900 Multi-Application Cell Sorter to empower their stem cell research.

[Download Publications List](#)

SONY



Bmi1 Maintains the Self-Renewal Property of Innate-like B Lymphocytes

This information is current as of July 29, 2021.

Michihiro Kobayashi, Yang Lin, Akansha Mishra, Chris Shelly, Rui Gao, Colton W. Reeh, Paul Zhiping Wang, Rongwen Xi, Yunlong Liu, Pamela Wenzel, Eliver Ghosn, Yan Liu and Momoko Yoshimoto

J Immunol 2020; 204:3262-3272; Prepublished online 24 April 2020;
doi: 10.4049/jimmunol.2000030
<http://www.jimmunol.org/content/204/12/3262>

Supplementary Material <http://www.jimmunol.org/content/suppl/2020/04/23/jimmunol.2000030.DCSupplemental>

References This article **cites 37 articles**, 18 of which you can access for free at: <http://www.jimmunol.org/content/204/12/3262.full#ref-list-1>

Why *The JI*? Submit online.

- **Rapid Reviews! 30 days*** from submission to initial decision
- **No Triage!** Every submission reviewed by practicing scientists
- **Fast Publication!** 4 weeks from acceptance to publication

**average*

Subscription Information about subscribing to *The Journal of Immunology* is online at: <http://jimmunol.org/subscription>

Permissions Submit copyright permission requests at: <http://www.aai.org/About/Publications/JI/copyright.html>

Email Alerts Receive free email-alerts when new articles cite this article. Sign up at: <http://jimmunol.org/alerts>

The Journal of Immunology is published twice each month by The American Association of Immunologists, Inc., 1451 Rockville Pike, Suite 650, Rockville, MD 20852
Copyright © 2020 by The American Association of Immunologists, Inc. All rights reserved.
Print ISSN: 0022-1767 Online ISSN: 1550-6606.



Bmi1 Maintains the Self-Renewal Property of Innate-like B Lymphocytes

Michihiro Kobayashi,* Yang Lin,[†] Akansha Mishra,[†] Chris Shelly,[†] Rui Gao,[†] Colton W. Reeh,* Paul Zhiping Wang,[‡] Rongwen Xi,[§] Yunlong Liu,[‡] Pamela Wenzel,* Eliver Ghosn,^{¶,||} Yan Liu,[†] and Momoko Yoshimoto*

The self-renewal ability is a unique property of fetal-derived innate-like B-1a lymphocytes, which survive and function without being replenished by bone marrow (BM) progenitors. However, the mechanism by which IgM-secreting mature B-1a lymphocytes self-renew is poorly understood. In this study, we showed that *Bmi1* was critically involved in this process. Although *Bmi1* is considered essential for lymphopoiesis, the number of mature conventional B cells was not altered when *Bmi1* was deleted in the B cell lineage. In contrast, the number of peritoneal B-1a cells was significantly reduced. Peritoneal cell transfer assays revealed diminished self-renewal ability of *Bmi1*-deleted B-1a cells, which was restored by additional deletion of *Ink4-Arf*, the well-known target of *Bmi1*. Fetal liver cells with B cell-specific *Bmi1* deletion failed to repopulate peritoneal B-1a cells, but not other B-2 lymphocytes after transplantation assays, suggesting that *Bmi1* may be involved in the developmental process of B-1 progenitors to mature B-1a cells. Although *Bmi1* deletion has also been shown to alter the microenvironment for hematopoietic stem cells, fat-associated lymphoid clusters, the reported niche for B-1a cells, were not impaired in *Bmi1*^{-/-} mice. RNA expression profiling suggested lysine demethylase 5B (*Kdm5b*) as another possible target of *Bmi1*, which was elevated in *Bmi1*^{-/-} B-1a cells in a stress setting and might repress B-1a cell proliferation. Our work has indicated that *Bmi1* plays pivotal roles in self-renewal and maintenance of fetal-derived B-1a cells. *The Journal of Immunology*, 2020, 204: 3262–3272.

Murine B-1 cells are innate-like mature B lymphocytes distinct from conventional adoptive immune B lymphocytes (B-2 cells). B-1 cells harbor unique characteristics, including specific surface markers (IgM^{high}IgD^{low}CD19^{hi}B220^{lo}), production of natural IgM Abs, and their primal localization in the

pleural and peritoneal cavities (1). One of the most striking characteristics of CD5⁺ B-1 cells (referred to as B-1a cells) is their unique origin and self-replenishing ability. Cell transfer studies using fetal liver (FL) and bone marrow (BM) progenitors demonstrated that only FL progenitors, not BM cells, efficiently reconstitute peritoneal B-1a cells upon transplantation (2). Lin⁻AA4.1⁺CD19⁺B220^{lo-neg} B-1-specific progenitors have been found in the FL, and neonatal BM and were shown to decline in number during aging, suggesting that B-1 cells are mostly derived from fetal and neonatal progenitors (3, 4) and represent a distinct lineage from conventional B-2 cells. Additionally, long-term hematopoietic stem cells (LT-HSCs) in the FL and adult BM reportedly failed to reconstitute peritoneal B-1a cells in transplantation assays (5, 6), indicating that some (if not most) B-1a cells develop independently of hematopoietic stem cells (HSCs) (7, 8) and are maintained throughout life without being replenished by adult HSC-derived progenitors (9). Finally, adoptive transfer of mature B-1a cells into congenic recipient mice was demonstrated to be sufficient to repopulate and maintain the B-1a cell compartment in the long term, supporting the notion that B-1a cells are maintained in vivo by self-renewal mechanisms.

The self-renewal ability is one of the most important features of stem cells. Both HSCs and neural stem cells rely on the *Bmi1* polycomb ring finger proto-oncogene (*Bmi1*) for their long-term self-renewal (10–12). BMI1 consists of the polycomb repressor complex 1 (PRC1), which represses gene expression. In *Bmi1*^{-/-} mice, the number of HSCs and all lymphoid cell subsets were shown to be significantly reduced, and the self-renewal ability of HSCs upon transplantation was lost (11). The *Ink4-Arf* locus is a known target of *Bmi1* in both HSCs and neural stem cells, and deletion of *Ink4-Arf* in *Bmi1*^{-/-} mice was demonstrated to dramatically correct the number and self-renewal ability of HSCs (13). Moreover, *Bmi1* has also been shown to regulate the regeneration of

*Center for Stem Cell Research and Regenerative Medicine, Institute for Molecular Medicine, McGovern Medical School, The University of Texas Health Science Center at Houston, Houston, TX 77030; [†]Wells Center for Pediatric Research, Department of Pediatrics, Indiana University School of Medicine, Indianapolis, IN 46202; [‡]Center for Computational Biology and Bioinformatics, Department of Medical and Molecular Genetics, Indiana University School of Medicine, Indianapolis, IN 46202; [§]National Institute of Biological Science, Beijing 102206, China; [¶]Department of Medicine, Lowance Center for Human Immunology, Emory Vaccine Center, Emory University, Atlanta, GA 30322; and ^{||}Department of Pediatrics, Lowance Center for Human Immunology, Emory Vaccine Center, Emory University, Atlanta, GA 30322
ORCID: 0000-0003-3574-5777 (A.M.); 0000-0002-5927-903X (C.W.R.); 0000-0002-2699-626X (Yunlong Liu); 0000-0001-7258-906X (E.G.); 0000-0002-7272-6682 (M.Y.).

Received for publication January 9, 2020. Accepted for publication April 6, 2020.

This work was supported by National Institute of Allergy and Infectious Diseases R56AI110831 and R01AI121197 (to M.Y.).

The microarray data presented in this article have been submitted to the Gene Expression Omnibus (<https://www.ncbi.nlm.nih.gov/geo/>) under accession number GSE97202.

Address correspondence and reprint requests to Dr. Yan Liu or Dr. Momoko Yoshimoto, Well Center for Pediatric Research, Indiana University School of Medicine, Indianapolis, IN 46202 (Yan Liu) or Institute of Molecular Medicine, University of Texas Health Science Center at Houston, McGovern Medical School, 1825 Pressler Street, Suite 637B, Houston, TX 77030 (M.Y.). E-mail addresses: liu219@iu.edu (Yan Liu) or Momoko.Yoshimoto@uth.tmc.edu (M.Y.).

The online version of this article contains supplemental material.

Abbreviations used in this article: B/J, Boy/J; BM, bone marrow; *Bmi1*^{f/f}, *Bmi1*-flox/flox; ChIP, chromatin immunoprecipitation; DE, differential expression; DKO, double knockout; F, forward; FALC, fat-associated lymphoid cluster; FL, fetal liver; HSC, hematopoietic stem cell; *Kdm5b*, lysine demethylase 5B; LT-HSC, long-term hematopoietic stem cell; MNC, mononuclear cell; NSG, NOD/SCID/IL-2R γ ^{-/-}; PRC1, polycomb repressor complex 1; qPCR, quantitative PCR; R, reverse; WT, wild-type.

Copyright © 2020 by The American Association of Immunologists, Inc. 0022-1767/20/\$37.50

skeletal muscles (14) and the proliferation and self-renewal of intestinal stem cells (15). Additionally, it has been reported that overexpression of *Bmi1* induced an extensive capacity for self-renewal in adult BM erythroblasts to similar levels as those seen in embryo-derived self-renewing erythroblasts (16). We recently reported that overexpressing *Bmi1* in mouse embryonic stem cell-derived B-1 cells enhanced long-term engraftment in recipient mice upon transplantation (17). Therefore, we hypothesized that *Bmi1* might play an important role in the homeostatic ability of self-renewal in B-1a cells.

In this study, we report the critical role of *Bmi1* in the maintenance of B-1a cells in vivo. We found that, compared with levels in other lymphoid cell subsets, *Bmi1* is highly expressed in B-1a cells. We confirmed that the total number of T and B lymphocytes were reduced in the spleen and BM of *Bmi1*^{-/-} mice, as previously reported (18). However, the percentage and number of total peritoneal B-1a cells were specifically decreased at a higher rate than those of B-2 and B-1b cells. Importantly, in B cell-specific *Bmi1* knockout mice, only B-1a cells, not other mature B cell subsets (follicular, marginal zone, and B-1b B cells), showed a reduction in their number and frequency. Accordingly, *Bmi1*-deficient peritoneal B-1a cells lost their self-renewal ability upon transplantation, which was restored by overexpression of *Bmi1* or deletion of a well-known target of *Bmi1*, *Ink4-Arf*. Although this restoration by *Ink4-Arf* deletion is consistent with previous reports on HSCs (13), microarray analysis suggested lysine demethylase 5B (*Kdm5b*) as another novel candidate target gene for *Bmi1*. Our results indicated that mature B-1a lymphocytes use *Bmi1* for their maintenance of self-renewal ability.

Materials and Methods

Mice

All mice were bred and maintained under specific pathogen-free conditions in the Indiana University School of Medicine Laboratory Animal Resource Center and the Center for Laboratory Animal Medicine and Care at University of Texas Health Science Center at Houston. C57BL/6J, Boy/J (B/J), NOD/SCID/IL-2R γ c^{-/-} (NSG), *Bmi1*-flox/flox (*Bmi1*^{f/f}), and CD19-Cre knock-in mice (CD19^{Cre/Cre}) were purchased from The Jackson Laboratory. *Bmi1*^{f/f} mice were also provided by Dr. X. Liu (National Institute of Biological Science, Beijing, China). *Bmi1*^{-/-} mice were provided by Dr. M. van Lohuizen (The Netherlands Cancer Institute). *Ink4a-Arf*^{-/-} mice were provided by Dr. R. A. DePinho (MD Anderson Cancer Center). *Bmi1*^{-/-} and *Bmi1*^{-/-}*Ink4-Arf*^{-/-} mice had CD45.1⁺CD45.2⁺ or CD45.2⁺ (depending on the experiment). The experimental procedures were approved by the Institutional Animal Care and Use Committee at Indiana University and the Animal Welfare Committee in University of Texas Health Science Center at Houston.

Flow cytometry

FL, spleen, BM, and peritoneal cells were prepared as single-cell suspension. For analysis and sorting of hematopoietic subsets (Supplemental Table I), the following Abs were used at different fluorescent color combinations: anti-mouse AA4.1 (AA4.1), CD19 (1D3), B220 (RA3-6B2), IgM (II/41), CD21 (8D9), CD23 (B3B4), CD11b (M1/70), Gr1 (RB6-8C5), CD5 (53-7.3), CD3e (145-2C11), Ter119 (TER-119), c-kit (2B8), Sca-1 (D7), CD150 (TC15-12F12.1), CD48 (HM48-1), IL-7Ra (A7R34), and annexin V (all purchased from eBioscience or BioLegend). Cells were analyzed on LSR II or sorted on FACS Aria (Becton Dickinson).

Real-time PCR

Briefly, total RNA was extracted with RNeasy Micro (QIAGEN), followed by reverse-transcription with SuperScript III (Invitrogen). The input cDNA was standardized and then amplified with an ABI Prism 7500 HT (Applied Biosystems) with SYBR Green Master Mix (Applied Biosystems); the following primer sets were used: β -actin forward (F), 5'-CCTAAGGCCAACCCTGAAAAG-3' and reverse (R), 5'-CAGAGGCATACAGGGACAGCA-3'; *HPRT* F, 5'-TCCTCCTCAGACCGCTTTT-3' and R, 5'-CCTGGTTCATCATCGTAATC-3'; *Bmi1* F, 5'-CAGGTTCAACAACCAGACCAC-3' and R, 5'-TGACGGGTGAGCTGCATAAA-3'; *Arf*

F, 5'-CATGTTGTTGAGGCTAGAGAGGA-3' and R, 5'-CTGCACCGTAGTTGAGCAGA-3'; *Kdm5b* F, 5'-TCAGGGACATTATGAGCGAA-3' and R, 5'-TCGGAGGTCAGGTTAGGCTC-3'; p21 F, 5'-AACATCTCAGGGCCGAAAAC-3' and R, 5'-TCCTGACCCACAGCAGAA-3'; and *Bcl-2* F, 5'-TGAGTACTGAACCGGCATCT-3' and R, 5'-TCAAACAGAGTTCGCATGCTG-3'.

Retrovirus production and infection

The knockdown plasmid pMKO was purchased from Addgene (no. 10676) and pMKO-shLuc or -sh-Kdm5b (sh1-3) were prepared with standard cloning strategy. For retrovirus production, pMigR1-Mock or -*Bmi1* or knockdown plasmids were transfected into Phoenix-ECO producer cells respectively, followed by collection and concentration of the virus supernatant with the standard method (19). The established spin-infection was used for infection into FL cells. Target sequences are the following: control (luciferase) 5'-TAAGGCTATGAAGAGATAC-3', Ms_Kdm5b-sh1 5'-GCAGAGGCATGAATATTA-3', Ms_Kdm5b-sh3 5'-CGCCAGTGTGTGGAGCA-TTA-3', and Ms_Kdm5b-shB 5'-GAGATGCACTCCGATACAT-3'.

Transplantation

For peritoneal cell transplantation, donor peritoneal cells (CD45.2 or CD45.1⁺CD45.2⁺) were injected into the peritoneal cavity of sublethally irradiated (250 rad) NSG mice (CD45.1). FL lineage⁻ cells with or without *Bmi1*-expressing vector were injected into the tail vein of lethally irradiated (950 rad) B/J mice. FL B-1 progenitor cells were injected into the peritoneal cavity of sublethally irradiated (150 rad) NSG neonates.

Microarray analysis

Peritoneal B-1a cells were collected from *Bmi1*^{-/-} and wild-type (WT) mice, and RNA was extracted using RNeasy Micro Kit (QIAGEN) and submitted to Miltenyi Biotec for gene expression analysis using Agilent Whole Mouse Genome Oligo Microarrays. Each seven samples were examined. Complete raw dataset and normalized data were produced by Miltenyi Biotec. The microarray data were submitted to Gene Expression Omnibus (accession code: GSE97202; <https://www.ncbi.nlm.nih.gov/geo/>).

Bioinformatics analysis of microarray

The normalized expression data from Miltenyi Biotec were first filtered by the expression level with a cutoff value of 5. If a gene is expressed higher than this cutoff level in four or more WT/knockout samples, it is kept for the downstream differential expression (DE) analysis. The DE analysis was performed on Partek Genomic Suite (Partek, St. Charles, MO). We then calculated Benjamini-Hochberg multitest adjusted false discovery rate based on the *p* values from the DE analysis. Genes with a false discovery rate <0.2 were used for the Ingenuity Pathway Analysis.

For hierarchical clustering, filtered data were imported into GenePattern (v. 3.9.9; Broad Institute) for hierarchical clustering. Clustering and distance measurements were calculated using pairwise complete linkage and Pearson correlation. Output was used to render heat map data.

Chromatin immunoprecipitation

Chromatin immunoprecipitation (ChIP) was done with standard protocols. DNA from Baf-3 cell (1×10^7) was cross-linked with 1% formaldehyde and was sheared into fragments ~200–500 bp in length with a sonicator (505 Sonic Dismembrator; Thermo Fisher Scientific). All immunoprecipitation used 5 μ g control IgG, anti-Bmi1 (AF27; Active Motif) or ring finger protein 1b (Ring-1b) (D139-3; MBL International) Ab with Protein A Dynabeads (Invitrogen). Quantification of precipitated genomic DNA relative to input was done in triplicate after real-time PCR with SYBR Green Master Mix (Applied Biosystems). The following primer sets were used: Ms_Kdm5b/ChIP/+700 F, 5'-GTCTGGAGCGGCTGGTTGAG-3' and R, 5'-CCCACATCCTCAAAGTGTGCG-3'; Ms_Kdm5b/ChIP/-200 F, 5'-GTCTGTCC-TTGCTGCTCCTTG-3' and R, 5'-AAACCCGAGAAGCAGAGTACT-3'; Ms_Kdm5b/ChIP/-2000 F, 5'-TCAGGCTCCAAATCCCTGTAGA-3' and R, 5'-GCTCTATCGAAGTACCTGGCC-3'; Ms_Kdm5b/ChIP/-3300 F, 5'-ACTGAGATGGTGCATTTGCTGA-3' and R, 5'-CCTGGCCTTACTGT-TAGTGCG-3'; Ms_Arf/ChIP F, 5'-AAAACCCCTCTTGGAGTGGG-3' and R, 5'-GCAGGTTCTTGGTCACTGTGAG-3'; Ms_Ink4a/ChIP F, 5'-GCCCGAGAATCTAGAGAAATCC-3' and R, 5'-GGATCTCTAGGATTTCTCGGGC-3'; and Ms_GAPDH/ChIP F, 5'-CCCACTTGCCTCTGTAT-TGG-3' and R, 5'-CTGTGGGGAGTCTTTTCAG-3'.

Fat-associated lymphoid cluster staining

Fat tissues were removed from the peritoneal cavity and fixed with 4% paraformaldehyde for 1 h at 4°C. The samples were stained with 1:200

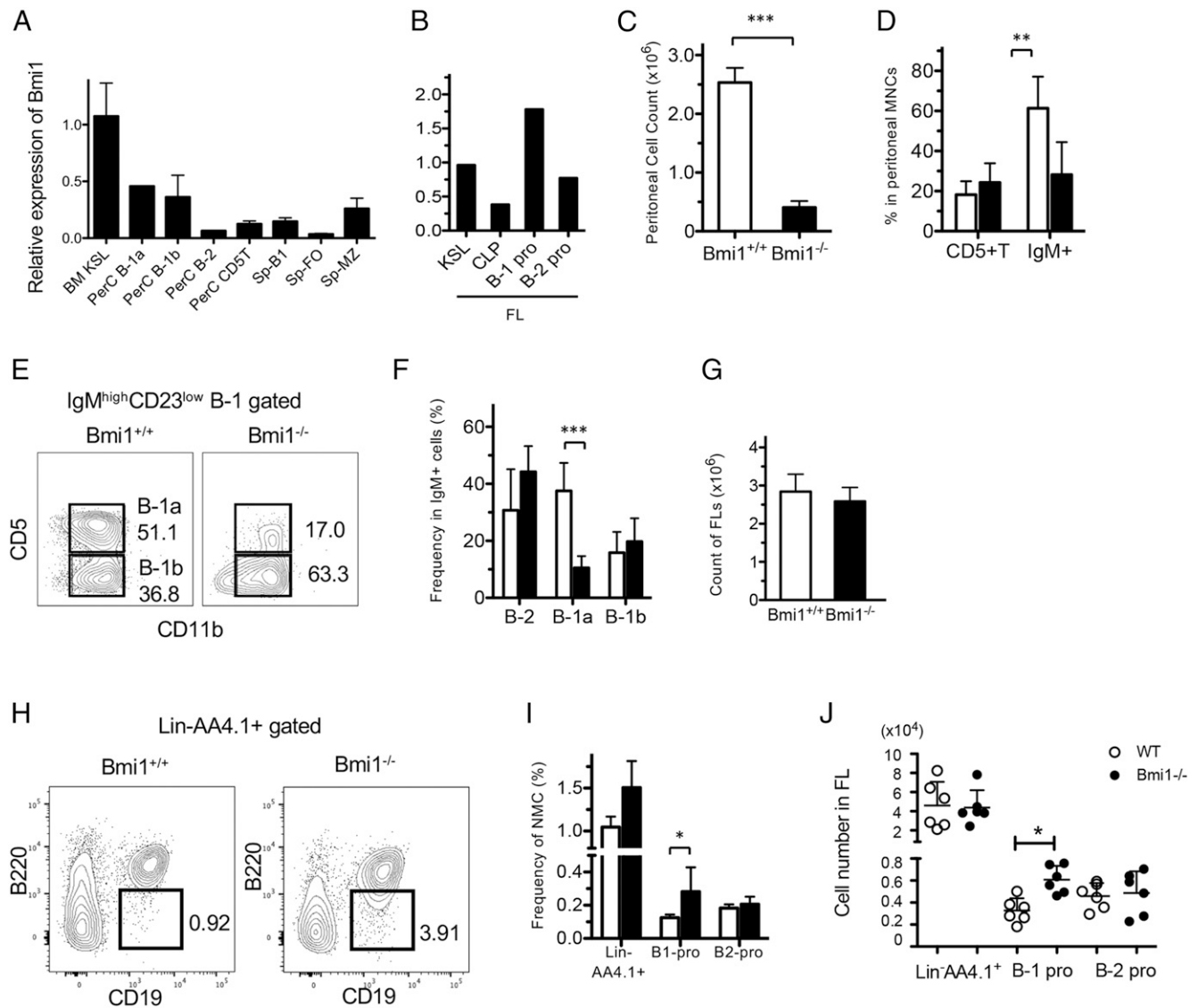


FIGURE 1. Peritoneal B-1a cells have higher *Bmi1* dependency than other lymphoid subsets. **(A)** *Bmi1* mRNA expression measured by qPCR in various sorted populations from adult BM, peritoneal cells (PerC), or spleen (Sp). **(B)** *Bmi1* expressions in various FL progenitor populations. **(C)** Marked reduction of PerC count in *Bmi1*^{-/-} mice ($n = 6$). **(D)** The frequency of IgM⁺ B cell and CD5⁺ T cells in the WT and *Bmi1*^{-/-} peritoneal cavity is depicted ($n = 5$). **(E)** Representative FACS plots for peritoneal B-1a cells in WT and *Bmi1*^{-/-} mice are depicted. The percentage of B-1a cells is reduced ($n = 5$). **(F)** The frequency of B cell subsets among the peritoneal IgM⁺ cells is depicted. The percentage of B-1a cells is reduced ($n = 5$). **(G–J)** Total cell number of FLs (G), representative FACS plots for lin⁻AA4.1⁺CD19⁺B220⁻ B-1 progenitor population in the FL (H), and the frequency (I) and absolute number (J) of FL B-1 and B-2 progenitor cells in WT and *Bmi1*^{-/-} embryos are depicted. B-1 progenitor cell number is increased in the *Bmi1*^{-/-} FL ($n = 6$). * $p < 0.03$. White bar and circle, WT; black bar and circle, *Bmi1*^{-/-}. All data were obtained from experiments more than three times. * $p < 0.05$, ** $p < 0.01$, *** $p < 0.001$. CLP, common lymphoid progenitor; FO, follicular B cell; KSL, kit⁺Sca-1⁺lin⁻ HSC population; MZ, marginal zone B cell.

Alexa Fluor 555-conjugated anti-mouse IgM Ab (SouthernBiotech) and FITC-conjugated anti-CD31 Ab or FITC-conjugated anti-CD11b Ab in 0.1% Triton X-100-PBS for 1 h at room temperature. Then Alexa Fluor 555⁺ (red) areas were dissected out under a Leica mz9.5 fluorescent stereomicroscope and then mounted on Superfrost Plus Gold Slides (Thermo Fisher Scientific) with ProLong Gold Antifade solution with DAPI (Thermo Fisher Scientific). Confocal images were taken using an Olympus II microscope with UApoN340 20×/0.7W objectives (Olympus). ImageJ software was used to adjust and output the images.

Ag stimulation assays

The sorted B-1a cells ($20\text{--}30 \times 10^3$) from each genogroup were plated in the 96-well plate in IMDM with 10% FBS, 10 ng/ml IL-5, 5 μg/ml R848 (TLR7/8 ligand), and 5 μg/ml LPS. Forty-eight hours later, cells were collected, and cell numbers were counted.

Statistical analysis

Student *t* test was used for all statistical analysis.

Results

B-1a cells show higher dependency on *Bmi1* than do other lymphoid subsets

We examined the expression of the *Bmi1* gene by quantitative PCR (qPCR) in various FACS-sorted lymphocyte subsets as shown in Supplemental Table I. Notably, *Bmi1* was highly expressed in peritoneal B-1a and B-1b cells compared with other lymphocyte subsets (Fig. 1A). In the FL, *Bmi1* was highly expressed in B-1-specific progenitors (lin⁻AA4.1⁺CD19⁺B220^{lo/-}) compared with other progenitor subsets (Fig. 1B). Although previous reports have indicated that the lymphoid compartment is globally reduced in the lymphoid organs of *Bmi1*^{-/-} mice, the effect of *Bmi1* deletion on peritoneal B-1 cells has not been reported. Therefore, we examined the peritoneal cavity and found that the total number of peritoneal cells was markedly reduced in *Bmi1*^{-/-} mice (Fig. 1C).

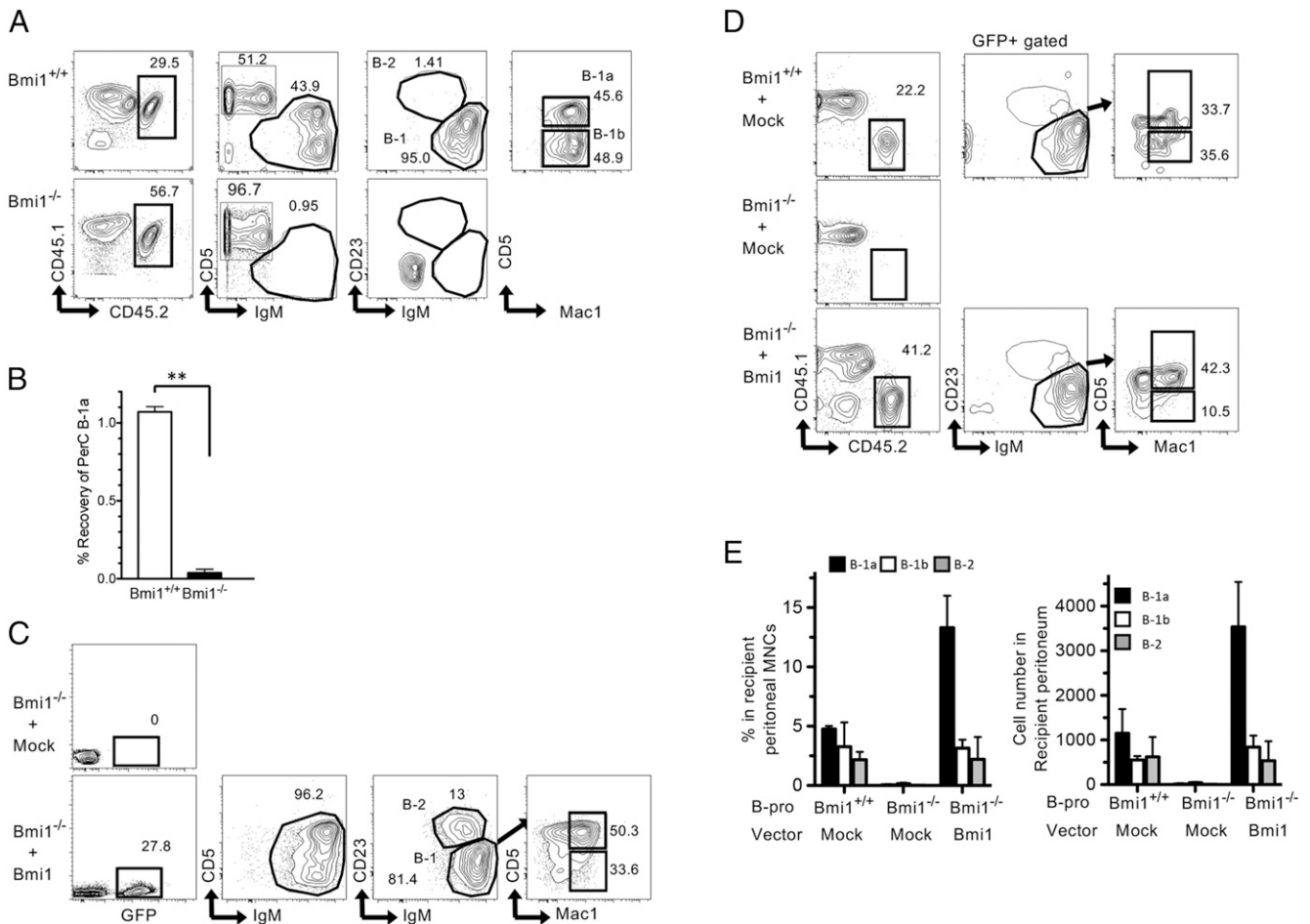


FIGURE 2. Loss of B-1a self-renewal by *Bmi1* disruption. **(A)** Representative FACS plots of recipient peritoneal cells at 12 wk posttransplant. The peritoneal cells of the recipient NSG mice transplanted with *Bmi1*^{+/+} (upper panel) or *Bmi1*^{-/-} (lower panel) peritoneal cells are depicted ($n = 3$). **(B)** Recovery ratio of WT and *Bmi1*^{-/-} B-1a cells after transplantation, calculated by (number of recovered B-1a cells)/(number of injected B-1a cells) 12 wk after transplantation ($n = 3$ for each group). Around 4,000–80,000 B-1a cells were injected. $**p < 0.01$. **(C)** Retrovirus with mock or *Bmi1* vector was infected into *Bmi1*^{-/-} FL Lin⁻ cells. Subsequently, infected cells were transplanted into sublethally irradiated (250 rad) NSG mice. Representative FACS plots at 4 mo posttransplant are depicted ($n = 3$). **(D)** WT and *Bmi1*^{-/-} FL B-1 progenitor cells with a mock or *Bmi1*-overexpressing retrovirus were injected into sublethally irradiated NSG mice. The recipient peritoneal cell analysis 4 mo after transplantation is depicted ($n = 3$). **(E)** The percentage (left) and cell number (right) of donor-derived B cell population in the peritoneal cavity of NSG mice transplanted with *Bmi1*^{-/-} FL B-1 progenitor cells with or without *Bmi1*-overexpressing vector are depicted ($n = 3$). All data were obtained from experiments more than three times.

Although the frequency of CD5⁺ T cells was not altered, the frequency of IgM⁺ B cells was significantly reduced (Fig. 1D). Interestingly, among the peritoneal IgM⁺ cells, the percentage of B-1a cells was specifically reduced, whereas B-2 and B-1b subsets showed similar percentages to those in WT mice (Fig. 1E, 1F). The absolute number of B-1a cells was also dramatically reduced. Both the frequency and absolute number of B-1 progenitors in the *Bmi1*^{-/-} FL were modestly increased compared with those of WT FL (Fig. 1G–J). Thus, loss of *Bmi1* resulted in a profound reduction in both the frequency and absolute number of peritoneal B-1a cells.

Loss of *Bmi1* impairs self-renewal ability of peritoneal B-1a cells

B-1a cells have a self-renewal ability; their numbers are maintained without being replenished by BM progenitors. Because *Bmi1* is crucial for the self-renewal capacity of various stem cells (10–15), we hypothesized that *Bmi1* might also play a critical role in self-renewal ability of peritoneal B-1 cells using transplantation assays in which peritoneal cells containing the same number of B-1a cells (4,000–80,000 cells) from either WT or *Bmi1*^{-/-} mice

were transplanted into sublethally irradiated (250 rad) NSG mice. Our results showed that 3 wk after transplantation, WT donor peritoneal B-1 cells repopulated both B-1a and B-1b subsets, whereas *Bmi1*^{-/-} donor B-1a cells showed poor engraftment (Supplemental Fig. 1A). Furthermore, 12 wk after transplantation, WT B-1a cells were fully reconstituted in the recipient peritoneal cavity, whereas *Bmi1*^{-/-} B-1a cells were diminished (Fig. 2A, 2B). Taken together, these results indicate that B-1a cells lost the self-renewal ability in the absence of *Bmi1*.

Overexpression of *Bmi1* rescues the self-renewal ability of B-1a cells

To confirm that *Bmi1* deficiency is the primary cause of the defect in B-1a cell self-renewal in *Bmi1*^{-/-} mice, we retrovirally overexpressed *Bmi1* in *Bmi1*^{-/-} FL lineage-negative cells (Supplemental Fig. 1B) and transplanted them into sublethally irradiated NSG mice. Although *Bmi1*^{-/-} FL cells transduced with mock vector failed to reconstitute in recipient mice, *Bmi1*^{-/-} FL cells overexpressing *Bmi1* efficiently repopulated all lineages in the BM, including HSCs (Supplemental Fig. 1C). Donor-derived B-1a, B-1b, and B-2 cells were all reconstituted in the peritoneal cavity of the recipient (Fig. 2C).

Next, *Bmi1*^{-/-} FL B-1-specific progenitors retrovirally transduced with *Bmi1* were injected into sublethally irradiated NSG mice to determine the requirement for *Bmi1* in B-1 progenitors. We found that 4 mo after transplantation, *Bmi1*^{-/-} B-1 progenitors transduced with mock vector failed to repopulate B-1a cells, as expected (Fig. 2D). However, *Bmi1*-overexpressing *Bmi1*^{-/-} B-1 progenitors exhibited efficient B-1a cell repopulation in recipient NSG mice (Fig. 2E). Interestingly, donor-derived B-1a cells were more frequent in mice transplanted with *Bmi1*-expressing *Bmi1*^{-/-} B-1 progenitors relative to those transplanted with WT B-1 progenitors (Fig. 2D). Thus, *Bmi1* overexpression not only restored, but also enhanced the self-renewal ability of *Bmi1*^{-/-} B-1a cells.

B cell-restricted deletion of Bmi1 leads to B-1a-specific reduction and loss of self-renewal ability

To exclude the potential influence of defects in either HSCs or the microenvironment on the reduction of B-1a cells in *Bmi1*^{-/-} mice, we used a mouse model in which *Bmi1* was conditionally deleted in the B cell lineage by crossing *CD19*^{Cre/+} and *Bmi1*^{F/F} mice. Notably, because homozygous *CD19*^{Cre/Cre} knock-in mice show defects in B-1a cells (20–22), we used *CD19*^{Cre/+} heterozygous mice to examine B cell-specific depletion of *Bmi1* to avoid any confusing results. Efficient deletion of *Bmi1* alleles was confirmed in sorted peritoneal B-1 cells from *CD19*^{Cre/+}*Bmi1*^{F/F} mice by genomic PCR, as well as by Western blotting of sorted spleen B220⁺ cells, including B-1, marginal zone, and follicular B cells (Fig. 3A, 3B).

Because CD19 is known to play a key role in BCR signaling, we investigated any adverse effects of CD19 heterozygosity on B-1a cells by comparing the frequency and absolute numbers of B-1a cells and other lymphoid subsets in the peritoneal cavity and spleen of WT, *CD19*^{Cre/+}, *CD19*^{Cre/+}*Bmi1*^{F/+}, and *CD19*^{Cre/+}*Bmi1*^{F/F} mice at different developmental ages (Fig. 3C). Although the numbers of peritoneal B-1a cells were significantly lower in any of the *CD19*^{Cre/+} groups at <3 mo old compared with those in WT mice, after 3 mo, only *CD19*^{Cre/+}*Bmi1*^{F/F} knockout mice showed a significant reduction in the numbers of peritoneal B-1a cells among the four groups (Fig. 3C, 3D). When we compared the numbers of B-1a cells in *CD19*^{Cre/+}*Bmi1*^{F/+} control and *CD19*^{Cre/+}*Bmi1*^{F/F} mice in the same litter, the reduction of B-1a cells was clear (Fig. 3E). Therefore, we evaluated the effect of B cell-specific deletion of *Bmi1* in mice older than 3 mo. The frequency and absolute number of peritoneal and splenic B-1a cells were significantly reduced in *CD19*^{Cre/+}*Bmi1*^{F/F} mice among the four groups, whereas no significant change was seen in the other B cell subsets (B-1b and B-2 cells) (Fig. 3F–H, Supplemental Fig. 2A). In addition, no significant change was observed in FL B-1 progenitors (Supplemental Fig. 2B).

To compare the self-renewal ability of B-1a cells from *CD19*^{Cre/+}*Bmi1*^{F/F} and WT mice in the same microenvironment, we performed competitive transplantation assays. To this end, 1×10^5 peritoneal B-1a cells from *Bmi1*^{F/F} or *CD19*^{Cre/+}*Bmi1*^{F/F} mice (CD45.2) were injected into the peritoneal cavities of NSG mice along with an equal number of congenic B/J WT B-1a cells (CD45.1, competitor). We noted that 12 wk after the injection, *CD19*^{Cre/+}*Bmi1*^{F/F} B-1a cells were able to reconstitute only ~8% of total B-1a cells in recipient mice, whereas both the control *Bmi1*^{F/F} and WT B/J B-1a cells achieved comparable levels of reconstitution (Fig. 3I, 3J). Thus, the self-renewal ability of B-1a cells was severely impaired in the absence of *Bmi1*.

The in vivo environment in Bmi1^{-/-} mice permits development and maintenance of B-1a cells

The difference between the severities of the reductions in B-1a cells of *Bmi1*^{-/-} and *CD19*^{Cre/+}*Bmi1*^{F/F} mice led us to hypothesize

that the microenvironment supporting maintenance of B-1a cells might be altered in *Bmi1*^{-/-} mice, similar to the impaired *Bmi1*^{-/-} BM environment that reportedly failed to support HSC self-renewal (13, 23, 24). Fat-associated lymphoid clusters (FALCs) have been reported as a niche for B-1 cells (25, 26), with IgM⁺ cell colonies surrounded by CD31⁺ endothelial cells (Fig. 4A). In *Bmi1*^{-/-} mice, the IgM⁺ lymphoid clusters/colonies were smaller in size and number than were those in WT mice ($p < 0.01$; Fig. 4B, 4C). Interestingly, FALCs in the omentum of *Bmi1*^{-/-}*Ink4a-Arf*^{-/-} mice were partially rescued in size compared with those in *Bmi1*^{-/-} mice (Fig. 4D, 4E). However, it was not clear whether the reduced number and size of FALCs in *Bmi1*^{-/-} mice was the result of environmental defects or of the reduction of B-1a cells itself. To investigate this, we examined the peritoneal environment of *Bmi1*^{-/-} mice using reciprocal transplantation assays. Sorted WT B-1a cells were injected into the peritoneal cavity of sublethally irradiated *Bmi1*^{-/-} and *Bmi1*^{F/+} mice. Against our expectations, the percentage of donor-derived B-1a cells was greater in *Bmi1*^{-/-} than in *Bmi1*^{F/+} recipient mice, although the actual cell numbers were similar (Fig. 4F, 4G). These results indicated that there were no environmental defects related to the engraftment/maintenance of B-1a cells in the peritoneal cavities of *Bmi1*^{-/-} mice.

Development of B-1a cells from FL progenitors is impaired in the absence of Bmi1

Next, to understand the effect of *Bmi1* deletion during development of B-1a cells, we transplanted E14.5 FL mononuclear cells (MNCs) containing B-1 progenitors from *Bmi1*^{F/F}, *CD19*^{Cre/+}, or *CD19*^{Cre/+}*Bmi1*^{F/F} embryos into sublethally irradiated adult NSG mice. Accordingly, 9 mo after transplantation, *CD19*^{Cre/+}*Bmi1*^{F/F} FL MNCs failed to repopulate the peritoneal B-1a cells but successfully repopulated the B-2 and B-1b cells to the same levels as did *Bmi1*^{F/F} FL MNCs (Fig. 3L). Strikingly, defects in the reconstitution of B-1a cells in both the peritoneum and spleen of recipient mice could be observed as early as 6 wk after transplantation (Fig. 3K, Supplemental Fig. 2C), suggesting that *Bmi1* might also be important for the development of B-1a cells from B-1 progenitors in the FL.

TLR-dependent proliferation of B-1a is impaired in the absence of Bmi1

Based on our findings that *Bmi1* was essential to B-1a cell self-renewal, we hypothesized that *Bmi1*-deficient B-1a cells might lose their proliferation ability upon Ag stimulation. To this end, we examined the ability of B-1 cells to proliferate upon stimulation with TLRs. FACS-sorted B-1a cells from each genotype were stimulated in vitro using 5 μg/ml R848 (TRL7/8 agonist) (27). Our results showed that 48 h after stimulation, *Bmi1*-deficient B-1a cells failed to proliferate and, instead, decreased in number, whereas B-1a cells from all control groups showed robust proliferation (Fig. 3M). Taken together, these data suggested that, in addition to its role in self-renewal, *Bmi1* was essential for the proliferation of B-1a cells upon stimulation.

Ink4-Arf locus is a target of Bmi1 in B-1a cells

Because the *Ink4a-Arf* locus is a well-known target of *Bmi1* in HSCs and loss of *Ink4-Arf* in *Bmi1*^{-/-} mice has been shown to rescue the numbers of HSCs and their ability to self-renew (13), we hypothesized that *Ink4-Arf* might also be a target of *Bmi1* in B-1a cells. Correspondingly, qPCR analysis showed a marked elevation of the expression of *Arf* in *Bmi1*^{-/-} peritoneal B-1a cells (Fig. 5A). In *Bmi1*^{-/-}*Ink4-Arf*^{-/-} (double knockout [DKO]) mice, the absolute number of peritoneal cells was significantly higher than that in *Bmi1*^{-/-} mice but still lower than that in WT

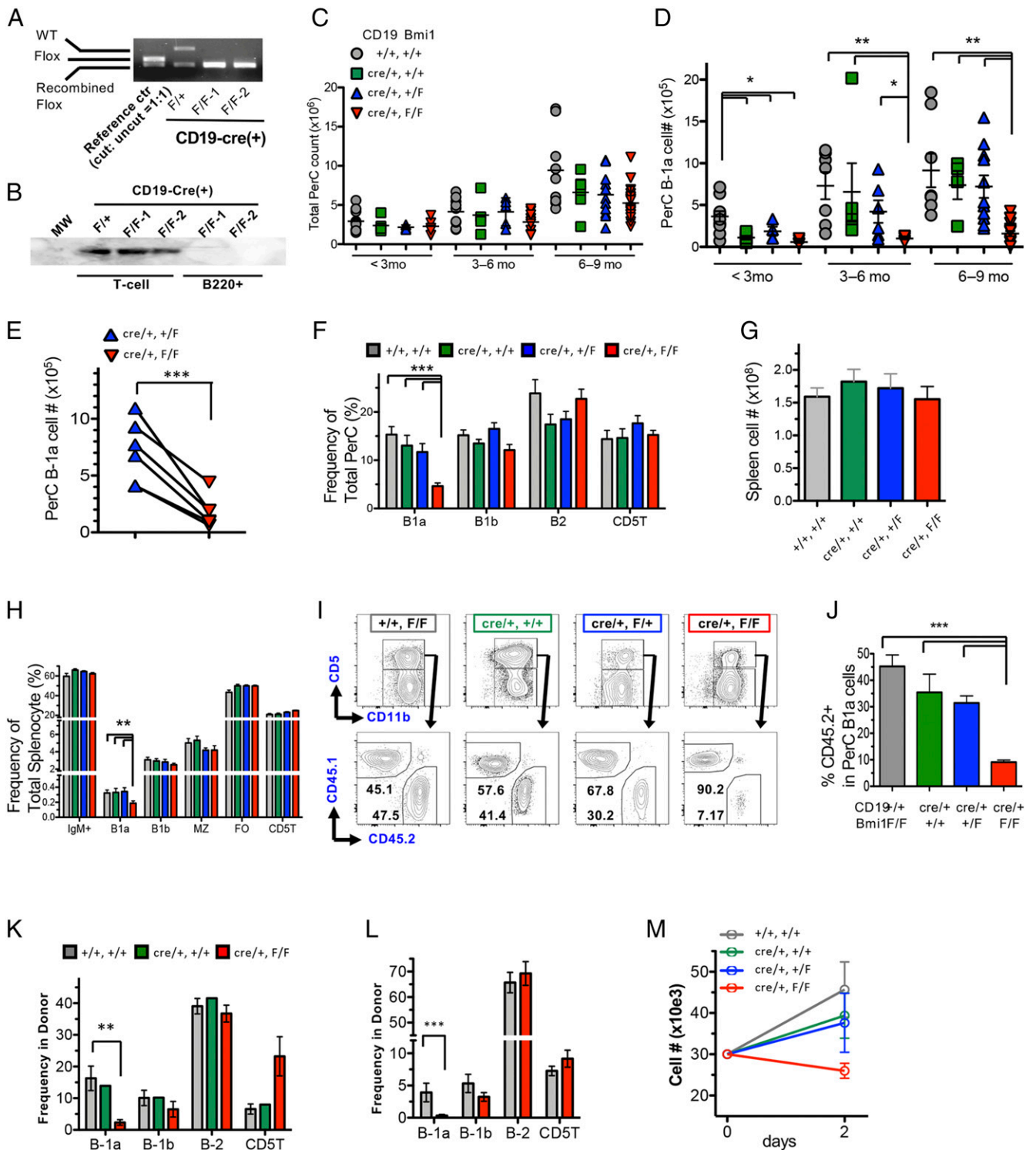


FIGURE 3. B cell-specific deletion of *Bmi1* leads to reduction in the B-1a cell pool and loss of self-renewal ability. The efficiency of CD19-Cre recombinase was confirmed by genomic PCR (**A**) in FACS-sorted B-1 cells or bead-selected spleen B cells (**B**). (**C**) Total peritoneal cell numbers in WT, *CD19^{Cre/+}*, *CD19^{Cre/+}Bmi1^{F/+}*, and *CD19^{Cre/+}Bmi1^{F/F}* mice are shown. No obvious difference was found among the four groups. (**D**) The numbers of peritoneal B-1a cells from four groups at different ages are shown. (*n* = 7–12 for each genotype for each age point). (**E**) The number of B-1a cells in *CD19^{Cre/+}Bmi1^{F/+}* and *CD19^{Cre/+}Bmi1^{F/F}* mice at 3–9 mo of age in the same litter is depicted. The line connects the mice in the same litter. The frequency of lymphoid subsets in the peritoneal cavities (**F**) and the spleens (**G** and **H**) of WT, *CD19^{Cre/+}*, *CD19^{Cre/+}Bmi1^{F/+}*, and *CD19^{Cre/+}Bmi1^{F/F}* mice are shown (*n* = 6). (**I** and **J**) Competitive peritoneal cell transplantation assays. The FACS plots of peritoneal B-1 cells of competitive peritoneal cell-transplanted mice (**I**) and the donor percentage (**J**) are shown. (**K** and **L**) FL MNC transplantation assays. The percentage of donor-derived lymphoid subsets in the peritoneal cavities of transplanted mice with WT or *CD19^{Cre/+}Bmi1^{F/F}* FL MNCs at 6 wk (**K**) and 9 mo (**L**) posttransplant (*n* = 3 for each genotyping, at each time point). (**M**) B-1a cell proliferation upon stimulation with TRL7 agonist. Cell number was counted 48 h after stimulation (*n* = 3). All data were obtained from experiments more than three times. **p* < 0.05, ***p* < 0.01, ****p* < 0.001. CD5T, CD5⁺ T cell; FO, follicular B cell; MZ, marginal zone B cell.

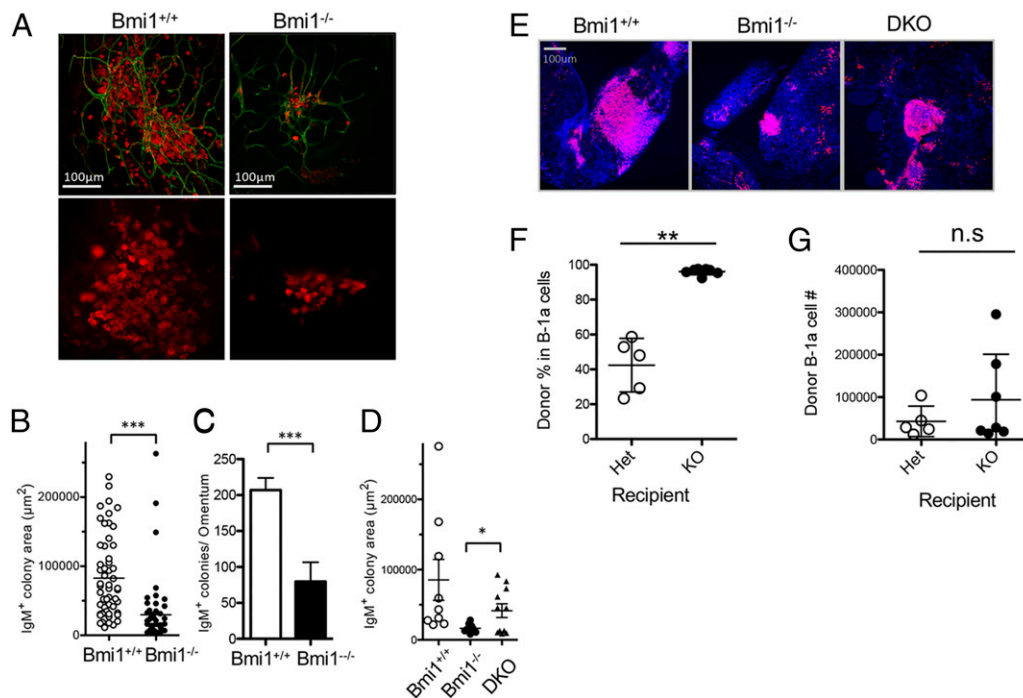


FIGURE 4. FALCs in *Bmi1*^{-/-} peritoneum and reciprocal transplantation assays. **(A)** Representative pictures of FALCs marked by IgM staining (red) in WT or *Bmi1*^{-/-} peritoneum. CD31⁺ endothelial cells are also stained (green). The size **(B)** and number **(C)** of FALCs in the omentum are depicted. **(D)** IgM⁺ colony areas in the omentum among WT, *Bmi1*^{-/-}, and DKO mice. **(E)** Representative pictures of FALCs in WT, *Bmi1*^{-/-}, or DKO mice are shown. The percentage **(F)** and number **(G)** of donor-derived B-1a cells in recipient peritoneal cavity 6 wk after reciprocal transplantation assays. Scale bar, 100 μ m. The data were obtained from three to four animals for each genotype from three experiments. * $p < 0.05$, ** $p < 0.01$, *** $p < 0.001$.

mice probably because of their smaller body sizes (WT: $2.7 \pm 0.1 \times 10^6$, DKO: $1.2 \pm 0.2 \times 10^6$, and *Bmi1*^{-/-}: $0.5 \pm 0.2 \times 10^6$; $p < 0.01$ between DKO and *Bmi1*^{-/-}). The percentage of B-1a cells in DKO mice was similar to that in WT mice (Fig. 5B, 5C), suggesting that deletion of *Ink4-Arf* in *Bmi1*^{-/-} mice was able to rescue the maintenance of B-1a cells, although the recovery of absolute numbers of B-1a cells in DKO was only partial (Fig. 5D). When we performed a competitive assay by transplanting DKO along with B/J WT peritoneal B-1a cells into sublethally irradiated NSG mice, DKO cells achieved similar chimerism to that in WT cells, whereas *Bmi1*^{-/-} B-1a cells failed to repopulate, indicating that deletion of *Ink4-Arf* in *Bmi1*^{-/-} B-1a cells completely restored the self-renewal ability of B-1a cells (Fig. 5E). These results demonstrated that the *Ink4-Arf* locus appears to be a critical target of *Bmi1* in B-1a cells and might play a key role in the self-renewal ability of peritoneal B-1a cells.

Dysregulation of epigenetic gene modifiers in *Bmi1*^{-/-} B-1a cells suggested *Kdm5b* as a target of *Bmi1*

To investigate the *Bmi1*-related genes involved in the maintenance of B-1a cells, we performed microarray analysis of sorted peritoneal B-1a cells from WT and *Bmi1*^{-/-} mice. We identified 364 genes that were shown to be significantly changed (>2-fold) between the two groups. Significantly upregulated and downregulated genes are shown in Fig. 6. Multiple genes mediating genome integrity and translational control, including AT-rich interaction domain 1B (*Arid1b*) and PHD finger protein 12 (*Phf12*), were downregulated (Fig. 6C). Interestingly, various epigenetic modifiers, including DNA methyltransferase 3 α (*Dnmt3a*), 3 β , enhancer of zeste 1 polycomb repressive complex 2 subunit 2 (*Ezh1*), and chromobox 1 (*Cbx1*), were also downregulated (Fig. 6D).

Because *Bmi1* represents a PRC1 gene repressor, many transcription factors were elevated in *Bmi1*^{-/-} B-1a cells. Among

them, we were interested in *Kdm5b* because it has been reported to play a role in the self-renewal and proliferation of cells (28). The expression of *Kdm5b* was significantly increased in the peritoneal B-1a cells, adult LT-HSCs, FL B-1 progenitors, and FL LT-HSCs in the *Bmi1*^{-/-} mice (Fig. 7A, 7B). However, the expression of *Kdm5b* was not elevated in *CD19*^{Cre/+} *Bmi1*^{F/F} B-1a cells in steady states (pre in Fig. 7C). Forty-eight hours after transplantation into sublethally irradiated NSG mice, *Kdm5b* expression significantly increased, and *Arf* expression in *CD19*^{Cre/+} *Bmi1*^{F/F} peritoneal B-1a cells markedly increased (Fig. 7C). In addition, the expression of p21 (cell cycle repressor) at 48 h was not repressed in *CD19*^{Cre/+} *Bmi1*^{F/F} peritoneal B-1a cells as it was in the control cells (Fig. 7C). Moreover, a higher percentage of dead cells was observed among *CD19*^{Cre/+} *Bmi1*^{F/F} B-1a cells (Fig. 7D). These results suggested that *Bmi1*-deficient B-1a cells could not proliferate after transplantation, presumably because of overexpression of *Arf* and *p21*.

To understand the molecular role of *Kdm5b* in cell proliferation, we knocked down the expression of *Kdm5b* in the Baf3 pro-B cell line using a sh-*Kdm5b* retroviral construct (Fig. 7E). sh-*Kdm5b*-transduced cells showed more proliferation than did control cells (sh-Luc) (Fig. 7F). Next, we introduced the viral sh construct into *Bmi1*^{-/-} FL cells and performed colony-forming assays. The number of colonies that formed from *Bmi1*^{-/-} FL cells was significantly lower than that formed from WT cells, as previously reported (12) (Fig. 7G). However, the knockdown of *Kdm5b* in *Bmi1*^{-/-} FLs induced an increase in the number of colonies formed (Fig. 7G). Thus, knockdown of *Kdm5b* led to enhanced cell proliferation in Baf3 and FL cells. In addition, a ChIP assay showed that *Bmi1* bound to the upstream region of *Kdm5b* (Fig. 7H), as well as *Arf*, a known target of *Bmi1* (Fig. 7I). We also confirmed that *Ring1b*, a main component of the PRC1 complex protein, bound to the same regions. Collectively, our data suggested that *Kdm5b* appears to be a downstream target of *Bmi1*, and

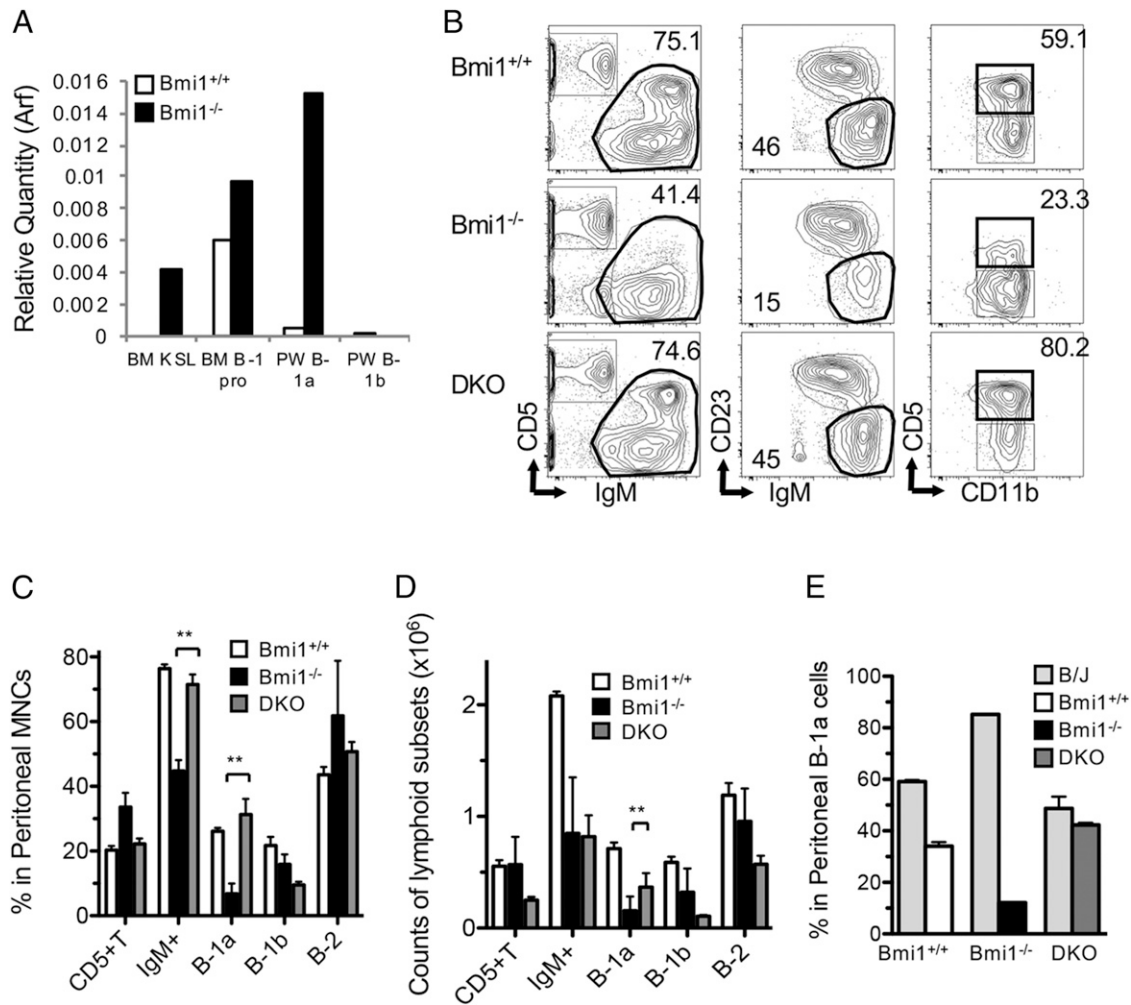


FIGURE 5. Arf-Ink4a is a major target for self-renewal of *Bmi1*^{-/-} B-1a cells. **(A)** Arf expression in WT and *Bmi1*^{-/-} B cells was measured by qPCR. **(B)** Representative FACS plots of peritoneal cells from WT, *Bmi1*^{-/-}, and *Bmi1*^{-/-}Arf-Ink4^{-/-} (DKO) mice are depicted. **(C)** Frequencies of CD5⁺ T cell and B cell subsets in the peritoneal cavity of WT, *Bmi1*^{-/-}, and DKO mice are shown (*n* = 3). **(D)** Absolute numbers of the peritoneal subpopulation from the same three groups (C) were measured. **(E)** Equal numbers of sorted B-1a cells from WT, *Bmi1*^{-/-}, and DKO mice were injected into sublethally irradiated NSG mice in a competitive manner against B/J B-1a cells, followed by analysis at 6 wk. The results of donor contribution are shown. The *Bmi1*^{-/-} B-1a cells failed to repopulate, whereas the DKO cells achieved repopulation similar to that of WT (*n* = 3 for each genotyping). The data were obtained from three experiments. ***p* < 0.01. PW, peritoneal wash.

an optimal low expression level of *Kdm5b* seems to be important for cell proliferation.

Discussion

B-1a lymphocytes are derived from embryonic precursors and maintained in the long-term through their self-renewal ability independently of HSCs (5–9). However, despite extensive studies on the development and function of B-1 cells, the molecular mechanism of B-1a cell self-renewal remains largely unknown. Traditionally, the spleen is known as the organ important for the maintenance of B-1a cells, in addition to their specific BCR and CD19 signaling, all of which continuously stimulate B-1a cells (22, 29–31). A recent study showed that deletion of the basic helix-loop-helix family member E41 (*Bhlhe41*) transcription factor significantly reduced the number of peritoneal B-1a cells, likely by altering BCR signaling and preventing the maturation of transitional B-1 progenitors in the spleen (32). Another interesting report has demonstrated that the autophagy-related 7 (*Atg7*) gene was required for the self-renewal of B-1a cells because of their specific metabolic status that is different from that of B-2 cells (33). These findings have gradually started to elucidate the mechanisms

that support B-1a cell self-renewal and suggest its complexity. In this study, we demonstrated that expression of *Bmi1* was indispensable for the self-renewal ability of peritoneal B-1a cells. The importance of this finding is that mature IgM-secreting B-1a lymphocytes use BMI1 for their self-renewal ability in a similar way to HSCs.

Bmi1, a component of PRC1, is a widely known critical factor in the self-renewal of various stem cells. Importantly, *Bmi1* is also considered to be involved in lymphopoiesis because a large reduction has been observed in lymphocyte counts in the spleen and thymus of *Bmi1*^{-/-} mice (18). However, the frequency and number of B-2 lymphocytes were not altered when *Bmi1* was deleted in the B cell lineage (using CD19-Cre mice). Therefore, it seems that a defect in stem cells (differentiation to B progenitors) mainly contributed to the reduction of B-2 cells in *Bmi1*^{-/-} mice and that, among the mature B cell subsets, only B-1a cells depend on *Bmi1* expression. In the field of HSC biology, self-renewal ability is confirmed only by transplantation assays. Therefore, we carried out peritoneal cell transfer assays in which WT peritoneal B-1a cells repopulate the recipient peritoneal cavity in the long-term, and we further demonstrated a defect in the self-renewal

A Top Canonical Pathways

name	p-value	Ratio
CXCR4 Signaling	3.28E-04	9/152 (0.059)
Signaling by Rho Family GTPases	6.17E-04	11/244 (0.045)
RhoGDI Signaling	9.01E-04	9/184 (0.049)
Role of NFAT in Regulation of the Immune Response	2.56E-03	8/173 (0.046)
Cholecystokinin/Gastrin-mediated Signaling	3.08E-03	6/97 (0.062)

B Molecular and Cellular Functions

name	p-value	# Molecules
Cellular Development	0.0006-0.04	29
Cell-to-Cell Signaling and Integration	6.17E-04	17
Cellular Assembly and organization	9.01E-04	23
Gene Expression	2.56E-03	55
Cellular Function and Maintenance	3.08E-03	35

C Fold change downregulated

Molecules	Exp. Value
Agbl1	-159.10
Ms4a4a	-102.24
Wipf1	-70.39
Dido1	-59.09
Rlim	-58.93
Zcchc2	-56.11
Plekhb2	-46.63
Slbp	-43.02
Gtf2h2	-40.81
Fzd6	-39.05
Nup188	-36.04
Phf12	-31.28
Rab27a	-29.63
Phf8	-19.34
Arid1b	-17.36
phf13	-12.70
phf3	-7.84
Eif5b	-6.54

Fold change upregulated

Molecules	Exp. Value
Hoxc9	84.49
Hcn3	14.38
Zfp873	12.44
Anxa9	8.96
Msrb1	8.83
Cript	7.28
Zeb1	7.09
Eef1g	4.35
Jmjd1c	4.01
Kdm5b	3.70
Il9r	3.47

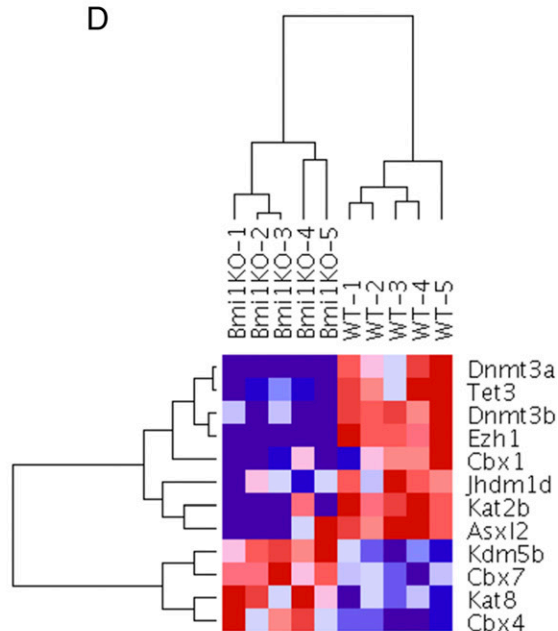
D

FIGURE 6. Gene expression profiling of *Bmi1*^{-/-} reveals dysregulation of epigenetic genes. B-1a cells were sorted from WT and *Bmi1*^{-/-} peritoneal cavity and subjected to microarray analysis. Affected canonical signaling pathways (**A**) and affected biofunctions (**B**) analyzed by Ingenuity Pathway Analysis are listed. (**C**) Differentially upregulated and downregulated transcripts are listed. (**D**) Hierarchical clustering of epigenetic genes is shown ($n = 5$ for each group).

ability of *Bmi1*-deficient B-1a cells, which was restored by additional deletion of *Ink4-Arf*. Proliferation of *Bmi1*-deficient B-1a cells was also impaired after exposure to a TLR7/8 agonist, as well as after transplantation. *Bmi1*-deficient B-1a cells showed upregulation of *Arf* and failure to downregulate p21 after stimulation, which suggested that *Bmi1* maintains the self-renewal ability of B-1a cells through the *Arf-p21* axis. Although *Bmi1* seems to play a role in the self-renewal of B-1a cells similar to its role in HSCs, we have further identified *Kdm5b* as a possible target of *Bmi1* in B-1a cells. The KDM5B histone modifier specifically demethylates H3 at lysine 4 and is known to be required for self-renewal of embryonic stem cells, HSC function, and leukemia/cancer progression and plays different roles depending on cell type and physiological context (28, 34–36). Our results showed that *Kdm5b* was upregulated in *Bmi1*-deficient B-1a cells in a stress setting, but not in steady state, suggesting that *Kdm5b* suppresses proliferation of B-1a cells in the absence of *Bmi1*. Indeed, knockdown of *Kdm5b*-enhanced proliferation of Baf3 cells and rescued the colony-forming ability of *Bmi1*^{-/-} FL cells (Fig. 7F, 7G). Therefore, it can be speculated that B-1a cells fail to proliferate and undergo apoptosis upon Ag exposure in the absence of *Bmi1* followed by upregulated *Kdm5b*. As such, further

investigation on the precise roles of *Kdm5b* in B-1a cells will be required.

Furthermore, FL MNCs that contain *Bmi1*-deleted B progenitors failed to repopulate only B-1a cells, and not other mature B cell subsets, even at an early time point after transplantation. This result suggests a possibility that *Bmi1* may also be required for the developmental process of fetal B-1 progenitor cells into mature B-1a cells. In addition, it is notable that overexpressing *Bmi1* in *Bmi1*^{-/-} FL MNCs not only rescued, but further enhanced B-1a cell repopulation ability (Fig. 2E). This result is consistent with previous reports showing enhanced self-renewal after overexpressing *Bmi1* in BM HSCs and erythroblasts (12, 16). Thus, *Bmi1* seems to enhance both B-1a cell differentiation from FL progenitors and self-renewal of mature B-1a cells. Because the developmental pathway from FL B-1 progenitors to mature peritoneal B-1a cells has not been fully characterized, further study to determine the stage at which *Bmi1* might be involved in the differentiation into B-1a cells is required.

Recent reports have shown the important role of *Bmi1* in controlling the fat volume in the HSC niche (23, 24). We also sought to investigate the effect of the lack of *Bmi1* on FALCs, a niche for B-1a cells, but found that the microenvironment of B-1a cells was

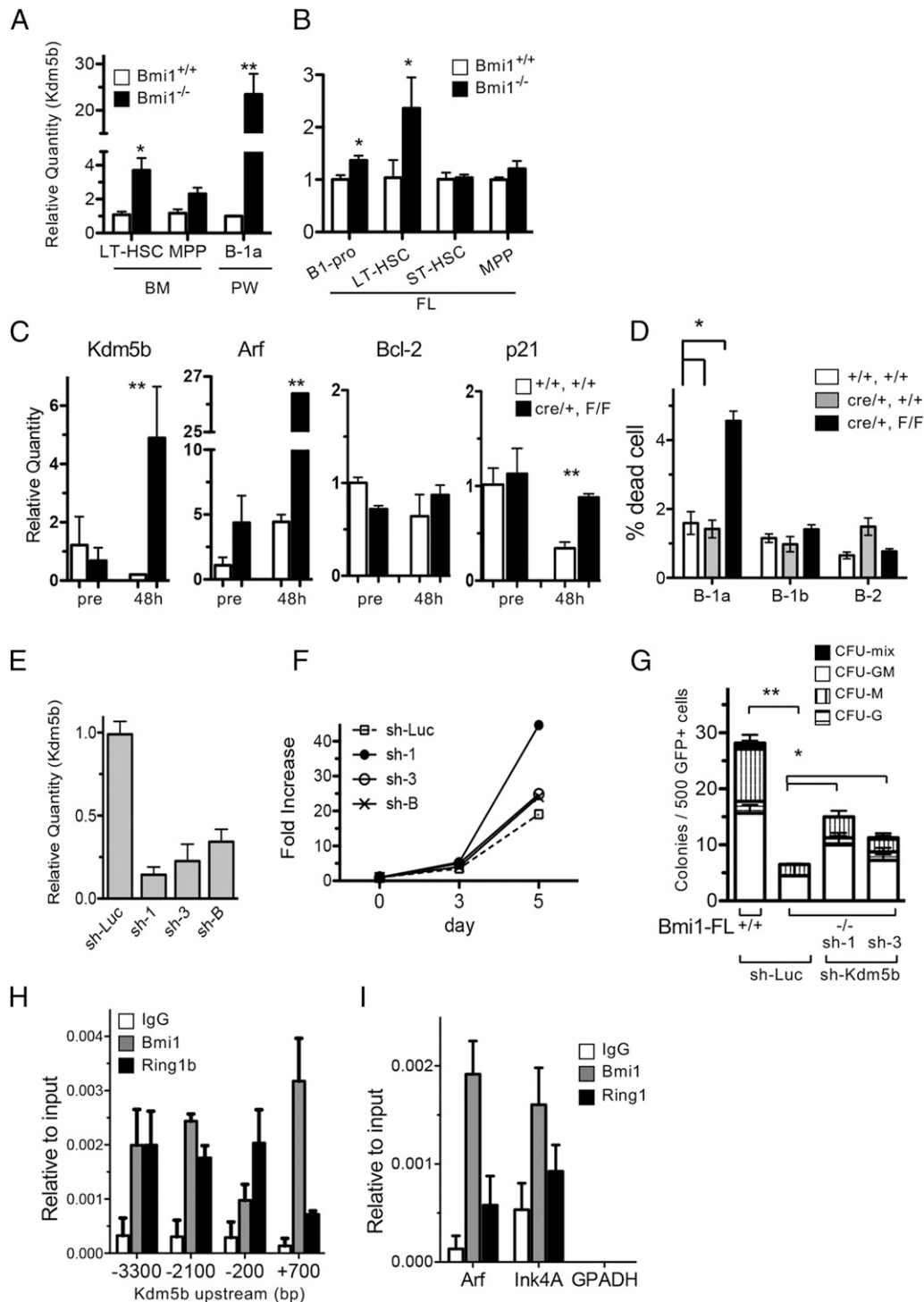


FIGURE 7. *Kdm5b* is a possible *Bmi1* target and crucial for posttransplant B-1a cell expansion. Expression of *Kdm5b* in various cell fractions from WT and *Bmi1*^{-/-} BM and peritoneum (**A**) or FL (**B**) (*n* = 3). **p* < 0.03, ***p* < 0.01. (**C**) Sorted B-1a cells from *CD19*^{Cre/+}*Bmi1*^{F/F} or control mice were injected into sublethally irradiated NSG mice, followed by harvesting of B-1a cells 48 h after transplantation by FACS sorting. Changes in the expression of various mRNAs before and after transplantation (day 2) were measured (*n* = 3). ***p* < 0.01. (**D**) Cell death in experiment (C) was measured by annexin V and DAPI staining (*n* = 3). **p* < 0.05. (**E**) Confirmation of knockdown of *Kdm5b*. Short hairpin RNAs (sh-RNAs) targeting *kdm5b* or control (sh-Luc) were introduced retrovirally into Baf/3 pro-B cells, and GFP⁺ cells were sorted. The quantity of *Kdm5b* mRNA in each clone is shown. (**F**) Cell proliferation of each Baf/3 subline targeting *Kdm5b* is shown. (**G**) Colony-forming assays of *Kdm5b* knockdown *Bmi1*^{-/-} FL cells. *Bmi1*^{-/-} FLs with *sh-Kdm5b* formed more colonies than did the sh-control (*n* = 3). ***p* < 0.01, **p* < 0.05. (**H** and **I**) ChIP assays were performed in Baf3 cells to confirm Bmi1 binding to the *Kdm5b* or *Arf-Ink4* regions. Binding to upstream regions of *Kdm5b* (**H**) and *Arf-Ink4* (**I**) is shown. The data were obtained from three experiments.

not altered. Therefore, *Bmi1* appears to maintain the self-renewal ability of B-1a cells in a cell-intrinsic manner.

In summary, our studies reviewed in this report showed that the self-renewal ability of B-1a lymphocytes depends heavily on

Bmi1 expression, and this dependency is not observed in other mature lymphocyte subsets. Because B-1a cells are not replenished by adult BM progenitors, the loss of B-1a cells after BM transplantation might thus result in acquired immunodeficiency

(37). The knowledge presented in this study could pave the way to fully elucidate the mechanisms of the *in vivo* self-renewal of B-1a cells, an important step toward producing pluripotent stem cell-derived B-1 cells for immune cell therapy (17).

Disclosures

The authors have no financial conflicts of interest.

References

- Herzenberg, L. A., A. M. Stall, P. A. Lalor, C. Sidman, W. A. Moore, D. R. Parks, and L. A. Herzenberg. 1986. The Ly-1 B cell lineage. *Immunol. Rev.* 93: 81–102.
- Hardy, R. R., and K. Hayakawa. 1991. A developmental switch in B lymphopoiesis. *Proc. Natl. Acad. Sci. USA* 88: 11550–11554.
- Montecino-Rodriguez, E., H. Leathers, and K. Dorshkind. 2006. Identification of a B-1 B cell-specified progenitor. *Nat. Immunol.* 7: 293–301.
- Barber, C. L., E. Montecino-Rodriguez, and K. Dorshkind. 2011. Reduced production of B-1-specified common lymphoid progenitors results in diminished potential of adult marrow to generate B-1 cells. *Proc. Natl. Acad. Sci. USA* 108: 13700–13704.
- Ghosh, E. E., R. Yamamoto, S. Hamanaka, Y. Yang, L. A. Herzenberg, H. Nakauchi, and L. A. Herzenberg. 2012. Distinct B-cell lineage commitment distinguishes adult bone marrow hematopoietic stem cells. *Proc. Natl. Acad. Sci. USA* 109: 5394–5398.
- Ghosh, E. E., J. Waters, M. Phillips, R. Yamamoto, B. R. Long, Y. Yang, R. Gerstein, C. A. Stoddart, H. Nakauchi, and L. A. Herzenberg. 2016. Fetal hematopoietic stem cell transplantation fails to fully regenerate the B-lymphocyte compartment. *Stem Cell Reports* 6: 137–149.
- Kobayashi, M., W. C. Shelley, W. Seo, S. Vemula, Y. Lin, Y. Liu, R. Kapur, I. Taniuchi, and M. Yoshimoto. 2014. Functional B-1 progenitor cells are present in the hematopoietic stem cell-deficient embryo and depend on Cbfb for their development. *Proc. Natl. Acad. Sci. USA* 111: 12151–12156.
- Yoshimoto, M., E. Montecino-Rodriguez, M. J. Ferkowicz, P. Porayette, W. C. Shelley, S. J. Conway, K. Dorshkind, and M. C. Yoder. 2011. Embryonic day 9 yolk sac and intra-embryonic hemogenic endothelium independently generate a B-1 and marginal zone progenitor lacking B-2 potential. *Proc. Natl. Acad. Sci. USA* 108: 1468–1473.
- Sawai, C. M., S. Babovic, S. Upadhaya, D. J. H. F. Knapp, Y. Lavin, C. M. Lau, A. Goloborodko, J. Feng, J. Fujisaki, L. Ding, et al. 2016. Hematopoietic stem cells are the major source of multilineage hematopoiesis in adult animals. *Immunity* 45: 597–609.
- Molofsky, A. V., R. Pardal, T. Iwashita, I. K. Park, M. F. Clarke, and S. J. Morrison. 2003. Bmi-1 dependence distinguishes neural stem cell self-renewal from progenitor proliferation. *Nature* 425: 962–967.
- Park, I. K., D. Qian, M. Kiel, M. W. Becker, M. Pihalja, I. L. Weissman, S. J. Morrison, and M. F. Clarke. 2003. Bmi-1 is required for maintenance of adult self-renewing haematopoietic stem cells. *Nature* 423: 302–305.
- Iwama, A., H. Oguro, M. Negishi, Y. Kato, Y. Morita, H. Tsukui, H. Ema, T. Kamijo, Y. Katoh-Fukui, H. Koseki, et al. 2004. Enhanced self-renewal of hematopoietic stem cells mediated by the polycomb gene product Bmi-1. *Immunity* 21: 843–851.
- Oguro, H., A. Iwama, Y. Morita, T. Kamijo, M. van Lohuizen, and H. Nakauchi. 2006. Differential impact of Ink4a and Arf on hematopoietic stem cells and their bone marrow microenvironment in Bmi1-deficient mice. *J. Exp. Med.* 203: 2247–2253.
- Di Foggia, V., X. Zhang, D. Licastro, M. F. Gerli, R. Phadke, F. Muntoni, P. Mourikis, S. Tajbakhsh, M. Ellis, L. C. Greaves, et al. 2014. Bmi1 enhances skeletal muscle regeneration through MT1-mediated oxidative stress protection in a mouse model of dystrophinopathy. *J. Exp. Med.* 211: 2617–2633.
- Yan, K. S., L. A. Chia, X. Li, A. Ootani, J. Su, J. Y. Lee, N. Su, Y. Luo, S. C. Heilshorn, M. R. Amieva, et al. 2012. The intestinal stem cell markers Bmi1 and Lgr5 identify two functionally distinct populations. *Proc. Natl. Acad. Sci. USA* 109: 466–471.
- Kim, A. R., J. L. Olsen, S. J. England, Y. S. Huang, K. H. Fegan, L. F. Delgadillo, K. E. McGrath, P. D. Kingsley, R. E. Waugh, and J. Palis. 2015. Bmi-1 regulates extensive erythroid self-renewal. *Stem Cell Reports* 4: 995–1003.
- Lin, Y., M. Kobayashi, N. Azevedo Portilho, A. Mishra, H. Gao, Y. Liu, P. Wenzel, B. Davis, M. C. Yoder, and M. Yoshimoto. 2019. Long-term engraftment of ESC-derived B-1 progenitor cells supports HSC-independent lymphopoiesis. *Stem Cell Reports* 12: 572–583.
- Bruggeman, S. W., M. E. Valk-Lingbeek, P. P. van der Stoop, J. J. Jacobs, K. Kieboom, E. Tanger, D. Hulsman, C. Leung, Y. Arsenijevic, S. Marino, and M. van Lohuizen. 2005. Ink4a and Arf differentially affect cell proliferation and neural stem cell self-renewal in Bmi1-deficient mice. *Genes Dev.* 19: 1438–1443.
- Gao, R., S. Chen, M. Kobayashi, H. Yu, Y. Zhang, Y. Wan, S. K. Young, A. Soltis, M. Yu, S. Vemula, et al. 2015. Bmi1 promotes erythroid development through regulating ribosome biogenesis. *Stem Cells* 33: 925–938.
- Rickert, R. C., J. Roes, and K. Rajewsky. 1997. B lymphocyte-specific, Cre-mediated mutagenesis in mice. *Nucleic Acids Res.* 25: 1317–1318.
- Rickert, R. C., K. Rajewsky, and J. Roes. 1995. Impairment of T-cell-dependent B-cell responses and B-1 cell development in CD19-deficient mice. *Nature* 376: 352–355.
- Sato, S., N. Ono, D. A. Steeber, D. S. Pisetsky, and T. F. Tedder. 1996. CD19 regulates B lymphocyte signaling thresholds critical for the development of B-1 lineage cells and autoimmunity. *J. Immunol.* 157: 4371–4378.
- Hu, T., A. Kitano, V. Luu, B. Dawson, K. A. Hoegenauer, B. H. Lee, and D. Nakada. 2019. Bmi1 suppresses adipogenesis in the hematopoietic stem cell niche. *Stem Cell Reports* 13: 545–558.
- Kato, Y., L. B. Hou, S. Miyagi, E. Nitta, K. Aoyama, D. Shinoda, S. Yamazaki, W. Kuribayashi, Y. Isshiki, S. Koide, et al. 2019. Bmi1 restricts the adipogenic differentiation of bone marrow stromal cells to maintain the integrity of the hematopoietic stem cell niche. *Exp. Hematol.* 76: 24–37.
- Bénézech, C., N. T. Luu, J. A. Walker, A. A. Kruglov, Y. Loo, K. Nakamura, Y. Zhang, S. Nayar, L. H. Jones, A. Flores-Langarica, et al. 2015. Inflammation-induced formation of fat-associated lymphoid clusters. *Nat. Immunol.* 16: 819–828.
- Moro, K., T. Yamada, M. Tanabe, T. Takeuchi, T. Ikawa, H. Kawamoto, J. Furusawa, M. Ohtani, H. Fujii, and S. Koyasu. 2010. Innate production of T(H)2 cytokines by adipose tissue-associated c-Kit(+)Sca-1(+) lymphoid cells. *Nature* 463: 540–544.
- Genestier, L., M. Taillardet, P. Mondiere, H. Gheit, C. Bella, and T. Defrance. 2007. TLR agonists selectively promote terminal plasma cell differentiation of B cell subsets specialized in thymus-independent responses. *J. Immunol.* 178: 7779–7786.
- Cellot, S., K. J. Hope, J. Chagraoui, M. Sauvageau, É. Deneault, T. MacRae, N. Mayotte, B. T. Wilhelm, J. R. Landry, S. B. Ting, et al. 2013. RNAi screen identifies Jarid1b as a major regulator of mouse HSC activity. *Blood* 122: 1545–1555.
- Kretschmer, K., J. Stopkovicz, S. Scheffer, T. F. Greten, and S. Weiss. 2004. Maintenance of peritoneal B-1a lymphocytes in the absence of the spleen. *J. Immunol.* 173: 197–204.
- Pedersen, G. K., X. Li, S. Khoenkhoen, M. Ádori, B. Beutler, and G. B. Karlsson Hedestam. 2018. B-1a cell development in splenectomized neonatal mice. *Front. Immunol.* 9: 1738.
- Wardemann, H., T. Boehm, N. Dear, and R. Carsetti. 2002. B-1a B cells that link the innate and adaptive immune responses are lacking in the absence of the spleen. *J. Exp. Med.* 195: 771–780.
- Kreslavsky, T., B. Vilagos, H. Tagoh, D. K. Poliakova, T. A. Schwickert, M. Wöhner, M. Jaritz, S. Weiss, R. Taneja, M. J. Rossner, and M. Busslinger. 2017. Essential role for the transcription factor Bhlhe41 in regulating the development, self-renewal and BCR repertoire of B-1a cells. *Nat. Immunol.* 18: 442–455.
- Clarke, A. J., T. Riffelmacher, D. Braas, R. J. Cornall, and A. K. Simon. 2018. B1a B cells require autophagy for metabolic homeostasis and self-renewal. *J. Exp. Med.* 215: 399–413.
- Kidder, B. L., G. Hu, Z. X. Yu, C. Liu, and K. Zhao. 2013. Extended self-renewal and accelerated reprogramming in the absence of Kdm5b. *Mol. Cell. Biol.* 33: 4793–4810.
- Wang, H., C. Song, Y. Ding, X. Pan, Z. Ge, B. H. Tan, C. Gowda, M. Sachdev, S. Muthusami, H. Ouyang, et al. 2016. Transcriptional regulation of JARID1B/KDM5B histone demethylase by Ikaros, histone deacetylase 1 (HDAC1), and casein kinase 2 (CK2) in B-cell acute lymphoblastic leukemia. *J. Biol. Chem.* 291: 4004–4018.
- Stewart, M. H., M. Albert, P. Sroczynska, V. A. Cruickshank, Y. Guo, D. J. Rossi, K. Helin, and T. Enver. 2015. The histone demethylase Jarid1b is required for hematopoietic stem cell self-renewal in mice. *Blood* 125: 2075–2078.
- Moins-Teisserenc, H., M. Busson, A. Herda, S. Apete, R. Peffault de Latour, M. Robin, A. Xhaard, A. Toubert, and G. Socié. 2013. CD19+CD5+ B cells and B1-like cells following allogeneic hematopoietic stem cell transplantation. *Biol. Blood Marrow Transplant.* 19: 988–991.

Bmi1 regulates Wnt signaling in hematopoietic stem and progenitor cells

Hao Yu,^{1*} Rui Gao,^{1*} Sisi Chen,^{2*} Xicheng Liu,³ Qiang Wang,⁴ Wenjie Cai,¹ Sasidhar Vemula,¹ Aidan C. Fahey,¹ Danielle Henley,¹ Michihiro Kobayashi,¹ Stephen Z. Liu,¹ Zhijian Qian,⁵ Reuben Kapur,¹ Hal E. Broxmeyer,⁶ Zhonghua Gao,⁴ Rongwen Xi,³ Yan Liu^{1,2,7,8}

¹Department of Pediatrics, Herman B Wells Center for Pediatric Research, Indiana University School of Medicine, Indianapolis, IN 46202, USA; ²Department of Biochemistry and Molecular Biology, Indiana University School of Medicine, Indianapolis, IN 46202, USA; ³National Institute of Biological Science, Beijing, China; ⁴Department of Biochemistry and Molecular Biology, College of Medicine, Pennsylvania State University, Hershey, PA 17033, USA; ⁵Department of Medicine, University of Florida, Gainesville, Florida 32610, USA; ⁶Department of Microbiology and Immunology, Indiana University, Indianapolis, IN 46202, USA; ⁷Department of Medicine, Northwestern University Feinberg School of Medicine, Chicago, IL 60611; ⁸Robert H. Lurie Comprehensive Cancer Center, Chicago, IL 60611.

*These authors contributed equally to the paper.

Correspondence: Rongwen Xi, Ph.D., National Institute of Biological Science, Beijing, China. Email: xirongwen@nibs.ac.cn; Yan Liu, Ph.D., Department of Medicine, Northwestern University Feinberg School of Medicine, Robert H. Lurie Comprehensive Cancer Center, Chicago, IL 60611. Email: yan.liu@northwestern.edu

Summary

Polycomb group protein Bmi1 is essential for hematopoietic stem cell (HSC) self-renewal and terminal differentiation. However, its target genes in hematopoietic stem and progenitor cells are largely unknown. We performed gene expression profiling assays and found that genes of the Wnt signaling pathway are significantly elevated in Bmi1 null hematopoietic stem and progenitor cells (HSPCs). Bmi1 is associated with several genes of the Wnt signaling pathway in hematopoietic cells. Further, we found that Bmi1 represses Wnt gene expression in HSPCs. Importantly, loss of β -catenin, which reduces Wnt activation, partially rescues the HSC self-renewal and differentiation defects seen in the Bmi1 null mice. Thus, we have identified Bmi1 as a novel regulator of Wnt signaling pathway in HSPCs. Given that Wnt signaling pathway plays an important role in hematopoiesis, our studies suggest that modulating Wnt signaling may hold potential for enhancing HSC self-renewal, thereby improving the outcomes of HSC transplantation.

Keywords Bmi1, HSC, self-renewal, differentiation, Wnt, and β -catenin

Introduction

Hematopoietic stem cells (HSCs) are multipotent, self-renewing progenitors that generate all mature blood cells [1-2]. In order to maintain hematopoietic homeostasis throughout the lifetime of an organism, the HSC pool must be maintained, which is achieved by the process of self-renewal [3-4]. Although practiced clinically for more than 40 years, the use of HSC transplants remains limited by the ability to expand functional HSCs *ex vivo* [5]. Deciphering the molecular mechanisms controlling HSC self-renewal is essential for developing clinical strategies that can enhance *ex vivo* HSC expansion [3-5].

Polycomb group (PcG) proteins are epigenetic gene silencers that have been implicated in stem cell maintenance and cancer development [6-11]. Genetic and biochemical studies indicate that Polycomb group proteins exist in at least two protein complexes, Polycomb repressive complex 2 (PRC2) and Polycomb repressive complex 1 (PRC1), that act in concert to initiate and maintain stable gene repression [10-11]. Bmi1, a key component of the Polycomb repressive complex 1 (PRC1), is essential for both HSC and leukemia stem cell (LSC) self-renewal [12-15]. We demonstrate that Bmi1 is a substrate of AKT and that AKT-mediated phosphorylation of Bmi1 inhibits HSC self-renewal [16]. In addition to HSC self-renewal, Bmi1 also plays key roles in multi-lineage differentiation [17]. We found that Bmi1 enhances erythroid differentiation through upregulating ribosomal genes [18]. We also found that Bmi1 maintains the self-renewal property of innate-like B lymphocytes [19]. While Bmi1 plays critical roles in hematopoiesis [12-19], its target genes in hematopoietic stem and progenitor cells (HSPCs) are largely unknown. Bmi1 is a potent negative regulator of the *Ink4a/Arf* locus, which encodes the cell cycle regulator and tumor suppressor p16^{Ink4a} and p19^{Arf} proteins [20-21]. In *Bmi1*^{-/-} bone marrow (BM) cells, there is an upregulation of both *p16*^{Ink4a} and *p19*^{Arf} [22]. However, loss of both *p16* and *p19* only partially rescues the self-renewal defects of *Bmi1*^{-/-} HSCs [22], suggesting that Bmi1 may regulate the expression of other genes in HSPCs.

The Wnt signaling pathway has pivotal roles during the development of many organ systems, and dysregulated Wnt signaling is a key factor in the initiation of various tumors [23]. In the canonical Wnt pathway, Wnt ligand binds to its receptor Frizzled at the cell surface and inhibits glycogen synthase kinase-

3 β (GSK-3 β)-mediated phosphorylation and degradation of β -catenin. Stabilized β -catenin then translocates to the nucleus where it binds to T cell factor (TCF)/lymphoid enhancer factor (LEF) transcription factors and induces the expression of Wnt target genes, such as *Tcf* and *Axin2*. In the absence of Wnt ligand, GSK-3 β phosphorylates β -catenin and targets it for ubiquitination and degradation [23]. Canonical Wnt signaling is differentially activated during hematopoiesis [24-26], suggesting an important regulatory role for specific Wnt signaling levels [27-29]. The Adenomatous polyposis coli gene (*Apc*) is a negative modulator of the canonical Wnt pathway and loss of *Apc* in hematopoietic compartment leads to stabilization of β -catenin and activation of the Wnt signaling pathway [29-30]. By combining different targeted hypomorphic alleles and a conditional deletion allele of *Apc*, a gradient of five different Wnt signaling levels were obtained *in vivo* [26]. By analyzing the effect of different mutations of *Apc* on hematopoiesis, Luis and colleagues demonstrated that the canonical Wnt signaling regulates hematopoiesis in a dosage-dependent fashion: Low levels of Wnt signaling activation (2-fold increase above normal) result in the maintenance of a multipotent state, therefore resulting in increased reconstitution in stem cell transplantation assays, and that high level of Wnt signaling (more than 10-fold increase above normal) results in impaired HSC self-renewal and a block in differentiation [26]. While Wnt signaling plays an important role in hematopoiesis [24-26], how Wnt signaling is regulated in HSCs remains elusive. Identify key regulators of Wnt signaling in HSCs may lead to novel approaches to expand human HSCs *ex vivo* and improve transplantation efficiency.

In this study, we discovered that several genes of the Wnt signaling pathway are upregulated in *Bmi1* null hematopoietic stem and progenitor cells (HSPCs). *Bmi1* binds to several Wnt genes on the chromatin and represses their transcription in HSPCs. Importantly, we found that loss of β -catenin partially rescues the HSC self-renewal and differentiation defects seen in the *Bmi1*^{-/-} mice. Thus, we have identified *Bmi1* as a novel regulator of Wnt signaling pathway in hematopoietic stem and progenitor cells.

Materials and Methods

Mice

Global *Bmi1* knockout mice were provided by Dr. Martin van Lohuizen at the Netherlands Cancer Institute, the Netherlands [20]. Conditional *Bmi1* knockout mice (*Bmi1^{F/F}*) in the *C57BL6* background were generated at the National Institute of Biological Science, Beijing, China. The *Ctnnb1^{F/F}* mice were obtained from the Jackson Labs and have been backcrossed to the *C57BL6* background for at least 8 generations. Wild type *C57BL/6* (CD45.2⁺), B6.SJL (CD45.1⁺) and F1 mice (CD45.2⁺ CD45.1⁺) mice were obtained from an on-site core breeding colony. All mice were maintained in the Indiana University Animal Facility according to IACUC-approved protocols.

Flow cytometry

Flow cytometry analysis of hematopoietic stem and progenitor cells was performed as described previously [31-32]. Murine hematopoietic stem and progenitor cells were identified and evaluated by flow cytometry using a single cell suspension of bone marrow mononuclear cells (BMMCs). Hematopoietic stem and progenitors are purified based upon the expression of surface markers. Bone marrow (BM) cells were obtained from femurs by flushing cells out of the bone using a syringe and phosphate-buffered saline (PBS) with 2mM EDTA. Red blood cells (RBCs) were lysed by RBC lysis buffer (eBioscience) prior to staining. Experiments were performed on FACS LSR IV cytometers (BD Biosciences) and analyzed by using the FlowJo Version 9.3.3 software (TreeStar).

Gene expression and Pathways Analyses

Transcript profiling of HSCs and MPPs from *Bmi1^{+/+}* and *Bmi1^{-/-}* mice were analyzed by Agilent Whole Mouse Genome Oligo Microarrays. Raw data will be available for download from Gene Expression Omnibus (<http://ncbi.nlm.nih.gov/geo/>, accession number in progress). Genes whose expressions are increased or decreased more than 2-fold in *Bmi1^{-/-}* cells compared to wild-type cells are shown. The Microarray data were analyzed using the Ingenuity Pathways Analysis program (Ingenuity Systems,

www.ingenuity.com); to identify the pathways that met the $<$ or $>$ 2-fold change cutoff and were associated with a canonical pathway in the Ingenuity Pathways Knowledge base were considered for the analysis. The significance of the association between the data set and the identified canonical pathway was measured in 2 ways: (1) A ratio of the number of genes from the data set that map to the pathway divided by the total number of genes from the data set that map to the canonical pathway and (2) Fischer's exact test, to calculate a p value determining the probability that the association between the genes in the data set and the canonical pathway is explained by chance alone.

ChIP assays

For ChIP assays, Kit⁺ BM cells and Baf3 cells were fixed with 1% (vol/vol) formaldehyde for 10 min at room temperature. ChIP assays were performed using the EZ-Magna ChIP A/G Kit (Millipore). Anti-Bmi1 antibody (Active Motif, AF27) and normal mouse IgG were used for immunoprecipitation. ChIP DNA was then subjected to real-time PCR analysis using primers targeting different region of genes of the canonical Wnt pathway and *Ink4a/Arf* locus.

Reporter assays

The Top-Flash luciferase construct encodes the firefly luciferase reporter gene under the control of a minimal CMV promoter and 8 tandem repeats of the TCF/LEF transcriptional response element (TRE). A Top-Flash mutant plasmid, containing defective TCF/LEF transcriptional response element, was used as a negative control in this assay. Each reporter is premixed with constitutively expressing Renilla luciferase, which serves as an internal control for normalizing transfection efficiencies and monitoring cell viability. 293T cells were transfected using Lipofectamine 2000 transfection reagent (ThermoFisher), according to the manufacturer's instructions. Transfected cells were harvested 24 hours later, and processed using Dual-Luciferase Reporter Assay (Promega).

Generation of retroviruses and infection of murine HSCs and MPPs

Retroviral vectors were produced by transfection of Phoenix E cells with the MIGR1 control (MSCV-IRES-GFP) or MIGR1 full-length Bmi1 c-DNA plasmid (MSCV-Bmi1-IRES-GFP), according to

standard protocols [16]. Murine HSCs and MPPs were infected with high-titer retroviral suspensions in the presence of 8 µg/mL polybrene (Sigma-Aldrich). Forty-eight hours after infection, the GFP-positive cells were sorted by FACS.

Transplantation

We transplanted 500,000 BM mononuclear cells isolated from *Bmi1^{F/F}-Ctnnb1^{F/F}-Mx1Cre⁻*, *Bmi1^{+/+}-Ctnnb1^{F/F}-Mx1Cre⁺*, *Bmi1^{F/F}-Ctnnb1^{+/+}-Mx1Cre⁺*, and *Bmi1^{F/F}-Ctnnb1^{F/F}-Mx1Cre⁺* mice (CD45.2⁺) together with 250,000 competitor BM cells (CD45.1⁺) into lethally irradiated recipient mice (CD45.1⁺CD45.2⁺). Eight weeks following transplantation, we injected pI:pC to delete *Bmi1* and/or *Ctnnb1* from hematopoietic cells. Peripheral blood was obtained by tail vein bleeding every 4-week after pI:pC treatment, RBC lysed, and the PB mononuclear cells stained with anti-CD45.2 FITC and anti-CD45.1 PE, and analyzed by flow cytometry. 20 weeks following transplantation, bone marrow cells from recipient mice were analyzed to evaluate donor chimerism in bone marrows. For secondary transplantation, 3 x 10⁶ BM cells from primary recipient mice reconstituted with *Bmi1^{F/F}-Ctnnb1^{F/F}-Mx1Cre⁻*, *Bmi1^{+/+}-Ctnnb1^{F/F}-Mx1Cre⁺*, *Bmi1^{F/F}-Ctnnb1^{+/+}-Mx1Cre⁺*, and *Bmi1^{F/F}-Ctnnb1^{F/F}-Mx1Cre⁺* BM cells were injected into lethally irradiated F1 mice (CD45.1⁺CD45.2⁺).

Statistical Analysis

Statistical analysis was performed with GraphPad Prism 8 software (GraphPad software, Inc). All data are presented as mean ± standard error of the mean (SEM). The sample size for each experiment are included in the figure legends. Statistical analyses were performed using unpaired, two-tailed Student's t test where applicable for comparison between two groups, and a One-way ANOVA test or Two-way ANOVA was used for experiments involving more than two groups. Statistical significance was defined as *p < 0.05, **p < 0.01, ***p < 0.001; ns, not significant.

Results

Genes of the Wnt signaling pathway are upregulated in *Bmi1* null hematopoietic stem and progenitor cells

To understand how Bmi1 regulates HSC self-renewal and differentiation, we performed gene expression profiling assays (using microarray analysis and quantitative RT-PCR analysis) to identify Bmi1 target genes in HSCs (CD48⁻CD150⁺Lin⁻Sca1⁺Kit⁺ cells) and MPPs (CD48⁺CD150⁻Lin⁻Sca1⁺Kit⁺ cells). Microarray analysis revealed that several genes in the canonical Wnt signaling pathway are significantly elevated in both HSCs and MPPs from *Bmi1*^{-/-} mice (Fig. 1A-B), suggesting that Wnt signaling may be activated in the absence of Bmi1. We first confirmed upregulation of several genes of the canonical Wnt pathway, including *Fzd4*, *Fzd7*, *Fzd9*, *Tcf3*, and *Axin2*, in *Bmi1*^{-/-} HSCs compared to *Bmi1*^{+/+} HSCs using quantitative RT-PCR analysis (Fig. 1C). *Fzd4*, *Lgr4*, *Lef1*, *Tcf3*, and *Axin2* are significantly upregulated in *Bmi1*^{-/-} MPPs compared to *Bmi1*^{+/+} MPPs. (Fig. 1D). These findings suggest that Bmi1 may be associated with genes in the Wnt pathway, thereby repressing their expression in HSPCs.

Bmi1 is associated with Wnt genes in hematopoietic cells

To determine if Bmi1 is directly associated with genes in the Wnt pathway, we performed chromatin immunoprecipitation (ChIP) assays using an antibody against Bmi1 or normal mouse IgG. As expected, Bmi1 was associated with the *Ink4a/Arf* locus in both Kit⁺ BM and Baf3 cells (Fig. 2A-B). We detected the association of Bmi1 with the *Lef1*, *Fzd4*, and *Axin2* promoters in these cells (Fig. 2A-B). Ring1b is the catalytic component of the PRC1 complex and genome-wide ChIP-seq analysis showed Ring1b binding to several Wnt target genes, including *Ccnd2*, *Fzd7*, *Ckn2a* and *Tcf3*, in murine L8057 megakaryoblastic cells (Fig. 2C) [33]. Thus, we demonstrate that Bmi1/PRC1 is associated with Wnt genes in hematopoietic cells.

Bmi1 represses Wnt gene expression in hematopoietic stem and progenitor cells

To determine the impact of Bmi1 expression on Wnt activation in cells, we used the Top-Flash Wnt reporter system. The Top-Flash reporter system is designed to monitor the activity of Wnt signal

transduction pathway in cultured cells [34]. While Wnt3a readily activates the Wnt reporter in 293T cells, Wnt activation is efficiently repressed by ectopic *Bmi1* expression, demonstrating that *Bmi1* indeed can inhibit Wnt signaling activation in cultured cells (Fig. 3A).

To determine whether *Bmi1* represses the expression of Wnt signaling genes in HSPCs, we introduced *Bmi1* (MSCV-*Bmi1*-IRES-GFP) or GFP (MSCV-IRES-GFP) into HSCs and MPPs purified from *Bmi1*^{+/+} and *Bmi1*^{-/-} mice using retroviruses mediated transduction. 48 hours after transduction, we isolated mRNA from transduced cells (GFP⁺) and performed qRT-PCR assays for genes involved in the canonical Wnt signaling pathway. We found that that ectopic *Bmi1* expression results in downregulation of *Fzd4*, *Fzd7*, and *Lef1* expression in *Bmi1*^{+/+} HSCs compared to that of the control viruses (MSCV-IRES-GFP) transduced cells (Fig. 3B). We also found that that ectopic *Bmi1* expression leads to downregulation of *Fzd4*, *Fzd7*, *Fzd9*, *Lef1*, and *Axin2* expression in *Bmi1*^{+/+} MPPs compared to that of the control viruses transduced cells (Fig. 3C). In addition, ectopic *Bmi1* expression represses *Fzd4*, *Fzd7*, and *Fzd9* expression in *Bmi1*^{-/-} HSCs compared to that of the control viruses transduced cells (Fig. 3D). Further, ectopic *Bmi1* expression leads to downregulation of *Fzd4*, *Fzd9*, and *Lef1* in *Bmi1*^{-/-} MPPs (Fig. 3E). Thus, we demonstrate that *Bmi1* represses Wnt gene expression in HSPCs.

Loss of β -catenin partially rescued HSC self-renewal and differentiation defects seen in *Bmi1* null mice

The *Ctnnb1* gene encodes β -catenin and loss of β -catenin reduces Wnt activation [35]. To determine the impact of β -catenin deficiency on *Bmi1*^{-/-} HSPCs, we generated *Bmi1*^{F/F}-*Ctnnb1*^{F/F}-*Mx1Cre*⁺ mice. We transplanted 500,000 BM cells isolated from *Bmi1*^{F/F}-*Ctnnb1*^{F/F}-*Mx1Cre*⁻, *Bmi1*^{+/+}-*Ctnnb1*^{F/F}-*Mx1Cre*⁺, *Bmi1*^{F/F}-*Ctnnb1*^{+/+}-*Mx1Cre*⁺, and *Bmi1*^{F/F}-*Ctnnb1*^{F/F}-*Mx1Cre*⁺ mice (CD45.2⁺) together with 250,000 competitor BM cells (CD45.1⁺) into lethally irradiated recipient mice (CD45.1⁺CD45.2⁺). Eight weeks following transplantation, we injected pI:pC to delete *Bmi1* and/or *Ctnnb1* from hematopoietic cells and examined the frequency of donor-derived cells (CD45.2⁺) in peripheral blood every 4 weeks for twenty

weeks. Conditional deletion of *Ctnnb1* does not affect the repopulating ability of BM cells (Fig. 4A). While the percentage of donor-derived cells in PB of recipient mice repopulated with *Bmi1*^{-/-} BM cells decreases, loss of *Ctnnb1* significantly increased the engraftment of *Bmi1*^{-/-} BM cells at twenty weeks following pI:pC treatment (Fig. 4A). We observed increased number of donor-derived HSCs in the BM of recipient mice repopulated with *Bmi1*^{-/-}*Ctnnb1*^{-/-} BM cells compared to that of the *Bmi1*^{-/-} cells (Fig. 4B-C). Loss of *Bmi1* resulted in decreased myeloid differentiation and increased lymphoid differentiation in the BM, whereas *Ctnnb1* deficiency rescued differentiation defects seen in *Bmi1*^{-/-} mice (Fig. 4D).

To determine the impact of genetic deletion of *Ctnnb1* on *Bmi1*^{-/-} HSC self-renewal, we performed secondary BM transplantation assays. We found that *Bmi1*^{-/-}*Ctnnb1*^{-/-} BM cells show increased engraftment compared to *Bmi1*^{-/-} cells following secondary transplantation (Fig. 4E). Thus, we demonstrate that loss of β -catenin, which reduces Wnt activation, partially rescues HSC self-renewal and differentiation defects seen in *Bmi1*^{-/-} mice.

Discussion

Hematopoietic stem cell (HSC) self-renewal requires a complex crosstalk between extrinsic signals from the microenvironment and the HSC-intrinsic regulators to maintain an undifferentiated state [1-4]. However, the crosstalk between signaling pathways and HSC-intrinsic regulators has not been well defined at the molecular level [1-4]. Thus, there remains a critical need to improve our understanding of the interactions between signaling pathways and HSC-intrinsic regulators and develop novel strategies that can enhance *ex vivo* HSC expansion and improve the efficiency and outcome of HSC transplantation [5].

The role of Wnt signaling in adult hematopoiesis has been controversial [24-25]. While loss of Wnt3a impairs HSCs self-renewal and differentiation [37-38], blocking the secretions of Wnt proteins in the hematopoietic system does not affect hematopoiesis [39]. Constitutive beta-catenin activation impairs HSC self-renewal and blocks terminal differentiation [36]; however, mice lacking β - and γ -catenin have normal stem cell self-renewal and differentiation [35]. These findings indicate canonical Wnt signaling is far more complicated than expected. Indeed, the canonical Wnt signaling appears to regulate adult hematopoiesis in a dosage-dependent manner: low level of canonical Wnt activation enhances HSC self-renewal, whereas high level of canonical Wnt activation impairs HSC self-renewal and blocks terminal differentiation [26].

Polycomb group protein Bmi1 plays an important role in cellular homeostasis by maintaining a balance between proliferation and senescence [12-15, 20]. It is often overexpressed in cancer cells and is required for stem cell self-renewal [14-15]. However, the downstream targets that mediate Bmi1 function remain elusive. To explore the mechanism by which Bmi1 enhances hematopoiesis, we performed transcript profiling assays to compare gene expression in HSCs and MPPs isolated from wild type and Bmi1^{-/-} mice. We found that the expression of several genes of the Wnt signaling pathway was upregulated in hematopoietic stem and progenitor cells (HSPCs). Further, Bmi1 directly associates with the promoter of these genes in hematopoietic cells. Importantly, we found that loss of β -catenin partially rescued self-renewal defects seen in Bmi1 null mice. Given that activation of the canonical Wnt pathway leads to loss of hematopoietic stem cell repopulation and multilineage differentiation block [26, 29-30, 36], our studies uncover a novel mechanism by which Bmi1 enhances HSC self-renewal and promotes terminal differentiation,

Previous studies have implicated Bmi1 in regulating WNT signaling in some cancer cells [40-41]. BMI1 has been shown to autoactivate its own promoter via an E-box present in its promoter. Further, BMI1 activates the WNT pathway by repressing DKK family of WNT inhibitors. BMI1 mediated repression of DKK1 results in up-regulation of WNT target c-Myc, leading to transcriptional

autoactivation of BMI1 [36]. This positive feedback loop regulating BMI1 expression may be relevant to the role of BMI1 in promoting cancer and maintaining stem cell phenotype [40]. For example, BMI1 is upregulated in colon cancer tissues and cell lines. Overexpression of BMI1 in primary epithelial colon cells promotes cellular growth and activates WNT pathway, whereas knocking down of BMI1 expression in colon cancer cells represses these effects [41]. Mechanistically, BMI1 activates WNT signaling in colon cancer by negatively regulating the WNT antagonist IDAX [41]. These findings suggest that Bmi1 may play a context-dependent role in regulating Wnt signaling during development and tumorigenesis.

Although BMI1 is upregulated in many cell types, very little is known about the signaling pathways that regulate its expression. Wnt signaling plays a key role in intestinal stem cells and Bmi1 has been shown to be a potential marker for intestinal stem cells [42]. The expression of Bmi1 in human colon cancers is associated with nuclear β -catenin, a hallmark for the activated Wnt signaling. Thus, these studies suggest that Wnt signaling may regulate the expression of Bmi1 in colon cancer cells [42]. Whether Wnt signaling regulates Bmi1 expression in hematopoietic stem and progenitor cells is not known, thereby awaiting future investigation.

In summary, we have identified Bmi1 as a negative regulator of canonical Wnt signaling pathway in hematopoietic stem and progenitor cells. Our studies suggest that modulating canonical Wnt signaling may hold potential for enhancing HSC self-renewal, thereby improving the outcomes of HSC transplantation,.

Acknowledgements The authors would like to acknowledge the Flow Cytometry Core and In vivo Therapeutic Core Laboratories at the Indiana University School of Medicine, which were sponsored, in part, by the NIDDK Cooperative Center of Excellence in Hematology (CCEH) grant U54 DK106846. This work was supported, in part, by a Project Development Team within the ICTSI NIH/NCRR Grant Number UL1TR001108.

Declarations

Ethical Approval All mouse experiments were approved by the Indiana University Institutional Animal Use and Care Committee.

Consent to Participate None.

Consent to Publish All authors concur with the publication of the manuscript.

Author Contributions H.Y., R.G., S.C., R.X., and Y.L. Designed the research. H.Y., R.G., S.C., X.L., Q.W., W.C., S.V., A.C.F., D.H., M.K., and S.Z.L. Performed the research; H.Y., R.G., S.C., Q.W., and Y.L. Analyzed the data and performed the statistical analysis. Z.Q., R.K., H.E.B., and Z.G. Provided reagents and constructive advice to the study. S.C., R.X., and Y.L. Wrote the manuscript. All authors read, commented on, and approved the manuscript.

Funding This work was supported by R01 HL150624, R56 DK119524, R56 AG052501, DoD W81XWH-18-1-0265, and DoD W81XWH-19-1-0575 awards to YL. This work was supported in part by the Leukemia & Lymphoma Society Translational Research Program award 6581-20 and the St. Baldrick's Foundation Scholar Award to YL.

Competing Interests The authors declared that no conflict interest exists.

Availability of data and materials Raw data will be available for download from Gene Expression Omnibus (<http://ncbi.nlm.nih.gov/geo/>, accession number in progress).

References

1. Kondo, M., Wagers, A.J., Manz, M.G., Prohaska, S.S., Scherer, D.C., Beilhack, G.F., Shizuru, J.A. and Weissman, I.L. (2003). Biology of Hematopoietic Stem Cells and Progenitors: Implications for Clinical Application. *Annu Rev Immunol*, 21,759-806.
2. Attar, E.C., and Scadden, D.T. (2004). Regulation of hematopoietic stem cell growth. *Leukemia*, 18, 1760-8.
3. Akala, O.O., and Clarke, M.F. (2006). Hematopoietic stem cell self-renewal. *Curr Opin Genet Dev*,16,496-501.
4. Zon, L.I. (2008). Intrinsic and extrinsic control of haematopoietic stem-cell self-renewal. *Nature*, 453,306-13.
5. Walasek, M.A., van Os, R., de Haan, G. (2012). Hematopoietic stem cell expansion: challenges and opportunities. *Ann N Y Acad Sci*, 1266,138-50.
6. Valk-Lingbeek, M.E., Bruggeman, S.W., van Lohuizen, M. (2004). Stem cells and cancer; the polycomb connection. *Cell*, 118, 409-18.
7. Sparmann, A., and van Lohuizen, M. (2006). Polycomb silencers control cell fate, development and cancer. *Nat Rev Cancer*, 6, 846-856.
8. Schuettengruber, B., Chourrout, D., Vervoort, M., Leblanc, B., and Cavalli, G. (2007). Genome Regulation by Polycomb and Trithorax Proteins. *Cell*, 128, 735-45.
9. Pietersen, A.M., and van Lohuizen, M. (2008). Stem cell regulation by polycomb repressors: postponing commitment. *Curr Opin Cell Biol*, 20, 201-207.
10. Bracken, A.P., and Helin, K. (2009). Polycomb Group Proteins: Navigators of Lineage Pathways Led Astray in Cancer. *Nature Review of Cancer*, 9, 773-84.
11. Simon, J. A., and Kingston, R. E. (2009). Mechanisms of Polycomb Gene Silencing: Knowns and Unknowns. *Nat Rev Mol Cell Biol*, 10, 697-708.

12. Sauvageau, M., and Sauvageau, G. (2010). Polycomb Group Proteins: Multi-Faceted Regulators of Somatic Stem Cells and Cancer. *Cell Stem Cell*, 7, 299-313.
13. Konuma, T., Oguro, H., Iwama, A. (2010). Role of the polycomb group proteins in hematopoietic stem cells. *Dev Growth Differ*, 52,505-16.
14. Park, I.K., Qian, D., Kiel, M., Becker, M.W., Pihalja, M., Weissman, I.L., Morrison, S.J., Clarke, M.F. (2003). Bmi-1 is required for maintenance of adult self-renewing haematopoietic stem cells. *Nature*, 423,302-5.
15. Lessard, J., Sauvageau, G. (2003). Bmi-1 determines the proliferative capacity of normal and leukaemic stem cells. *Nature*, 423,255-60.
16. Liu, Y., Liu, F., Yu, H., Zhao, X., Sahsida, G., Deblasio, A., Chen, Z., Lin, H.K., Di Giandomenico, S., Elf, S.E., Yang, Y.Y., Miyata, Y., Huang, G., Menendez, S., Mellinghoff, I., Pandolfi, P.P., Hedvat, C.V. and Nimer, S.D. (2012). Akt Phosphorylates the Transcriptional Repressor Bmi1 to Block Its Association with Tumor Suppressing *Ink4a-Arf* locus. *Science Signaling*, 5, ra77.
17. Oguro, H., Yuan, J., Ichikawa, H., Ikawa, T., Yamazaki, S., Kawamoto, H., Nakauchi, H., Iwama, A. (2010). Poised lineage specification in multipotential hematopoietic stem and progenitor cells by the polycomb protein Bmi1. *Cell Stem Cell*, 6,279-86.
18. Gao, R., Chen, S., Kobayashi, M., Yu, H., Young, S.K., Soltis, A., Zhang, Y., Wan, Y., Vemula, S., Fraenkel, E., Cantor, A., Xu, Y., Yoder, M.C., Wek, R., Ellis, S., Kapur, R., Zhu, X. and Liu, Y. (2015). Bmi1 promotes erythroid development through regulating ribosome biogenesis. *Stem Cells*, 33,925-38.
19. Kobayashi, M., Lin, Y., Mishra, A., Shelly, C., Gao, R., Reeh, C.W., Wang, P.Z., Xi, R., Liu, Y., Wenzel, P., Ghosn, E., Liu, Y., Yoshimoto, M. (2020). Bmi1 Maintains the Self-Renewal Property of Innate-like B Lymphocytes. *J Immunol*, 204,3262-3272.
20. Jacobs, J. J., Kieboom, K., Marino, S., DePinho, R. A., van Lohuizen, M. (1999). The oncogene and Polycomb-group gene bmi-1 regulates cell proliferation and senescence through the ink4a locus. *Nature*, 397, 164-168.

21. Bracken, A.P., Kleine-Kohlbrecher, D., Dietrich, N., Pasini, D., Gargiulo, G., Beekman, C., Theilgaard-Mönch, K., Minucci, S., Porse, B.T., Marine, J.C., Hansen, K.H., Helin, K. (2007). The Polycomb group proteins bind throughout the INK4A-ARF locus and are disassociated in senescent cells. *Genes Dev*, 21, 525-30.
22. Oguro, H., Iwama, A., Morita, Y., Kamijo, T., van Lohuizen, M., Nakauchi, H. (2006). Differential impact of Ink4a and Arf on hematopoietic stem cells and their bone marrow microenvironment in Bmi1-deficient mice. *J Exp Med*, 203, 2247-53.
23. Reya T, Clevers H. (2005). Wnt signalling in stem cells and cancer. *Nature*. 434(7035):843-50.
24. Staal FJ, Sen JM. (2008). The canonical Wnt signaling pathway plays an important role in lymphopoiesis and hematopoiesis. *Eur J Immunol*, 38,1788-94.
25. Staal, F.J., Chhatta, A., Mikkers, H. (2016). Caught in a Wnt storm: Complexities of Wnt signaling in hematopoiesis. *Exp Hematol*, 44, 451-7.
26. Luis, T.C., Naber, B.A., Roozen, P.P., Brugman, M.H., de Haas, E.F., Ghazvini, M., Fibbe, W.E., van Dongen, J.J., Fodde, R., Staal, F.J. (2011). Canonical wnt signaling regulates hematopoiesis in a dosage-dependent fashion. *Cell Stem Cell*, 9,345-56.
27. Reya T, Duncan AW, Ailles L, Domen J, Scherer DC, Willert K, Hintz L, Nusse R, Weissman IL. (2003). A role for Wnt signalling in self-renewal of haematopoietic stem cells. *Nature*, 423,409-14.
28. Duncan AW, Rattis FM, DiMascio LN, Congdon KL, Pazianos G, Zhao C, Yoon K, Cook JM, Willert K, Gaiano N, Reya T. (2005). Integration of Notch and Wnt signaling in hematopoietic stem cell maintenance. *Nat Immunol*, 6,314-22.
29. Qian Z, Chen L, Fernald AA, Williams BO, Le Beau MM. (2008). A critical role for Apc in hematopoietic stem and progenitor cell survival. *J Exp Med*, 205,2163-75.
30. Wang J, Fernald AA, Anastasi J, Le Beau MM, Qian Z. (2010). Haploinsufficiency of Apc leads to ineffective hematopoiesis. *Blood*,115,3481-8.

31. Liu, Y., Elf, S.E., Miyata, Y., Sashida, G., Liu, Y.H., Huang, G., Di Giandomenico, S., Lee, J.M., Deblasio, A., Menendez, S., Antipin, J., Reva, B., Koff, A. and Nimer, S.D. (2009). p53 Regulates Hematopoietic Stem Cell Quiescence. *Cell Stem Cell*, 4, 37-48.
32. Chen, S., Wang, Q., Yu, H., Capitano, M.L., Vemula, S., Nabinger, S.C., Gao, R., Yao, C., Kobayashi, M., Geng, Z., Fahey, A., Henley, D., Liu, S.Z., Barajas, S., Cai, W., Wolf, E.R., Ramdas, B., Cai, Z., Gao, H., Luo, N., Sun, Y., Wong, T.N., Link, D.C., Liu, Y., Boswell, H.S., Mayo, L.D., Huang, G., Kapur, R., Yoder, M.C., Broxmeyer, H.E., Gao, Z., Liu, Y. (2019). Mutant p53 drives clonal hematopoiesis through modulating epigenetic pathway. *Nat Commun*, 10,5649.
33. Yu, M., Mazor, T., Huang, H., Huang, H.T., Kathrein, K.L., Woo, A.J., Chouinard, C.R., Labadorf, A., Akie, T.E., Moran, T.B., Xie, H., Zacharek, S., Taniuchi, I., Roeder, R.G., Kim, C.F., Zon, L.I., Fraenkel, E., Cantor, A.B. (2012). Direct recruitment of polycomb repressive complex 1 to chromatin by core binding transcription factors. *Mol Cell*, 45, 330-43.
34. Yu, J., Liu, D., Sun, X., Yang, K., Yao, J., Cheng, C., Wang, C., Zheng, J. (2019). CDX2 inhibits the proliferation and tumor formation of colon cancer cells by suppressing Wnt/beta-catenin signaling via transactivation of GSK-3beta and Axin2 expression. *Cell Death Dis*, 10,26.
35. Jeannot, G., Scheller, M., Scarpellino, L., Duboux, S., Gardiol, N., Back, J., Kuttler, F., Malanchi, I., Birchmeier, W., Leutz, A., Huelsken, J., Held, W. (2008). Long-term, multilineage hematopoiesis occurs in the combined absence of beta-catenin and gamma-catenin. *Blood*, 111,142-9.
36. Scheller, M., Huelsken, J., Rosenbauer, F., Taketo, M.M., Birchmeier, W., Tenen, D.G., Leutz, A. (2006). Hematopoietic stem cell and multilineage defects generated by constitutive beta-catenin activation. *Nat Immunol*, 7,1037-47.
37. Luis, T.C., Weerkamp, F., Naber, B.A., Baert, M.R., de Haas, E.F., Nikolic, T., Heuvelmans, S., De Krijger, R.R., van Dongen, J.J., Staal, F.J. (2009). Wnt3a deficiency irreversibly impairs hematopoietic stem cell self-renewal and leads to defects in progenitor cell differentiation. *Blood*, 113, 546-54.

38. Luis, T.C., Naber, B.A., Fibbe, W.E., van Dongen, J.J., Staal, F.J. (2010). Wnt3a nonredundantly controls hematopoietic stem cell function and its deficiency results in complete absence of canonical Wnt signaling. *Blood*, *116*, 496-7.
39. Kabiri, Z., Numata, A., Kawasaki, A., Tenen, D.G., Virshup, D.M. (2015). Wnts are dispensable for differentiation and self-renewal of adult murine hematopoietic stem cells. *Blood*, *126*, 1086-94.
40. Cho, J.H., Dimri, M., Dimri, D.P. (2013). A positive feedback loop regulates the expression of polycomb group protein BMI1 via WNT signaling pathway. *J Biol Chem*, *288*, 3406-18.
41. Yu, F., Zhou, C., Zeng, H, Liu, Y., Li, S. (2018). BMI1 activates WNT signaling in colon cancer by negatively regulating the WNT antagonist IDAX. *Biochem Biophys Res Commun*, *496*, 468-474.
42. Yu, T., Chen, X., Zhang, W., Colon, D., Shi, J. Napier, D., Rychahou, P., Lu, W., Lee, E.Y., Weiss, H.L., Evers, B.M., Liu, C. (2012). Regulation of the potential marker for intestinal cells, Bmi1, by β -catenin and the zinc finger protein KLF4: implications for colon cancer. *J Biol Chem*, *287*, 3760-8.

FIGURE LEGENDS

Fig. 1 Genes of the Wnt signaling pathway are upregulated in hematopoietic stem and progenitor cells.

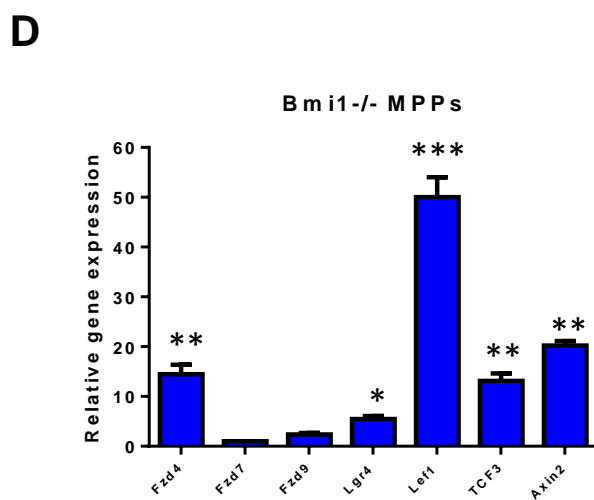
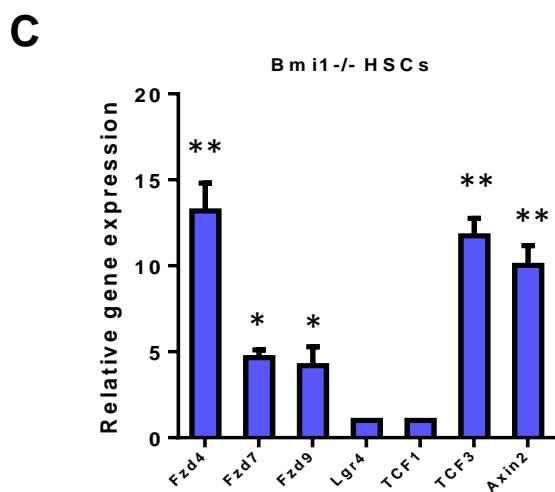
(A) Transcript profiling of HSCs (CD48⁻CD150⁺LSKs) from *Bmi1*^{+/+} and *Bmi1*^{-/-} mice were analyzed by Agilent Whole Mouse Genome Oligo Microarrays. Genes that are differentially expressed in *Bmi1*^{-/-} HSCs compared to wild-type cells are shown. We utilized Ingenuity pathways Analysis (Ingenuity Systems) to group genes into specific canonical pathways. Values are shown for three biological replicates. Color red indicates genes that are upregulated in *Bmi1*^{-/-} HSCs and color blue indicates genes that are downregulated in *Bmi1*^{-/-} HSCs. (B) Transcript profiling of MPPs (CD48⁺CD150⁻LSKs) from *Bmi1*^{+/+} and *Bmi1*^{-/-} mice were analyzed by Agilent Whole Mouse Genome Oligo Microarrays. Genes that are differentially expressed in *Bmi1*^{-/-} MPPs compared to wild-type cells are shown. We utilized Ingenuity pathways Analysis (Ingenuity Systems) to group genes into specific canonical pathways. Values are shown for three biological replicates. Color red indicates genes that are upregulated in *Bmi1*^{-/-} MPPs and color blue indicates genes that are downregulated in *Bmi1*^{-/-} MPPs. (C) Real-time RT-PCR analysis of gene expression in *Bmi1*^{+/+} and *Bmi1*^{-/-} HSCs. Data shown are relative expression as compared to *Bmi1*^{+/+} HSCs (set as 1), n = three biological replicates, *p<0.05, **p<0.01. (D) Real-time RT-PCR analysis of gene expression in *Bmi1*^{+/+} and *Bmi1*^{-/-} MPPs. Data shown are relative expression as compared to *Bmi1*^{+/+} MPPs (set as 1), n = three biological replicates, *p<0.05, **p<0.01, ***p<0.001.

Fig. 2 *Bmi1* is associated with Wnt genes in hematopoietic cells. (A) *Bmi1* binds to promoters of genes of the Wnt pathway *in vivo*. Chromatin bound DNA from Kit⁺ BM cells was immunoprecipitated with a *Bmi1*-specific antibody or with normal mouse IgG. qRT-PCR amplification was performed on corresponding templates using primers for indicated genes, n = three biological replicates, **p<0.01. (B) *Bmi1* binds to promoters of genes of the Wnt pathway *in vivo*. Chromatin bound DNA from Baf3 cells was immunoprecipitated with a *Bmi1*-specific antibody or with normal mouse IgG. qRT-PCR amplification was performed on corresponding templates using primers for indicated genes, n = three biological replicates, *p<0.05, **p<0.01. (C) Representative *Ring1b* and IgG ChIP-seq profiles of loci

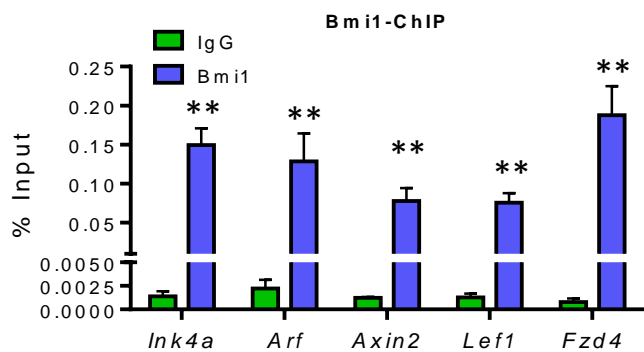
occupied by Ring1b in murine L8057 megakaryoblastic cells. It appears that Ring1b associates with several Wnt target genes, including *Ccnd2*, *Fzd7*, *Cdkn2a* and *Tcf3*, in L8057 cells.

Fig. 3 Bmi1 regulates Wnt gene expression in hematopoietic stem and progenitor cells. **(A)** Bmi1 represses Wnt3a-induced Wnt reporter activation. Luciferase activity was assayed 24 hours after transfection of 293T cells. Values are means (\pm SEM), n = three biological replicates, *p<0.05. **(B)** Ectopic Bmi1 expression represses Wnt gene expression in *Bmi1*^{+/+} HSCs. Data shown are relative expression compared to control viruses (MSCV-IRES-GFP) transduced HSCs, n = three biological replicates, *p<0.05, **p<0.01. **(C)** Ectopic Bmi1 expression represses Wnt gene expression in *Bmi1*^{+/+} MPPs. Data shown are relative expression compared to control viruses transduced MPPs, n = three biological replicates, *p<0.05, **p<0.01. **(D)** Ectopic Bmi1 expression represses Wnt gene expression in *Bmi1*^{-/-} HSCs. Data shown are relative expression compared to control viruses transduced *Bmi1*^{-/-} HSCs, n = three biological replicates, *p<0.05, **p<0.01. **(E)** Ectopic Bmi1 expression represses Wnt gene expression in *Bmi1*^{-/-} MPPs. Data shown are relative expression compared to control viruses transduced *Bmi1*^{-/-} MPPs, n = three biological replicates, *p<0.05, ***p<0.001.

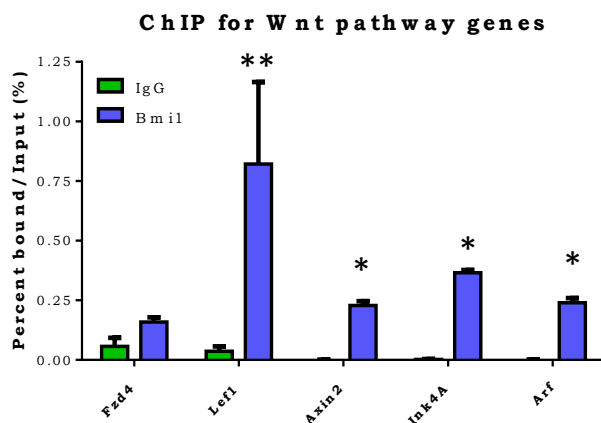
Fig. 4 Loss of β -catenin partially rescued HSC self-renewal and differentiation defects seen in Bmi1 null mice. **(A)** Percentage of donor-derived cells (CD45.2⁺) in the peripheral blood of recipient mice following pI:pC treatment. n=7 mice per group, **p<0.01. **(B)** Percentage of donor-derived cells (CD45.2⁺) in the BM of recipient mice at 20 weeks following pI:pC treatment. n=4 mice per group, **p<0.01. **(C)** The frequency of donor-derived HSCs in the BM of recipient mice at 20 weeks following pI:pC treatment. n=4 mice per group, *p<0.05. **(D)** Lineage distribution of donor-derived cells in the bone marrow of primary recipient mice at 20 weeks following pI:pC treatment. n=4 mice per group, **p<0.01, ***p<0.001. **(E)** Percentage of donor-derived cells (CD45.2⁺) in the peripheral blood of recipient mice at 8 weeks following secondary transplantation. n=7-8 mice per group, ***p<0.001.



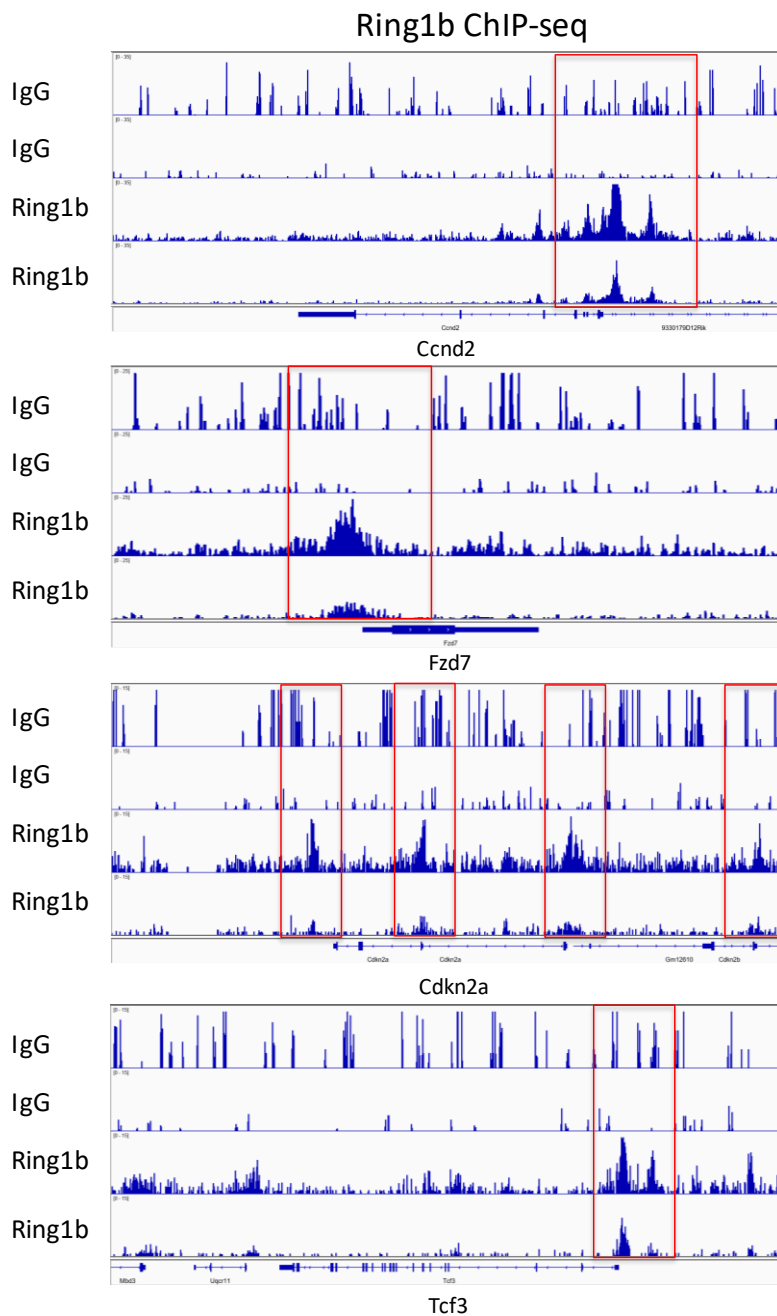
A



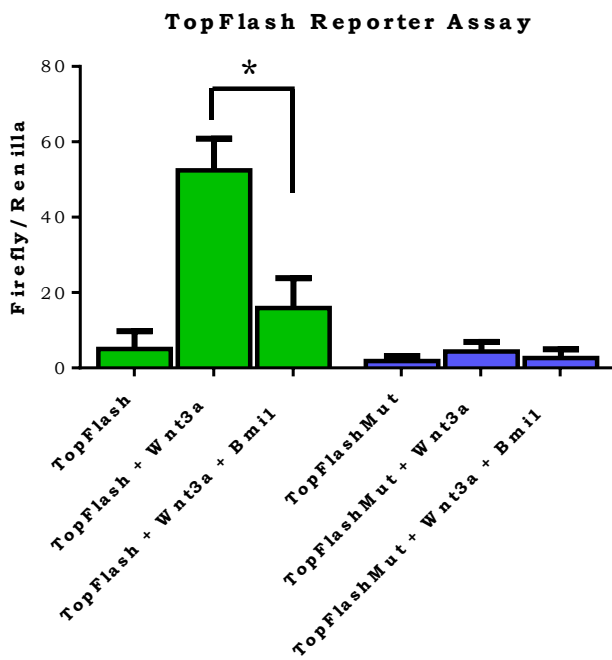
B



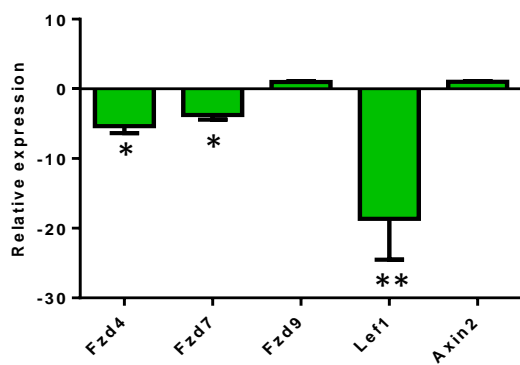
C



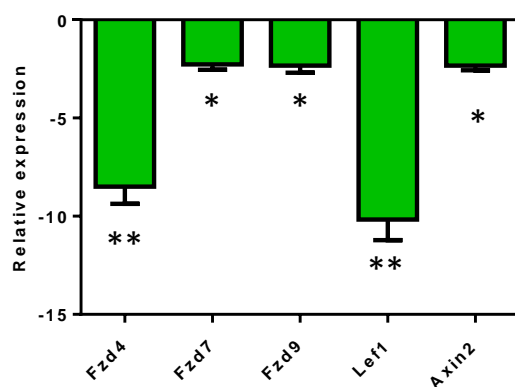
A



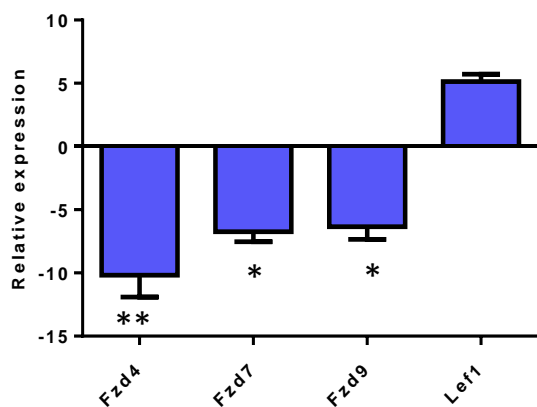
B

Ectopic Bmi1 expression in Bmi1^{+/+} HSCs

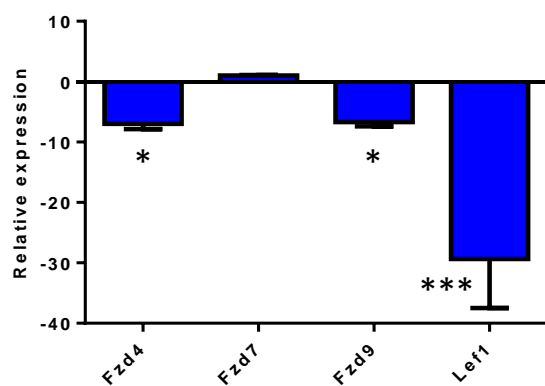
C

Ectopic Bmi1 expression in Bmi1^{+/+} MPPs

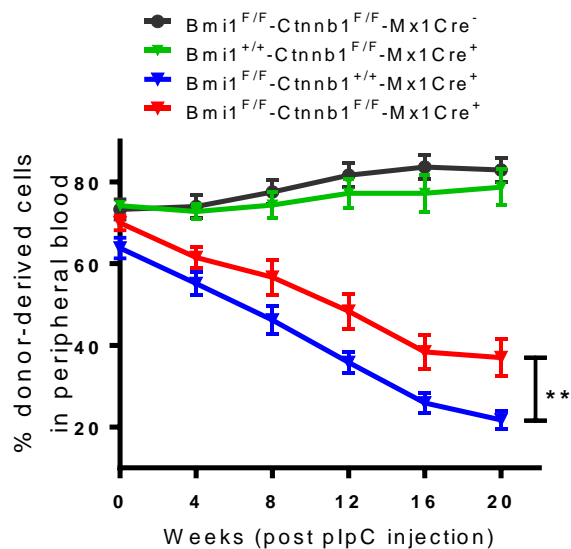
D

Ectopic Bmi1 expression in Bmi1^{-/-} HSCs

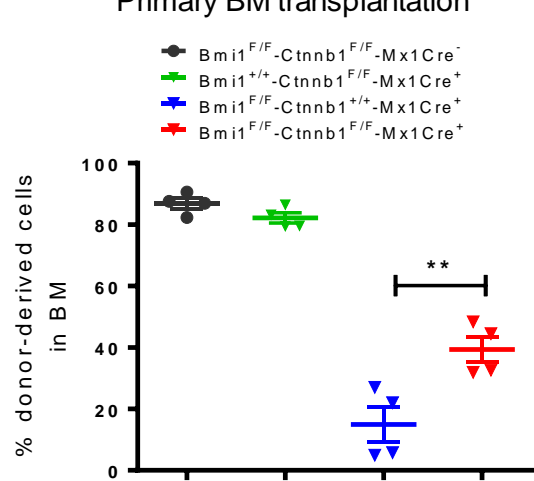
E

Ectopic Bmi1 expression in Bmi1^{-/-} MPPs

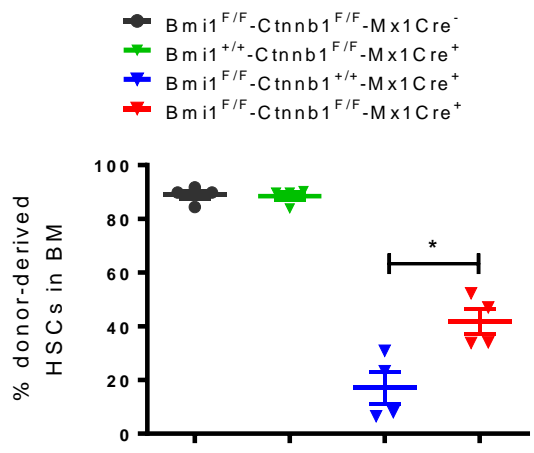
A Primary BM transplantation



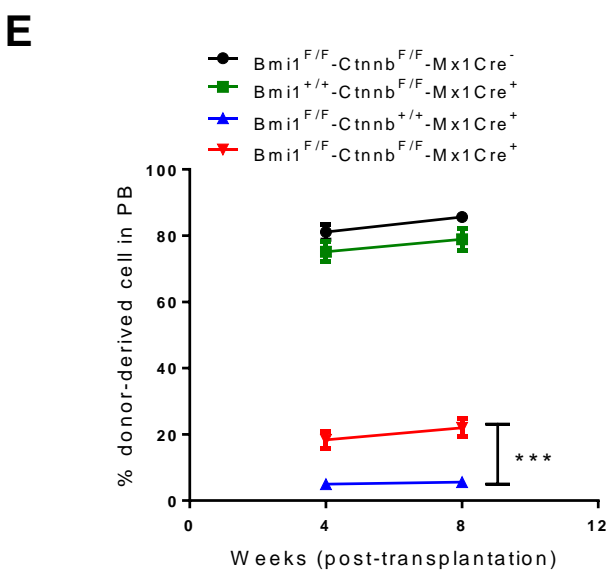
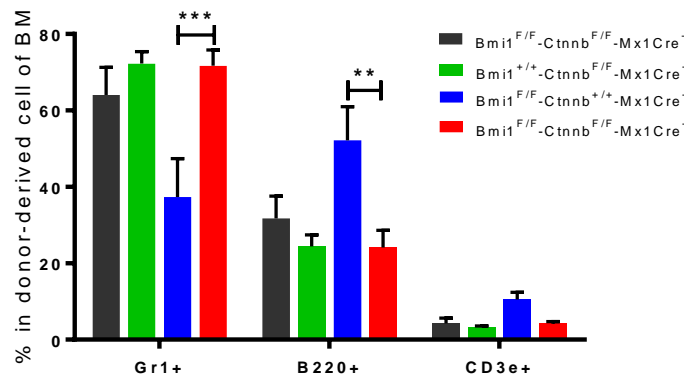
B Primary BM transplantation



C Primary BM transplantation



D Multilineage differentiation in BM at 20 week after plpC





Fate of Hematopoiesis During Aging. What Do We Really Know, and What are its Implications?

Hal E. Broxmeyer¹ · Yan Liu² · Reuben Kapur² · Christie M. Orschell³ · Arafat Aljoufi¹ · James P. Ropa¹ · Thao Trinh¹ · Sarah Burns² · Maegan L. Capitano¹

Accepted: 19 October 2020 / Published online: 3 November 2020
© Springer Science+Business Media, LLC, part of Springer Nature 2020

Abstract

There is an ongoing shift in demographics such that older persons will outnumber young persons in the coming years, and with it age-associated tissue attrition and increased diseases and disorders. There has been increased information on the association of the aging process with dysregulation of hematopoietic stem (HSC) and progenitor (HPC) cells, and hematopoiesis. This review provides an extensive up-to date summary on the literature of aged hematopoiesis and HSCs placed in context of potential artifacts of the collection and processing procedure, that may not be totally representative of the status of HSCs in their *in vivo* bone marrow microenvironment, and what the implications of this are for understanding aged hematopoiesis. This review covers a number of interactive areas, many of which have not been adequately explored. There are still many unknowns and mechanistic insights to be elucidated to better understand effects of aging on the hematopoietic system, efforts that will take multidisciplinary approaches, and that could lead to means to ameliorate at least some of the dysregulation of HSCs and HPCs associated with the aging process.

Keywords Hematopoiesis · Hematopoietic stem and progenitor cells · Aging · Cytokines/Chemokines · Microenvironment · Oxygen · Inflammation · Microbiome · CHIP

Aging is an inevitable process if one lives long enough. There is an ongoing shift in demographics such that older persons will outnumber young persons in the coming years, and with it age-associated tissue attrition and increased diseases and disorders. There has been an increased influx in literature on the association of the aging process with dysregulation of hematopoietic stem (HSC) and progenitor (HPC) cells, and hematopoiesis. Most such hematopoietic aging studies have been carried out in mice, where it has been reported that the aging process (in this case mice in the range of 2 years old)

compared to that of younger mice is associated with increased absolute numbers of phenotypically defined HSCs identified by cell surface antigens in the bone marrow (BM). Yet, the functional capacities of these increased numbers of HSCs are grossly deficient in their engrafting capability in competitive and non-competitive HSC transplants in lethally irradiated mice. Moreover, the differentiation capacity of the engrafted donor BM cells from the old mice is different from that of young donor BM cells; there is a shift in the lymphoid/myeloid ratio of engrafting cells such that the older donor BM cells manifest greater numbers of myeloid to lymphoid cell output. This is the opposite of that of young engrafting mouse BM HSCs. How informative this and other information on aged hematopoiesis is remains to be determined by further investigation. Recent work from our laboratory [1] has observed that at least some of the abnormalities of HSCs from old mice may be more of an artifact of the collection and processing of mouse BM cells, rather than how they manifest their numbers and functional capacities *in vivo*.

This review provides an extensive, although not necessarily complete, summary on the literature of aged hematopoiesis, HSCs and HPCs. When placed in context of potential artifacts of the collection and processing procedure, that may

✉ Hal E. Broxmeyer
hbroxmey@iupui.edu

✉ Maegan L. Capitano
malcapit@iupui.edu

¹ Department of Microbiology and Immunology, Indiana University School of Medicine, 950 West Walnut Street, R2-302, Indianapolis, IN 46202-5181, USA

² Department of Pediatrics, Indiana University School of Medicine, Indianapolis, IN, USA

³ Department of Medicine, Indiana University School of Medicine, Indianapolis, IN, USA

not be totally representative of the status of HSCs in the *in vivo* microenvironment of BM, the site in which HSCs, HPCs, and hematopoiesis are nurtured for self-renewal, proliferation, survival, and differentiation some of what we know may have to be re-evaluated. This review encompasses the following sections: A) Aging and Stem Cells in General, B) Age-Related Changes in HSCs/HPCs and Hematopoiesis, C) Age-Related Clonal Hematopoiesis of Indeterminant Potential (CHIP) and Inflammation, D) DNA Damage, Transcriptional and Epigenetic Changes During Aging, E) Metabolic Processes, Mitochondria and Reactive Oxygen Species (ROS) During Aging, F) Apoptosis, Autophagy, Radiation and a Role for the Sirtuin Family of Proteins During Aging, G) The Microbiome, Hematopoiesis, and Aging, H) Additional Age-Related Information, The Microenvironment, Exosomes, Leptin (Lep) and Leptin Receptors (R), and Means to Better Evaluate and Understand Hematopoiesis During Aging in part in context of our recent studies [1], I) COVID-19, SARS-CoV-2, Aging and Hematopoiesis, and J) Conclusions in Context of Potential Future Interventions for Better Health of the Hematopoietic System During Aging. One of the authors (HEB) of this review had an interest in Gerontology, the study of aging, over 50 years ago, but it is only most recently, that he, his lab members, and collaborators have been involved in actual experiments in this area, having previously focused on the regulation of hematopoiesis in the young.¹

A) Aging and Stem Cells in General

It has been suggested that aging is not caused by active gene programming, but that it rather evolved through limitations in maintenance of somatic cells in which there was a build up of damage [2], which in fact is associated with gene mutations that affect endocrine signaling, stress responses, metabolism and telomere length [3]. Thus, aging is believed to entail

¹ While HEB was pursuing a Masters degree in microbiology, prior to his PhD studies in blood cell development and regulation, he was especially interested in reading the literature on Gerontology. In 1969, he attended as an on-looker an International Conference on Gerontology, the first conference he ever attended. The conference was held in Washington, DC, where he heard talks by all the leading experts in this area of research, including Leonard Hayflick, the original proponent on identifying the limited life-span of normal cells. On a whim, HEB registered to attend a closed discussion group of 20 individuals in the conference to discuss the ramifications of what was then currently known about the biology of aging. While he was the only one in the discussion group without an advanced degree, the others in the group were understanding when the Discussion participants were asked to describe their academic background and interest in the field of Gerontology. When it came time for him to talk he apologized, as he had not worked in the area, but noted his interest in the field, and told them his very limited academic training to that time. To his surprise, he was warmly welcomed into the discussion group, which included amongst those present, Dr. Hayflick. The other participants made it clear that the field of Gerontology was still in its infancy, and their words of advice to him, in not so many words, was to find a field to work in that was more advanced and then when he became an expert in that field to integrate the knowledge from that field into the studies of aging. This he did, a half century later.

“damage” due to multiple mechanisms, some information of which may possibly be used to slow some of the “damage” during aging for healthier outcome. Covered in these papers [2, 3] are the areas of: why aging occurs, is it programmed, how does evolutionary genetics and physiology fit into these processes, how aging is “caused” in terms of molecular mechanisms, mitochondria, and network themes. Whether we yet know enough about the aging process of cells, their organelles, and organisms is still open for debate, although more insight into problems and causes associated with aging could provide the means to potentially intervene at least partially in the future.

Human aging is associated with a number of diseases and defects including the heart, muscle wasting, osteoporosis, and in some cases mental deterioration [4]. Senescent cells and their accumulating damage can contribute to aging, through a number of intracellular signaling pathways including the p53 and RB tumor suppressors, and the influences of neighboring cells in the environment [5]. These, and a number of other genetic pathways have been implicated in aging [6], including nutrient sensing pathways. Over thirty genetic mutations have been reported to extend the lifespan of mice, and a number of genes have been associated in genome wide association studies with longevity of humans [6]. Ames Dwarf mice which harbor a spontaneous mutation in the *Prop1^{df}* gene resulting in the lack of growth hormone, prolactin, and thyroid-stimulating hormone are known to live close to two times the lifespan of other mouse strains [7–10], a situation mimicking certain conditions in humans. Why we age has been commented on from an evolutionary point of view [11]. While somatic cells have a limited lifespan, the lifespan of stem cells, which have the property of making more of themselves (self-renewal) and being able under the appropriate stimuli for differentiation to more mature cell types has not yet been conclusively defined, although transcriptional fingerprinting and other pathway analyses suggest that stem cells do themselves age as one gets older [12, 13].

B) Age-Related Changes in HSCs/HPCs and Hematopoiesis

A number of articles and reviews appeared in this area of research since 2005 [14–37] which will be mainly described in chronological order so that the reader can see what research was reported first and then subsequently, as not all research findings may agree. It was reported that the aging of long-term (LT) HSCs was associated with autonomous changes that increased the self-renewal of these cells, but that these HSCs manifested decreased potential for lymphoid cell differentiation and production [14]. This was associated with down-modulation of genes that mediate lymphoid specification, and up-modulation of myeloid fate decisions and functions

[14]. Competitive transplants were done using the congenic CD45.1/CD45.2 mouse system with relatively purified populations of donor HSCs to assess engraftment, and self-renewal was estimated by secondary transplants. This paper [14] did not note the decreased engrafting capacity of HSCs from BM of older mice that most of the other numerous publications in this area have reported, and lacked detailed month by month chimerism data comparing engraftment of old vs. young mice; nor did it quantitate numbers of functional HSCs using limiting dilution analysis to calculate competitive repopulating units (CRUs, a measure of the numbers of functional HSCs [38]). Age-related defects in lymphoid-bias [15] and B-lymphopoiesis [16] have been reported by others, and have been suggested to underlie the dominance of myeloid cells in adult leukemia [17]. In order for HSCs to engraft, they must first home to the BM after IV injection. This process of homing for BM cells of old mouse CRUs was about 3-fold lower than the homing efficiency of CRUs from young mice [18], hence one potential reason for decreased engrafting capability noted by others. Of some interest, although not completely understood, the ability to mobilize HSCs from old mice with G-CSF to the blood was increased compared to that of G-CSF mobilization of HSCs from younger mice [19]. This correlated with a reduced adhesion capacity of an immature cell population (not a purified HSC population) to stromal cells, and with increased activation of Cdc42, a small RhoGTPase. This work has not yet been reproduced to the knowledge of the authors of this review, and more rigorous analysis is needed to fully understand this interesting phenomenon. What has not been defined yet is the mobilization of lymphoid vs. myeloid-biased HSCs in old vs. young mice. It will also be of interest to assess the mobilizing capacity of bonified HSCs to the combination of G-CSF plus AMD3100 (Plerixafor), as G-CSF and AMD3100 synergize to mobilize HSCs and HPCs from young mice [39].

Other reviews have noted age-related changes in hematopoiesis of old vs. young mice [20, 21], with one short report [22] not seeing differences in engraftment of sorted populations of HPCs from elderly (>70 years old vs. young) human BM in immune deficient NSG mice. This clearly needs more rigorous investigation in terms of numbers and engrafting capability of rigorously purified populations of functional human BM HSCs (not HPCs) from old and young donors.

While an earlier report [14] suggested increased self-renewal of HSCs from BM of old mice, a later report by others with more in-depth analysis demonstrated that HSCs from the BM of old mice manifested significantly reduced self-renewal in secondary transplants using highly purified populations of LT-HSCs [23] for both primary and secondary engraftment. They [23] as did others [18] showed decreased homing efficiency of HSCs from the BM of old mice. Moreover, they [23] showed significantly delayed proliferative responses of old vs. young BM HSCs.

What is clear is that all studies thus far that have assessed old vs. young BM engrafting HSCs have shown a bias of the myeloid vs. lymphoid production capability of HSCs from old mice [14, 16–18, 20–24]. Whether this apparent bias of donor HSCs from old mice might be due to potential artifacts in how donor cells were collected, processed, and injected into recipient mice [1] will be discussed in Section H.

The impact of hematopoiesis in aging primates was investigated by clonal tracking in which clonal output of thousands of genetically barcoded HSCs and HPCs was determined in old vs. young macaques after autologous transplantation [25, 26]. Delayed output from multipotent clones was observed in old macaques with persistence of lineage biased clones noted; in contrast to aging studies in mice which showed persistence of myeloid-biased clones with old age, there was persistent output from both B-lymphoid- and myeloid-biased clones. Whether or not macaque vs. mouse differences were due to aging differences between species requires further investigation as these studies [25] were based on only two old macaques 18 and 25 years of age, which were considered “aged” on their lifespans of captivity of 20–30 years.

The multipotential progenitor (MPP) cell compartment is a composite of 4 different cell types, with the MPP4 compartment being considered to be lymphoid-primed [27]. A yet to be understood observation in context of lymphoid-biased aging studies is the progressive loss and increased cycling of the MPP4 population with aging; other cells and factors may be involved in lymphoid-biased output from engrafted aged HSCs.

Two intriguing reviews on HSC aging are entitled: “The slippery slope of hematopoietic stem cell aging” [30], and “Age-related clonal hematopoiesis: Stem cells tempting the devil” [29]. The latter review touches on clonal hematopoiesis of indeterminate potential (CHIP), an area that will be covered in detail in Section C, and is associated with increased risk of hematological cancers, as well as that of the mortality associated with cardiovascular problems. A number of other more recent reviews are worth noting including: “Aging of hematopoietic stem cells” [31], “Anemia at older age: etiologies, clinical implications and management” [32], “Aged murine stem cells drive aging-associated immune remodeling” [33], “The global complexity of the murine blood system declines throughout life and after serial transplantation” [34], “Hematopoietic stem cells aging, life span and transplantation” [35], “The ageing hematopoietic stem cell compartment” [36], and “Relationships between aging and hematopoietic cell transplantation” [37]. All these reviews suggest that intervention in age-related dysfunction of HSCs may be possible, in part by targeting selected intracellular regulatory pathways. We suggest in Section H, the potential use based on studies in mice of HSCs and HPCs from older individuals for efficient hematopoietic cell transplantation (HCT), if the cells are more appropriately collected and processed under conditions that

maintain their *in vivo* numbers and functional characteristics [40–42]. How these cells are collected may be crucial, as cells are currently collected in almost all mouse studies, except those noted by us [40–42], and in all human studies, in ambient air (~21% O₂ tension). Collection of cells in ambient air subjects them to a phenomenon which we termed Extra Physiological Oxygen Shock Stress (EPHOSS) [40, 41]. Ambient air causes the very rapid loss of HSCs and a concomitant increase in numbers of HPCs due to EPHOSS-induced differentiation of HSCs [40]. This differentiation process during collection of cells in air occurs within minutes, and may likely be needed to be considered in interpretation of at least some of the published information presented. This may require some re-evaluation of past studies to ensure that studies accurately describe the situation of numbers and functions of these cells as when they are present in their BM microenvironment, before removal for collection and analysis, as we reported in [1] and discuss in Section H.

C) Age-Related Clonal Hematopoiesis of Indeterminant Potential (CHIP) and Inflammation

Age-Related Clonal Hematopoiesis

CHIP, also known as age-related clonal hematopoiesis (ARCH), is characterized by expansion of somatic mutations in various hematopoietic lineages of older persons and is associated with risks of developing leukemia [43], as well as other age-associated disorders including cardiovascular disease [44]. Human aging is associated with an exponential increase in the occurrence of CHIP in aged individuals. It is an emerging public health issue that affects at least 15–20% of individuals aged 70 or above [43–59]. A number of reviews and reports on clonal hematopoiesis have been published [45–59]. This is currently a heavily researched area of investigation, with the causes still relatively unknown. Clarity is needed on why some cells with mutations, likely involving and caused by several factors [57] noted in the below Sections, persist and/or expand with resultant disorders such as leukemias, myelodysplasias, and cancers associated with aging individuals.

The vast majority of the mutations identified in CHIP are dispersed across the genome. However, five genes, including *DNMT3A*, *TET2*, *ASXL1*, *JAK2*, and *TP53*, have high numbers of somatic mutations [54–59]. The most common base-pair change in the somatic variants identified in CHIP was a cytosine to thymine (C to T) transition, a somatic mutational signature of aging [54–56]. CHIP is an age-dependent risk factor for both hematological malignancies and cardiovascular disease [53–59]. Thus, preventing CHIP progression may prove to be beneficial for human health. However,

mechanisms by which somatic mutations in HSCs and other blood cells contribute to the pathogenesis of age-related diseases are largely unknown.

Clinical studies revealed that hematopoietic clones harboring specific mutations in individuals with CHIP may expand over time [54–58]. However, how different cellular stressors affect clonal expansion is largely unknown. Recently, three different stressors, including hematopoietic transplantation, cytotoxic therapy and inflammation, have been shown to expand hematopoietic clones. *TP53* mutations identified in CHIP confer a competitive advantage to HSCs and HPCs following transplantation through modulating epigenetic pathways [52]. Considering that common mutations identified in CHIP affect epigenetic modulators, including *DNMT3A*, *ASXL1*, and *TET2*, these findings underscore the importance of dysregulated epigenetic control in CHIP development.

PPM1D is a phosphatase that negatively regulates p53 and several proteins involved in the DNA damage response (DDR) pathway [60]. Recently, *PPM1D* mutations were found in CHIP [54–58]. *PPM1D* mutations result in the expansion of *PPM1D*-mutant hematopoietic cells following chemotherapy treatment. However, they do not confer competitive advantage to HSCs and HPCs following bone marrow transplantation [61, 62]. *TP53* mutations are associated with prior exposure to chemotherapy [63]. Genotoxic stresses selectively expand *TP53*-mutant HSPCs [50, 64]. While both p53 and *PPM1D* are involved in the DDR pathway, they appear to play distinct roles in promoting of HSCs and HPCs expansion.

The Effects of Chronic, Low-Grade Inflammation Associated with Aging

During aging, chronic and low-grade inflammation - inflammaging - develops, which contributes to the pathogenesis of age-related diseases [65, 66]. Aberrant innate immune activation and pro-inflammatory signaling within the malignant clone and the BM microenvironment have been identified as key pathogenic drivers of myelodysplastic syndrome (MDS), an age-related disease [67]. Mutations identified in CHIP may utilize cell extrinsic mechanisms to promote clonal hematopoiesis. For example, *TET2*-deficient macrophages exhibit an increased in *NLRP3* inflammasome-mediated interleukin-1 β secretion [68]. Inflammasomes are multiprotein complexes that activate Caspase-1 and increase the release of pro-inflammatory cytokines such as IL-1 β , leading to caspase-1-dependent death, known as pyroptosis [69]. HSCs and HPCs from low to high-risk human patients with MDS manifest activated *NLRP3* inflammasome [70]. *NLRP1* inflammasome activation increases IL-1 β secretion that inhibits wild-type HSPC function through inducing pyroptosis [71]. The *NLRP1* inflammasome, but not the *NLRP3* inflammasome, is specifically activated in p53 mutant

HSPCs, leading to increased secretion of IL-1 β , which induces pyroptosis of wild-type HSPCs in a paracrine fashion (YL and HEB, unpublished data). Tet2-deficient hematopoietic stem and progenitor cells manifest a hyperactive IL-6 pathway, which promotes cell survival under basal conditions and in response to inflammatory stress. Inhibiting inflammatory signaling in Tet2 mutant preleukemic cells mitigates stress-induced abnormalities and clonal hematopoiesis [72].

Splicing of pre-mRNAs by the spliceosome plays a key role in tissue development [73, 74]. Genome wide splicing analysis revealed an increased number of spliced genes during aging [75, 76]. Changes in spliceosome gene expression and alterations in pre-mRNA splicing are associated with lifespan in mice and humans [77]. Notably, both human and mouse HSPCs display dysregulated pre-mRNA splicing with age [78, 79]. Further, spliceosome gene mutations, including *SF3B1*, *SRSF2* and *U2AF1*, were frequently found in CHIP and MDS [54–57, 80–82], implicating that aberrant splicing in hematopoietic cells may contribute to CHIP and pathogenesis of MDS. Although both *SRSF2* and *SF3B1* mutations alter mRNA splicing, these mutations functionally converge with hyperactivation of NF- κ B, a key mediator of the inflammatory response [83]. These findings underscore the importance of chronic inflammation in promoting CHIP development during aging.

Inflammation

Inflammation is a double-edged sword in hematopoiesis and disease. The hematopoietic system gives rise to the immune cells of the body and is, therefore, closely linked to inflammation. Even at early stages of hematopoietic development, inflammatory cytokines, such as interleukin-1 (IL-1), interferon- γ (IFN- γ), tumor necrosis factor (TNF), and granulocyte colony stimulating factor (G-CSF), play critical roles in the specification of hematopoietic stem cells (HSCs) [84]. Remarkably, different levels and combinations of inflammatory signaling molecules can elicit opposing responses, suggesting that context may be significant. For example, while IFN- γ and TNF are linked to bone marrow failure and decreased self-renewal capacity in adults, they enable hematopoiesis during development [84]. Under normal conditions in the mature hematopoietic system, cytokines influence HSC proliferation, differentiation, and self-renewal [84]. IFN- γ , IL-3, and IL-1 can influence the differentiation of HSCs toward myeloid lineages by activating myeloid transcription factors [84]. These same inflammatory factors stimulate hematopoiesis to support the immune system during infection and injury in a process called emergency granulopoiesis [85]. This process leads to the expansion of myeloid cells, which serve as the first line of defense against foreign pathogens [85]. These mechanisms rely on inflammatory mediators and are essential for maintaining homeostasis.

While inflammation enables hematopoietic development and stimulation of HSCs during illness and injury, it also contributes to pathogenesis and disease progression. During infection, inflammatory signals, such as IFN- γ and IL-27, trigger the proliferation and differentiation of HSCs to bolster the immune response either by acting directly on HSCs or indirectly via mature hematopoietic cells, endothelial cells, or the bone marrow microenvironment [86–90]. However, prolonged bacterial or viral infection can hinder self-renewal and competitive repopulation capacity, leading to HSC depletion [91, 92]. This exhaustion of HSCs during chronic inflammation may be attributed to increased myeloid differentiation [93]. Notably, dysregulation of the myeloid cell compartment also occurs in patients with severe COVID-19 [94]. This inflammation-mediated HSC dysfunction may occur via the TLR4-TRIF-ROS-p38 signaling pathway rather than Myd88 signaling, suggesting that the mechanism underlying chronic inflammation may be distinct from that of emergency granulopoiesis [91]. In the context of sepsis, activation of Myd88 caused myelosuppression without significant effects on HSCs, whereas activation of TRIF strongly inhibited HSC self-renewal without direct effects on myeloid cells, inferring cell type-specific effects of these inflammatory mechanisms [95]. Targeting these two pathways may have therapeutic value. While foreign infections can alter hematopoiesis by triggering inflammation, the normal microbiome can also influence the hematopoietic system. See more on this in Section G. Antibiotic-treated mice exhibit depletion of HSCs and progenitor cells as well as anemia, thrombocytosis, pan-lymphopenia, and leukopenia [96]. The complexity of the intestinal microbiome regulates the size of the myeloid cell population in the bone marrow via Myd88 signaling [97]. The disruption of these interactions may have implications for the potential contribution of infection to the progression of preleukemic conditions to hematological disease. For example, disruption of the intestinal barrier promotes myeloproliferation in mice lacking the preleukemic gene Tet2, whereas germ-free Tet2-deficient mice do not exhibit myeloproliferation [98]. Germline Tet2 loss of function is associated with immunodeficiency and lymphoma in children [99, 100]. Importantly, myeloproliferation was alleviated in Tet2-deficient mice with loss of intestinal integrity by treatment with antibiotics [98, 101]. Similarly, bacterial signals cause the expansion of HSCs lacking Tet2 and induce the production of IL-6 from HSCs, bolstering the role of infection and inflammation in the pathogenesis of hematological malignancy [102]. A link to these effects in aged animals remains to be better elucidated, with effects of bacteria on tumor progression and metastasis covered in Section I.

Remarkably, many of the same inflammatory pathways that guide hematopoietic development and strengthen the immune system under normal conditions can also drive leukemia in the context of infection or other inflammatory conditions.

For example, IL-6 facilitates the development of chronic myelogenous leukemia in mice, and IL-33 contributes to myeloproliferative neoplasms by altering myelopoiesis [103, 104]. In addition, inflammation can cause genotoxic stress, the accumulation of mutations, and the progression of preleukemic conditions to leukemia [105, 106]. An unexplored area is the elucidation of the factors and events responsible for the transition from the normal inflammatory response to the deleterious inflammation that can promote hematological disease. As during hematopoietic development, the context of the inflammatory response may be important in shaping disease outcomes. For example, chronic IL-1 signaling can reduce HSC self-renewal, limit hematopoietic lineages, and impair the response of HSCs to replicative challenges [107]. A recent study of MDS indicates that inflammation acts as a selective pressure that specifically fosters expansion of preleukemic or malignant HSCs compared to normal HSCs [108]. Distinct hematopoietic cell subtypes may exhibit differential responses to specific inflammatory signaling molecules, further supporting heterogeneous HSC populations that can drive leukomogenesis [84, 109].

The effect of inflammation on HSCs has valuable implications for age-associated diseases, as older individuals exhibit elevated levels of inflammation [110]. Inflammation plays a significant role in expansion of HSC clones carrying preleukemic mutations in CHIP. Characterized by acquisition of somatic mutations in hematopoietic lineages with age, CHIP is associated with both hematological malignancy and cardiovascular disease (CVD), broadening the role of preleukemic mutations in disease states [111, 112]. The pro-inflammatory response observed in HSCs carrying preleukemic mutations indicates the existence of intrinsic mechanisms of inflammation for HSCs [102, 113, 114]. The addition of a pro-inflammatory preleukemic mutation can alter the presentation of hematological malignancy [115]. It has been proposed that HSCs and mature hematopoietic lineages propagate the inflammatory response via a feedforward mechanism, in which inflammatory signals from one cell type amplifies the other [116]. Pro-inflammatory macrophages secreting IL-1 α enable CHIP-associated CVD, underscoring that some of the same pathways involved in hematopoietic homeostasis and leukemogenesis also contribute to the non-hematopoietic manifestations of CHIP [68]. In addition, as in emergency granulopoiesis, aging promotes myeloid expansion, further emphasizing potential mechanistic overlap [109]. While intrinsic factors appear to be important to the inflammatory response involved in the pathogenesis of CHIP-associated diseases, extrinsic mechanisms may also influence this process as the conditioned media from aged mesenchymal stromal cells impairs the function of young HSCs [117]. In addition to acting directly on HSCs, inflammation can also remodel the bone marrow microenvironment, which regulates

hematopoiesis [118]. Additional studies are needed to understand the ways in which these pathways are altered during aging and pathogenesis, and how they may be modified for health benefit.

Elderly populations may be uniquely susceptible to the effects of inflammation and CHIP as comorbidities and CHIP are more common in aging individuals. Several comorbidities with inflammatory components, such as ulcerative colitis, rheumatoid arthritis, and systemic sclerosis, have been linked to increased clonal hematopoiesis [119–121]. Pro-inflammatory features of CHIP-associated HSCs/HPCs may influence outcomes of hematopoietic stem cell transplants, leading to cytopenias, chronic graft vs. host disease, and/or donor-derived leukemia (DDL) [122]. These patient populations may especially be vulnerable to development of hematological malignancies and CHIP-associated diseases following infection, as infection may exacerbate the existing inflammatory response in these patients. Inflammation may be a key factor contributing to the heterogeneity observed in hematological malignancies and CHIP-associated diseases and should be considered in the clinical management of patients with these conditions. In particular, differences in the clinical presentation between donors and recipients that develop DDL highlight the potential role of inflammation and comorbidities in promoting leukemogenesis. It is yet not known if these different sources of inflammation influence hematological malignancies and CHIP-associated diseases via common mechanisms.

Intrinsic and extrinsic sources of inflammation may represent potential therapeutic targets for hematological malignancies and CHIP-associated diseases. Inhibition of inflammation can impede clonal expansion in response to inflammatory stimuli [102]. Blocking inflammation may also be a valuable therapeutic approach in CVD, as inhibiting IL-1 receptor signaling from pro-inflammatory macrophages can prevent CHIP-associated CVD in mice [68]. It is currently unclear whether suppressing inflammatory HSCs or mature hematopoietic lineages is more effective. Inflammatory signals from the bone marrow microenvironment may also be viable therapeutic targets but have not yet been investigated. A more thorough understanding of the timing of the inflammatory response and the cell types involved will facilitate the effective inhibition of inflammation in hematological malignancies and CHIP-associated diseases. Strategies to both prevent pathogenesis and to treat existing disease will be valuable. A critical aspect of targeting inflammation in these disease contexts will be to maintain the normal inflammatory response necessary for responses to infection and injury while targeting aberrant inflammatory pathways that promote disease; however, additional studies are needed to elucidate factors governing these processes. Thus, Inflammation acts as a dysregulator of tissue maintenance and regeneration during aging as evidenced by

the fact that HSC do not regenerate well after inflammatory challenge [123].

D) DNA Damage, Transcriptional, and Epigenetic Changes During Aging

DNA damage accumulates with age, and defects in DNA repair can cause cellular changes that resemble a premature aging phenomenon [124–127]. Tables on selected models of premature aging in mice and their common features have been summarized in a review [126] and p53 implicated in DNA damage [87]. While DNA damage to HSCs and HPCs during aging is clearly impacted, such damage to the microenvironmental niche cannot be overlooked [124]. Transcriptional changes in stem cell populations have been profiled for HSCs and other stem cell types, but it is not clear yet if a common age-related signature has been identified [12]. A role for epigenetics in the aging process is also considered [128]. Epigenetic hallmarks of aging and senescence have been diagrammed, as have been the pros and cons of using model systems to study aging and senescence in a variety of species, along with a short listing of repositories and tools for evaluating a role for research in the aging process [128].

Repair of damage has been shown to offset deficient HSC function during aging [129]. This was especially apparent under stress conditions, in which DNA damage led to loss of the potential of HSC reconstitution, proliferative capacity, self-renewal activity, enhanced apoptosis, and then exhaustion of function [129]. It was suggested that the accrual of DNA damage may be a means contributing to HSC functional defects of these cells to respond to acute stress or injury [129].

A shift from canonical to non-canonical signaling by Wnt, in response to elevated expression of Wnt5a was associated with the process of HSC aging [130]. Treatment of cells from young mice with Wnt5a induced aging associated HSC apolarity, reduced their capacity for regeneration, and resulted in a age-related shift in myeloid/lymphoid differentiation, that was associated with activation of the GTPase Cdc42 [130]. Moreover, haploinsufficiency of Wnt5a resulted in the attenuation of the aging phenotype of HSCs [130]. Other studies defined replication stress as a driver of functional declines in HSCs during aging [131]. This was associated with decreased expression of mini-chromosomal maintenance helicase components and altered DNA replication fork dynamics [132].

There are reports on a role for epigenetics in abnormalities associated with HSCs in old mice [132–135]. While the decline of HSC function seemed to be dependent on their proliferative history, it was noted to be independent of the length of their telomeres [133]. HSCs from old mice manifested reduced signaling of transforming growth factor-beta with changes in genes involved in proliferation and differentiation of HSCs [135]. HSCs from old mice had broader peaks of

H3K4me3 with increased methylation of DNA at the transcription factor binding sites that were associated with genes involved in promotion of differentiation, and a reduction of genes associated with maintenance of HSCs [135]. Ribosomal biogenesis was found to be a particular target of this age-related HSC phenotype; there was increased transcription of ribosomal protein and RNA genes, and the hypomethylation of genes for ribosomal RNA [135].

Proteosome analysis [136] and single-cell RNA sequencing [137] have been performed on HSCs from old mice. How much these analyses really inform us about the prime drivers in HSC dysfunction remains to be determined, especially since the cells were collected in ambient air prior to analysis, which may not be optimal for assessing physioxia associated effects [1]. Of some interest, deletion of inhibition of DNA binding1 (Id1), a helix-loop-helix transcription factor protected HSCs from both the effects of stress-induced exhaustion and that of aging [138].

E) Metabolic Processes, Mitochondria and Reactive Oxygen Species (ROS) During Aging

Metabolism, mitochondria and ROS are important aspects of HSC function [40, 41], as well as for other stem and progenitor cell types [139–141]. Aging is associated with extensive changes in metabolism [75–77]. A short report questioned whether or not metabolic mechanisms of stem cell maintenance might explain aging and its associated impact on stem cells [142]. Another review concentrated on mitochondrial contributions to dysfunction of somatic stem cells in general and in context of aging [143] and a review on mitochondrial metabolic checkpoints and aging of HSCs implicated mitochondrial maintenance mechanisms including mitophagy and asymmetric segregation of “aged” mitochondria [144]. This is an area that clearly requires more detailed investigation, although it has been suggested that mutations in mitochondrial DNA are not a primary driver of stem cell aging [145].

ROS has been implicated in various stem cell functions [40, 41, 146–148], and STAT3, mitochondrial dysfunction, and overproduction of ROS has been associated with a rapid aging-like phenotype [149]. Symmetric divisions of stem cells, including HSCs, results in increased stem cell numbers with maintenance of stem cell characteristics of the original “mother” cell. However, asymmetric division of stem cells can result in one daughter cell maintaining the original stem cell characteristics of the “mother” stem cell, while the other cell can be a more differentiated progenitor cell. To assess selective apportioning of subcellular contents between “daughter” cells using mammary stem like cells, it was found that “daughter” cells that received fewer “old” mitochondria were associated with maintenance of stem cell traits; inhibition of mitochondrial

fission disrupted age-dependent subcellular localization and segregation of mitochondria with resultant loss of stem cell properties in the progeny [150]. It is not clear if such studies with mitochondria apportioning between HSCs undergoing symmetric or asymmetric divisions have yet been done, but it is certainly an area of interest if done in context of HSC from young and old bone marrow HSCs, and their collection and processing under physioxia conditions as noted [1].

There is still much to be learned regarding how stem cells maintain metabolic homeostasis. The unfolded protein response has been implicated as modulating the HSC pool during stress [151], but has apparently not yet been evaluated in HSCs from aged mice. However, a regulatory branch of the mitochondrial unfolded protein response, mediated by the interplay of the sirtuin, SIRT7 (more on sirtuins in Section F), and nuclear respiratory factor 1 (NRF1) which is a master regulator of mitochondria, was interrogated in HSCs [152]. It was noted that inactivation of SIRT7 resulted in reduced quiescence, increased mitochondrial protein folding stress, and decreased regenerative capacity of HSCs. Moreover, expression of SIRT7 was decreased in HSCs from old mice, and up-regulation of SIRT7 in the aged HSCs improved their regenerative capacity. This implicated the mitochondrial unfolded protein response-mediated metabolic checkpoint as a contributor to HSCs in old mice [152]. In addition, mitochondrial DNA polymerase, when defective, has been associated with premature aging in mice [153], but how, if at all, this relates to HSC function from old mice remains to be determined.

Thioredoxin-interacting protein (TXNIP) is a 397 amino acid residue, belonging to the arrestin family of proteins. It has been reported to regulate HSC quiescence and mobilization after stress [154–156], and is likely to be involved in HSC function, but has not to our knowledge been extensively investigated. Reasons to evaluate this during aging is that *Txnip*^{-/-} mice have decreased HSC reconstitution resulting in HSC exhaustion, effects associated with hyperactive signaling of Wnt, an active cell cycle, and reduced expression of p21^{cip1}. These stresses also affect the BM microenvironment resulting in decreased expression of CXCL12 (a chemotactic and homing chemokine)- and osteopontin-mediated interactions between HSCs and the BM [154]. TXNIP helps to maintain the pool of HSCs by functional switching of p53 after oxidative stress, effects that have been reviewed [155].

There is much to be learned regarding metabolic influences in aging, and molecular mechanisms underlying aging effects on HSCs still remain unclear. Elevated activity of the small RhoGTPase cdc42, previously noted by the investigators in another paper was linked casually to effects on HSCs in old mice [152], with a correlation of the loss of polarity in these cells. Moreover, by inhibiting cdc42 activity by pharmacological means, it “rejuvenated” the aged populations of HSCs by increasing the percent of polarized cells and restoring the level and spatial distribution of histone H4 lysine16 acetylation

such that it was similar to that in HSCs isolated from young mice [152, 157]. This information further identified epigenetic regulatory changes in functional effects of HSCs from old mice, and may relate to metabolic changes.

Other studies linked the interaction of ROS dependent DNA damage, mitochondria, and p38 MAPK with senescence of adult mesenchymal stem/stroma cells (MSCs) from humans, with pharmacological inhibition of p38 MAPK partially recovered the senescence phenotype by partial prevention of hydrogen peroxide-induced senescence [158]. How linked senescence phenotypes are to the function of HSCs in aged persons remains to be determined. Somatic cell mitochondrial DNA (mtDNA) mutations contribute to such age-related disorders as those associated with myelodysplasia (MDS), and it was noted that the mito-protective effect of autophagy was impaired in erythroid cells of old mice [159]. mtDNA-mutated mice had somatic mtDNA mutations that were a targeted defect in the function of proofreading mtDNA polymerase, PolgA, and developed macrocytic anemia similar that seen in MDS patients. Mechanistic insight into these processes was reported [159], but whether or not these processes reflected changes in HSCs from old mice was not explored.

F) Apoptosis, Autophagy, Radiation, and a Role for the Sirtuin Family of Proteins During Aging

Ageing-Related Apoptosis and Autophagy

Apoptosis, the phenomenon of programmed cell death, and autophagy, a self-degradative process responsible for eliminating cytosolic constituents such as long-lived proteins, aggregated proteins, and damaged organelles (mitochondria, ribosomes, peroxysomes) [160] have been linked to functional changes noted during aging [161, 162] and HCT [163]. Autophagy is associated with repair pathways that can protect hematopoiesis from injury due to nuclear radiation [164, 165]. Inhibition of autophagy by genetic manipulation was associated with normal and pathological aging, with its inhibition compromising the “longevity-promoting” effects of restriction of calories, the activation of SIRT1, inhibition of insulin and insulin growth factor signaling, and the administration of rapamycin, resveratrol, or spermine [161]. Autophagy was shown to maintain the metabolism of HSCs from both young and old mice [164]. These influences were not noted in all HSCs from old mice, with about a third of HSCs from aged mice demonstrating high autophagy levels being associated with a low metabolic state and high potential for regeneration [165]. This suggests that not all HSCs in aged mice are functionally compromised, an important point in aging HSC research that can be overlooked when studying HSCs from old mice at a total HSC population level. It is known that there are

subsets of rigorously purified HSC populations that differ in mitotic history [166], and intracellular characteristics [1]. FOXO4 was suggested as a pivotal agent in the area of cellular senescence [167]. Using a FOXO4 peptide that disrupted the FOXO4 interactions with p53 *in vivo* where it was tolerated, restored certain functions in naturally aged and in fast aging Xpd^{TTD/TTD} mice. How this relates to HSCs in old mice remains to be evaluated.

Mitophagy is a process that is evolutionary conserved involving autophagic targeting and clearance of mitochondria that are destined for removal [168]. It is induced by short ubiquitin chains on the mitochondria [169]. Reviews on this process have been reported [168, 169] and discuss how metformin, an oral diabetes medication, both enhances and normalizes mitochondrial function that leads to alleviation of inflammation associated with aging [170]. What remains to be determined is if there is a role for mitophagy in HSC and HPC during aging, and if this can be modulated for health benefit.

Radiation Effects and Aging

Like aging, exposure to radiation is an additional stressor to the hematopoietic (H) system, the most sensitive tissue in the body to radiation damage. Therapeutic radiation, nuclear accidents, and malicious exposure from radiologic-warfare put mankind at risk for life-threatening acute radiation syndromes (ARS) and the delayed effects of acute radiation exposure (DEARE) in those fortunate to survive ARS. H-ARS, due to direct and indirect effects of radiation exposure on all classes of hematopoietic cells, leads to death within weeks if untreated [171, 172].

Hematopoietic DEARE, also known as residual bone marrow damage (RBMD), is characterized by diminished immunity and decreased production of blood cells persisting for years after radiation exposure [173–179]. Survivors of H-ARS exhibit severe lifelong damage to HSC, characterized by significantly decreased complete blood count, loss of HSC repopulating potential, loss of HSC quiescence, decreased numbers of HPC, and dramatic myeloid skewing, all most evident under stress [173–183]. An increased incidence of lymphoid malignancies, shortened life span, decreased mesenchymal stem/progenitor cell (MSC) number, and aberrant levels of endothelial cell-derived HSC niche proteins in aged H-ARS survivors have also been documented (Orschell, unpublished data). Long-term damage to the HSC-supportive niche also likely contributes to HSC dysfunction and RBMD. As enhanced cycling of HSC is believed to lead to loss of self-renewal potential and is detrimental to engraftment potential [184], it seems likely that the enhanced cycling of HSC from H-ARS survivors is a major contributor to RBMD. These data illustrate an unrecoverable loss of HSC self-renewal and differentiation potential, the two hallmarks of HSC [185–191], in survivors of H-ARS and suggest that compensatory

mechanisms of hematopoietic support cannot overcome the “second hit” imparted by aging [14, 124, 129, 192, 193].

The DEARE are generally thought to result from persistent inflammation and chronic oxidative stress [194–201], leading to fibrosis [202] and loss of stem cell self-renewal functions. Indeed, elevated levels of pro-inflammatory cytokines associated with oxidative stress [203] have been reported in Japanese atomic bomb survivors [198, 202]. Other studies in atomic bomb survivors have shown possible reductions in self-renewal capability of HSC secondary to dose-dependent DNA damage [204], as well as detriments in immune function [205], corroborating mouse H-ARS data. NAD(P)H oxidase, xanthine oxidase, and mitochondria have all been implicated as primary oxidant sources in various models and conditions [203, 206–208], and ROS has been documented in HSC post-irradiation as well [181]. NF- κ B, one of several transcription factors activated by ionizing radiation [209], plays a central role in inflammation [210], is activated by oxidative stress and induces oxidative stress through interactions with cytokines [211], creating a potential feed-forward mechanisms to maintain chronic inflammation and oxidative stress.

Cellular senescence, and its associated oxidative/pro-inflammatory phenotype, has recently emerged as a causative mechanism of DEARE [211–214], making senescent cells a new therapeutic target for RBMD and other DEARE. Importantly, senolytic drugs have the potential to be used as an effective treatment for DEARE even after DEARE becomes a progressive disease [212], but it is not yet clear how this might be used in and for elderly exposed individuals.

As mice age, like humans, health issues and phenotypic changes begin to manifest and variability in experimental endpoints increases, necessitating the need for larger group sizes for sufficient statistical power. For example, mice of similar strains have been shown to exhibit significantly different life spans [215, 216] and radiation sensitivities when aged (Orschell, unpublished data), as well as differing susceptibilities to radiation-induced swollen muzzle syndrome [217], all depending on the vendor from which they were sourced. Mice from different vendors have also been shown to possess different fecal microbiota [218], which may contribute to vendor-specific phenotypic differences. For these reasons, investigators should consider stringent control of the vendor and barrier of their mice for aging studies to ensure optimal stability of their experimental models.

It is noted that more profound effects of aging may be produced not by life-threatening ARS (where the majority of those are exposed to high dose radiation), but rather by moderate or even low dose exposure.

The Role of Sirtuins in Regulating Aged HSC Function

Sirtuins are part of a large family of molecules, some of which have been linked in longevity/aging studies. The role of the

sirtuin SIRT1 in stem cell biology, the aging process and in HSC function in old mice had been reviewed [219]. In this review it was noted that although the role of SIRT1 in telomere maintenance was not resolved, its role in mitochondria and generation of ROS was highly implicated. It was observed that the genetic, hormonal, or drug manipulation of stem cell mitochondria may be useful as an intervening tool for manipulating HSCs from old mice. It was later reported that deficiency of SIRT1 compromised mouse embryonic stem cell hematopoietic cell differentiation in addition to embryonic and adult mouse hematopoiesis [220]. SIRT1 was reported to be required for maintenance of HSCs and lineage specification, in part by the transcription factor FOXO3 [221]. These investigators also suggested that SIRT1 may be involved in HSC function during aging by “delaying” HSC functional abnormalities [221], but this has not been rigorously studied. Although the role of SIRT1 and other sirtuins in the caloric restriction of modifying the aging process have been extensively reviewed [222–224], such studies do not always take into account the sex and mouse strains utilized [225] which could influence the reported results. SIRT3, while found to be dispensable for maintenance of HSCs and homeostasis of tissues during young age, was reported to be essential following stress and with the aging process [226]. SIRT3 expression was decreased with aging and upregulation of SIRT3 expression in HSCs of old mice improved their regenerative capacity, effects involving a role for mitochondrial homeostasis [226]. As noted above in Section E, SIRT7 in the mitochondrial unfolded protein response and aging-associated changes in HSCs in the old mice were linked [152]. This was discussed more thoroughly in a short commentary [227].

G) The Microbiome, Hematopoiesis, and Aging

The microbiome describes microorganisms such as bacteria, viruses, and fungi that colonize the human and animal body and influence various biological processes. Most studies that explored microbiome–hematopoiesis interactions are based on characterizing HSC and HPC populations in germ-free (GF) or broad-spectrum antibiotic-treated mice and in human subjects under prolonged antibiotic regimens or diagnosed with gut dysbiosis such as inflammatory bowel syndrome [228–230]. GF mice demonstrated myelosuppression, smaller HSC, MPP, and common lymphoid progenitor (CLP) populations, and impaired neutrophils, monocytes, and T-cell functions. Recolonization of GF mice restored immune response to infection [96, 228, 231]. However, a closer evaluation of HSCs and HPCs in oral antibiotic-treated mice revealed normal HSC and HPC populations but reduced mature T cell, B cell, and granulocyte populations, suggesting impaired differentiation of mature immune cells in microbiota-depleted mice

after oral antibiotics treatment and introduced some discrepancies between animal models used to study the microbiome [232]. Following HCT, microbiota-depleted recipient mice immune reconstitution was significantly lower than their control counterparts [232] supporting the conclusion that the microbiome plays a role in regulating mature immune cell development. Several studies have linked the human gut microbiome imbalance or dysbiosis in conditions such as inflammatory bowel syndrome, malnutrition, and obesity to altered hematopoiesis [229].

The microbiome and hematopoiesis have been intimately linked [233–238]. Gut microbiota are known to sustain hematopoiesis [233], microbiota can regulate HSC differentiation by altering the BM niche [234], and CX3CR1⁺ mononuclear cells influence HPCs [235]. Reduced mPB is noted in mice receiving antibiotics [236] and microbiota modification has been discussed in context of hematology [237]. Moreover, gut microbiota are known to control bacterial infection by promoting hematopoiesis [238], but definitive and rigorous comparative studies on a role of the microbiome on hematopoiesis in the young and old are yet to be done.

Bacteria and the microbiome present a not uncomplicated scenario that has not been adequately addressed in context of aged hematopoiesis and this needs adequate attention. Certain bacteria, using that of *Fusobacterium nucleatum* as an example, have been implicated in enhancing metastasis of cancer cells [239–248]. If such bacteria have this capacity for cancer cell metastasis, then why not for HSC and HPC, migration and/or homing an area worthy of investigation.

Up to 15% of patients with a history of prolonged antibiotic use have suffered hematological adverse effects in the form of neutropenia, anemia, and pancytopenia [249, 250]. Although associations between the hematopoietic system and microbiota imbalance is apparent in mice and humans, mechanistic understanding of this interaction is limited. In the signal transducer and activator of transcription protein 1 (STAT1) knockout mouse, the antibiotic effects on HSC and HPC numbers were abrogated [96]. In another report, administering a ligand of the pathogen recognition receptor 1 (NOD1) restored HSC and HPC numbers in GF mice [251]. To the authors' knowledge, aged-HSC and HPC function and phenotyping in relation to the microbiome have not yet been reported in mice or humans. Aging is associated with perturbation of intestinal epithelial integrity and upregulation of permeability, allowing microbiota entrance to the circulation and induces a chronic inflammatory state in the aged subject. Aging results in microbiota-associated increases in pro-inflammatory cytokine levels (e.g., TNF- α , TGF- β , IL-6, etc), changes in T-cell numbers (e.g., Treg, Th1, and Th2 T-cell subsets), and activation of TLR2, NF- κ B and mTOR [252]. Considering how the well-characterized low-grade, chronic inflammation associated with aging affects the hematopoietic system, a role for microbiota promoting such inflammation is a strong

possibility. How this might regulate hematopoiesis in the young and old remains an unexplored area to be better studied in steady- and stressed-states.

H) Additional Age-Related Information and Means to Better Evaluate/Understand Hematopoiesis During Aging

Role of Collection/Processing of Cells

Many studies have acknowledged the probable effects of oxidative stress on functional changes in stem cells during aging [253]. This oxidative stress is associated with damage to macromolecules including that of nucleic acids, proteins, lipids, and carbohydrates that could contribute to changes in HSC function. This however, did not consider how even the mere removing of HSC-containing populations of cells from mouse BM [40], mouse mobilized peripheral blood (mPB) [42], or human cord blood [40] could so quickly change HSC numbers and impinge on the function of the removed HSCs. As previously mentioned, collecting and processing cells under ambient air conditions for as little as 15 minutes exposes the cells to extra physiological oxygen stress/shock or EPHOSS. EPHOSS is associated with increased differentiation of HSCs to HPCs through a sequence of events involving p53, the opening of the mitochondrial permeability transition pore, cyclophilin D, hypoxia inducing factor (HIF)1- α and the hypoxamir, miR210 [40, 41]. By collecting and processing BM and mPB from mice and cord blood from humans in a hypoxic chamber set at 3% O₂ and taking care to make sure that the cells are never exposed to ambient air conditions, it is possible to obtain many more phenotyped and functional HSCs [40–42]. Increased numbers of collected HSCs under hypoxia has also been reported for BM cells from *Fanca*^{-/-} and *Fancc*^{-/-} mice [254]. It is possible that some of the EPHOSS-related effects on HSCs exposed to ambient air can be compensated for by collection and processing of these cells at ~4°C [255]. Such cold collections and processing of human cord blood and mouse BM cells mimic at least some of the effects seen during hypoxia collection/processing of cells including increased numbers of collected HSCs. However, the mechanisms involved with preserving HSC numbers/function following cold collection/processing of cord blood cells have not yet been worked out and may differ somewhat from that of physioxia/hypoxia collected/processed cell populations.

Collecting/processing BM cells from old vs. young mice under different oxygen tensions [1], allowed us to demonstrate that functional engrafting HSCs from old mouse BM collected/processed at 3% O₂ were equal in number to that of ambient air (~21% O₂) collected/processed young mouse BM HSCs. Perhaps more importantly, the abnormal myeloid to lymphoid ratio seen when aged BM cells were engrafted into lethally

irradiated recipient mice in a competitive transplant setting was not noticeable and completely resembled that seen after engraftment of young mouse BM. This was consistent with increased CLP numbers and decreased CMP and GMP numbers in the donor BM from old mice following their collection in hypoxia. These phenomena seen with old BM HSCs collected/processed in hypoxia, were associated with decreased total and mitochondria ROS, and decreased expression of stress-induced proteins [1]. Hence, aged mouse BM HSC function may not be as dysregulated as many others have reported, with differences perhaps due to their increased response to EPHOSS following *ex vivo* analysis in ambient air. A corollary of this may suggest that with the more physiological collection and processing of HSCs (a.k.a. in hypoxia conditions, or by means of a physiological strategy (e.g. collecting cells in the cold [255]) from BM of older individuals may be more functional in context of clinical HCT than if they were collected/processed as usual in ambient air O₂. It is known that there are distinct populations of even rigorously purified populations of HSCs [1, 256]. Which of these HSC populations survive EPHOSS effects when cells are collected/processed in ambient air from young and old mouse BM remains to be better elucidated. While much more obviously needs to be done to more mechanistically and physiologically understand the true state of HSCs isolated from older human individuals or mice, it may be that much of the literature on aged HSCs needs to be re-evaluated for their functional status as they are within their *in vivo* physioxia microenvironment. Studies to be done with hypoxia vs. ambient collected HSCs include more in-depth intracellular events and signaling pathways that include gene and protein expression profiles, as well as epigenetic changes, work currently ongoing.

Molecular chaperones and heat shock responses have been postulated to play a role in longevity and aging [257], but rigorous studies in the area of aged HSCs are lacking. Age and organ specific differences in bioenergetics in Brown Norway rats have been noted [258], and p53 deficiency induces diverse dysregulated processes under physiological oxygen/physioxia [259], but we know that such events are influenced by modes of cell collection and processing [40, 41].

The Microenvironment

Not to be ignored in studies of aged HSCs is the role that their microenvironment *in vivo* plays in the functional cellular and intracellular abnormalities/defects associated with their engrafting deficiencies and biased differentiation patterns. The microenvironment niche for HSCs has been studied for young mice [260], but more in-depth studies of the aged BM microenvironment is warranted, especially in context of oxygen content [260], as we noted [1]. There is a report of the rejuvenation of progenitors from old mice when placed into and exposed to a young BM environment [261], and a more

recent report demonstrated that degeneration of adrenergic nerves in BM affects aging of the HSC niche [262], and that aging in humans alters the special organization between populations of CD34⁺ cells (contains mainly HPCs, but also a small percentage of HSCs) and adipocytes in the BM [263]; this is of potential relevance as increased adiposity is associated with the aged BM microenvironment and can alter the functionality of surrounding cells. MSCs showed aging related expression of *cxc4* [264], a “homing” HSC/HPC receptor, but this has not yet been evaluated under conditions of hypoxia collection and processing such as in [40, 41].

Leptin (Lep) and Lep Receptors (R)

Metabolic activities of cells are adaptively regulated by systemic signals that reflect the nutritional status of an organism throughout its life [265, 266]. This is particularly crucial in the case of HSCs as they are rare, and they maintain the integrity of the entire hematopoietic organ system. One way that the body communicates nutritional cues to HSCs is via systemic hormonal regulations. Various metabolic hormones have been documented to influence hematopoiesis, and aging can significantly alter these metabolic messengers, hence indirectly affecting HSC functional behavior [267–269].

Among them, leptin controls the body energy expenditure and storage through both central and peripheral mechanisms [270]. As an adipokine, it is recognized to have broad spectrum effects on numbers and functions of different immune cells under homeostasis [271]. Aging is known to be associated with multiple dysregulations of the immune system, including a declined adaptive immune response [272]. Lep induces gene expression of p16, a marker of cellular immunosenescence in human B cells from young lean adults. These cells also exhibited lowered class switching activity and ability to produce influenza-specific IgG [273, 274]. Unfortunately, the study was limited to *in vitro* treatment only and did not provide full mechanistic insights. In line with this finding, it was demonstrated that lep induced significantly higher levels of IL-10, TNF- α , and IL-6 from aged human B cells as compared to young controls, and this effect was mediated through the STAT3 signaling pathway downstream of lepR activation [275]. Another group reported that sustainably higher lep levels were found in LPS-treated older (24 month) compared to young (2 month) rats, and the old rats showed delayed but longer febrile response. Elevated lep concentrations were accompanied by increased levels of pro-inflammatory cytokines including IL-6 and IL-1R α ; however, it was not determined whether the increase in lep level was causative and how [276]. Although lep signaling was consistently reported to be altered in aged animals, more rigorously designed studies are needed to help us understand how this well-known proinflammatory neuroendocrine adipokine may play any roles in aging-associated immunological changes [277, 278].

Beyond its role in immunity, lepR-expressing MSCs in murine hematopoiesis have been well-characterized as an indispensable source of stem cell factor for maintenance of both HSCs and more differentiated progenitor cells [279–282]. In addition, it has been demonstrated that BM adipose tissue possessed brown fat properties that declined in old or diabetic mice [283]. It was demonstrated that during the process of aging or in obesity, MSCs preferentially differentiated into adipocytes, which impaired hematopoietic recovery [284]. Since BM adipocytes could be a potential source of lep, it is important to know how BM adipocyte-derived lep can directly or indirectly alter hematopoiesis as the animal ages. In the context of HSC biology, we recently discovered that Lepr marks a small subset of robustly repopulating and self-renewing long-term HSCs in adult murine BM; Lepr⁺ HSCs (defined as LSKCD150⁺CD48⁻) were found to generate equal myeloid-lymphoid outputs as compared to Lepr⁻ HSCs [285]. Given that lep (OB-R) was also reported to be expressed by different types of both myeloid and lymphoid leukemic cells [286–289], it will be intriguing and important to determine whether aging has a differential selection pressure on Lepr⁺ HSCs as compared to the rest of total BM HSCs, particularly in the context of clonal hematopoiesis. Although RNA-seq data suggested that Lepr⁺ HSCs and Lepr⁺ MPPs (defined as LSKCD150⁻CD48⁻) predominantly expressed the truncated short isoforms *OB-Ra* and *OB-Rc*, it remains to be determined whether aged HSCs or leukemic cells can express the long functional isoform *OB-Rb* (*LepR*). Future studies with more mechanistic insight should be able to address these questions, perhaps providing potential meaningful clinical implications.

More on Inflammation

Aging-related inflammation promoted aging characteristics of HSCs through a tumor necrosis (TNF)- α , ERK, ETS1, IL-27 receptor (R) pathway [290]. TNF- α increases during aging and induced expression of HSC IL-27R- α by ERK-ETS-1 intracellular signaling, with deletion of IL-27R- α rescuing functional decline and myeloid bias of HSCs. Old IL-27R- α knockout mice had reduced proportions of myeloid-biased HSCs. Thus, this is another report implicating factors external to HSCs that effect the functional capacity of HSCs from old mice. Somatotrophic/Insulin-Like Growth Factor has also been implicated in aging effects on stem cells as well, in these cases on a population of very small embryonic like stem cells [291, 292].

Exosomes

Exosomes are a subset of small extracellular vesicles that range in size from 30–150nm, that are produced by normal and malignant cells [293, 294], originate from the endocytic compartment of producer cells [295], and have emerged as a

universal intercellular communication system [296, 297]. Exosomes are in a protective protein/lipid bilayer, are delivered to recipient cells without degradation, and freely cross biological barriers [296, 297]. Exosomes [298] influence proliferation of HPCs [299], but there is no information on effects of exosomes on HSCs and HPCs during aging.

Biological Time Keeping and Circadian Rhythms

Biological time keeping [300] and circadian variations are known to influence numbers of HSCs and HPCs in BM and blood, but how this might occur in old mice has not yet been explored. Such studies may be of interest, based on when it is best to collect HSCs and HPCs from older individuals from BM and mPB for use in HCT. Studies of circadian deep sequencing revealed stress-response genes that adapted to high rhythmic expression during aging [301], and daily onset of light and darkness have been reported to manifest control over HSC maintenance and differentiation [302]. Moreover, circadian host and microbiome interactions have been suggested to play relevant roles [303]. There is a noted sexual dimorphism in body clock regulation [304] which has not been adequately addressed, especially in context of aging, and aged HSCs and HPCs.

HSC homing to the BM plays an important role in the engrafting capability of the HSCs [305], and more consideration needs to be given to this capacity of aged HSCs. There are a number of means to enhance the homing of HSCs for enhanced engraftment [306–309], but these have not yet been evaluated in context of HSCs from old mice, or when cells are collected/processed in hypoxia vs. ambient air. Notably, there are a number of animal models to study aging, with an example being the Ames hypopituitary dwarf mice [7–10], that live approximately two times longer than that of most other mice. Imbalanced myelopoiesis was noted in myelopoiesis between BM and spleen in Ames dwarf mice [310].

I) COVID-19/SARS-CoV-2, Aging, and Hematopoiesis

Severe Acute Respiratory Syndrome Coronavirus 2 (SARS-CoV-2) is the pathogen responsible for causing Coronavirus Disease 2019 (COVID-19), a disease which has spread worldwide, infected over 32 million people and claimed the lives of nearly 1 million people as of September 2020 [311]. SARS-CoV-2 is a virus which infects cells by binding to cell surface proteins via its Spike protein that extends out from the viral envelope, facilitating entry to the host cell and allowing for viral replication within the cell [312–314]. The most well-studied presentation of COVID-19 is an infection of the lungs, with symptoms ranging from a mild cough and fever to a severe pneumonia [315, 316].

The prognosis and severity of COVID-19 in patients appears strongly tied to the age of the patient [317]. The risk for SARS-CoV-2 infection leading to symptomatic disease rises dramatically with age. According to the Center for Disease Control (CDC), as age increases the likelihood of being hospitalized for COVID-19 increases, with adults over 65 having 5–13x higher hospitalization rate [318]. Older people are, as presently known, also more likely to die from the disease, with a 90–630x higher death rate in patients over 65 [318], although it is likely that the full story on this is not yet known. This is not likely due to older people being more susceptible to infection, as RT-PCR tests for the presence of SARS-CoV-2 in mild to moderate cases of COVID-19 demonstrate that the host cells of younger patients contain more viral RNA than older patients [319]. A potential interpretation of this is that a higher viral load is necessary for younger people to display symptoms compared to older people. This suggests that children are equally likely to be infected, but may be less likely to display symptoms of the disease, likely due to a general lack of additional contributing factors, possibly including a predisposition to hematologic disorders.

Understandably, many studies of SARS-CoV-2 have focused on its infection of and impact on the lungs. However, it has become increasingly evident that COVID-19 is systemic in nature [320], affecting many different systems including primitive and mature hematopoietic cells [317, 321–324]. The impact that the disease has on the hematopoietic system is evident in the hematological manifestations of COVID-19. A review looking at hematological factors in COVID-19 patients found that both lymphocytopenia and thrombocytopenia are common symptoms with hospitalized patients [322]. It is also evident that more severe cases of COVID-19 were more frequently associated with these hematological factors [322]. Further, one of the more devastating effects of SARS-CoV-2 infection is the induction of a "cytokine storm" [325, 326]. Cytokine storm refers to a toxic excessive release of immune cytokines leading to an autoimmune response. Thus, there is a strong need to address the mechanisms and effects of SARS-CoV-2 exposure on primitive and mature hematopoietic cells and the impact it may have for COVID-19 patients, especially in older individuals.

Recently it was demonstrated that ACE2 is expressed on the cell surface of small numbers of HPCs and mature immune cells [324] and moderate to large numbers of HSCs [323, 324]. Importantly, exposure of human HSCs to SARS-CoV-2 Spike protein induces increases in expression of inflammatory molecules such as *NLRP3* and *IL-1beta* [323], indicating that the cytokine storm may be mediated in part through primitive hematopoietic cells. Further, human HSCs and HPCs exposed to Spike protein *ex vivo* have decreased capacity for functional HPC colony formation, exhibit decreased cell growth, and decreased expansion of HSCs, HPCs, and functional HPC colony forming units compared to cells that were unexposed to the

viral protein [324]. These effects can be neutralized by co-treatment with Angiotensin1-7 [323, 324], a peptide linked to ACE2 regulation of hypertension [327]. The effects of the SARS-CoV-2 Spike protein on colony forming capacity and expansion can also be neutralized by treatment with an antibody targeting SARS-CoV-2 Spike protein or by treatment with soluble human ACE2 [324]. Human peripheral blood mature immune cells also exhibit a response to exposure to Spike protein *ex vivo*, with monocytes upregulating CD14 and undergoing aberrant changes in morphology [324]. It is clear that SARS-CoV-2 does not have to infect HSCs and HPCs to cause some of the above noted effects of the SARS-CoV-2 Spike protein [323, 324]. These, and that yet to be reported, data are important because they may help to explain the origin of hematological manifestations of COVID-19 such as lymphocytopenia and thrombocytopenia and provide insight into neutralizing these effects on the hematopoietic system.

It is very possible that one of the contributing factors to COVID-19 disease severity in the aged population is due to the impact of the disease on a hematopoietic system that has already been accumulating alterations and damage for many years. Additionally, effects of cytokine storm associated inflammation may further damage aged hematopoietic cells, possibly making them even more vulnerable to the development of hematological disorders even after recovery from COVID-19. The relationships between hematologic manifestations of COVID-19 and age should be further studied, as should the effects of SARS-CoV-2 exposure on HSC/HPC and mature immune cells from the aged versus young. It will also be important to determine whether the hematological manifestations of COVID-19 may be neutralized by specifically targeting the effects on the hematopoietic system, thus potentially relieving some of the disease burden on more severely affected patients, including older patients.

J) Conclusions in Context of Potential Future Intervention for Better Health of the Hematopoietic System During Aging

A number of studies have reviewed the aging process in general including protein sequestration at the nuclear periphery, and pathways of cellular proteostasis, the effects of aging on stem cell populations, and potential therapeutic interventions including that for aged HSCs [328–334]. Organoids have been suggested as experimental means to study the process of cellular aging [335], but much more rigorous work is needed in this area, especially with analysis *ex vivo* of HSCs in a relevant physioxia microenvironment BM niche model.

It has been noted that there are molecules in aged blood that promote the spread of cancer [336] and the accumulation of methylmalonic acid promotes tumor progression in the aged

[337]. How these phenomenon relate to HSC, HPC, and hematopoiesis and pre-leukemia and leukemia, and to effects on cells collected in hypoxia/physioxia remains to be determined. A recent book [338] has described the aging process from the perspective of a long-time investigator in this field and noted the mTOR, AMPK and sirtuin pathways as main longevity signaling pathways.

Other considerations in context of aging and hematopoiesis to be elucidated are: how mitochondrial ROS acts as a double-edged conundrum for that of host defense in contrast to infection associated pathological inflammation [339] and its effects on HSC and HPC [340]. More in-depth insights can be gained from approaches incorporating single cell multiomics [341] and what role the mechanoregulation [342] of hematopoiesis might play during aging and disorders associated with aging. There is also the question of a role for mitochondrial transfer from Cx43-expressing HPC to stroma [343] during aging of the hematopoietic system and its interaction with the bone marrow microenvironment during regeneration. As noted in more recent reviews on CHIP [344–346], there is still much we do not understand about this phenomenon and its relationship to aging and aged hematopoiesis.

Cytokines, Chemokines and Intracellular Signaling

HSCs, HPCs, and hematopoiesis are regulated by numerous interacting cytokines and chemokines [347], effects mediated by receptor-induced intracellular signaling [348; Broxmeyer; submitted solicited review on Cytokines/Chemokines/Other Growth Regulators and their Receptors, 8th Edition, Hematology: Basic Principles and Practice, Eds. R. Hoffman, et. al., 2020). Some recent intracellular players involved in HSC and HPC function have been reported [307–309, 349, 350]. However, all such intracellular signaling events have been carried out with HSCs, HPCs, and immune cells of young mice, or human CB or human BM or mPB from younger individuals. Whether or not such regulatory intracellular signaling is similar in cells from old vs. the young remains to be determined, and such studies need to be assessed with purified populations of HSCs and HPCs, and in context of such cells isolated and processed under physioxia conditions, so that they are not exposed to ambient air oxygen which will likely modify the signaling events.

Dipeptidylpeptidase (DPP)4

We had noted that it may be feasible to use HSCs from older individuals for hematopoietic cell transplantation (HCT) if the cells are collected so that they are not induced by EPHOSS to decrease HSC numbers [1] when stressed by ambient air collection [40–42], but are there means to decrease the acute GVHD associated with allogeneic HCT, which perhaps has the potential to be more aggressive when donor cells are from

more aged individuals? Inhibition of the enzyme dipeptidylpeptidase (DPP)4/CD26 has been shown to enhance mouse BM HCT and to accelerate recovery after radiation and selected chemotherapeutic drugs [351, 352] and to enhance time to engraftment of cord blood (CB) HCT [353–355]. This enhancement in time to neutrophil engraftment was also associated with a decrease in the already low acute GVHD noted for CB HCT [356]. It is now clear that the orally active DPP4 inhibitor, sitagliptin used in the CB Trials also greatly dampens acute GVHD in the setting of clinical mPB HCT [357]. Hence, there may be a role for DPP4 inhibitors such as sitagliptin in context of aged hematopoiesis and HCT. DPP4 has also been implicated in exosomes from patients with acute myeloid leukemia [299]. More in depth information on DPP4 during the aging process is clearly warranted. There are many proteins that have purported DPP4-truncation sites [358, 359]. This is of relevance as DPP4-truncated proteins can have decreased activity and block the effects of the full length molecules [352, 360]. Hence, a better undertaking of DPP4 on hematopoiesis in the old, as well as young, could uncover additional means to enhance hematopoiesis during health, aging and disease.

Concluding Thoughts

There are still many unknowns, and still to be elucidated mechanistic insights to understand changes in hematopoiesis during aging. Enhanced genomics may provide additional clues to age-related hematopoiesis [361]. Some of these areas for further investigation are noted in Table 1. It will likely take

Table 1 Suggested areas of investigation requiring more thorough and rigorous analysis to better understand HSC and HPC function and hematopoiesis during the aging process

Listing [In context of physioxia (<i>in vivo</i> microenvironmental hypoxia) Collection and Processing Analysis [1, 40–42, 254] or perhaps non-physiological cold collection and processing [255] using purified subset populations of HSCs, HPCs, stromal and accessory cells]:
• Cytokine, chemokine and other growth regulatory factors, and their receptor-mediated intracellular signaling events
• Role for the enzyme dipeptidylpeptidase (DPP)4/CD26 and perhaps other enzymes for modifying protein actions
• Gene Expression
• Epigenetics
• Age-Related Clinal Hematopoiesis of Indeterminant Potential (CHIP), Preleukemia (MDS, MPN), Leukemia
• Metabolism, mitochondria, ROS, apoptosis, autophagy, mitophagy
• Microenvironmental and accessory cells
• Inflammation
• Microbiome

Legend: This is not meant to be a complete listing but a start on areas needing further investigation.

a multidisciplinary approach to fully understand the causes of abnormalities associated with the aging process, not only of the hematopoietic system. This information might at least partially control what might not be the inevitable consequences of the time- and disease-induced aging process. Future studies of hematopoiesis and HSCs during the aging process that investigate these processes in context of their status in an *in vivo*/physioxia environment, and *ex-vivo* under conditions that more closely mimic their *in vivo* condition of O₂ tension and with microenvironmental niche cell interactions [362] will bring us closer to better understanding aged HSCs and what their true functional capacities and abnormalities are. Only with this enhanced understanding can we truly know how this information can best be used and better modified, if necessary and possible, for health benefit.

Acknowledgements Some of the studies reported in this review, and the writing of this review were supported by the following U.S. Public Health Grants from the National Institutes of Health to H.E.B.: R35 HL139599 (Outstanding Investigator Award), R01 DK109188, U54 DK106846; A.A., J.P.R., and T.T. were supported by T32 DK007519 to H.E.B. R01 HL150624, R56 DK119524, R56 AG052501, DoD W81XWH-13-1-0187, DoD W81XWH-18-1-0265 and DoD W81XWH-19-1-0575, the Leukemia and Lymphoma Society Translational Research Program award 6581-20 and the St. Baldrick's Foundation Scholar Award to Y.L. MLC was supported by R01 DK109188. CO was supported by National Institute of Allergy and Infectious Diseases (NIAID) contracts HHSN266200500043C and HHSN272201000046C and grants 1U01AI107340-01 and 2R44 AI088288-03A1, National Institute on Aging (NIA) grant R01AG046246-01, and Department of Defense grants PR140896, PR141527, and PR140433P1.

References

1. Capitano, M. L., Mohamad, S. F., Cooper, S., Guo, B., Huang, X., Gunawan, A. M., Sampson, C., Ropa, J., Srour, E. F., Orschell, C. M., & Broxmeyer, H.E. (2020). Mitigating oxygen stress enhances aged mouse hematopoietic stem cell numbers and function. *Journal of Clinical Investigation*. In Press.
2. Kirkwood, T. B. (2005). Understanding the odd science of aging. *Cell*, 120(4), 437–447. <https://doi.org/10.1016/j.cell.2005.01.027>.
3. Kenyon, C. (2005). The plasticity of aging: insights from long-lived mutants. *Cell*, 120(4), 449–460. <https://doi.org/10.1016/j.cell.2005.02.002>.
4. Chien, K. R., & Karsenty, G. (2005). Longevity and lineages: toward the integrative biology of degenerative diseases in heart, muscle, and bone. *Cell*, 120(4), 533–544. <https://doi.org/10.1016/j.cell.2005.02.006>.
5. Campisi, J. (2005). Senescent cells, tumor suppression, and organismal aging: good citizens, bad neighbors. *Cell*, 120(4), 513–522. <https://doi.org/10.1016/j.cell.2005.02.003>.
6. Singh, P. P., Demmitt, B. A., Nath, R. D., & Brunet, A. (2019). The genetics of aging: a vertebrate perspective. *Cell*, 177(1), 200–220. <https://doi.org/10.1016/j.cell.2019.02.038>.
7. Bartke, A. (2000). Delayed aging in Ames dwarf mice. Relationships to endocrine function and body size. Results and problems in cell differentiation, 29, 181–202. https://doi.org/10.1007/978-3-540-48003-7_10.
8. Bartke, A., Coschigano, K., Kopchick, J., Chandrashekar, V., Mattison, J., Kinney, B., & Hauck, S. (2001). Genes that prolong

- life: relationships of growth hormone and growth to aging and life span. *The Journals of gerontology. Series A, Biological Sciences and Medical Sciences*, 56(8), B340–B349. <https://doi.org/10.1093/gerona/56.8.b340>.
9. Brown-Borg, H. M., Borg, K. E., Meliska, C. J., & Bartke, A. (1996). Dwarf mice and the ageing process. *Nature*, 384(6604), 33. <https://doi.org/10.1038/384033a0>.
 10. Bartke, A. (1964). Histology of the anterior hypophysis, thyroid and gonads of two types of dwarf mice. *The Anatomical Record*, 149, 225–235. <https://doi.org/10.1002/ar.1091490206>.
 11. Shahrestani, P. (2012). Aging: an evolutionarily derived condition. *Frontiers in Genetics*, 3, 187. <https://doi.org/10.3389/fgene.2012.00187>.
 12. Keyes, B. E., & Fuchs, E. (2018). Stem cells: aging and transcriptional fingerprints. *The Journal of Cell Biology*, 217(1), 79–92. <https://doi.org/10.1083/jcb.201708099>.
 13. Sharpless, N. E., & DePinho, R. A. (2007). How stem cells age and why this makes us grow old. *Nature reviews. Molecular Cell Biology*, 8(9), 703–713. <https://doi.org/10.1038/nrm2241>.
 14. Rossi, D. J., Bryder, D., Zahn, J. M., Ahlenius, H., Sonu, R., Wagers, A. J., & Weissman, I. L. (2005). Cell intrinsic alterations underlie hematopoietic stem cell aging. *Proceedings of the National Academy of Sciences of the United States of America*, 102(26), 9194–9199. <https://doi.org/10.1073/pnas.0503280102>.
 15. Cho, R. H., Sieburg, H. B., & Muller-Sieburg, C. E. (2008). A new mechanism for the aging of hematopoietic stem cells: aging changes the clonal composition of the stem cell compartment but not individual stem cells. *Blood*, 111(12), 5553–5561. <https://doi.org/10.1182/blood-2007-11-123547>.
 16. Signer, R. A., Montecino-Rodriguez, E., Witte, O. N., McLaughlin, J., & Dorshkind, K. (2007). Age-related defects in B lymphopoiesis underlie the myeloid dominance of adult leukemia. *Blood*, 110(6), 1831–1839. <https://doi.org/10.1182/blood-2007-01-069401>.
 17. Miller, J. P., & Allman, D. (2005). Linking age-related defects in B lymphopoiesis to the aging of hematopoietic stem cells. *Seminars in Immunology*, 17(5), 321–329. <https://doi.org/10.1016/j.smim.2005.05.003>.
 18. Liang, Y., Van Zant, G., & Szilvassy, S. J. (2005). Effects of aging on the homing and engraftment of murine hematopoietic stem and progenitor cells. *Blood*, 106(4), 1479–1487. <https://doi.org/10.1182/blood-2004-11-4282>.
 19. Xing, Z., Ryan, M. A., Daria, D., Nattamai, K. J., Van Zant, G., Wang, L., Zheng, Y., & Geiger, H. (2006). Increased hematopoietic stem cell mobilization in aged mice. *Blood*, 108(7), 2190–2197. <https://doi.org/10.1182/blood-2005-12-010272>.
 20. Warren, L. A., & Rossi, D. J. (2009). Stem cells and aging in the hematopoietic system. *Mechanisms of Ageing and Development*, 130(1–2), 46–53. <https://doi.org/10.1016/j.mad.2008.03.010>.
 21. Beerman, I., Maloney, W. J., Weissman, I. L., & Rossi, D. J. (2010). Stem cells and the aging hematopoietic system. *Current Opinion in Immunology*, 22(4), 500–506. <https://doi.org/10.1016/j.coi.2010.06.007>.
 22. Kuranda, K., Vargaftig, J., de la Rochere, P., Dosquet, C., Charron, D., Bardin, F., Tonnel, C., Bonnet, D., & Goodhardt, M. (2011). Age-related changes in human hematopoietic stem/progenitor cells. *Aging Cell*, 10(3), 542–546. <https://doi.org/10.1111/j.1474-9726.2011.00675.x>.
 23. Dykstra, B., Olthof, S., Schreuder, J., Ritsema, M., & de Haan, G. (2011). Clonal analysis reveals multiple functional defects of aged murine hematopoietic stem cells. *The Journal of Experimental Medicine*, 208(13), 2691–2703. <https://doi.org/10.1084/jem.20111490>.
 24. Pang, W. W., Price, E. A., Sahoo, D., Beerman, I., Maloney, W. J., Rossi, D. J., Schrier, S. L., & Weissman, I. L. (2011). Human bone marrow hematopoietic stem cells are increased in frequency and myeloid-biased with age. *Proceedings of the National Academy of Sciences of the United States of America*, 108(50), 20012–20017. <https://doi.org/10.1073/pnas.1116110108>.
 25. Yu, K. R., Espinoza, D. A., Wu, C., Truitt, L., Shin, T. H., Chen, S., Fan, X., Yabe, I. M., Panch, S., Hong, S. G., Koelle, S., Lu, R., Bonifacino, A., Krouse, A., Metzger, M., Donahue, R. E., & Dunbar, C. E. (2018). The impact of aging on primate hematopoiesis as interrogated by clonal tracking. *Blood*, 131(11), 1195–1205. <https://doi.org/10.1182/blood-2017-08-802033>.
 26. Di Micco, R., & Montini, E. (2018). De(bar)coding aged hematopoiesis in primates. *Blood*, 131(11), 1157–1159. <https://doi.org/10.1182/blood-2018-02-826412>.
 27. Pietras, E. M., Reynaud, D., Kang, Y. A., Carlin, D., Calero-Nieto, F. J., Leavitt, A. D., Stuart, J. M., Göttgens, B., & Passegué, E. (2015). Functionally distinct subsets of lineage-biased multipotent progenitors control blood production in normal and regenerative conditions. *Cell Stem Cell*, 17(1), 35–46. <https://doi.org/10.1016/j.stem.2015.05.003>.
 28. Young, K., Borikar, S., Bell, R., Kuffler, L., Philip, V., & Trowbridge, J. J. (2016). Progressive alterations in multipotent hematopoietic progenitors underlie lymphoid cell loss in aging. *The Journal of Experimental Medicine*, 213(11), 2259–2267. <https://doi.org/10.1084/jem.20160168>.
 29. Busque, L., Buscarlet, M., Mollica, L., & Levine, R. L. (2018). Concise review: age-related clonal hematopoiesis: stem cells tempting the devil. *Stem Cells (Dayton, Ohio)*, 36(9), 1287–1294. <https://doi.org/10.1002/stem.2845>.
 30. Wahlestedt, M., & Bryder, D. (2017). The slippery slope of hematopoietic stem cell aging. *Experimental Hematology*, 56, 1–6. <https://doi.org/10.1016/j.exphem.2017.09.008>.
 31. de Haan, G., & Lazare, S. S. (2018). Aging of hematopoietic stem cells. *Blood*, 131(5), 479–487. <https://doi.org/10.1182/blood-2017-06-746412>.
 32. Stauder, R., Valent, P., & Theurl, I. (2018). Anemia at older age: etiologies, clinical implications, and management. *Blood*, 131(5), 505–514. <https://doi.org/10.1182/blood-2017-07-746446>.
 33. Leins, H., Mulaw, M., Eiwien, K., Sakk, V., Liang, Y., Denking, M., Geiger, H., & Schirmbeck, R. (2018). Aged murine hematopoietic stem cells drive aging-associated immune remodeling. *Blood*, 132(6), 565–576. <https://doi.org/10.1182/blood-2018-02-831065>.
 34. Ganuza, M., Hall, T., Finkelstein, D., Wang, Y. D., Chabot, A., Kang, G., Bi, W., Wu, G., & McKinney-Freeman, S. (2019). The global clonal complexity of the murine blood system declines throughout life and after serial transplantation. *Blood*, 133(18), 1927–1942. <https://doi.org/10.1182/blood-2018-09-873059>.
 35. Van Zant, G., & Liang, Y. (2012). Concise review: hematopoietic stem cell aging, life span, and transplantation. *Stem Cells Translational Medicine*, 1(9), 651–657. <https://doi.org/10.5966/sctm.2012-0033>.
 36. Geiger, H., de Haan, G., & Florian, M. C. (2013). The ageing haematopoietic stem cell compartment. *Nature Reviews Immunology*, 13(5), 376–389. <https://doi.org/10.1038/nri3433>.
 37. Cupit-Link, M. C., Arora, M., Wood, W. A., & Hashmi, S. K. (2018). Relationship between aging and hematopoietic cell transplantation. *Biology of Blood and Marrow Transplantation: Journal of the American Society for Blood and Marrow Transplantation*, 24(10), 1965–1970. <https://doi.org/10.1016/j.bbmt.2018.08.015>.
 38. Cooper, S. H., Broxmeyer, H. E., & Capitano, M. L. (2020). Experimental mouse models of mouse and human hematopoietic stem cell transplantation. In L. M. Pelus & J. Hoggatt (Eds.), *Methods in molecular biology: Hematopoietic stem cells*. New York: Springer Nature In Press.
 39. Broxmeyer, H. E., Orschell, C. M., Clapp, D. W., Hangoc, G., Cooper, S., Plett, P. A., Liles, W. C., Li, X., Graham-Evans, B.,

- Campbell, T. B., Calandra, G., Bridger, G., Dale, D. C., & Srour, E. F. (2005). Rapid mobilization of murine and human hematopoietic stem and progenitor cells with AMD3100, a CXCR4 antagonist. *The Journal of Experimental Medicine*, 201(8), 1307–1318. <https://doi.org/10.1084/jem.20041385>.
40. Mantel, C. R., O'Leary, H. A., Chitteti, B. R., Huang, X., Cooper, S., Hangoc, G., Brustovetsky, N., Srour, E. F., Lee, M. R., Messina-Graham, S., Haas, D. M., Falah, N., Kapur, R., Pelus, L. M., Bardeesy, N., Fitamant, J., Ivan, M., Kim, K. S., & Broxmeyer, H. E. (2015). Enhancing hematopoietic stem cell transplantation efficacy by mitigating oxygen shock. *Cell*, 161(7), 1553–1565. <https://doi.org/10.1016/j.cell.2015.04.054>.
 41. Broxmeyer, H. E., O'Leary, H. A., Huang, X., & Mantel, C. (2015). The importance of hypoxia and extra physiologic oxygen shock/stress for collection and processing of stem and progenitor cells to understand true physiology/pathology of these cells ex vivo. *Current Opinion in Hematology*, 22(4), 273–278. <https://doi.org/10.1097/MOH.0000000000000144>.
 42. Aljoufi, A., Cooper, S., & Broxmeyer, H.E. (2020). Collection and processing of mobilized mouse peripheral blood at lowered oxygen tension yields enhanced numbers of hematopoietic stem cells. *Stem Cell Reviews and Reports*. In Press.
 43. Burns, S. S., & Kapur, R. (2020). Clonal hematopoiesis of indeterminate potential as a novel risk factor for donor-derived leukemia. *Stem Cell Reports*, 15(2), 279–291. <https://doi.org/10.1016/j.stemcr.2020.07.008>.
 44. Burns, S. S., & Kapur, R. (2020). Putative mechanisms underlying cardiovascular disease associated with clonal hematopoiesis of indeterminate potential. *Stem Cell Reports*, 15(2), 292–306. <https://doi.org/10.1016/j.stemcr.2020.06.021>.
 45. Shlush, L. I. (2018). Age-related clonal hematopoiesis. *Blood*, 131(5), 496–504. <https://doi.org/10.1182/blood-2017-07-746453>.
 46. Fabre, M. A., McKerrell, T., Zwiebel, M., Vijayabaskar, M. S., Park, N., Wells, P. M., Rad, R., Deloukas, P., Small, K., Steves, C. J., & Vassiliou, G. S. (2020). Concordance for clonal hematopoiesis is limited in elderly twins. *Blood*, 135(4), 269–273. <https://doi.org/10.1182/blood.2019001807>.
 47. Hansen, J. W., Pedersen, D. A., Larsen, L. A., Husby, S., Clemmensen, S. B., Hjelmberg, J., Favero, F., Weischenfeldt, J., Christensen, K., & Grønbaek, K. (2020). Clonal hematopoiesis in elderly twins: concordance, discordance, and mortality. *Blood*, 135(4), 261–268. <https://doi.org/10.1182/blood.2019001793>.
 48. Steensma, D. P., Bejar, R., Jaiswal, S., Lindsley, R. C., Sekeres, M. A., Hasserjian, R. P., & Ebert, B. L. (2015). Clonal hematopoiesis of indeterminate potential and its distinction from myelodysplastic syndromes. *Blood*, 126(1), 9–16. <https://doi.org/10.1182/blood-2015-03-631747>.
 49. Pardali, E., Dimmeler, S., Zeiher, A. M., & Rieger, M. A. (2020). Clonal hematopoiesis, aging, and cardiovascular diseases. *Experimental Hematology*, 83, 95–104. <https://doi.org/10.1016/j.exphem.2019.12.006>.
 50. Chen, S., Gao, R., Yao, C., Kobayashi, M., Liu, S. Z., Yoder, M. C., Broxmeyer, H., Kapur, R., Boswell, H. S., Mayo, L. D., & Liu, Y. (2018). Genotoxic stresses promote clonal expansion of hematopoietic stem cells expressing mutant p53. *Leukemia*, 32(3), 850–854. <https://doi.org/10.1038/leu.2017.325>.
 51. Nabinger, S. C., Chen, S., Gao, R., Yao, C., Kobayashi, M., Vemula, S., Fahey, A. C., Wang, C., Daniels, C., Boswell, H. S., Sandusky, G. E., Mayo, L. D., Kapur, R., & Liu, Y. (2019). Mutant p53 enhances leukemia-initiating cell self-renewal to promote leukemia development. *Leukemia*, 33(6), 1535–1539. <https://doi.org/10.1038/s41375-019-0377-0>.
 52. Chen, S., Wang, Q., Yu, H., Capitano, M. L., Vemula, S., Nabinger, S. C., Gao, R., Yao, C., Kobayashi, M., Geng, Z., Fahey, A., Henley, D., Liu, S. Z., Barajas, S., Cai, W., Wolf, E. R., Ramdas, B., Cai, Z., Gao, H., Luo, N., et al. (2019). Mutant p53 drives clonal hematopoiesis through modulating epigenetic pathway. *Nature Communications*, 10(1), 5649. <https://doi.org/10.1038/s41467-019-13542-2>.
 53. Sperling, A. S., Gibson, C. J., & Ebert, B. L. (2017). The genetics of myelodysplastic syndrome: from clonal haematopoiesis to secondary leukaemia. *Nature Reviews Cancer*, 17(1), 5–19. <https://doi.org/10.1038/nrc.2016.112>.
 54. Jaiswal, S., Fontanillas, P., Flannick, J., Manning, A., Grauman, P. V., Mar, B. G., Lindsley, R. C., Mermel, C. H., Burt, N., Chavez, A., Higgins, J. M., Moltchanov, V., Kuo, F. C., Kluk, M. J., Henderson, B., Kinnunen, L., Koistinen, H. A., Ladenvall, C., Getz, G., Correa, A., et al. (2014). Age-related clonal hematopoiesis associated with adverse outcomes. *The New England Journal of Medicine*, 371(26), 2488–2498. <https://doi.org/10.1056/NEJMoa1408617>.
 55. Genovese, G., Köhler, A. K., Handsaker, R. E., Lindberg, J., Rose, S. A., Bakhoum, S. F., Chambert, K., Mick, E., Neale, B. M., Fromer, M., Purcell, S. M., Svantesson, O., Landén, M., Höglund, M., Lehmann, S., Gabriel, S. B., Moran, J. L., Lander, E. S., Sullivan, P. F., Sklar, P., et al. (2014). Clonal hematopoiesis and blood-cancer risk inferred from blood DNA sequence. *The New England Journal of Medicine*, 371(26), 2477–2487. <https://doi.org/10.1056/NEJMoa1409405>.
 56. Xie, M., Lu, C., Wang, J., McLellan, M. D., Johnson, K. J., Wendl, M. C., McMichael, J. F., Schmidt, H. K., Yellapantula, V., Miller, C. A., Ozenberger, B. A., Welch, J. S., Link, D. C., Walter, M. J., Mardis, E. R., Dipersio, J. F., Chen, F., Wilson, R. K., Ley, T. J., & Ding, L. (2014). Age-related mutations associated with clonal hematopoietic expansion and malignancies. *Nature Medicine*, 20(12), 1472–1478. <https://doi.org/10.1038/nm.3733>.
 57. Young, A. L., Challen, G. A., Birman, B. M., & Druley, T. E. (2016). Clonal haematopoiesis harbouring AML-associated mutations is ubiquitous in healthy adults. *Nature Communications*, 7, 12484. <https://doi.org/10.1038/ncomms12484>.
 58. Zink, F., Stacey, S. N., Norddahl, G. L., Frigge, M. L., Magnusson, O. T., Jonsdottir, I., Thorgeirsson, T. E., Sigurdsson, A., Gudjonsson, S. A., Gudmundsson, J., Jonasson, J. G., Tryggvadottir, L., Jonsson, T., Helgason, A., Gylfason, A., Sulem, P., Rafnar, T., Thorsteinsdottir, U., Gudbjartsson, D. F., Masson, G., et al. (2017). Clonal hematopoiesis, with and without candidate driver mutations, is common in the elderly. *Blood*, 130(6), 742–752. <https://doi.org/10.1182/blood-2017-02-769869>.
 59. Xia, J., Miller, C. A., Baty, J., Ramesh, A., Jotte, M., Fulton, R. S., Vogel, T. P., Cooper, M. A., Walkovich, K. J., Makaryan, V., Bolyard, A. A., Dinauer, M. C., Wilson, D. B., Vlachos, A., Myers, K. C., Rothbaum, R. J., Bertuch, A. A., Dale, D. C., Shimamura, A., Boxer, L. A., et al. (2018). Somatic mutations and clonal hematopoiesis in congenital neutropenia. *Blood*, 131(4), 408–416. <https://doi.org/10.1182/blood-2017-08-801985>.
 60. Fiscella, M., Zhang, H., Fan, S., Sakaguchi, K., Shen, S., Mercer, W. E., Vande Woude, G. F., O'Connor, P. M., & Appella, E. (1997). Wip1, a novel human protein phosphatase that is induced in response to ionizing radiation in a p53-dependent manner. *Proceedings of the National Academy of Sciences of the United States of America*, 94(12), 6048–6053. <https://doi.org/10.1073/pnas.94.12.6048>.
 61. Hsu, J. I., Dayaram, T., Tovy, A., De Braekeleer, E., Jeong, M., Wang, F., Zhang, J., Heffernan, T. P., Gera, S., Kovacs, J. J., Marszalek, J. R., Bristow, C., Yan, Y., Garcia-Manero, G., Kantarjian, H., Vassiliou, G., Futreal, P. A., Donehower, L. A., Takahashi, K., & Goodell, M. A. (2018). PPM1D mutations drive clonal hematopoiesis in response to cytotoxic chemotherapy. *Cell Stem Cell*, 23(5), 700–713.e6. <https://doi.org/10.1016/j.stem.2018.10.004>.
 62. Kahn, J. D., Miller, P. G., Silver, A. J., Sellar, R. S., Bhatt, S., Gibson, C., McConkey, M., Adams, D., Mar, B., Mertins, P.,

- Fereshtetian, S., Krug, K., Zhu, H., Letai, A., Carr, S. A., Doench, J., Jaiswal, S., & Ebert, B. L. (2018). PPM1D-truncating mutations confer resistance to chemotherapy and sensitivity to PPM1D inhibition in hematopoietic cells. *Blood*, *132*(11), 1095–1105. <https://doi.org/10.1182/blood-2018-05-850339>.
63. Coombs, C. C., Zehir, A., Devlin, S. M., Kishtagari, A., Syed, A., Jonsson, P., Hyman, D. M., Solit, D. B., Robson, M. E., Baselga, J., Arcila, M. E., Ladanyi, M., Tallman, M. S., Levine, R. L., & Berger, M. F. (2017). Therapy-related clonal hematopoiesis in patients with non-hematologic cancers is common and associated with adverse clinical outcomes. *Cell Stem Cell*, *21*(3), 374–382.e4. <https://doi.org/10.1016/j.stem.2017.07.010>.
 64. Wong, T. N., Miller, C. A., Jotte, M., Bagegni, N., Baty, J. D., Schmidt, A. P., Cashen, A. F., Duncavage, E. J., Helton, N. M., Fiala, M., Fulton, R. S., Heath, S. E., Janke, M., Luber, K., Westervelt, P., Vij, R., DiPersio, J. F., Welch, J. S., Graubert, T. A., Walter, M. J., et al. (2018). Cellular stressors contribute to the expansion of hematopoietic clones of varying leukemic potential. *Nature Communications*, *9*(1), 455. <https://doi.org/10.1038/s41467-018-02858-0>.
 65. Franceschi, C., Garagnani, P., Parini, P., Giuliani, C., & Santoro, A. (2018). Inflammaging: a new immune-metabolic viewpoint for age-related diseases. *Nature Reviews Endocrinology*, *14*(10), 576–590. <https://doi.org/10.1038/s41574-018-0059-4>.
 66. Franceschi, C., Garagnani, P., Vitale, G., Capri, M., & Salvioli, S. (2017). Inflammaging and ‘Garb-aging’. *Trends in Endocrinology and Metabolism: TEM*, *28*(3), 199–212. <https://doi.org/10.1016/j.tem.2016.09.005>.
 67. Sallman, D. A., & List, A. (2019). The central role of inflammatory signaling in the pathogenesis of myelodysplastic syndromes. *Blood*, *133*(10), 1039–1048. <https://doi.org/10.1182/blood-2018-10-844654>.
 68. Fuster, J. J., MacLauchlan, S., Zuriaga, M. A., Polackal, M. N., Ostriker, A. C., Chakraborty, R., Wu, C. L., Sano, S., Muralidharan, S., Rius, C., Vuong, J., Jacob, S., Muralidhar, V., Robertson, A. A., Cooper, M. A., Andrés, V., Hirschi, K. K., Martin, K. A., & Walsh, K. (2017). Clonal hematopoiesis associated with TET2 deficiency accelerates atherosclerosis development in mice. *Science (New York, N.Y.)*, *355*(6327), 842–847. <https://doi.org/10.1126/science.aag1381>.
 69. Guo, H., Callaway, J. B., & Ting, J. P. (2015). Inflammasomes: mechanism of action, role in disease, and therapeutics. *Nature Medicine*, *21*(7), 677–687. <https://doi.org/10.1038/nm.3893>.
 70. Basiorka, A. A., McGraw, K. L., Eksioglu, E. A., Chen, X., Johnson, J., Zhang, L., Zhang, Q., Irvine, B. A., Cluzeau, T., Sallman, D. A., Padron, E., Komrokji, R., Sokol, L., Coll, R. C., Robertson, A. A., Cooper, M. A., Cleveland, J. L., O’Neill, L. A., Wei, S., & List, A. F. (2016). The NLRP3 inflammasome functions as a driver of the myelodysplastic syndrome phenotype. *Blood*, *128*(25), 2960–2975. <https://doi.org/10.1182/blood-2016-07-730556>.
 71. Masters, S. L., Gerlic, M., Metcalf, D., Preston, S., Pellegrini, M., O’Donnell, J. A., McArthur, K., Baldwin, T. M., Chevrier, S., Nowell, C. J., Cengia, L. H., Henley, K. J., Collinge, J. E., Kastner, D. L., Feigenbaum, L., Hilton, D. J., Alexander, W. S., Kile, B. T., & Croker, B. A. (2012). NLRP1 inflammasome activation induces pyroptosis of hematopoietic progenitor cells. *Immunity*, *37*(6), 1009–1023. <https://doi.org/10.1016/j.immuni.2012.08.027>.
 72. Cai, Z., Kotzin, J. J., Ramdas, B., Chen, S., Nelanuthala, S., Palam, L. R., Pandey, R., Mali, R. S., Liu, Y., Kelley, M. R., Sandusky, G., Mohseni, M., Williams, A., Henao-Mejia, J., & Kapur, R. (2018). Inhibition of inflammatory signaling in Tet2 mutant preleukemic cells mitigates stress-induced abnormalities and clonal hematopoiesis. *Cell Stem Cell*, *23*(6), 833–849.e5. <https://doi.org/10.1016/j.stem.2018.10.013>.
 73. Wahl, M. C., Will, C. L., & Lührmann, R. (2009). The spliceosome: design principles of a dynamic RNP machine. *Cell*, *136*(4), 701–718. <https://doi.org/10.1016/j.cell.2009.02.009>.
 74. Saltzman, A. L., Pan, Q., & Blencowe, B. J. (2011). Regulation of alternative splicing by the core spliceosomal machinery. *Genes & Development*, *25*(4), 373–384. <https://doi.org/10.1101/gad.2004811>.
 75. Harries, L. W., Hernandez, D., Henley, W., Wood, A. R., Holly, A. C., Bradley-Smith, R. M., Yaghootkar, H., Dutta, A., Murray, A., Frayling, T. M., Guralnik, J. M., Bandinelli, S., Singleton, A., Ferrucci, L., & Melzer, D. (2011). Human aging is characterized by focused changes in gene expression and deregulation of alternative splicing. *Aging Cell*, *10*(5), 868–878. <https://doi.org/10.1111/j.1474-9726.2011.00726.x>.
 76. Deschênes, M., & Chabot, B. (2017). The emerging role of alternative splicing in senescence and aging. *Aging Cell*, *16*(5), 918–933. <https://doi.org/10.1111/acel.12646>.
 77. Lee, B. P., Pilling, L. C., Emond, F., Flurkey, K., Harrison, D. E., Yuan, R., Peters, L. L., Kuchel, G. A., Ferrucci, L., Melzer, D., & Harries, L. W. (2016). Changes in the expression of splicing factor transcripts and variations in alternative splicing are associated with lifespan in mice and humans. *Aging Cell*, *15*(5), 903–913. <https://doi.org/10.1111/acel.12499>.
 78. Crews, L. A., Balaian, L., Delos Santos, N. P., Leu, H. S., Court, A. C., Lazzari, E., Sadarangani, A., Zipeto, M. A., La Clair, J. J., Villa, R., Kulidjian, A., Storb, R., Morris, S. R., Ball, E. D., Burkart, M. D., & Jamieson, C. (2016). RNA splicing modulation selectively impairs leukemia stem cell maintenance in secondary human AML. *Cell Stem Cell*, *19*(5), 599–612. <https://doi.org/10.1016/j.stem.2016.08.003>.
 79. Sun, D., Luo, M., Jeong, M., Rodriguez, B., Xia, Z., Hannah, R., Wang, H., Le, T., Faull, K. F., Chen, R., Gu, H., Bock, C., Meissner, A., Göttgens, B., Darlington, G. J., Li, W., & Goodell, M. A. (2014). Epigenomic profiling of young and aged HSCs reveals concerted changes during aging that reinforce self-renewal. *Cell Stem Cell*, *14*(5), 673–688. <https://doi.org/10.1016/j.stem.2014.03.002>.
 80. McKerrell, T., Park, N., Moreno, T., Grove, C. S., Pongstingl, H., Stephens, J., Understanding Society Scientific Group, Crawley, C., Craig, J., Scott, M. A., Hodkinson, C., Baxter, J., Rad, R., Forsyth, D. R., Quail, M. A., Zeggini, E., Ouwehand, W., Varela, I., & Vassiliou, G. S. (2015). Leukemia-associated somatic mutations drive distinct patterns of age-related clonal hemopoiesis. *Cell Reports*, *10*(8), 1239–1245. <https://doi.org/10.1016/j.celrep.2015.02.005>.
 81. Yoshida, K., Sanada, M., Shiraishi, Y., Nowak, D., Nagata, Y., Yamamoto, R., Sato, Y., Sato-Otsubo, A., Kon, A., Nagasaki, M., Chalkidis, G., Suzuki, Y., Shiosaka, M., Kawahata, R., Yamaguchi, T., Otsu, M., Obara, N., Sakata-Yanagimoto, M., Ishiyama, K., Mori, H., et al. (2011). Frequent pathway mutations of splicing machinery in myelodysplasia. *Nature*, *478*(7367), 64–69. <https://doi.org/10.1038/nature10496>.
 82. Papaemmanuil, E., Cazzola, M., Boultonwood, J., Malcovati, L., Vyas, P., Bowen, D., Pellagatti, A., Wainscoat, J. S., Hellstrom-Lindberg, E., Gambacorti-Passerini, C., Godfrey, A. L., Rapado, I., Cvejic, A., Rance, R., McGee, C., Ellis, P., Mudie, L. J., Stephens, P. J., McLaren, S., Massie, C. E., et al. (2011). Somatic SF3B1 mutation in myelodysplasia with ring sideroblasts. *The New England Journal of Medicine*, *365*(15), 1384–1395. <https://doi.org/10.1056/NEJMoa1103283>.
 83. Lee, S. C., North, K., Kim, E., Jang, E., Obeng, E., Lu, S. X., Liu, B., Inoue, D., Yoshimi, A., Ki, M., Yeo, M., Zhang, X. J., Kim, M. K., Cho, H., Chung, Y. R., Taylor, J., Durham, B. H., Kim, Y. J., Pastore, A., Monette, S., et al. (2018). Synthetic lethal and convergent biological effects of cancer-associated spliceosomal gene

- mutations. *Cancer Cell*, 34(2), 225–241.e8. <https://doi.org/10.1016/j.ccell.2018.07.003>.
84. Pietras, E. M. (2017). Inflammation: a key regulator of hematopoietic stem cell fate in health and disease. *Blood*, 130(15), 1693–1698. <https://doi.org/10.1182/blood-2017-06-780882>.
 85. Boettcher, S., & Manz, M. G. (2017). Regulation of inflammation- and infection-driven hematopoiesis. *Trends in Immunology*, 38(5), 345–357. <https://doi.org/10.1016/j.it.2017.01.004>.
 86. Boettcher, S., Gerosa, R. C., Radpour, R., Bauer, J., Ampenberger, F., Heikenwalder, M., Kopf, M., & Manz, M. G. (2014). Endothelial cells translate pathogen signals into G-CSF-driven emergency granulopoiesis. *Blood*, 124(9), 1393–1403. <https://doi.org/10.1182/blood-2014-04-570762>.
 87. Ziegler, P., Boettcher, S., Takizawa, H., Manz, M. G., & Brümmerdorf, T. H. (2016). LPS-stimulated human bone marrow stroma cells support myeloid cell development and progenitor cell maintenance. *Annals of Hematology*, 95(2), 173–178. <https://doi.org/10.1007/s00277-015-2550-5>.
 88. Fernandez, L., Rodriguez, S., Huang, H., Chora, A., Fernandes, J., Mumaw, C., Cruz, E., Pollok, K., Cristina, F., Price, J. E., Ferkowicz, M. J., Scadden, D. T., Clauss, M., Cardoso, A. A., & Carlesso, N. (2008). Tumor necrosis factor- α and endothelial cells modulate Notch signaling in the bone marrow microenvironment during inflammation. *Experimental Hematology*, 36(5), 545–558. <https://doi.org/10.1016/j.exphem.2007.12.012>.
 89. Furusawa, J., Mizoguchi, I., Chiba, Y., Hisada, M., Kobayashi, F., Yoshida, H., Nakae, S., Tsuchida, A., Matsumoto, T., Ema, H., Mizuguchi, J., & Yoshimoto, T. (2016). Promotion of expansion and differentiation of hematopoietic stem cells by interleukin-27 into myeloid progenitors to control infection in emergency myelopoiesis. *PLoS Pathogens*, 12(3), e1005507. <https://doi.org/10.1371/journal.ppat.1005507>.
 90. Baldrige, M. T., King, K. Y., Boles, N. C., Weksberg, D. C., & Goodell, M. A. (2010). Quiescent haematopoietic stem cells are activated by IFN- γ in response to chronic infection. *Nature*, 465(7299), 793–797. <https://doi.org/10.1038/nature09135>.
 91. Takizawa, H., Fritsch, K., Kovtonyuk, L. V., Saito, Y., Yakkala, C., Jacobs, K., Ahuja, A. K., Lopes, M., Hausmann, A., Hardt, W. D., Gomariz, Á., Nombela-Arrieta, C., & Manz, M. G. (2017). Pathogen-induced TLR4-TRIF innate immune signaling in hematopoietic stem cells promotes proliferation but reduces competitive fitness. *Cell Stem Cell*, 21(2), 225–240.e5. <https://doi.org/10.1016/j.stem.2017.06.013>.
 92. Hirche, C., Frenz, T., Haas, S. F., Döring, M., Borst, K., Tegtmeyer, P. K., Brizic, I., Jordan, S., Keyser, K., Chhatbar, C., Pronk, E., Lin, S., Messerle, M., Jonjic, S., Falk, C. S., Trumpp, A., Essers, M., & Kalinke, U. (2017). Systemic virus infections differentially modulate cell cycle state and functionality of long-term hematopoietic stem cells in vivo. *Cell Reports*, 19(11), 2345–2356. <https://doi.org/10.1016/j.celrep.2017.05.063>.
 93. Matatall, K. A., Jeong, M., Chen, S., Sun, D., Chen, F., Mo, Q., Kimmel, M., & King, K. Y. (2016). Chronic infection depletes hematopoietic stem cells through stress-induced terminal differentiation. *Cell Reports*, 17(10), 2584–2595. <https://doi.org/10.1016/j.celrep.2016.11.031>.
 94. Schulte-Schrepping, J., Reusch, N., Paclik, D., Baßler, K., Schlickeiser, S., Zhang, B., Krämer, B., Krammer, T., Brumhard, S., Bonaguro, L., De Domenico, E., Wendisch, D., Grasshoff, M., Kapellos, T. S., Beckstette, M., Pecht, T., Saglam, A., Dietrich, O., Mei, H. E., Schulz, A. R., et al. (2020). Severe COVID-19 is marked by a dysregulated myeloid cell compartment. *Cell*, 182(6), 1419–1440.e23. Advance online publication. <https://doi.org/10.1016/j.cell.2020.08.001>.
 95. Zhang, H., Rodriguez, S., Wang, L., Wang, S., Serezani, H., Kapur, R., Cardoso, A. A., & Carlesso, N. (2016). Sepsis induces hematopoietic stem cell exhaustion and myelosuppression through distinct contributions of TRIF and MYD88. *Stem Cell Reports*, 6(6), 940–956. <https://doi.org/10.1016/j.stemcr.2016.05.002>.
 96. Josefsson, K. S., Baldrige, M. T., Kadmon, C. S., & King, K. Y. (2017). Antibiotics impair murine hematopoiesis by depleting the intestinal microbiota. *Blood*, 129(6), 729–739. <https://doi.org/10.1182/blood-2016-03-708594>.
 97. Balmer, M. L., Schürch, C. M., Saito, Y., Geuking, M. B., Li, H., Cuenca, M., Kovtonyuk, L. V., McCoy, K. D., Hapfelmeier, S., Ochsenbein, A. F., Manz, M. G., Slack, E., & Macpherson, A. J. (2014). Microbiota-derived compounds drive steady-state granulopoiesis via MyD88/TICAM signaling. *Journal of Immunology (Baltimore, Md. : 1950)*, 193(10), 5273–5283. <https://doi.org/10.4049/jimmunol.1400762>.
 98. Meisel, M., Hinterleitner, R., Pacis, A., Chen, L., Earley, Z. M., Mayassi, T., Pierre, J. F., Ernest, J. D., Galipeau, H. J., Thuille, N., Bouziat, R., Buscariet, M., Ringus, D. L., Wang, Y., Li, Y., Dinh, V., Kim, S. M., McDonald, B. D., Zurenski, M. A., Musch, M. W., et al. (2018). Microbial signals drive pre-leukaemic myeloproliferation in a Tet2-deficient host. *Nature*, 557(7706), 580–584. <https://doi.org/10.1038/s41586-018-0125-z>.
 99. Zhang, Q., & Casanova, J. L. (2020). Human TET2 bridges cancer and immunity. *Blood*, 136(9), 1018–1019. <https://doi.org/10.1182/blood.2020006881>.
 100. Stremenova Spegarova, J., Lawless, D., Mohamad, S., Engelhardt, K. R., Doody, G., Shrimpton, J., Rensing-Ehl, A., Ehl, S., Rieux-Laucat, F., Cargo, C., Griffin, H., Mikulasova, A., Acres, M., Morgan, N. V., Poulter, J. A., Sheridan, E. G., Chetcuti, P., O'Riordan, S., Anwar, R., Carter, C. R., et al. (2020). Germline TET2 loss of function causes childhood immunodeficiency and lymphoma. *Blood*, 136(9), 1055–1066. <https://doi.org/10.1182/blood.2020005844>.
 101. Zeng, H., He, H., Guo, L., Li, J., Lee, M., Han, W., Guzman, A. G., Zang, S., Zhou, Y., Zhang, X., Goodell, M. A., King, K. Y., Sun, D., & Huang, Y. (2019). Antibiotic treatment ameliorates Ten-eleven translocation 2 (TET2) loss-of-function associated hematological malignancies. *Cancer Letters*, 467, 1–8. <https://doi.org/10.1016/j.canlet.2019.09.013>.
 102. Cai, Z., Kotzin, J. J., Ramdas, B., Chen, S., Nelanuthala, S., Palam, L. R., Pandey, R., Mali, R. S., Liu, Y., Kelley, M. R., Sandusky, G., Mohseni, M., Williams, A., Henao-Mejia, J., & Kapur, R. (2018). Inhibition of inflammatory signaling in tet2 mutant preleukemic cells mitigates stress-induced abnormalities and clonal hematopoiesis. *Cell Stem Cell*, 23(6), 833–849.e5. <https://doi.org/10.1016/j.stem.2018.10.013>.
 103. Reynaud, D., Pietras, E., Barry-Holson, K., Mir, A., Binnewies, M., Jeanne, M., Sala-Torra, O., Radich, J. P., & Passegué, E. (2011). IL-6 controls leukemic multipotent progenitor cell fate and contributes to chronic myelogenous leukemia development. *Cancer Cell*, 20(5), 661–673. <https://doi.org/10.1016/j.ccr.2011.10.012>.
 104. Mager, L. F., Riether, C., Schürch, C. M., Banz, Y., Wasmer, M. H., Stuber, R., Theodorides, A. P., Li, X., Xia, Y., Saito, H., Nakae, S., Baerlocher, G. M., Manz, M. G., McCoy, K. D., Macpherson, A. J., Ochsenbein, A. F., Beutler, B., & Krebs, P. (2015). IL-33 signaling contributes to the pathogenesis of myeloproliferative neoplasms. *The Journal of Clinical Investigation*, 125(7), 2579–2591. <https://doi.org/10.1172/JCI77347>.
 105. Zambetti, N. A., Ping, Z., Chen, S., Kenswil, K., Mylona, M. A., Sanders, M. A., Hoogenboezem, R. M., Bindels, E., Adisty, M. N., Van Strien, P., van der Leije, C. S., Westers, T. M., Cremers, E., Milanese, C., Mastroberardino, P. G., van Leeuwen, J., van der Eerden, B., Touw, I. P., Kuijpers, T. W., Kanaar, R., et al. (2016). Mesenchymal inflammation drives genotoxic stress in hematopoietic stem cells and predicts disease evolution in human pre-

- leukemia. *Cell Stem Cell*, 19(5), 613–627. <https://doi.org/10.1016/j.stem.2016.08.021>.
106. Hasselbalch, H. C. (2013). Chronic inflammation as a promoter of mutagenesis in essential thrombocythemia, polycythemia vera and myelofibrosis. A human inflammation model for cancer development? *Leukemia Research*, 37(2), 214–220. <https://doi.org/10.1016/j.leukres.2012.10.020>.
 107. Pietras, E. M., Mirantes-Barbeito, C., Fong, S., Loeffler, D., Kovtonyuk, L. V., Zhang, S., Lakshminarasimhan, R., Chin, C. P., Techner, J. M., Will, B., Nerlov, C., Steidl, U., Manz, M. G., Schroeder, T., & Passegué, E. (2016). Chronic interleukin-1 exposure drives haematopoietic stem cells towards precocious myeloid differentiation at the expense of self-renewal. *Nature Cell Biology*, 18(6), 607–618. <https://doi.org/10.1038/ncb3346>.
 108. Muto, T., Walker, C. S., Choi, K., Hueneman, K., Smith, M. A., Gul, Z., Garcia-Manero, G., Ma, A., Zheng, Y., & Starczynowski, D. T. (2020). Adaptive response to inflammation contributes to sustained myelopoiesis and confers a competitive advantage in myelodysplastic syndrome HSCs. *Nature Immunology*, 21(5), 535–545. <https://doi.org/10.1038/s41590-020-0663-z>.
 109. Mann, M., Mehta, A., de Boer, C. G., Kowalczyk, M. S., Lee, K., Haldeman, P., Rogel, N., Knecht, A. R., Farouq, D., Regev, A., & Baltimore, D. (2018). Heterogeneous responses of hematopoietic stem cells to inflammatory stimuli are altered with age. *Cell Reports*, 25(11), 2992–3005.e5. <https://doi.org/10.1016/j.cellrep.2018.11.056>.
 110. Kovtonyuk, L. V., Fritsch, K., Feng, X., Manz, M. G., & Takizawa, H. (2016). Inflamm-aging of hematopoiesis, hematopoietic stem cells, and the bone marrow microenvironment. *Frontiers in Immunology*, 7, 502. <https://doi.org/10.3389/fimmu.2016.00502>.
 111. Jaiswal, S., Fontanillas, P., Flannick, J., Manning, A., Grauman, P. V., Mar, B. G., Lindsley, R. C., Mermel, C. H., Burt, N., Chavez, A., Higgins, J. M., Moltchanov, V., Kuo, F. C., Kluk, M. J., Henderson, B., Kinnunen, L., Koistinen, H. A., Ladenvall, C., Getz, G., Correa, A., et al. (2014). Age-related clonal hematopoiesis associated with adverse outcomes. *The New England Journal of Medicine*, 371(26), 2488–2498. <https://doi.org/10.1056/NEJMoa1408617>.
 112. Jaiswal, S., Natarajan, P., Silver, A. J., Gibson, C. J., Bick, A. G., Shvartz, E., McConkey, M., Gupta, N., Gabriel, S., Ardissino, D., Baber, U., Mehran, R., Fuster, V., Danesh, J., Frossard, P., Saleheen, D., Melander, O., Sukhova, G. K., Neuberg, D., Libby, P., et al. (2017). Clonal hematopoiesis and risk of atherosclerotic cardiovascular disease. *The New England Journal of Medicine*, 377(2), 111–121. <https://doi.org/10.1056/NEJMoa1701719>.
 113. Abegunde, S. O., Buckstein, R., Wells, R. A., & Rauh, M. J. (2018). An inflammatory environment containing TNF α favors Tet2-mutant clonal hematopoiesis. *Experimental Hematology*, 59, 60–65. <https://doi.org/10.1016/j.exphem.2017.11.002>.
 114. Yu, V., Yusuf, R. Z., Oki, T., Wu, J., Saez, B., Wang, X., Cook, C., Baryawno, N., Ziller, M. J., Lee, E., Gu, H., Meissner, A., Lin, C. P., Kharchenko, P. V., & Scadden, D. T. (2016). Epigenetic memory underlies cell-autonomous heterogeneous behavior of hematopoietic stem cells. *Cell*, 167(5), 1310–1322.e17. <https://doi.org/10.1016/j.cell.2016.10.045>.
 115. Ramdas, B., Mali, R. S., Palam, L. R., Pandey, R., Cai, Z., Pasupuleti, S. K., Burns, S. S., & Kapur, R. (2020). Driver mutations in leukemia promote disease pathogenesis through a combination of cell-autonomous and niche modulation. *Stem Cell Reports*, 15(1), 95–109. <https://doi.org/10.1016/j.stemcr.2020.05.002>.
 116. Chavakis, T., Mitroulis, I., & Hajishengallis, G. (2019). Hematopoietic progenitor cells as integrative hubs for adaptation to and fine-tuning of inflammation. *Nature Immunology*, 20(7), 802–811. <https://doi.org/10.1038/s41590-019-0402-5>.
 117. Gnani, D., Crippa, S., Della Volpe, L., Rossella, V., Conti, A., Lettera, E., Rivis, S., Ometti, M., Frascini, G., Bernardo, M. E., & Di Micco, R. (2019). An early-senescence state in aged mesenchymal stromal cells contributes to hematopoietic stem and progenitor cell clonogenic impairment through the activation of a pro-inflammatory program. *Aging Cell*, 18(3), e12933. <https://doi.org/10.1111/ace1.12933>.
 118. Batsivari, A., Haltalli, M., Passaro, D., Pospori, C., Lo Celso, C., & Bonnet, D. (2020). Dynamic responses of the haematopoietic stem cell niche to diverse stresses. *Nature Cell Biology*, 22(1), 7–17. <https://doi.org/10.1038/s41556-019-0444-9>.
 119. Dragoljevic, D., Westerterp, M., Veiga, C. B., Nagareddy, P., & Murphy, A. J. (2018). Disordered haematopoiesis and cardiovascular disease: a focus on myelopoiesis. *Clinical Science (London, England : 1979)*, 132(17), 1889–1899. <https://doi.org/10.1042/CS20180111>.
 120. Zhang, C., Nix, D., Gregory, M., Ciorba, M. A., Ostrander, E. L., Newberry, R. D., Spencer, D. H., & Challen, G. A. (2019). Inflammatory cytokines promote clonal hematopoiesis with specific mutations in ulcerative colitis patients. *Experimental Hematology*, 80, 36–41.e3. <https://doi.org/10.1016/j.exphem.2019.11.008>.
 121. Ricard, L., Hirsch, P., Largeaud, L., Deswarte, C., Jachiet, V., Mohty, M., Rivière, S., Malard, F., Tenon, M., de Vassogne, F., Fain, O., Gaugler, B., Rossignol, J., Delhommeau, F., & Mekinian, A. (2020). Clonal haematopoiesis is increased in early onset in systemic sclerosis. *Rheumatology (Oxford, England)*, keaa282. <https://doi.org/10.1093/rheumatology/keaa282>. Advance online publication.
 122. Burns, S. S., & Kapur, R. (2020). Clonal hematopoiesis of indeterminate potential as a novel risk factor for donor-derived leukemia. *Stem Cell Reports*, 15(2), 279–291. <https://doi.org/10.1016/j.stemcr.2020.07.008>.
 123. Bogeska, R., Kaschutnig, P., Fawaz, M., Mikecin, A.-M., Büchler-Schäff, M., Paffenholz, S., Asada, N., Frauhammer, F., Buettner, F., Ball, M., Knoch, J., Stäble, S., Walter, D., Petri, A., Carreño-Gonzalez, M.J., Wagner, V., Brors, B., Haas, S., Lipka, D.B., Essers, M.A.G., Holland-Letz, T., Mallm, J.-P., Rippe, K., Frenette, P.S., Rieger, M.A., & Milsom, M.D. (2020). Hematopoietic stem cells fail to regenerate following inflammatory challenge. *bioRxiv* 2020.08.01.230433. <https://doi.org/10.1101/2020.08.01.230433>.
 124. Rossi, D. J., Jamieson, C. H., & Weissman, I. L. (2008). Stem cells and the pathways to aging and cancer. *Cell*, 132(4), 681–696. <https://doi.org/10.1016/j.cell.2008.01.036>.
 125. Moehrl, B. M., & Geiger, H. (2016). Aging of hematopoietic stem cells: DNA damage and mutations? *Experimental Hematology*, 44(10), 895–901. <https://doi.org/10.1016/j.exphem.2016.06.253>.
 126. Lombard, D. B., Chua, K. F., Mostoslavsky, R., Franco, S., Gostissa, M., & Alt, F. W. (2005). DNA repair, genome stability, and aging. *Cell*, 120(4), 497–512. <https://doi.org/10.1016/j.cell.2005.01.028>.
 127. Ou, H. L., & Schumacher, B. (2018). DNA damage responses and p53 in the aging process. *Blood*, 131(5), 488–495. <https://doi.org/10.1182/blood-2017-07-746396>.
 128. Sen, P., Shah, P. P., Nativity, R., & Berger, S. L. (2016). Epigenetic mechanisms of longevity and aging. *Cell*, 166(4), 822–839. <https://doi.org/10.1016/j.cell.2016.07.050>.
 129. Rossi, D. J., Bryder, D., Seita, J., Nussenzweig, A., Hoeijmakers, J., & Weissman, I. L. (2007). Deficiencies in DNA damage repair limit the function of haematopoietic stem cells with age. *Nature*, 447(7145), 725–729. <https://doi.org/10.1038/nature05862>.
 130. Florian, M. C., Nattamai, K. J., Dörr, K., Marka, G., Uberle, B., Vas, V., Eckl, C., Andrä, I., Schiemann, M., Oostendorp, R. A., Scharffetter-Kochanek, K., Kestler, H. A., Zheng, Y., & Geiger,

- H. (2013). A canonical to non-canonical Wnt signalling switch in haematopoietic stem-cell ageing. *Nature*, 503(7476), 392–396. <https://doi.org/10.1038/nature12631>.
131. Flach, J., Bakker, S. T., Mohrin, M., Conroy, P. C., Pietras, E. M., Reynaud, D., Alvarez, S., Diolaiti, M. E., Ugarte, F., Forsberg, E. C., Le Beau, M. M., Stohr, B. A., Méndez, J., Morrison, C. G., & Passegué, E. (2014). Replication stress is a potent driver of functional decline in ageing haematopoietic stem cells. *Nature*, 512(7513), 198–202. <https://doi.org/10.1038/nature13619>.
132. Adams, P. D., Jasper, H., & Rudolph, K. L. (2015). Aging-induced stem cell mutations as drivers for disease and cancer. *Cell Stem Cell*, 16(6), 601–612. <https://doi.org/10.1016/j.stem.2015.05.002>.
133. Beerman, I., Bock, C., Garrison, B. S., Smith, Z. D., Gu, H., Meissner, A., & Rossi, D. J. (2013). Proliferation-dependent alterations of the DNA methylation landscape underlie hematopoietic stem cell aging. *Cell Stem Cell*, 12(4), 413–425. <https://doi.org/10.1016/j.stem.2013.01.017>.
134. Beerman, I., & Rossi, D. J. (2015). Epigenetic control of stem cell potential during homeostasis, aging, and disease. *Cell Stem Cell*, 16(6), 613–625. <https://doi.org/10.1016/j.stem.2015.05.009>.
135. Sun, D., Luo, M., Jeong, M., Rodriguez, B., Xia, Z., Hannah, R., Wang, H., Le, T., Faull, K. F., Chen, R., Gu, H., Bock, C., Meissner, A., Göttgens, B., Darlington, G. J., Li, W., & Goodell, M. A. (2014). Epigenomic profiling of young and aged HSCs reveals concerted changes during aging that reinforce self-renewal. *Cell Stem Cell*, 14(5), 673–688. <https://doi.org/10.1016/j.stem.2014.03.002>.
136. Hennrich, M. L., Romanov, N., Horn, P., Jaeger, S., Eckstein, V., Steeples, V., Ye, F., Ding, X., Poisa-Beiro, L., Lai, M. C., Lang, B., Boultonwood, J., Luft, T., Zaugg, J. B., Pellagatti, A., Bork, P., Aloy, P., Gavin, A. C., & Ho, A. D. (2018). Cell-specific proteome analyses of human bone marrow reveal molecular features of age-dependent functional decline. *Nature Communications*, 9(1), 4004. <https://doi.org/10.1038/s41467-018-06353-4>.
137. Grover, A., Sanjuan-Pla, A., Thongjuea, S., Carrelha, J., Giustacchini, A., Gambardella, A., Macaulay, I., Mancini, E., Luis, T. C., Mead, A., Jacobsen, S. E., & Nerlov, C. (2016). Single-cell RNA sequencing reveals molecular and functional platelet bias of aged haematopoietic stem cells. *Nature Communications*, 7, 11075. <https://doi.org/10.1038/ncomms11075>.
138. Singh, S. K., Singh, S., Gadomski, S., Sun, L., Pfannenstien, A., Magidson, V., Chen, X., Kozlov, S., Tessarollo, L., Klarmann, K. D., & Keller, J. R. (2018). Id1 ablation protects hematopoietic stem cells from stress-induced exhaustion and aging. *Cell Stem Cell*, 23(2), 252–265.e8. <https://doi.org/10.1016/j.stem.2018.06.001>.
139. Chandel, N. S., Jasper, H., Ho, T. T., & Passegué, E. (2016). Metabolic regulation of stem cell function in tissue homeostasis and organismal ageing. *Nature Cell Biology*, 18(8), 823–832. <https://doi.org/10.1038/ncb3385>.
140. Balaban, R. S., Nemoto, S., & Finkel, T. (2005). Mitochondria, oxidants, and aging. *Cell*, 120(4), 483–495. <https://doi.org/10.1016/j.cell.2005.02.001>.
141. Wiley, C. D., & Campisi, J. (2016). From ancient pathways to aging cells-connecting metabolism and cellular senescence. *Cell Metabolism*, 23(6), 1013–1021. <https://doi.org/10.1016/j.cmet.2016.05.010>.
142. Snoeck, H. W. (2015). Can metabolic mechanisms of stem cell maintenance explain aging and the immortal germline? *Cell Stem Cell*, 16(6), 582–584. <https://doi.org/10.1016/j.stem.2015.04.021>.
143. Ahlqvist, K. J., Suomalainen, A., & Hämmäläinen, R. H. (2015). Stem cells, mitochondria and aging. *Biochimica et Biophysica Acta*, 1847(11), 1380–1386. <https://doi.org/10.1016/j.bbabi.2015.05.014>.
144. Mohrin, M., & Chen, D. (2016). The mitochondrial metabolic checkpoint and aging of hematopoietic stem cells. *Current Opinion in Hematology*, 23(4), 318–324. <https://doi.org/10.1097/MOH.0000000000000244>.
145. Norddahl, G. L., Pronk, C. J., Wahlestedt, M., Sten, G., Nygren, J. M., Ugale, A., Sigvardsson, M., & Bryder, D. (2011). Accumulating mitochondrial DNA mutations drive premature hematopoietic aging phenotypes distinct from physiological stem cell aging. *Cell stem cell*, 8(5), 499–510. <https://doi.org/10.1016/j.stem.2011.03.009>.
146. Shao, L., Li, H., Pazhanisamy, S. K., Meng, A., Wang, Y., & Zhou, D. (2011). Reactive oxygen species and hematopoietic stem cell senescence. *International Journal of Hematology*, 94(1), 24–32. <https://doi.org/10.1007/s12185-011-0872-1>.
147. Khatri, R., Krishnan, S., Roy, S., Chattopadhyay, S., Kumar, V., & Mukhopadhyay, A. (2016). Reactive oxygen species limit the ability of bone marrow stromal cells to support hematopoietic reconstitution in aging mice. *Stem Cells and Development*, 25(12), 948–958. <https://doi.org/10.1089/scd.2015.0391>.
148. Yang, S. R., Park, J. R., & Kang, K. S. (2015). Reactive oxygen species in mesenchymal stem cell aging: implication to lung diseases. *Oxidative Medicine and Cellular Longevity*, 2015, 486263. <https://doi.org/10.1155/2015/486263>.
149. Mantel, C., Messina-Graham, S., Moh, A., Cooper, S., Hangoc, G., Fu, X. Y., & Broxmeyer, H. E. (2012). Mouse hematopoietic cell-targeted STAT3 deletion: stem/progenitor cell defects, mitochondrial dysfunction, ROS overproduction, and a rapid aging-like phenotype. *Blood*, 120(13), 2589–2599. <https://doi.org/10.1182/blood-2012-01-404004>.
150. Katajisto, P., Döhla, J., Chaffer, C. L., Pentinmikko, N., Marjanovic, N., Iqbal, S., Zoncu, R., Chen, W., Weinberg, R. A., & Sabatini, D. M. (2015). Stem cells. Asymmetric apportioning of aged mitochondria between daughter cells is required for stemness. *Science (New York, N.Y.)*, 348(6232), 340–343. <https://doi.org/10.1126/science.1260384>.
151. van Galen, P., Kreso, A., Mbong, N., Kent, D. G., Fitzmaurice, T., Chambers, J. E., Xie, S., Laurenti, E., Hermans, K., Eppert, K., Marciniak, S. J., Goodall, J. C., Green, A. R., Wouters, B. G., Wienholds, E., & Dick, J. E. (2014). The unfolded protein response governs integrity of the haematopoietic stem-cell pool during stress. *Nature*, 510(7504), 268–272. <https://doi.org/10.1038/nature13228>.
152. Mohrin, M., Shin, J., Liu, Y., Brown, K., Luo, H., Xi, Y., Haynes, C. M., & Chen, D. (2015). Stem cell aging. A mitochondrial UPR-mediated metabolic checkpoint regulates hematopoietic stem cell aging. *Science (New York, N.Y.)*, 347(6228), 1374–1377. <https://doi.org/10.1126/science.aaa2361>.
153. Trifunovic, A., Wredenberg, A., Falkenberg, M., Spelbrink, J. N., Rovio, A. T., Bruder, C. E., Bohlooly-Y, M., Gidlöf, S., Oldfors, A., Wibom, R., Törnell, J., Jacobs, H. T., & Larsson, N. G. (2004). Premature ageing in mice expressing defective mitochondrial DNA polymerase. *Nature*, 429(6990), 417–423. <https://doi.org/10.1038/nature02517>.
154. Jeong, M., Piao, Z. H., Kim, M. S., Lee, S. H., Yun, S., Sun, H. N., Yoon, S. R., Chung, J. W., Kim, T. D., Jeon, J. H., Lee, J., Kim, H. N., Choi, J. Y., & Choi, I. (2009). Thioredoxin-interacting protein regulates hematopoietic stem cell quiescence and mobilization under stress conditions. *Journal of Immunology (Baltimore, Md. : 1950)*, 183(4), 2495–2505. <https://doi.org/10.4049/jimmunol.0804221>.
155. Jung, H., Kim, M. J., Kim, D. O., Kim, W. S., Yoon, S. J., Park, Y. J., Yoon, S. R., Kim, T. D., Suh, H. W., Yun, S., Min, J. K., Lee, H. G., Lee, Y. H., Na, H. J., Lee, D. C., Kim, H. C., & Choi, I. (2013). TXNIP maintains the hematopoietic cell pool by switching the function of p53 under oxidative stress. *Cell Metabolism*, 18(1), 75–85. <https://doi.org/10.1016/j.cmet.2013.06.002>.

156. Jung, H., & Choi, I. (2014). Thioredoxin-interacting protein, hematopoietic stem cells, and hematopoiesis. *Current Opinion in Hematology*, 21(4), 265–270. <https://doi.org/10.1097/MOH.000000000000037>.
157. Florian, M. C., Dörr, K., Niebel, A., Daria, D., Schrezenmeier, H., Rojewski, M., Filippi, M. D., Hasenberg, A., Gunzer, M., Scharffetter-Kochanek, K., Zheng, Y., & Geiger, H. (2012). Cdc42 activity regulates hematopoietic stem cell aging and rejuvenation. *Cell Stem Cell*, 10(5), 520–530. <https://doi.org/10.1016/j.stem.2012.04.007>.
158. Borodkina, A., Shatrova, A., Abushik, P., Nikolsky, N., & Burova, E. (2014). Interaction between ROS dependent DNA damage, mitochondria and p38 MAPK underlies senescence of human adult stem cells. *Aging*, 6(6), 481–495. <https://doi.org/10.18632/aging.100673>.
159. Li-Harms, X., Milasta, S., Lynch, J., Wright, C., Joshi, A., Iyengar, R., Neale, G., Wang, X., Wang, Y. D., Prolla, T. A., Thompson, J. E., Opferman, J. T., Green, D. R., Schuetz, J., & Kundu, M. (2015). Mito-protective autophagy is impaired in erythroid cells of aged mtDNA-mutator mice. *Blood*, 125(1), 162–174. <https://doi.org/10.1182/blood-2014-07-586396>.
160. Klionsky, D. J., Abdelmohsen, K., Abe, A., Abedin, M. J., Abeliovich, H., Acevedo Arozena, A., Adachi, H., Adams, C. M., Adams, P. D., Adeli, K., Adihetty, P. J., Adler, S. G., Agam, G., Agarwal, R., Aghi, M. K., Agnello, M., Agostinis, P., Aguilar, P. V., Aguirre-Ghiso, J., Airoidi, E. M., et al. (2016). Guidelines for the use and interpretation of assays for monitoring autophagy (3rd edition). *Autophagy*, 12(1), 1–222. <https://doi.org/10.1080/15548627.2015.1100356>.
161. Rubinsztein, D. C., Mariño, G., & Kroemer, G. (2011). Autophagy and aging. *Cell*, 146(5), 682–695. <https://doi.org/10.1016/j.cell.2011.07.030>.
162. García-Prat, L., Martínez-Vicente, M., Perdiguero, E., Ortet, L., Rodríguez-Ubrea, J., Rebollo, E., Ruiz-Bonilla, V., Gutarra, S., Ballestar, E., Serrano, A. L., Sandri, M., & Muñoz-Cánoves, P. (2016). Autophagy maintains stemness by preventing senescence. *Nature*, 529(7584), 37–42. <https://doi.org/10.1038/nature16187>.
163. Leveque, L., Le Texier, L., Lineburg, K. E., Hill, G. R., & MacDonald, K. P. (2015). Autophagy and haematopoietic stem cell transplantation. *Immunology and Cell Biology*, 93(1), 43–50. <https://doi.org/10.1038/icb.2014.95>.
164. Lin, W., Yuan, N., Wang, Z., Cao, Y., Fang, Y., Li, X., Xu, F., Song, L., Wang, J., Zhang, H., Yan, L., Xu, L., Zhang, X., Zhang, S., & Wang, J. (2015). Autophagy confers DNA damage repair pathways to protect the hematopoietic system from nuclear radiation injury. *Scientific Reports*, 5, 12362. <https://doi.org/10.1038/srep12362>.
165. Ho, T. T., Warr, M. R., Adelman, E. R., Lansinger, O. M., Flach, J., Verovskaya, E. V., Figueroa, M. E., & Passequé, E. (2017). Autophagy maintains the metabolism and function of young and old stem cells. *Nature*, 543(7644), 205–210. <https://doi.org/10.1038/nature21388>.
166. Säwén, P., Lang, S., Mandal, P., Rossi, D. J., Soneji, S., & Bryder, D. (2016). Mitotic history reveals distinct stem cell populations and their contributions to hematopoiesis. *Cell Reports*, 14(12), 2809–2818. <https://doi.org/10.1016/j.celrep.2016.02.073>.
167. Baar, M. P., Brandt, R., Putavet, D. A., Klein, J., Derks, K., Bourgeois, B., Stryeck, S., Rijksen, Y., van Willigenburg, H., Feijtel, D. A., van der Pluijm, I., Essers, J., van Cappellen, W. A., van IJcken, W. F., Houtsmuller, A. B., Pothof, J., de Bruin, R., Madl, T., Hoeijmakers, J., Campisi, J., et al. (2017). Targeted apoptosis of senescent cells restores tissue homeostasis in response to chemotoxicity and aging. *Cell*, 169(1), 132–147.e16. <https://doi.org/10.1016/j.cell.2017.02.031>.
168. Killackey, S. A., Philpott, D. J., & Girardin, S. E. (2020). Mitophagy pathways in health and disease. *The Journal of Cell Biology*, 219(11), e202004029. <https://doi.org/10.1083/jcb.202004029>.
169. Ikeda, F. (2020). Mitophagy is induced by short ubiquitin chains on mitochondria. *The Journal of Cell Biology*, 219(9), e202008031. <https://doi.org/10.1083/jcb.202008031>.
170. Bharath, L. P., Agrawal, M., McCambridge, G., Nicholas, D. A., Hasturk, H., Liu, J., Jiang, K., Liu, R., Guo, Z., Deeney, J., Apovian, C. M., Snyder-Cappione, J., Hawk, G. S., Fleeman, R. M., Pihl, R., Thompson, K., Belkina, A. C., Cui, L., Proctor, E. A., Kern, P. A., et al. (2020). Metformin enhances autophagy and normalizes mitochondrial function to alleviate aging-associated inflammation. *Cell Metabolism*, 32(1), 44–55.e6. <https://doi.org/10.1016/j.cmet.2020.04.015>.
171. Coleman, C. N., Blakely, W. F., Fike, J. R., MacVittie, T. J., Metting, N. F., Mitchell, J. B., Moulder, J. E., Preston, R. J., Seed, T. M., Stone, H. B., Tofilon, P. J., & Wong, R. S. (2003). Molecular and cellular biology of moderate-dose (1–10 Gy) radiation and potential mechanisms of radiation protection: report of a workshop at Bethesda, Maryland, December 17–18, 2001. *Radiation Research*, 159(6), 812–834. <https://doi.org/10.1667/rr3021>.
172. Dainiak, N., Waselenko, J. K., Armitage, J. O., MacVittie, T. J., & Farese, A. M. (2003). The hematologist and radiation casualties. Hematology. American Society of Hematology. Education Program, 473–496. <https://doi.org/10.1182/asheducation-2003.1.473>.
173. Chua, H. L., Plett, P. A., Sampson, C. H., Katz, B. P., Carnathan, G. W., MacVittie, T. J., Lenden, K., & Orschell, C. M. (2014). Survival efficacy of the PEGylated G-CSFs Maxy-G34 and neulasta in a mouse model of lethal H-ARS, and residual bone marrow damage in treated survivors. *Health Physics*, 106(1), 21–38. <https://doi.org/10.1097/HP.0b013e3182a4df10>.
174. Chua, H. L., Plett, P. A., Sampson, C. H., Joshi, M., Tabbey, R., Katz, B. P., MacVittie, T. J., & Orschell, C. M. (2012). Long-term hematopoietic stem cell damage in a murine model of the hematopoietic syndrome of the acute radiation syndrome. *Health Physics*, 103(4), 356–366. <https://doi.org/10.1097/HP.0b013e3182666d6f>.
175. Chua, H. L., Plett, P. A., Fisher, A., Sampson, C. H., Vemula, S., Feng, H., Sellamuthu, R., Wu, T., MacVittie, T. J., & Orschell, C. M. (2019). Lifelong residual bone marrow damage in murine survivors of the hematopoietic acute radiation syndrome (H-ARS): a compilation of studies comprising the Indiana University Experience. *Health Physics*, 116(4), 546–557. <https://doi.org/10.1097/HP.0000000000000950>.
176. Botnick, L. E., Hannon, E. C., & Hellman, S. (1979). A long lasting proliferative defect in the hematopoietic stem cell compartment following cytotoxic agents. *International Journal of Radiation Oncology, Biology, Physics*, 5(9), 1621–1625. [https://doi.org/10.1016/0360-3016\(79\)90785-5](https://doi.org/10.1016/0360-3016(79)90785-5).
177. Mauch, P., Rosenblatt, M., & Hellman, S. (1988). Permanent loss in stem cell self renewal capacity following stress to the marrow. *Blood*, 72(4), 1193–1196.
178. Wu, T., Plett, P.A., Chua, H.L., Jacobsen, M., Sandusky, G.E., MacVittie, T.J., & Orschell, C.M. (2020). Immune reconstitution and thymic involution in the acute and delayed hematopoietic radiation syndromes. *Health Physics*. 2020 (in press).
179. Patterson, A. M., Plett, P. A., Chua, H. L., Sampson, C. H., Fisher, A., Feng, H., Unthank, J. L., Miller, S. J., Katz, B. P., MacVittie, T. J., & Orschell, C. M. (2020). Development of a model of the acute and delayed effects of high dose radiation exposure in Jackson diversity outbred mice; comparison to inbred C57BL/6 Mice. *Health Physics*. <https://doi.org/10.1097/HP.0000000000001344>. Advance online publication.
180. Hellman, S., & Botnick, L. E. (1977). Stem cell depletion: an explanation of the late effects of cytotoxins. *International*

- Journal of Radiation Oncology, Biology, Physics*, 2(1-2), 181–184. [https://doi.org/10.1016/0360-3016\(77\)90028-1](https://doi.org/10.1016/0360-3016(77)90028-1).
181. Wang, Y., Schulte, B. A., LaRue, A. C., Ogawa, M., & Zhou, D. (2006). Total body irradiation selectively induces murine hematopoietic stem cell senescence. *Blood*, 107(1), 358–366. <https://doi.org/10.1182/blood-2005-04-1418>.
 182. Meng, A., Wang, Y., Van Zant, G., & Zhou, D. (2003). Ionizing radiation and busulfan induce premature senescence in murine bone marrow hematopoietic cells. *Cancer Research*, 63(17), 5414–5419.
 183. Fish, B. L., Gao, F., Narayanan, J., Bergom, C., Jacobs, E. R., Cohen, E. P., Moulder, J. E., Orschell, C. M., & Medhora, M. (2016). Combined hydration and antibiotics with lisinopril to mitigate acute and delayed high-dose radiation injuries to multiple organs. *Health Physics*, 111(5), 410–419. <https://doi.org/10.1097/HP.0000000000000554>.
 184. Traycoff, C., Yoder, M., Hiatt, K., & Srour, E. (1996). Cell cycle stage-specific expression of adhesion molecules may augment engraftment potential of quiescent but not mitotically active hematopoietic progenitor cells. *Blood*, 88(10), 475.
 185. Abramson, S., Miller, R. G., & Phillips, R. A. (1977). The identification in adult bone marrow of pluripotent and restricted stem cells of the myeloid and lymphoid systems. *The Journal of Experimental Medicine*, 145(6), 1567–1579. <https://doi.org/10.1084/jem.145.6.1567>.
 186. Jones, R. J., Celano, P., Sharkis, S. J., & Sensenbrenner, L. L. (1989). Two phases of engraftment established by serial bone marrow transplantation in mice. *Blood*, 73(2), 397–401.
 187. Jones, R. J., Wagner, J. E., Celano, P., Zicha, M. S., & Sharkis, S. J. (1990). Separation of pluripotent haematopoietic stem cells from spleen colony-forming cells. *Nature*, 347(6289), 188–189. <https://doi.org/10.1038/347188a0>.
 188. Keller, G., & Snodgrass, R. (1990). Life span of multipotential hematopoietic stem cells in vivo. *The Journal of Experimental Medicine*, 171(5), 1407–1418. <https://doi.org/10.1084/jem.171.5.1407>.
 189. Visser, J. W. M., Bauman, J. G. J., Mulder, A. H., Eliason, J. F., & DeLeeuw, A. M. (1984). Isolation of murine pluripotent hematopoietic stem cells. *The Journal of Experimental Medicine*, 159, 1576.
 190. Hall, E. (2000). Acute effects of total-body irradiation. In E. Hall (Ed.), *Radiobiology for the radiologist* (pp. 124–135). Philadelphia: Lippincott Williams & Wilkins.
 191. Till, J. E., & McCulloch, E. A. (1961). A direct measurement of the radiation sensitivity of normal mouse bone marrow cells. *Radiation Research*, 14, 213–222.
 192. Yahata, T., Takanashi, T., Muguruma, Y., Ibrahim, A. A., Matsuzawa, H., Uno, T., Sheng, Y., Onizuka, M., Ito, M., Kato, S., & Ando, K. (2011). Accumulation of oxidative DNA damage restricts the self-renewal capacity of human hematopoietic stem cells. *Blood*, 118(11), 2941–2950. <https://doi.org/10.1182/blood-2011-01-330050>.
 193. Simonnet, A. J., Nehmé, J., Vaigot, P., Barroca, V., Leboulch, P., & Tronik-Le Roux, D. (2009). Phenotypic and functional changes induced in hematopoietic stem/progenitor cells after gamma-ray radiation exposure. *Stem Cells (Dayton, Ohio)*, 27(6), 1400–1409. <https://doi.org/10.1002/stem.66>.
 194. Zhao, W., Diz, D. I., & Robbins, M. E. (2007). Oxidative damage pathways in relation to normal tissue injury. *The British Journal of Radiology*, 80 Spec No 1, S23–S31. <https://doi.org/10.1259/bjr/18237646>.
 195. Delanian, S., & Lefaix, J. L. (2007). Current management for late normal tissue injury: radiation-induced fibrosis and necrosis. *Seminars in Radiation Oncology*, 17(2), 99–107. <https://doi.org/10.1016/j.semradonc.2006.11.006>.
 196. Yarnold, J., & Brotons, M. C. (2010). Pathogenetic mechanisms in radiation fibrosis. *Radiotherapy and Oncology : Journal of the European Society for Therapeutic Radiology and Oncology*, 97(1), 149–161. <https://doi.org/10.1016/j.radonc.2010.09.002>.
 197. Zhao, W., & Robbins, M. E. (2009). Inflammation and chronic oxidative stress in radiation-induced late normal tissue injury: therapeutic implications. *Current Medicinal Chemistry*, 16(2), 130–143. <https://doi.org/10.2174/092986709787002790>.
 198. Stone, H. B., Coleman, C. N., Anscher, M. S., & McBride, W. H. (2003). Effects of radiation on normal tissue: consequences and mechanisms. *The Lancet. Oncology*, 4(9), 529–536. [https://doi.org/10.1016/s1470-2045\(03\)01191-4](https://doi.org/10.1016/s1470-2045(03)01191-4).
 199. Yan, X., Sasi, S. P., Gee, H., Lee, J., Yang, Y., Mehrzad, R., Onufrak, J., Song, J., Enderling, H., Agarwal, A., Rahimi, L., Morgan, J., Wilson, P. F., Carrozza, J., Walsh, K., Kishore, R., & Goukassian, D. A. (2014). Cardiovascular risks associated with low dose ionizing particle radiation. *PLoS ONE*, 9(10), e110269. <https://doi.org/10.1371/journal.pone.0110269>.
 200. Sasi, S. P., Yan, X., Lee, J., Sisakyan, H., Carrozza, J., & Goukassian, D. A. (2014). Radiation-associated degenerative cardiovascular risks during normal aging and after adverse CV event 10 months post-initial exposure. *Journal of Radiation Research*, 55(Suppl 1), i111–i112.
 201. Di Maggio, F. M., Minafra, L., Forte, G. I., Cammarata, F. P., Lio, D., Messa, C., Gilardi, M. C., & Bravatà, V. (2015). Portrait of inflammatory response to ionizing radiation treatment. *Journal of Inflammation (London, England)*, 12, 14. <https://doi.org/10.1186/s12950-015-0058-3>.
 202. Fliedner, T. M., Nothdurft, W., & Calvo, W. (1986). The development of radiation late effects to the bone marrow after single and chronic exposure. *International Journal of radiation biology and Related Studies in Physics, Chemistry, and Medicine*, 49(1), 35–46. <https://doi.org/10.1080/09553008514552211>.
 203. Soucy, K. G., Lim, H. K., Attarzadeh, D. O., Santhanam, L., Kim, J. H., Bhunia, A. K., Sevinc, B., Ryoo, S., Vazquez, M. E., Nyhan, D., Shoukas, A. A., & Berkowitz, D. E. (2010). Dietary inhibition of xanthine oxidase attenuates radiation-induced endothelial dysfunction in rat aorta. *Journal of Applied Physiology (Bethesda, Md. : 1985)*, 108(5), 1250–1258. <https://doi.org/10.1152/japplphysiol.00946.2009>.
 204. Kajimura, J., Kyoizumi, S., Kubo, Y., Misumi, M., Yoshida, K., Hayashi, T., Imai, K., Ohishi, W., Nakachi, K., Weng, N. P., Young, L. F., Shieh, J. H., Moore, M. A., van den Brink, M. R., & Kusunoki, Y. (2016). Relationship between spontaneous γ H2AX foci formation and progenitor functions in circulating hematopoietic stem and progenitor cells among atomic-bomb survivors. *Mutation research. Genetic toxicology and environmental mutagenesis*, 802, 59–65. <https://doi.org/10.1016/j.mrgentox.2016.04.006>.
 205. Kusunoki, Y., & Hayashi, T. (2008). Long-lasting alterations of the immune system by ionizing radiation exposure: implications for disease development among atomic bomb survivors. *International Journal of Radiation Biology*, 84(1), 1–14. <https://doi.org/10.1080/095530007016161606>.
 206. Soucy, K. G., Lim, H. K., Kim, J. H., Oh, Y., Attarzadeh, D. O., Sevinc, B., Kuo, M. M., Shoukas, A. A., Vazquez, M. E., & Berkowitz, D. E. (2011). HZE ^{56}Fe -ion irradiation induces endothelial dysfunction in rat aorta: role of xanthine oxidase. *Radiation Research*, 176(4), 474–485. <https://doi.org/10.1667/rr2598.1>.
 207. Datta, K., Suman, S., Kallakury, B. V., & Fornace Jr., A. J. (2012). Exposure to heavy ion radiation induces persistent oxidative stress in mouse intestine. *PLoS ONE*, 7(8), e42224. <https://doi.org/10.1371/journal.pone.0042224>.
 208. Collins-Underwood, J. R., Zhao, W., Sharpe, J. G., & Robbins, M. E. (2008). NADPH oxidase mediates radiation-induced oxidative stress in rat brain microvascular endothelial cells. *Free Radical*

- Biology & Medicine*, 45(6), 929–938. <https://doi.org/10.1016/j.freeradbiomed.2008.06.024>.
209. Raju, U., Gumin, G. J., & Tofilon, P. J. (2000). Radiation-induced transcription factor activation in the rat cerebral cortex. *International Journal of Radiation Biology*, 76(8), 1045–1053. <https://doi.org/10.1080/09553000050111514>.
210. Tak, P. P., & Firestein, G. S. (2001). NF-kappaB: a key role in inflammatory diseases. *The Journal of Clinical Investigation*, 107(1), 7–11. <https://doi.org/10.1172/JCI11830>.
211. Donato, A. J., Pierce, G. L., Lesniewski, L. A., & Seals, D. R. (2009). Role of NFkappaB in age-related vascular endothelial dysfunction in humans. *Aging*, 1(8), 678–680. <https://doi.org/10.18632/aging.100080>.
212. Pan, J., Li, D., Xu, Y., Zhang, J., Wang, Y., Chen, M., Lin, S., Huang, L., Chung, E. J., Citrin, D. E., Wang, Y., Hauer-Jensen, M., Zhou, D., & Meng, A. (2017). Inhibition of Bcl-2/xl with ABT-263 selectively kills senescent type II pneumocytes and reverses persistent pulmonary fibrosis induced by ionizing radiation in mice. *International Journal of Radiation Oncology, Biology, Physics*, 99(2), 353–361. <https://doi.org/10.1016/j.ijrobp.2017.02.216>.
213. He, Y., Thummuri, D., Zheng, G., Okunieff, P., Citrin, D. E., Vujaskovic, Z., & Zhou, D. (2019). Cellular senescence and radiation-induced pulmonary fibrosis. *Translational Research: the Journal of Laboratory and Clinical Medicine*, 209, 14–21. <https://doi.org/10.1016/j.trsl.2019.03.006>.
214. Chang, J., Wang, Y., Shao, L., Laberge, R. M., Demaria, M., Campisi, J., Janakiraman, K., Sharpless, N. E., Ding, S., Feng, W., Luo, Y., Wang, X., Aykin-Burns, N., Krager, K., Ponnappan, U., Hauer-Jensen, M., Meng, A., & Zhou, D. (2016). Clearance of senescent cells by ABT263 rejuvenates aged hematopoietic stem cells in mice. *Nature Medicine*, 22(1), 78–83. <https://doi.org/10.1038/nm.4010>.
215. Yuan, R., Tsaih, S. W., Petkova, S. B., Marin de Evsikova, C., Xing, S., Marion, M. A., Bogue, M. A., Mills, K. D., Peters, L. L., Bult, C. J., Rosen, C. J., Sundberg, J. P., Harrison, D. E., Churchill, G. A., & Paigen, B. (2009). Aging in inbred strains of mice: study design and interim report on median lifespans and circulating IGF1 levels. *Aging Cell*, 8(3), 277–287. <https://doi.org/10.1111/j.1474-9726.2009.00478.x>.
216. Turturro, A., Witt, W. W., Lewis, S., Hass, B. S., Lipman, R. D., & Hart, R. W. (1999). Growth curves and survival characteristics of the animals used in the Biomarkers of Aging Program. The journals of gerontology. *Series A, Biological Sciences and Medical Sciences*, 54(11), B492–B501. <https://doi.org/10.1093/gerona/54.11.b492>.
217. Garrett, J., Sampson, C. H., Plett, P. A., Crisler, R., Parker, J., Venezia, R., Chua, H. L., Hickman, D. L., Booth, C., MacVittie, T., Orschell, C. M., & Dynlacht, J. R. (2019). Characterization and etiology of swollen muzzles in irradiated mice. *Radiation Research*, 191(1), 31–42. <https://doi.org/10.1667/RR14724.1>.
218. Ericsson, A. C., Davis, J. W., Spollen, W., Bivens, N., Givan, S., Hagan, C. E., McIntosh, M., & Franklin, C. L. (2015). Effects of vendor and genetic background on the composition of the fecal microbiota of inbred mice. *PLoS ONE*, 10(2), e0116704. <https://doi.org/10.1371/journal.pone.0116704>.
219. Mantel, C., & Broxmeyer, H. E. (2008). Sirtuin 1, stem cells, aging, and stem cell aging. *Current Opinion in Hematology*, 15(4), 326–331. <https://doi.org/10.1097/MOH.0b013e3283043819>.
220. Ou, X., Chae, H. D., Wang, R. H., Shelley, W. C., Cooper, S., Taylor, T., Kim, Y. J., Deng, C. X., Yoder, M. C., & Broxmeyer, H. E. (2011). SIRT1 deficiency compromises mouse embryonic stem cell hematopoietic differentiation, and embryonic and adult hematopoiesis in the mouse. *Blood*, 117(2), 440–450. <https://doi.org/10.1182/blood-2010-03-273011>.
221. Rimmelé, P., Bigarella, C. L., Liang, R., Izac, B., Dieguez-Gonzalez, R., Barbet, G., Donovan, M., Brugnara, C., Blander, J. M., Sinclair, D. A., & Ghaffari, S. (2014). Aging-like phenotype and defective lineage specification in SIRT1-deleted hematopoietic stem and progenitor cells. *Stem Cell Reports*, 3(1), 44–59. <https://doi.org/10.1016/j.stemcr.2014.04.015>.
222. Guarente, L., & Picard, F. (2005). Calorie restriction—the SIR2 connection. *Cell*, 120(4), 473–482. <https://doi.org/10.1016/j.cell.2005.01.029>.
223. Ocampo, A., & Izpisua Belmonte, J. C. (2015). Stem cells. Holding your breath for longevity. *Science (New York, N.Y.)*, 347(6228), 1319–1320. <https://doi.org/10.1126/science.aaa9608>.
224. Baur, J. A., Ungvari, Z., Minor, R. K., Le Couteur, D. G., & de Cabo, R. (2012). Are sirtuins viable targets for improving healthspan and lifespan? *Nature Reviews Drug Discovery*, 11(6), 443–461. <https://doi.org/10.1038/nrd3738>.
225. Mitchell, S. J., Madrigal-Matute, J., Scheibye-Knudsen, M., Fang, E., Aon, M., González-Reyes, J. A., Cortassa, S., Kaushik, S., González-Freire, M., Patel, B., Wahl, D., Ali, A., Calvo-Rubio, M., Burón, M. I., Guterrez, V., Ward, T. M., Palacios, H. H., Cai, H., Frederick, D. W., Hine, C., et al. (2016). Effects of sex, strain, and energy intake on hallmarks of aging in mice. *Cell Metabolism*, 23(6), 1093–1112. <https://doi.org/10.1016/j.cmet.2016.05.027>.
226. Brown, K., Xie, S., Qiu, X., Mohrin, M., Shin, J., Liu, Y., Zhang, D., Scadden, D. T., & Chen, D. (2013). SIRT3 reverses aging-associated degeneration. *Cell Reports*, 3(2), 319–327. <https://doi.org/10.1016/j.celrep.2013.01.005>.
227. Wrighton, K. H. (2015). Stem cells: SIRT7, the UPR and HSC ageing. *Nature Reviews Molecular Cell Biology*, 16(5), 266–267. <https://doi.org/10.1038/nrm3981>.
228. Yan, H., Baldrige, M. T., & King, K. Y. (2018). Hematopoiesis and the bacterial microbiome. *Blood*, 132(6), 559–564. <https://doi.org/10.1182/blood-2018-02-832519>.
229. Manzo, V. E., & Bhatt, A. S. (2015). The human microbiome in hematopoiesis and hematologic disorders. *Blood*, 126(3), 311–318. <https://doi.org/10.1182/blood-2015-04-574392>.
230. Broxmeyer, H. E., Cooper, S., Cacalano, G., Hague, N. L., Bailish, E., & Moore, M. W. (1996). Involvement of Interleukin (IL) 8 receptor in negative regulation of myeloid progenitor cells in vivo: evidence from mice lacking the murine IL-8 receptor homologue. *The Journal of Experimental Medicine*, 184(5), 1825–1832. <https://doi.org/10.1084/jem.184.5.1825>.
231. Khosravi, A., Yáñez, A., Price, J. G., Chow, A., Merad, M., Goodridge, H. S., & Mazmanian, S. K. (2014). Gut microbiota promote hematopoiesis to control bacterial infection. *Cell Host & Microbe*, 15(3), 374–381. <https://doi.org/10.1016/j.chom.2014.02.006>.
232. Staffas, A., Burgos da Silva, M., Slingerland, A. E., Lazrak, A., Bare, C. J., Holman, C. D., Docampo, M. D., Shono, Y., Durham, B., Pickard, A. J., Cross, J. R., Stein-Thoeringer, C., Velardi, E., Tsai, J. J., Jahn, L., Jay, H., Lieberman, S., Smith, O. M., Pamer, E. G., Peled, J. U., et al. (2018). Nutritional support from the intestinal microbiota improves hematopoietic reconstitution after bone marrow transplantation in mice. *Cell Host & Microbe*, 23(4), 447–457.e4. <https://doi.org/10.1016/j.chom.2018.03.002>.
233. Theilgaard-Mönch, K. (2017). Gut microbiota sustains hematopoiesis. *Blood*, 129(6), 662–663. <https://doi.org/10.1182/blood-2016-12-754481>.
234. Luo, Y., Chen, G. L., Hannemann, N., Ipseiz, N., Krönke, G., Bäuerle, T., Munos, L., Wirtz, S., Schett, G., & Bozec, A. (2015). Microbiota from obese mice regulate hematopoietic stem cell differentiation by altering the bone niche. *Cell Metabolism*, 22(5), 886–894. <https://doi.org/10.1016/j.cmet.2015.08.020>.
235. Lee, S., Kim, H., You, G., Kim, Y. M., Lee, S., Le, V. H., Kwon, O., Im, S. H., Kim, Y. M., Kim, K. S., Sung, Y. C., Kim, K. H., Surh, C. D., Park, Y., & Lee, S. W. (2019). Bone marrow

- CX3CR1+ mononuclear cells relay a systemic microbiota signal to control hematopoietic progenitors in mice. *Blood*, 134(16), 1312–1322. <https://doi.org/10.1182/blood.2019000495>.
236. Velders, G. A., van Os, R., Hagoort, H., Verzaal, P., Guiot, H. F., Lindley, I. J., Willemze, R., Opendakker, G., & Fibbe, W. E. (2004). Reduced stem cell mobilization in mice receiving antibiotic modulation of the intestinal flora: involvement of endotoxins as cofactors in mobilization. *Blood*, 103(1), 340–346. <https://doi.org/10.1182/blood-2002-07-2270>.
237. Severyn, C. J., Brewster, R., & Andermann, T. M. (2019). Microbiota modification in hematology: still at the bench or ready for the bedside? *Hematology. American Society of Hematology. Education Program*, 2019(1), 303–314. <https://doi.org/10.1182/hematology.2019000365>.
238. Khosravi, A., Yáñez, A., Price, J. G., Chow, A., Merad, M., Goodridge, H. S., & Mazmanian, S. K. (2014). Gut microbiota promote hematopoiesis to control bacterial infection. *Cell Host & Microbe*, 15(3), 374–381. <https://doi.org/10.1016/j.chom.2014.02.006>.
239. Wallis, C. (2020). New player in cancer's spread. A commonplace mouth bacterium now is tied to metastasis of some tumors. *Scientific American*, 323(4), 28.
240. Thaiss, C. A., Levy, M., Korem, T., Dohnalová, L., Shapiro, H., Jaitin, D. A., David, E., Winter, D. R., Gury-BenAri, M., Tatrovsky, E., Tuganbaev, T., Federici, S., Zmora, N., Zeevi, D., Dori-Bachash, M., Pevsner-Fischer, M., Kartvelishvili, E., Brandis, A., Harmelin, A., Shibolet, O., et al. (2016). Microbiota diurnal rhythmicity programs host transcriptome oscillations. *Cell*, 167(6), 1495–1510.e12. <https://doi.org/10.1016/j.cell.2016.11.003>.
241. Kostic, A. D., Chun, E., Robertson, L., Glickman, J. N., Gallini, C. A., Michaud, M., Clancy, T. E., Chung, D. C., Lochhead, P., Hold, G. L., El-Omar, E. M., Brenner, D., Fuchs, C. S., Meyerson, M., & Garrett, W. S. (2013). *Fusobacterium nucleatum* potentiates intestinal tumorigenesis and modulates the tumor-immune microenvironment. *Cell Host & Microbe*, 14(2), 207–215. <https://doi.org/10.1016/j.chom.2013.07.007>.
242. Sears, C. L., & Garrett, W. S. (2014). Microbes, microbiota, and colon cancer. *Cell Host & Microbe*, 15(3), 317–328. <https://doi.org/10.1016/j.chom.2014.02.007>.
243. Abed, J., Emgård, J. E., Zamir, G., Faroja, M., Almogy, G., Grenov, A., Sol, A., Naor, R., Pikarsky, E., Atlan, K. A., Mellul, A., Chaushu, S., Manson, A. L., Earl, A. M., Ou, N., Brennan, C. A., Garrett, W. S., & Bachrach, G. (2016). Fap2 mediates *Fusobacterium nucleatum* colorectal adenocarcinoma enrichment by binding to tumor-expressed Gal-GalNAc. *Cell Host & Microbe*, 20(2), 215–225. <https://doi.org/10.1016/j.chom.2016.07.006>.
244. Yan, X., Liu, L., Li, H., Qin, H., & Sun, Z. (2017). Clinical significance of *Fusobacterium nucleatum*, epithelial-mesenchymal transition, and cancer stem cell markers in stage III/IV colorectal cancer patients. *OncoTargets and Therapy*, 10, 5031–5046. <https://doi.org/10.2147/OTT.S145949>.
245. Shang, F. M., & Liu, H. L. (2018). *Fusobacterium nucleatum* and colorectal cancer: a review. *World Journal of Gastrointestinal Oncology*, 10(3), 71–81. <https://doi.org/10.4251/wjgo.v10.i3.71>.
246. Sun, C. H., Li, B. B., Wang, B., Zhao, J., Zhang, X. Y., Li, T. T., Li, W. B., Tang, D., Qiu, M. J., Wang, X. C., Zhu, C. M., & Qian, Z. R. (2019). The role of *Fusobacterium nucleatum* in colorectal cancer: from carcinogenesis to clinical management. *Chronic Diseases and Translational Medicine*, 5(3), 178–187. <https://doi.org/10.1016/j.cdtm.2019.09.001>.
247. Kang, W., Ji, X., Zhang, X., Tang, D., & Feng, Q. (2019). Persistent exposure to *Fusobacterium nucleatum* triggers chemokine/cytokine release and inhibits the proliferation and osteogenic differentiation capabilities of human gingiva-derived mesenchymal stem cells. *Frontiers in Cellular and Infection Microbiology*, 9, 429. <https://doi.org/10.3389/fcimb.2019.00429>.
248. Chen, Y., Chen, Y., Zhang, J., Cao, P., Su, W., Deng, Y., Zhan, N., Fu, X., Huang, Y., & Dong, W. (2020). *Fusobacterium nucleatum* promotes metastasis in colorectal cancer by activating autophagy signaling via the upregulation of CARD3 expression. *Theranostics*, 10(1), 323–339. <https://doi.org/10.7150/thno.38870>.
249. Furtek, K. J., Kubiak, D. W., Barra, M., Varughese, C. A., Ashbaugh, C. D., & Koo, S. (2016). High incidence of neutropenia in patients with prolonged ceftaroline exposure. *The Journal of Antimicrobial Chemotherapy*, 71(7), 2010–2013. <https://doi.org/10.1093/jac/dkw062>.
250. Vinh, D. C., & Rubinstein, E. (2009). Linezolid: a review of safety and tolerability. *The Journal of Infection*, 59(Suppl 1), S59–S74. [https://doi.org/10.1016/S0163-4453\(09\)60009-8](https://doi.org/10.1016/S0163-4453(09)60009-8).
251. Iwamura, C., Bouladoux, N., Belkaid, Y., Sher, A., & Jankovic, D. (2017). Sensing of the microbiota by NOD1 in mesenchymal stromal cells regulates murine hematopoiesis. *Blood*, 129(2), 171–176. <https://doi.org/10.1182/blood-2016-06-723742>.
252. Shintouo, C. M., Mets, T., Beckwee, D., Bautmans, I., Ghogomu, S. M., Souopgui, J., Leemans, L., Meriki, H. D., & Njemini, R. (2020). Is inflammaging influenced by the microbiota in the aged gut? A systematic review. *Experimental Gerontology*, 141, 111079. Advance online publication. <https://doi.org/10.1016/j.exger.2020.111079>.
253. Chen, F., Liu, Y., Wong, N. K., Xiao, J., & So, K. F. (2017). Oxidative stress in stem cell aging. *Cell Transplantation*, 26(9), 1483–1495. <https://doi.org/10.1177/0963689717735407>.
254. Broxmeyer, H. E., Capitano, M. L., Cooper, S., Potchanant, E. S., & Clapp, D. W. (2020). Numbers of long-term hematopoietic stem cells from bone marrow of fanca and fancx knockout mice can be greatly enhanced by their collection and processing in physioxia conditions. *Blood Cells, Molecules & Diseases*, 86, 102492. Advance online publication. <https://doi.org/10.1016/j.bcmd.2020.102492>.
255. Broxmeyer, H. E., Cooper, S., & Capitano, M. L. (2020). Enhanced collection of phenotypic and engrafting human cord blood hematopoietic stem cells at 4°C. *Stem Cells (Dayton, Ohio)*, 38(10), 1326–1331. <https://doi.org/10.1002/stem.3243>.
256. Säwén, P., Lang, S., Mandal, P., Rossi, D. J., Soneji, S., & Bryder, D. (2016). Mitotic history reveals distinct stem cell populations and their contributions to hematopoiesis. *Cell Reports*, 14(12), 2809–2818. <https://doi.org/10.1016/j.celrep.2016.02.073>.
257. Calderwood, S. K., Murshid, A., & Prince, T. (2009). The shock of aging: molecular chaperones and the heat shock response in longevity and aging—a mini-review. *Gerontology*, 55(5), 550–558. <https://doi.org/10.1159/000225957>.
258. Pandya, J. D., Valdez, M., Royland, J. E., MacPhail, R. C., Sullivan, P. G., & Kodavanti, P. (2020). Age- and organ-specific differences in mitochondrial bioenergetics in brown norway rats. *Journal of Aging Research*, 2020, 7232614. <https://doi.org/10.1155/2020/7232614>.
259. Valente, L. J., Tarangelo, A., Li, A. M., Naciri, M., Raj, N., Boutelle, A. M., Li, Y., Mello, S. S., Biegging-Rolett, K., DeBerardinis, R. J., Ye, J., Dixon, S. J., & Attardi, L. D. (2020). p53 deficiency triggers dysregulation of diverse cellular processes in physiological oxygen. *The Journal of Cell Biology*, 219(11), e201908212. <https://doi.org/10.1083/jcb.201908212>.
260. Nombela-Arrieta, C., Pivarnik, G., Winkel, B., Canty, K. J., Harley, B., Mahoney, J. E., Park, S. Y., Lu, J., Protopopov, A., & Silberstein, L. E. (2013). Quantitative imaging of haematopoietic stem and progenitor cell localization and hypoxic status in the bone marrow microenvironment. *Nature Cell Biology*, 15(5), 533–543. <https://doi.org/10.1038/ncb2730>.

261. Conboy, I. M., Conboy, M. J., Wagers, A. J., Girma, E. R., Weissman, I. L., & Rando, T. A. (2005). Rejuvenation of aged progenitor cells by exposure to a young systemic environment. *Nature*, *433*(7027), 760–764. <https://doi.org/10.1038/nature03260>.
262. Maryanovich, M., Zahalka, A. H., Pierce, H., Pinho, S., Nakahara, F., Asada, N., Wei, Q., Wang, X., Ciero, P., Xu, J., Leftin, A., & Frenette, P. S. (2018). Adrenergic nerve degeneration in bone marrow drives aging of the hematopoietic stem cell niche. *Nature Medicine*, *24*(6), 782–791. <https://doi.org/10.1038/s41591-018-0030-x>.
263. Aguilar-Navarro, A. G., Meza-León, B., Gratzinger, D., Juárez-Aguilar, F. G., Chang, Q., Ornatsky, O., Tsui, H., Esquivel-Gómez, R., Hernández-Ramírez, A., Xie, S. Z., Dick, J. E., & Flores-Figueroa, E. (2020). Human aging alters the spatial organization between CD34+ hematopoietic cells and adipocytes in bone marrow. *Stem Cell Reports*, *15*(2), 317–325. <https://doi.org/10.1016/j.stemcr.2020.06.011>.
264. Singh, P., Kacena, M. A., Orschell, C. M., & Pelus, L. M. (2020). Aging-related reduced expression of CXCR4 on bone marrow mesenchymal stromal cells contributes to hematopoietic stem and progenitor cell defects. *Stem Cell Reviews and Reports*, *16*(4), 684–692. <https://doi.org/10.1007/s12015-020-09974-9>.
265. Wang, Y. P., & Lei, Q. Y. (2018). Metabolite sensing and signaling in cell metabolism. *Signal Transduction and Targeted Therapy*, *3*, 30. <https://doi.org/10.1038/s41392-018-0024-7>.
266. Shapira, S. N., & Christofk, H. R. (2020). Metabolic regulation of tissue stem cells. *Trends in Cell Biology*, *30*(7), 566–576. <https://doi.org/10.1016/j.tcb.2020.04.004>.
267. Xia, P., Wang, S., Du, Y., Huang, G., Satoh, T., Akira, S., & Fan, Z. (2015). Insulin-InsR signaling drives multipotent progenitor differentiation toward lymphoid lineages. *The Journal of Experimental Medicine*, *212*(13), 2305–2321. <https://doi.org/10.1084/jem.20150618>.
268. Zhang, Y., Xue, Y., Cao, C., Huang, J., Hong, Q., Hai, T., Jia, Q., Wang, X., Qin, G., Yao, J., Wang, X., Zheng, Q., Zhang, R., Li, Y., Luo, A., Zhang, N., Shi, G., Wang, Y., Ying, H., Liu, Z., et al. (2017). Thyroid hormone regulates hematopoiesis via the TR-KLF9 axis. *Blood*, *130*(20), 2161–2170. <https://doi.org/10.1182/blood-2017-05-783043>.
269. Stewart, M. H., Gutierrez-Martinez, P., Beerman, I., Garrison, B., Gallagher, E. J., LeRoith, D., & Rossi, D. J. (2014). Growth hormone receptor signaling is dispensable for HSC function and aging. *Blood*, *124*(20), 3076–3080. <https://doi.org/10.1182/blood-2014-05-575308>.
270. Friedman, J. M., & Halaas, J. L. (1998). Leptin and the regulation of body weight in mammals. *Nature*, *395*(6704), 763–770. <https://doi.org/10.1038/27376>.
271. La Cava, A., & Matarese, G. (2004). The weight of leptin in immunity. *Nature Reviews Immunology*, *4*(5), 371–379. <https://doi.org/10.1038/nri1350>.
272. Ongrádi, J., & Kövesdi, V. (2010). Factors that may impact on immunosenescence: an appraisal. *Immunity & Ageing: I & A*, *7*, 7. <https://doi.org/10.1186/1742-4933-7-7>.
273. Frasca, D., Diaz, A., Romero, M., & Blomberg, B. B. (2020). Leptin induces immunosenescence in human B cells. *Cellular Immunology*, *348*, 103994. <https://doi.org/10.1016/j.cellimm.2019.103994>.
274. Frasca, D., & Blomberg, B. B. (2017). Adipose tissue inflammation induces B cell inflammation and decreases B cell function in aging. *Frontiers in Immunology*, *8*, 1003. <https://doi.org/10.3389/fimmu.2017.01003>.
275. Gupta, S., Agrawal, S., & Gollapudi, S. (2013). Increased activation and cytokine secretion in B cells stimulated with leptin in aged humans. *Immunity & Ageing: I & A*, *10*(1), 3. <https://doi.org/10.1186/1742-4933-10-3>.
276. Koenig, S., Luheshi, G. N., Wenz, T., Gerstberger, R., Roth, J., & Rummel, C. (2014). Leptin is involved in age-dependent changes in response to systemic inflammation in the rat. *Brain, Behavior, and Immunity*, *36*, 128–138. <https://doi.org/10.1016/j.bbi.2013.10.019>.
277. Gabriely, I., Ma, X. H., Yang, X. M., Rossetti, L., & Barzilai, N. (2002). Leptin resistance during aging is independent of fat mass. *Diabetes*, *51*(4), 1016–1021. <https://doi.org/10.2337/diabetes.51.4.1016>.
278. Filippi, B. M., & Lam, T. K. (2014). Leptin and aging. *Aging*, *6*(2), 82–83. <https://doi.org/10.18632/aging.100637>.
279. Zhou, B. O., Yu, H., Yue, R., Zhao, Z., Rios, J. J., Naveiras, O., & Morrison, S. J. (2017). Bone marrow adipocytes promote the regeneration of stem cells and haematopoiesis by secreting SCF. *Nature Cell Biology*, *19*(8), 891–903. <https://doi.org/10.1038/ncb3570>.
280. Himburg, H. A., Termini, C. M., Schlüssel, L., Kan, J., Li, M., Zhao, L., Fang, T., Sasine, J. P., Chang, V. Y., & Chute, J. P. (2018). Distinct bone marrow sources of pleiotrophin control hematopoietic stem cell maintenance and regeneration. *Cell stem cell*, *23*(3), 370–381.e5. <https://doi.org/10.1016/j.stem.2018.07.003>.
281. Comazzetto, S., Murphy, M. M., Berto, S., Jeffery, E., Zhao, Z., & Morrison, S. J. (2019). Restricted hematopoietic progenitors and erythropoiesis require SCF from leptin receptor+ niche cells in the bone marrow. *Cell stem cell*, *24*(3), 477–486.e6. <https://doi.org/10.1016/j.stem.2018.11.022>.
282. Ding, L., Saunders, T. L., Enikolopov, G., & Morrison, S. J. (2012). Endothelial and perivascular cells maintain haematopoietic stem cells. *Nature*, *481*(7382), 457–462. <https://doi.org/10.1038/nature10783>.
283. Krings, A., Rahman, S., Huang, S., Lu, Y., Czernik, P. J., & Lecka-Czernik, B. (2012). Bone marrow fat has brown adipose tissue characteristics, which are attenuated with aging and diabetes. *Bone*, *50*(2), 546–552. <https://doi.org/10.1016/j.bone.2011.06.016>.
284. Ambrosi, T. H., Scialdone, A., Graja, A., Gohlke, S., Jank, A. M., Bocian, C., Woelk, L., Fan, H., Logan, D. W., Schürmann, A., Saraiva, L. R., & Schulz, T. J. (2017). Adipocyte accumulation in the bone marrow during obesity and aging impairs stem cell-based hematopoietic and bone regeneration. *Cell Stem Cell*, *20*(6), 771–784.e6. <https://doi.org/10.1016/j.stem.2017.02.009>.
285. Trinh, T., Ropa, J., Aljoufi, A., Cooper, S., Sinn, A., Srour, E. F., & Broxmeyer, H. E. (2020). Leptin receptor as a marker for long-term functional hematopoietic stem cells. *Leukemia*. In Press.
286. Nakao, T., Hino, M., Yamane, T., Nishizawa, Y., Morii, H., & Tatsumi, N. (1998). Expression of the leptin receptor in human leukaemic blast cells. *British journal of haematology*, *102*(3), 740–745. <https://doi.org/10.1046/j.1365-2141.1998.00843.x>.
287. Lu, Z., Xie, J., Wu, G., Shen, J., Collins, R., Chen, W., Kang, X., Luo, M., Zou, Y., Huang, L. J., Amatrua, J. F., Slone, T., Winick, N., Scherer, P. E., & Zhang, C. C. (2017). Fasting selectively blocks development of acute lymphoblastic leukemia via leptin-receptor upregulation. *Nature Medicine*, *23*(1), 79–90. <https://doi.org/10.1038/nm.4252>.
288. Wex, H., Pönelis, E., Wex, T., Dressendörfer, R., Mittler, U., & Vorwerk, P. (2002). Plasma leptin and leptin receptor expression in childhood acute lymphoblastic leukemia. *International Journal of Hematology*, *76*(5), 446–452. <https://doi.org/10.1007/BF02982810>.
289. Ozturk, K., Avcu, F., & Ural, A. U. (2012). Aberrant expressions of leptin and adiponectin receptor isoforms in chronic myeloid leukemia patients. *Cytokine*, *57*(1), 61–67. <https://doi.org/10.1016/j.cyto.2011.10.004>.
290. He, H., Xu, P., Zhang, X., Liao, M., Dong, Q., Cong, T., Tang, B., Yang, X., Ye, M., Chang, Y., Liu, W., Wang, X., Ju, Z., & Wang,

- J. (2020). Aging-induced IL27Ra signaling impairs hematopoietic stem cells. *Blood*, *136*(2), 183–198. <https://doi.org/10.1182/blood.2019003910>.
291. Kucia, M., Masternak, M., Liu, R., Shin, D. M., Ratajczak, J., Mierzejewska, K., Spong, A., Kopchick, J. J., Bartke, A., & Ratajczak, M. Z. (2013). The negative effect of prolonged somatotrophic/insulin signaling on an adult bone marrow-residing population of pluripotent very small embryonic-like stem cells (VSELs). *Age (Dordrecht, Netherlands)*, *35*(2), 315–330. <https://doi.org/10.1007/s11357-011-9364-8>.
292. Ratajczak, M. Z., Bartke, A., & Darzynkiewicz, Z. (2017). Prolonged growth hormone/insulin/insulin-like growth factor nutrient response signaling pathway as a silent killer of stem cells and a culprit in aging. *Stem Cell Reviews and Reports*, *13*(4), 443–453. <https://doi.org/10.1007/s12015-017-9728-2>.
293. Boyiadzis, M., & Whiteside, T. L. (2017). The emerging roles of tumor-derived exosomes in hematological malignancies. *Leukemia*, *31*(6), 1259–1268. <https://doi.org/10.1038/leu.2017.91>.
294. Shah, R., Patel, T., & Freedman, J. E. (2018). Circulating extracellular vesicles in human disease. *The New England Journal of Medicine*, *379*(10), 958–966. <https://doi.org/10.1056/NEJMr1704286>.
295. Kowal, J., Tkach, M., & Théry, C. (2014). Biogenesis and secretion of exosomes. *Current Opinion in Cell Biology*, *29*, 116–125. <https://doi.org/10.1016/j.ceb.2014.05.004>.
296. Dreyer, F., & Baur, A. (2016). Biogenesis and functions of exosomes and extracellular vesicles. *Methods in Molecular Biology (Clifton, N.J.)*, *1448*, 201–216. https://doi.org/10.1007/978-1-4939-3753-0_15.
297. Kalluri, R. (2016). The biology and function of exosomes in cancer. *The Journal of Clinical Investigation*, *126*(4), 1208–1215. <https://doi.org/10.1172/JCI81135>.
298. Guo, W., Li, Y., Pang, W., & Shen, H. (2020). Exosomes: a potential therapeutic tool targeting communications between tumor cells and macrophages. *Molecular Therapy : the Journal of the American Society of Gene Therapy*, *28*(9), 1953–1964. <https://doi.org/10.1016/j.ymthe.2020.06.003>.
299. Namburi, S., Broxmeyer, H. E., Hong, C. S., Whiteside, T. L., & Boyiadzis, M. (2020). DPP4+ exosomes in aml patient's plasma suppress proliferation of hematopoietic progenitor cells. *Leukemia*. In Press.
300. Glielich, C. R., & Holland, A. J. (2020). Keeping track of time: the fundamentals of cellular clocks. *The Journal of Cell Biology*, *219*(11), e202005136. <https://doi.org/10.1083/jcb.202005136>.
301. Kuintzle, R. C., Chow, E. S., Westby, T. N., Gvakharia, B. O., Giebultowicz, J. M., & Hendrix, D. A. (2017). Circadian deep sequencing reveals stress-response genes that adopt robust rhythmic expression during aging. *Nature Communications*, *8*, 14529. <https://doi.org/10.1038/ncomms14529>.
302. Golan, K., Kumari, A., Kollet, O., Khatib-Massalha, E., Subramaniam, M. D., Ferreira, Z. S., Avemaria, F., Rzeszotek, S., Garcia-García, A., Xie, S., Flores-Figueroa, E., Gur-Cohen, S., Itkin, T., Ludin-Tal, A., Massalha, H., Bernshtein, B., Ciechanowicz, A. K., Brandis, A., Mehlman, T., Bhattacharya, S., et al. (2018). Daily onset of light and darkness differentially controls hematopoietic stem cell differentiation and maintenance. *Cell Stem Cell*, *23*(4), 572–585.e7. <https://doi.org/10.1016/j.stem.2018.08.002>.
303. Butler, T. D., & Gibbs, J. E. (2020). Circadian host-microbiome interactions in immunity. *Frontiers in Immunology*, *11*, 1783. <https://doi.org/10.3389/fimmu.2020.01783>.
304. Anderson, S. T., & FitzGerald, G. A. (2020). Sexual dimorphism in body clocks. *Science (New York, N.Y.)*, *369*(6508), 1164–1165. <https://doi.org/10.1126/science.abd4964>.
305. Liesveld, J. L., Sharma, N., & Aljotawi, O. S. (2020). Stem cell homing: from physiology to therapeutics. *Stem cells (Dayton, Ohio)*. <https://doi.org/10.1002/stem.3242>. Advance online publication.
306. Huang, X., & Broxmeyer, H. E. (2019). Progress towards improving homing and engraftment of hematopoietic stem cells for clinical transplantation. *Current Opinion in Hematology*, *26*(4), 266–272. <https://doi.org/10.1097/MOH.0000000000000510>.
307. Guo, B., Huang, X., Cooper, S., & Broxmeyer, H. E. (2017). Glucocorticoid hormone-induced chromatin remodeling enhances human hematopoietic stem cell homing and engraftment. *Nature Medicine*, *23*(4), 424–428. <https://doi.org/10.1038/nm.4298>.
308. Huang, X., Guo, B., Liu, S., Wan, J., & Broxmeyer, H. E. (2018). Neutralizing negative epigenetic regulation by HDAC5 enhances human haematopoietic stem cell homing and engraftment. *Nature Communications*, *9*(1), 2741. <https://doi.org/10.1038/s41467-018-05178-5>.
309. Xu, D., Yang, M., Capitano, M., Guo, B., Liu, S., Wan, J., Broxmeyer, H. E., & Huang, X. (2020). Pharmacological activation of nitric oxide signaling promotes human hematopoietic stem cell homing and engraftment. *Leukemia*. <https://doi.org/10.1038/s41375-020-0787-z>. Advance online publication.
310. Capitano, M. L., Chitteti, B. R., Cooper, S., Srouf, E. F., Bartke, A., & Broxmeyer, H. E. (2015). Ames hypopituitary dwarf mice demonstrate imbalanced myelopoiesis between bone marrow and spleen. *Blood Cells, Molecules & Diseases*, *55*(1), 15–20. <https://doi.org/10.1016/j.bcmd.2015.03.004>.
311. Dong, E., Du, H., & Gardner, L. (2020). An interactive web-based dashboard to track COVID-19 in real time. *The Lancet. Infectious Diseases*, *20*(5), 533–534. [https://doi.org/10.1016/S1473-3099\(20\)30120-1](https://doi.org/10.1016/S1473-3099(20)30120-1).
312. Banerjee, A., Nasir, J. A., Budyłowski, P., Yip, L., Aftanas, P., Christie, N., Ghalami, A., Baid, K., Raphenya, A. R., Hirota, J. A., Miller, M. S., McGeer, A. J., Ostrowski, M., Kozak, R. A., McArthur, A. G., Mossman, K., & Mubareka, S. (2020). Isolation, sequence, infectivity, and replication kinetics of severe acute respiratory syndrome coronavirus 2. *Emerging Infectious Diseases*, *26*(9), 2054–2063. <https://doi.org/10.3201/eid2609.201495>.
313. Korber, B., Fischer, W. M., Gnanakaran, S., Yoon, H., Theiler, J., Abfalterer, W., Hengartner, N., Giorgi, E. E., Bhattacharya, T., Foley, B., Hastie, K. M., Parker, M. D., Partridge, D. G., Evans, C. M., Freeman, T. M., de Silva, T. I., Sheffield COVID-19 Genomics Group, McDanal, C., Perez, L. G., Tang, H., et al. (2020). Tracking changes in SARS-CoV-2 Spike: evidence that D614G increases infectivity of the COVID-19 virus. *Cell*, *182*(4), 812–827.e19. <https://doi.org/10.1016/j.cell.2020.06.043>.
314. Hoffmann, M., Kleine-Weber, H., Schroeder, S., Krüger, N., Herrler, T., Erichsen, S., Schiergens, T. S., Herrler, G., Wu, N. H., Nitsche, A., Müller, M. A., Drosten, C., & Pöhlmann, S. (2020). SARS-CoV-2 cell entry depends on ACE2 and TMPRSS2 and is blocked by a clinically proven protease inhibitor. *Cell*, *181*(2), 271–280.e8. <https://doi.org/10.1016/j.cell.2020.02.052>.
315. Chan, J. F., Yuan, S., Kok, K. H., To, K. K., Chu, H., Yang, J., Xing, F., Liu, J., Yip, C. C., Poon, R. W., Tsoi, H. W., Lo, S. K., Chan, K. H., Poon, V. K., Chan, W. M., Ip, J. D., Cai, J. P., Cheng, V. C., Chen, H., Hui, C. K., et al. (2020). A familial cluster of pneumonia associated with the 2019 novel coronavirus indicating person-to-person transmission: a study of a family cluster. *Lancet (London, England)*, *395*(10223), 514–523. [https://doi.org/10.1016/S0140-6736\(20\)30154-9](https://doi.org/10.1016/S0140-6736(20)30154-9).
316. Huang, C., Wang, Y., Li, X., Ren, L., Zhao, J., Hu, Y., Zhang, L., Fan, G., Xu, J., Gu, X., Cheng, Z., Yu, T., Xia, J., Wei, Y., Wu, W., Xie, X., Yin, W., Li, H., Liu, M., Xiao, Y., et al. (2020). Clinical features of patients infected with 2019 novel coronavirus

- in Wuhan, China. *Lancet (London, England)*, 395(10223), 497–506. [https://doi.org/10.1016/S0140-6736\(20\)30183-5](https://doi.org/10.1016/S0140-6736(20)30183-5).
317. Pence, B. D. (2020). Severe COVID-19 and aging: are monocytes the key? *GeroScience*, 42(4), 1051–1061. <https://doi.org/10.1007/s11357-020-00213-0>.
 318. COVID-19 Hospitalization and Death by Age | CDC [Online]. Available at: <https://www.cdc.gov/coronavirus/2019-ncov/covid-data/investigations-discovery/hospitalization-death-by-age.html>. Accessed 25 Sept 2020.
 319. Heald-Sargent, T., Muller, W. J., Zheng, X., Rippe, J., Patel, A. B., & Kociolek, L. K. (2020). Age-related differences in nasopharyngeal severe acute respiratory syndrome coronavirus 2 (SARS-CoV-2) levels in patients with mild to moderate coronavirus disease 2019 (COVID-19). *JAMA Pediatrics*, 174(9), 902–903. Advance online publication. <https://doi.org/10.1001/jamapediatrics.2020.3651>.
 320. Zhang, Y., Geng, X., Tan, Y., Li, Q., Xu, C., Xu, J., Hao, L., Zeng, Z., Luo, X., Liu, F., & Wang, H. (2020). New understanding of the damage of SARS-CoV-2 infection outside the respiratory system. *Biomedicine & Pharmacotherapy = Biomedecine & Pharmacotherapie*, 127, 110195. <https://doi.org/10.1016/j.biopha.2020.110195>.
 321. Wen, W., Su, W., Tang, H., Le, W., Zhang, X., Zheng, Y., Liu, X., Xie, L., Li, J., Ye, J., Dong, L., Cui, X., Miao, Y., Wang, D., Dong, J., Xiao, C., Chen, W., & Wang, H. (2020). Immune cell profiling of COVID-19 patients in the recovery stage by single-cell sequencing. *Cell Discovery*, 6, 31. <https://doi.org/10.1038/s41421-020-0168-9>.
 322. Terpos, E., Ntanasis-Stathopoulos, I., Elalamy, I., Kastritis, E., Sergentanis, T. N., Politou, M., Psaltopoulou, T., Gerotziakas, G., & Dimopoulos, M. A. (2020). Hematological findings and complications of COVID-19. *American Journal of Hematology*, 95(7), 834–847. <https://doi.org/10.1002/ajh.25829>.
 323. Ratajczak, M. Z., Bujko, K., Ciechanowicz, A., Sielatycka, K., Cymer, M., Marlicz, W., & Kucia, M. (2020). SARS-CoV-2 entry receptor ACE2 is expressed on very small CD45- precursors of hematopoietic and endothelial cells and in response to virus spike protein activates the Nlrp3 inflammasome. *Stem Cell Reviews and Reports*, 1–12. <https://doi.org/10.1007/s12015-020-10010-z>. Advance online publication.
 324. Ropa, J., Cooper, S., Capitano, M.L., Van't Hof, W., & Broxmeyer, H.E. (2020). Human hematopoietic stem, progenitor, and immune cells respond ex vivo to SARS-CoV-2 spike protein. *Stem Cell Reviews and Reports*. In Press.
 325. Mehta, P., McAuley, D. F., Brown, M., Sanchez, E., Tattersall, R. S., Manson, J. J., & HLH Across Speciality Collaboration, UK. (2020). COVID-19: consider cytokine storm syndromes and immunosuppression. *Lancet (London, England)*, 395(10229), 1033–1034. [https://doi.org/10.1016/S0140-6736\(20\)30628-0](https://doi.org/10.1016/S0140-6736(20)30628-0).
 326. Yang, Y., Shen, C., Li, J., Yuan, J., Wei, J., Huang, F., Wang, F., Li, G., Li, Y., Xing, L., Peng, L., Yang, M., Cao, M., Zheng, H., Wu, W., Zou, R., Li, D., Xu, Z., Wang, H., Zhang, M., et al. (2020). Plasma IP-10 and MCP-3 levels are highly associated with disease severity and predict the progression of COVID-19. *The Journal of Allergy and Clinical Immunology*, 146(1), 119–127.e4. <https://doi.org/10.1016/j.jaci.2020.04.027>.
 327. Jiang, F., Yang, J., Zhang, Y., Dong, M., Wang, S., Zhang, Q., Liu, F. F., Zhang, K., & Zhang, C. (2014). Angiotensin-converting enzyme 2 and angiotensin 1-7: novel therapeutic targets. *Nature Reviews Cardiology*, 11(7), 413–426. <https://doi.org/10.1038/nrcardio.2014.59>.
 328. Hadley, E. C., Lakatta, E. G., Morrison-Bogorad, M., Warner, H. R., & Hodes, R. J. (2005). The future of aging therapies. *Cell*, 120(4), 557–567. <https://doi.org/10.1016/j.cell.2005.01.030>.
 329. Montecino-Rodriguez, E., Berent-Maoz, B., & Dorshkind, K. (2013). Causes, consequences, and reversal of immune system aging. *The Journal of Clinical Investigation*, 123(3), 958–965. <https://doi.org/10.1172/JCI64096>.
 330. McHugh, D., & Gil, J. (2018). Senescence and aging: causes, consequences, and therapeutic avenues. *The Journal of Cell Biology*, 217(1), 65–77. <https://doi.org/10.1083/jcb.201708092>.
 331. Campisi, J., Kapahi, P., Lithgow, G. J., Melov, S., Newman, J. C., & Verdin, E. (2019). From discoveries in ageing research to therapeutics for healthy ageing. *Nature*, 571(7764), 183–192. <https://doi.org/10.1038/s41586-019-1365-2>.
 332. Spehar, K., Pan, A., & Beerman, I. (2020). Restoring aged stem cell functionality: current progress and future directions. *Stem Cells (Dayton, Ohio)*. <https://doi.org/10.1002/stem.3234>. Advance online publication.
 333. Serebryanny, L., & Misteli, T. (2018). Protein sequestration at the nuclear periphery as a potential regulatory mechanism in premature aging. *The Journal of Cell Biology*, 217(1), 21–37. <https://doi.org/10.1083/jcb.201706061>.
 334. Klaips, C. L., Jayaraj, G. G., & Hartl, F. U. (2018). Pathways of cellular proteostasis in aging and disease. *The Journal of Cell Biology*, 217(1), 51–63. <https://doi.org/10.1083/jcb.201709072>.
 335. Hu, J. L., Todhunter, M. E., LaBarge, M. A., & Gartner, Z. J. (2018). Opportunities for organoids as new models of aging. *The Journal of Cell Biology*, 217(1), 39–50. <https://doi.org/10.1083/jcb.201709054>.
 336. Wang, H., & Zhang, X. H. (2020). Molecules in the blood of older people promote cancer spread. *Nature*, 585(7824), 187–188. <https://doi.org/10.1038/d41586-020-02381-7>.
 337. Gomes, A. P., Ilter, D., Low, V., Endress, J. E., Fernández-García, J., Rosenzweig, A., Schild, T., Broekaert, D., Ahmed, A., Planque, M., Elia, I., Han, J., Kinzig, C., Mullarky, E., Mutvei, A. P., Asara, J., de Cabo, R., Cantley, L. C., Dephore, N., Fendt, S. M., et al. (2020). Age-induced accumulation of methylmalonic acid promotes tumour progression. *Nature*, 585(7824), 283–287. <https://doi.org/10.1038/s41586-020-2630-0>.
 338. Sinclair, D., LaPlante, M. D., & Delphia, C. (2019). *Lifespan: why we age—and why we don't have to*. Publisher: New York: Atria Books, 2019.
 339. Silwal, P., Kim, J. K., Kim, Y. J., & Jo, E. K. (2020). Mitochondrial reactive oxygen species: double-edged weapon in host defense and pathological inflammation during infection. *Frontiers in Immunology*, 11, 1649. <https://doi.org/10.3389/fimmu.2020.01649>.
 340. Hormaechea-Agulla, D., Le, D. T., & King, K. Y. (2020). Common sources of inflammation and their impact on hematopoietic stem cell biology. *Current Stem Cell Reports*, 1–12. <https://doi.org/10.1007/s40778-020-00177-z>. Advance online publication.
 341. Haas, S. (2020). Hematopoietic stem cells in health and disease—insights from single-cell multi-omic approaches. *Current Stem Cell Reports*, 6, 67–76. <https://doi.org/10.1007/s40778-020-00174-2>.
 342. Horton, P. D., Dumbali, S., & Wenzel, P. L. (2020). Mechanoregulation in hematopoiesis and hematologic disorders. *Current Stem Cell Reports*, 6, 86–95. <https://doi.org/10.1007/s40778-020-00172-4>.
 343. Golan, K., Singh, A. K., Kollet, O., Bertagna, M., Althoff, M., Khatib-Massalha, E., Petrovich-Kopitman, E., Wellendorf, A., Massalha, H., Levin-Zaidman, S., Dadosh, T., Bohan, B., Gawali, M. V., Dasgupta, B., Lapidot, T., & Cancelas, J. A. (2020). Bone marrow regeneration requires mitochondrial transfer from donor Cx43-expressing hematopoietic progenitors to stroma. *Blood*, 2020005399. <https://doi.org/10.1182/blood.2020005399>. Advance online publication.
 344. Challen, G. A., & Goodell, M. A. (2020). Clonal hematopoiesis: mechanisms driving dominance of stem cell clones. *Blood*, 136(14), 1590–1598. <https://doi.org/10.1182/blood.2020006510>.

345. Warren, J. T., & Link, D. C. (2020). Clonal hematopoiesis and risk for hematologic malignancy. *Blood*, *136*(14), 1599–1605. <https://doi.org/10.1182/blood.2019000991>.
346. Jaiswal, S. (2020). Clonal hematopoiesis and nonhematologic disorders. *Blood*, *136*(14), 1606–1614. <https://doi.org/10.1182/blood.2019000989>.
347. Shaheen, M., & Broxmeyer, H. E. (2013). Principles of cytokine signaling. In R. Hoffman, E. J. Benz, L. E. Silberstein Jr., H. Heslop, J. I. Weitz, & J. Anastasi (Eds.), *Hematology: Basic principles and practice* (6th Edition, Chapter 14 ed., pp. 136–146). Philadelphia: Elsevier Saunders.
348. Shaheen, M., & Broxmeyer, H. E. (2018). Cytokine/Receptor families and signal transduction. In R. Hoffman, E. Benz, L. Silberstein, H. Heslop, J. I. Weitz, J. Anastasi, M. E. Salama, & S. A. Abutalib (Eds.), *Hematology: Basic principles and practice* (7th Edition, Chapter 16 ed., pp. 163–175).
349. Shao, L., Elujoba-Bridenstine, A., Zink, K. E., Sanchez, L. M., Cox, B. J., Pollok, K. E., Sinn, A., Bailey, B. J., Sims, E., Cooper, S., Broxmeyer, H. E., Pajcini, K. V., & Tamplin, O. J. (2020). The neurotransmitter receptor Gabbr1 regulates proliferation and function of hematopoietic stem and progenitor cells. *Blood*, *2019004415*. <https://doi.org/10.1182/blood.2019004415>. Advance online publication.
350. Wang, X. and Broxmeyer, H.E. (2020). DUSP16 is a regulator of hematopoietic stem and progenitor cells and promotes their expansion ex-vivo. *Leukemia*. In Press.
351. Christopherson 2nd, K. W., Hangoc, G., Mantel, C. R., & Broxmeyer, H. E. (2004). Modulation of hematopoietic stem cell homing and engraftment by CD26. *Science (New York, N.Y.)*, *305*(5686), 1000–1003. <https://doi.org/10.1126/science.1097071>.
352. Broxmeyer, H. E., Hoggatt, J., O'Leary, H. A., Mantel, C., Chitteti, B. R., Cooper, S., Messina-Graham, S., Hangoc, G., Farag, S., Rohrabough, S. L., Ou, X., Speth, J., Pelus, L. M., Srour, E. F., & Campbell, T. B. (2012). Dipeptidylpeptidase 4 negatively regulates colony-stimulating factor activity and stress hematopoiesis. *Nature Medicine*, *18*(12), 1786–1796. <https://doi.org/10.1038/nm.2991>.
353. Farag, S. S., Srivastava, S., Messina-Graham, S., Schwartz, J., Robertson, M. J., Abonour, R., Cornetta, K., Wood, L., Secrest, A., Strother, R. M., Jones, D. R., & Broxmeyer, H. E. (2013). In vivo DPP-4 inhibition to enhance engraftment of single-unit cord blood transplants in adults with hematological malignancies. *Stem Cells and Development*, *22*(7), 1007–1015. <https://doi.org/10.1089/scd.2012.0636>.
354. Vélez de Mendizábal, N., Strother, R. M., Farag, S. S., Broxmeyer, H. E., Messina-Graham, S., Chitnis, S. D., & Bies, R. R. (2014). Modelling the sitagliptin effect on dipeptidyl peptidase-4 activity in adults with haematological malignancies after umbilical cord blood haematopoietic cell transplantation. *Clinical Pharmacokinetics*, *53*(3), 247–259. <https://doi.org/10.1007/s40262-013-0109-y>.
355. Farag, S. S., Nelson, R., Cairo, M. S., O'Leary, H. A., Zhang, S., Huntley, C., Delgado, D., Schwartz, J., Zaid, M. A., Abonour, R., Robertson, M., & Broxmeyer, H. (2017). High-dose sitagliptin for systemic inhibition of dipeptidylpeptidase-4 to enhance engraftment of single cord umbilical cord blood transplantation. *Oncotarget*, *8*(66), 110350–110357. <https://doi.org/10.18632/oncotarget.22739>.
356. Broxmeyer, H. E., Farag, S. S., & Rocha, V. (2016). Cord blood hematopoietic cell transplantation. In S. J. Forman, R. S. Negrin, J. H. Antin, & F. R. Appelbaum (Eds.), *Thomas Hematopoietic Cell Transplantation* (5th Edition, Chapter 39 ed., pp. 437–455). Oxford, England: John Wiley & Sons, Ltd.
357. Farag, S., Zaid, M. A., Nelson, R. P., Schwartz, J. E., Thakran, T. C., Blakley, A. J., Broxmeyer, H. E., & Zhang, S. (2020). Dipeptidyl peptidase-4 inhibition for the prevention of acute graft versus host disease following myeloablative allogeneic peripheral blood stem cell transplantation. *New England Journal of Medicine*. In Press.
358. Ou, X., O'Leary, H. A., & Broxmeyer, H. E. (2013). Implications of DPP4 modification of proteins that regulate stem/progenitor and more mature cell types. *Blood*, *122*(2), 161–169. <https://doi.org/10.1182/blood-2013-02-487470>.
359. Ropa, J., & Broxmeyer, H. E. (2020). An expanded role for dipeptidylpeptidase4 (DPP4) in cell regulation. *Current Opinion in Hematology*, *27*(4), 215–224. <https://doi.org/10.1097/MOH.0000000000000590>.
360. Broxmeyer, H. E., Capitano, M., Campbell, T. B., Hangoc, G., & Cooper, S. (2016). Modulation of hematopoietic chemokine effects in vitro and in vivo by DPP-4/CD26. *Stem Cells and Development*, *25*(8), 575–585. <https://doi.org/10.1089/scd.2016.0026>.
361. Liggett, L. A., & Sankaran, V. G. (2020). Unraveling hematopoiesis through the lens of genomics. *Cell*, *182*(6), 1384–1400. <https://doi.org/10.1016/j.cell.2020.08.030>.
362. Morrison, S. J., & Scadden, D. T. (2014). The bone marrow niche for haematopoietic stem cells. *Nature*, *505*(7483), 327–334. <https://doi.org/10.1038/nature12984>.

Publisher's Note Springer Nature remains neutral with regard to jurisdictional claims in published maps and institutional affiliations.